



**FACULTY OF MECHANICAL ENGINEERING KRALJEVO
UNIVERSITY OF KRAGUJEVAC
KRALJEVO - SERBIA
SERBIA & MONTENEGRO**

THE FIFTH INTERNATIONAL CONFERENCE

HEAVY MACHINERY HM 2005

PROCEEDINGS

ORGANIZATION SUPPORTED BY:

Ministry of Science and environmental protection of the Republic of Serbia

KRALJEVO, 28 JUNE – 03 JULY 2005



FACULTY OF MECHANICAL ENGINEERING KRALJEVO
UNIVERSITY OF KRAGUJEVAC
KRALJEVO - SERBIA
SERBIA & MONTENEGRO

PUBLISHER:

Faculty of Mechanical Engineering, Kraljevo

EDITORS:

Prof. Dr Milomir Gašić, mech. eng.

Prof. Dr Ljubomir Lukić, mech. eng.

PRINTOUT:

PP Komino Trade, Kraljevo

TECHNICAL COMMITTEE

Dr Zlatan Šoškić

Dr Dragan Petrović

M.Sc. Dragan Pršić

M.Sc. Radovan Bulatović

M.Sc. Goran Miodragović

M.Sc. Slobodan Ivanović

M.Sc. Ljubiša Dubonjić

M.Sc. Miljan Marašević

M.Sc. Goran Marković

M.Sc. Rade Karamarković

Nebojša Bogojević

Slobodan Bukarica

Milorad Stambolić

No. of copies: 200

REVIEWS:

All papers have been reviewed by members of scientific committee



FACULTY OF MECHANICAL ENGINEERING KRALJEVO
UNIVERSITY OF KRAGUJEVAC
KRALJEVO - SERBIA
SERBIA & MONTENEGRO

CONFERENCE CHAIRMAN

Prof. Dr Milomir Gašić, mech. eng.

INTERNATIONAL PROGRAM COMMITTEE

President: Prof. Dr Milomir Gašić, FME Kraljevo

Vice President: Prof. Dr Milan Dedić, FME Kraljevo

Secretary: M.Sc. Snežana Ćirić Kostić, FME Kraljevo

- | | |
|--|--|
| 1. Prof. Dr E. M. Kudrjavcev, Russia | 26. Prof. Dr D. Ostrić, FME Belgrade |
| 2. Prof. Dr P. I. Nikulin, Russia | 27. Prof. Dr Z. Petković, FME Belgrade |
| 3. Prof. Dr K. Ehmann, USA | 28. Prof. Dr Z. Ribar, FME Belgrade |
| 4. Prof. Dr A. Freddi, Italy | 29. Prof. Dr V. Lučanin, FME Belgrade |
| 5. Prof. Dr N. Shapira, USA | 30. Prof. Dr S. Tošić, FME Belgrade |
| 6. Prof. Dr M. Guidoboni, Italy | 31. Prof. Dr B. Obrović, FME Kragujevac |
| 7. Prof. Dr M. Alamoreanu, Romania | 32. Prof. Dr M. Stefanović, FME Kragujevac |
| 8. Prof. Dr H. M. Bogdevicius, Lithuania | 33. Prof. Dr M. Demić, FME Kragujevac |
| 9. Prof. Dr I. A. Emeljanova, Ukraine | 34. Prof. Dr Z. Jugović, FTS Čačak |
| 10. Prof. Dr L.V. Nazarov, Ukraine | 35. Prof. Dr R. Mijajlović, FME Niš |
| 11. Prof. Dr V. N. Meščerin, Russia | 36. Prof. Dr V. Jevtić, FME Niš |
| 12. Prof. Dr M. A. Stepanov, Russia | 37. Prof. Dr R. Rakanović, FME Kraljevo |
| 13. Prof. Dr I. Filonov, Belarus | 38. Prof. Dr M. Vesković, FME Kraljevo |
| 14. Prof. Dr N. Nenov, Bulgaria | 39. Prof. Dr V. Karamarković, FME Kraljevo |
| 15. Prof. Dr A. Bruja, Romania | 40. Prof. Dr N. Nedić, FME Kraljevo |
| 16. Prof. Dr J. Polajnar, Canada | 41. Prof. Dr M. Rajović, FME Kraljevo |
| 17. Prof. Dr K. Weinert, Deutschland | 42. Prof. Dr V. Mečanin, FME Kraljevo |
| 18. Prof. Dr V. Čović, FME Belgrade | 43. Prof. Dr D. Jevtić, FME Kraljevo |
| 19. Prof. Dr D. Ružić, FME Belgrade | 44. Prof. Dr M. Milojević, FME Kraljevo |
| 20. Prof. Dr R. Durković, FME Podgorica | 45. Prof. Dr T. Pantelić, FME Kraljevo |
| 21. Prof. Dr V. Gajić, FTS Novi Sad | 46. Prof. Dr LJ. Djordjević, FME Kraljevo |
| 22. Prof. Dr M. Kalajdžić, FME Belgrade | 47. Prof. Dr S. Radović, FME Kraljevo |
| 23. Prof. Dr Ž. Spasić, FME Belgrade | 48. Prof. Dr M. Vukićević, FME Kraljevo |
| 24. Prof. Dr V. Milačić, FME Belgrade | 49. Prof. Dr S. Trifunović, FME Kraljevo |
| 25. Prof. Dr Dj. Zrnić, FME Belgrade | 50. Prof. Dr M. Pavličić, FME Kraljevo |



FACULTY OF MECHANICAL ENGINEERING KRALJEVO
UNIVERSITY OF KRAGUJEVAC
KRALJEVO - SERBIA
SERBIA & MONTENEGRO

ORGANIZING COMMITTEE

Charman: Prof. Dr Ljubomir Lukić, FME Kraljevo

Vice charman: Doc. Dr Zoran Petrović, FME Kraljevo

Secretary: M. Sc. Nataša Pavlović, FME Kraljevo

Members: Doc. Dr A. Babić, FME Kraljevo
Doc. Dr M. Savković, FME Kraljevo
Doc. Dr R. Petrović, FME Kraljevo
Doc. Dr D. Petrović, FME Kraljevo
Doc. Dr Z. Šoškić, FME Kraljevo
Doc. Dr M. Kolarević, FME Kraljevo
M.Sc. D. Pršić, M.Sc. S. Ivanović,
M.Sc. G. Miodragović, M.Sc. R. Bulatović,
M.Sc. J. Nešović, M.Sc. G. Marković,
M.Sc. S. Šalinić, M.Sc. R. Nikolić,
M.Sc. Lj. Lalović, M.Sc. Z. Glavčić,
M.Sc. R. Karamarković (FME Kraljevo)
M.Sc. M. Marašević (FME Kraljevo)
M.Sc. Lj. Dubonjić (FME Kraljevo)



CONTENTS

PLENARY SESSION

Lj.Lukić, M.Gašić, R.Rakanović, N.Nedić, V.Karamarković, Lj.Djordjević APPLICATION OF UP-TO-DATE INFORMATION TECHNOLOGIES IN REVITALIZING OF PRODUCTION SYSTEMS	P.1
--	-----

I DESIGN IN MACHINERY

SESSION A: EARTH MOVING AND MINIG MACHINES AND TRANSPORTATION SYSTEMS

И.С. Суровцев, П.И. Никулин, Р.С. Солодов ВЛИЯНИЕ РАДИУСА ПОВОРОТА НА ТОПЛИВНО-ЭКОНОМИЧЕСКИЕ ПОКАЗАТЕЛИ ДИФФЕРЕНЦИАЛЬНОГО МОСТА СНАБЖЁННОГО КРУПНОГАБАРИТНЫМИ ПНЕВМАТИЧЕСКИМИ ШИНАМИ	I A.1
Prof. dr Radan Durković MOBILE WORKING MACHINES AND THEIR ELEMENTS: CALCULATION OF LIFETIME	I A.5
Никулин Павел Иванович, Топалов Эдуард Львович СТЕНД ДЛЯ ИСПЫТАНИЯ СИСТЕМЫ ПНЕВМОКАТКОВЫЙ ДВИЖИТЕЛЬ - ГРУНТ	I A.9
Емельянова И.А. , Баранов А.Н , Задорожный А.А, Непорожнев А.С, Грачев Ф.А. ПУТИ СОВЕРШЕНСТВОВАНИЯ МАЛОГАБАРИТНОГО ОБОРУДОВАНИЯ ДЛЯ УСЛОВИЙ СТРОИТЕЛЬНОЙ ПЛОЩАДКИ	I A.13
П.И.Никулин, Е.И.Никаноров МЕТОДИКА ОЦЕНКИ ТОРМОЗНЫХ КАЧЕСТВ КОЛЕСНОГО ДВИЖИТЕЛЯ ЗЕМЛЕРОЙНО-ТРАНСПОРТНЫХ МАШИН	I A.17
М. Gašić, M. Savković, G. Marković, N. Zdravković, S. Igrutinović MACHINES AND PLANTS OF BUILDING AND TRANSPORT MECHANIZATION- TECHNICAL REGULATIONS CONDITION	I A.19
П.И. Никулин, В.А. Нилов, А.А. Косенко ИСПЫТАНИЯ СКРЕПЕРНОГО АГРЕГАТА	I A.23
Ljubinko D. Savić, Miloje D. Rajović, Vukmir O. Mijajlović DISPOSITION OF THE DIGGING RESISTANCE ON THE OPEN PIT EXCAVATOR TYPE SRS – 1300, AT THE KOSOVO'S COAL-MINE	I A.27
П.И. Никулин, А.П. Никулин, В.Л. Тюнин ВЛИЯНИЕ КОНСТРУКЦИИ КРУПНОГАБАРИТНОЙ ШИНЫ НА ТОПЛИВНО- ЭКОНОМИЧЕСКИЕ ПОКАЗАТЕЛИ КОЛЁСНОГО ДВИЖИТЕЛЯ ПРИ КРИВОЛИНЕЙНОМ ДВИЖЕНИИ	I A.31

Ph. D. Dragoslav Janosevic, Stevan Nedeljkovic SYNTHESIS OF SLEWING PLATFORMS DRIVES OF HYDRAULIC EXCAVATORS	I A.35
П.И. Никулин, Д.А. Удодов, А.Н. Пришуттов ВЛИЯНИЕ РАДИУСА ПОВОРОТА НА ТОПЛИВНО-ЭКОНОМИЧЕСКИЕ ПОКАЗАТЕЛИ ДВУХОСНОГО ДВИЖИТЕЛЯ СНАБЖЁННОГО КРУПНОГАБАРИТНЫМИ ПНЕВМАТИЧЕСКИМИ ШИНАМИ	I A.39
Milosav Georgijević, Nenad Zrnić, Andreja Arsenijević, Vlada Gašić MACHINES FOR HANDLING CONTAINERS AND BULK MATERIALS, ARE WE READY FOR THE INTERNATIONAL COMPETITION?	I A.43
Mircea Alămoreanu EVALUATION OF THE AVAILABLE RESOURCES OF THE SELF-SUPPORTING STRUCTURES OF HOISTING MACHINES DURING EXPLOITATION	I A.49
Gašić M , Savković M, Marković G, Zdravković N THE APPROXIMATION OF THE EQUATION FOR BENDING STIFFNESS OF TRUSS CONSTRUCTION	I A.55
Petković Z., Gašić V., Bošnjak S., Zrnić N. DYNAMIC BEHAVEOUR SIMULATION OF STRUCTURE OF BRIDGE-TYPE STACKER-RECLAIMER	I A.59
Univ. Prof. Dr. Sc. Đorđe Zrnić INFLUENCE OF MAINTENANCE ON THE PERFORMANCES OF LARGE SCALE SYSTEMS	I A.65
Univ. Ass. Dr.-Ing. Nenad Đ. Zrnić, Univ. Prof. Dr.-Ing. Zoran Petković QUAYSIDE CONTAINER CRANES - GENERAL CLASSIFICATION, STATE-OF-THE-ART AND SOME EXPECTATION IN DEVELOPMENT	I A.69
Zoran Marinković, Predrag Milić, Dragan Marinković, Goran Petrović, Saša Marković MODELING AND SIMULATION OF THE WORK OF TRANSPORT MACHINES DRIVING MECHANISMS WITH FREQUENCY MODULATED ELECTROMOTOR DRIVE	I A.73
Gašić V., Petković Z., Bošnjak S. SETTING UP THE DYNAMIC MODEL OF BOOM STRUCTURE AT BRIDGE-TYPE STACKER-RECLAIMER	I A.77
Univ. Ass. Dr.-Ing. Nenad Đ. Zrnić EVALUATION OF PERFORMANCES AND PROPOSAL OF CONCEPT OF QUAYSIDE CONTAINER CRANES IN FUTURE	I A.81
Георги Генадиев РЕСУРС ДЕТАЛЕЙ ТРАНСПОРТНЫХ МАШИН – В ЗАВИСИМОСТИ ОТ НАГРУЗОЧНЫХ РЕЖИМОВ	I A.85
Miloradović N., Slavković R., Vujanac R. BEHAVIOR OF OVERHEAD TRAVELING CRANE'S CARRYING STRUCTURE DURING JOINT OPERATION OF HOISTING AND TROLLEY MECHANISMS	I A.89
Brkić A., Petrović Z., Bugarić U. ADVANTAGES OF CONTEMPORARY, MODULAR, LIGHTWEIGHT PROFILE BRIDGE CRANE AND MONORAIL SYSTEMS	I A.93

I DESIGN IN MACHINERY

SESSION B: AUTOMATIC CONTROL AND FLUID TECHNIQUE

Vojislav Filipovic

ROBUST STABILITY OF NETWORKED CONTROL SYSTEMS BASED ON
LYAPUNOV-RAZUMIKHIN THEORY

I B.1

Zoran Boričić, Dragisa Nikodijević, Dragica Milenković and Stamenković Živojin

UNIVERSAL EQUATIONS OF UNSTEADY MHD INCOMPRESSIBLE FLOW ON
HEATED MOVING PLATE OF FLUID WHICH ELECTRO-CONDUCTIVITY IS
FUNCTION OF VELOCITY RATIO

I B.5

Vlastimir Nikolić, Žarko Čojbašić and Katarina Aleksić

CONVENTIONAL AND INTELLIGENT TEMPERATURE CONTROL COMPARISON
FOR THE MULTIZONE CRYSTAL GROWTH FURNACE

I B.9

Bogdevicius Marijonas

DYNAMIC PROCESSES OF BRAKING THE VEHICLE WITH THE HYDRAULIC
BRAKING SYSTEM

I B.13

Ž. Jakovljević, P. B. Petrović

A NEW SYSTEM FOR TEXTILE WEB FEEDING AT CALENDERING LINES IN
TIREMAKING INDUSTRY

I B.17

Vojislav Filipovic

FEEDBACK OVER WIRELESS CHANNEL

I B.21

Radovan Petrovic, Svetislav Cantrak, Zoran Glavcic

COMPUTER PROGRAM FOR MATHEMATICAL MODELING AND IDENTIFICATION
OF HYDRODINAMIC PROCESSES OF A PISTON RADIAL PUMP

I B.25

Radovan Petrovic, Zoran Glavcic, Nebojsa Zdravkovic

MATHEMATICAL MODEL OF THE VANE PUMP WORKING FLUID

I B.29

Zoran Boričić, Dragisa Nikodijević, Dragica Milenković and Stamenković Živojin

NUMERICAL AND EXPERIMENTAL DETERMINATION OF VENTURI TUBE
FLOWMETER DISCHARGE COEFFICIENT

I B.33

D.H. Pršić and N.N. Nedić

CAUSALITY OF 0-JUNCTIONS IN ENERGY BASED MODELING

I B.37

S. Lj. Biočanin, V. D. Veljković

EXPERIMENTAL ANALYSIS OF FIRE CONTROL SYSTEM

I B.41

M. Živković, G. Mihajlović, D. Golubović

SIMULATION MODEL FOR THE ANALYSIS OF BEHAVIOUROF HYDROSTATIC
FORCE TRANSDUCER (HFT)

I B.45

N.N.Nedić, D.H.Pršić, L.J.M.Dubonjić

PRESSURE EQUIPMENTS SAFETY UNITS TESTING ACCORDING TO EUROPEAN
DIRECTIVE (PED) 97/23 EC

I B.49

I DESIGN IN MACHINERY

SESSION C: CONSTRUCTION AND MECHANICS

В.П. Баранчик, В.А. Васильев

ДИНАМИЧЕСКИЕ ПРОЦЕССЫ В КОМБИНИРОВАННОМ ПРИВОДЕ МАШИН С
СУММИРОВАНИЕМ ПАРАЛЛЕЛЬНЫХ СИЛОВЫХ ПОТОКОВ

I C.1

Miroslav Zivkovic, Milos Kojic, Vlade Vukadinovic, Ivo Vlastelica THE ELEMENT-FREE GALERKIN METHOD	I C.5
Prof. Dr. Adrian BRUJA, Marian DIMA, Catalin FRANCU INFLUENCE OF THE GEOMETRICAL PARAMETERS CONCERNING THE DISTRIBUTION OF MESHING FORCES ON HARMONICAL GEARINGS WITH RIGID FRONTAL ELEMENT	I C.9
Ognjanović M., Ćirić-Kostić S. GEAR HOUSING MODAL BEHAVIOUR AND NOISE EMISSION	I C.13
Prof. dr Božidar Rosić, dr Aleksandar Marinkovic, mr Aleksandar Venc OPTIMUM DESIGN OF MULTISPEED GEARBOXES AND MODELING OF TRANSMISSION COMPONENTS	I C.17
Prof. Dr. Adrian BRUJA, Marian DIMA, Catalin FRANCU ANALYSIS OF THE INDUCED STRESS AND STRAIN OF TEETH FLANKS OF FRONTAL HARMONIC GEARINGS WITH RIGID ELEMENT	I C.21
Dr Milorad Milovančević, Dr Milan Dedić CRITICAL TRANSVERSE PRESSURE OF A COMPOSITE PLATE WITH MID-LAYER MADE OF LONGITUDINAL STRIPS	I C.25
Ruzica R. Nikolic, Jelena M. Veljkovic THE ANALYSIS OF DESIGNING COLUMNS CENTRICALLY LOADED BY AXIAL COMPRESSIVE LOAD	I C.29
Dr Milan Dedic AN ANALYSIS OF LOCAL STABILITY OF COMPOSITE PLATE WITH STRIPPED MID-LAYER	I C.33
Svetislav Radovic APPLICATION OF DYNAMICS OF RIGID BODIES TO MECHANISMS WITH CLOSED CHAIN FORMS	I C.37
Cristiano Fragassa, Leonardo Frizziero, Martin Villanueva USING QUALITY METHODOLOGIES FOR INNOVATIVE DESIGN	I C.41
M.Sc. Boban Andjelković, Ph. D. Vlastimir Đokić, Ph. D. Dragan Milčić THE MODEL FOR GENERATING THE STRUCTURE OF THE NEURO – FAZI INFERENCE SYSTEM	I C.45
Jovanović M., Milić P., Mijajlović D. NONLINEAR CONTACT ANALYSIS OF THE HEAVY STRUCTURE SUPPORT	I C.49
Nikola Janković CALCULATION OF DOUBLE PARABOLOID SPRINGS	I C.53
Dr Svetislav Lj. Markovic, Dr Danica Josifovic, Dr Slobodan Tanasijevic, M.Sc. Snezana Ciric-Kostic QUALITATIVE PARAMETRES OF THE REGENERATION OF THE DAMAGED GEARS OF THE FIRST GEAR AND REVERSE IN GEAR BOX OF THE HEAVY LOAD TRUCKS	I C.57
Ana Pavlović, Prof. dr Vera Nikolić-Stanojević, Mr. Dejan Dimitrijević DYNAMIC ANALYSIS OF MULTIPLY GEAR	I C.61
I DESIGN IN MACHINERY	
SESSION D: RAILWAY ENGINEERING	
Ranko Rakanović PRESENT STATE OF RAILWAY VEHICLES CENTER KRALJEVO	I D.1

Dobrinka Borisova Atmadzhova A MODEL FOR DYNAMICS OF WAGON-TRACK SYSTEMS	I D.5
Marko Djukić, Srdjan Rusov THE DETERMINING OF THE PERMITTED VELOCITY OF RAILWAY VEHICLES OVER SWITCHES	I D.11
Nebojša Ivković, Zoran Marinković FUNDAMENTAL PROBLEMS IN THE MODELLING OF WAGONS' DYNAMICS	I D.15
Майя Г. Иванова ВЛИЯНИЕ ПАРАМЕТРОВ ТРАССЫ ПРИ ПРОЕКТИРОВАНИИ ЖЕЛЕЗНОДОРОЖНОГО ПУТИ	I D.19
Румен Иванов, Валентин Николов, Коста Костов СОВРЕМЕННЫЕ ГЕОДЕЗИЧЕСКИЕ ТЕХНОЛОГИИ ДЛЯ ОПРЕДЕЛЕНИЯ ГЕОМЕТРИИ ЖЕЛЕЗНОЙ ДОРОГИ	I D.23
Dr. Sc Dragutin Jovanovic CHARACTERISTICS OF DANGEROUS GOODS – THE SOURCE OF CONSTRUCTIVE REQUESTS IN PRODUCTION OF RAILWAYS	I D.25
Vladimir Aleksandrov STATIC AND DYNAMIC THERMAL ENGINEERING TESTS OF RAILWAY VEHICLES	I D.29
Иван Миленов, Георги Павлов ИЗМЕРЕНИЕ И ОЦЕНКА ВИБРАЦИЙ В КАБИНЕ ЛОКОМОТИВОВ И МОТОРВАГОННЫХ ПОЕЗДОВ	I D.33
Георги Павлов, Иван Миленов ИЗМЕРЕНИЕ И ОЦЕНКА УРОВНЯ ШУМА В КАБИНАХ ЛОКОМОТИВОВ И МОТОРВАГОННЫХ ПОЕЗДОВ	I D.37
Anna Dzhaleva-Chonkova THE EXPERIENCE OF SERBIA AND THE ESTABLISHMENT OF STATE OWNERSHIP IN THE BULGARIAN RAILWAYS	I D.41
Margarita Georgieva, Ivan Nenov HARMONIZATION OF THE BULGARIAN TELECOMMUNICATION AND SAFETY SYSTEMS ALONG THE EUROPEAN TRANSPORT CORRIDORS	I D.43
Rajko Radonjić DYNAMICS OF TANK VEHICLES WITH LIQUID CARGO	I D.47
Rajko Radonjić OPTIMIZATION OF VEHICLE SHOCK ABSORBER	I D.51
Lalovic R Ljubica, Lalovic M Dragomir, Knezevic-Miljanovic Julka DYNAMICS OF BRAKED VEHICLE ON REAL SURFACE	I D.55
Dr Tomislav Simović TO DO UP AND GAIN	I D.61
Zlatan Šoškić QUASI-CALIBRATED BRIDGE MEASUREMENT ERRORS	I D.63
Dragan Petrović, Ranko Rakanović, Zlatan Šoškić, Nebojša Bogojević PROBLEMS AT EXPLOATATION OF DDAM AND FBD WAGONS, AND SUGGESTIONS FOR THEIR RESOLUTIONS	I D.67

Nebojša Bogojević, Zlatan Šoškić, Dragan Petrović, Ranko Rakanović
TORQUE RIGIDITY FOR TRIPL-AXEL wagons I D.71

R.Rakanović, D.Petrović, M.Pavličić
TECHNICAL AND ECONOMIC EFFECTS OF ELASTIC ELEMENT BUILT IN
SUSPENSION SYSTEMS OF FREIGHT WAGONS I D.75

II PRODUCTION TECHNOLOGIES

SESSION A: DESIGNING OF MACHINING PROCESSES

И.С. Суровцев, В.М. Рубинштейн, В.Б. Тригуб
ПЛАЗМОХИМИЧЕСКОЕ НАНЕСЕНИЕ СЛОЕВ SiC ДЛЯ УПРОЧНЕНИЯ
ИНСТРУМЕНТАЛЬНЫХ СТАЛЕЙ II A.1

Radun Vulović, Vukić Lazić, Milorad Jovanović, Ružica Nikolić, Dragan Adamović
SELECTION OF THE WELDING TECHNOLOGY OF RELIABLE JOINTS USING
GMAW PROCESS II A.5

Рангел К. Рангелов, Денъо А. Георгиев, Крум Л. Петров и Боряна Д. Съйкова
ВОЗМОЖНОСТИ ВАКУУМНОЙ ФОРМОВКИ ДЛЯ ВЫРАБОТКИ
ФОРМООБРАЗУЮЩИХ ИНСТРУМЕНТОВ II A.9

Денъо Алипиев
ПЛАСТМАССОВЫЕ МОДЕЛИ, ИЗГОТОВЛЕННЫЕ В ВАКУУМНЫХ ФОРМАХ II A.13

Vukić Lazić, Miroslav Zivković, Dragan Rakić, Milorad Jovanović, Dragan Adamović
THEORETICAL-EXPERIMENTAL DETERMINING OF COOLING TIME ($t_{8/5}$) IN HARD
FACING II A.17

B. Nedić, M. Kaplarević
FLEXIBLE TOOL FOR POSITIONING AND CLAMPING THE ASSEMBLY THE CAR-
BODY AND OTHER COMPLEX THREE DIMENSIONAL FORMS II A.21

К.Л. Петров, П. Добрев, Р. Петков
МОДЕЛИРОВАНИЕ ПРОЦЕССОВ ПРИ ЗАЛИВКЕ ЛИТЕЙНЫХ ФОРМ ЖИДКИМ
МЕТАЛЛОМ II A.25

J. Kaleicheva, N. Kemilev, V. Mishev
AUSTEMPERING OF ALLOY SPHEROIDAL GRAPHITE CAST IRONS II A.27

Dragan Milčić, Miroslav Mijajlović, Boban Anđelković
APPLIANCE OF TRIZ METHOD IN CHOICE OF TECHNOLOGY FOR SOLVING
PROBLEM OF WOODEN WASTE II A.31

Predrag Dašić, Sava Đurić, Michal Štefánek
CHOICE ANALYSIS OF REGRESSION DEPENDED OF YIELD POINT AND
ELONGATION OF WELDED CONNECTIONS OF STEEL NIONICRAL-70 AND
TEMPERATURE OF THERMAL TREATMENT II A.35

Radmila Pljakić, Radica Prokić-Cvetković, Anđelka Milosavljević
THE TESTING OF BORIDING FOR THE CASE-HARDENING STEEL QUALITY
DETERMINATION II A.39

Radmila Pljakić, Anđelka Milosavljević, Jovan Manasijević
THE ASPECTS OF QUALITY AND ECOLOGY IN THE PROCESS OF BORONIZING
STEEL MATERIALS II A.43

Lj. Đorđević, I. Filipović, D. Đorđević
EXPLORATION OF POSSIBILITIES FOR REENGINEERING OF TECHNOLOGICAL
PROCESSES AND MACHINES II A.47

Dragan Živković, Đorđe Zrnić ECONOMY AS ONE CRITERION FOR THE SELECTION OF THE AUTOMATION LEVEL OF PRODUCTION EQUIPMENT	II A.51
Predrag Janković, Miroslav Radovanović NONTRADITIONAL MACHINING BY ABRASIVE WATER JET CUTTING	II A.55
Vasić Ž., Kalajdžić M. DRILL STIFFNESS ANALYSIS	II A.59
Kokotović B., Puzović R., Tanović Lj., Kalajdžić M. MODEL OF THRUST FORCE AND TORQUE IN TAPPING OPERATIONS	II A.63
P. Popovic, Lj. Djordjevic, B Radicevic, M. Bjelic THE UNIFICATION OF THE MECHANICAL PRESS DRIVING MECHANISM	II A.67
Predrag. Dašić, Ratomir Ječmenica, Valeriy Kuzin CLASSIFICATION, CHARACTERISTICS AND APPLICATION OF THE CERAMIC CUTTING TOOLS	II A.71
Predrag. Dašić, Ratomir Ječmenica, Valeriy Kuzin CLASSIFICATION, CHARACTERISTICS AND APPLICATION OF THE CERAMIC CUTTING TOOLS	II A.75
Ph.D. Predrag Popovic, Ph.D. Ljubodrag Djordjevic, B.Sc. Branko Radicevic, B.Sc. Miso Bjelic THE UNIFICATION OF THE MECHANICAL PRESS DRIVINGMECHANISM	II A.79

II PRODUCTION TECHNOLOGIES

SESSION B: COMPUTER-INTEGRATED PROCESSES

Arandjel Babic, Aleksandar Zukovski MODERN APPROACH IN DESIGN AND EXCHANGE OF INFORMATION WITHIN THE MATTER OF A PRODUCT LIFECYCLE	II B.1
Miroslav Pilipović, Dejan Vučković, Žarko Spasić CONTRIBUTION TO VIRTUAL MANUFACTURING MODELLING	II B.5
D. Erić, G. Miodragović KNOWLEDGE BASE IN DEVELOPMENT EXPERT-CAPP SYSTEMS FOR ELECTRICAL DISCHARGE MACHINING TECHNOLOGY	II B.9
G. Miodragović, A. Petrović, A. Žukovski THE METHODS OF MODELLING OF ASSEMBLY SRUCTURES IN CA ENVIROMENT	II B.13
G. Vujačić, S. Ristić, Ž. Marjanović ONE APPROACH OF DEVELOPING THE NETWORK SOFTWARE USED IN CIM TECHNOLOGIES	II B.17
M. Popovic, M. Kalajdzic NONLINEARITY IN FINITE ELEMENT ANALYSIS	II B.21

II PRODUCTION TECHNOLOGIES

SESSION C: ENGINEERING OF ENTREPRENEURSHIP

Cristiano Fragassa, Filippo Marzio RELIABILITY EVALUATION USED FOR THE REDESIGN OF THE ELECTROSPINDLE IN A CNC TOOL MACHINE	II C.1
--	--------

Viara Pozhidaeva, Dragan Živković, Milorad Rančić PREVENTIVE MAINTENANCE OF MECHANICAL SCISSORS USED IN METAL PROCESSING INDUSTRY	II C.5
Ilija Latinovic, Predrag Kezele, Volodja Pezo TOOL WEAR STATUS AND WAVELETSSUCCESSFUL TECHNIQUES IN AN OLD PROBLEM	II C.9
Dr Mirko Đapić, Dr Vladimir Zeljković EUROPEAN APPROACH TO PRODUCT CONFORMITY ASSESSMENT	II C.13
Z. Radojević, D. Stojanović, J. Avakumović BUSINESS PLAN FOR WORKSHOP FOUNDING	II C.17
Cedomir Avakumovic, Julija Avakumovic DEVELOPMENT OF BUSINES POSSIBILITIES IN FORMATION AND RE- FORMATION OF ORGANIZATION	II C.21
Dr Savo Trifunović BUSINESS ETHICS AND FREE ENTERPRISING SYSTEM	II C.25
Dr Savo Trifunović, Dr Milorad Pavličić, Mr Dušan Babović ABOUT ETHICAL CODEX OF MANAGERS	II C.29
Smiljković S. DEFINITIVE SUM OF SOME SERIES	II C.33
III URBAN ENGINEERING	
Bukumirović M., Gašić M., Savković M., G. Marković REGIONAL CITY LOGISTICS AND SUPPLY CHAINS IN MACHINERY	III 1
И.С.Суровцев, О.Б. Рудаков, В.Т. Перцев, Т.Д. Никулина ТЕРМОСТОЙКИЕ ПОКРЫТИЯ НА ОСНОВЕ СИЛИКАТОВ ЩЕЛОЧНЫХ МЕТАЛЛОВ	III 7
D.V. Polyakov, S.M. Merdanov, G.G. Zakirzakov GENERAL ASSOCIATION OF SNOW MASS' MELTING'S TIME UNDER ACTION OF THE ELECTRIC ENERGY	III 11
Radivoje Djurin Mančić, Dragan J. Gavrilović THE LAW OF THE LIVING MATTER CONSTANT (THE SIXTH ECOMAN LAW)	III 15
Vladan Karamarković, Miljan Marašević, Rade Karamarković THE MODEL FOR DETERMINATION OF THE TEMPERATURE AND THE GAS COMPOSITION OF BIOMASS GASIFICATION PRODUCTS BY THE USE OF MATERIAL AND ENERGY BALANCES	III 19
Dr Zoran Petrovic, Branko Radicevic, Miso Bjelic INCREASE OF ENERGETIC EFFICIENCY AT CENTRIFUGAL PUMP	III 23
Rade Biocanin ENVIRONMENT PROTECTION AND CHEMICAL ACCIDENTS	III 27
Prof. Dr Dragoljub Vujić OIL DEBRIS MONITORING AS A DIAGNOSTIC METHOD FOR FAILURES DETECTION AT AIRCRAFT ENGINES	III 33
Rade Karamarković, Miljan Marašević COMPARATIVE ANALYSIS OF THE THERMAL EFFICIENCIES FOR THE USE OF DOWNDRAFT GASIFICATION PRODUCTS BY FUEL CELL AND GAS TURBINE	III 37

APPLICATION OF UP-TO-DATE INFORMATION TECHNOLOGIES IN REVITALIZING OF PRODUCTION SYSTEMS

Lj.Lukić, M.Gašić, R.Rakanović, N.Nedić, V.Karamarković, Lj.Djordjević¹

Abstract

In last 15 years there have been no investments in production, technology and industry plants in Serbia. Production, transport and energetic equipment can not satisfy requirements of high productive and competitive production according to world standards. Modernization and revitalizing of our factories must be done in order to reach technical and technological level of factories in developed countries. The most efficient results in revitalizing are obtained by application of up-to-date information technologies, computer control system and modulus of programmable automatization in production lines.

The Faculty of Mechanical Engineering in Kraljevo has oriented its scientific activities and cooperation with economy towards application of up-to-date information technologies in the field of computer science and development of industrial software, technology and product designing, technical diagnostics, examination of complex mechanical systems and application of programmable controllers in various fields of production systems integrated by computers. The paper shows some realized results in Innovation Centers which will serve as a basis for forming small scientific and technological park at the Faculty of Mechanical Engineering in Kraljevo. It will serve as transfer and diffusion of new technologies and knowledge in enterprises and it will be a significant figure in reviving economy system in the region.

Key words: *information technologies, revitalizing, programmable automatization, digital systems*

1. INTRODUCTION

The Faculty of Mechanical Engineering in Kraljevo has a long experience in cooperation with economy in the field of scientific, research and development work. In accordance with economy surroundings it has specialized its research and scientific programs in development and innovation centers and it has obtained acknowledged results in the field of production machinery, automatization of production systems, mining and building machines, railway transport means, energetic efficiency, and especially in the field of software development and application of up-to-date information technologies in industry. Supported by the Ministry of Science and Environment Protection of the Republic of Serbia, the Faculty of Mechanical Engineering in Kraljevo develops the Innovative Center for information technologies which represents an integral basis for computer and communication infrastructure for application of up-to-date method for production development, designing and testing, introducing computer control systems and programmable automatization in industry, development of application software for business and industrial application. Feasibility study of technologic incubator is currently

being done at the Faculty of Mechanical Engineering in Kraljevo, which is a part of strategic project " Feasibility study for forming scientific and technologic parks in Serbia" financed by the Ministry of Science and Environment Protection. In the future present innovation centers should become a small scientific and technologic park, which would connect the faculty, being an important scientific and educational institution in the region, with not only large enterprises but small and medium ones as well. Thus, there will be a needed number of well trained and enterprising oriented engineers and technology transfer and economy development in the region will be accelerated, too. Because of that the Faculty of Mechanical Engineering in Kraljevo in its research and development programs is directed toward methods and technologies that in our conditions can be mastered with minimum investment costs and maximum effects. World experiences show that so called outsourcing businesses are the most efficient method for obtaining the first significant results that are very important for economy system of countries in transition. In following chapters some practical and realized results are presented which are the basis for future activities of the Faculty of Mechanical

¹ Prof. Ljubomir Lukić, Ph.D.Mech.Eng., Prof. Milomir Gašić, Ph.D.Mech.Eng., Prof. Ranko Rakanović, Ph.D.Mech.Eng., Prof. Novak Nedić, Ph.D.Mech.Eng., Prof. Vladan Karamarković, Ph.D.Mech.Eng., Prof. Ljubodrag Djordjević, Ph.D.Mech.Eng., University of Kragujevac, Faculty of Mechanical Engineering Kraljevo, 36000 Kraljevo, Dositejeva 19, tel. +381 36 336 866, e-mail: office@maskv.edu.yu.

Engineering in Kraljevo for up-to-date digital system to be introduced in our economy practice.

2. CIM SYSTEM OF CARDBOARD FACTORY

"Umka" cardboard factory in Belgrade is the only producer of multilayer chromic cardboard in the territory of former Yugoslavia. The factory worked with four decade old technologic equipment and 750 employees produced about 120 tones of cardboard a day. "Umka" was privatized in 2002 and major owner invested the assets in modernization of facilities in order to increase daily production for 30%, to enlarge production assortment, to increase plant flexibility, to decrease the number of employees, to improve quality and energetic efficiency according to European standards.

Cardboard production is based on a technologic line (fig.1) so its modernization has been done in many technologic and working centers. These are the most important ones:

- Digital systems and electronic scales for measurement of incoming raw material for mass preparation,
- Computer laboratory system,
- Up-to-date PLC controllers for control of section for mass preparation, cardboard machine and dryer,
- Regulators for control of operating systems at cardboard machine and dryer,
- Microprocessing measurement systems for analysis of cardboard characteristics,
- Vision systems for paint quality.

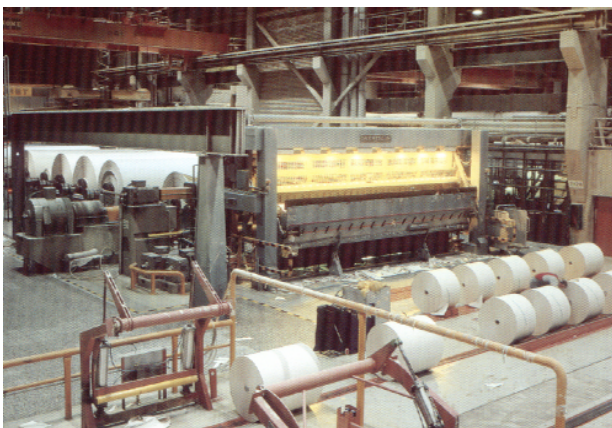


Fig.1 Part of technologic line for cardboard production

Technologic conditions being satisfied, original CIM system (Computer Integrated Manufacturing System) has been developed and applied as one of the projects of Innovation Center for information technologies at the Faculty of Mechanical Engineering in Kraljevo. It is a new software product, meant to meet the needs of process industry. It integrates complete production system of the factory, starting with production planning,

its realization and product delivery. Production process in technologic sense (optimal recipes for various cardboard types) has been integrated, parameters from PLC controller are directly put in the system for production control, they are compared to measured parameter values in the lab, and on the basis of the system for automatic control of cardboard quality at the technologic plant exit optimization of cardboard cutting is being done according to working and buyers' orders. Integrated computer production system for multilayer chromic cardboard production is based on many working centers but at each center specific phase of technologic process is being realized (fig.2). Working centers have following technologic scheme:

1. Section for mass preparation (PM) of defined recipe which is controlled in the lab and put in layers of various thickness on continual textile conveyor belt moving by former rollers,
2. Formers (FO) for making the layer of mass being put by centrifugal distributors and diffusion on formers,
3. Dryer (SU) for cardboard drying in defined heat regime which is in correlation with humidity percentage,
4. Plant for putting the third paint (TP) of fine quality and
5. Automatic plant for control of cardboard quality characteristics during forming cardboard tape (Q).

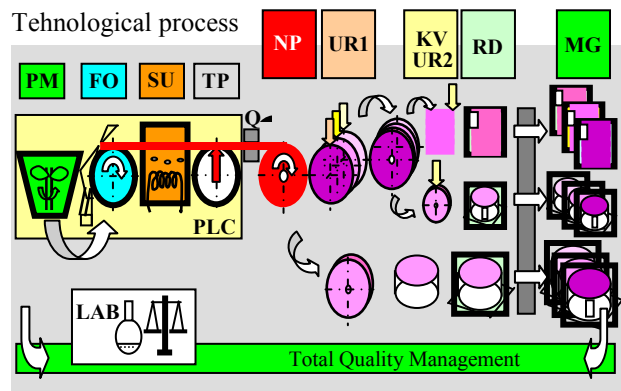


Fig.2 Schematic display of technologic production of multilayer cardboard

These phases of technologic process relate to forming of cardboard tape which winds up on winding plant in big rolls whose width is 3.500 mm. Following phases of technologic process include cutting and processing of big roll in final products being delivered to buyers packed on pallets (rolls, small rolls, tapes, sheets of various formats). Processing of cardboard tape is done on special plants:

- Winding plant (NP) on which big roll of cardboard tape is being formed.
- Longitudinal cutter (UR1) on which big roll is being cut. After that production line has two branches: cross cutter (KV) for cross cutting of tapes out of rolls in order to produce sheets of

wanted format and other longitudinal cutter (UR2) for production of small rolls.

- Manual finishing is a sorting, packing and measurement process. Packed products go to stockroom (MG) and wait to be delivered to buyers

In all working processes system quality control, which also includes technologic laboratory, controls technologic process starting with raw materials, mass preparation, packing and delivery to buyers, according to ISO9001 standard.

Software system integrates all working centers in technologic process (fig.3) and compares all production data to parameters controlled by PLC controller and to measured values in the lab (fig.4). On the basis of computer integration of production system, management has all elements for analysis and production control at a certain moment so that factory capacities would be optimally used, so that waste would be minimum, products of high quality, planned terms to be fulfilled and buyers' needs to be satisfied with high product economy.

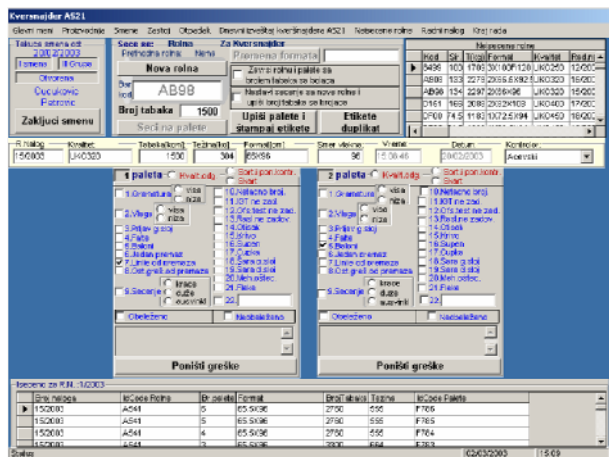


Fig.3 Application software at working station of cross cutter

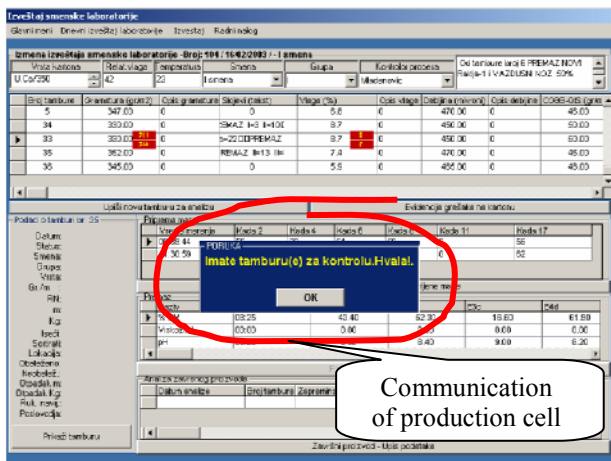


Fig.4 Working station in the laboratory

At all working stations there is a report system. From all working centers system reports are also generated for top management and they give a real picture of all working processes in the factory. Report system in working centers in the best way illustrates integral report on daily production at winding plant (fig.5).

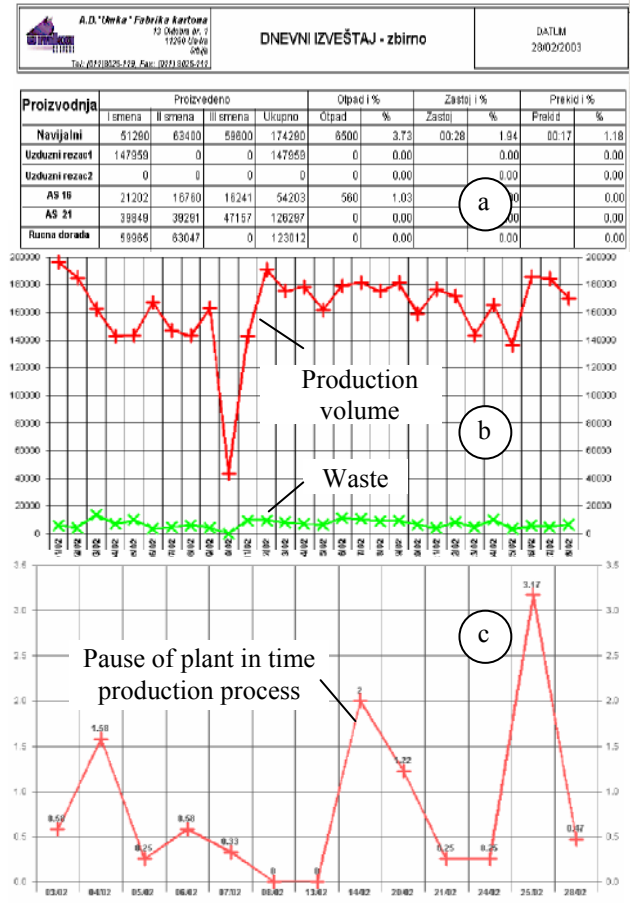


Fig.5 Report system on winding plant

Structure of integral report is defined so that it gives information data on production of all working centers during shifts, days, weeks, months, years. Beside production results the report gives the quantity of cardboard waste at certain working center and its percentage in total production for specific day. Through report system management also gets the insight of stoppage hours and percentage in relation to working time of working center. There is a report on breaks at working centers, too. The breaks at working centers do not need production line nor other working center to be stopped. The methodology for breaks analysis is the same as for stoppages. Fig.5 shows realized result during winding plant operation. Report presents trends for chosen month and shows comparative results analysis of produced cardboard and waste. Thus management and executive directors can, in due time, increase production and decrease wastes. Reports also enable stoppage analysis at working center, the insight of their frequency with possible prediction of next stoppages and measures for prevention maintenance. Reports are being study

simultaneously because their common analysis enables bringing optimal decisions.

Beside information on realized results in production there are other important parameters for optimal production process. So that management could efficiently do all necessary analyses, original software package Workflow is developed as a part of CIM system (Fig.6).

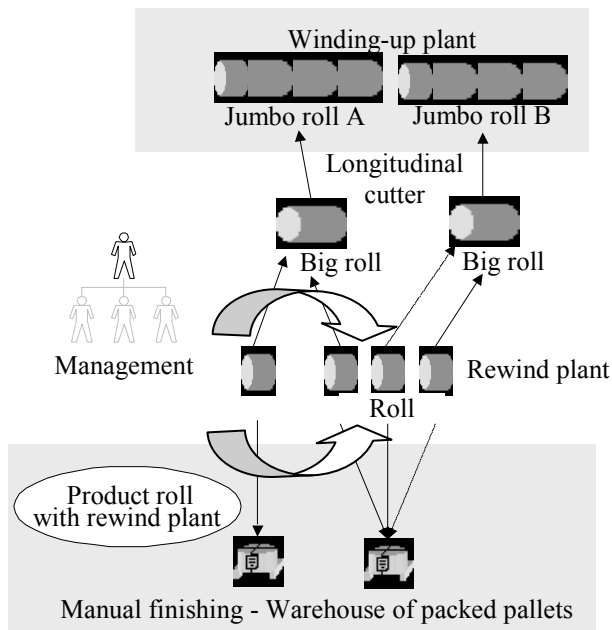


Fig.6 Workflow system for two-direction search

Three methods in Workflow concept are implemented. They enable: forward search, back search and two direction search. Two direction search is a combined and complete method based on simultaneous analysis of product making by forward and back search. Methodology is an original manner for generation of reports for management and executive directors and it can be successfully applied in any kind of production, with products structured like "consistuent parts of a product".

By introducing CIM system "Umka" cardboard factory had a daily production of 200 tones of cardboard (the value of 100.000 euros), there are 275 employees, it has optimized consumption of energy and raw materials, reached cardboard quality according to world standards, widened product assortment, conquered new markets and became competitor to famous producers in the world

3. METHODS OF CAD DESIGNING IN DISTRIBUTED PRODUCTION

Complex products in the process of production development need integration of a large number of parts, additional components and modulus into a unique functional whole. When there were huge industrial and

production complexes, with great design and development sectors, experienced designers, technologic departments that were thoroughly acquainted with technology of production manufacture, with all production resources available, organized departments for quality control and labs for specialized testing and verification of functional production characteristics, documentation was based on these facts. But nowadays the only possible way to make more complex products is by enforced coordination of production phases and by documentation in synthesized form at CAD working stations in our industrial surroundings in many small or medium enterprises (in distributed production) which are specialized in partial technologic processes.

Methodology of CAD/CAM designing in distributed production conditions is based on synthesis of construction and technologic documentation so the enterprise which realizes some technologic operations gets clear and complete construction, technologic, control and assembly documentation, but only for the activities assigned to the enterprises for realization.

Design documentation for production is printed selectively only with parameters that are important for manufacture phase related to work range in an enterprise so that taking over a phase and control of realized operation would be correctly done according to technical documentation.

For example, project of working part of forming machine for manufacture of paper packing elements is stated (fig.7). It consists of three plates connected by four guides. Pneumatic cylinder piston, which is also fixed, is connected to middle plate. Up and down plates move together with cylinder and guides while machine works.

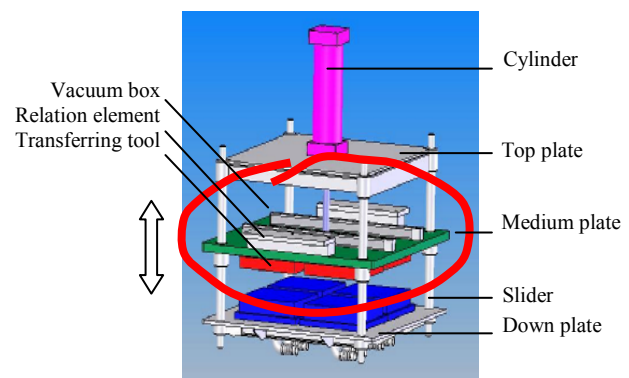


Fig.7 Working part of forming machine-3D model

For distributed production conditions of this technologically complex product, project and production documentation was done (fig.8) by application of CAD/CAM system.

Today's conditions of production development directly influence on the change of access in designing and production development in relation to traditional

manner. Methodology of CAD/CAM designing should be partly oriented to application of cheaper software packages which are available to enterprises and which do not need computer and communication infrastructure of high performances while the manner of product modelling and production technologies is based on distributed production.

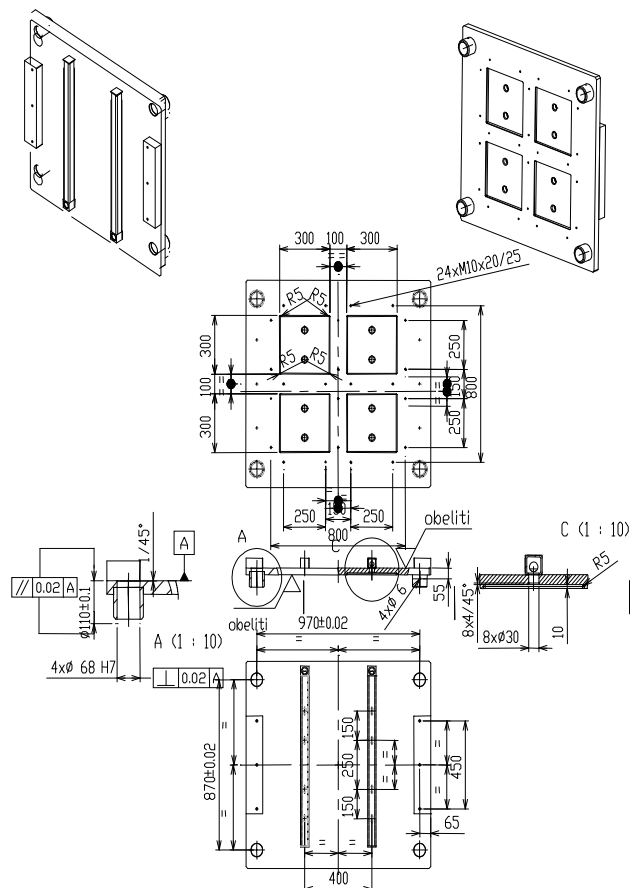


Fig.8 A detail of CAD design and production documentation for middle plate

Production phases being done, by coordination, surveyance and production control in all enterprises, that take part in production process, forming machine was integrated and put into operations as part of production line in a small production enterprise in Kraljevo (fig.9).



Fig.9 Middle plate with transfer tools as part of forming machine

4. CAE SYSTEMS IN MACHINE CONSTRUCTION DESIGNING

CAD/CAM/CAE systems for designing and engineering analyses enable very efficient calculation of stresses, modelling of heat processes, 3D product modelling and generation of NC program, analysis of welding and casting processes,... which is very important for efficient integral development of new products and design of machine construction. In projects of the Faculty of Mechanical Engineering in Kraljevo CAD/CAM systems of intermediate level are used (AutoCAD 2000, Mechanical Desktop, Autodesk Inventor, SolidWorks, Solid Edge, Catia, ProEngineer, MasterCAM, EdgeCAM, PowerMill,...). They are relatively cheap and enable high efficiency. Their application replaces many designers and offers more additional effects for designing in enterprises (fig.10). Application of internet service in designing and development, enables very fast calculations, dimensioning and selection of additional components.



Fig.10 Railway transport system of coal in "TENT" steam power station

Application of CAE system, internet technology and further development of computer and communication infrastructure of Innovation Center for information technologies at the Faculty of Mechanical Engineering in Kraljevo are the basis for education of engineering staff, knowledge transfer and up-to-date methods for automatic designing in economy in the region.

5. SYSTEM EXAMINATION OF WAGONS AND INDUSTRIAL PLANTS

The Center for railway vehicles at the Faculty of Mechanical Engineering in Kraljevo has become a leading research, development and diagnostic center in the country by long cooperation with railway transport enterprises and wagon building factories. Special wagon laboratory, with modern computer equipment for direct signal acquisition and new developed methods for wagon modulus designing on the basis of up-to-date

information technologies made the Center for railway vehicles become leader of revitalization and modernization of railway transport system in Serbia as well as an important figure for technologic development and international scientific technical cooperation. Revitalization of railway for coal transport from "Kolubara" strip mining to "TENT" steam power station (450 wagons and 30 locomotives transport 25 million tones of coal a year) mostly relies on results of system examination and technical solutions of the Faculty of Mechanical Engineering in Kraljevo (fig.11).

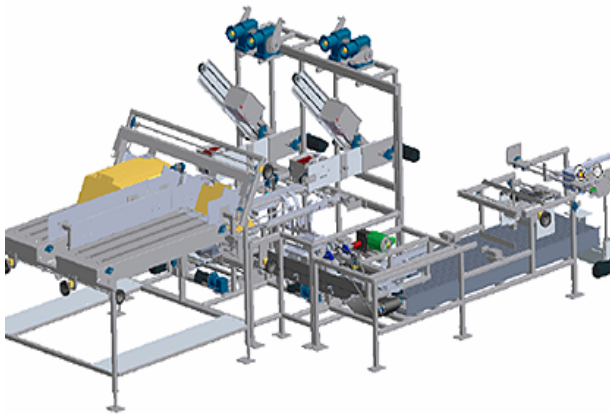


Fig.11 Plant designed in 3D model by Autodesk Inventor

Development of new transport wagons and additional modulus, research of phenomena and dynamic wagon stability with great loads and moving speeds are based on application of up-to-date diagnostic systems, microprocessing measure instruments and specialized software packages. It makes the Center for railway vehicles at the Faculty of Mechanical Engineering in Kraljevo an important partner in modernization of Serbian railway transport system and in reviving of wagon production in our factories after restructuring and privatization process.

6. CONCLUSION

Up-to-date information technologies enable the most efficient way for present knowledge and research results to be implemented and directly applied in industrial and production practice, giving relatively fast and important business results with minimum investment.

Development of industrial software and information systems, integration of production systems on the basis of digital technologies, application of PLC controllers in automatization of technologic process, development of new methods for CAD/CAM designing in conditions of distributed production, application of microprocessing measurement systems in examination of machine constructions, development and application of modern methods for calculation and engineering analyses in designing of mining and building machines and hoisting devices, are main activities at the Faculty of Mechanical Engineering in Kraljevo along with cooperation with

economy, equipment revitalization and reviving of production activities in industrial production in big economy systems, small and medium enterprises.

Scientific and technologic park at the Faculty of Mechanical Engineering in Kraljevo can become a significant manufacturer of industrial software. NT software parks in India- STPI, EHTP and Bangalore are "East silicon valley" where the best known companies in the world in the field of computers have their own firms. Those companies became prime international investors in India. The same thing happened in France (Technopole Sophia Antipolis), Israel (MATAM Scientific Industry Center Haifa) and other countries.

In previous chapters only some of realized results were shown. They prove today's transformation outline at the Faculty of Mechanical Engineering in Kraljevo and its orientation toward creation of technologic incubators for development of industrial software and application of information technologies in plant revitalization in economy enterprises.

7. LITERATURE

- [1] Lj.Lukić and researcher group: Development and Implementation of CIM system in cardboard factory A.D. "Umka" in Belgrade, Innovation center for information technologies Faculty of Mechanical Engineering Kraljevo & "PBS" Project Business System, Belgrade (2002-2004).
- [2] M.Gašić, M.Vesković, Z.Petrović: The Faculty of Mechanical Engineering in Kraljevo in function of Strategy of Economic and Scientific Development of Environment, Proc. 4th International Conference Heavy Machinery-HM'02, Kraljevo (2002), pp.P.7-P.11.
- [3] R.Rakanović: Roll of the Centre for Railway vehicles at the Faculty of Mechanical Engineering in the time to come, Proc. 4th International Conference Heavy Machinery-HM'02, Kraljevo (2002), pp.C.1-C.4.
- [4] N.Nedić: Istraživanje i razvoj elektrohidrauličkih i elektropneumatskih servo sistema, Mašinstvo za XXI vek, Monografija, Novi Sad, 1995.
- [5] LJ.Lukić, M.Kalajdžić, R.Rakanović: Development and application of CAD/CAM system design of complex projects in conditions of distributed production, 31st JUPITER Conference, 18th Symposium "CAD/CAM", Zlatibor(2005), CD medium.
- [6] V. Karamarković: Energetski stepen korisnosti pri sagorevanju i gasifikaciji biomase, Procesna tehnika, br.1 (2003) pp. 145-149.
- [7] LJ.Lukić, Z.Andelković, S.Stamatović: Computer Integration of Cardboard Production, Chemical Industry 5 (2004), Vol.58, pp.221-227.

ВЛИЯНИЕ РАДИУСА ПОВОРОТА НА ТОПЛИВНО-ЭКОНОМИЧЕСКИЕ ПОКАЗАТЕЛИ ДИФФЕРЕНЦИАЛЬНОГО МОСТА СНАБЖЁННОГО КРУПНОГАБАРИТНЫМИ ПНЕВМАТИЧЕСКИМИ ШИНАМИ.

И.С. Суровцев, П.И. Никулин, Р.С. Солодов

В статье представлены результаты теоретических исследований по влиянию радиуса поворота на топливно-экономические показатели дифференциального моста снабжённого крупногабаритными пневматическими шинами, позволившие разработать научно обоснованную методику расчёта тяговых и топливно-экономических показателей колёсного движителя землеройно-транспортных машин при движении по дуге окружности.

Одноосный колёсный движитель, дифференциальный мост, скольжение, топливно-экономические показатели.

Два и более ведущих колёс землеройно-транспортной машины (ЗТМ), соединённых трансмиссией, образуют сложную механическую систему, закономерности движения которой в общем случае отличаются от закономерностей, характеризующих качение одиночного колеса. Анализ колёсных схем ЗТМ позволяет выделить наиболее часто встречающиеся сочетания колёс в ходовом оборудовании в виде дифференциального и блокированного моста (одноосный движитель), балансира, сдвоенных колёс и четырёх колёс (двухосный движитель), имеющих также дифференциальный или блокированный привод.

Тяговая динамика колёсных ЗТМ при криволинейном движении по недеформирующейся, а особенно по деформирующейся поверхностям, исследована недостаточно [1]. Принимая во внимание особенности колёсных схем ЗТМ, необходимо на основании исследования кинематики качения многоколёсного движителя решить задачу по определению силы тяги и распределению её по колёсам движителя с учётом деформации как пневматических шин, так и опорной поверхности, а так же исследовать влияние данных параметров на топливно-экономические показатели колёсного движителя.

В данном примере рассматривается работа одноосного колёсного движителя имеющего межколёсный дифференциал. Особенностью кинематики движения одноосного колёсного движителя является то, что центральная опорная точка для системы колёс принята условно.

Дополнительным параметром по сравнению с одиночным колесом, влияющим на кинематику движения одноосного колёсного движителя является значение $2B$, т.е. колея машины, а также различная частота вращения внутреннего и внешнего колёс ($\omega_{\kappa 1} \neq \omega_{\kappa 2}$).

Следует отметить, что при движении колёс моста $\theta_{oy} \geq l + b / (R_o + B)$ и $\theta_{oy} \geq l + b / (R_o - B)$ с межколёсным дифференциалом по деформирующейся поверхности элементы шин соответственно внешнего и внутреннего колеса движутся в области контакта только с буксованием. При этом параболы выходят за пределы контактов колёс, смещаясь от центра поворота.

$$\text{При } \theta_{oy} < \frac{(1 + B_2 \cdot a_1^2)}{(1 + B_1 \cdot a_1^2)} \left(1 - \frac{b}{R_o + B} \right) \text{ и}$$
$$\theta_{oy} < \frac{(1 + B_2 \cdot a_1^2)}{(1 + B_1 \cdot a_1^2)} \left(1 - \frac{b}{R_o - B} \right)$$

элементы шин соответственно внешнего и внутреннего колеса движутся в области контакта юзом и параболы выходят за пределы контактов колёс, смещаясь к центру поворота (рис. 1).

Проведённый анализ кинематики движения одноосного колёсного движителя с межколёсным дифференциалом по дуге окружности показывает, что процесс проскальзывания зависит от коэффициента проскальзывания условной центральной опорной точки, радиуса поворота, размеров области контакта шин с опорной

поверхностью, расстояния между колёсами движителя $2B$, типа привода колёс.

матических шин колёс моста с межколёсным дифференциалом на деформирующейся поверхности заключается в

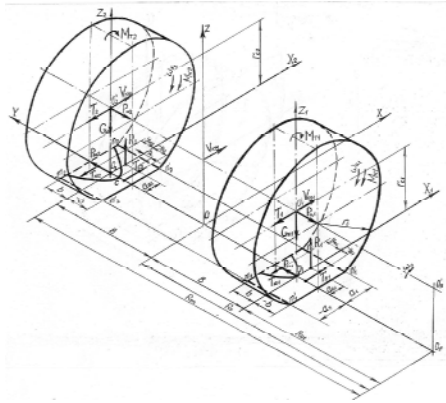


Рис. 1. Схема сил и моментов действующих на одноосный колёсный движитель с пневматическими шинами, при работе в ведущем режиме.

нахождении зависимости равнодействующей элементарных сил трения и нормальных сил, спроектированной на горизонтальную ось x , от коэффициента проскальзывания условной центральной опорной точки θ_{oy} и радиуса поворота R_0 , т. е. $T_{\mu} = T_{\mu}(\theta_{oy}, R_0)$.

В расчётной схеме, соответствующей движению ведущего моста с межколёсным дифференциалом по дуге окружности и деформирующейся поверхности, оси координат располагаем в областях контактов колёс моста, поскольку частота вращения колёс разная (рис. 1).

Исходное выражение для определения проекций равнодействующей элементарных сил dF и равнодействующей нормальных элементарных сил dN на горизонтальную ось x колёс ведущего моста с межколёсным дифференциалом записываем следующим образом:

$$T_{\mu} = T_{\mu H} + T_{\mu B},$$

где $T_{\mu H}$ – суммарная равнодействующая элементарных сил трения в области контакта шины внешнего колеса ведущего моста; $T_{\mu B}$ – суммарная равнодействующая элементарных сил трения в области контакта шины внутреннего колеса ведущего моста.

$$T_{\mu} = \int_{-a_3}^{a_1} \sigma \left(\mu'_{сид} - \frac{2\epsilon x_1}{\sqrt{R_i^2 - x_i^2}} \right) dx_1 +$$

Тогда

$$+ \int_{-a_3}^{a_1} \sigma \left(\mu''_{сид} - \frac{2\epsilon x_2}{\sqrt{R_i^2 - x^2}} \right) dx_2,$$

Решение задачи по определению сил трения в области контакта пнев

где $\mu'_{сид}$, $\mu''_{сид}$ – коэффициент трения скольжения, соответственно внешнего и внутреннего колёс дифференциального моста, величина которого зависит от коэффициента проскальзывания центральной опорной точки θ_0 , области контакта шины с опорной поверхностью и радиуса поворота колёсного движителя R_0

Анализ теоретических зависимостей характеристик проскальзывания одноосного колесного движителя на деформирующейся поверхности (рис. 2), полученных на основании расчётов, выполненных для моста с межколёсным дифференциалом с шинами размером 21.00-33Рт и следующих исходных данных: $G=116$ кН, $r_0=97,5$ см, $E_I=1$ Мпа, $2B=240$ см, $\mu_{c\theta 0}=0,84$, $\mu_{n\sigma}=0,4$, $u_n=0,06$, $u_c=0,04$, $n=4$ при различных радиусах поворота R_0 показывает, что: во-первых, разность в значениях сил T_H и T_B при $T_{\mu}=0$ практически равна нулю, т.е. кривые скольжения как внутреннего так и внешнего колеса моста совпадают; во-вторых, с уменьшением радиуса поворота, при постоянной силе тяги, скольжение шин моста увеличивается (кривая 2).

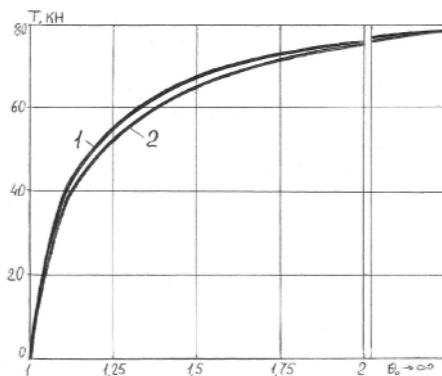


Рис. 2. Кривые скольжения одноосного движителя с крупногабаритными шинами размером 21.00-33Рт при различных радиусах поворота R_0 на деформирующемся грунте ($E_I=1$ Мпа, $P_0=0,6$ Мпа, $G_k=116$ кН): 1 – $R_0=750$ см, 2 – $R_0=250$ см.

Для определения топливно-экономических показателей дифференциального моста необходимо рассмотреть совместную работу двигателя внутреннего сгорания и колёсного движителя. Рассмотрим случай с механической трансмиссией.

С этой целью в первом квадранте размещаем регуляторную характеристику дизельного двигателя, перестроенную в функции крутящего момента M_e , а во втором строим тяговую характеристику дифференциального моста с шинами

размером 21.00-33Рт модели ВФ-166А при различных радиусах поворота (рис. 3).

Значение коэффициента буксования для построения тяговой характеристики получено с использованием кривых скольжения при различных радиусах поворота и конструкции шин. Формула перехода от коэффициента проскальзывания к коэффициенту буксования имеет вид

$$\delta = (1 - \theta_{oc} / \theta_o) \cdot 100\%,$$

где θ_o – коэффициент проскальзывания центральной опорной точки; θ_{oc} – коэффициент проскальзывания центральной опорной точки при $T=0$.

Рассчитываем силу сопротивления качению колёсного движителя P_f по формуле

$$P_f = G_k f_k, \text{ кН},$$

где G_k – вертикальная нагрузка на колеса моста, кН; f_k – коэффициент сопротивления качению колёсного движителя.

Откладываем её значение влево от точки O .

Строим график $M_e = M_e(P_k)$, применяя формулу

$$M_e = \frac{(T + P_f)r_c}{i_m \eta_m}, \text{ кН} \cdot \text{м},$$

где r_c – силовой радиус колеса, м; i_m – передаточное число механической трансмиссии; η_m – КПД механической трансмиссии. Для каждого радиуса данная зависимость выражается прямой, проходящей через точку O_I .

Строим основную зависимость $v_d = v_d(T)$.

$$v_{di} = 0,377 \frac{n_{ei} r_c}{i_m} \left(1 - \frac{\delta_i}{100}\right), \text{ км/ч},$$

где n_{ei} – частота вращения коленчатого вала двигателя, об/мин; r_c – силовой радиус колеса, м; i_m – передаточное число трансмиссии.

Строим основную зависимость $G_T = G_T(T)$ графическим способом, перенося эти значения с регуляторной характеристики на тяговую характеристику, с учетом величины P_k и масштаба построения.

Построение производных зависимостей $N_T = N_T(T)$, $g_T = g_T(T)$ и $\eta_T = \eta_T(T)$ производится следующим образом. Кривая тяговой мощности строится на основании расчетов по формуле

$$N_T = T v_d, \text{ кВт},$$

где T – сила тяги, кН, v_d – действительная скорость движения моста, м/с.

Кривая удельного расхода топлива g_T строится с применением формулы

$$g_T = 10^3 \frac{G_T}{N_T}, \text{ г/кВт} \cdot \text{ч}.$$

Кривую тягового КПД строим, пользуясь зависимостью

$$\eta_T = \frac{N_T}{N_e}.$$

Располагая тяговой характеристикой, можно определить параметры характеризующие основные режимы работы одноосного движителя: максимальную силу тяги T_ϕ , определяемую условиями сцепления шин пневмоколёсного движителя с поверхностью качения; силу тяги T_{NT} при максимальной тяговой мощности; силу тяги T_η , соответствующую максимальному значению тягового КПД; силу тяги $T_{g \min}$, при минимальном значении удельного тягового расхода топлива.

С учётом вышеизложенного была построена тяговая характеристика дифференциального моста с шинами размером 21.00-33Рт модели ВФ-166А при различных радиусах поворота на плотном связанном грунте.

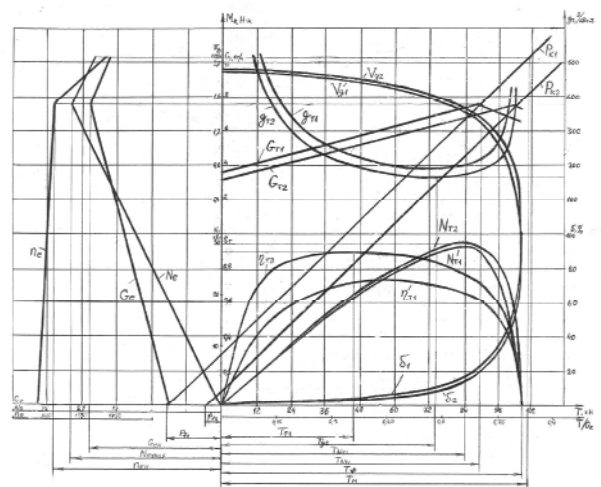


Рис.3. Тяговая характеристика одноосного колёсного движителя с шинами 21,00-33Рт модели ВФ-166А на плотном связанном грунте при $P_\omega=0,6$ Мпа, $G_k=116$ кН и различных R_0 : $P_1, P_1, \delta_1, N_{T1}, \eta_{T1}, G_{T1}, g_{T1}, V_{T1} - R_0=2,5$ м; $P_2, P_2, \delta_2, N_{T2}, \eta_{T2}, G_{T2}, g_{T2}, V_{T2} - R_0=7,5$ м.

Проведя анализ полученной тяговой характеристики одноосного колёсного движителя построенной по вышеизложенной методике можно сделать выводы по влиянию радиуса поворота на тяговые и топливно-экономические показатели ведущего моста. Уменьшение радиуса поворота в исследуемых пределах приводит к существенному

возрастанию коэффициента проскальзывания условной центральной опорной точки шины θ_{oy} , в результате чего при постоянной величине силы тяги снижается $v_{кд}$, уменьшаются N_m и η_T .

На плотном грунте при среднем радиусе поворота $R_0=2,5$ м (т.е. внутреннее колесо двигалось по радиусу $R_{o1}=1,25$ м, наружное – по $R_{o2}=3,65$ м) и $P_\omega=0,6$ МПа величины N_{Tmax} и η_{Tmax} одноосного колёсного движителя меньше, чем при $R_0=7,5$ м (радиус качения внутреннего колеса $R_{o1}=6,25$ м, наружного- $R_{o2}=8,7$ м) соответственно на 2% и 17% (рис. 3). Минимальное значение удельного тягового расхода топлива g_{Tmin} при $R_0=7,5$ м меньше на 10%, чем при $R_0=2,5$ м, а часовой расход топлива G_T достигает своего максимума при меньшей силе тяги на радиусе $R_0=2,5$ м.

Список литературы

1. Никулин П.И. Теория криволинейного движения колёсного движителя / П.И. Никулин. – Воронеж: Изд-во ВГУ, 1992. – 212 с.
2. Ульянов Н.А. Самоходные колёсные землеройно-транспортные машины / Н.А. Ульянов, Э.Г. Ронинсон, В.Г. Соловьёв. – М.: Машиностроение, 1976. – 366 с.

MOBILE WORKING MACHINES AND THEIR ELEMENTS: CALCULATION OF LIFETIME

Prof. dr Radan Durković, Faculty of Mechanical Engineering, Podgorica, SCG

Abstract: The present study deals with the calculation of lifetime of mobile working machines which is grounded on the implementation of material damage hypotheses. It contains the relevant expressions for the lifetime of elements expressed by the number of cycles of stress variation and working time/hours. The paper outlines the necessity of reducing working and critical stresses to the same degree of asymmetry and demonstrates relevant procedures. The expressions for the number of stress variation cycles in a time unit are set forth here, as well. Finally, there is also an illustration of a concrete example of the method of probability calculation.

Keywords: mobile working machine, lifetime, hypotheses on material damage, working and critical stresses, probability calculation.

1. INTRODUCTORY PART

Mobile working machines represent very complex dynamic systems composed of several interconnected constructional i.e. functional systems. In the course of work of these machines, loads of specific systems and elements occur which represent random functions of time. The loads originate from the driving engine, foundation and the work process, and are dependant on constructional characteristics and working regime of the machine and working resistances. Characteristics of transmission and working equipment load in mobile construction machinery are illustrated by the data of exploitation tests, Figures 1 and 2.

The Figure 1 exhibits an oscillogram of transmission load in power shovels during their movement towards a waste area, shoveling and removal of material [1].

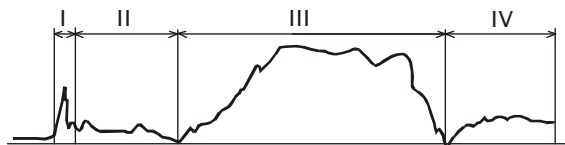


Figure 1. Oscillogram of variations in the power shovel transmission load [1]; I – starting from the place, II – movement towards a waste area, III – shoveling of material, IV – removal of material.

The oscillogram of deformations of the hydraulic excavator holder is obtained by application of measuring tapes as shown in Figure 2 [2].

Oscillograms exhibited in the above Figures indicate to a random character of load i.e. stress variations. By the oscillogram analysis with the implementation of corresponding systematic methods, curves of load i.e. stress amplitude distribution are obtained, generally as shown in Figure 3.

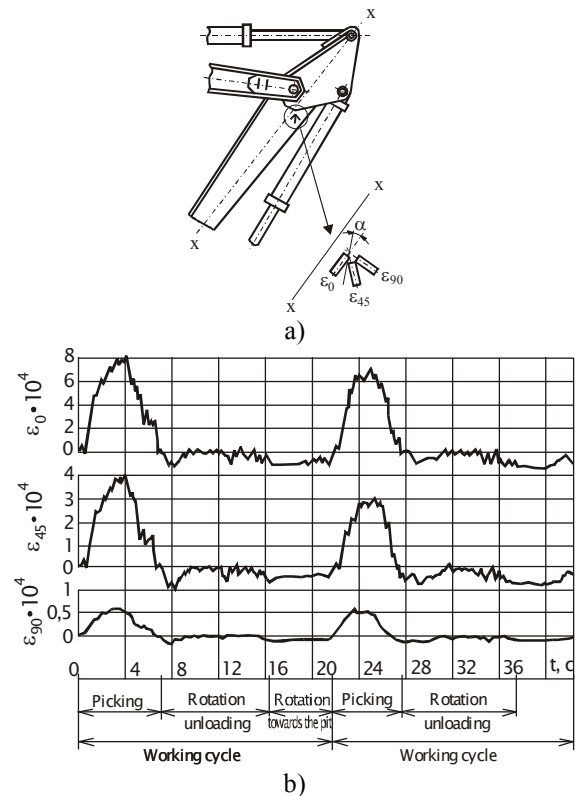


Figure 2. [2] a) Position of measuring tapes on the hydraulic excavator holder, b) Oscillogram of variations in holder deformations.

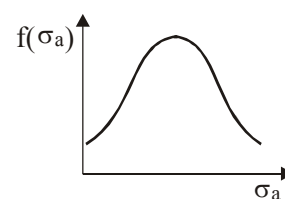


Figure 3. Stress amplitude distribution curve.

where:

$$K = \frac{1}{a_r} \cdot \sum_{i=1}^k \frac{n_{ib}}{n_b} \cdot \left(\frac{\sigma_{ai}}{\sigma_{aR}} \right)^m \quad (7)$$

Analogously, the amplitude of the equivalent working stress for a continuous spectrum, presented by the expression (4), is being transformed into the following:

$$\sigma_{aekv.}^m = \frac{1}{a_r} \cdot \sigma_{aR}^m \cdot \frac{\int_{\sigma_{a min}}^{\sigma_{aR}} \sigma_{ai}^m \cdot f(\sigma_{ai}) \cdot d\sigma_{ai}}{\sigma_{aR}^m} = K \cdot \sigma_{aR}^m \quad (8)$$

where:

$$K = \frac{\frac{1}{a_r} \cdot \int_{\sigma_{a min}}^{\sigma_{aR}} \sigma_{ai}^m \cdot f(\sigma_{ai}) \cdot d\sigma_{ai}}{\sigma_{aR}^m} \quad (9)$$

Applying the expressions (6) and (8), the expression (5) for the number of working hours can be written in the following form:

$$T = \frac{N_D \cdot \sigma_D^m}{n_{Tekv.} \cdot \sigma_{aR}^m} \quad (10)$$

where:

$n_{Tekv.} = n_T \cdot K$ - equivalent number of cycles.

It is obvious that in the expression (5) there is an equivalent stress, while in the expression (10) an equivalent number of cycles.

2.1. Lifetime Analysis

Expressions (5) and (10) for the lifetime of elements, can be written in a general form:

$$T = \frac{R}{R_1} \quad (11)$$

where:

- $R = N_D \cdot \sigma_D^m$, total available working capability (resource) of elements,
- $R_1 = n_T \cdot \sigma_{aekv.}^m$ or $R_1 = n_{Tekv.} \cdot \sigma_{aR}^m$ required working capability of elements per 1 [h] of work (unit working capability or unit resource).

It should be emphasized that in concrete calculations, critical and working stresses, due to their comparability, should have the same character of change i.e. degree of asymmetry.

For example, the working stress of shaft torsion is asymmetrical to some mean stress τ_m and amplitude τ_a . Reduction of working and critical stresses to the same degree of asymmetry may be achieved in two manners, [2]:

Naprimjer radni napon uvijanja vratila je nesimetričan sa nekim srednjim naponom τ_m i amplitudom τ_a . Svođenje radnih i kritičnih napona na isti stepen asimetrije moguće je postići na dva načina, [2]:

- for a critical stress, take $\tau_{D(-1)}$, and reduce the asymmetrical working stress to the symmetrical one by a reduced amplitude

$$\tau_{aRed.} = \tau_a + \psi \cdot \tau_m \quad (12)$$

where: ψ is a coefficient of sensibility of material to the asymmetry of a cycle

- keep the asymmetrical working stress with the degree of asymmetry R and determine the critical stress using the same degree of asymmetry:

$$\tau_{DR} = \frac{2 \cdot \tau_{D(-1)}}{(1-R) + \psi(1+R)} \quad (13)$$

The number of cycles of working stresses variation per one working hour of element is determined for specific elements in different manners, [1], [6].

For the teeth of gear wheels and jaw couplings, as well as for shafts and other elements of transmission with a bending load, the number of cycles per one working hour shall be:

$$n_T = 60 \cdot n \left[\frac{\text{ciklus}}{\text{čas}} \right] \quad (14)$$

where: n [min^{-1}] is a number of revolutions per minute.

For transmission elements, at the movement of mobile working machines along an earth surface, the number of cycles of a torsion moment variation per one hour of work shall be:

$$n_T = \frac{3600}{2\pi} \cdot \sqrt{\frac{C_f}{m}} \left[\frac{\text{ciklus}}{\text{čas}} \right] \quad (15)$$

where:

C_f [KN/m] - rigidity of the machine support system,
 m [t] - a part of the machine mass which is being transmitted through the support system to the driving wheels.

The number of cycles n_T can be ascertained by implementation of the theory of random functions using the stress oscillogram, what is of special relevance for the calculation of working equipment.

In this case, the number of cycles n_T is:

$$n_T = \frac{1}{T_e} = \frac{1}{2\pi} \sqrt{\frac{D_{vx}}{D_x}} \left[\frac{\text{ciklus}}{\text{čas}} \right] \quad (16)$$

where:

T_e - the effective period of stress change,
 D_x i D_{vx} - dispersion of amplitudes of workings stresses and speeds of its change.

3. LIFETIME PROBABILITY CALCULATION

In the expression (11) given for the lifetime of elements, values R and R_1 are generally of an undeterministic character, and therefore are given as distribution curves and variations of such curves. It is on the basis of these

curves in the probability calculation that a curve of distribution of lifetime indicators and its mean square deviation is determined.

Furthermore, the present study demonstrates the procedure and possibilities of the probability calculation of working time of elements, analogously to the calculation of the displacement in [4].

By an algorithm of the expression (11), we arrive at:

$$\lg T = \lg R - \lg R_1 \quad (17)$$

Let us now analyze the case when values $\lg R$ and $\lg R_1$ are described by the normal distribution law. Then a random value $\lg T$ is also subject to the normal law. A mean value of the random value $\overline{\lg T}$ and its mean square deviation $S_{\lg T}$ are:

$$\overline{\lg T} = \overline{\lg R} - \overline{\lg R_1} \quad (18)$$

$$S_{\lg T} = \sqrt{S_{\lg R}^2 + S_{\lg R_1}^2} \quad (19)$$

The above ascertained values $\lg T$ and $S_{\lg T}$ enable the calculation of the following significant working lifetime indicators in elements:

- probability of faultless operation of an element for the projected lifetime $P(T_0)$,
- minimum guaranteed lifetime of an element $\lg T_{\min}$,
- lifetime of an element for any probability of faultless operation, the so called gamma percentage resource or gamma percentage lifetime $T_{\gamma\%}$.

For the normal law of distribution of the random value $\lg T$, the probability of faultless operation of an element for its projected lifetime shall be determined on the basis of the standardized value of a random value (quantile of normal distribution)

$$u = \frac{\lg T_0 - \overline{\lg T}}{S_{\lg T}} \quad (20)$$

For the calculated value u , the corresponding probability of faultless operation during the projected lifetime T_0 is ascertained by the use of relevant tabular data.

The minimum i.e. guaranteed lifetime of elements is obtained by the implementation of the following three-sigma rule:

$$\lg T_{\min} = \overline{\lg T} - 3 \cdot S_{\lg T} \quad (21)$$

In this case, the lifetime has the probability of 99.73%, [7].

The gamma percentage lifetime of an element is determined in such a manner as to determine, first of all, the value u_{γ} , which corresponds to the selected probability $P_{\gamma\%}$ of a continuous work, and then to calculate $\lg T_{\gamma}$:

$$\lg T_{\gamma} = \overline{\lg T} + u_{\gamma} \cdot S_{\lg T} \quad (22)$$

An example of calculation of the gamma percentage lifetime of the semi-shaft in a power shovel is exhibited in the paper [8]. For distribution of working stresses, the two-parameter Weibull's law is used, while for distribution of critical stresses, the inscribed (carved) normal law is applied. For the concrete numerical values of initial data, values of reliability $P_{\gamma\%}$ and working time T_{γ} are arrived at:

$P_{\gamma} [\%]$	80	90	95
$T_{\gamma} [h]$	11300	8780	6700

4. CONCLUDING REMARKS

It is possible, by implementation of the probability calculation at the stage of designing, to ensure the required reliability of elements for a given lifetime and exploitation requirements by a relevant design solution. It is also possible to envisage for a given design solution the lifetime of elements for varied conditions of exploitation. The possibility to make a projection of the lifetime of elements is of great significance for the development of new machinery of high technological level, as well as for preventive maintenance of the existing machinery by replacement of their corresponding parts and elements.

5. LITERATURE

- [1] Grinević G.P. i dr.: Nadežnost stroiteljnih mašin, "Strojizdat", Moskva, 1983.
- [2] Rjahin V.A., Moškarev G.H.: Dolgovečnost i ustrojčivost svarnih konstrukcii stroiteljnih i dorožnih mašin, "Mašinostroenije", Moskva, 1984.
- [3] Durković R., Damjanović M.: Radni vijek prenosnika snage motornih vozila – sistemske metode proračuna elemenata, Monografija povodom 30 godina časopisa International Jurnal for Mechanics, Engins and Transportation Systems Mobility & Vehicles Mechanics, Kragujevac, 2005.
- [4] Bočarov N.F., Citović I.S., Polungjan A.A. i dr.: Konstruirovanie i rasčet kolesnih mašin visokoj prohodnosti, "Mašinostroenije", Moskva, 1983.
- [5] Citović I.S., Mitin V.E., Džun V.A.: Nadežnost transmisii avtomobilej i traktorov, "Nauka i tehnika", Minsk, 1985.
- [6] Buharin N.A., Prozorov V.S., Šćukin M.M.: Avtomobili, "Mašinostroenije", Leningrad, 1973.
- [7] Pavlić I.: Matematička statistika (primjena u proizvodnji), "Privreda", Zagreb, 1962.
- [8] Durković R., Pajković V., Damjanović M.: Prgoniziranje pouzdanosti elemenata transmisije kao sistemski doprinos obezbjeđenju tehničkog nivoa i ekonomske efektivnosti mobilnih radnih mašina, Zbornik radova Međunarodne naučne konferencije "Teška Mašinogradnja – TM '96", Kraljevo, 1996.

СТЕНД ДЛЯ ИСПЫТАНИЯ СИСТЕМЫ ПНЕВМОКАТКОВЫЙ ДВИЖИТЕЛЬ-ГРУНТ

Никулин Павел Иванович, Топалов Эдуард Львович ¹⁾

В данном докладе представляется конструкция стенда, результаты экспериментальных исследований, взаимодействие пневмокаткового движителя с грунтами с различными физико-механическими характеристиками.

Пневмокатковый движитель, сопротивление качению, физико-механические характеристики грунтов

В основу исследований положены часто применяемые в мировой практике параметры пневмоколесных движителей и их тяговые характеристики: сила тяги, коэффициент сцепления, крутящие моменты, а также внешнее и внутреннее давление в пневмокатках и деформации грунтов. Данные объекта исследований представлены в табл.1.

Коэффициентами подобия для каждого параметра являлись $m_D=12$; $m_B=6$; $m_{p_0}=1$; $m_{GK}=450$; $m_v=18$. Экспериментальные исследования проводились на стенде, схема которого показана на рис.1.

Катками служили гладкие эластичные оболочки соответствующих шиноразмеров. Давление в оболочке создавалось введением объема воздуха методом шприцевания с последующей герметизацией отверстия.

Стенд состоит из основания 1, на котором закреплены четыре стойки для рамы 2, которая подпружинена снизу и сверху. Нагрузка на каток обеспечивается мерными грузами 3, грунты уложены в специальные кюветы 5, сваренные из 2-х миллиметровой полосовой стали. Одноручьевый шкив 6 служит для передачи вращательного движения ленте привода катка. Колебания исследуемой системы записывались при помощи тензометрирования. Тензометры сопротивления устанавливали на ленте в точке контакта, на поверхности оболочки катка, на расстоянии a_3 и x от осевой линии.

Усиленный сигнал от тензостанции 8 – АНЧ -7м попадал на осциллоскоп GOS-305. Обработка полученных результатов производилась с помощью ЭВМ. Для полученных зависимостей находились доверительные интервалы с вероятностью попадания в них 0,95.

Таблица 1
Характеристика объекта исследований

№ п/п	Основные показатели					
	Диаметр, D, мм	Ширина, B, мм	Давление, $P_{ш}$, Па	Нагрузка, G_k , Н	Скорость, V, м/с	Грунт
1	50	24	5	10	0,8	I-V
2	60	30	10	15	1,1	I-V
3	65	40	15	18	1,5	I-V
4	70	50	20	20	2,0	I-V
5	80	60	30	22,5	2,22	I-V
6	85	70	50	24	2,52	I-V
7	90	80	80	26	2,78	I-V
8	100	90	100	28	3,33	I-V

1) Никулин Павел Иванович - д.т.н., Воронежский государственный архитектурно-строительный университет профессор Россия. Воронеж.
Топалов Эдуард Львович – к.т.н. доцент Тюменская государственная архитектурно-строительная академия, Тюмень.

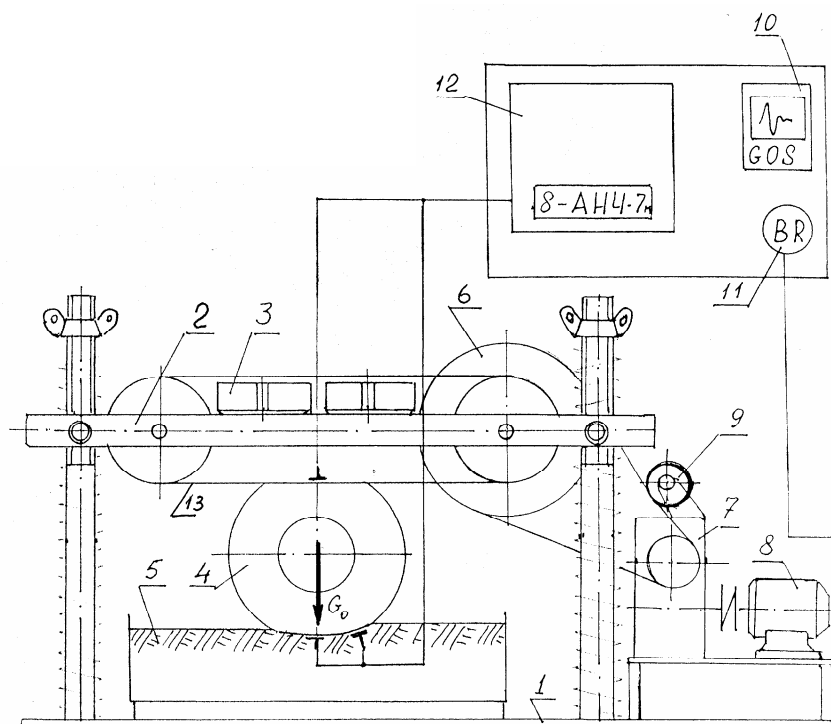


Рис.1 Схема стана

- 1 – основание; 2 – подвижная рама с натяжным устройством; 3 – сменные грузы;
 4 – пневмокаток; 5 – исследуемые грунты; 6 – приводной шкив; 7 – редуктор;
 8 – регулируемый электрический двигатель; 9 – механизм натяжения ремня;
 10 – осциллоскоп; 11 – счетчик оборотов; 12 – тензостанция; 13 – лента

Для каждого шиноразмера катка проводилась серия опытов, в которых поочередно менялись нагрузка на каток и давление воздуха в шине. По полученным данным для каждой шины строились зависимости взаимодействия катков с сопряженными грунтами, характеристика которых в табл.2.

Зависимость тягового усилия от изменения диаметра катка при сопряжении с влажным песком и внутренним давлением воздуха в катке 0,01 МПа при скорости вращения 0,8 м/с представлены на рис.2.

Зависимость тягового усилия от ширины катка при тех же условиях эксперимента на рис.3.

Изменение тягового усилия в зависимости от геометрических параметров катка зависят от характеристики сопряженного грунта. Для влажного песка характерным являются гранулометрический состав и плавучность.

Таблица 2
 Характеристика и классификационные признаки грунтов

Грунт	$t, ^\circ\text{C}$	Плотность $\rho, \text{г/см}^3$	Сопротивле- ние сдвигу $\tau, \text{кПа}$	Коэффициент сцепления ϕ	Удельная сила тяги $F_{\text{кр}}$ при давлении в шинах, кПа			Нормальные напряжения, МПа	Сопротивле- ние качению, $f_{\text{к}}$
					5	20	50		
Песок сухой I	20	1,51	0,6	0,20	0,09	0,11	0,12	1,43	0,15
Песок влажный II	20	1,62	2,0	0,35	0,10	0,12	0,127	1,21	0,12
Суглинок влажный III	20	1,51	2,0	0,35	0,29	0,31	0,32	2,45	0,16
Суглинок тяжелый IV	0	1,60	0,6	0,40	0,29	0,30	0,31	2,81	0,14
Снег рыхлый V	0	0,6	0,1	0,08					0,07

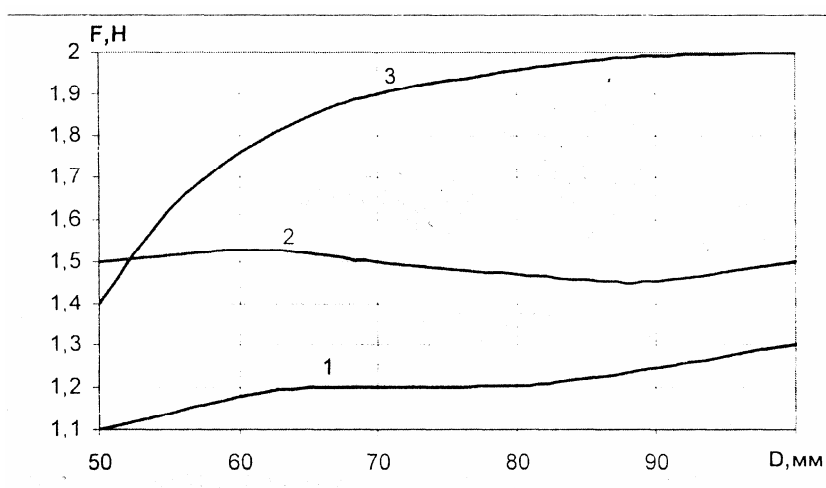


Рис.2. Зависимость тягового усилия от диаметра катка при сопряжении с влажным песком:
1 - ширина катка 24 мм; 2 - ширина катка 50 мм; 3 - ширина катка 90 мм

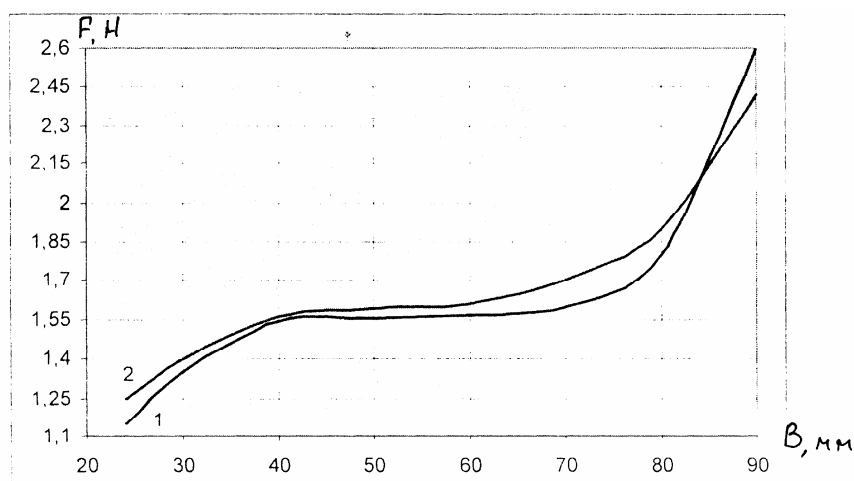


Рис.3. Зависимость тягового усилия от ширины катка в сопряжении с влажным песком:
1 - диаметр катка 60 мм; 2 - диаметр катка 90 мм

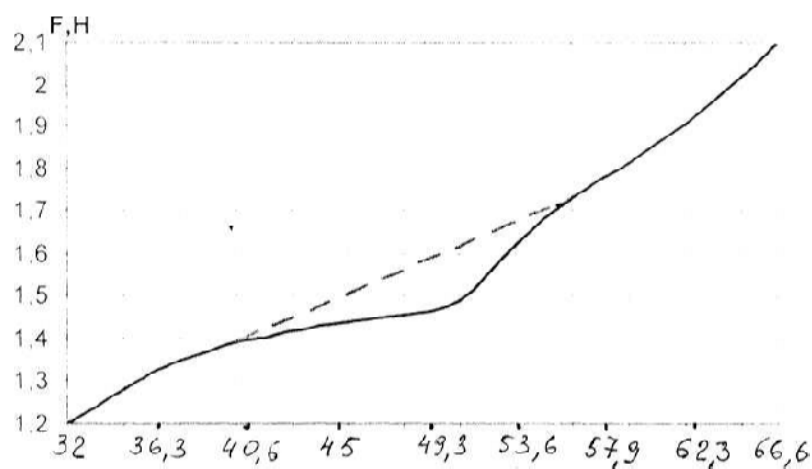


Рис.4 Зависимость тягового усилия от угловой скорости катка

Сжимаемость песчаных грунтов значительно ниже, чем связанных. Под влиянием статических нагрузок происходит едва заметное уплотнение, но при малых скоростях вращения катков происходит интенсивное виброуплотнение песчаных грунтов, особенно сухих. Модуль деформации песчаных грунтов не превышает 50 МПа, который резко уменьшается с уменьшением дисперсности и увеличением плотности. Деформацией песчаной основы можно объяснить сложность зависимости на рис. 2 и 3. Для определения зависимости тягового усилия от скорости вращения катка проведен эксперимент сопряжения каток - песчаный грунт увлажненный. Размеры катка: диаметр 80 мм и ширина 60 мм, давление воздуха 50 МПа и нагрузка составляла 22,5 Н. Результаты испытаний на рис. 4.

Характер зависимости в области от 40,6 до 57,9 1/с обусловлен резонансными частотами, вызывающими дополнительные затраты энергии на деформационное уплотнение грунта.

Возможно, при определенных допущениях такую зависимость можно рассматривать как линейную, что в принципе подтверждается в работах отечественных исследователей.

ПУТИ СОВЕРШЕНСТВОВАНИЯ МАЛОГАБАРИТНОГО ОБОРУДОВАНИЯ ДЛЯ УСЛОВИЙ СТРОИТЕЛЬНОЙ ПЛОЩАДКИ.

Емельянова И.А. , Баранов А.Н. , Задорожный А.А, Непорожнев А.С, Грачев Ф.А.

Abstract

Освещаются различные виды нового малогабаритного оборудования, которое за период 1999-2005гг. внедрено на различных стройках Украины. Все оборудование, разработанное на основе результатов многочисленных теоретических и экспериментальных исследований, запатентовано в Украине.

Ключевые слова: малогабаритное оборудование, растворобетононасос, технологический комплект, композиционное транспортирование, струйный аппарат, бетоносмеситель.

При возведении новых зданий, реконструкции и ремонте действующих часто требуется оборудование, которое легко устанавливается на строительной площадке и может быть использовано для различных строительных работ без переналадки. Так был создан ряд машин и оборудования, из которых в конкретных условиях строительства можно сформировать технологические комплекты, выполняющие строго определенные виды работ. Такие комплекты можно использовать при:

- нанесении бетонных покрытий на усиленные старые перекрытия жилых домов;
- бетонировании полов, сейфов с приготовлением и укладкой сталефибробетонных смесей;
- транспортировании малоподвижных строительных смесей на дальние расстояния;
- выполнении гидроизоляционных работ при строительстве и ремонте бассейнов, фонтанов, резервуаров способами сухого и мокрого торкретирования;
- заделке стыков в возводимых зданиях и сооружениях;
- приготовлении и подаче пенобетонных смесей и т.д.

В случае необходимости из разработанного нового оборудования при различном насыщении могут быть созданы системы узкого целевого назначения. [1] Это технологические комплекты для:

- нанесения бетонных покрытий способом сухого торкретирования: «передвижная компрессорная установка- набрызг-машина- рабочее сопло с кольцевым насадком»;
- приготовления и транспортирования пенобетонных смесей: «передвижная компрессорная установка-набрызг-машина- струйный аппарат»;
- нанесения бетонных покрытий способом мокрого торкретирования: «передвижная компрессорная

установка- двухпоршневой растворобетононасос-компенсатор пульсаций- рабочее сопло с кольцевым насадком»;

- транспортирования композиционным способом строительных смесей: «растворобетононасос-передвижная компрессорная установка-дополнительная камера смешения- гаситель»;
- приготовления, транспортирования и нанесения сталефибробетонных смесей: «передвижная компрессорная установка- цемент-пушка или набрызг- машина- автомат-резчик фибры- рабочее сопло для сталефибробетонной смеси».

Некоторые виды оборудования, входящие в вышеперечисленные комплекты оборудования, представлены на рекламном листке, прилагаемом к данной статье.

Одной из определяющих машин в технологических комплектах является растворобетононасос, прошедший за последние годы ряд усовершенствований, которые позволили существенно расширить диапазон рабочих строительных смесей для этих машин ($P=4...12\text{см}$), улучшить их конструкцию. На Рис.1 представлены принципиальные схемы насосов в той последовательности как они подвергались модернизации. Эффективной машиной, созданной в последнее время, является насос двухпоршневой с горизонтальным расположением цилиндров и принудительной шнековой загрузкой, который работает на бетонных смесях подвижностью $P=3...4\text{см}$. [2.] Все растворобетононасосы, представленные на Рис.1, могут быть использованы при композиционном транспортировании бетонных смесей [3], особенность которого заключается в том, что, используя на первоначальном пути транспортирования подвижные смеси, на выходе за

1) Емельянова И.А. , Украина Проф. ХГТУСА-Харьков
Баранов А.Н. , Украина Проф. ХГТУСА-Харьков
Задорожный А.А. , Украина Доц. ХГТУСА-Харьков
Непорожнев А.С., Украина Асп. ХГТУСА-Харьков

счет оригинальной конструкции гасителя потребитель получает малоподвижную смесь с существенно сниженной первоначальной подвижностью. Малогабаритная набрызг-машина

успешно заменяет громоздкую цемент-пушку (её масса в 4...5раз меньше) и эффективно работает с автоматом-резчиком, который в условиях стройплощадки

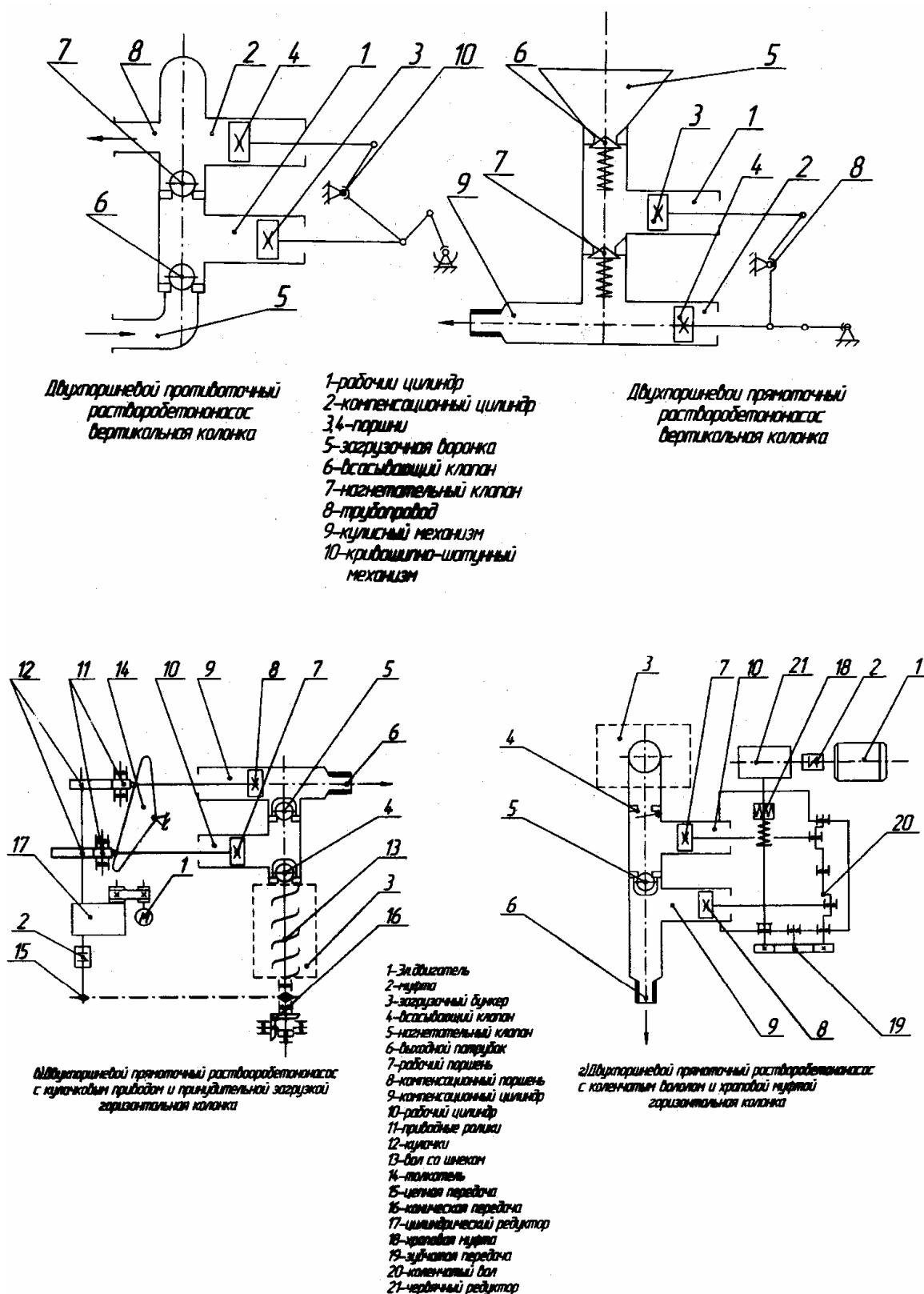


Рис.1 Принципиальные схемы растворобетонасосов

непосредственно используется для нарезания фибровых элементов. Благодаря среде сжатого воздуха в камере смешения машины образуется сухая сталефибробетонная смесь, которая, поступая в рабочее сопло, взаимодействует с водой. Эта машина интересна также и тем, что при подсоединении к ней струйного аппарата появляется возможность получать пенобетонные смеси.

Опыт первой эксплуатации новых машин показал, что существуют трудности с получением качественных малоподвижных строительных смесей, на которых работает предлагаемое оборудование. В связи с этим, разработан бетоносмеситель нетрадиционной конструкции, который может быть использован и как самостоятельная машина, и как составная часть растворобетононасоса (Рис.2),

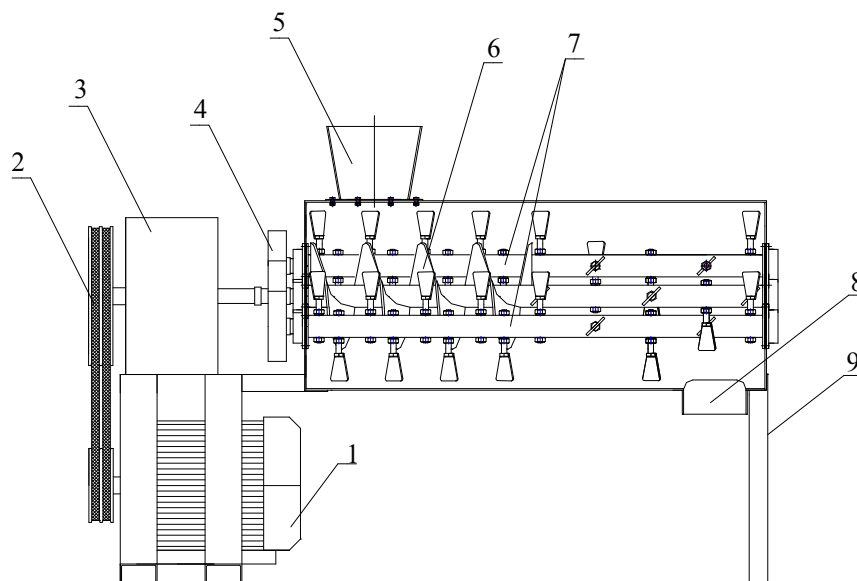


Рис.2 Трехвальный бетоносмеситель непрерывного действия для приготовления строительных смесей

1. двигатель; 2. клиноременная передача; 3. редуктор;
4. открытая зубчатая передача; 5. загрузочный бункер; 6. шнековый вал; 7. лопастные валы;
8. разгрузочный патрубок; 9. рама

который организует режим трехконтурного движения смеси в корпусе, что существенно интенсифицирует процесс перемешивания [4] и позволяет получить однородную смесь. Таким образом, новое оборудование, из отдельных видов которого легко собираются технологические комплекты целевого назначения, позволяет существенно улучшить многие рабочие процессы на строительной площадке.

Выводы

Представлено новое малогабаритное эффективное оборудование для строительной площадки, которое в составе отдельных технологических комплектов позволяет выполнять широкий фронт строительных работ.

Литература

1. Емельянова И.А. Особенности малогабаритного оборудования для строительной площадки. // Наукoвий вісник будівництва.-Харків: Вид. ХДТУБА-2005-Вип.№30-с.1-67 – 1-72.
2. Емельянова И.А., Баранов А.Н., Задорожный А.А., Непорожнев А.С. Технологический комплект оборудования для торкрет-работ с использованием двухпоршневых растворобетононасосов // Вісник криворізького технічного університету.-Кривий Ріг: Вид. КГУ-2004-Вип№4-С.15-18.
3. Емельянова И.А., Баранов А.Н., Никонов Д.В. Теоретические основы создания оборудования для композиционного транспортирования бетонных смесей. // Научно-технический сборник «Коммунальное хозяйство городов.-Киев: Издательство «Техника».-2002-С.63-69.
4. Емельянова И.А., Бражко В.В. Технологический комплект оборудования для торкрет-работ с бетоносмесителем принудительного действия. // Наукoвий вісник будівництва. Харків: Вид. ХДТУБА.-2004.-Вип.27.-С.147-150

МЕТОДИКА ОЦЕНКИ ТОРМОЗНЫХ КАЧЕСТВ КОЛЕСНОГО ДВИЖИТЕЛЯ ЗЕМЛЕРОЙНО-ТРАНСПОРТНЫХ МАШИН

П.И.Никулин, Е.И.Никаноров

Изложена методика оценки тормозных качеств колесного движителя на транспортном режиме, в которой приведены исходные данные и порядок расчета показателей тормозных качеств; полученные аналитические выражения позволяют проводить на стадии проектирования анализ влияния параметров шины и поверхности на тормозные качества.

Пневматическая шина, параметры, тормозные качества, расчет

В условиях интенсивной эксплуатации пневматические шины землеройно-транспортных машин наряду с высокими тягово-сцепными качествами должны обеспечивать и надежную безопасность движения на транспортном режиме. Безопасность в значительной степени определяется их тормозными качествами, которые зависят от максимальной величины относительной силы торможения в контакте с опорной поверхностью и области устойчивого торможения, т.е. меньшей склонности колеса к блокированию.

Для расчета зависимости $\psi_t = \psi_t(S)$ относительной силы торможения ψ_t от коэффициента скольжения S на недеформирующейся опорной поверхности необходимы следующие данные:

а) вертикальная нагрузка на ось колеса G_k ;
б) поступательная скорость оси колеса V_{kd} ;
в) параметры поверхности: коэффициент трения покоя резины протектора об опорную поверхность μ_n , коэффициент влияния скорости скольжения на коэффициент трения скольжения K_c ;

г) нормальное максимальное напряжение в контакте σ_{max} , показатель, определяющий форму эпюры продольных нормальных напряжений K ;
д) параметры пневматической шины: наружные радиусы пневматической шины r_o и ее каркаса R_k , высота слоя протектора h_o , ширина протектора B_n , коэффициент насыщенности рисунка протектора K_n , модуль упругости резины протектора E ; коэффициенты, зависящие от соотношения геометрических размеров выступа протектора, давления воздуха P_w в шине $-\psi_1, \psi_2$, жесткость протектора на сдвиг C_n , жесткость протектора относительно шины на сдвиг γ_n .

Расчет проводится в следующей последовательности:

1. Определяется половина длины области контакта пневматической шины с опорной поверхностью l_n :

$$a = \sqrt[3]{\frac{3G_k r_o}{B_n (\kappa_1 + \kappa_2)}},$$

где κ_1 - коэффициент деформации шины при сжатии недеформированной формы, κ_2 - коэффициент восстановления недеформируемой формы.

2. Рассчитывается зависимость $\psi_t = \psi_t(S)$ при равномерном установившемся движении колеса с определенной степенью затормаживания:

при $a \geq l_n > 0$:

$$\begin{aligned} \Psi_T = & \frac{h_o k^2}{6a^2 \Psi_1 \Psi_2 (k-1)} \cdot \\ & \cdot \left[l_n \left(1 - \frac{l_n}{2a} \right) - \frac{a}{k} \left(1 - \exp \frac{-kl_n}{a} \right) \right] + \\ & + \frac{B_n k_n l_n^2 E}{6h_o \Psi_1 G_k} \left[\frac{S}{(1-S)\gamma_n} - \right. \\ & - \frac{G_k h_o^2 k^2}{2a^2 B_n k_n E \Psi_2 l_n (k-1)} \cdot \\ & \cdot \left(\frac{a-l_n}{a} - i \cdot \exp -k \left(1 - \frac{a-l_n}{a} i \right) \right) \left. \right] + \\ & + \frac{k(\mu_n - k_c V_{kd} S)}{2a(k-1)} \left[(2a-l_n) - \frac{a}{k} \cdot \right. \\ & \cdot \left. \left(1 + \exp \frac{-kl_n}{a} \right) \right] \end{aligned} \quad (1)$$

и при $2a \geq l_n > a$

$$\begin{aligned} \Psi_T = & \frac{h_o k^2}{6a^2 \Psi_1 \Psi_2 (k-1)} \cdot \left[l_n \left(1 - \frac{l_n}{2a} \right) - \frac{a}{k} \left(1 - \exp \frac{-k(2a-l_n)}{a} \right) \right] + \\ & + \frac{B_n k_n l_n^2 E}{6h_o \Psi_1 G_K} \left[\frac{S}{(1-S)\gamma_n} - \frac{G_K h_o^2 k^2}{2a^2 B_n k_n E \Psi_2 l_n (k-1)} \cdot \left(\frac{a-l_n}{a} - i \cdot \exp -k \left(1 - \frac{a-l_n}{a} i \right) \right) \right] + \\ & + \frac{k(\mu_n - k_c V_{кд} S)}{2a(k-1)} \left[(2a-l_n) - \frac{a}{k} \cdot (1 + \exp \frac{-k(2a-l_n)}{a}) \right] \end{aligned} \quad (2)$$

где l_n – длина области покоя в контакте; $i=-1$, если $x<0$ и $i=+1$, если $x>0$, где x – продольная координата элемента протектора в области контакта, измеряемая от центра контакта. Расчет по формулам (1) и (2) производится в следующем порядке. В начале задаются рядом значений l_n в пределах $2a > l_n > 0$, определяют коэффициент скольжения S , соответствующий каждому заданному l_n :

$$S = \frac{\mu_n \gamma_n \sigma_{\max} [1 - \exp(-k(1 - \frac{l_n - a}{a} i))]}{l_n C_n + \mu_n \gamma_n \sigma_{\max} [1 - \exp(-k(1 - \frac{l_n - a}{a} i))]}$$

и рассчитывают значения Ψ_T по выражению (1) при S , соответствующем $a \geq l_n > 0$ и по выражению (2) при S , соответствующем $2a \geq l_n > a$.

На рис.1 показаны графические зависимости $\Psi_T = \Psi_T(S)$, полученные по выражениям (1) и (2) (сплошные линии), по уравнениям регрессии (штриховые линии), полученным методом планирования эксперимента, а также нанесены точками средние опытные значения при скоростях движения затормаживаемого колеса $V_{кд}=5$ км/ч и $V_{кд}=35$ км/ч на асфальтобетоне а) и грунтовой накатанной дороге б).

По зависимости $\Psi_T = \Psi_T(S)$ можно определить показатели, позволяющие оценить тормозные качества колесного движителя при расчете и

анализе влияния параметров пневматической шины на этапе проектирования и при эксплуатации. Этими показателями являются: максимальная относительная сила торможения $\Psi_{T\max}$, критический коэффициент скольжения $S_{кр}$ соответствующий $\Psi_{T\max}$ и коэффициент степени реализации тормозной

силы при блокировке колеса $K_T = - \frac{\Psi_{TS}}{\Psi_{T\max}}$, где

Ψ_{TS} – относительная сила торможения при $S=1$.

Показатели $S_{кр}$ и K_6 определяют величину области устойчивого торможения колесного движителя и склонность его к блокировке и возможному заносу.

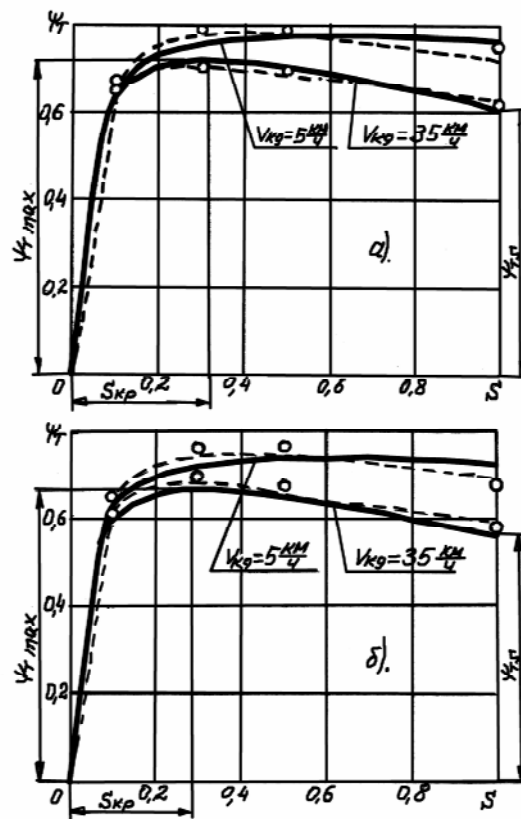


Рис.1. Зависимости относительной силы торможения $\Psi_T = \Psi_T(S)$ при скоростях движения затормаживаемого колеса $V_{кд}=5$ км/ч и $V_{кд}=35$ км/ч на асфальтобетонной поверхности а) и грунтовой накатанной дороге б).

Список литературы

1. Ульянов Н.А. Колесные движители строительных и дорожных машин: Теория и расчет. - М.: Машиностроение, 1982.

MACHINES AND PLANTS OF BUILDING AND TRANSPORT MECHANIZATION- TECHNICAL REGULATIONS CONDITION¹⁾

M. Gašić, M. Savković, G. Marković, N. Zdravković²⁾, S. Igrutinović³⁾

Product distribution at market of the Member States of the European Union is restricted by application of new directives that regulate the product quality. In order to increase the export Serbia and Montenegro should take part in assuming and applying the EU technical regulations so that state administration could be reorganized and trained. In this paper key directive requirements related to machines are shown and analyzed. Relations between directives and national legislation are also given as well as starting assumptions and actions for technical regulation harmonization.

Key words: UE directives, standards, harmonization, machines.

1. INTRODUCTION

Free flow of goods enables pretty larger offer for consumers and induces competition. of The European Union market, defined as a space with no borders, was formed in order to enable free flow of goods, people, service and assets.

This market is of great importance for economy of Serbia and Montenegro. The condition for placing the goods on this market is strictly observing the legislative and technical regulations.

On the basis of defined rules of the EU market organization, the interests of the EU members are being protected through environment protection, occupational health, property protection etc.

The enterprises that intend to export the products on the EU market must apply and be acquainted with the EU regulations before the country from which the enterprise comes become the EU member. The country should assume these regulations into national legislation as soon as possible. They also include harmonized EU regulations related to technical regulations and marking the products with CE mark.

In order to be exported into UE countries the product must satisfy following conditions:

- functioning
- design
- price
- delivery terms
- quality
- appropriate marketing.

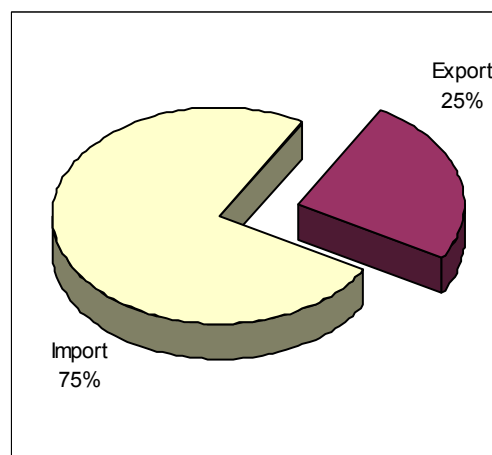
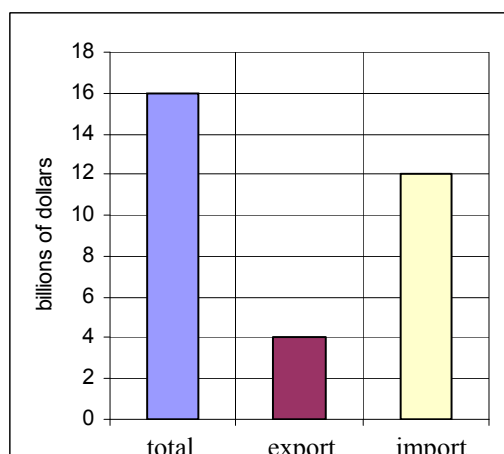


Fig.1- Trade exchange in Serbia and Montenegro in 2004

- 1) This work is a part of the scientific and research project: "Research, development and application of methods and procedures of testing, controlling and certifying the products and processes according to the International standards" supported by Ministry of Science and Environmental Protection of the Republic of Serbia for period 2005-2007, evidention number TD007068A
- 2) Ph. D Gašić Milomir, Faculty of Mechanical Engineering Kraljevo, Dositejeva 19, 36000 Kraljevo, gasic.m@maskv.edu.yu
Ph. D Savković Mile, Faculty of Mechanical Engineering Kraljevo, Dositejeva 19, 36000 Kraljevo, savkovic.m@maskv.edu.yu
Msc. Marković Goran, Faculty of Mechanical Engineering Kraljevo, Dositejeva 19, 36000 Kraljevo, markovic.n@maskv.edu.yu
Zdravković Nebojša, Faculty of Mechanical Engineering Kraljevo, Dositejeva 19, 36000 Kraljevo, zdravkovic.n@maskv.edu.yu
- 3) Igrutinović Smiljana, The Mechanics and Technics School, Trstenik, sgasic@ptt.yu

The stated conditions are not legally obligatory but they must be fulfilled if the producer wants a part of the market.

Last year total foreign-trade exchange of Serbia and Montenegro was about 16 billion dollars, the export was about 4 billion dollars and import was about 12 billion dollars. It is obvious that there was a great deficit in foreign-trade exchange (fig.1). In order to decrease the mentioned deficit it is essential to carry out the harmonization with legal obligatory conditions for placing the products on the EU market from the aspect of people's health and safety.

Before the product is being placed on the market the producer must carry out procedure of harmonization with valid technical regulations regarding safety.

All these activities must be done through appropriate institutions, accredited and notification bodies regarding machines.

The EU legislation on industrial product safety can be grouped as follows:

- a) General approach directives such as directives for agriculture, food industry, chemical products, medicines, motor vehicles...
- b) New approach directives

2. NEW APPROACH DIRECTIVES

The aim of new approach directives is to enable free flow of products according to requirements determined by particular directives. The directives were stated by the Council's resolution on new approach to technical harmonization and standardization and they introduced following principles:

- Harmonization of legislation is restricted by important requirements that products must satisfy in order to have free flow inside community.
- Technical specifications on product harmonization with important requirements, are given in harmonized standards.
- Application of harmonized or other standards is not obligatory. The producer can always use other technical specifications that satisfy important requirement.
- The assumption on harmonization with important requirements applies to all products made in accordance with harmonized standards
- Producers can chose among different procedures for harmonization determination.

Relation between new approach directives, national legislation and harmonized standards is shown in fig.2.

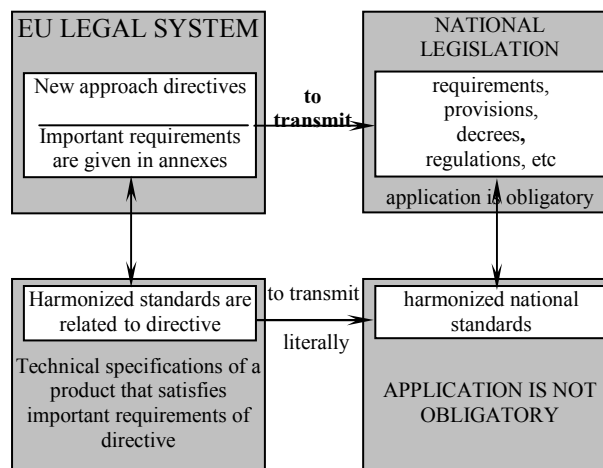


Fig.2- Relation between new approach directives, national legislation and harmonized standards

New approach directives are applied for new products made in the Member States as well as for new and used products imported from the third countries into the EU countries.

New approach directives point to product marking with CE mark. Twenty-one directives for technical products that require CE marking are in practice as well as four directives that do not allow CE marking.

3. REVIEW OF MACHINE PRODUCTION IN SERBIA AND DIRECTIVES RELATED TO MACHINES

Key products of "IMK 14.oktobar" in Kruševac are building machines. Production started in 1954 and reached the maximum from 1984-1986. The number of produced machines in types in three periods is shown in table1:

Table 1

year	caterpillars	wheel loaders	ex-cavators	rollers	other machines
1981	658	254	205	90	33
1982	652	248	168	81	10
1983	461	208	29	50	49
1984	1 200	280	99	60	21
1985	1 112	290	57	44	29
1986	1 165	331	51	35	30
1987	542	367	70	50	36
1988	510	392	93	50	58
1989	354	336	75	26	44
1990	268	319	73	37	18

The percentage of total number of produced machines in types is shown in fig. 3.

Since these machines operate on uneven ground or on the fields with canals for irrigation, roll-overs with accidents were very frequent.

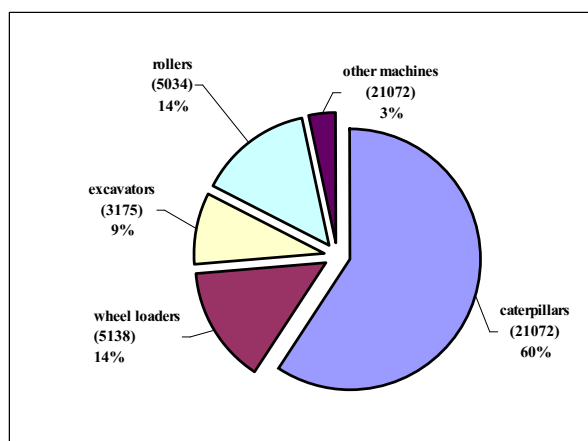


Fig.3- The percentage of total number of produced machines from 1954-2003

The first international regulation related to this field was brought by OECD (Organization for Economic Cooperation and Development) in 1967. In the USA a year later SAE standards (Society of Automotive Engineers) are brought treating operator's protection (SAE J333) as well as requirements and conditions of testing for tractor frame (SAE J334). We also brought the Regulations on occupational health in agriculture, by which tractors must have a cab or protection frame which protects the operator in case of roll-overs.

ROPS (Roll-over protective structures) is included in the standard defining structure for protection during machine roll-over (figures 4 and 5). FOPS (Fall-over protective structures) is included in ISO 3449 standard and testing scheme is shown in fig. 6. In both cases protective zone of the operator must not be endangered, which is defined by ISO 3164 standard.

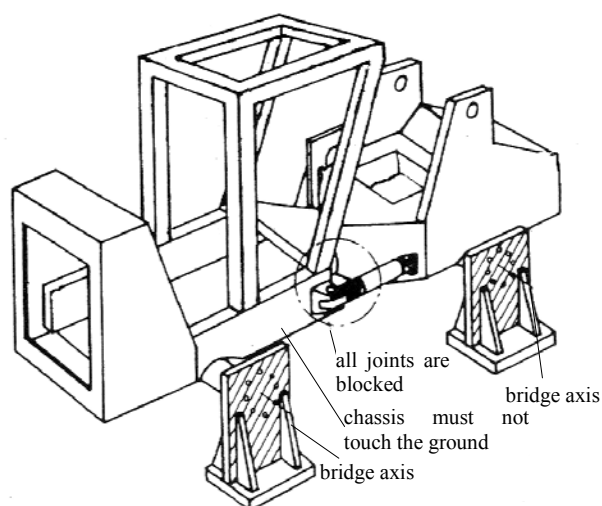


Fig.4- Fixing of joint loader chassis

Directives of the European Council and European Parliament No. 98/37/EC dated 22nd June 1998, points out the approaching in law harmonization of the EU states related to machines, their construction, exploitation and maintenance, failure prevention, protection of environment and occupational health.

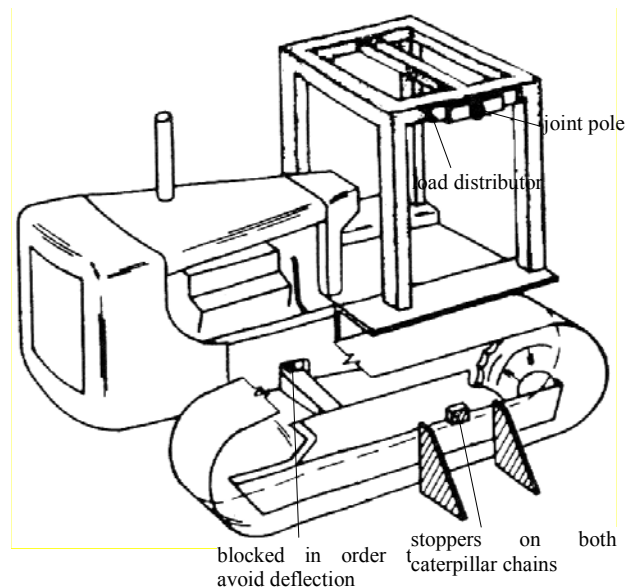


Fig. 5- Fixing of caterpillar chasis

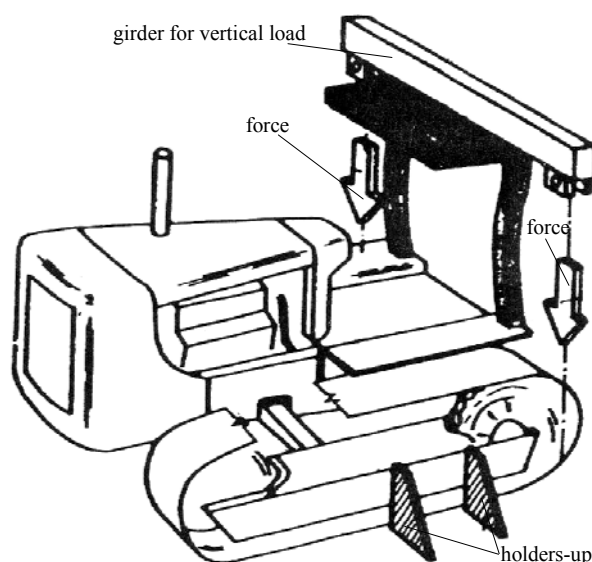


Fig. 6- Frame exposure to vertical load

The requirements of this directive are given in following chapters:

Chapter I: Goods placing on market and free flow of goods

Chapter II: Procedure of harmonization estimation

Chapter III: CE mark

Chapter IV: Final regulations.

In chapter I machines are defined as:

- assembly of connected parts or components so that particular process, work, movement or material packing could be done
- assembly of many machines which are operated so that they are a whole and function as a whole
- changeable equipment (modulus). The main machine can operate without the mentioned equipment and the machine function is changed if the equipment is changed (tractor with additional modulus).

So, safety components, as constituent parts of machines, are defined and built in by producer so that in the case of breakdown or failure safety or health of the persons near machine will not be brought into danger.

During the estimation process of application range it is essential to notice that EU Directive No.98/37/EC excludes particular groups of machines.

In chapter II procedures for harmonization estimation are defined as well as fulfillment of conditions and form of CE certificate, graphic presentation of the certificate, data on producer and authorized agent, what the certificate should include. All this is defined in 9 annexes where application of protection depending on machine type and components type is also defined.

Minimum criteria that must be fulfilled by staff are defined as well as necessary equipment so that administrative activities related to verification should be properly done.

Chapter II deals with CE marking and obligations that must be satisfied so that a product could get and keep CE mark.

Domestic standardization follows world trends in accordance with society development. The act on standardization (The Official Gazette No.30/1996, 59/1998 and 57/2001) regulates the following: standard bringing and its application, technical and other regulations, checkout the harmonization of process, products and services with technical and other regulations, that is with standards, product declaration, marking, packing as well as supervision of law realization.

Basic theses of this act are:

- standard is a technical norm and it should be in accordance with international and European standards or with standards of developed industrial countries;
- technical regulations are brought by the ministries, in the first place by citing the state demands;
- technical recommendations are done for faster application of new knowledge and technologies;
- making of national system for checkout and estimation of harmonization of process, product and service based on international documents;
- system realization of accredited laboratories, first of all the ones needed for obligatory checkout of harmonization with technical regulations and standards;
- forming of state accredited body, issuing of manner and conditions of accreditation and supervision of accredited legal persons by which conditions for internationally harmonized concept of accreditation is accomplished;
- cooperation with international and European organizations for standardization, working bodies of the United Nations dealing in standardization and national organizations for other countries standardization;

- establishing of fast and accurate information system in the field of standardization, both in the country and abroad;
- supervision of carrying out the act is regulated for competent institutions.

4. CONCLUSION

Since Declaration No.98/37/EC corresponds to over 500 harmonized standards and other technical regulations (EN and EN ISO) the significance of work on further harmonization of domestic regulations with international ones is obvious.

A large number of producers, some of them being the leaders, makes machines and devices that are in domain of this Directive. Present technical regulations mostly are not in accordance with the appropriate ones in the EU.

Beside acceptance and standard making in Serbia and Montenegro the following should be done:

- Work out of methods and procedures for testing, control and certificates in accordance with procedures for harmonization estimation.
- Development of laboratory capacities in various neutral and independent institutions (faculties and institutes) but:
 - a) Plant for measurement and testing should be reactivated
 - b) If something is missing it should be acquired or completed
 - c) New devices for testing and measurement should be designed and produced.

One should look at directive application as a transformational process which would turn the economy and whole society the quality, consumers' protection, environment protection, and which would enable free flow of goods and assets. Directives also have some characteristics of previous transformational process, such as energy saving, limitless competition and quality. They especially influence on the market transformation, that is on producer-consumer relation but also on the employees' attitude toward a product or service.

5. REFERENCES

- [1] Prešern S.: Unutrašnje tržište evropske unije i CE oznaka, SIQ Ljubljana 2003. Agencija za razvoj malih i srednjih preduzeća – Euroinfo-korespondentni centar, EICC, Podgorica 2004.
- [2] Mitrović R., Ristivojević M., Stamenić Z., Lazović T.: Analiza stanja tehničke regulative u oblasti mašina u skladu sa zahtevima evropskih standarda i propisa, Festival kvaliteta 2005., 32. Nacionalna konferencija o kvalitetu, Kragujevac, 19-21. maj, 2005.
- [3] Đorđević Lj.: Kako dalje, bez strategije, bez strateških partnera, IMK 14. oktobar, Istraživanje i razvoj, časopis instituta IMK 14. oktobar Kruševac, broj (16-17) 1-2/2003.

ИСПЫТАНИЯ СКРЕПЕРНОГО АГРЕГАТА

П.И. Никулин, В.А. Нилов, А.А. Косенко

Аннотация

Наиболее универсальными по области применения являются прицепные скреперы к энергонасыщенным колесным тягачам, позволяющие осуществлять эффективный самонабор грунта без толкача. В настоящей работе изложены результаты полевых испытаний прицепного скрепера, сцепной вес тягача которого на время копания увеличивается специальным тягово-сцепным устройством.

Тягач, сцепной вес, догрузка, испытания, гидравлическая система

Для увеличения сцепных качеств колесных тягачей, работающих с прицепными скреперами, целесообразно применение специальных тягово-сцепных догружающих устройств (ТСДУ) различной конструкции [1]. Их работа основана на передачи части вертикальной нагрузки, приходящейся на передний мост ковша прицепного скрепера, на колесный тягач. ТСДУ позволяют увеличивать сцепной вес тягача, как при разработке грунта, так и на транспортном режиме в тяжелых дорожных условиях.

Для изучения процесса копания грунта прицепным скрепером, имеющим колесный тягач с изменяемым сцепным весом в Воронежском государственном архитектурно-строительном университете (ВГАСУ) были проведены экспериментальные и теоретические исследования скреперного агрегата (табл. 1), включавшего прицепной скрепер ДЗ-111 и колесный тягач Т-150К.

В табл. 1 приведена техническая характеристика экспериментального скреперного агрегата.

Таблица 1

Техническая характеристика скреперного агрегата

Параметр	Единицы измерения	Величина
1. Мощность двигателя	кВт	122
2. Вместимость ковша: геометр. / с «шапкой»	м ³	4,5/5,5
3. Ширина резания	м	2,43
4. Максимальная глубина резания	м	0,13
5. Сцепной вес тягача	кН	76,8
6. Увеличение сцепного веса тягача при копании	%	15...25

ТСДУ [2] включает (рис. 1) тягач 1, соединенный с прицепным скрепером 2, сцепным устройством 3.

Между тяговым брусом 4 и аркой-хоботом прицепного скрепера 2 установлен на шаровых опорах гидроцилиндр 5. При наборе грунта в гидроцилиндр 5 подают регулируемое давление масла, которое автоматически поддерживается напорным клапаном.

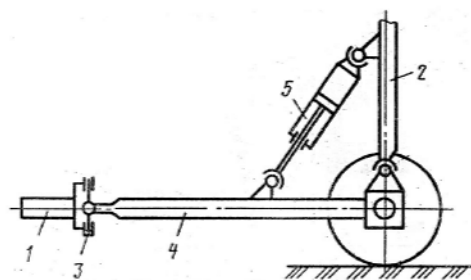


Рис. 1. Схема тягово-сцепного догружающего устройства скрепера

При этом шток гидроцилиндра 5 выдвигается и через тяговой брус 4 осуществляет нажатие на сцепное устройство 3 тягача 1. В результате происходит перераспределение нормальных реакций между колесами тягача 1 и передним мостом скрепера 2 вплоть до его полного вывешивания.

На транспортном режиме тягача 1 гидроцилиндр 5 переводят в плавающее положение, что обеспечивает все необходимые перемещения тягового бруса 4 и прицепного скрепера 2 при езде по пересеченной местности.

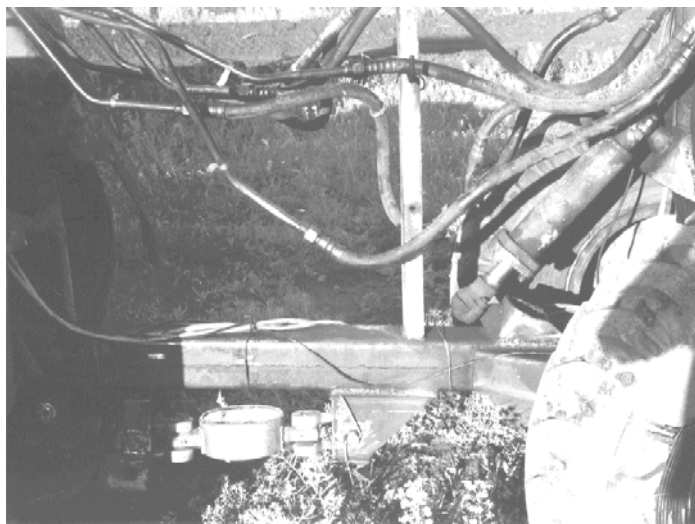


Рис. 2. Экспериментальное ТСДУ

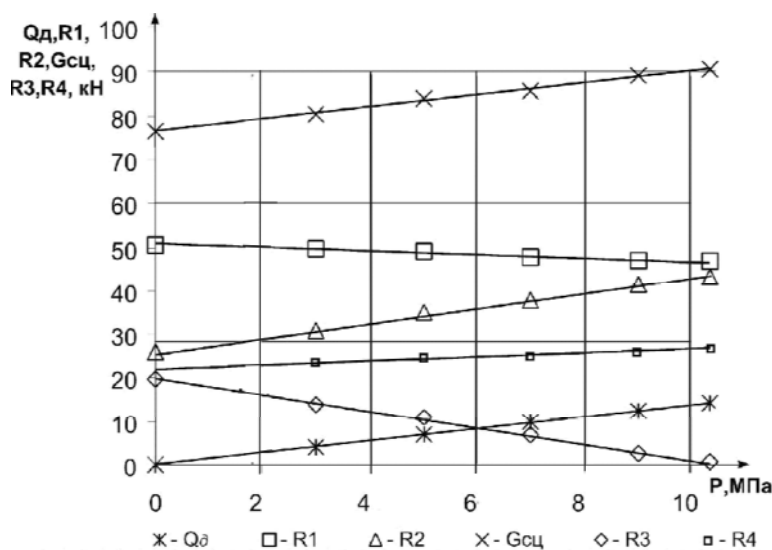


Рис. 3. Изменение вертикальных нагрузок на мосты скреперного агрегата в статике при работе ТСДУ

(Вертикальные нагрузки на мосты: тягача R_1 , R_2 ; скрепера R_3 , R_4 ; сцепной вес тягача G_{sc} ; давление в гидроцилиндре – Q_d)

Экспериментальный скреперный агрегат (табл. 1) был оснащен ТСДУ (рис. 2) и показал, что при полном вывешивании переднего моста прицепного скрепера с порожним ковшом в статике сцепной вес тягача увеличивается на 19 % (рис. 3). При этом, что немаловажно, происходило выравнивание вертикальных нагрузок R_1 и R_2 на мосты колесного тягача.

Испытания скреперного агрегата на полигоне ВГАСУ показали следующие результаты [4]. При копании грунта с догрузкой (давление в гидроцилиндре 5 (рис. 1) 10 МПа) зарегистрировано существенное увеличение объема набираемого грунта (в среднем на 19%, рис. 4), сцепного веса тягача на 20%, максимальной тяговой мощности на 16%.



а) копание без догрузки



б) копание с догрузкой

Рис. 4. Заполнение ковша при копании с постоянной глубиной резания 80 мм

Отмечено также, что при заполнении ковша происходит увеличение вертикальной нагрузки на передний мост прицепного скрепера на 15...30%, несмотря на то, что часть его статического веса использована ТСДУ для увеличения сцепного веса тягача в самом начале копания. Это обстоятельство дает основания для разработки новой гидросистемы ТСДУ, которая позволяла бы осуществлять двухступенчатую догрузку тягача: первая треть заполнения ковша происходит при меньшей догрузке тягача; вторая – при увеличенной на 10...20% догрузке.

С этой целью разработана новая гидросистема ТСДУ [4], рис. 5. Она работает следующим образом. Начиная копание грунта, оператор тягача секцией гидрораспределителя 2 подает масло из бака 3 в рабочую (бесштоковую) полость гидроцилиндра 8 ТДСУ, что обеспечивает первую ступень увеличения сцепного веса тягача. В таком положении гидросистемы оператор фиксирует подачу масла в гидроцилиндр 8 на время набора 30...40% вместимости ковша.

Давление в гидроцилиндре 8 в этот период автоматически поддерживается напорным клапаном 9 (рис. 5) через левую позицию гидроуправляемого золотника 11.

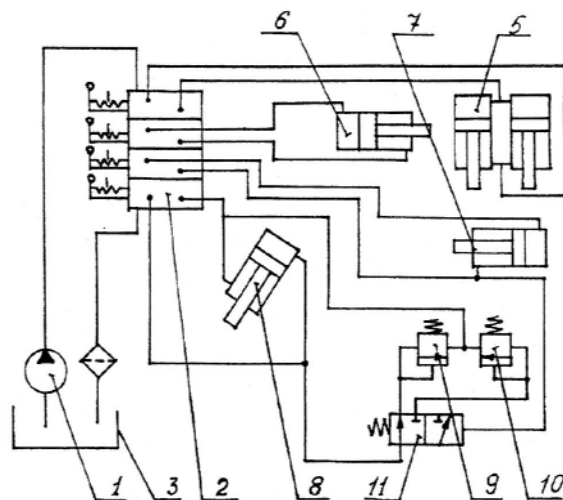


Рис. 5 Гидросистема ТДСУ (догрузка двухступенчатая)

После набора грунта, объемом 0,4...0,5 вместимости ковша, оператор тягача на короткий срок подает масло в гидроцилиндр 7 задней стенки и включает (запирает) его. Задняя стенка в крайнем положении копания назад перемещаться не может. Такого импульса давления достаточно для переключения позиций гидроуправляемого золотника 11. В результате функция поддержания давления в рабочей полости гидроцилиндра 8 ТДСУ передается напорному клапану 10, настроенному на более высокое давление, а напорный клапан 9 отключается. В результате повышения давления в гидроцилиндре 8 ТДСУ увеличивается сцепной вес тягача, который на заключительной стадии копания развивает повышенную силу тяги.

Проведенные исследования показывают, что применение ТСДУ [1] с усовершенствованной гидросистемой [3] позволяет увеличить геометрическую вместимость ковша прицепного скрепера к тягачу Т-150К до 5 м³ (самонабор грунта II категории).

Список литературы

1. Патент 2182948 RU, МПК⁷ E02F3/64. Скрепер с догружающим устройством / В.А. Нилов, А.А. Косенко (РФ); Воронеж. гос. техн. ун-т (РФ). 2000119280/03; Заявлено 19.07.2000; Оpubл. 27.05.2002, Бюл. №15.
2. А.С. 1239213 СССР, МКИ⁴ A1 E02F3/64. Прицепной скрепер с догружающим устройством /. В.А. Нилов, А.В. Гаврилов, В.П. Меньшиков (СССР); Воронеж. политехн. ин-т. 3711704/29; Заявлено 13.03.84; Оpubл. 23.06.86, Бюл. № 23.
3. Никулин П.И., Нилов В.А., Терехов А.А., Косенко А.А. // Сборник трудов международной научно-практической конференции «HEAVY MACHINERY NM 2002». - Кralьево, Сербия, Югославия: Изд-во Kraljevo University of Kraguevac, 2002.
4. Пат. 2243329 RU, МПК⁷ C1 E02F 9/22. Гидропривод рабочего оборудования прицепного скрепера / В.А. Нилов, П.И. Никулин, А.А. Косенко, и др. (РФ); Воронеж. гос. техн. ун-т. (РФ). 2003118027/03; Заявлено 16.06.2003; Оpubл. 27.12.2004, Бюл. № 36

DISPOSITION OF THE DIGGING RESISTANCE ON THE OPEN PIT EXCAVATOR TYPE SRS – 1300, AT THE KOSOVO'S COAL-MINE

Ljubinko D. Savić¹⁾, Miloje D. Rajović¹⁾, Vukmir O. Mijajlović¹⁾

Abstract

During the selection of the equipment for the Kosovo's open pit coal-mine there were no relevant facts about mine – geological conditions of the coal bearing. During exploitation we come to now that on the open pit is complex conditions, so the equipment wasn't adjusted for the existing conditions. For that reason there were researching of the digging resistance, which are the base for the answer about required power on the working wheel and for the construction of the excavator. Research were done in the measuring of the digging resistance at the open pit excavator type SRS – 1300 but the results helps for the selection of the rotor excavator on the Kosovo's coal – mine

1. INTRODUCTION

Construction of rotor excavator must to overpower total resistance of the material being excavated. Total resistance of material is decomposed to: tangential (P_t), lateral (P_b) and normal (P_n) components of resistance to excavation.

Tangential component to excavation of material acts in the plane of working wheel, is opposite to the direction of its rotation, has the course of tangent onto scotching path and is being overpowered by the power of engine on working wheel.

Lateral component of resistance to excavation acts in the plane of the rotational motion of the working wheel's boom, is opposite to the direction of its rotation, has the course of tangent onto path of the working wheel's rotation and is being overpowered by the power of engine for rotational motion of the excavator's upper part.

Normal component of resistance to excavation acts in the plane of working wheel, within scotching angle, has the course of normal onto path of the working wheel's rotation and is being overpowered by the power of engine for the excavator's transport.

At construction of the an excavator, only the tangential component of resistance to excavation is being calculated; lateral and normal component of resistance to excavation are assumed as percentages of either edge force applied to working wheel (P), or tangential component of resistance to excavation (excavation force).

Total resistance to excavation of material is manifested as a resistance at the working wheel's shaft. The power of engine on working wheel is defined by the following expression:

$$N = \frac{1}{\eta} (N_k + N_d), \quad [kW] \quad (1)$$

where:

N_k – the power of engine needed for the excavation of material [kW];

N_d – the power of engine needed for the elevation of material to the height of releasing [kW];

η – grade of productive effect of the working wheel's engine.

The power of engine needed for the excavation of material equals to:

$$N_k = N \cdot \eta - N_d, \quad [kW] \quad (2)$$

The power of engine needed for the elevation to the height of releasing can be determined from the following expression:

$$N_d = \frac{Q_t \cdot \gamma \cdot g \cdot h_d}{3600}, \quad [kW] \quad (3)$$

where:

Q_t – the theoretical capacity of excavator, [$m^3 \cdot r.m./h$];

γ – the filling mass of material, [$t/m^3 \cdot r.m$];

g – acceleration of the Earth's gravity, [m/s^2];

h_d – the height of the elevation of the material in bucket up to the height of releasing, [m].

The power of engine needed for the excavation of material can be determined from the following expression:

1) Prof. dr Ljubinko D. Savić FTN, 38220 Kosovska Mitrovica,
Prof. dr Miloje Rajović, dipl.mat., Faculty of Mechanical engineering, Dositejeva 19, 36000 Kraljevo
Vukmir O. Mijajlović EPS,

$$N_k = \frac{P_t \cdot V_k}{1000}, [kW] \quad (4)$$

i.e.:

$$P_t = \frac{1000 \cdot N_k}{V_k}, [N] \quad (5)$$

where

V_k – the edge velocity of working wheel, $[m/s]$.

The specific resistance to excavation of material (K_L or K_F) is defined by the following expression:

$$K_L = \frac{P_t}{L_{sr}}, [kW] \quad (6)$$

$$K_F = \frac{P_t}{F_{sr}}, [N/cm^2]$$

where:

L_{sr} – mean aggregate length of all the pails, which are in the same time engaged in the excavation process. It can be, with a sufficient accuracy, computed by the means of the following expression:

$$L_{sr} = \frac{m}{2\pi} [(2 \cdot S_0 + 0,7 r_V) \cdot (0,9549 \rho - 0,425)], [cm] \quad (7)$$

where

m – the number of pails on the working wheel;
 S – the thickness of slice, measured in the course of the longitudinal axis of excavator and at the height of working wheel's radius, $[cm]$;
 r_V – radius of the curvature of pail;
 ρ – scotching angle, $[rad]$.

The mean aggregate surface of the cross sections of all the pails being simultaneously in the excavating process can be determined by means of the following expression:

$$F_{sr} = \frac{S_0 \cdot b_0}{a} (1 - \cos \rho) = \frac{h \cdot S_0 \cdot b_0}{r \cdot a}, [N/cm^2] \quad (8)$$

where

b_0 – the width of slice, measured at the height of the working wheel's radius, $[cm]$;
 a – angle between pails, $[rad]$;
 h – the height of sub – section, i.e. slice, $[cm]$;
 r – the working wheel's radius, $[cm]$.

2. MEASURING THE RESISTANCE TO EXCAVATION BY ROTOR EXCAVATOR SR_S – 1300 · 24/5

Measurements of the resistance to excavation by rotor excavator SR_S – 1300 · 24/5 were done at the open pit “Belačevac”. The excavator had the following features:

- Theoretical capacity at 100% charge of pails and 50% of annular section 4370/5250(m^3/h)
- Diameter of working wheel 9(m)
- Number of pails 18
- Number of inter-cutters 18
- Volume of a pail 470(l)
- Volume of annular section 230(l)
- The number of the pails' releasings 104/125(min^{-1})
- Velocity of the working wheel's scotching 2,73/3,27(m/s)
- Installed power of the working wheel's engine 630(kW)

Measuring of the resistance to excavation by angular pails was done by the excavator SR_S – 1300 · 24/5, with electromotor of 630 (kW) on the working wheel and with six variants of teeth angles' adjustment. Some of the results are shown in the table 1.

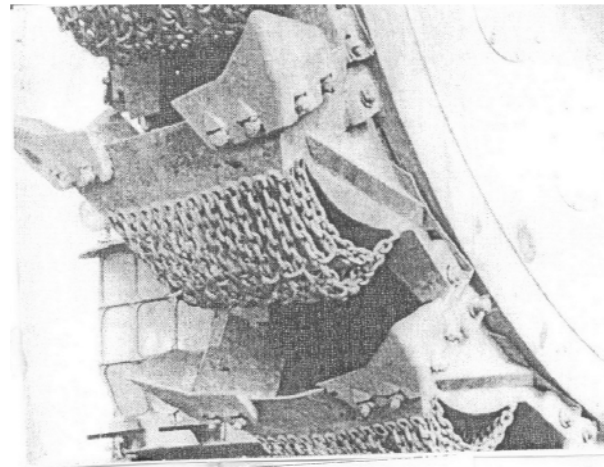


Fig. 1 Angular pails of the excavator

Meas. num.	h (m)	C (cm)	V _s (m·min)	Q (m ³ /h)	N (kW)	K (N/cm)	kWh/m ³
1	5,1	16	15,3	761	277	654	0,36
2	5,1	17	15,8	829	238	522	0,29
3	5,1	18	15,6	870	242	516	0,28
4	5,1	16	16,1	802	216	476	0,27
5	5,1	25	15,2	1142	248	441	0,22
6	5,1	23	15,8	1098	280	523	0,26
7	5,1	23	19,5	1354	315	521	0,23
8	5,1	32	19,4	1354	235	363	0,17
9	5,1	28	18,8	1616	380	577	0,23
10	5,1	30	19,6	1797	370	518	0,21
11	5,1	29	19,7	1748	392	566	0,22
12	5,1	30	20,2	1851	390	541	0,21
13	5,1	28	19,4	2259	502	637	0,22
14	5,1	36	19,9	2215	465	589	0,21
15	5,1	38	17,6	2048	428	563	0,21
16	5,1	36	20,3	2258	448	555	0,20
17	5,1	50	16,3	2477	557	677	0,22
18	5,1	45	20,2	2745	495	543	0,18
19	5,1	44	19,6	2611	468	525	0,18
20	5,1	45	19,6	2304	414	495	0,18
21	5,1	49	19,5	2918	483	502	0,17
22	5,1	51	18,1	2806	463	500	0,17
23	5,1	49	19,6	2937	596	650	0,20
24	5,1	50	16,8	2571	435	484	0,17
25	5,1	54	19,7	3251	530	519	0,16
26	5,1	55	18,2	3079	533	546	0,17
27	5,1	54	19,6	3212	452	424	0,14
28	5,1	55	18,9	3149	478	465	0,15
29	5,1	29	39,6	3511	425	359	0,12
30	5,1	29	39,3	3491	496	448	0,14
31	5,1	28	38,4	3305	402	350	0,12
32	5,1	36	39,8	4312	680	572	0,16
33	5,1	24	38,7	4065	492	386	0,12
34	5,1	45	37,6	5201	658	492	0,13
35	5,1	49	29,2	4396	643	523	0,15

Rotor excavator SR_S – 1300 non disturb zone

participation [%]	5	9	20	26	26	8	2	4	100
number of measurement	9	15	24	45	45	14	4	7	173
				x	x				
				xx	xx				
				xx	xx				
				xx	xx				
				xx	xx				
			xx	xx	xx				
			xx	xx	xx				
			xx	xx	xx				
			xx	xx	xx				
			xx	xx	xx				
			xx	xx	xx				
			xx	xx	xx				
			xx	xx	xx				
			xx	xx	xx				
			xx	xx	xx				
		x	xx	xx	xx				
		xx	xx	xx	xx	xx			
	x	xx	xx	xx	xx	xx			
	xx	xx	xx	xx	xx	xx			
	xx	xx	xx	xx	xx	xx			
	xx	xx	xx	xx	xx	xx		x	
	xx	xx	xx	xx	xx	xx		xx	
	xx	xx	xx	xx	xx	xx	xx	xx	
	xx	xx	xx	xx	xx	xx	xx	xx	
interval	1	2	3	4	5	6	7	8	
class	30	40	50	60	70	80	90	100-120·10 N/cm	

3. DEDUCTION

Measuring of the digging resistance, on our best knowledge, there were two basic zones for different resistance in the gray clay, so: - normal blocks zone (non disturbe zone) and zone with cracks. On the base of the digging resistance measuring, there were arithmetically madden results for surmount of the separately measured biggest resistance, cutting power for the excavator type $SR_S - 1300 \cdot 24/5$ for the normal blocks zone and for the zone with cracks is $660 [N/cm]$.

Cutting speed for the same excavator is $3,27 [m/s]$.

In the Kosovo coal basin an excavator must have a declared specific scotching force higher than $1000 [N/cm]$.

4. REFERENCE

1. M.Makar, Teorija bagerovanja rotornim bagerima, Rudarski institut, Beograd, (1990).
2. Lj. Savić, I. Jakovljević, Zbirka rešenih zadataka iz Tehnologije površinske eksploatacije mineralnih sirovina, RMF, Kosovska Mitrovica, (1997).
3. JPPK "Kosovo" – Obilić, Studija istraživanja otpora kopanja na otkrivci i određivanju specifične sile bagera za kosovski ugljeni basen, IRI, Priština, (1995).
4. N. Spasić, Tehnologija površinske eksploatacije mineralnih sirovina, Zavod za udžbenike i nastavna sredstva SAP Kosovo, Priština, (1982).

П.И. Никулин, А.П. Никулин, В.Л. Тюнин

Колёсный движитель, скольжение, топливно-экономические показатели.

Таким образом, исследование топливно-экономических показателей колёсного движителя снабжённого крупногабаритными шинами

Исследование кинематики качения колеса с пневматической шиной по дуге окружности (рис. 1) позволили установить, что нескользжащие элементы шины в области контакта располагаются на параболической кривой, которая делит её на зоны буксования и юза [1].

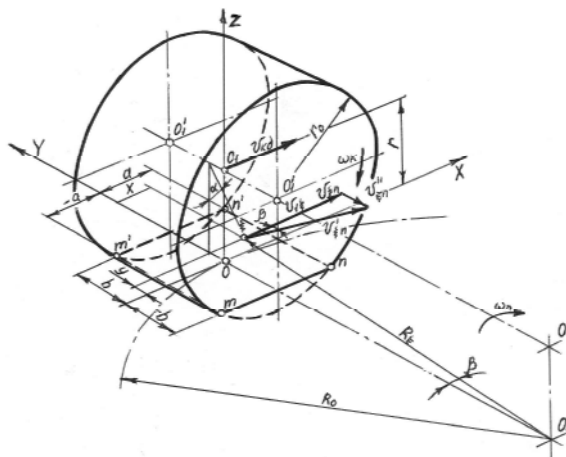


Рис. 1. Кинематика качения колеса с пневматической шиной по дуге окружности.

При работе колеса в ведущем режиме сила тяги T_μ будет представлять собой равнодействующую элементарных сил трения, возникающих вследствие проскальзывания элементов протектора пневматической шины относительно опорной поверхности, и элементарных нормальных сил, действующих в области контакта протектора шины с грунтом, в проекции на горизонтальную ось. При очень малых значениях T_μ , когда $\theta_0 \leq 1$, эпюра скоростей проскальзывания изменяет свой знак, что обусловлено кинематикой качения колеса по дуге окружности. При больших значениях силы тяги, когда $\theta_0 > 1$, скорость проскальзывания элементов протектора шины с координатами $-y, \pm x$ будет иметь только один знак – положительный. И наконец, когда $\theta_0 \gg 1$, все элементы протектора шины в области контакта проскальзывают только в одном направлении – с буксованием.

Решение задачи об определении сил трения в области контакта пневматической шины при качении колеса по деформирующейся опорной поверхности заключается в определении зависимости равнодействующей элементарных сил трения и нормальных элементарных сил, спроектированной на горизонтальную ось x , от коэффициента проскальзывания центральной опорной точки шины θ_0 и радиуса поворота колеса R_0 , т.е. $T_\mu = T_\mu(\theta_0, R_0)$.

Элементарная сила трения dF , возникающая в области контакта пневматической шины, вследствие проскальзывания относительно опорной поверхности,

в зоне буксования

$$dF = \mu_c \sigma dx dy,$$

в зоне юза

$$-dF = \mu_c \sigma dx dy,$$

где μ_c – коэффициент трения скольжения резины протектора, σ – нормальное контактное напряжение.

Нормальная элементарная сила, действующая на участке контакта протектора пневматической шины вследствие вертикальной нагрузки в зонах загрузки и разгрузки

$$dN = \sigma dy ds.$$

Элементарные силы трения dF в области контакта при θ_0 менее единицы (рис. 1) имеют различное направление, противоположное скорости проскальзывания.

Проекция суммарной равнодействующей элементарных сил трения и нормальных сил на участке области контакта шины будет

$$T_\mu = \int_{-a_3}^{a_1} \sigma \left(\mu_{cu} - \frac{2\theta x}{\sqrt{R_0^2 - x^2}} \right) dx,$$

где μ_{cu} – коэффициент трения скольжения, величина которого зависит от коэффициента проскальзывания центральной опорной точки θ_0 , области контакта шины с опорной поверхностью и радиуса поворота колёсного движителя R_0 / l .

Данное уравнение позволяет рассчитать проекцию суммарной равнодействующей элементарных сил трения и нормальных сил, определяющей силу тяги колёсного движителя для различных характеристик трения резины протектора и состояния опорной поверхности, характеризуемой модулем E_l .

Рассмотрим результаты теоретических характеристик проскальзывания колеса на деформирующейся поверхности. На рис. 2 приведены характеристики проскальзывания колеса с пневматической шиной размером 21,00-33 модели ВФ-166А диагональной и радиальной комбинированной конструкции на деформирующейся поверхности.

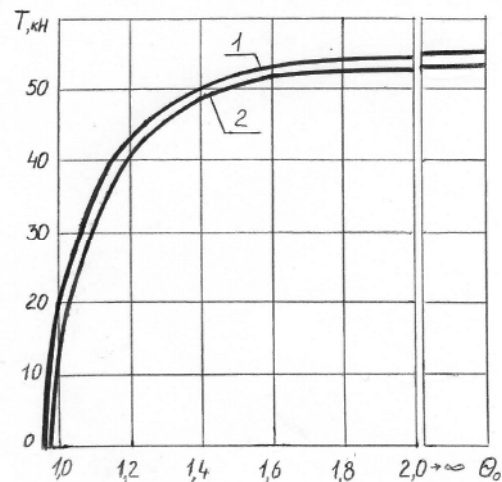


Рис. 2. Характеристики скольжения колеса с крупногабаритной шиной размером 21,00-33 радиальной комбинированной (1) и диагональной (2) конструкции на деформирующемся грунте ($P_w = 0,6$ МПа, $G_k = 68,67$ кН).

Анализ полученных характеристик показывает, что при постоянном значении коэффициента проскальзывания сила тяги колёсного движителя с диагональной шиной снижается.

Значение коэффициента буксования для построения тяговой характеристики получено с использованием кривых скольжения при различных радиусах поворота. Формула перехода от коэффициента проскальзывания к коэффициенту буксования имеет вид

$$\delta = (1 - \theta_{oc} / \theta_o) \cdot 100\%,$$

где θ_o – коэффициент проскальзывания центральной опорной точки; θ_{oc} – коэффициент проскальзывания центральной опорной точки при $T=0$.

Для определения топливно-экономических показателей необходимо рассмотреть совместную работу двигателя внутреннего сгорания и колёсного движителя. Рассмотрим случай с механической трансмиссией. С этой целью строим тяговую характеристику колёсного движителя (рис. 3).

Коэффициент буксования рассчитывается по уже приведённой формуле.

Рассчитываем силу сопротивления качению колёсного движителя P_f по формуле

$$P_f = G_k \cdot f_k, \text{ кН},$$

где G_k – вертикальная нагрузка на колесо, кН; f_k – коэффициент сопротивления качению колёсного движителя.

Откладываем значение P_f влево от точки O .

Строим график $M_e = M_e(P_k)$, применяя формулу

$$M_e = \frac{(T + P_f) r_c}{i_m \eta_m}, \text{ кН} \cdot \text{м},$$

где r_c – силовой радиус колеса, м; i_m – передаточное число механической трансмиссии; η_m – КПД механической трансмиссии. Для каждого радиуса данная зависимость выражается прямой, проходящей через точку O_1 .

Строим основную зависимость $v_d = v_d(T)$.

$$v_{di} = 0,377 \frac{n_{ei} r_c}{i_m} \left(1 - \frac{\delta_i}{100}\right), \text{ км/ч},$$

где n_{ei} – частота вращения коленчатого вала двигателя, об/мин; r_c – силовой радиус колеса, м; i_m – передаточное число трансмиссии.

Строим основную зависимость $G_T = G_T(T)$ графическим способом, перенося эти значения с регуляторной характеристики на тяговую характеристику, с учетом величины P_k и масштаба построения.

Построение производных зависимостей $N_T = N_T(T)$, $g_T = g_T(T)$ и $\eta_T = \eta_T(T)$ производится следующим образом. Кривая тяговой мощности строится на основании расчётов по формуле

$$N_T = T v_d, \text{ кВт},$$

где T – сила тяги колёсного движителя, кН; v_d – действительная скорость колёсного движителя, м/с.

Кривая удельного расхода топлива g_T строится с применением формулы

$$g_T = 10 \frac{G_T}{N_T}, \text{ г/кВт} \cdot \text{ч}.$$

Кривую тягового КПД строим, пользуясь зависимостью

$$\eta_T = \frac{N_T}{N_e}.$$

Располагая тяговой характеристикой, можно определить следующие характерные значения силы тяги: максимальную силу тяги T_ϕ , определяемую условиями сцепления шин пневмоколёсного движителя с поверхностью качения; силу тяги T_{NT} при максимальной тяговой мощности; силу тяги T_η , соответствующую максимальному значению тягового КПД; силу тяги $T_{g \min}$, при минимальном значении удельного тягового расхода топлива.

С учётом вышеизложенного была построена тяговая характеристика колёсного движителя с шиной 21.00-33 модели ВФ-166А диагональной и радиальной комбинированной конструкции (рис. 3).

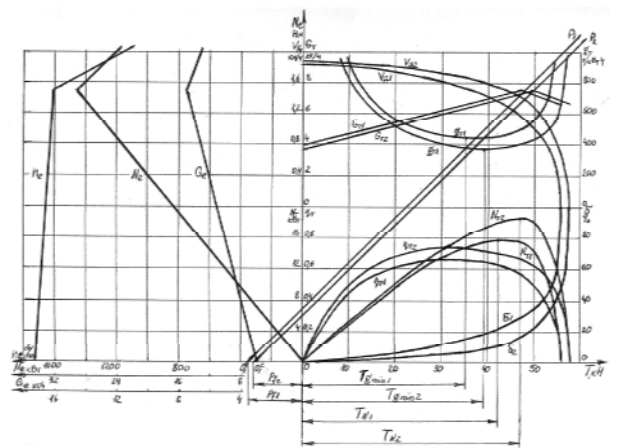


Рис. 3. Тяговая характеристика колёсного движителя: $P_{\phi 1}$, $P_{\phi 2}$, δ_1 , N_{T1} , η_{T1} , G_{T1} , g_{T1} , V_{T1} – диагональная; $P_{\phi 2}$, $P_{\phi 2}$, δ_2 , N_{T2} , η_{T2} , G_{T2} , g_{T2} , V_{T2} – радиальная комбинированная.

Проведя анализ полученных тяговых характеристик колёсного движителя с шинами различной конструкции можно сделать некоторые выводы по влиянию конструкции шин на их тяговые и топливно-экономические показатели: на плотном связном грунте при $R_0 = 1,25\text{ м}$ и $R_0 = 6,25\text{ м}$, и $P_{\omega} = 0,6\text{ МПа}$ минимальное значение удельного тягового расхода топлива $g_{T \min}$ у комбинированной шины ниже чем у диагональной на 14 и 11% соответственно, а максимальная тяговая мощность колёсного движителя с радиальным комбинированной шиной модели ВФ-166А выше, чем движителя с диагональной шиной, на 15 и 7% (рис. 4), его КПД – на 11 и 4,5%.

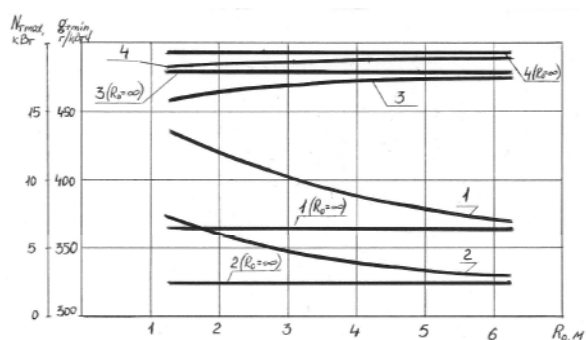


Рис.4. Зависимость минимального значения удельного расхода топлива $g_{T \min}$ и максимальной тяговой мощности $N_{T \max}$ на плотном связном грунте колёсного движителя с шиной 21.00-33: 1,2 – минимальное значение удельного тягового расхода топлива $g_{T \min}$ соответственно для диагональной и радиальной комбинированной; 3,4 – максимальное значение тяговой мощности $N_{T \max}$ соответственно для диагональной и радиальной комбинированной.

Список литературы

1. Никулин П.И. Теория криволинейного движения колёсного движителя / П.И. Никулин. – Воронеж: Изд-во ВГУ, 1992. – 212 с.
2. Ульянов Н.А. Самоходные колёсные землеройно-транспортные машины / Н.А. Ульянов, Э.Г. Ронинсон, В.Г. Соловьёв. – М.: Машиностроение, 1976. – 366 с.

SYNTHESIS OF SLEWING PLATFORMS DRIVES OF HYDRAULIC EXCAVATORS

Ph. D. Dragoslav Janosevic, professor, Faculty of Mechanical Engineering, Nis
Stevan Nedeljkovic, Graduate Mechanical Engineer

Summary: Numerous mobile machines (construction, transport, mining, agricultural, communal...) are characterized with possibility of space manipulation while performing various functions. In principle, the necessary space manipulation these machines attain by complex configuration of linkage where at least one kinematic couple in the chain is connected by the fifth-class joint to the vertical revolving axis. Frequently, that kinematic couple consists of first two links in linkage: thrust-motion mechanism and slewing platform of machine linked with axial bearing. Abutted on the base, the thrust-motion mechanism is relatively fixed link regarding the platform which can obtain the full rotation in both directions. This paper presents the process of synthesis of slewing platforms drive of hydraulic excavators. Given methodology of estimate can also apply on synthesis of swinging platforms drive of other mobile machines.

Key words: slewing platforms drive

1. INTRODUCTION

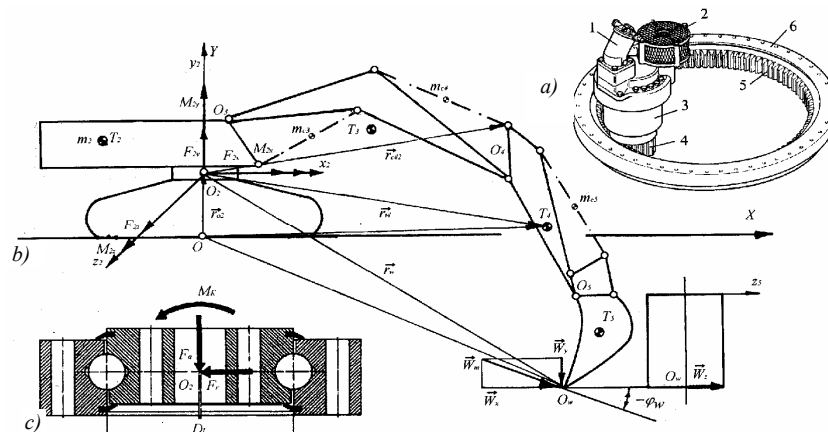
Generally, the concept of swinging platforms drive of hydraulic excavators of all sizes, in principal is consisted of: hydraulic motor (1) (fig 1,a), reducing gear (3) which on output shaft has a gear wheel (4) conjugated with ring gear (5) of axial bearing. All components of the drive are produced by specialized world manufacturers in standardization with numerous models of different parameters.

According to the given function parameters, during the synthesis of whole slewing platforms drive of excavator and other mobile machines it is necessary to carry out the following activities: a) to select axial bearing according to through analysis of bearing load in the whole working area of the machine /1/; b) to analyse the elements of screw joint and supporting structure to which the bearing is linked /2/ and c) to select hydraulic motor and drive reducing gear.

2. SELECTION OF AXIAL BEARING

Hydraulic excavators are characterised by universality of application, which can be accomplished by possibility of equipping the excavators with different manipulators (depth, loading) and numerous executive tools (spoons, grabs). It is necessary to perform the analysis of bearing load for all possible combinations of manipulators work and tools along with the estimation of application of each of these in the working life of the machine. Because of numerous tools and possible working conditions, the general mathematical model of excavator has been developed for the analysis of bearing load by the computer. The basic elements of excavator model are: by fictitious breakdown of excavator linkage in the joint (bearing) O_2 (fig. 1,b) of kinematic couple: motion mechanism-slewing platform, and by reduction of all loads in its centre, the following resulting bearing loads are obtained: force F_2 and moment M_2 :

$$\begin{aligned} \vec{M}_2 = & [\vec{r}_w - \vec{r}_2, \vec{W}_r] + g \cdot \sum_{i=2}^5 m_i \cdot [\vec{r}_{ti} - \vec{r}_2, -\vec{j}] + \\ & + g \cdot \sum_{i=3}^5 \frac{m_{ci}}{2} [\vec{r}_{ci1} - \vec{r}_2, -\vec{j}] + g \cdot \sum_{i=3}^5 \frac{m_{ci}}{2} [\vec{r}_{ci2} - \vec{r}_2, -\vec{j}] \end{aligned} \quad (1)$$



that is, the components of load moment M_2 :

$$\begin{aligned} M_{2x} &= (\vec{i}, \vec{M}_2) \\ M_{2y} &= (\vec{j}, \vec{M}_2) \\ M_{2z} &= (\vec{k}, \vec{M}_2) \end{aligned} \quad (2)$$

components of the force F_2 :

$$\begin{aligned} F_{2x} &= W_m \cdot \cos \varphi_w \\ F_{2y} &= W_m \cdot \sin \varphi_w + g \cdot \sum_{i=2}^5 m_i + g \cdot \sum_{i=3}^5 m_{ci} \\ F_{2z} &= W_z \end{aligned} \quad (3)$$

where: W_r - is the resulting excavation resistance, m_i - is mass of links of excavator linkage, m_{ci} - is mass of manipulator's actuator, $\vec{i}, \vec{j}, \vec{k}$ - is unit vectors of absolute coordinate system, W_m - is possible excavation resistance that enables the drive manipulator mechanism and allows the excavator stability, W_z - is the component of side excavation resistance.

Vector of resulting excavation resistance is equal to:

$$\vec{W}_r = W_w \cdot \cos \varphi_w \cdot \vec{i} + W_w \cdot \sin \varphi_w \cdot \vec{j} + W_z \cdot \vec{k} \quad (4)$$

where side excavation resistance W_z has the value:

$$W_z = \frac{M_o}{(\vec{i}, \vec{r}_w - \vec{r}_2)} \quad (5)$$

where: M_o - is the resistance swivelling moment of thrust-motion link on the base of support.

The components of bearing load are (Fig.1,c): axial force F_a , radial force F_r and moment M_k whose vector support lies in the horizontal plane of the bearing, where:

$$F_a = F_{2y} \quad (6)$$

$$F_r = (F_{2x}^2 + F_{2z}^2)^{1/2} \quad (7)$$

$$M_k = (M_{2x}^2 + M_{2y}^2)^{1/2} \quad (8)$$

The component of the moment M_{2z} whose vector support coincides with the bearing axis, has been balanced by the moment of mechanism of platform slewing.

The selection of the bearing is made according to admissible static and time carrying capacity, which are given by the manufacturers of the bearings as the diagrams of dependency of admissible equivalent static force (F_{es}) (fig. 2, curves: 1, 2, 3 and 4) and admissible equivalent static moment (M_{es}), that is, the time admissible force (F_{ed}) and time admissible moment (M_{ed}) of bearing load.

The equivalent axial forces and equivalent moment of bearing load can be determined according to the equation:

a) according to the criteria of testing the static carrying capacity:

$$\begin{aligned} F_{es}^{(r)} &= (a \cdot F_a + b \cdot F_r) \cdot f_s \\ M_{es}^{(r)} &= f_s \cdot M_k \end{aligned} \quad (9)$$

where: a - is the factor of influence of axial force, b - is the factor of influence of radial force, f_s - is the factor of bearing working conditions. The values of the factors a, b, f_s are given by the manufacturers for their bearings. b) according to the criteria of time bearing testing:

$$\begin{aligned} F_{ed}^{(r)} &= f_L \cdot \sqrt[k]{\frac{\sum_{i=1}^n p_i (F_i)^k}{100}} \\ M_{ed}^{(r)} &= f_L \cdot \sqrt[k]{\frac{\sum_{i=1}^n p_i (M_i)^k}{100}} \end{aligned} \quad (10)$$

where: $f_L = \sqrt[k]{N / 30000}$ - is load factor, k - is exponent dependent on the shape of rolling bodies of the bearing, ($k = 3$ - for balls, $k = 10/3$ - for cylinders), N - is desired number of revolutions (cycle) of bearing, F_i, M_i - is the axial force and the load moment of certain collectives of bearing loads, p_i - is proportional share of certain load collectives.

During the selection of bearing, the condition is that values of calculated equivalents of bearing loads do not exceed the limit curves (fig. 2) of admissible carrying capacity of bearing.

Due to the numerous different working conditions of excavator, the programme for analysis of bearing load has been developed. This programme offers possibility for determination of equivalent bearing loads (moment M_{es} , force F_{es}).

Figure 2 shows the results of bearing load of excavator, mass 25 000 kg, where clearly can be seen which of the bearings satisfies the carrying capacity.

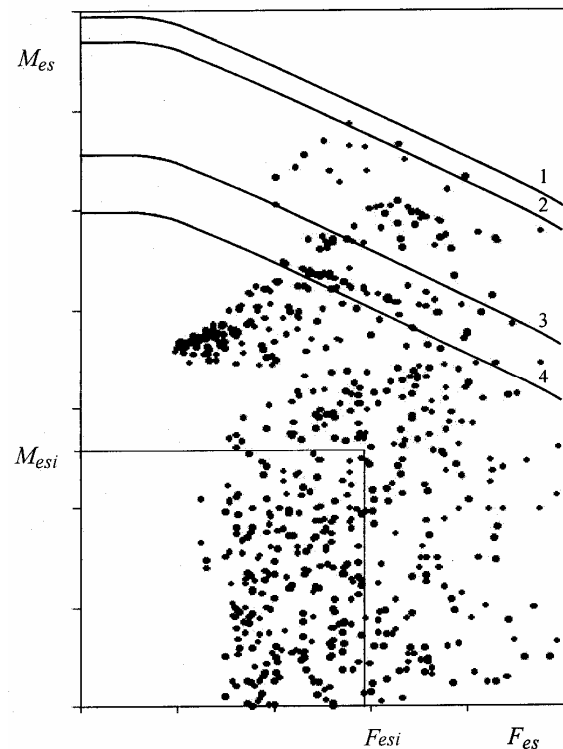


Fig. 2 Equivalent bearing loads in the whole working area of hydraulic excavator for desired number of positions

3. SYNTHESIS OF DRIVES OF PLATFORMS SLEWING

In addition of this paper is given the procedure of calculation and criteria of selection of hydraulic motors and drive reducing gear of mobile machines slewing platforms.

In principal, hydraulic motor (C_2) (fig. 3,a,b) of drive mechanism of mobile machines slewing platforms can, with hydraulic pump that supplies it, build open or closed circuit in hydrostatic system of the machine. In open circuit (fig. 3,a) hydraulic motor (C_2) is through transfer connected to one-way hydraulic pump (2). In closed circuit (fig. 3,b) hydraulic motor (C_2) of the drive is directly connected to two-way hydraulic pump (2).

In defining the drive, the following function parameters are given: maximal number of revolutions n_{max} and desired acceleration time t_u of the platform.

Where we know the number of teeth z_5 of ring gear of selected axial bearing, according to which the admissible minimal number of teeth z_4 of gear wheel on output shaft of the reducing gear is selected. First step is determination of maximal moment M_{max} which has to overcome the resistance of the platform in the phase of initial accelerated revolution:

$$M_{max} = k \cdot J_{max} \cdot \dot{\omega} \leq M_o \quad (11)$$

where: J_{max} - the maximal moment of inertia of the platform and links of manipulator's linkage for axis of rotation of machine's platform, kgm^2 ; $\dot{\omega}$ - is angle acceleration of platform slewing, s^{-2} ; k - is coefficient of moment increasing due to other resistances which occur during the turning (wind resistance, frictional resistances in axial bearing); M_o - is resistance moment of swivelling of thrust-motion link on the plane support.

Angle acceleration $\dot{\omega}$ of the platform presents the relation:

$$\dot{\omega} = \frac{\omega}{t_p} = \frac{n_{max} \cdot \pi}{30 t_p} \quad (12)$$

Maximal moment M_{rmax} on output shaft of slewing drive reducing gear:

$$M_{rmax} = \frac{M_{max}}{i} \quad (13)$$

where: i - is transmission ratio between bearing ring gear and gear wheel on output shaft of the reducing gear.

Transmission ratio i has the following value: for external conjugation (fig. 3,c):

$$i = \frac{z_5 + z_4}{z_4} \quad (14)$$

and internal conjugation of gear wheel (fig. 3,c):

$$i = \frac{z_5 - z_4}{z_4} \quad (15)$$

According to calculated moment M_{rmax} we select the size of drive reducing gear of platform slewing from the types of available sizes whose maximal admissible output moment M_{dmax} is equal or larger than the maximal moment needed::

$$M_{rmax} \leq M_{dmax} \quad (16)$$

However, with the selection of the size, the gearbox hasn't been determined yet, because the same size of gearbox can be derived with the different sizes of the hydraulic motor and with reducing gears of different transmission ratio.

3.1. Determination of the drive in the open hydrostatic circuit system

3.1.1. Determination of the drive according to the slewing moment - For the definition of the gearbox, the first step is the condition that the maximal moment needed for platform slewing can be reached at maximal working pressure p_{max} of the pump that supplies the drive hydraulic motor (fig. 3).

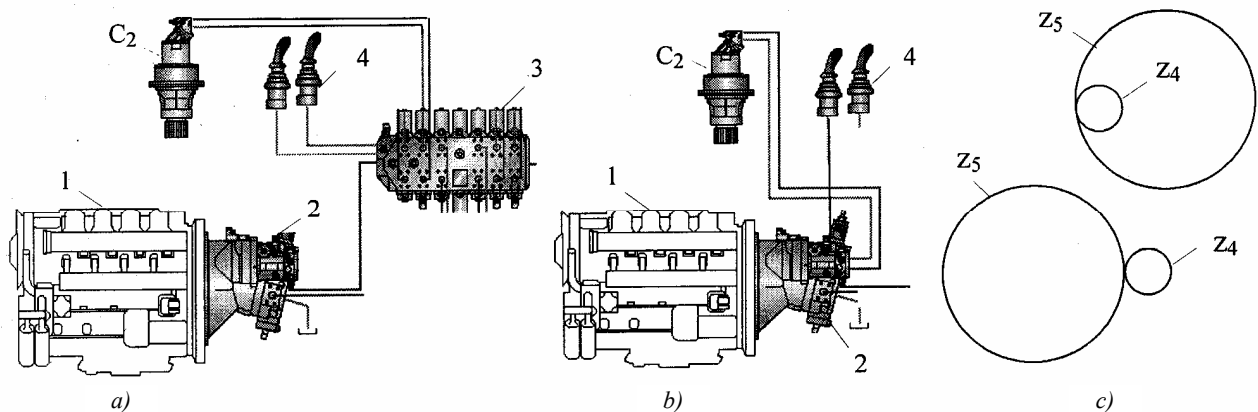


Fig. 3 Drives of slewing platforms: a) with open hydrostatic circuit, b) with closed hydrostatic circuit, c) with internal or external conjunction of gear wheel of reducing gear and ring gear of axial bearing

For the adopted size of the gearbox, the selection of hydraulic motor of certain constant specific flow q_m is made out of the set of recommended hydraulic motors. Usually due to unification, if possible, the same size of hydraulic motor, which has already been selected for other drives on the machine, is selected.

Maximal moment M_{mmax} on output shaft of selected hydraulic motor:

$$M_{mmax} = \frac{(p_{max} - p_o) \cdot q_m \cdot \eta_{mm}}{2\pi} \quad (17)$$

where: p_{max} - is maximal working pressure of the pump, MPa; q_m - is specific flow of the hydraulic motor, cm^3 ; η_{mm} - the mechanical efficiency of hydraulic motor; p_o - is pressure in the reverse pipe of hydraulic motor, MPa.

Needed transmission ratio i_r^M of reducing gear, by which M_{rmax} is obtained:

$$i_r^M = \frac{M_{rmax}}{M_{mmax}} \cdot \frac{1}{\eta_r} \quad (18)$$

where: η_r - is the efficiency of the reducing gear.

3.1.2. Determination of the drive according to the number of slewing of the platform - In determination of the gearbox, the first step is the condition that the given maximal number of platform slewing n_{max} is obtained at maximal flow Q_{max} of the pump, which supplies hydraulic motor of slewing drive.

Maximal number of revolutions n_{mmax} on output shaft of adopted hydraulic motor is:

$$n_{mmax} = \frac{1000 Q_{max}}{q_m} \cdot \eta_{mv} \leq n_{md} \quad (19)$$

where: Q_{max} - is the maximal pump flow, l/min ; q_m - is specific flow of the hydraulic motor, cm^3 ; η_{mv} - is volume efficiency of hydraulic motor; n_{md} - admissible maximal number of hydraulic motor revolutions.

The needed transmission ratio i_r^n of reducing gear by which n_{max} is reached, corresponds to the maximal number of hydraulic motor revolutions n_{mmax} :

$$i_r^n = \frac{n_{mmax}}{i \cdot n_{max}} \quad (20)$$

In the case that the values $i_r^M \approx i_r^n$, are for the adopted size of reducing gear, the closest value of available transmission ratio $i_r \approx i_r^n$ is selected.

If $i_r^M < i_r^n$ are for the adopted size of reducing gear, then the closest value of available transmission ratio $i_r \approx i_r^n$ is selected, where maximal pressure loss in hydraulic motor should have the value:

$$(p_{rmax} - p_o) = (p_{max} - p_o) \cdot \frac{i_r^M}{i_r} \quad (21)$$

where: p_{rmax} - is the maximal needed pressure in delivery hydraulic motor pipe.

In the case that $i_r^M > i_r^n$ is for adopted size of reducing gear, the closest value of available transmission ratio $i_r \approx i_r^M$ is selected, but adopts the hydraulic motor of acceptable specific flow that has maximal specific flow ($q_{mmax} = q_m$) same as already adopted hydraulic motor of constant specific flow q_m and minimal specific flow q_{mmin} , whose value is:

$$q_{mmin} = q_{mmax} \cdot \frac{i_r^n}{i_r} \quad (22)$$

3.2. Determination of the drive in the closed hydrostatic circuit system

In the case of drive of slewing platform in the closed hydraulic circuit system, the calculation procedure is similar as in the open circuit.

Namely, first step is determination of transmission ratio of reducing gear according to the needed moment of platform slew, and afterwards the needed number of hydraulic motor revolutions:

$$n_{mmax} = n_{max} \cdot i_r^M \cdot i \leq n_{md} \quad (23)$$

The needed maximal hydraulic pump delivery is determined according to the maximal number of hydraulic motor revolutions:

$$Q_{max} = \frac{q_m \cdot n_{mmax}}{1000 \eta_{mv}} \quad (24)$$

that is, specific hydraulic pump delivery:

$$q_p = \frac{1000 Q_{max}}{n_p \cdot \eta_{pv}} \quad (25)$$

where: n_p - is the number of pump revolutions, min^{-1} , η_{pv} - is the volume efficiency of pump.

The appropriate size of the pump is selected according to the calculated specific flow.

4. CONCLUSION

This paper describes the procedure of analysis and determination of needed sizes and parameters for selection and defining of components of the drive of revolution of slewing platforms of hydraulic excavators. The procedure has the general character and can be applied at synthesis of drives and other mobile machines, which in their linkage have slewing platform.

Literature

- /1/ Д. Јаношевић, В. Јевтић: Прилог анализи лежаја зглоба; обртна платформа-кретни механизам код хидрауличких багера, XIII меународна научно-стручни скуп Транспорт у индустрији, Београд, 1994.
- /2/ Д. Јаношевић, В. Јевтић: Анализа оптерећења елемената за везу аксијалног лежаја хидрауличких багера, Начно-стручни скуп ИРМЕС 2000, Котор, 2000.
- /3/ С. Недељковић: Хидрауличке компоненте и системи мобилних машина, семинарски рад, Машински факултет, Ниш, 2005.

ВЛИЯНИЕ РАДИУСА ПОВОРОТА НА ТОПЛИВНО-ЭКОНОМИЧЕСКИЕ ПОКАЗАТЕЛИ ДВУХОСНОГО ДВИЖИТЕЛЯ СНАБЖЁННОГО КРУПНОГАБАРИТНЫМИ ПНЕВМАТИЧЕСКИМИ ШИНАМИ.

П.И. Никулин, Д.А. Удодов, А.Н. Пришуттов

Представлены результаты теоретических исследований по влиянию радиуса поворота на топливно-экономические показатели двухосного движителя снабжённого крупногабаритными пневматическими шинами, позволившие разработать методику расчёта тяговых и топливно-экономических показателей колёсного движителя землеройно-транспортных машин при движении по дуге окружности.

Двухосный колёсный движитель, скольжение, топливно-экономические показатели.

Основным направлением повышения эффективности землеройно-транспортных машин (ЗТМ) следует считать создание самоходных колесных машин большой единичной мощности и производительности. С повышением единичной мощности ЗТМ значительно увеличивается расход топлива двигателем /1/.

Движение колесных ЗТМ при выполнении операции рабочего цикла (копания и транспортирования грунта, маневрирования) осуществляется за счет взаимодействия колесного движителя с опорной поверхностью, в результате которого вращательное движение колеса преобразуется в поступательное прямолинейное или криволинейное движение машины. В реальных условиях эксплуатации колесные ЗТМ движутся по различным видам опорных поверхностей: деформирующейся и недеформирующейся /1/.

Тяговая динамика колесных ЗТМ при прямолинейном движении исследована в достаточном объеме, а при криволинейном – недостаточно. На основании исследования кинематики качения многоколесного движителя необходимо решить задачу по определению тяговых и топливно-экономических показателей колесного движителя с учетом деформации как пневматических шин так и опорной поверхности при криволинейном движении /1/.

Для решения поставленной задачи рассмотрим работу двухосного колесного движителя (балансир) с заблокированным приводом при криволинейном движении по недеформирующейся опорной поверхности, обладающей более стабильными свойствами.

При решении задач о проскальзывании пневматической шины при качении колеса исходим

из того, что равнодействующая элементарных сил, возникающая в результате взаимодействия шины с недеформирующейся опорной поверхностью, создается силами трения, действующими в области контакта. Такое допущение учитывает влияние насыщенности рисунка протектора на рассматриваемый процесс. Очевидно, что оно обосновано для случая взаимодействия пневматической шины с недеформирующейся опорной поверхностью /2/.

Основываясь на исследованиях кинематики качения колеса с пневматической шиной по недеформирующейся опорной поверхности, рассмотрим трение элементов протектора, находящихся в пределах области контакта /2/.

При работе колеса в ведущем режиме сила тяги T_μ представляет собой равнодействующую элементарных сил трения, возникающих в следствии проскальзывания элементов протектора шины относительно опорной поверхности. Нескользящие элементы шины в области контакта располагаются на параболической кривой, которая делит её на зоны буксования и юза (рис. 1). Если при этом колесо будет развивать значительную силу тяги, то элементы протектора пневматической шины будут проскальзывать только в одном направлении, противоположном направлению движения колеса. Скорости проскальзывания элементов протектора пневматической шины будут положительными и, кроме того, будут возрастать по мере удаления от точки O_i к периферии области контакта, достигая максимального значения в крайних опорных точках n_i'' , m_i'' . Элементарные силы трения dT_μ будут также иметь только одно положительное направление. Итак, при работе балансира на ведущем режиме и значительной силе тяги $\theta_0 > 1$ /2/.

Решение задачи о проскальзывании центральной опорной точки θ_0 балансира заключается в установлении зависимости равнодействующих элементарных сил трения dT_μ , возникающих в области контакта пневматических шин двухосного движителя с недеформирующейся опорной поверхностью, и нормальных элементарных сил, спроектированной на горизонтальную ось x , от коэффициентов проскальзывания центральных опорных точек шин θ_{01} , θ_{02} и радиуса поворота движителя R_0 , то есть $T_\mu = T_\mu(\theta_0, R_0)$.

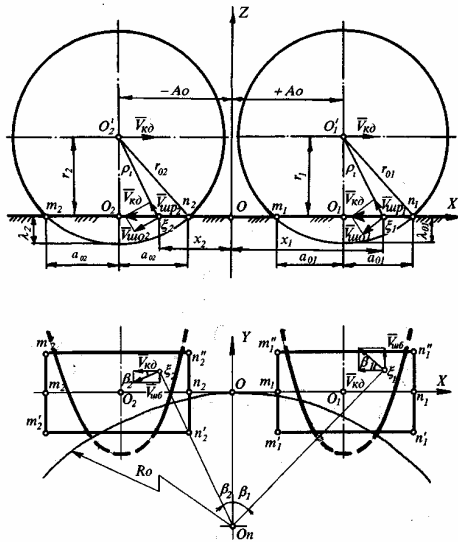


Рис. 1. Кинематика качения двухосного движителя по недеформирующейся опорной поверхности.

Элементарная сила трения dT_μ , возникающая на участке контакта протектора пневматической шины длиной dS и шириной dy в следствии его проскальзывания относительно его поверхности, будет:

в зоне буксования

$$dT_\mu = \mu_c \sigma dS dy,$$

в зоне юза

$$-dT_\mu = \mu_c \sigma dS dy,$$

где μ_c – коэффициент трения скольжения резины протектора, σ – нормальное контактное напряжение.

Нормальная элементарная сила, действующая на участке контакта протектора пневматической шины вследствие вертикальной нагрузки в зонах загрузки и разгрузки:

$$dN = \sigma dS dy.$$

Сила тяги, развиваемая колесным движителем, складывается из суммарных сил тяги каждого колеса

$$T_\mu = \sum_{i=1}^2 \int_{(-1)^i A_0 - a_{3i}}^{(-1)^i A_0 + a_{1i}} \int_{(-b, y_i)}^{(b, y_i)} \sigma_i \left(\mu_{ci} - \frac{dz_i}{dx} \right) dx dy$$

где μ_{ci} – коэффициент трения скольжения, величина которого зависит от коэффициента проскальзывания центральной опорной точки θ_0 , области контакта шины с опорной поверхностью и радиуса поворота колёсного движителя $R_0/2$.

Анализ теоретических зависимостей характеристик проскальзывания двухосного колесного движителя на недеформирующейся поверхности (рис. 2), полученных на основании расчётов, выполненных для балансира с шинами размером 20.5-25 модели Ф-92 при различных радиусах поворота R_0 показывает, что с уменьшением радиуса поворота, при постоянной относительной силе тяги, скольжение шин балансира увеличивается.

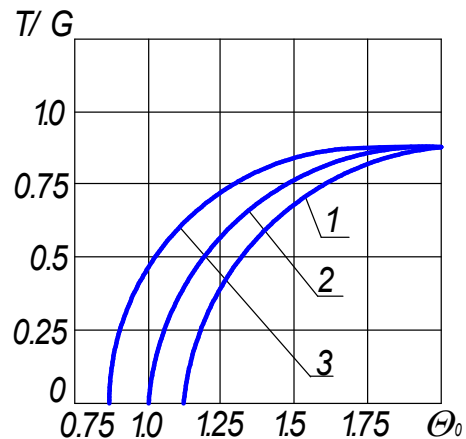


Рис. 2. Безразмерные кривые скольжения двухосного движителя с шинами размером 20.5-25 модели Ф-92 при качении по недеформирующейся поверхности при $P_{\omega 1} = P_{\omega 2} = 0,6$ МПа: 1- $R_0=2$ м, 2- $R_0=4$ м, 3- $R_0=6$ м.

Для определения топливно-экономических показателей балансира необходимо рассмотреть совместную работу двигателя внутреннего сгорания и колёсного движителя. Рассмотрим случай с механической трансмиссией. С этой целью в первом квадранте размещаем регуляторную характеристику дизельного двигателя, перестроенную в функции крутящего момента M_e , а во втором строим тяговую характеристику двухосного колесного движителя с шинами размером 20.5-25 модели Ф-92 при различных радиусах поворота (рис. 3).

Значение коэффициента буксования для построения тяговой характеристики получено с использованием кривых скольжения при различных радиусах поворота. Формула перехода от

коэффициента проскальзывания к коэффициенту буксования имеет вид

$$\delta = (1 - \theta_{oc} / \theta_o) \cdot 100\%,$$

где θ_o – коэффициент проскальзывания центральной опорной точки; θ_{oc} – коэффициент проскальзывания центральной опорной точки при $T=0$.

Рассчитываем силу сопротивления качению колёсного движителя P_f по формуле

$$P_f = G_k f_k, \text{ кН},$$

где G_k – вертикальная нагрузка на колеса балансира, кН; f_k – коэффициент сопротивления качению колёсного движителя.

Откладываем её значение влево от точки O .

Строим график $M_e = M_e(P_k)$, применяя формулу

$$M_e = \frac{(T + P_f) r_c}{i_m \eta_m}, \text{ кН}\cdot\text{м},$$

где r_c – силовой радиус колеса, м; i_m – передаточное число механической трансмиссии; η_m – КПД механической трансмиссии. Для каждого радиуса данная зависимость выражается прямой, проходящей через точку O_1 .

Строим основную зависимость $v_d = v_d(T)$.

$$v_{di} = 0,377 \frac{n_{ei} r_c}{i_m} \left(1 - \frac{\delta_i}{100}\right), \text{ км/ч},$$

где n_{ei} – частота вращения коленчатого вала двигателя, об/мин; r_c – силовой радиус колеса, м; i_m – передаточное число трансмиссии.

Строим основную зависимость $G_T = G_T(T)$ графическим способом, перенося эти значения с регуляторной характеристики на тяговую характеристику, с учетом величины P_k и масштаба построения.

Построение производных зависимостей $N_T = N_T(T)$, $g_T = g_T(T)$ и $\eta_T = \eta_T(T)$ производится следующим образом. Кривая тяговой мощности строится на основании расчетов по формуле

$$N_T = T v_d, \text{ кВт},$$

где T – сила тяги, кН, v_d – действительная скорость движения моста, м/с.

Кривая удельного расхода топлива g_T строится с применением формулы

$$g_T = 10 \frac{N_T}{N_T}, \text{ г/кВт}\cdot\text{ч}.$$

Кривую тягового КПД строим, пользуясь зависимостью

$$\eta_T = \frac{N_T}{N_e}.$$

Располагая тяговой характеристикой, можно определить показатели, характеризующие основные режимы работы двухосного движителя: максимальную силу тяги по сцеплению T_{φ} , определяемую условиями сцепления шин пневмоколёсного движителя с поверхностью качения, силу тяги при максимальной тяговой мощности T_{NT} , силу тяги соответствующую максимальному значению тягового КПД η_T , силу тяги при минимальном значении удельного тягового расхода топлива $T_{g \min}$ [3].

С учётом вышеизложенного была построена тяговая характеристика двухосного колёсного движителя с шинами размером 20.5-25 модели Ф-92 при различных радиусах поворота на недеформирующейся опорной поверхности.

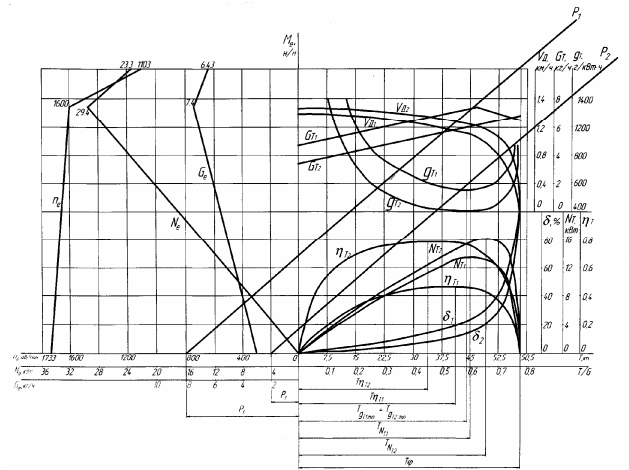


Рис.3. Тяговая характеристика двухосного колёсного движителя с шинами 20.5-25 модели Ф-92 на асфальтобетоне при $P_{\omega 1} = P_{\omega 2} = 0,6$ МПа, $G_k = 75$ кН и различных R_0 : $P_1, P_2, \delta_1, \delta_2, N_{T1}, N_{T2}, \eta_{T1}, \eta_{T2}, g_{T1}, g_{T2}, V_{T1}, V_{T2}$ – $R_0 = 2$ м; $P_1, P_2, \delta_1, \delta_2, N_{T1}, N_{T2}, \eta_{T1}, \eta_{T2}, g_{T1}, g_{T2}, V_{T1}, V_{T2}$ – $R_0 = 6$ м.

Проведя анализ полученной тяговой характеристики двухосного колёсного движителя построенной по вышеизложенной методике можно сделать выводы по влиянию радиуса поворота на тяговые и топливно-экономические показатели балансира. Уменьшение радиуса поворота в исследуемых пределах приводит к существенному возрастанию коэффициента проскальзывания центральной опорной точки θ_o , в результате чего при постоянной величине силы тяги снижается v_d , уменьшаются N_m и η_T .

С уменьшением радиуса поворота на асфальтобетоне с $R_o = 6$ м до $R_o = 2$ м при $P_{\omega 1} = P_{\omega 2} = 0,6$ МПа и $G_k = 75$ кН величины N_{Tmax} и η_{Tmax} двухосного колёсного движителя уменьшаются соответственно на 17% и 41%.

При этом минимальное значение удельного тягового расхода топлива g_{\min} увеличивается на 27%, а часовой расход топлива G_t достигает своего максимума при $R_0=2\text{м}$. (рис. 3).

Список литературы

1. Никулин П.И. Теория криволинейного движения колёсного движителя / П.И. Никулин. – Воронеж: Изд-во ВГУ, 1992. – 212 с.
2. Ульянов Н.А. Колесные движители строительных и дорожных машин / Н.А. Ульянов. – М.: Машиностроение, 1982. – 278 с.
3. Ульянов Н.А. Самоходные колёсные землеройно-транспортные машины / Н.А. Ульянов, Э.Г. Ронинсон, В.Г. Соловьёв. – М.: Машиностроение, 1976. – 366 с.

MACHINES FOR HANDLING CONTAINERS AND BULK MATERIALS, ARE WE READY FOR THE INTERNATIONAL COMPETITION?

Milosav Georgijević¹, Nenad Zrnić², Andreja Arsenijević³, Vlada Gašić⁴

Abstract

The paper gives a short survey and state-of-the-art on the equipment for handling containers in sea ports terminals, river ports terminals, and inland terminals. The paper also discusses the possibility of Serbian manufacturers (specially GOŠA) and researches to create the first ever built domestic construction of container crane. A short analysis of techno-economic parameters, also as decision support algorithm are presented.

Keywords: container crane, seaport, riverport, inland terminal, decision algorithm

1. INTRODUCTION

Development in seaports and river ports take place against the background of three different but related processes [12]: globalization, privatization, and modernization. Globalization in ports means the clear trend towards the global ownership and management of port terminals. Modernization includes introduction of new cargo handling technologies and automation of cargo handling and transport, also as development of information technologies in ports. Recently, the information technology (IT) has made remarkable progress, and the informations can be provided instantaneously. On the other hand, due to globalization of industrial production, speedy material handling is needed, and the material handling systems are now being subject of change [15]. Globalization of market after the Second World War has definitely transferred logistic, set up in ancient Greece, from the military into the civilian sector. According to this, necessities for large transportation of goods have reasserted the container as transportation unit, although it has occurred in middle of the 19-th century (1831 on railroad Liverpool-Manchester). In our country, before the 1990 there's been manufacturers so-called ISO container (Factory of coaches in Kraljevo and others), along with equipment for container transshipment. Unfortunately, policy of that time in Serbia had no plan for potential container manufacturers like Goša, MIN and LOLA to enable constructing the first machine for container manipulation, help overcoming initial difficulties which all would imply with good rating for world market competition. Question of perspective lays in a fact that range of container transportation increase with rate 10% a year, which means double enlargement for less other

10 years. Also, it is necessary to emphasize the importance of geographical and traffic position of our country, including land corridor X and Danube river corridor VII, which will result in a top-priority reconstruction, modernization and development of traffic infrastructure for all types of traffic transiting [2]. But, the current situation in transport system of Serbia is characterized, in addition to other factors, by low presence of contemporary transport systems. With internationalization and globalization shipping has obtained a central role in world trade. More than 90% of the world transport volume is being transported by ship [16]. In industrially developed countries like Japan, e.g. before the 1990 more than 90% of all goods were transported with containers. It is expected that exports and imports in Japan will be increased about 60% in 2010, and about 90% in 2015, compared with 1999 [15]. In Europe all the goods transportation on relations over 500 km are most efficient by containers, etc. War and chaos interrupted yet started era of containerization in this area. In order to enable usage of intermodalism, in cooperation with GOŠA, first author has prepared in 1992 design of truck container with hydraulic crane that would perform transportation of containers between terminal and loading/unloading location, Fig. 1. Cranes in Danube ports were bought in eastern countries, regardless the fact that Serbia produced better cranes. Hence, we still don't have adequate loading/unloading equipment for container manipulation. Likewise at rail container terminals, except Belgrade (capacity 40,000 TEU per year [2]), there are no places that disserves name of terminal. Actual political establishment expect fast incorporation in world tendencies, which is imperative that demands containerization in overall economy.

¹Prof. Dr.-Ing. Milosav Georgijević, Faculty of Technical Sciences Novi Sad, Trg Dositeja Obradovića 6, 21000 Novi Sad, Serbia, E-mail: georgije@uns.ns.ac.yu

² Ass. Dr.-Ing. Nenad Zrnić, Faculty of Mech. Engineering Belgrade, Kraljice Marije 16, 11000 Belgrade, Serbia, E-mail: nznric@mas.bg.ac.yu

³ Program Director Dipl.-Ing. Andreja Arsenijević, GOŠA FOM, Industrijska 70, 11420 Smederevska Palanka, Serbia, E-mail: gosafom@eunet.yu

⁴ Ass. Mag.-Ing. Vlada Gašić, Faculty of Mech. Engineering Belgrade, Kraljice Marije 16, 11000 Belgrade, Serbia, E-mail: vgasic@mas.bg.ac.yu

Concerning the fact that equipment for container manipulation on river ports and land terminals costs from 0,5 up to 3 million €, and for sea ports more than 5 million € (up to 10 mill. €), questions of initial management occur, along with necessary help for our industry capable to produce it. This research gained by Ministry of Science and Environmental Protection should make the first step to help domestic industry to build first container crane, made in Serbia and created in Serbia.

2. Problem definition and goals

If the problem for Serbia is to make container crane, research goals are to gain adequate technical solution of machine for loading/unloading containers that is most needed for our terminals and concurrent for commercial usage. Within this research there are used analysis and synthesis methods, i.e. analysis of demands for usage with simulation of terminal processes, which results with technical demands for construction of device and command unit, that complies with simulations as optimization method.

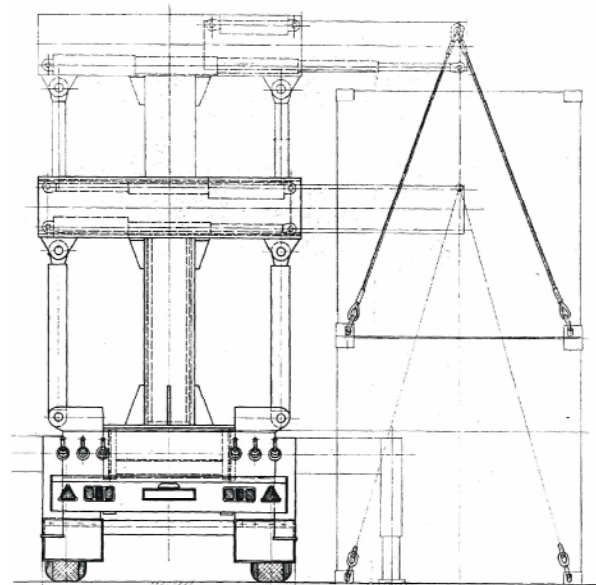


Figure1. Container manipulator

3. Present state within technical domain

3.1. Quayside cranes for sea ports

ECT generation

- cranes No.4,5,6 and 7, capacities of 45 t
- cranes No. 9 and 10, capacities 50 t
- crane for Delta terminal, capacity of 55 t

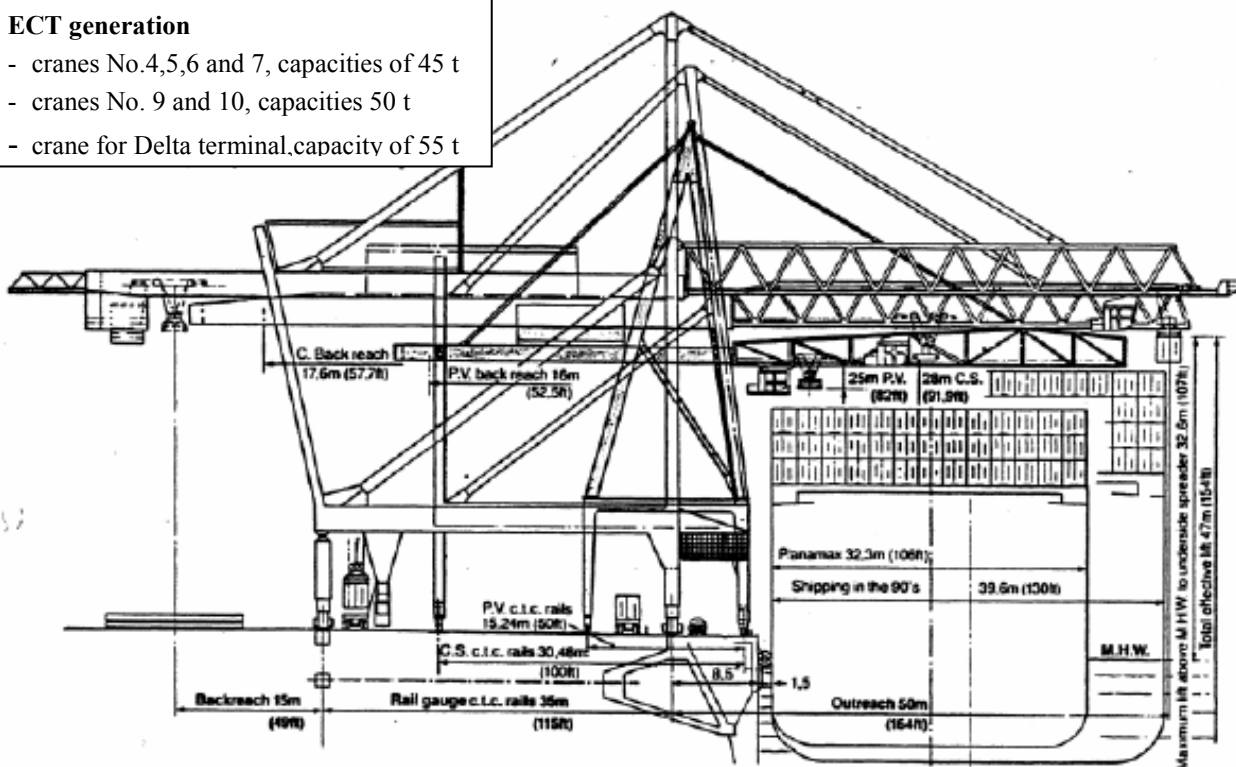


Figure 2. Development of ECT quayside cranes in Rotterdam port

Arrival of first ship from New York to Europe in 1966, with 226 containers of 35 ft, presents the beginning of intermodalism and globalization, despite the facts that present era of containerization began in 1956 in USA (The first voyage of a SeaLand container ship commenced on April 26, 1956 between Newark, New

Jersey, and Puerto Rico, [19]), and transporting lines between the US and Australia even before 1966. Quayside cranes for common cargo since then has transformed into new kind of machines with outreach up to 70 m or even more, capacities over 70 t, and weight close to 1600 t. Fig. 2 shows development of structures

of quayside cranes at Europe Container Terminal (ECT) in Rotterdam, which was the biggest port in world until 1990. In last ten years sizes of ships for container transportation has enlargement from 5,000 TEU to 10,000 TEU, which demands redesign of present structures and driving systems, and mostly the control. For instance in mid 2003 the largest container ship afloat was a little more than 8,000 TEU and some argue that is inevitable that 12,000 TEU ships will come [17]. Mega (Jumbo or Large) container ships, lead up into exploitation, present the ships of the future with the capacity more than 7,000 TEU, and with expectations of capacity of 15,000 TEU (even 18,000 TEU for Malacca-Max ships). Present criterion for Mega container cranes is to service ships that capacity is 9,000 TEU (500,000 TEU per year - transshipment during 24h, [11]) and at least 20 containers across deck. An outline of a mega container crane in operation is presented in Fig. 3 [13].

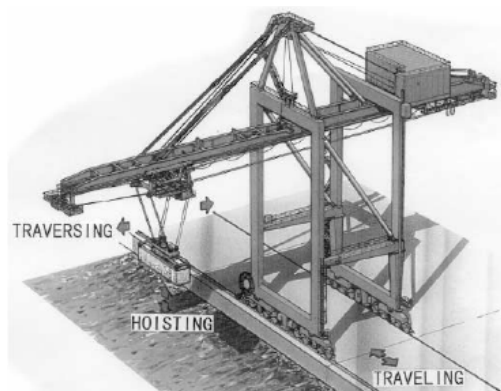


Figure 3. An outline of mega crane in operation

Technical parameters of existing machines and expectations in the future are, Fig. 4 [18, 14]:

- Lifting capacity (current 67-73, expected 80 t);
- Outreach (current 60-65 m, expected 65-70 m);
- Backreach (current and expected 15,24 m);
- Gage (current and expected 30,48 m);
- Maximum lifting height (current and expected more than 60 m);
- Trolley velocity (current 250 m/min, expected 300 m/min);
- Hoisting velocity (current and expected 100 m/min).

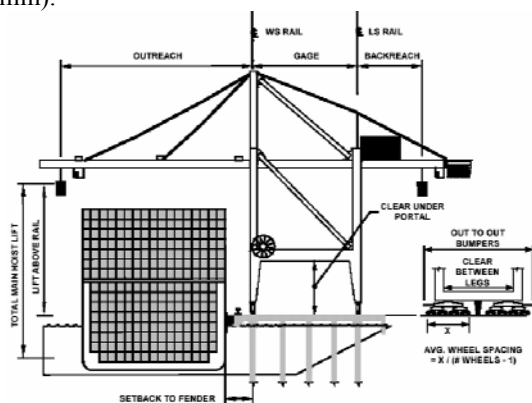


Figure 4. Principal dimensions of quay container cranes

3.2 Quayside cranes of river ports

River ports demands still starts from general cargos up to container terminals and don't give right determinants. User demands are main factor that leads to spectra of possible technical solutions. At these structures driving systems are, by default, mounted on trolley. Fig. 5 shows technically most light structure, 3D frame, with rotating trolleys. Crane serves both the cost and terminal.



Figure 5. Lightweight structure of quay crane for river port terminals

Fig. 6 shows concept of double girder quayside crane with box girders that serve cost and terminal, and solutions for trolleys varies from expected level of usage. Rotary part can be simpler with curved rail or hanging structure at small radi-axial bearing up to structures (c) with big radi-axial bearing at lifting driving system common for cranes with big efficiency, i.e. intensive usage.

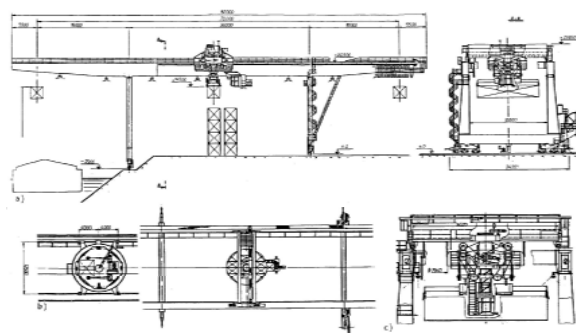


Figure 6. Quayside crane for river ports

Gage is up to 40m, and length of main girder goes over 80m. This basic concept is very interesting for Danube ports. Technical parameters of these machines are:

- Lifting velocity, to 1 m/s
- Trolley velocity, over 2 m/s
- Crane velocity, over 2 m/s
- Price can be up to 4 million EUR.

3.3 Yard equipment

Container terminal of seaports requires cranes that serve storage part of terminal. For this purpose there has been developed rail mounted cranes, which were Europe favorites, and rubber-wheel mounted cranes from Pacific region. Rail mounted cranes serve own field, are not mobile, and often needed 10 or more of them. Often they have overhanging (cantilever) covering bigger area and they are easy for automation. Automatic terminals with Rail Mounted Cranes in storages are present for 20 years. This concept of cranes is suitable also for inland terminals, like railway terminals, but without automation. They have systems for container sway damping and rough positioning. Fig. 7 shows gantry crane in inland container terminal with box girders and rotary trolleys.



Figure 7. Container crane in inland terminal

Fig. 8 shows developed crane for seaports terminal, fully automated and single girder without overhanging. Double girder structures with overhanging also exist.



Figure 8. Fully automated gantry crane for storage

Technical parameters of these machines are:

- Lifting velocity, to 0,5 m/s
- Trolley velocity, over 1 m/s
- Crane velocity, over 2 m/s

Regarding that price for these cranes is from 2 up to 3 million EUR, big initial investment encouraged development of mobile cranes for container terminal on rubber wheels, where enlargement through time of cargo flow can always lead to investment in new cranes. Power engine is internal combustion motor, with electric generator, so the driving systems are similar to above mentioned. They are supported on 4 pneumatic

wheels (rarely 8), and half of them can have hydraulic drive. Also, they can rotate for $\pm 90^\circ$, so can be manipulate easy in terminal area. These cranes are mostly without overhanging, have smaller spans and fully automated for 20 years. Control is done by induction cable in terminal floor. Fig. 9 presents this type of cranes.

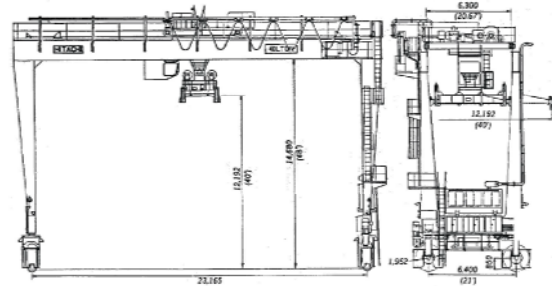


Figure 9. Rubber-Tired Gantry container crane

Technical parameters of these machines are:

- lifting velocity, over 0,5 m/s
- trolley velocity, over 1 m/s
- crane movement, over 2 m/s
- girder span up to 25 m

For serving the zone between the quayside crane and storage cranes, there are used special terminal vehicles for this purpose. Fig. 10 shows fully automated vehicle (AGV) that is already standard.



Figure 10. Terminal AGV

For serving the area between quayside cranes and storage, and especially in/out zone for road traffic, there are suitable straddle carrier, presented on Fig. 11. These machines can serve storage also, with expected stacking bigger than 1+2 containers. Hence, they are slower and not suitable for connecting cost and storage. They are powered by SUS motor, with hydraulic lifting and hydrostatic wheel driving. They are not suitable for automatization.

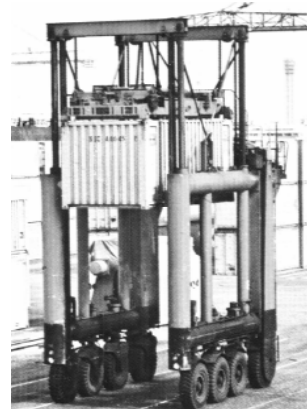


Figure 11. Straddle carrier

Since 1990, for storage serving there appeared machines following truck cranes (Fig. 12), without upper structure slewing, but with rotary container grab on boom top. They can put two full containers in two rows, and empty one in the third. They have problems with order in rows and demands wide hallway in terminal. Driving is hydraulic, and powered by internal combustion motor. Forklift machines with capacities round 40 t can not be considered as suitable machines for container terminals in spite their multi purpose.



Figure 12. Telescopic reach stacker

Technical parameters of these machines are:

- Lifting velocity, to 0,5 m/s
- Velocity, up to 25 km/h

4. Criteria for equipment selection

For sea ports quayside container cranes the basic idea is clear. Options are size of ships that will be served that directs technical solutions. Structures with box girder, 3D truss structures remain variable that depends from manufacturer technology and buyer demands. Control electronics for damping of cargo sway and monitoring is present in all of the options. Automated cargo positioning is possible option. Another trolley is desirable only for container high flow variant. Full working automation, because of complex demands, stays for future time; no matter Hitachi builds these kinds of cranes in Seattle 20 years ago. Quayside cranes for river ports can have full spectra of technical solutions that depend from: usage area, different cargos, expected capacities, storage usage, etc. In all the cases, system for sway damping is desirable and minimal monitoring that simplifies operator to work. Storage cranes depends mostly from the terminal layout and expected container flow. Rail mounted cranes has defined path. For whole storage it often needed more of them. They are easy for automation. Rubber-tired cranes are mobile on whole terminal-storage area, which is advantage but hard for automation. Selection of equipment has to start with analysis of usage demands with consideration of present state of following: terminal dimensions, container or general cargo operation, storage capacities for containers, how high they can be set (because of wind), connection with other form of transportation (road, railway), daily in/out loading and expecting ones in 5, 10 and eg. 15 years. According to present state and possible terminal concept and terminal container flow simulation of containers; it is determined

needed number of machines and their technical characteristics for multioptions, along with variation of velocities in sensible domains. Nominal options from techno-economic analysis lead to structural qualifications, working simulations, testing of control systems and basis for design. Fig. 13 presents decision algorithm with simulations as optimization method.

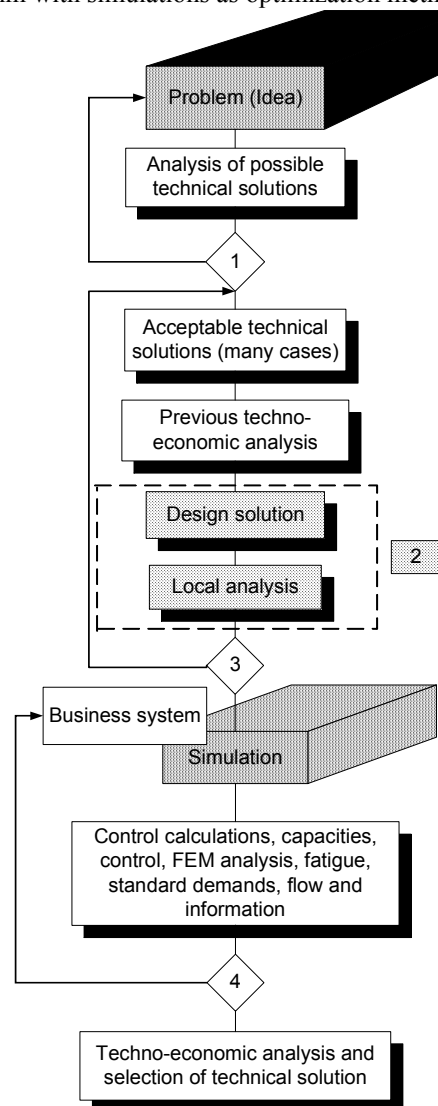


Figure 13. Decision algorithm for crane selection

5. Are we ready for making the concurrent machine?

Regarding our relative concurrent factors (not directly economy), it is for sure that we are less concurrent from 1990. Lack of information and society activities for 2 or 3 technological cycles (stands for 5 years for engineering), brought that we are losing the world match in many areas. Our manufacturer promising lies in offering the "Tailor-Made" concept, and not in the "Off the Shelf Approach". Both concepts are explained in details by [1]. It is clear that Serbian industry is unable to compete with well-known international manufacturers in producing serial constructions. Solely specific constructions give us the possibility to be equal

with them in the world market. Only brave tried to maintain and follow the world activities. Authors of this paper and research have many years of experience in this field [3,4,5,6,7,8,9,18,19]. Participant of this research (GOŠA-FOM) has maintained presence in this area thanks to business with unloading cranes for bulk materials for Siberian conditions. In Fig. 14 it is shown last crane with following performances.



Figure 14. RGP crane; $Q = 320 \text{ kN}$, $76,2+31,8+6 \text{ m}$; Manufacturer GOŠA

References

- [1] Bhimani, A. K., Jordan, M. A.: *Crane Purchase Specifications: Tailor-Made or Off-The-Shelf*, Presented at Conference "TOC '01", Lisbon, Portugal, June 20, 2001.
- [2] Drobac, M., Radović, M., Jovanov, D.: *Strategy of Development of Multimodal Transport and Infrastructure in "Belgrade" Port - Measures for Integration in the Transport System of Southeastern Europe*, 5th Summit Economic Forum, Skopje, Macedonia, November 13-15, 2002.
- [3] Georgijević M.: *Containers transshipment - Containers, Terminals, Container Cranes, Automation of operation*, book in Serbian prepared for publishing in 1992 by publisher "Naučna Knjiga" Belgrade, but still unpublished due to the publisher collapse.
- [4] Georgijević M.: *Anwendung von Rechenmodellen bei der dynamischen Analyse von Hebezeugen*, dhf - deutsche hebe und fordertechnik, Frankfurt, Nr.10, pp. 46-53, 1990.,.
- [5] Georgijević M.: *Einwirkung der konstruktiven Losung und Antriebsregulierung auf Dynamik von Hafenhebezeugen*, dhf-deutsche hebe und fordertechnik, Frankfurt, Nr. 6, pp. 64-69, 1991.
- [6] Georgijević M.: *Einfluss der Wippantrieb-Regulierung auf Lastpendel und Dynamik von Wippdrehe Krannen*, dhf - deutsche hebe und fordertechnik, Frankfurt, 1992, Nr. 3, pp. 74-81
- [7] Georgijević M., Milisavljević B.: *Pendeln des Containers bei der Katzenbewegung der Portalkrane*, dhf - deutsche hebe und fordertechnik, invited paper, Frankfurt, Nr.9, str. 41-47, 1994,
- [8] Georgijević M.: *Zur Regelung und Steuerung bei Kranen*, dhf- deutsche hebe und fordertechnik, Nr. 1/2-97, pp. 58-64, 1997.
- [9] Georgijević M.: *Matrix Method in Analysis of Stiff Systems and its Application to hostDrive Crane*, Pannonian Applied Mathematical Meetings, Balatonalmady, BAM 1086, pp. 193-200, 1995.
- [10] Goedhart, G. J.: *Criteria for (un)-loading Container ships*, Final Report, TU Delft, Netherlands, 2002.
- [11] Klaassens, J. B., Smid, G. E., Van Nauta Lemke, H. R., Honderd, G.: *Modeling and Control of Container Cranes*, IIR's Second Annual Developments in Container Handling Automation & Technologies, London, UK, February 28-29, 2000.
- [12] Marges, K.: *The Global Record and Outlook*, Lloyd's List Conference on Privatisation, Lisbon, Portugal, February, 22-23, 2000.
- [13] Masoud, Z.N., Nayfeh, A.H.: *Sway reduction on Container Cranes Using Delayed Feedback Controller*, Nonlinear Dynamics, 34, pp. 347-358, 2003.
- [14] Morris, C. A., Mc Carthy, P. W.: *The Impact of Jumbo Cranes on Wharves*, Proceedings of the Conference "PORTS '01", American Society of Civil Engineering, section 30, chapter 4, Norfolk, VA, USA, 2001.
- [15] Nishitake, S., Nakada, H., Karasuda, S., Osaki, Y.: *Cranes and Forklift Trucks - Material Handling systems Designed for Safe Transportation*, Mitsubishi Heavy Industries Technical Review, Vol. 40, No. 1, 2003.
- [16] Payer, H. G.: *Economic and Technical Aspects of Mega-Container Carriers*, IAME Annual Conference and General Meeting, International Association of Maritime Economists, Panama, November 13-15, 2002.
- [17] Robinson, B.: *Getting bigger and faster ship to shore cranes*, Cargo Systems, July, 2003
- [18] Zrnić, N.: *Influence of Trolley Motion to Dynamic behaviour of Ship-To-Shore Container Cranes*, Dr. Tech. Sc. dissertation in Serbian, Faculty of Mechanical Engineering Belgrade, 2005.
- [19] Zrnić, N., Hoffmann, K.: *Development of design of ship-to-shore container cranes:1959-2004*, In: History of Machines and Mechanisms, edited by Marco Ceccarelli, pp. 229-242, KLUWER ACADEMIC PUBLISHERS, Dordrecht, Netherlands, 2004.

This paper is a part of the research project TR 6344 "Research, development and construction of machines for handling and stocking of containers and bulk materials", and research project with specified topic TD 7005 "New methods for defining factors of optimal functioning of river shipping technological subsystems", both supported by Serbian Ministry of Science and Environmental Protection.

EVALUATION OF THE AVAILABLE RESOURCES OF THE SELF-SUPPORTING STRUCTURES OF HOISTING MACHINES DURING EXPLOITATION

Mircea Alămoreanu

Technical University of Civil Engineering Bucharest – Faculty of Technological Equipment, e-mail: alamor@utcb.ro

ABSTRACT

The subject of the study has been generated by the observation that nowadays in our country there is a large number of old hoisting cranes for which an objective answer is required in order to maintain them working.

The working period of such equipment is determined by its self-supporting structure, because other components can be replaced or repaired.

As a consequence this paper tries to give an answer to the following problem: being a structural element of hoisting crane in exploitation, for which the data concerning the history of the exploitation are not sufficient or are missing, to determine the available resource for a predictable period of exploitation. This will permit to evaluate a possible number of exploitation cycles during which the equipment can be used.

Key words: Hoisting machines, available resources, self-supporting structures.

1. SETTING THE PROBLEM

Hoisting machines are devices with high potential for accidents. Due to that, their design, construction and exploitation surveillance are done under specific normative prescriptions, by qualified persons and authorized institutions. In our country the authorized institution of the domain is The State Inspection for Recipients Boilers and Hoisting Equipment – ISCIR – Inspect. This institution verifies the new hoisting cranes and delivers the functional authorisations, makes periodical checking of the working devices extending or not the given authorisations

For a hoisting machines the exploitation period is determined by its self-supporting structure, because other components – such as action components, mechanical electrical or monitor ones can be repaired or replaced if they are no more safely. Evaluation of the available resources of the self-supporting structures of hoisting machines is quite difficult even in the case of a relatively good state (for example the absence of rust). They are dimensioned for a limited durability, expressed in stress cycles, for a particular stress spectrum, and at the checking moment the possible number of cycles as well as the spectrum can hardly be appreciated. That is due to the fact that the hoisting machines are not equipped with adequate monitor and register devices. Some times the working aspects expected by the designer, adequate to the device destination, should be changed (for example because

the technological process in which this one is involved is changed.)

The problem that should be solved is the following: *being a structural part of a hoisting machine under exploitation, for which the data about intensity and time period of exploitation are not enough or are unknown, the left disposability should be determined. In other words, the available loading cycle should be evaluated for a predictable way and manner of exploitation with a pre-set safety margins*

2. CLASIFICATION OF SELF-SUPPORTING STRUCTURES OF HOISTING MACHINES ACCORDING TO THE PARAMETERS OF EXPLOITING CONDITIONS

All modern design regulations in the hoisting machine field, among which the international ones ISO [1] the European Federation regulations [2] those in highly industrialised countries such as the German ones [3] and of course the Romanian ones [4] and [5] establish the working regulation according to two exploiting parameters *the impact load* and *the exploitation class*.

Exploitation class is characterised from the quality point of view by the exploitation frequency and from the quantity one by the amount of impact load cycles of the device working period. The subdivision of class exploitation according to regulations [3] and [4] is indicated in table 1.

Table 1. Subdivision of self-supporting structure of lifting machines in utility classes

Utility classes	Characteristics of exploitation frequency	Conventional domain of cycles stress
U ₁	Occasionally use, irregular, followed by long breaks.	$2 \cdot 10^4 \leq N \leq 2 \cdot 10^5$
U ₂	Regular use, but discontinuous	$2 \cdot 10^5 < N \leq 6 \cdot 10^5$
U ₃	Regular use, continuously	$6 \cdot 10^5 < N \leq 2 \cdot 10^6$
U ₄	Regular use under heavy exploitation	$N > 2 \cdot 10^6$

The **impact load** of a self-supporting structure is characterised by the level of stress and by the frequency of some stress repetition. The status of stress can be graphically represented, as in figure 1, taking as coordinate – in order to express a general variability – the non-dimensional variables. The abscissa is

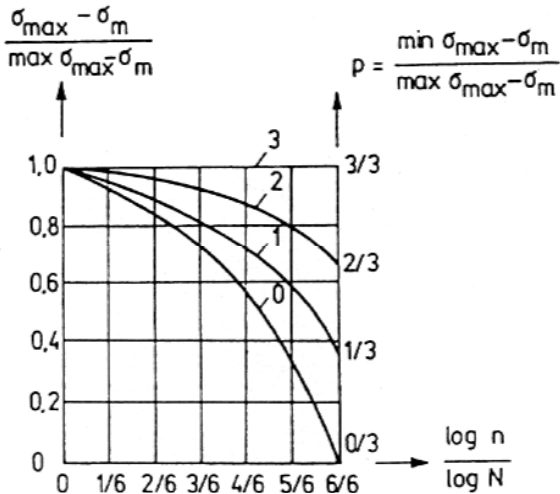


Fig. 1 The cumulate frequency curves of the typical stress status.

represented by the proportion $\log n / \log N$, in which N represents the number of cycles during the exploitation period, and n the number of cycles during which a certain level of stress is register. The ordinate is represented by

the proportion $\frac{\sigma_{\max} - \sigma_m}{\max \sigma_{\max} - \sigma_m}$ in which σ_m is the medium tension, level which is reached during each solicitation cycle, the amplitude of the most severe impact load cycle.

The points of each curve that characterizes one of the four typical impact load statuses can be used in order to establish the n number of cycles during which the amplitude of the impact load has at least the value $(\sigma_{\max} - \sigma_m)$. The typical impact load, as well as the characteristics of the relative levels of loading are represented in table 2 (according to STAS 8290-83 [4], identical with DIN 15018 [3]. Parameter p , associated to typical status, represents a part of the greatest impact loading amplitude, that being the amplitude reached during all the N solicitation cycles.

$$p = \frac{\min \sigma_{\max} - \sigma_m}{\max \sigma_{\max} - \sigma_m} \quad (1)$$

Table 2. Classification groups of cranes structures according with loading status

The impact loading status and the qualitative characteristics	p	$\log n / \log N$						
		0	1/6	2/6	3/6	4/6	5/6	6/6
		Values of: $(\sigma_{\max} - \sigma_m) / (\max \sigma_{\max} - \sigma_m)$						
S ₀ – very easy	0	1	0,927	0,836	0,723	0,576	0,372	0
S ₁ – easy	1/3	1	0,952	0,890	0,814	0,716	0,579	0,333
S ₂ – medium	2/3	1	0,975	0,944	0,906	0,856	0,787	0,666
S ₃ – heavy	3/3	1	1	1	1	1	1	1

The equations of the characteristic curves can be described by parameter p according to the following expression:

$$\frac{\sigma_{\max} - \sigma_m}{\max \sigma_{\max} - \sigma_m} = p + (1 - p) \sqrt{1 - \frac{\log n}{\log N}} \quad (2)$$

Combining the two parameters in a single condition of practice determines the **working groups** (according STAS 8290-83) or **classification groups** (new notion, introduced by SR ISO 4301). There are

six different groups. The interesting fact is that they are divided in utility groups (U), correlated with division in impact load (S) so that the couples (U_{i-1}, S_{j+1}) (U_i, S_j) and (U_{i+1}, S_{j-1}) means equivalent exploitation practice, globally characterised by the same classification group C_{ij} . This means that from the effect on a self-supporting structure point of view a higher exploitation class is the equivalent of a higher

stress and that harder exploitation conditions can be compensated by reducing the exploitation time.

3. TYPES OF PROBLEMS

During exploitation two main problems may occur, in connection with disposability reserve establishment.

Problems of Type 1 – the history of the working period is known and the length of the working period has to be determined, according to set way of exploitation. This can be the same with that previously known, or may be different, more or less stressing.

Problems of Type 2 – the history of exploitation is unknown and the requested task is the establishment of the left working period, in known practice conditions.

In both cases there is the risk that the left working period should be too short. In this case the machine is taken out of work, or the working process should be done under an inferior stress. A new working period is established according to these conditions. The descending with one or more steps of the impact load can be done in connection with descending the nominal load, the nominal moment and load – for jib cranes.

4. HYPOTESIS AND MAIN IDEAS

1. The determination of the left elements of self-supporting structure of the lifting machines (LM) should be done according to the existing regulations. Those are synthesised by cumulative frequencies curves of the four typical impact loading values (fig.1).

2. For a self-supporting structure of the LM, situated in a determined point on the axe which ends at the end of the whole working period of the crane, it should be assumed that when it passed through a significant number of loading cycles, the loading spectrum as well as the division of the frequency according to the loading levels is similar to the loading of the element. In other words the static division low concerning the different loading levels is the same. This means that the relative frequency curves cumulated in certain exploitation periods are identical to those in figure 1, the difference consisting in the fact that in the abscissa the number of the cycles relevant for proportion $\log n / \log N$ are smaller.

This represents the hypothesis, which had been the starting point for the proposed solution of the set problem. It should be noticed that this hypothesis is of statically origin. Is fulfilled if the number of loading cycles is bigger. That means that longer the hoisting machine exploitation has been, more adequate our theory is.

3. The objective evaluation of the resources at a given moment is due only to the use of experimental means. For this purpose some miniature test piece should be taken from the most stressed part of the

structure and tested on a dynamic testing machine, using testing units adequate to the way in which the machine was exploited. So the main problem is the adequate definition of that testing pieces. They are defined by level and loading cycles.

It should be mentioned that when there are not enough data concerning the history of exploitation this is the unique reasonable solution for achieving trustful results.

5. ESTABLISHING THE LEVEL OF THE TESTING UNITS

Supposing that the test piece is tested under puissant uniaxial loading, it is necessary to establish the σ_{\max} values of each unit, as well as the σ_m value – the same for all units. The starting point is the value of ordinates y of cumulative relative frequency curves which in the characteristics points of the abscissa has the values indicated in table 2. They are written $y_{ji}, j = 0 \dots 3$ being the index for marks the typical loading, and $i = 1 \dots 6$ being the index marking the characteristic point of the abscissa, the result being:

$$\frac{\sigma_{\max}^{ji} - \sigma_m}{\max \sigma_{\max} - \sigma_m} = y_{ji}.$$

The maximum values $\max \sigma_{\max}$ and σ_m can be determinate by calculation, if the necessary data are available for LM or if not by theoretical determination on the tested machine on the most loading part supposing the value of this structure. Supposing the values of this tension, the values σ_{\max}^{ji} of the units are the result of the following expression

$$\sigma_{\max}^{ji} = (\max \sigma_{\max} - \sigma_m) y_{ji} + \sigma_m \quad (3)$$

So the levels of the loading units can be represented graphically as in figure 2.

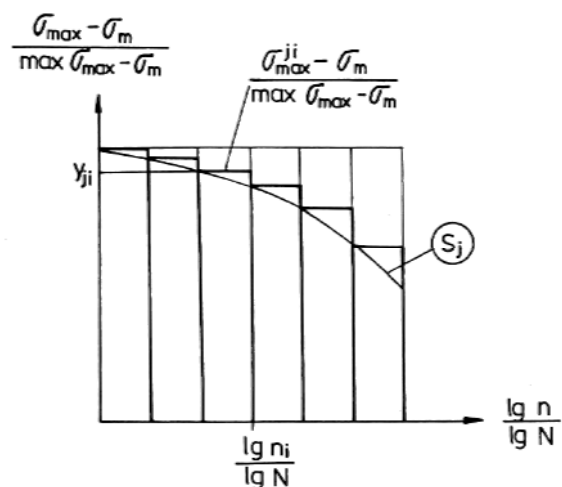


Fig 2 Graphic representation of maximum levels of testing units (expressed in relative amplitudes)

It was recorded that if units with determined levels (in the already mentioned way) are accepted, the obtained results will be protective. According to this situation the maximum exploitation of the testing units should be considered, the arithmetic geometrical, and potential mean of the values from the left and the right of intervals $(i-1)$, i .

If it is more easy to determine the values $\max \sigma_{\max}$ and $\min \sigma_{\max}$ instead of $\max \sigma_{\max}$ and σ_m , then σ_m can be determined according to the curved corresponding to point $r_6 = 6/6$: $\frac{\min \sigma_{\max} - \sigma_m}{\max \sigma_{\max} - \sigma_m} = p$. Later on the values can be calculated (3).

6. INDIVIDUALIZING THE CUMULATIVE RELATIVE FREQUENCY CURVES FOR CYCLE

NUMBERS OF TYPICAL UTILITY CLASSES.

The procedure is necessary for the establishing the number of cycles for the testing units.

Considering N_k , $k = 1 \dots 4$ the maximum value of the loading cycles of the typical units of use (tab.1) and i , $i = 1 \dots 6$ the values of the characteristics points of the abscissa figure 1 ($r_1 = 1/6$, $r_2 = 2/6 \dots$). For utility class k , the number of cycle corresponding to n_{ik} being the result of $\frac{\lg n_{ik}}{\lg N_k} = i$.

As a consequence

$$n_{ik} = N_k^{r_i} \quad (4)$$

n_{ik} values being calculated in this way, are related to the utility type in table 3.

Table 3. The values of numbers of cycle n_{ik} calculated in i points, corresponding of the utility classes.

i	0/6	1/6	2/6	3/6	4/6	5/6	6/6
Utility class	n_{ik}						
U_1	1	$0,7647 \cdot 10^1$	$0,5848 \cdot 10^2$	$0,4472 \cdot 10^3$	$0,342 \cdot 10^4$	$0,2615 \cdot 10^5$	$2 \cdot 10^5$
U_2	1	$0,9184 \cdot 10^1$	$0,8434 \cdot 10^2$	$0,7746 \cdot 10^3$	$0,7114 \cdot 10^4$	$0,65332 \cdot 10^5$	$6 \cdot 10^5$
U_3	1	$1,122 \cdot 10^1$	$1,260 \cdot 10^2$	$1,414 \cdot 10^3$	$1,587 \cdot 10^4$	$1,782 \cdot 10^5$	$2 \cdot 10^6$
U_4	1	$1,348 \cdot 10^1$	$1,817 \cdot 10^2$	$2,449 \cdot 10^3$	$3,302 \cdot 10^4$	$4,451 \cdot 10^5$	$6 \cdot 10^6$

7. THE PROBLEM SOLUTION: ESTABLISHING THE NUMBER OF CYCLES OF THE TESTING UNITS

7.1. Solving problem type 1

According to what was previously said in paragraph 3 the history of the machine exploitation is assumed as known and as sequence the total number of loading cycles of the self-structural part. Considering the loading N_e (e being the *already done* cycles) the loading j is known as well. The loading levels of the i testing units, are those assumed in paragraph 5.

The cumulative frequencies of the loading in which level σ_{\max}^{ji} were reached (from (3)) are calculated according to (4)

$$n_{ie} = N_e^{r_i} \quad (5)$$

The number of cycles σ_{\max} reached level σ_{\max}^{ji} but did not surpassed is according to figure 3

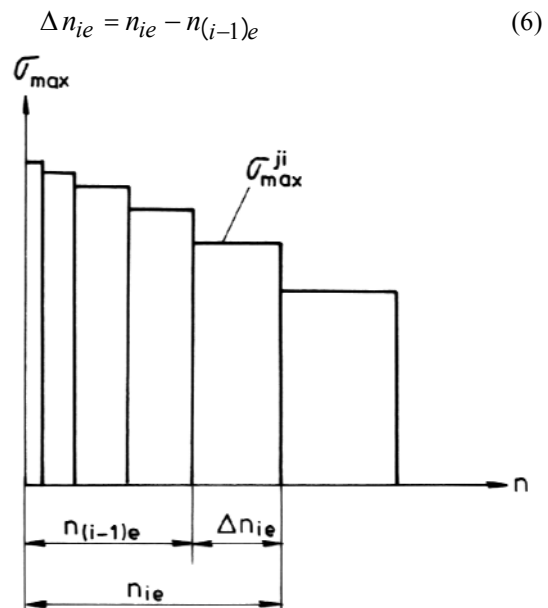


Fig. 3 Graphic representation of the number of cycles in which the maximum level of loading was reached.

If it is assumed that the exploitation will continue up to the fulfillment of the whole exploitation cycle according to the utility class k , N_k , which evidently should be greater than N_e class (this meaning that the resources are all used), then the n_{ik} with (4) are calculated before Δn_{ik} with (6):

$$\Delta n_{ik} = n_{ik} - n_{(i-1)k} \quad (7)$$

The number of cycles of testing steps i will be

$$n_i = \Delta n_{ik} - \Delta n_{ie} \quad (8)$$

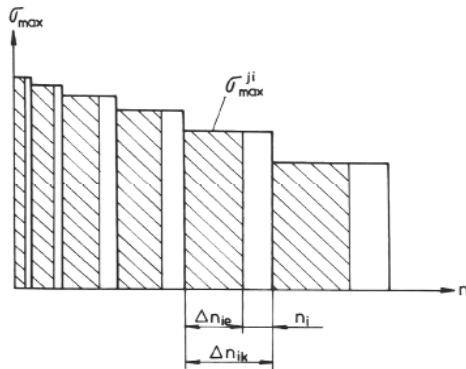


Fig. 4 Used cycles (notified zones) and remained loading cycles.

If at least one of the values (8) is negative, the conclusion is that the reassures of the machine have been all used, at least according to utility class k , the check being made according to a lower utility or loading grade (meaning a smaller nominal loading) or both.

The notification of the calculated values in a table as indicated below is recommended.

The graphic representation of the used cycles and remained ones, according each testing unit is indicated in figure 4.

Example of calculus. Knowing the total whole number of loading cycle of a hoisting crane $N_e = 1,2 \cdot 10^6$, the six number of cycles of the testing blocks can be established. According to this test the decision of maintaining the equipment in use until the complete number of cycles is reached, should be taken according to the utility class U_3 .

According to table 1, related to utility class U_3 , $N_k = 2 \cdot 10^6$ cycle. Using (5), (6), (7) and (8) the result is according to data written in table 4, where, in the last column are written the number of cycles related to the six testing units. Values n_{ik} are taken directly from table 3.

Table 4. Centralized table for testing units number of the loading cycles calculation

Unit index i	n_{ie}	Δn_{ie}	n_{ik}	Δn_{ik}	n_i
1	$1,031 \cdot 10^1$	$1,031 \cdot 10^1$	$1,122 \cdot 10^1$	$1,122 \cdot 10^1$	1
2	$1,063 \cdot 10^2$	$0,960 \cdot 10^2$	$1,260 \cdot 10^2$	$1,1478 \cdot 10^2$	19
3	$1,095 \cdot 10^3$	$0,989 \cdot 10^3$	$1,414 \cdot 10^3$	$1,288 \cdot 10^3$	299
4	$1,129 \cdot 10^4$	$1,0195 \cdot 10^4$	$1,587 \cdot 10^4$	$1,4456 \cdot 10^4$	4261
5	$1,164 \cdot 10^5$	$1,0511 \cdot 10^5$	$1,782 \cdot 10^5$	$1,6233 \cdot 10^5$	57220
6	$1,2 \cdot 10^6$	$1,0836 \cdot 10^6$	$2,0 \cdot 10^6$	$1,8218 \cdot 10^6$	738200

7.2. Solving problem type 2

The type of loading as well as its history is unknown. The maintenance in exploitation for a number N of cycle related to previously established loading, according to the given exploitation status, is desired.

For the beginning the utility class is established, as if the equipment is a new one, to this N_k a certain number of cycles is related. The problem is handled as if $N_e = N_k - N$ cycles have been already fulfilled and so the problem is one of type 1. If the problem supposed to be solved as shown before, has no solution, the two solutions already mentioned can be used: these are either the time limitation to an inferior number of cycle $N' < N$, or a lower number of nominal loading, or that of the loading and nominal moment for jib cranes.

8. SAFENESS APPRECIATION

Related to the well-known safeness margins concerning the elements under static stress or fatigue or cycles with a constant amplitude with set safeness coefficients defined according to established limited tensions, in the case of elements randomly loading and checked in case of limited durability. Safeness should be appreciated in relation to certain number of loading cycles, considered limited. It represents the number of cycles during which the sign of degradation appears.

If the mentioned number of cycles is marked with N_{lim} then the global safeness coefficient is

$$c_s = N_{lim} / N_k \quad (9)$$

where N_k is the number of all loading cycle during the whole exploitation period, according to the utility class of

the equipment. When N_k is set and the c_s being chose the test should be done for a number of c_s cycles $N_{lim} = c_s \cdot N_k$. They are split on loading units with an amplitude of σ_{max}^{ji} and according to methodology described in paragraph 7, and according to adapted formulae (5)...(8). It should be noticed that the intermediate coefficients

$$c_{si} = \Delta n_{i \lim} / \Delta n_{ik} \quad (10)$$

have different values compared to the global safeness coefficient.

9. COMMENTS AND CONCLUSIONS

The proposed methodology is on the first rank based on the static theoretical corpus which led to the integration of self-supporting structure elements of LM in typical loading and to the design of the cumulate frequency curves according to this non-dimensional stages, made of characteristic proportions of loading. They have general characteristics, each particular case can be identified according to a minimum of requested data. These are the number of the loading cycle, according to utility class of the given element) as well as an average tension (σ_m) and the maximum tension possible reached during exploitation ($\max \sigma_{max}$). It can be said that the cumulated frequency curves represents a synthesis containing a large number of pieces of information.

On the other hand the proposed methodology is based on the representation of the hypothesis described at point 2 of paragraph 4, according to which the loading spectrum during a part time exploitation is similar to that of a full time one.

Methodology indicates for remnant resources evaluation the taking out of structural test pieces and their testing on dynamic testing machines, the loading units are establish according to the previously mentioned

criteria. These methods guarantee the objectivity of the procedure.

Points r_i are taken as a criteria for the number of the sitting units and testing levels of each unit, can be different, if compared to those mentioned in the paper. Moreover their number can be different ($i \neq 6$) it is advisable to be greater, because 6 should be considered a minimum value. As a consequence the number of units should be increased. It is obviously that by this mean the results will be clearer, testing referring to different testing levels. It should be noticed that the increase of testing units does not lead to the increase of the whole amount of testing cycles. They are the same because

$$\sum_i n_i = \sum_i (\Delta n_{ik} - \Delta n_{ie}).$$

Indeed $\sum_i n_i = N_i$ and $\sum_i \Delta n_{ik} = N_k$,
respectively $\sum_i \Delta n_{ie} = N_e$. Is obtained

$\sum n_i = N_k - N_e$, which is not determined by the number of testing units. The only effect is N_i distribution in cycles to a larger number of units. As consequence a larger number of units means a larger number of tests, but less cycles on a certain level (units).

It should be noticed that hoisting equipment may have remnant resources even if its working period, previously predicted, seems to be finished. This is due to two main reasons. This is the consequence of the fact that the equipment is part of a *limited* number of utility classes and loading positions of each type (four for each). Indeed the design engineer taking into consideration the normal life-time of an equipment expressed in years and the effective exploitation conditions determines the total number of loading cycles and frames the element in the specific utility class, determined by the *superior* number of cycles. This can lead to a first limitation. The second one is due to the similar procedure of framing the element in the closest loading level, meaning *one superior* to the effective one.

REFERENCES

- | | |
|--|---|
| <p>[1] ISO 4301-1...5</p> <p>[2] FEM 1.001</p> <p>[3] DIN 15018: 1987</p> <p>[4] STAS 8290-83</p> <p>[5] SR ISO 4301-1...5</p> <p>[6] Alămoreanu, M.,
Coman, L.,
Nicolescu, Ş.</p> | <p><i>Cranes and lifting appliances, Classifications.</i> Part 1: General, Part 2: Mobile cranes, Part 3: Tower cranes, Part 4: Jib cranes, Part 5: Overhead traveling and portal bridge cranes.</p> <p><i>Règles pour le calcul des appareils de levage.</i> Cahier 2: Classement et sollicitations des charpentes et des mecanismes.</p> <p><i>Krane. Grundsätze für Stahltragwerke. Berechnung. Blatt 1.</i></p> <p><i>Instalații de ridicat. Principii de calcul și proiectare pentru construcția metalică.</i></p> <p><i>Idem ISO 4301-1...5, [1].</i></p> <p><i>Mașini de ridicat, Vol. I, Organele specifice, mecanismele și acționarea mașinilor de ridicat, Ed. Tehnică, București, 1996</i></p> |
|--|---|

THE APPROXIMATION OF THE EQUATION FOR BENDING STIFFNESS OF TRUSS CONSTRUCTION

Gašić M., Savković M., Marković G., Zdravković N.¹⁾

Abstract

The bending stiffness of the construction is one of the key factors for stress condition analysis, stability and dynamic behavior. The parameter that directly influences the stiffness of the construction is the cross-section moment of inertia, so its defining is necessary. The way of forming the truss filler is also a parameter that significantly influences the bending stiffness, so the research of its influence is also needed.

This paper shows the simplified model which approximately defines the moment of inertia of truss construction. The most usual ways of truss construction filler forming for different spans are analyzed. The truss construction deflection dependence on the way of filling and span of construction is defined.

Key words: truss construction, moment of inertia

1. INTRODUCTION

By varying the stiffness values you can influence the change of construction parameters, such as: increase of stability, decrease of stress and deformations, unfailing work of mechanism, i.e. machine, provision of wanted functionality.

The moment of inertia is a parameter that directly determines the stiffness. The overhead traveling crane and boom-crane truss constructions consist of a great number of truss rods: horizontal, slope and vertical, so it is complicated to evaluate the moment of inertia of truss construction cross-section because it varies depending on the truss construction cross section position. In the beginning phase of construction design, it is very important to obtain the information about geometrical characteristics of the truss construction elements in order to reduce the calculating procedure.

According to the researches [1], [2], [4], the moment of inertia is a sufficient parameter for truss construction stiffness analysis, i.e. the calculation of its deflection.

Except this parameter, it is very important to know the deflection dependence on the construction span and the way of forming the filler (i.e. the angle of the filler elements setting). This dependence enables determining the needed angle of the truss filler declension relating the tolerable deflection of the construction.

The problem was considered on particular examples of the portal revolving crane boom and the bridge crane, which does not diminish the generality for other types of space truss constructions. The simplified models for defining the dependence between the stiffness and the moment of inertia are shown in figure 1.

The construction greatest deflection values for the girders shown in figure 1 are evaluated as follows:

$$f_s = \frac{F_s \cdot L_s^3}{3 \cdot E \cdot I_s} ; f_m = \frac{F_m \cdot L_m^3}{48 \cdot E \cdot I_m} ; \quad (1)$$

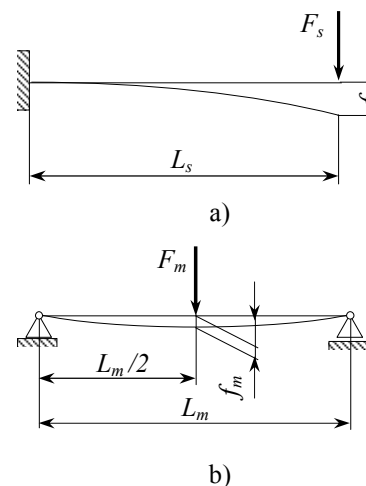


Figure 1

The forces by which the construction opposes the bending are calculated as follows:

$$F_s = c_s \cdot f_s ; F_m = c_m \cdot f_m ; \quad (2)$$

so that the corresponding stiffness are defined by following expressions:

$$c_s = \frac{3 \cdot E \cdot I_s}{L_s^3} = K_s \cdot I_s ; c_m = \frac{48 \cdot E \cdot I_m}{L_m^3} = K_m \cdot I_m ; \quad (3)$$

1) Ph. D Gašić Milomir, Faculty of Mechanical Engineering Kraljevo, Dositejeva 19, 36000 Kraljevo, gasic.m@maskv.edu.yu
Ph. D Savković Mile, Faculty of Mechanical Engineering Kraljevo, Dositejeva 19, 36000 Kraljevo, savkovic.m@maskv.edu.yu
Msc. Marković Goran, Faculty of Mechanical Engineering Kraljevo, Dositejeva 19, 36000 Kraljevo, markovic.n@maskv.edu.yu
Zdravković Nebojša, Faculty of Mechanical Engineering Kraljevo, Dositejeva 19, 36000 Kraljevo, zdravkovic.n@maskv.edu.yu

2. DEFINING THE SIMPLIFIED EXPRESSION FOR BENDING STIFFNESS EVALUATION

The aim of defining the simplified expression for bending stiffness evaluation is to achieve the truss construction moment of inertia (i.e. stiffness) value in a simple and quick way, so the designer, in as short term as possible, could determine the main parameters of the construction.

The complex space truss construction moment of inertia can be defined by the following expressions [1],[3],[4] (fig. 2):

$$I_x = \sum_{i=1}^4 (I_{\xi_i} + A_i \cdot y_i^2) \quad (4)$$

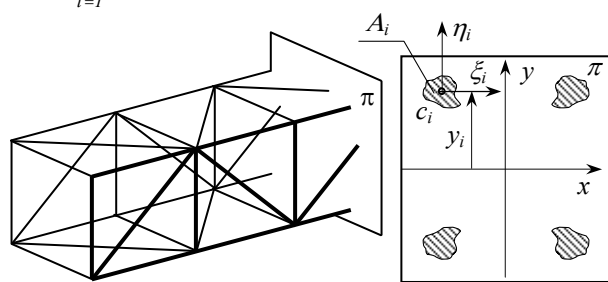


Figure 2

In the previous expression the influence of truss filler was neglected, so for evaluation a relatively simple expression is used. Error that is made by using of such expression for evaluating the moment of inertia (equation 4) can be significantly reduced by proper factors of correction ψ_s and ψ_m so that calculating values of the moment of inertia and bending stiffness are:

$$\begin{aligned} I_{rs} &= I_x \cdot \psi_s & I_{rm} &= I_x \cdot \psi_m \\ c_s &= K_s \cdot \psi_s \cdot I_x ; & c_m &= K_m \cdot \psi_m \cdot I_x ; \end{aligned} \quad (5)$$

3. DEFINING THE CORRECTION FACTOR VALUES

The correction factor value analysis ψ_s is thoroughly illustrated in [4] so that only some conclusions of analysis will be mentioned here. For analyzed values of stiffness $c_s \in (0,7 \div 5,4)$ correction factor value is : $\psi_s \in (1,03 \div 1,1)$ (Table1).

Table 1

stiffness c_s (kNcm)	calculated deflection f_r (cm)	deflection from MKE f_{MKE} (cm)	correction factor ψ_s
0.70	1.43	1.468	0.97
1.01	1.0	1.029	0.97
1.97	0.64	0.668	0.96
1.73	0.58	0.6	0.96
2.53	0.4	0.422	0.95

3.47	0.29	0.301	0.95
3.95	0.25	0.278	0.89
4.8	0.22	0.231	0.95
5.43	0.18	0.198	0.90

This analysis is shown in figure 3.

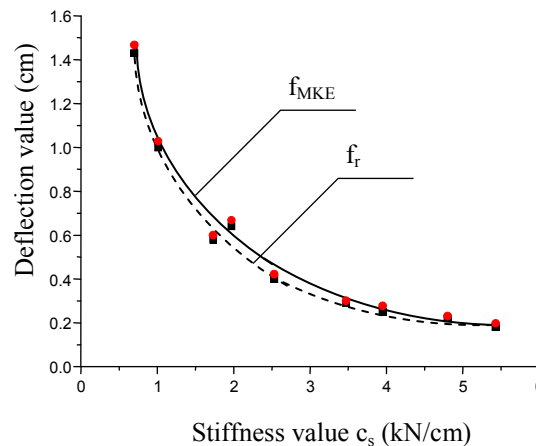


Figure 3

The practiced analysis [4] shows that the value ψ_s does not exceed 1,1 for analyzed boom spans $L \in (20 \div 35)$ m nor the stiffness value exceeds $c_s \in (0,3 \div 7)$.

For determining the correction factor value ψ_m the models from figure 4 are used.

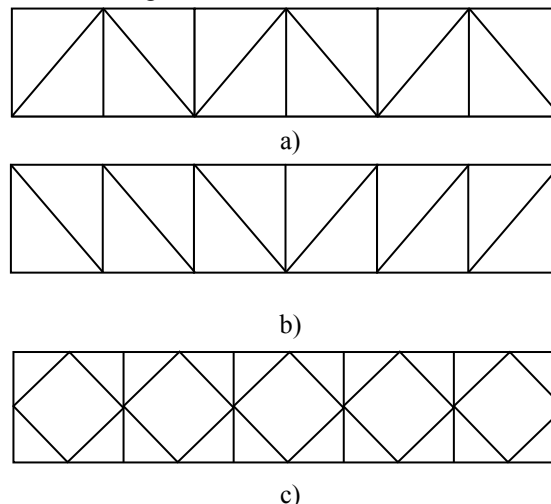


Figure 4

Table 2

L(m)	20	25	30	35
f_{MKE} (mm)	36	46.1	56	66.6
f_r (mm)	44.5	55.8	67.0	78.3
f_{kr} (mm)	37.1	46.5	55.9	65.2
ψ_m	1.2			
Error (%)	3	1	0	2

The results of the analysis for the truss type shown in figure 4a are given in the Table 2. The deflection f_{kr} is

obtained by correcting the moment of inertia value (4) i.e. by using the equation (5), where the correction factor is $\psi_m = 1,2$. The obtained results of deflection, by correcting the moment of inertia values, show a great accuracy for wide range of truss girder span.

Table 3

L(m)	20	25	30	35
f_{MKE} (mm)	42.5	54.5	66.3	78.8
f_r (mm)	44.5	55.8	67.0	78.3
f_{kr} (mm)	43.2	54.1	65.1	76.0
ψ_m	1.03			
Error (%)	2	1	2	4

The results of truss type analysis shown in figure 4b are given in table 3. The deflection f_{kr} is obtained by using the equation (5), where the correction factor $\psi_m = 1,3$. The deflection results obtained by correcting the moment of inertia values show a great accuracy so one can even tell that for this type the correction is not necessary.

Table 4

L(m)	20	25	30	35
f_{MKE} (mm)	33	42.5	51.9	62.2
f_r (mm)	44.5	55.8	67.0	78.3
f_{kr} (mm)	34.2	42.9	51.6	60.2
ψ_m	1.3			
Error (%)	4	1	1	3

The table 4 gives the results of truss type analysis shown in figure 4c. In this case, as well, the deflection f_{kr} is obtained by using the equation (5), where the correction factor is $\psi_m = 1,3$. The evaluated deflection results, by correcting the moment of inertia values, overlap in a great degree with the results of practiced finite element analysis.

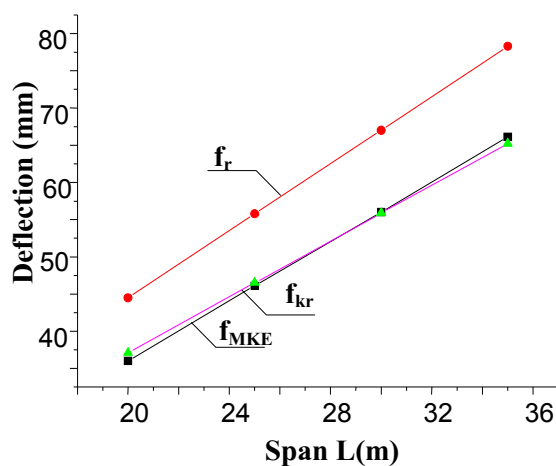


Figure 5

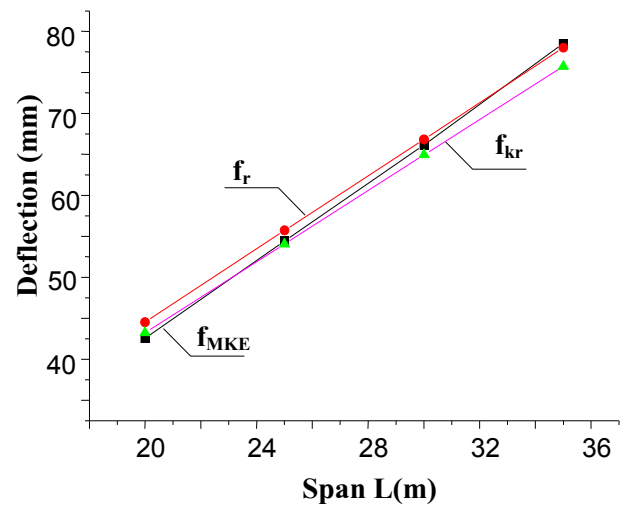


Figure 6

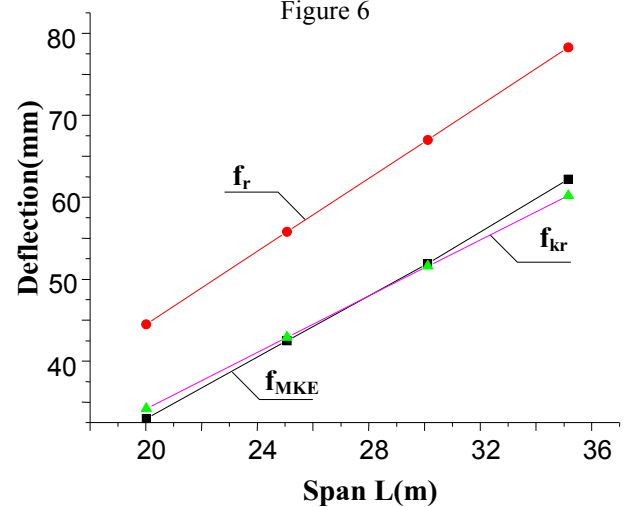


Figure 7

Figures 5,6 and 7 depict comparative values of maximum truss construction deflection. Figure 5,6 and 7 show the results of the construction type shown in figure 4a, 4b and 4c respectively. The deviations for other truss construction types [5] do not exceed the limits shown in tables 2,3 and 4.

In reference [1] the recommended correction factor value is $\mu \in (1,15 \div 1,4)$, but it is not more precisely defined for the construction type and span.

Also, it is important to consider the influence of the way the trusses are filled on their stiffness. The considerations are done for the diagonal angle toward the horizontal line $\alpha \in (30 \div 60)$ and the spans $L = 20; 25; 30; 35$ m, where the truss heights are equal. In figures 8÷11 we can see the influence of the way the truss is filled on its stiffness. Also, we can establish the relation between truss construction deflection and the way of filling the truss in relation to the filling angle, equation (6).

$$f = k_l \cdot 2 \cdot L \cdot e^{\frac{-\alpha}{5 \cdot L}} \quad (6)$$

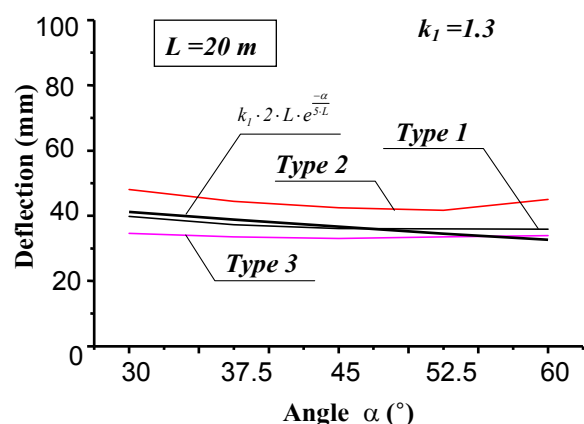


Figure 8

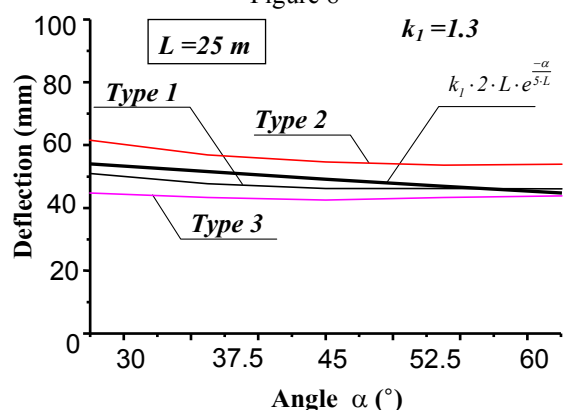


Figure 9

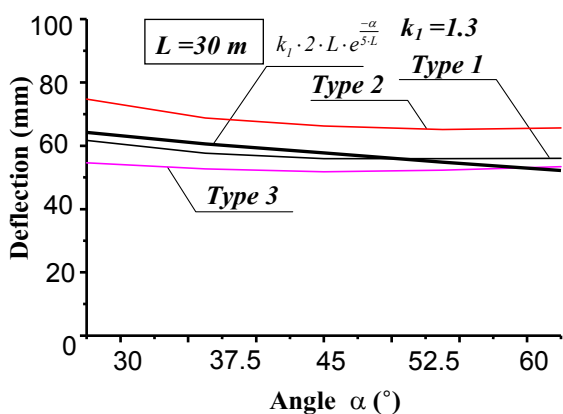


Figure 10

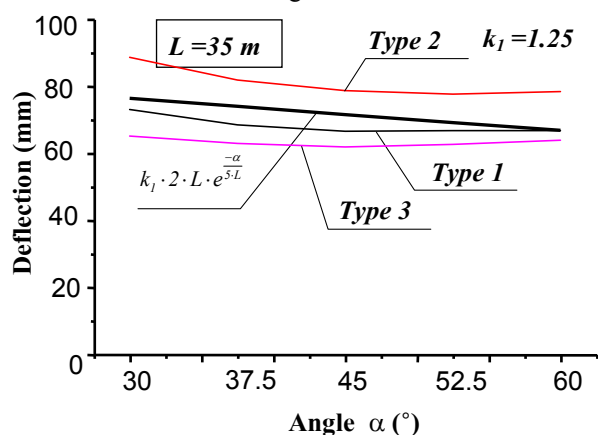


Figure 11

The analysis was also done for truss construction boom [5] where dependance between deformation and the way of filling the truss is established by following relation:

$$f_k = \left(\frac{L}{L_k} \right) \cdot \frac{k_1 \cdot L}{e^{m \cdot \alpha}} \quad (7)$$

where L_k – the distance between the revolving pillar and the location where the boom is connected with the brace. Approximation practiced by the equation (7) gives a great accuracy [5], which can be noticed in the case of crane reach of $L=14m$ (figure 12).

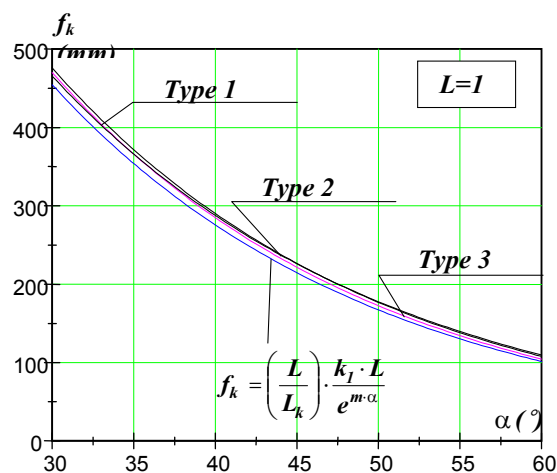


Figure 12

4. CONCLUSION

Performed expression for the bending stiffness enables its relatively simple calculation. This approximation allows the designer to relatively quickly define the basic parameters of the construction with the smallest possible deviation in deformation and stress analyses.

The defined construction stiffness correction factors give a great accuracy in calculating and include the basic geometric parameters of construction.

5. LITERATURE

- [1] Gohberg M.M. "Metalicheskie konstrukcii pod'emno-transportnyh mašin", Ma{ino-stroenie, Leningrad 1976. g.
- [2] Gohberg M.M., i dr. "Spravo~nik po kranam I,II ", Ma{inostroenie, Moskva 1988. g.
- [3] Lang A.G. i dr. "Portalnye kranj", Gosudarstvennoe nau~no-tehni~eskoe izdatel'stvo ma{inostroitel'noj literatury, Moskva 1962.
- [4] Savković M., Gašić M., Ostrić D. "Metoda uprošćavanja izraza za savojnu krutost prostornih rešetkastih konstrukcija", XXIII JUPITER konferencija, Beograd 1997.
- [5] Savković M., Gašić M., Marković G. "Analiza uticaja načina formiranja ispune rešetke na ugib

strele rešetkaste konstrukcije”, XXVIII JUPITER
konferencija, Beograd 2002.

DYNAMIC BEHAVIOUR SIMULATION OF STRUCTURE OF BRIDGE-TYPE STACKER-RECLAIMER

Petković Z., Gašić V., Bošnjak S., Zrnić N.

Abstract

This paper presents dynamic analysis of structure of bridge-type stacker-reclaimer subjected to external loads caused by resistances to coal reclaiming. Dynamic model is presented with four lumped masses and developed along with finite element model of structure of unloading bridge. There are gained natural frequencies and mode shapes, along with adequate dynamic responses of structure.

Key words: Dynamic behaviour, bridge-type stacker-reclaimer, bucket chain booms, FEM, modes

1. INTRODUCTION

Reclaimers are basic link of bulk transportation system in thermal plants. They are, generally, categorized according to their functional and constructional characteristics [9]. Within the class of bridge-type equipment with blending effect, a type of special designed bridge-type stacker-reclaimer with bucket chain booms is shown at fig.1.



Figure 1 – Bridge-type stacker-reclaimer; Power plant “Kolubara” – Veliki Crljeni

Capability for changing the position of reclaiming bucket chain booms and central belt conveyor, along the bridge, enables such machine to have 4 working regimes:

- reclaiming the coal from tranches and transportation to the main belt conveyor (which goes in to the plant), Fig. 2(a)
- reclaiming the coal from tranches and stacking on stockyard, Fig. 2(b)
- reclaiming the coal both from tranche and from stockyard and further transportation to the main belt conveyor, Fig. 2(c)
- reclaiming the coal from stockyard and transportation to the main belt conveyor, Fig. 2(d)

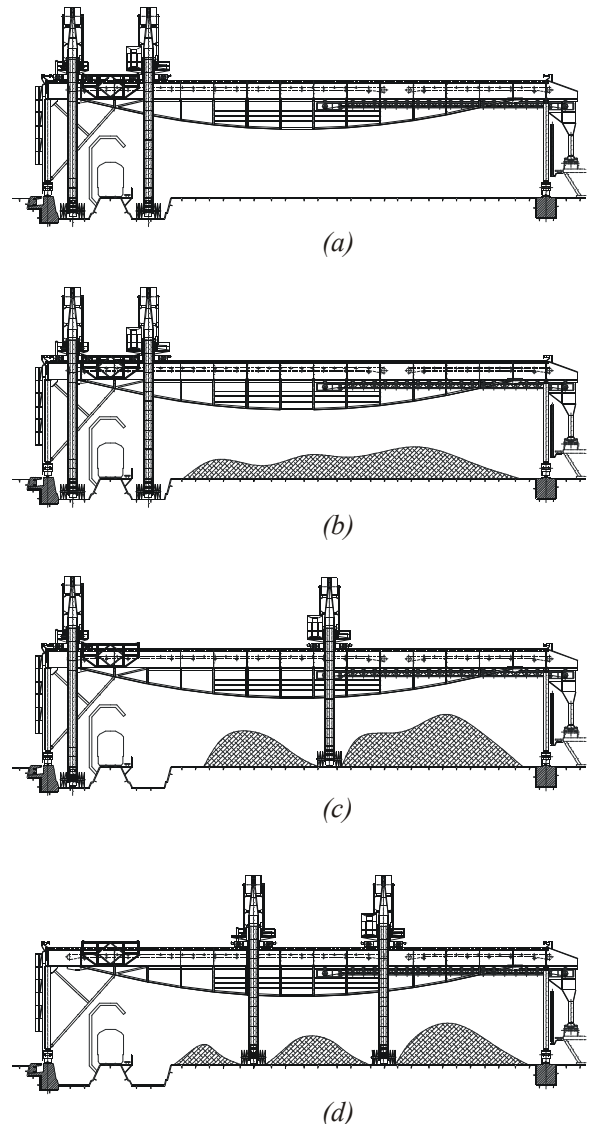


Figure 2 [6] – Working regimes of bridge-type stacker-reclaimer

¹Prof. Dr.-Ing. Zoran Petković, Faculty of Mech.Engineering, Kraljice Marije 16, 11000 Belgrade, E-mail: zpetkovic@mas.bg.ac.yu

²Ass.Mag.-Ing. Vlada Gašić, Faculty of Mech.Engineering, Kraljice Marije 16, 11000 Belgrade, E-mail: vgasic@mas.bg.ac.yu

³Ao. Prof. Dr.-Ing. Srđan Bošnjak, Faculty of Mech.Engineering, Kraljice Marije 16, 11000 Belgrade, E-mail: sbosnjak@mas.bg.ac.yu

⁴Ass.Dr.-Ing. Nenad Zrnić, Faculty of Mech.Engineering, Kraljice Marije 16, 11000 Belgrade, E-mail: nzrnic@mas.bg.ac.yu

2. SETTING OF DYNAMIC MODEL OF BOOM STRUCTURE

Dynamic behaviour caused by resistances to reclaiming process is analyzed for uniform work of unloading bridge for two cases, shown in Figures 2-c and 2-d. Setting up the dynamic model of structure of unloading bridge is fully analogous with modeling of cranes, especially gantry cranes. Dynamic models of the supporting structure is presented with four lumped masses that includes concentrated masses of booms, Fig.3 and 4.

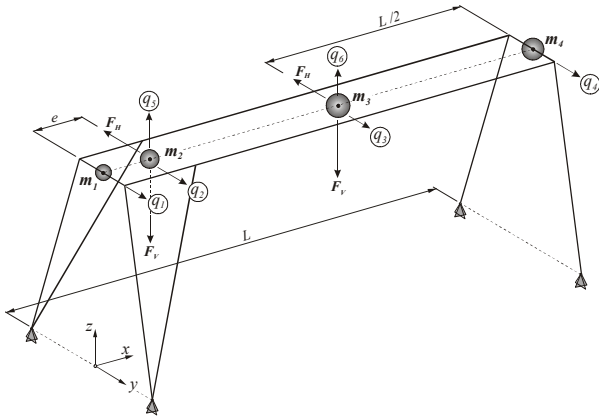


Figure 3. Case I, one boom at rigid leg

$$m_1 = \frac{1}{3} m_{KN} + \frac{1}{2} \frac{e}{L} (m_{mo} + m_{TR})$$

$$m_2 = \frac{1}{2} \frac{e}{L} (m_{mo} + m_{TR}) + m_{ZU} + \frac{1}{2} \frac{L-2e}{2L} (m_{mo} + m_{TR})$$

$$m_3 = \frac{1}{2} \frac{L-2e}{2L} (m_{mo} + m_{TR}) + m_{ZU} + \frac{1}{2} \frac{1}{2} (m_{mo} + m_{TR}) + \frac{1}{2} m_{PTR}$$

$$m_4 = \frac{1}{2} \frac{1}{2} (m_{mo} + m_{TR}) + \frac{1}{3} m_{PN} + \frac{1}{2} m_{PTR}$$

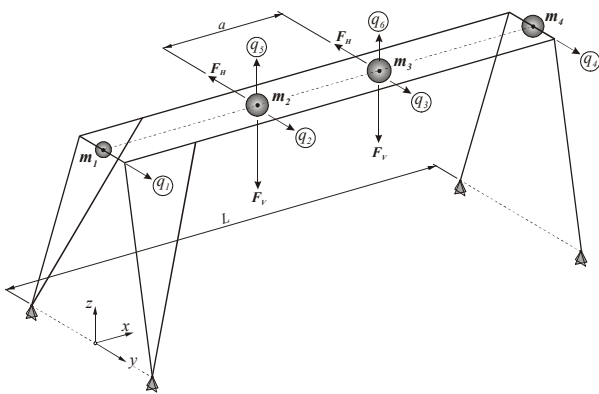


Figure 4. Case II, two booms at middle of the structure

$$m_1 = \frac{1}{3} m_{KN} + \frac{1}{2} \frac{1}{2} \frac{L-a}{L} (m_{mo} + m_{TR})$$

$$m_2 = \frac{1}{2} \frac{1}{2} \frac{L-a}{L} (m_{mo} + m_{TR}) + m_{ZU} + \frac{1}{2} \frac{a}{L} (m_{mo} + m_{TR})$$

$$m_3 = \frac{1}{2} \frac{a}{L} (m_{mo} + m_{TR}) + m_{ZU} + \frac{1}{2} \frac{1}{2} \frac{L-a}{L} (m_{mo} + m_{TR}) + \frac{1}{2} m_{PTR}$$

$$m_4 = \frac{1}{2} \frac{1}{2} \frac{L-a}{L} (m_{mo} + m_{TR}) + \frac{1}{3} m_{PN} + \frac{1}{2} m_{PTR}$$

3. MATHEMATICAL FORMULATION OF FORCED VIBRATION OF BRIDGE STRUCTURE

Mass matrix is easily determined as:

$$A = \begin{bmatrix} m_1 & 0 & 0 & 0 & 0 & 0 \\ & m_2 & 0 & 0 & 0 & 0 \\ & & m_3 & 0 & 0 & 0 \\ & & & m_4 & 0 & 0 \\ Sim. & & & & m_2 & 0 \\ & & & & & m_3 \end{bmatrix}$$

Due to complexity of structure of unloading bridge there's been made a finite element model of supporting structure (Figure 9.) Potential energy is determined through influence coefficients, gained as static response to unit forces in characteristic places and direction, as shown at Figure 5.

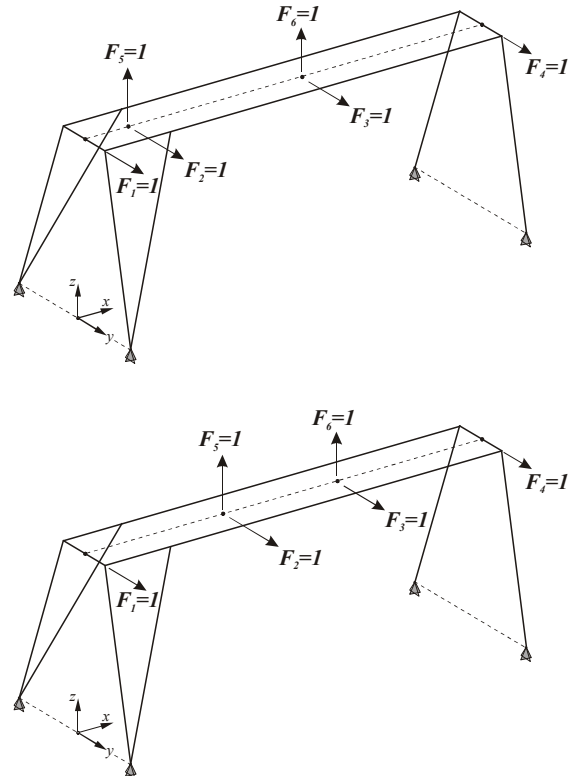


Figure 5. Determination of influential coefficients for cases I and II, respectively

As a result there are obtained displacement in characteristic joints that represent influential coef., and following matrix:

$$\alpha = \begin{bmatrix} \alpha_{11} & \alpha_{12} & \alpha_{13} & \alpha_{14} & 0 & 0 \\ & \alpha_{22} & \alpha_{23} & \alpha_{24} & 0 & 0 \\ & & \alpha_{33} & \alpha_{34} & 0 & 0 \\ & & & \alpha_{44} & 0 & 0 \\ Sim. & & & & \alpha_{55} & \alpha_{56} \\ & & & & & \alpha_{66} \end{bmatrix}$$

External loads acting upon structure of bridge reclaimer which are caused by resistances to coal reclaiming process are dynamic loads and consider the problems related to: ship section, specific resistance to digging and position of components of force resisting excavation [1]. Their determination is presented in [2,5].

Vector of generalized forces is:

$$\mathbf{Q} = \{0 \quad -F_H \quad -F_H \quad 0 \quad -F_V \quad -F_V\}^T$$

The mathematical model is set through Lagrange's equations of the second-kind with following differential equation of forces vibration

$$\mathbf{A} \cdot \ddot{\mathbf{q}} + \mathbf{C} \cdot \dot{\mathbf{q}} = \mathbf{Q}$$

Natural frequencies are obtained from equation

$$\det(\mathbf{I} - \alpha \mathbf{A} \cdot \omega^2) = 0$$

Vibrational motion, in non-resonance case, has following form [7]

$$q_p = q_0 + \sum_1^{\infty} q_C^{(n)} \cos n\Omega t + \sum_1^{\infty} q_s^{(n)} \sin n\Omega t$$

Whole mathematical algorithm for both cases is done numerically, with software MathCad.

4. NUMERICAL EXAMPLE

Numerical example is performed for bridge-type stacker-reclaimer in power plant Kolubara, with parameters taken from [5]. The software provides nodal displacements, acceleration and frequencies of structure.

Acceleration values are obtained for the case II because of bigger dynamic importance for bridge (as concluded in chapter 6), Fig.8, with distance of 10 m between the booms.

Obtained frequencies for case I, are

$$f = [2.16 \quad 2.27 \quad 4.51 \quad 6.27 \quad 7.62 \quad 28] \text{ Hz}$$

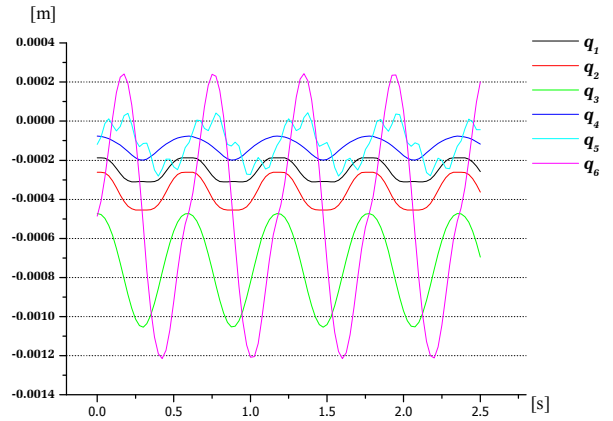


Figure 6. Nodal deflections for the case I

Obtained frequencies for case II, are

$$f = [1.9 \quad 1.95 \quad 6 \quad 7 \quad 7.08 \quad 7.5] \text{ Hz}$$

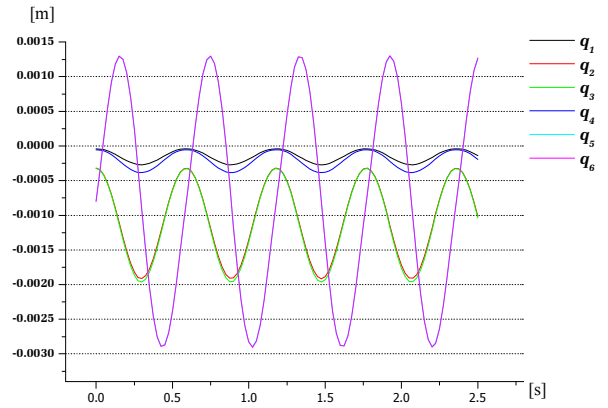


Figure 7. Nodal deflections for the case II; $a=7$ m

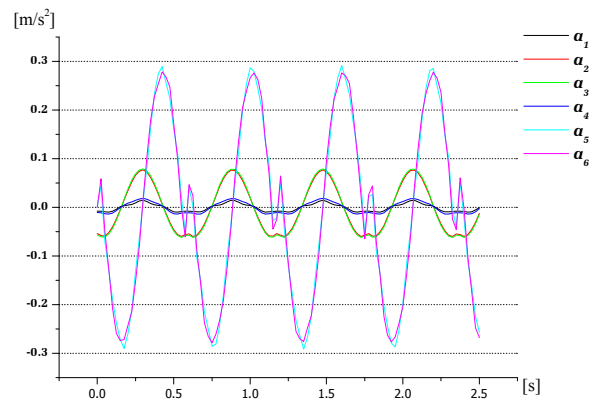


Figure 8. Nodal accelerations for case II, $a=10$ m

5. FINITE ELEMENT ANALYSIS OF BRIDGE STRUCTURE

Finite element model of the considered bridge is done with software SAP 2000, and consists of beam elements. Whole model, along with section characteristics is shown in Fig.9.

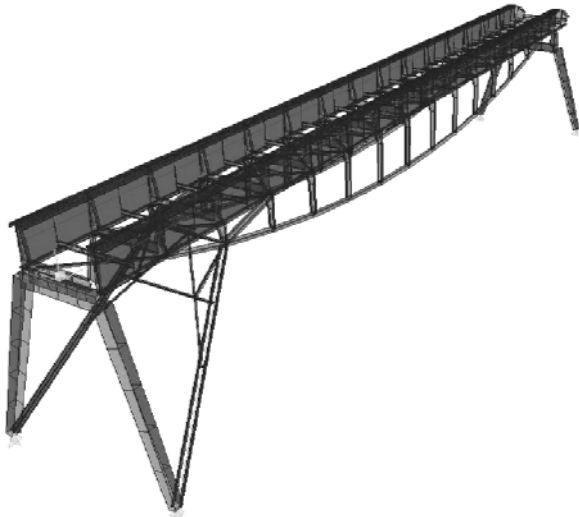


Figure 9. Finite element model of bridge structure

Modal analysis is performed on presented model and there are obtained natural frequencies of structure. On following pictures there are shown first 6 modes of vibration (Fig 9.1-9.6).

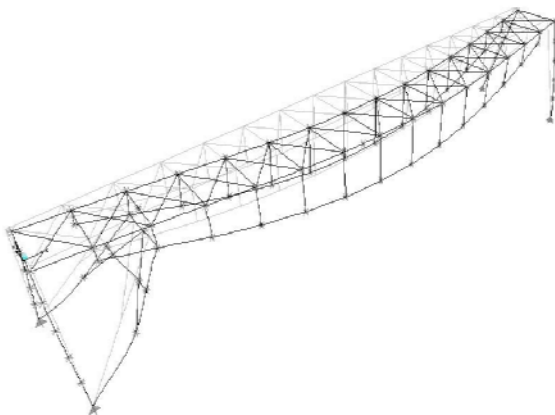


Figure 9.1 - 1. mode; $f = 2,35 \text{ Hz}$

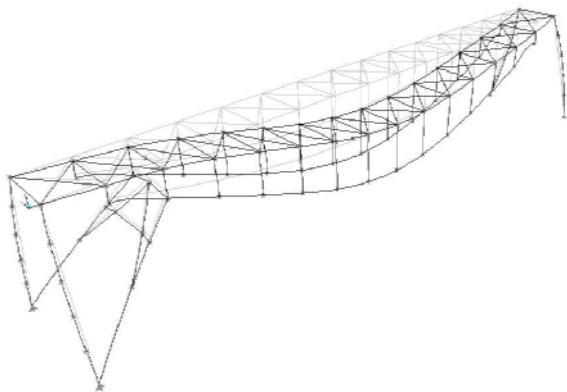


Figure 9.2 - 2. mode; $f = 2,91 \text{ Hz}$

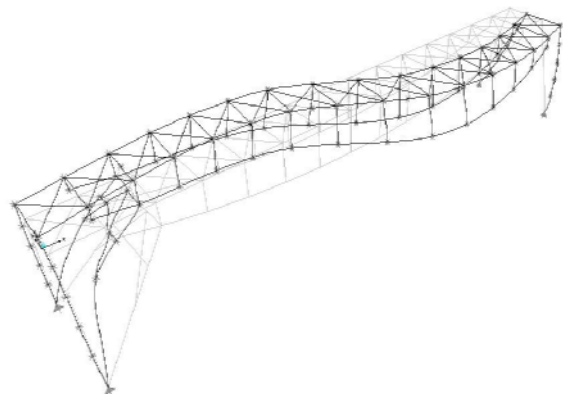


Figure 9.3 - 3. mode; $f = 6,86 \text{ Hz}$

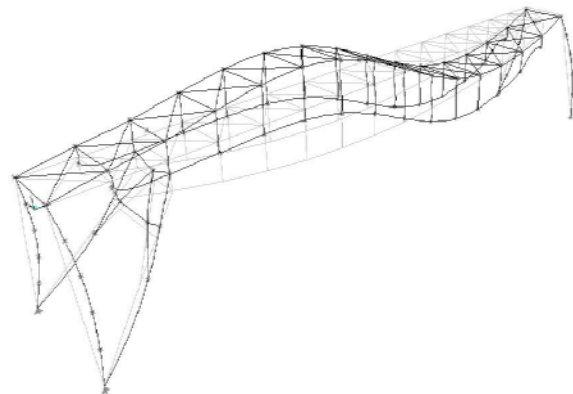


Figure 9.4 - 4. mode; $f = 7,2 \text{ Hz}$

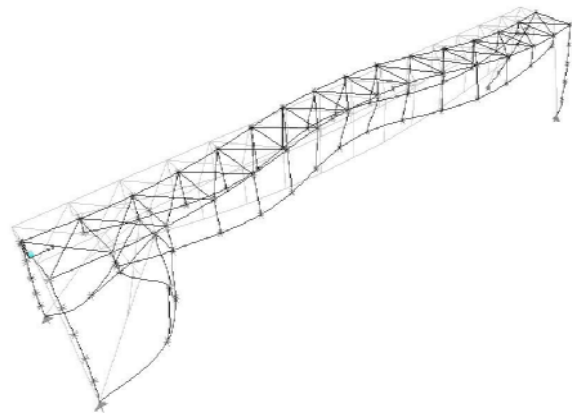


Figure 9.5 - 5. mode; $f = 11,5 \text{ Hz}$

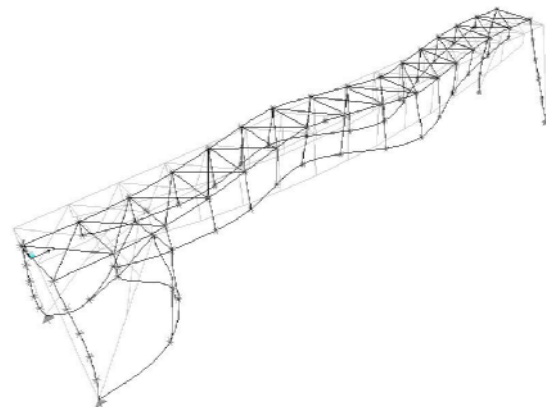


Figure 9.6 - 6. mode; $f = 12,5 \text{ Hz}$

Also, modal analysis is performed on lumped model of bridge structure. Comparison of frequencies gained from FEM and lumped system is presented in following table.

Frequencies [Hz]			
No.	FEM system	Lumped model	Absolute error [%]
1.	2.35	2.15	9
2.	2.91	2.63	9.6
3.	6.86	6.48	5.5
4.	7.2	6.81	5.4
5.	11.5	8.72	24.1
6.	12.5	9.16	26.7

It can be concluded that absolute errors for first 4 frequencies are less than 10%, what satisfies engineering accuracy. This approves recommended reduction of masses in dynamic models.

6. RESULT ANALYSIS

By comparison of values from Figures 6 and 7, it can be concluded that structure of bridge-type stacker-reclaimer is more subjected to dynamic influences for the case II. That could be expected because of static inconvenience when booms are positioned in the middle of the bridge. Also, it is obvious that bridge has smaller values of bridge frequencies for the case II that could reach forced frequency for this type of machine $\Omega = 10.65 \text{ s}^{-1}$ [5].

Due to ratio of forced and natural frequency, which is 0.88, it can be concluded that bridge is very close to enter the resonance domain, with known expression

$$0,9 \leq \frac{\Omega}{\omega_k} \leq 1,1.$$

This proves exploitation recommendation that minimal distance between the bucket chain booms, when they are positioned at the middle of the structure, (Fig. 2d), should be 10 m. In practice it is achieved with special bumpers positioned on booms.

Presented plots gives maximum deflection of bridge of 3 mm, and acceleration of $0,3 \text{ m/s}^2$. This shows small influence of external loads, especially because of their magnitude values that are small in comparison with masses of booms and selfweight of bridge. Only dynamic character of external loads can produce dynamic instability of bridge structure.

With gained dynamic values it can be obtained dynamic forces and moments. Total bridge loading in vertical plane for case II, that includes inertial forces, is presented in Figure 10.

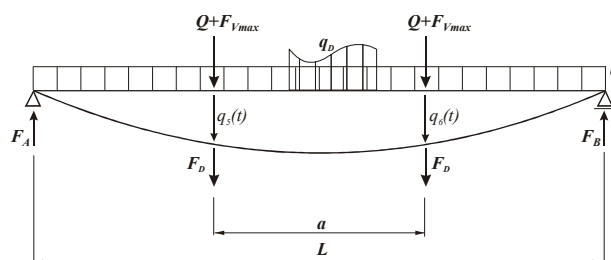


Figure 10. – Bridge loads in vertical plane

Dynamic coefficient, i.e. ratio of total loads and static loads, has the known form

$$K_D = \frac{M_{st} + M_{din}}{M_{st}} = 1 + \left| \frac{M_{din}}{M_{st}} \right|$$

In vertical plane bridge is primary subjected to bending. For this bridge, it is gained that dynamic coefficient in vertical plane is $K_D = 1,025$, that also prove little influence of external loads on to the structure.

7. CONCLUSION

Dynamic simulation is performed on real model of structure of bridge-type stacker-reclaimer subjected to external loads caused by resistances to coal reclaiming. It is shown that only dynamic character of loads has influence of structure behaviour and that main loads come from masses of reclaiming booms, belt conveyors and selfweight of crane. There are determined natural frequencies of structure and made comparison with forced frequency. It is shown that operating restriction has background in dynamic analysis, along with dominate static prerequisites. Given model has enough engineering accuracy and provides possibility for further dynamic analysis that includes variety of load cases, especially in non-stationary movement of crane. Presented analysis enables good insight in behaviour of such machines, along with contribution in extension of references concerning the bulk bridge & slewing devices with blending effect.

REFERENCES

- [1] Bošnjak, S.: Bucket wheel trenchers (in Serbian), Faculty of Mechanical Engineering, Belgrade, 2001.
- [2] Bošnjak, S., Jovković, M., Gašić, V.: PREMO, Software for calculating the external loads caused by coal reclaiming process at bridge-type reclaimers, Faculty of Mechanical Engineering, Belgrade, 2004.
- [3] Computers and Structures, Inc.: SAP 2000 Analysis reference manual, Berkeley, California, USA, 2002.
- [4] Dedijer, S., Petković, Z., Grujić, B.: Project T-107, Working processes of heavy machinery (in

- Serbian), Faculty of Mechanical Engineering, Belgrade, 1990.
- [5] Gašić V.: Dynamic behaviour identification of bridge type stacker – reclaimer with bucket chain booms in power plants, Mag.Tech.Sc.Thesis, Faculty of Mechanical Engineering, Belgrade, 2004.
- [6] Petkovic Z., Ostrić D.: Steel structures (in Serbian), Faculty of Mechanical Engineering, Belgrade 1996.
- [7] Radosavljević, Lj.: Theory of vibrations (in Serbian), Faculty of Mechanical Engineering, Belgrade 1981.
- [8] Spyrakos, C.: Finite element modeling in engineering practice, West Virginia University, Morgantown, 1994.
- [9] Wöhlbier, R.H.: Stacking, Blending, Reclaiming of Bulk Materials, Trans Tech Publications, First Edition 1977.
- [10] Zrnić N.: Contribution to identification of dynamic behaviour of gantry crane, Mag.Tech. Sc.Thesis, Faculty of Mechanical Engineering, Belgrade, 1996.

This paper is a part of the research project TR 6344 "Research, development and construction of machines for handling and stocking of containers and bulk materials, supported by Serbian Ministry of Science and Environmental Protection.

INFLUENCE OF MAINTENANCE ON THE PERFORMANCES OF LARGE SCALE SYSTEMS

Univ. Prof. Dr. Sc. Đorđe Zrnić¹

Abstract: *Most of the transport systems are safety critical, small flaws in their construction may result in substantial risk to human lives and/or the environment. There is therefore a need to increase both, the safety and efficiency (high performances). The aim of this paper is to show some elements of developed procedure for modeling the LSS, and the influence of maintenance on design, and performances of the system and their particular elements. This paper presents the methods used to develop a structural inspection program and to evaluate the useful structural life using statistical analysis and the principles of fracture mechanics.*

Keywords: *Large Scale System, Cranes, Maintenance, Inspection program.*

1. INTRODUCTION

The term Large Scale System (LSS) is often used to refer to systems with multiple components that need to cooperate to achieve a common goal, trying to make efficient use of available resources. In general case LSS consists of many interacting sub-systems performing various planning and control functions. Designing of LSS presents a special challenge for the designer, because of the more complex systems with different level of links between elements (from very slack to very rigid), and with mutual influences, which could be deterministic or defined by, stochastic values [4,5,7]. Most of the transport systems discussed above are safety critical, small flaws in their construction may result in substantial risk to human lives and/or the environment. There is therefore a need to increase both, the safety and efficiency (high performances) of LSS [10,11]. The aim of this paper is to show some elements of developed procedure for maintenance of the LSS.

The need for performance evaluation and prediction exists from the initial concept of a system architectural design to its operation after installation. The accuracy of such prediction rests on our capability of mapping the performance characteristics of the system components into the overall system level performance characteristic. The system design requires clear understanding of complex interaction among system elements. Prediction of the overall system performance is difficult since the nature of the interactions in general are nonlinear and non deterministic, thus the problem could be reduced to the isolation and optimization of the knot points ("bottlenecks"), resources whose capability seriously disturb the whole system performance, taking into the account the interactions among the system and its elements and vice versa [4,7].

Knot point or Elementary Subsystem (ESS) represents a place of performing technological operations, transshipment, branching or collecting of transportation flows, etc. Sometimes, they are very expensive components. For example a container crane at the

terminal. By definition ESS is the subsystem, which is unable to be further, decompose without disturbing given function and which is suitable for optimization in system analysis. The basic aim for introducing notion ESS is to define boundaries in such manner to enable optimization of elementary subsystem in a most appropriate way.

Estimation of system performances in the design phase is a very complex and responsible task, so is developed methodology for service level evaluation. The basic idea of the procedure TPD – Total Performance Design is to coordinate methods of operations research, at the system level, and the methods of optimization at the component level [4,5,7]. Specially, in the case when the standard components are capable to be modified (reengineering process) or where it is reasonable to make a new design (construction) of the component. A pragmatic model is developed to combines simulation model and multiattributive evaluation methodology. The approach is based on the following concept: a simulation model developed is combined with a formal evaluation procedure to initiate an iterative solution finding process. The results of the simulation may at any point in time be submitted to a formalized evaluation procedure containing multi goal structure [4,5,7]. The procedure enables evaluation of system performance, as indicator of utility, including, for example the influence of the maintenance of the ESS.

2. MAINTENANCE OF ESS - THEORETICAL OVERVIEW

The useful structural life is the remaining time the crane can be operated with an acceptable risk of failure. When first asked to consider acceptable risk, the usual response is an acceptable risk is no risk. Using the damage tolerant design philosophy, the consequences of the failure of one detail may be limited with periodic inspection. This paper presents the methods used to develop a structural inspection program and to evaluate

¹ Univ. Prof. Dr. Sc. Đorđe Zrnić, academician of Academy of Engineering Sciences of Serbia and Montenegro, Faculty of Mechanical Engineering Belgrade, E-mail: nenadzrn@yubc.net, Kraljice Marije 16, 11120 Belgrade 35, Serbia & Montenegro

the useful structural life using statistical analysis and the principles of fracture mechanics [11]. The prediction of fatigue crack growth is based on statistical data and the principles of fracture mechanics. Cracks grow from initial discontinuities, usually at welded joints. The crack size increases with each cycle of loading, until the crack reaches a critical size and the member fails suddenly without warning. The study determines the actions needed to reduce the risk of such failures to acceptable levels and if such actions are economic. Crack prediction based on the statistical approach is not perfect. It provides a method of improving the reliability of the structure. The reliability can be estimated once the current condition of the structure and the operational demands are known. Improving details and increasing the intensity and frequency of the structural inspection may extend the useful life. However, the cost of the improvements may not be justified, in which case other options need to be considered. Other options range from changing the use or refurbishing the structure to scrapping the cranes.

A structural life assessment of a container crane follows the steps: perform a condition survey, perform a fatigue cumulative damage analysis of the cranes and determine the Non Destructive Testing (NDT) inspection intervals, make an initial estimate of the useful life, based on current maintenance levels, develop a structural maintenance program, develop the final estimate of the useful life based on new maintenance levels, explore options based on economics [6,10].

2.1. Condition Survey

The engineer's visual assessment provides valuable information regarding the crane's operations and the present crane condition. The condition survey provides a comparison between the as built condition of the crane and that shown on the manufacturer's drawings. The survey also provides a means for the engineer to assess the condition of Fracture Critical Members (FCMs) and determine whether they have any welded attachments that could accelerate fatigue crack growth. FCMs are tension members whose failure could lead to collapse of the crane. Welded attachments to FCMs can severely accelerate fatigue growth. A crack may initiate at a poor weld detail and grow into the parent metal of a fracture critical member. Since fatigue cracks grow perpendicular to the principal stress, the crack will grow across the member. During the condition survey, the engineer takes photographs of each joint. The photographs will be included in the inspection manual that will be used by the NDT inspector to understand what to inspect and to report his findings.

2.2. Cumulative Damage Analysis and Estimating Inspection Intervals

Current specifications for cyclically loaded structures adopt a damage tolerant design philosophy [8]. This means that if fatigue cracks were to occur in any given

member, the remaining structure should be able to safely carry the load until a routine periodic inspection detects the crack. Therefore, the periodic inspection interval should be long enough to make the inspection economically feasible, but short enough to detect the crack before it reaches an unstable state. The cumulative damage analysis provides a method to estimate the inspection intervals.

The fatigue and load spectrums were generated based on the theoretical vessel operation, the trolley loading, and the number of cycles of operation. The fatigue spectrum describes the vessel loading and unloading operation for the trolley. The load spectrum describes the trolley loading and the number of cycles of operation during the life of the crane. Liftech's inspection program [6] concentrates the inspection effort where it is most important. Only a few fracture critical members with high relative cumulative damage may require more frequent inspection, while all other joints could be inspected less frequently. Through cost-effective inspections, reliabilities can be greatly increased, and the life of a crane can be extended well beyond its original planned life.

2.3. Initial Assessment of Useful Life

The initial estimate of the useful life, prior to a NDT inspection of the cranes, is based on the current condition of the cranes and on predicting the number of fatigue cracks in a crane. First, the relative cumulative damage is calculated as discussed above. Typically, the estimate of remaining useful life will increase after the crane is inspected and cracks are repaired. So, the initial assessment provides the useful life of the crane, at its current maintenance levels, prior to repairing the cracks. The initial estimate of the useful life provides options to the owner. If the predicted number of cracks is excessive, the owner may scrap the cranes and forego a costly NDT inspection. If the estimate of the useful life is between eight to ten years, he may decide to proceed with the NDT inspection, crack repairs, and refurbishment of the cranes.

2.4. Structural Maintenance Program

Liftech's structural maintenance includes preparation of a NDT inspection manual for each crane. The manual addresses the structural details to be inspected: whether the detail is fracture critical or non-fracture critical; the method of locating each detail; the required method of inspection. Visual, Magnetic Particle, Ultrasonic, or Radiographic; the inspection interval for each weld detail; the inspector's qualifications; the required reporting procedure for the defect findings; and the repair procedure. An NDT inspector inspects the crane; the Engineer prepares a repair procedure or redesigns the connections, and the cracks are repaired. If a crack is detected in time and repaired before it becomes unstable, the metal in the vicinity of the repaired crack is rejuvenated, and the reliability of the repaired joint would be the same as new. However, as the cranes age,

the cracking pattern becomes more unpredictable, and the frequency of cracking increases nonlinearly (see Figure below). Thus, closer inspection intervals are required as the crane ages.

2.5. Final Assessment of the Useful Life of the Crane

The NDT inspection of the crane provides the actual number of fatigue cracks that have developed in the crane. Based on the actual number of cracks, the revised reliability, and the revised relative cumulative damage, are computed. The remaining life at current maintenance levels is then recalculated. When the cracks in the crane structure are repaired, the life typically improves by at least one inspection cycle, between three and six years.

2.6. Determination of Economic Benefits

Once the useful life data is determined, the crane owner can make an economic assessment of the cranes. Refurbishment could include new drives, outreach extension, and crane raise. If the remaining useful life is low, the owner may decide to scrap the cranes, relocate them to a lighter duty port, or sell the cranes.

3. AN EXAMPLE

An example of Liftech Consultants Inc. analysis is given [6,8] made for Hong Kong International Terminals to assess the structural useful life of eight dockside cranes manufactured by Paceco/MES, IHI, and Hitachi. The cranes had been operating for 14 to 28 years. HIT wished to operate the cranes for an additional 10 years if the structures have low risks of catastrophic failure.

Cranes	Commissioned	Outreach/ Backreach/ Gage (m)	Number of Lifts
Paceco 63	1972	36/9.14/24.38	$2.6 \cdot 10^6$
Paceco 71			$2.65 \cdot 10^6$
IHI 41	1976	36.6/9.14/24.38	$2.1 \cdot 10^6$
IHI 43			$2.2 \cdot 10^6$
IHI 61			$2.3 \cdot 10^6$
IHI 64			$2.4 \cdot 10^6$
Hitachi 42	1985	36.6/9.14/24.38	$1.5 \cdot 10^6$
Hitachi 62			$1.45 \cdot 10^6$

In general, the cranes were found to be in good condition. Indications of cracks were on all cranes and were noted in the NDT inspection manuals. Liftech performed cumulative damage analysis of the three different types of cranes based on the crane operating data provided by HIT and the assumed fatigue design criteria. In addition to an annual visual inspection of the cranes, the following table shows the recommended inspection interval. The table identifies non-fracture critical and fracture critical components. The inspection interval is either the number of container moves or the number of years from the latest inspection, whichever occurs first.

Component Frame	FCM/ NFCM	Inspec. Interval No. of moves	Lesser of years
Landside Trolley Girder Connection	FCM	300,000	3
Landside Trolley Girder Support Beams	FCM	600,000	6
Waterside Trolley Girder Support Beams	FCM	1,200,000	12
Portal Beam	NFCM	2,400,000	24

Only a few of the crane structural components require inspection once every three years. The remaining components need to be inspected at 6, 12 or 24-year inspection intervals. A three-year inspection interval for all joints is excessive and a six-year inspection interval is probably excessive for some joints and inadequate for others. Using the inspection intervals shown above, the required down time to inspect the cranes is also significantly reduced.

3.1. Estimated Fatigue Crack Frequency vs. Actual Fatigue Cracks Documented in NDT Inspection

Based on the crane operating data provided by HIT and the assumed fatigue design criteria for the MES, IHI, and Hitachi cranes, the expected frequency of detectable fatigue cracks was calculated at current maintenance levels, prior to an NDT inspection. An NDT inspection was then performed. The inspection provided data on the actual cracking pattern for the cranes. The table below compares the predicted number of fatigue cracks for each set of cranes at current maintenance levels vs. the actual fatigue cracks detected during the NDT inspection.

Cranes	Predicted no. of fatigue cracks	Fatigue cracks detected during NDT inspection
Paceco 63	33 to 36	13
IHI 41	3 to 5	3
IHI 61	4 to 6	12
Hitachi 42	0 to 1	2
Hitachi 62	0 to 1	3

There is a significant variation in different cranes. Since the relative cumulative damage varies as the cube of the stress range, a small variation in the stress range magnifies the relative cumulative damage significantly. The table below compares the estimated future structural life for each crane at reliabilities of 97.73%, prior to NDT inspection, after NDT inspection, and after all repairs are completed [6].

Cranes	Prior to NDT	Based on NDT inspection	After repairs inspection results
Paceco 63	0-1	6-7	11-12
IHI 41	12-13	16-18	20
IHI 61	10-11	5-7	10-12
Hitachi 42	15-16	10-11	15-16
Hitachi 62	16-17	8-10	13-14

QUAYSIDE CONTAINER CRANES - GENERAL CLASSIFICATION, STATE-OF-THE-ART AND SOME EXPECTATION IN DEVELOPMENT

Univ. Ass. Dr.-Ing. Nenad Đ. Zrnić¹, Univ. Prof. Dr.-Ing. Zoran Petković²

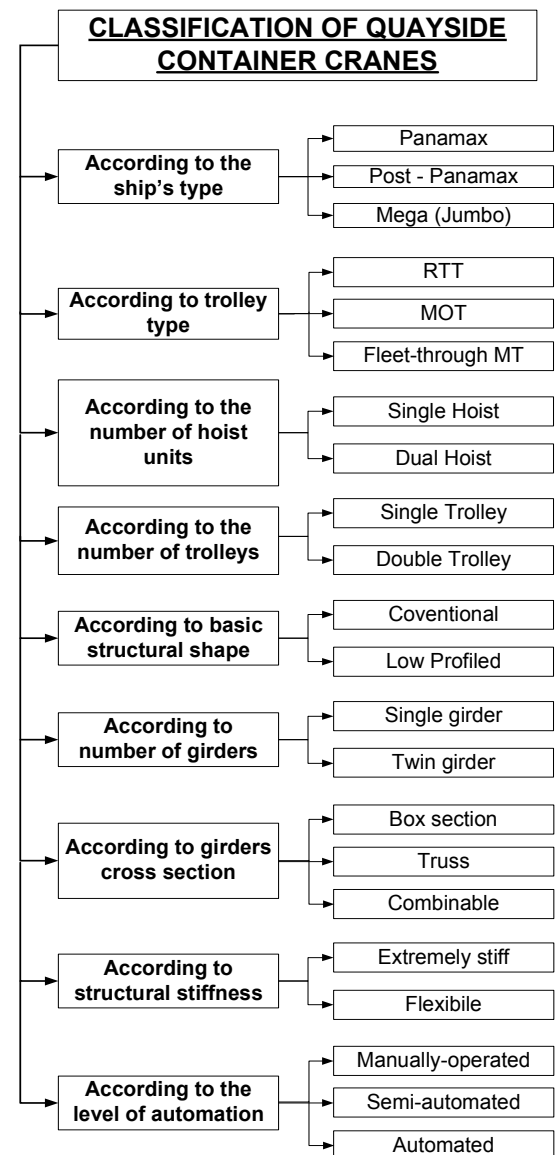
Abstract: Quayside container cranes are the biggest investment of total capital costs in ports and have a most significant effect on the efficiency of terminal operations. Up to nowadays no one's classification has been presented in authoritative references in the field. The paper presents a complete classification of quayside container cranes, and discusses the state-of-the art of container cranes and future trends in their development. The facts exposed in the paper should give a suggestion what type of quayside crane we tend towards, because the future mega cranes starts today

Keywords: quayside container cranes, classification, development, automation

1. Basic classification of quayside cranes

The development of efficient, automated, high-technology loading/unloading equipment has the potential of considerably improving the performance of terminal operations. Advances in quayside container cranes technologies, as the major part and the biggest investment (capital costs for container cranes are 70 % of total costs in ports [1]) of the cargo storage and retrieval system have a significant effect on the efficiency of port terminal operations once properly implemented, [2]. Up to now the classification of quayside container cranes has not been presented in authoritative references covering the field of quay container cranes. It is interesting that the references are dealing merely with some partial segments of classification, but no one has given a full-scale classification. It is worth-while to mention that the following factors, in addition to the tradition and philosophy of manufacturers, are working upon structural solutions of container cranes:

1. Outreach, depending on the ship's size;
2. Height above water, also depending on the ship's size;
3. Gage, distance between rails depending on the terminal's concept;
4. Number of trolleys working on crane;
5. Bacreach, depending on the servicing requirements, i.e. servicing the storage are, or transferring soleley containers between the transportation devices on the dock (e.g. Automated Guided Vehicles) and the ship;
6. Destination of port terminal, i.e. river or sea terminal;
7. Reasons for restricting the height of container cranes, e.g. in proximity of airport.



The basic classification of quayside container cranes is presented in Figure 1 [3].

Figure 1. Basic classification of quayside cranes

¹ Dr.-Ing. Nenad Zrnić, Faculty of Mechanical Engineering Belgrade, Kraljice Marije 16, 11000 Belgrade, Serbia, E-mail: nzmnic@mas.bg.ac.yu
² Prof. Dr.-Ing. Zoran Petković, Faculty of Mechanical Engineering Belgrade, Kraljice Marije 16, 11000 Belgrade, Serbia

2. State-of-the Art and expectations in development of quayside container cranes

The size of container cranes has almost tripled since the first container cranes were built in January 1959. The Matson container cranes built by PACECO in 1959 were designed to service Panamax ships and to lift 22.7-t boxes 15.6 m over the rails with an outreach of 23.8 m [4]. The development of container ships in the 60s of the last century resulted in expansion of Panamax container cranes. Increasing the number of containers across deck resulted in development of Post-Panamax ships and cranes. Mega (Jumbo or Large) container ships, lead up into exploitation, present the ships of the future with the capacity more than 7,000 TEU, and with expectations of capacity of 15,000 TEU (even 18,000 TEU for Malacca-Max ships). Present criterion for Mega container cranes is to service ships that capacity is 9,000 TEU (500,000 TEU per year - transshipment during 24h, [5]) and at least 20 containers across deck. Figure 2 presents the difference in size between the first container cranes and the currently largest container crane manufactured by Chinese ZPMC in 2004. Figure 3 presents the increasing of cranes weight in the last 45 years since the first crane was built [6].



Figure 2. Comparison of cranes dimensions (1959:2004)

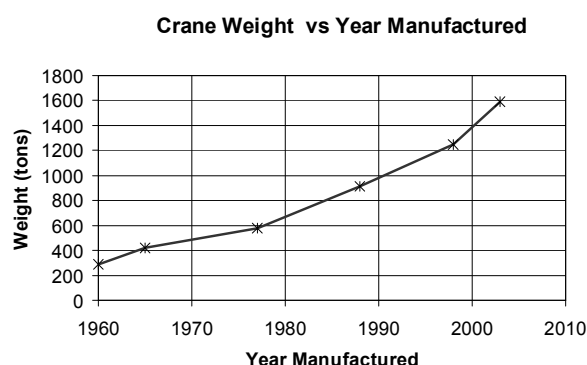


Figure 3. Increasing the cranes weight (1959:2004)

The basic features of existing mega quayside container cranes and the expected future trends in their development are presented the followings [3]:

1. Lifting capacity (current 67-73, expected 80 t);
2. Outreach (current 60-65 m, expected 65-70 m);

3. Backreach (current and expected 15,24 m);
4. Gage (current and expected 30,48 m);
5. Maximum lifting height (current and expected more than 60 m);
6. Trolley velocity (current 250 m/min, expected 300 m/min);
7. Hoisting velocity (current and expected 100 m/min).

The selection of a crane's trolley type is significant for the structure, as well as for the wheel loads. The trolley selection should be based on the needs at a particular location, as well as the preference of the owner and operators [7]. Basically the trolley can be Rope Towed Trolley (RTT) or Machinery On Trolley type (MOT). A hybrid of the two systems, commonly known as a Fleet Through Machinery Trolley (or Semi-Rope trolley [8]), was adopted by some manufacturers. In a more detailed subdivision the types of trolley can be classified as follows:

1. Rope Towed Trolley - Fleet Through - Catenary Support Trolleys;
2. Rope Towed Trolley - Fleet Through - Continuous Catenary Support;
3. Fleet Through Machinery Trolley - Self Powered Trolley;
4. Machinery On Trolley;
5. Rope Towed Machinery On Trolley - Semi-Machinery Trolley.

For the structural design, weight is the main difference between the two types of trolleys. The weight of the rope-towed trolley is approximately one-third that of a machinery trolley. The main disadvantage of the machinery trolley is the increase in crane weight and wheel loads on the wharf. Comparison in weight between RTT and MOT construction of trolley for 16 containers wide crane is presented in Table 1 [2, 9]:

	Type of Trolley	
	RTT	MOT
Trolley's mass, (t)	20,4	63,5
Total moving load, (t)	104	152
Total crane's mass	1050	1200
Maximum wheel load, (t/m)	49	57

Table 1. Comparison of data for trolley weight

The typical quay crane includes one main hoist on the frame. These typical cranes make up the overwhelming majority of cranes, and this will continue for many years. Rapidly developing improvements in electronics and optical and acoustical equipment will reduce dwell times and increase productivity. The real productivity of single hoist dockside cranes will be limited to 40 to 50 moves per hour because of service to the quay [10]. Advanced crane concepts have been developed to provide increased crane productivity. Dual hoist cranes have a second hoist located over the quay. Those cranes

were developed in the 1980's, first by ECT Rotterdam, and then by Virginia Port Authority [11]. This can increase productivity by about 50%, but also increases the initial costs of the crane by 30 to 50%, adds an operator, and increases maintenance and operating costs. The new solution of Dual hoist crane combined with elevating platform (Dual Elevating platform) crane is presented in Figure 4 [9].

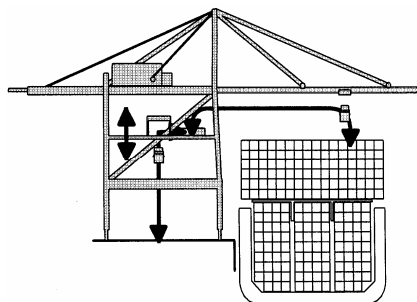


Figure 4. Dual hoist elevating platform

The double trolley will help the productivity of the crane. The suggestion is that two trolleys operate on the same runway, Figure 5 [9]. Operating double trolleys is not an entirely new idea. The SeaLand Ansaldo cranes in Taiwan are designed to carry two trolleys. The initial installation included only the ship trolley. The second trolley was planned so that it would operate only the landside of the waterside rail, but the shore trolley was never installed. The second trolley requires a second operator. Since the second trolley is at the crane girder level, the second trolley operator is far above the quay, making load control difficult [11]. Nowadays, a dual hoist crane will be more productive than a dual trolley crane. The initial and operating cost of two cranes solutions are the same. There is no apparent advantage to the dual trolley crane.

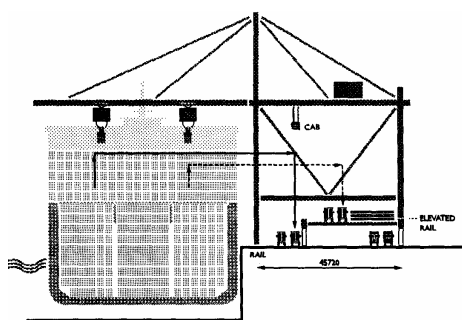


Figure 5. Double trolley crane

The basic structural form of STS container cranes (A-frame) remains practically unchangeable compared with the first structure built in 1959. The basic structural shape of STS cranes can be divided into two groups:

1. Conventional or modified conventional cranes;
2. Low profile cranes.

The conventional and modified A-frame crane with single trolley and one operator is still the workhorse of container cranes industry. The first low profile cranes emerged in the late 1960s. The boom is supported by a hanger system including support truck and wheels; it rides on the wheels at all times. For the PACECO standard, all machinery and electrical equipment is on the boom. The machinery travels with the boom and causes significant increases in the wheel loadings. Low profile cranes cost about 15% more than A-frame cranes and were used when it was necessary to restrict the height of the crane (under max. 46 m), i.e. because they have the advantage of keeping cranes profile below aircraft clearance lines, Figure 6. During the period 1970-1999 approximately 40 of these cranes were built, sized to service vessels between 13 and 16 containers wide. Except for the US, they are now found only in Italy [8].



Figure 6. Low profile crane

Supporting structure of quayside container cranes can be either single girder or twin girder. Also, the girder cross section can be box, truss, or combinable solution where the outreach is truss, and the girder between legs and backreach is box.

Full crane automation, from ship to shore, may be the answer to greater crane speeds and productivity demands. This is difficult to achieve for several reasons: accuracy will be required to automatically pick a container from a ship and set it on a truck on the quay; the new container cranes have increasing degrees of automation that increase crane productivity. For automation to operate correctly, the location of all system components must be known. For fixed object, this is an easy task. For moving objects, such as the crane structure flexing with the movement of the trolley, the task becomes more difficult. One approach is to require a very stiff structure with strict deflection limits. A stiff structure helps with load control and provides an easier ride for the operator. A detailed structural design process is required to minimize the weight and optimize the geometry and sections. The alternative is to account for crane movement in the load control system design and not specify deflection limits. This requires more complex software, but will result in an about 10% lighter crane structure [3].

The outline of the classification of existing STS cranes due to their degree of automation is shown in Figure 7 [3].

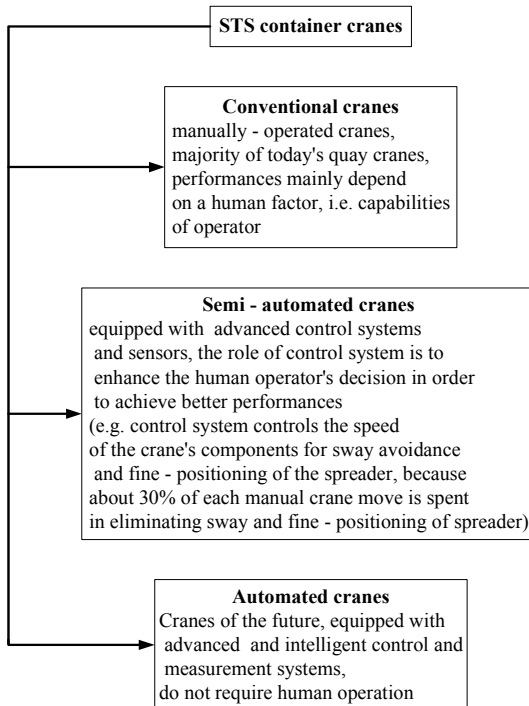


Figure 7. Classification of cranes by automation degree

3. Conclusion

The exposed classification, supplemented with the state-of-the art and some expectation in development, should give us a suggestion what type of quayside container cranes we tend towards, and what are the main subsystems for cranes functioning in the future, and what are the main problems that a designer of those cranes may encounter. This is essentially important, because the development of mega container cranes impose several new standards in their design. The future of mega quay cranes starts today and will last until 2030, what is the reasonable life of a container crane with a proper maintenance. An effective crane must be designed to suit the present and future needs of the end user. But if today's crane is built large enough to serve tomorrow's ships using future technology, the crane will not perform well on today's ship with today's technology. For years design team members have worked together to produce economical design that meet operational demands and that can be efficiently fabricated and erected. As always, the "best" ("optimum") design requires balance. The cost and benefits of each alternative should be considered in respect of the specific case.

References

- [1] Strandenes, S.P., 2004: Port Pricing Structures and Ship Efficiency, Review of Network Economics, Vol.3, Issue 2, pp. 134-144.

- [2] Zrnić, Đ., Kosanić, N., Čuprić, N., Zrnić, N., 2002: Total performance design of transportation systems, Proceedings of International Conference on Industrial Systems, IS'2002, Vrnjacka Banja, Serbia, pp. 164-171.
- [3] Zrnić, N., 2005: Influence of Trolley Motion to Dynamic behaviour of Ship-To-Shore Container Cranes, Dr. Tech. Sc. dissertation in Serbian, Faculty of Mechanical Engineering Belgrade.
- [4] Bhimani, A. K., Jordan, M. A., 2001: Crane Purchase Specifications: Tailor-Made or Off-The-Shelf, Presented at Conference "TOC '01", Lisbon, Portugal.
- [5] Klaassens, J. B., Smid, G. E., Van Nauta Lemke, H. R., Honderd, G., 2000: Modeling and Control of Container Cranes, IIR's Second Annual Developments in Container Handling Automation & Technologies, London, UK, February 28-29,
- [6] Vazifdar, F. R., Florin, J., 2004: Operating Jumbo Cranes on Existing Wharves, Presented at Conference "TOC Asia 2004", Singapore.
- [7] Zrnić, N., Petković, Z., 2002: Evaluation of Design Solutions for Trolley of Quayside Container Cranes, Proceedings of the "IRMES 2002" Conference, pp. 99-104, University of Srpsko Sarajevo, Republic Srpska, Bosnia and Herzegovina.
- [8] Zrnić, N., Hoffmann, K., 2004: Development of design of ship-to-shore container cranes:1959-2004, In: History of Machines and Mechanisms, edited by Marco Ceccarelli, pp. 229-242, KLUWER ACADEMIC PUBLISHERS, Dordrecht, Netherlands.
- [9] Morris, C. A., Hoite, S., 1997: The Future of Quayside Container Cranes, Presented at Post Conference Workshop "China Ports '97", China.
- [10] Zrnić, N., 2001: The Influence of Some Container Cranes Design Characteristics on Terminal System Performances, In: Modelling and Optimisation of Logistic Systems (edited by T. Banayai and J. Cselenyi), pp 159-171, University of Miskolc, Hungary.
- [11] Zrnić, N., Dragović, B., Petković, Z., 2003: Survey of Some New Concepts that Increase STS Container Cranes Productivity, Proceedings of "Miskolczer Gespraech 2003", Die Neuesten Ergebnisse auf dem Gebiet Foerdertechnik und Logistic, pp. 133-138, Miskolc, Hungary.

This paper is a part of the research project TR 6344 "Research, development and construction of machines for handling and stocking of containers and bulk materials", and research project with specified topic TD 7005 "New methods for defining factors of optimal functioning of river shipping technological subsystems", both supported by Serbian Ministry of Science and Environmental Protection.

MODELING AND SIMULATION OF THE WORK OF TRANSPORT MACHINES DRIVING MECHANISMS WITH FREQUENCY MODULATED ELECTROMOTOR DRIVE

Zoran Marinković¹⁾, Predrag Milić¹⁾, Dragan Marinković¹⁾, Goran Petrović¹⁾, Saša Marković¹⁾,

Abstract: The paper presents the modeling of driving mechanisms of the transport machines with cage electromotor. For that purpose a torsional elastic-kinetic model is used, the masses' movement of which is defined by second-order non-homogeneous differential equations. The natural characteristic and the curves of frequency modulated starting of the motor are accurately described in the analytical manner. The solution of the system of differential equations determines the laws of the motion of the masses as well as the torque function in the elastic constraints between the masses. By means of the available software packages and developed computer programs the work of these mechanisms is successfully simulated on a PC.

Key words: driving mechanism, cage electromotor, frequency modulation, modeling, simulation

1. Introduction

The electromotor is the most frequently used drive for a great number of internal transport machines. It represents an electromechanical system used to put the executive parts of driving mechanisms of these machines into motion. Two basic groups of internal transport machines can be distinguished. The first group consists of non-continuous transport machines, i.e. cranes, which perform a cyclic transport of the load through a combination of motion of several independent driving mechanisms. Machines that perform continuous transport (transporters, elevators, conveyers) belong to the second group. The former group is characterized by intermittent drive with pronounced dynamical loadings, and the latter one is characterized by stationary loadings [1, 2].

Electromotor drive consists of the electric energy supply system, control device and the mechanical transfer of energy to the executive parts of the transport machines driving mechanisms. Electromotors are characterized by simple and robust structure, high safety and constant readiness for operation, possibility of short overloading, easy maintenance, in other words they are highly economic in the exploitation. The electric energy supply is relatively simple and very reliable. The control system has the equipment that provides starting of the motor, speed regulation, electric braking and change of the rotation direction. A number of control modes has been developed depending on the type of the motor, efficiency of the control function realization and the price [3].

Nowadays, the asynchronous cage electromotors with the short-circuited rotor are quite often used in the transport technique. They are simpler, cheaper and easier for maintenance with respect to other electromotors, because of the lack of collectors, rings and brushes. Their starting is realized directly or in one of various other ways. However,

the frequency modulation as a control mode is getting on importance today due to the good results that are achieved and the acceptable price of frequency converters [3]. Therefore the paper presents the procedure of modeling and simulating the work of cranes driving mechanisms with cage motor, the starting and speed regulation of which is performed directly and by means of the frequency converter.

2. Modeling of driving mechanisms of cranes with cage motor

Modeling of the driving mechanisms of cranes comprises:

- the selection of an equivalent dynamic model,
- determination of the characteristics of the model and of the external excitations,
- setting an adequate mathematical model,
- solving the mathematical model and getting the laws of motion and loading functions.

Within the first phase the complex real system, i.e. the driving mechanism, is presented by a simpler equivalent model. The kind, the form and the complexity of the model depends on the kinematical structure of the driving mechanism, aims of the research, accuracy of the obtained results, etc. The procedure will be demonstrated on a concrete example (fig 1).

This mechanism is produced and is used as a driving mechanism of a laboratory apparatus, mass 4.0 t and speed 1.08 m/s, by means of which the movement of cranes is simulated. It consists of a break cage motor, type KBF-90 LA 2, power $P_M = 1.0$ kW, revolutions per minute $n_1 = 2510$ min⁻¹, nominal $M_n = 3.8$ Nm and breaking moment $M_B = 9.6$ Nm, vertical three-step reducer with gear ratio $i_R = 35.5$ and driving wheel with diameter $D_T = 250$ mm. In this example, the velocity function $v = f(t)$ and the torque function $M_t(t) = T(t)$

¹⁾ prof. dr Zoran Marinković (zoranm@masfak.ni.ac.yu), Predrag Milić, Dragan Marinković, Goran Petrović, mr Saša Marković, Mašinski fakultet Univerziteta u Nišu, ul. A. Medvedeva 14, 18000 Niš, Srbija i Crna Gora

of the referent – outlet shaft of the reducer are experimentally and analytically examined for a movement that consists of acceleration, stationary motion, breaking and suppression of vibrations of the system after the breaking.

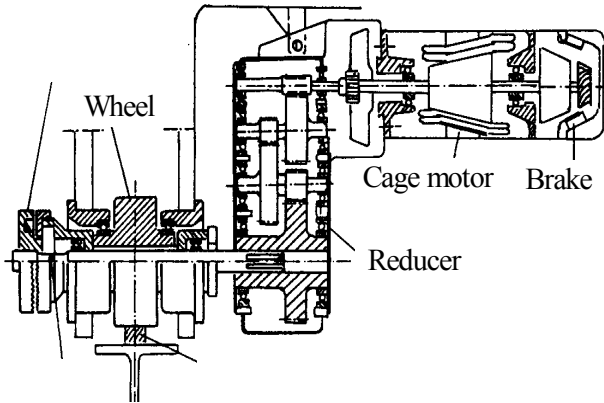


Fig. 1 Mechanism for moving the laboratory apparatus

Since the laws of motion and the torque function of the referent shaft are analytically examined for the mentioned real system, i.e. crane driving mechanism (fig 1), the system is replaced by a torsional elastic-kinetic model with a finite number of discrete revolving masses and elastic constraints between them. The masses are determined by the inertia moments J_i , and the constraints by the rigidity c_i and dumping coefficients b_i . Nevertheless, by performing appropriate reduction of the mentioned characteristics, the complex dynamic model can be reduced to a very simple model with only two revolving masses and an elastic constraint (fig 2), by means of which the relevant results for the analysis of the work of the mechanisms can be obtained [1, 2].

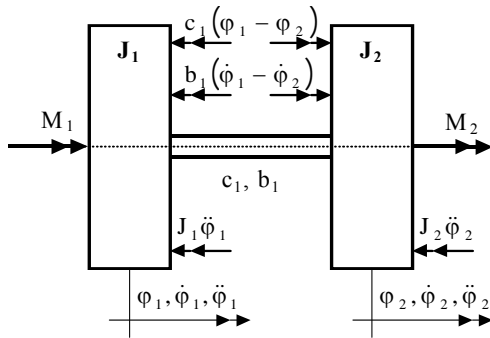


Fig. 2 Equivalent torsional elastic-kinetic model

Since the reduction is performed for the shaft for which the torque function $M_t = T(t)$ is sought, all the masses up to the shaft form the driving mass (J_1), and the remaining masses form the driven mass (J_2). The elastic constrained is described by the reduced rigidity c_1 and dumping constants b_1 . For the example at hand, the reduction is performed for the outlet shaft, so that: $J_1 = 27.35 \text{ kgm}^2$, $J_2 = 62.50 \text{ kgm}^2$, $c_1 = 24206 \text{ Nm}$ and $b_1 = 14.00 \text{ Nms}$ [1, 2].

Dynamical behavior of this driving mechanism depends also on the external distractions and excitations. Above all, those are the excitation of the cage motor $M_I = M_M = f(n)$ and the brake $M_I = M_B$ as well as the distractions of the various movement resistants $M_2 = M_W$.

The natural torque characteristic for the direct starting of the cage motor, type KBF – 90 LA 2, the curve torque (M_M) - revolutions per minute (n) on the diagram, is given on the fig. 3 [1]. Most frequently it is a higher order curve $M_M = f(n)$, which cannot be described by an explicit function. It is rarely specified by the producer, but the following torque values are always known: starting M_P , maximal M_K , nominal M_n and minimal (saddle) M_S for a concrete motor.

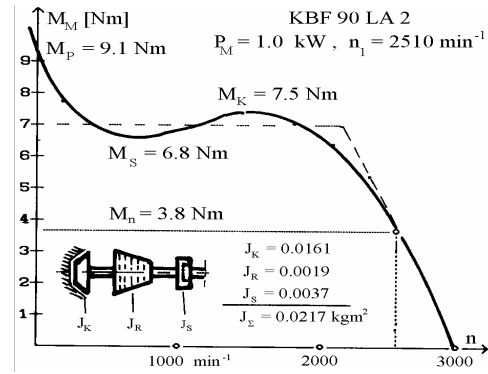


Fig. 3 Natural characteristic of the cage motor

In the paper the curve is modeled through a separate treatment of its two intervals (fig 3): between the starting M_P and the maximal moment M_K and between the maximal M_K and the nominal moment M_n . The first interval can be described by a 4th order polynomial:

$$M(n) = A_4 \cdot n^4 + A_3 \cdot n^3 + A_2 \cdot n^2 + A_1 \cdot n + A_0, \quad (1)$$

because the three points of the curve are known M_P , M_S and M_K , as well as the two points in which the curve has the horizontal slope M_S i M_K .

The second interval is best described by the so-called Clos equation:

$$M(s) = \frac{2 \cdot s \cdot s_k}{s^2 + s_k^2} \cdot M_K = M(n), \quad (2)$$

where we have:

$s = 1 - n/n_{sh}$ - sliding at any point of the interval,

$s_k = 1 - n_k/n_{sh}$ - sliding at the point of maximal moment,

n_k - number of revolutions at maximal moment,

n_{sh} - synchronous number of revolutions.

The modeled natural characteristic for the direct starting of the cage motor KBF – 90 LA 2, according to (1) i (2), is given on the fig. 4 as curve nr. 1.

As already pointed out, the starting and the speed regulation of the motor is today successfully realized by means of the frequency converter, i.e. continuous change of the current frequency f in certain limits. In this case the tendency is to perform starting of the motor with the maximal flux $\Phi = U/f$ in order to keep the maximal value of the maximal moment M_K . The motor characteristic with this kind of regulation is obtained starting from the known analytical relation (3), which describes the moment of the motor as a function of the voltage U and the frequency f [3]:

$$M_K(U, f) = (U/U_n)^2 \cdot (f_n/f)^2 \cdot M_{KN}, \quad (3)$$

where: M_K – the maximal value of the maximal moment with the variable voltage U and frequency f ; U_n and f_n – nominal values of the voltage ($U_n = 380$ V) and the frequency ($f_n = 50$ Hz) and M_{KN} – the maximal value of the maximal moment at U_n i f_n .

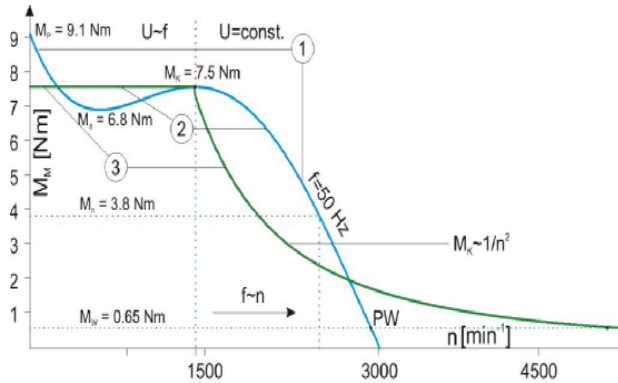


Fig. 4 Modeled curves of the cage motor KBF – 90 LA 2

Two basic cases are characteristic for the change of the frequency. The first case occurs when the frequency is changed in the limits $f = 2.5 \div 50$ Hz, and the second one occurs when the frequency is further increased, most often up to 100 Hz. This points out the fact that the number of revolutions of the motor is doubled with respect to the nominal value.

The first case represents the starting of the motor with the simultaneous change of the voltage U and the frequency f so as to keep the flux $\Phi = U/f$ constant and maximal. This means that the value of the expression $(U/U_n)^2 \cdot (f_n/f)^2$ in the equation (3) is equal to 1, i.e. the moment of the motor is constant and with the maximal value of the maximal moment M_{KN} . Upon reaching the nominal values of the voltage U_n and the frequency f_n the further change of the moment is described by the Clos equation (2) until the stationary regime is reached, i.e. the work point PW, which is at the intersection of the moment of the motor M_M and the moment of resistance M_W . On the fig. 4 it is the curve nr. 2, which consists of a straight line in the first part and of the Clos curve in the second part.

In the second case, when the nominal voltage U_n is reached with the increase of the frequency f above the nominal value f_n , the flux decreases with f^{-1} and the maximal moment with f^{-2} . According to the equation (3), in the interval $f = 50 \div 100$ Hz this change follows the law $M_K = (f_n/f)^2 \cdot M_{KN} = (n_k/n)^2 \cdot M_{KN}$. In the concrete case it is the curve nr. 3 on the fig. 4, which points out that the motor is not well used due to the large sliding at the point of the maximal moment ($s_k = 0.527$ for $n_k = 1420$ min⁻¹), with $f \geq 50$ Hz. Also, this regulation is not suitable for the two-pole cage motors because of the duplication of the number of revolutions (between 3000 ÷ 6000 min⁻¹).

Besides the excitation originating from the motor given as curves $M_M = f(n)$ on the fig. 4, the other excitations in the considered mechanism (fig. 1) are the breaking moment

M_B and the moment of resistance M_W . They are considered as constant in the present analysis. The former has the value $M_B = 9.6$ Nm and is related to the first – driving shaft, and the latter is $M_W = 22.4$ Nm and is related to the outlet shaft. The moments have their sign, i.e. the direction of acting.

After the selection of the elastic-kinetic model with two revolving masses (fig. 2) and determination of its characteristics and the external excitations, the adequate mathematical model is set in the 3rd phase of the modeling of the transport machines driving mechanisms. It is the fact that in the transient regimes the masses of the model perform a forced damped oscillatory motion under the influence of the external excitations, i.e. the moment of the motor $M_1 = M_M = f(n) = f(\dot{\varphi} = \pi \cdot n/30)$, the moment of the brake $M_1 = -M_B$ and the resistant moment $M_2 = -M_W$. Therefore, based on the kinetostatic method according to the d'Alembert's principle (fig. 2) the mathematical model used to describe the movement presents a system of two second-order non-homogeneous differential equations [1, 2]:

$$\begin{aligned} J_1 \ddot{\varphi}_1 + b_1 (\dot{\varphi}_1 - \dot{\varphi}_2) + c_1 (\varphi_1 - \varphi_2) &= M_1 \\ J_2 \ddot{\varphi}_2 - b_1 (\dot{\varphi}_1 - \dot{\varphi}_2) - c_1 (\varphi_1 - \varphi_2) &= M_2 \end{aligned} \quad (4)$$

where $\varphi_j, \dot{\varphi}_j, \ddot{\varphi}_j$ - are the generalized coordinates of the angle, angular velocity and the angular acceleration of the driving ($j = 1$) and the driven ($j = 2$) mass.

The 4th phase of the modeling implies solving the system of differential equations of motion (4). The solution for the initial conditions $t = t_0, \varphi_1(t_0) = \varphi_{10}, \dot{\varphi}_1(t_0) = \dot{\varphi}_{10}, \varphi_2(t_0) = \varphi_{20}$ and $\dot{\varphi}_2(t_0) = \dot{\varphi}_{20}$ gives the laws of motion of each mass $\varphi_1(t) = f(t)$ and $\varphi_2(t) = f(t)$. The torque function $M_t(t) = T(t)$ of the elastic constraint within the equivalent model (fig. 2), i.e. of the referent shaft of the driving mechanism (fig. 1), is [1, 2]:

$$M_t(t) = T(t) = c_1 \cdot (\varphi_1(t) - \varphi_2(t)) = c_1 \cdot \Delta\varphi(t), \quad (5)$$

$\Delta\varphi(t) = (\varphi_1(t) - \varphi_2(t))$ - deformation of the elastic constraint.

3. Work simulation of driving mechanisms of cranes with cage motors

Hereby the term simulation implies the procedure for imitating and analyzing the work of a real driving mechanism (fig. 1) by means of its equivalent dynamic model (fig. 2) and the analytical model in the form of system of differential equations (4). In this case, the velocity $v = f(t)$ and the torque function $M_t(t) = T(t)$ of the reducer outlet shaft, i.e. of the wheel shaft, are examined for one movement comprising acceleration, stationary motion and breaking. Since the mechanism is used in praxis for driving a laboratory apparatus, the sought functions are experimentally registered for directly driven break cage motor KBF – 90 LA 2 and are shown on the fig. 5 [1, 2].

In the case of analytical simulation of the motor excitation $M_1 = M_M = f(n) = f(\dot{\varphi})$ (fig. 4) it is necessary to reduce it to the driving mechanism outlet shaft (fig. 1). The following relations are used for that purpose:

$$M_{iz} = M_{ul} \cdot i_R \cdot \eta_{pr}, \quad \dot{\varphi}_{iz} = \dot{\varphi}_{ul} / i_R = (\pi \cdot n) / (30 \cdot i_R), \quad (6)$$

where: M_{iz} and M_{ul} – the outlet and inlet moment, $\dot{\varphi}_{iz}$ and $\dot{\varphi}_{ul}$ – the outlet and inlet angular velocity, η_{pr} – the reducer efficiency coefficient ($\eta = 0.95$).

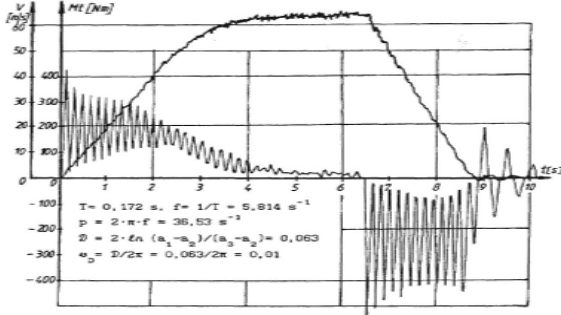


Fig. 5 Experimental results $v = f(t)$ and $M_t(t) = T(t)$ of the mechanism outlet shaft from the fig. 1

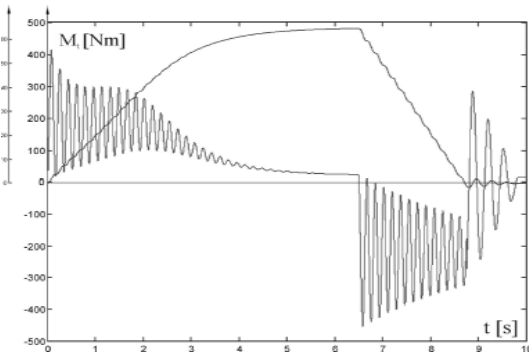


Fig. 6 Analytical simulation $v = f(t)$ and $M_t(t) = T(t)$ of the mechanism outlet shaft from the fig. 1

The fig. 6 shows simulated change of the velocity $v = f(t)$ and the torque moment $M_t(t) = T(t)$ for a movement consisting of acceleration, stationary motion and breaking. In the acceleration period the motor is directly started according to the modeled curve $M_M = f(n)$ nr. 1 on the fig. 4, which is by means of the relation (6) reduced to the outlet shaft in the form $M_M = f(\dot{\varphi})$. During the whole movement the resistance moment with the value of $M_W = -224 \text{ Nm}$ acts in the direction opposite to the velocity direction. In the breaking period the breaking moment acts in the direction opposite to the direction of motion, with a value of $M_B = -9.6 \cdot 355 / 0.95 \approx -360 \text{ Nm}$ after reduction on the wheel shaft.

Comparison of the functions obtained by the simulation $v = f(t)$ and $M_t(t) = T(t)$ on the fig. 6 with the experimental results on the fig. 5 shows a significant agreement. This justifies the proposed method of modeling and simulating the work of transport machines driving mechanisms. It gets on importance when a set of influencing parameters are varied with the aim of multi-variant designing and realization of the optimal solution. Therefore, the fig. 7 shows the simulation of the analyzed functions only for the acceleration period with the frequency modulated ($f = 2.5 \div 50 \text{ Hz}$) starting of the cage

motor (the curves of the motor nr. 2 on the fig. 4). Comparison with the direct starting of the motor (fig. 7.b) demonstrates the better usage of the motor in the former case and that a less effort is required from the motor.

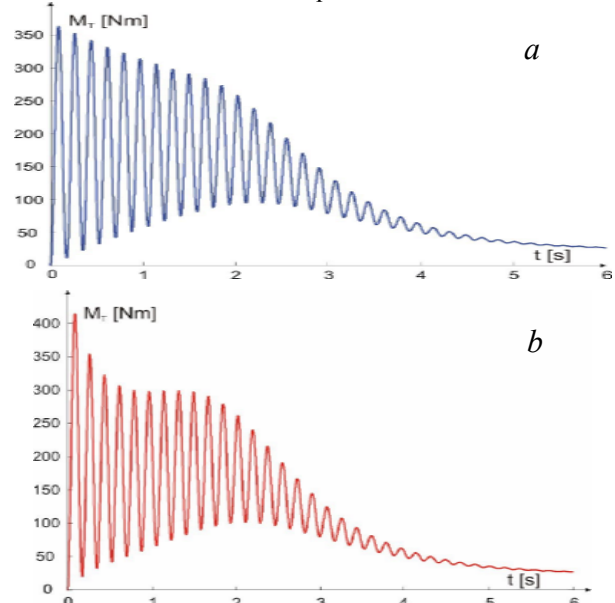


Fig. 7 Comparison of the simulations $M_t(t) = T(t)$

- with frequency modulation $f = 2.5 \div 50 \text{ Hz}$
- with direct starting of the motor

The simulation with the frequency change $f = 2.5 \div 100 \text{ Hz}$ is not done here, because the motor curve nr. 3 on the figure 4 is not suitable and because of the high number of revolutions of up to 6000 min^{-1} , which could have a negative influence on the work of the mechanism and the life-time of the elements.

4. Conclusions

Based on the previous text it can be concluded that the proposed modeling procedure offers a successful simulation of the work of crane mechanisms by means of the simple torsional elastic-kinetic model (fig 2) and the more accurate description of the cage motor excitations. By means of the frequency modulation of the cage motors the better performances of the mechanism are obtained. Analytically obtained functions of loads are important for the calculation and the analysis of the work of the mechanism in the designing phase, in which the changes in the design are still possible.

Literature

- [1] Mijajlović R., Marinković Z., Jovanović M.: *Dinamika i optimizacija dizalica*, monografija, Mašinski fakultet Univerziteta u Nišu, Niš, 2002.
- [2] Marinković Z., Jevtić V., Petrović G., Marković S., Milić P.: *Računske simulacije opterećenja mašina teške mašinogradnje*, Simpozijum YUINFO 2003 - Kopaonik, CD ROM, 2003.
- [3] Thomas F.: *Informaionstechnik für Logistiksysteme 2003, Skript zu Vorlesung*, TU, Karlsruhe, 2003.

Note: The paper was written as part of project No. 006363 financed by Ministry of Science and Environmental Protection of Repuplic of Serbia

EVALUATION OF PERFORMANCES AND PROPOSAL OF CONCEPT OF QUAYSIDE CONTAINER CRANES IN FUTURE

Univ. Ass. Dr.-Ing. Nenad Đ. Zrnić¹

Abstract: Container terminal should provide better services, handle materials more speedily and reduce costs. For those reasons is necessary to define factors for selection and evaluation of mega cranes performances. The paper gives the most significant factors and corresponding assumptions, and present comparison of some cranes performances and concepts for improving productivity. Finally, the paper discusses the level of structural performances and solutions that cranes should achieve in the future.

Keywords: quayside container cranes, evaluation, performances, concepts, future

1. Introduction

With the basic price of 5÷7 millions \$ (the price of modified constructions with modern electronic and advanced control systems approaches 11 millions \$), quayside container cranes present the biggest investment in the container terminal system, wherefore is necessary to apply particular attention in the process of their design in terms of selection the most "optimal" construction. Due to globalization of the society, companies all over the world are making efforts to further expand their business areas. So the needs for container transportation are being increased, and container terminals should satisfy such needs, Figure 1 [1]. For example they should provide better services to meet such needs, should handle materials more speedily, and should reduce the cost. The dimensions of ships are increasing, that impose requirements of designing new terminals for servicing those ships, and constructions of new container cranes operating in such terminals.

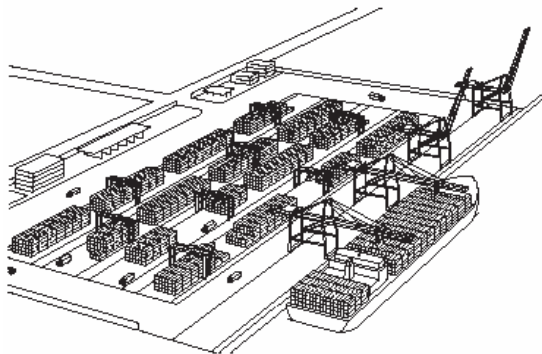


Figure 1. Container terminal

For a quayside container crane, the future starts today and will last until 2025 or 2030. This is the reasonable life of a container crane. The crane may be operational for 40 years with proper maintenance and protection

against corrosion, but the useful life will not be more than 25 or 30 years, and even then the crane will need occasional upgrades to perform to modern standards [2, 3]. The paper presents a proposal for the crane "of the future".

2. Factors for selection and evaluation of performances of mega container cranes

The most significant factors, although mutually often in conflict, are essential for selection and evaluation of performances of mega container cranes [4]:

1. **Price:** The manufacturer should be competitive with the offered price;
2. **Maximum pressure on wheels** (depends on the crane's and trolley's weight, and lifting capacity: We tend towards lightweight construction);
3. **Adopted type of trolley:** By thorough evaluation of existing solutions, and on the basis of setting up criteria for evaluation, we select a more "perspective" solution;
4. **Productivity:** From varied offered solutions for increasing productivity by successive elimination we should accept effective and feasible solutions: the basic measure of productivity is moves (cycle) per hour.

There are also some other factors governing the cranes selection, as are maintenance costs, reliability in operation, safety of personal, etc. [5].

Upon the beginning of setting up criteria for container crane selection the following assumptions have been adopted [4]:

1. The crane is intended to service mega container ships of the future in sea container terminals;

¹ Dr.-Ing. Nenad Zrnić, Faculty of Mechanical Engineering Belgrade, Kraljice Marije 16, 11000 Belgrade, Serbia, E-mail: nznric@mas.bg.ac.yu

2. The crane should operate in modern and not already built container terminal with no prior limits of maximum pressures on wheels;
3. The crane is not operating in the vicinity of airports, so there are no restrictions in maximum height;
4. The concept of terminal is traditional (Figure 1), and the ship is serviced by the crane from one side only;
5. The crane is not servicing the storage and is intended to handle container between ship and the shore;
6. The crane is manufactured in according with detailed specification of the bidder, but by using more of the standard components (combination of "Tailor-Made" and "Off the Shelf" strategies);
7. For increasing productivity are used viable concepts, without considering ideally concepts with unproven values;
8. The current trend in design of quayside container cranes is adopted (increasing productivity, dimensions and capacity, tendency towards full automation of operations, etc) [6].

3. Comparison of some cranes performances

The size of container cranes outreach has almost tripled since the first container cranes were built in January 1959. Other dimensions didn't have such increase. Figure 2 presents a comparison of respective characteristic dimensions of quay cranes with respect to number of containers across deck [4].

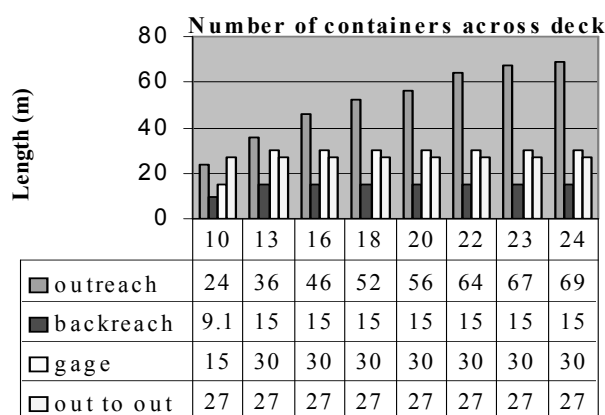


Figure 2. Comparison of respective cranes dimensions

The values from Figure 2 are pointing out the following:

1. In comparison with the first crane ever built the length of outreach is almost tripled;
2. The length of backreach stabilized to 15,24 m and don't show neither the trend of increasing nor payroll (very rare and in particular cases it reach the length of 18,3 m, 21 m, i.e. 22,9 m);

3. The gage stabilized to 30,48 m, herewith it can be shorter for monogirder cranes, e.g. 16,8 m;
4. Out to out bumpers dimension defining the leg width is unchangeable starting from the first crane up to now, with individual exceptions.

The designers have a problem to increase length of outreach because of "cantilever" nature of quayside container cranes [7]. In structural sense cantilever is not efficient because of its self-weight presenting a significant concern in proof of strength.

The comparison of maximum pressure on crane wheels on waterside rail is presented in Figure 3 [4, 8, 9].

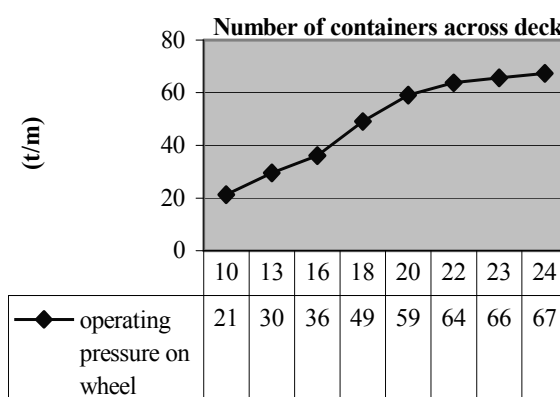


Figure 3. Comparison of maximum operating pressures

The analysis of data from Figure 3 shows linear increment of pressures for cranes servicing Panamax ships, and parabolic increment for servicing Post-Panamax ships.

Figure 4 depicts comparison of trolley velocities [4].

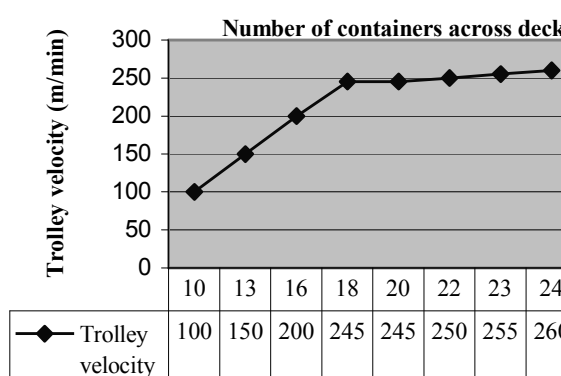


Figure 4. Comparison of trolley velocities

The data acquired from Figure 4 show saturation of velocities for cranes servicing ships with 18 and more containers wide. In future, although that are some expectations of achieving velocities of 300 m/min or even more, the most of the cranes will have the trolley velocity of 250÷260 m/min. Two years ago Chinese manufacturer ZPMC achieve velocity of 350 m/min for

its crane in Dubai, but this construction is still under industrial testing.

The comparative analysis of existing types of trolley is presented shortly in Table 1 [4, 8, 9]

Basic parameters for evaluation of solution	Advantage
Trolley reeving	MOT
Positioning of trolley	MOT
Trolley festoon	RTT
Trolley acceleration	—
Lubrication, ecology	MOT

Table 1. Comparison of trolley solutions

Both types of trolley systems, RTT and MOT have beneficial site-specific applications, and are viable. For each crane purchase, the owner have to evaluate each design and then choose the design which best suits the site and the all-round operational needs [10]. The premise of non-restricted values of maximum pressures on wheel gives the advantage to MOT concept.

Productivity of container cranes is always the critical component of port terminal productivity. In the next decades the crane productivity may become the limiting component of the terminal production. Some improvements in performances and new technical concepts increase the production incrementally (5-20%); other improvements make a quantum jump (25-40%) [11]. Incremental improvements of productivity can be achieved by [5, 11]:

1. Increasing speed and acceleration performances;
2. Automation of operations;
3. Concept of Elevating Girder Crane (EGC): The elevating girder crane is identical to the conventional crane with one notable exception. The upper works can be raised or lowered before vessel service operations begin. The upper works can be parked at five levels, so the lift height is 20, 25, 30, 35, or 40 m above the quay. This reduces the distance from the trolley to the spreader and improves load control. Production is increased about 5% for 17 containers wide ship, and about 21% for barges. Such crane weight and costs are about 20% greater than for conventional cranes. Only one operator is necessary, and additional maintenance is required for upper works lifting and locking components, Figure 5.
4. Concept of Tandem Forties Spreader (TFS), where spreader is created to lift simultaneously two 40 ft. containers, Figure 6.

The quantum jump improvements can be achieved by:

1. Introduction of Dual Hoist Concept;

2. Introduction of Dual Trolley Concept;
3. Introduction of Linear Crane Concept, employing only linear path of container: This adds time to the hoist time increment. Since the trolley does not travel, the load control is much better. The time added due to a longer lift will be more than made up by the time saved by better load control. Various linear crane concepts have been studied since the 1960's, all of these concepts are interesting, but detailed studies will be needed to fully understand the ramification of each on the quay, the initial and operating costs, and the productivity of each concept. This solution is shown in Figure 7.

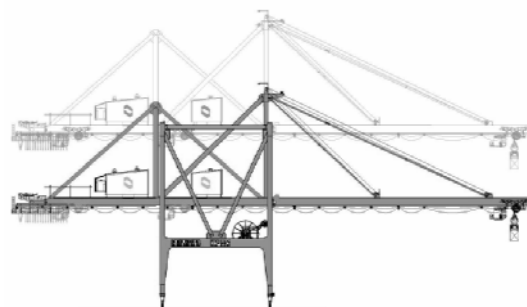


Figure 5. Elevating Girder Crane

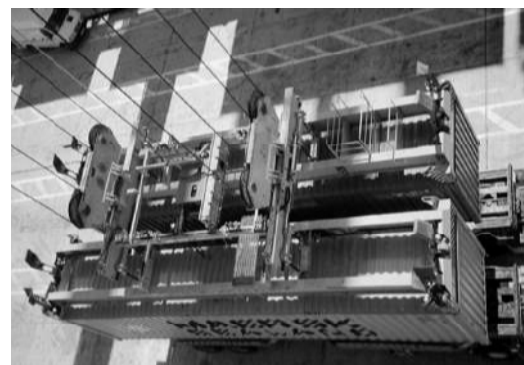


Figure 6. Tandem Forties Spreader

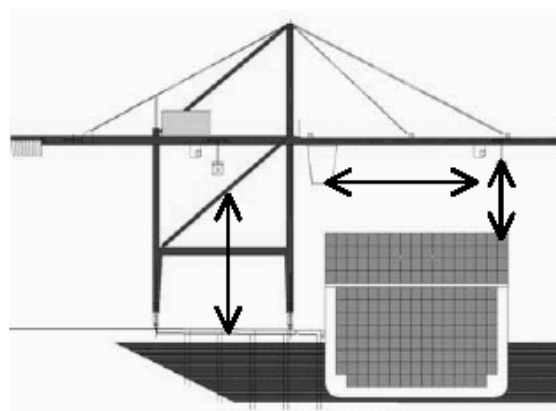


Figure 7. Linear Crane Concept

It is necessary to mention that the properly designed monogirder crane is always lighter than the twin girder

crane that impose the monogirder structure in order to minimize crane weight and optimize cross sections. Minimization of weight imposes truss structure, but on the other side simplicity and high quality of manufacturing impose box sections. For those reasons both solutions are considered equally, with the small advantage of box section. With respect to structural stiffness flexible structure without prior restrictions of deflection is proposed. These facts impose the necessity of doing a more detailed dynamic analysis of cranes structure, by introducing new and accurate dynamic models. Those new models are the basis for creating new advanced control strategies [4].

4. Conclusion

After analyzing the main facts for evaluating cranes performances presented in the paper, the future quayside container crane have to achieve the following level of structural solutions and performances [4]:

1. The basic structural concept is conventional;
2. The outreach should be at least 65 m, because afterward increasing of its length dramatically enrich the final price;
3. The backreach should remain its length of 15,24 m;
4. The gage remains its length of 30,48 m;
5. Trolley velocity have to be at least about 250 m/min, and the acceleration rates about 5 s;
6. The MOT concept of trolley is adopted;
7. The crane have to be at least supplied with semi-automation control system;
8. If necessary, Dual Hoist concept can be introduced;
9. The backreach cross section is box;
10. The outreach cross section is either box or truss, and the part of girder between legs is box.

The adopted quayside container crane belongs to the mega cranes. Dynamic behaviour of mega cranes is completely different comparing with cranes with smaller dimensions and performances. The outreach is most loaded structural part. Because of its huge dimensions and mass, it is most relevant from the aspect of analysis of dynamic behaviour done in [4].

References

- [1] Nishitake, S., Nakada, H., Karasuda, S., Osaki, Y., 2003: Cranes and Forklifts - Material Handling Systems Designed for Safe Transportation, Mitsubishi Heavy Industries Ltd. Technical Review, Vol. 40, No. 1, pp. 1-5.
- [2] Jordan, M. A., 2001: Future-Proof Your Crane, Presented at Conference "TOC Americas '01", Miami, FL, USA.
- [3] Petković Z., Zrnić N., 2002: The Expectations in the Trend of Development of Container Cranes for the XXI Century, Zbornik radova

drugog naučno – stručnog skupa: Vodni saobraćaj u 21. veku, str. 121-128, Saobraćajni fakultet Beograd, Beograd.

- [4] Zrnić, N., 2005: Influence of Trolley Motion to Dynamic behaviour of Ship-To-Shore Container Cranes, Dr. Tech. Sc. dissertation in Serbian, Faculty of Mechanical Engineering Belgrade.
- [5] Petković Z., Zrnić N., 2002: State of the Art of Post-Panamax Ship To Shore Conventional and Modified A-frame Container Cranes, Proceedings of the XVII International Conference on Material Flow, Machines and Devices in Industry "ICMFMDI 2002", pp. 1.78-1.81, Faculty of Mechanical Engineering Belgrade.
- [6] Ioannou, P.A., Kosmatopoulos, E.B., Jula, H., Collinge, A., Liu, C.I., Asef-Vaziri, A., Dougherty, E., 2000: Cargo handling technologies, Final report, Prepared for Task 1.2.3.2 for the Center for Commercial Deployment of Transportation Technologies.
- [7] Casper, W. L., 1999: Coping with Container Gantry Crane Wheel Loads, Port Technology International, No. 11, section 4, pp. 87-90.
- [8] Bhimani, A. K., Hoite, S., 1998: Machinery Trolley Cranes, Proceedings of the Conference "PORTS '98", American Society of Civil Engineering, pp. 603-613, Long Beach, USA.
- [9] Zrnić, N., Petković, Z., 2002: Evaluation of Design Solutions for Trolley of Quayside Container Cranes, Proceedings of the "IRMES 2002" Conference, pp. 99-104, University of Srpsko Sarajevo, Republic Srpska, Bosnia and Herzegovina.
- [10] Zrnić, N., Hoffmann, K., 2004: Development of design of ship-to-shore container cranes:1959-2004, In: History of Machines and Mechanisms, edited by Marco Ceccarelli, pp. 229-242, KLUWER ACADEMIC PUBLISHERS, Dordrecht, Netherlands.
- [11] Zrnić, N., Dragović, B., Petković, Z., 2003: Survey of Some New Concepts that Increase STS Container Cranes Productivity, Proceedings of "Miskolczer Gespraech 2003", Die Neuesten Ergebnisse auf dem Gebiet Foerdertechnik und Logistic, pp. 133-138, Miskolc, Hungary.

This paper is a part of the research project TR 6344 "Research, development and construction of machines for handling and stocking of containers and bulk materials", and research project with specified topic TD 7005 "New methods for defining factors of optimal functioning of river shipping technological subsystems", both supported by Serbian Ministry of Science and Environmental Protection.

SETTING UP THE DYNAMIC MODEL OF BOOM STRUCTURE AT BRIDGE-TYPE STACKER-RECLAIMER

Gašić V.¹, Petković Z.², Bošnjak S.³

Abstract

This paper presents an original concept for setting up the dynamic model of boom structure of coal bridge-type stacker-reclaimers. Given solution of forced vibrations has universal character. Dynamic model, as lumped system, include main constructive parameters, along with variability of boom cross-section and gives needed response for further dynamic analysis of this device. Also, it includes estimated dynamic loadings for bucket chain boom.

Keywords: Dynamic model, bucket chain boom, bridge-type stacker-reclaimer

1. INTRODUCTION

Working simulation of some machine is always performed on idealized models of that machine and, depending of its complexity, can present more or less real situation. Therefore, dynamic models of machines are very important for analysis and providing the insight into the behaviour of machine. Dynamic analysis and modeling are extra needed at material handling machines, especially at cranes, bucket wheel excavators/reclaimers and other heavy machinery. Past analysis of such machines showed dynamic instability even at world known producers of these machines. Also, optimization of constructive-technological parameters of material handling machines can't be performed without dynamic analysis.

Reclaiming bucket chain boom is reclaiming device of coal unloading bridges in thermal plants. These unloading bridges can't be easily classified according to known classification in literature, [7], and have special design characteristics. They belong to the group of bridge-type equipment with blending effect.



Figure 1. Bridge-type stacker-reclaimer; Power plant "Kolubara", V.Crljeni

According to following dynamic concept, it is needed to show main parts of reclaiming device: 1- Top boom

segment, 2 –Bottom boom segment, 3 - Counterweight, 4 – Counterweight carrier, 5 – Lever, 6 – Rope system, 8 – Bucket, 9 – Chain. Dynamic model of boom is set as for independent system.

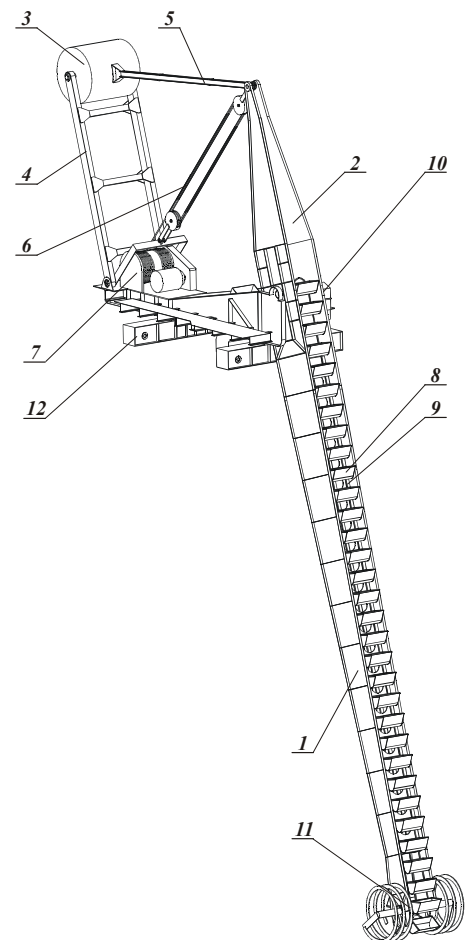


Figure 2. Reclaiming bucket chain boom

¹Ass.Mag.-Ing. Vlada Gašić, Faculty of Mech.Engineering, Kraljice Marije 16, 11000 Belgrade, E-mail: vgasic@mas.bg.ac.yu

²Prof. Dr.-Ing. Zoran Petković, Faculty of Mech.Engineering, Kraljice Marije 16, 11000 Belgrade, E-mail: zpetkovic@mas.bg.ac.yu

³Ao. Prof. Dr.-Ing. Srdan Bošnjak, Faculty of Mech.Engineering, Kraljice Marije 16, 11000 Belgrade, sbosnjak@mas.bg.ac.yu

Adequate influence coefficients are obtained with setting unit forces on to the joints 1 and 2, fig. 5a and 5b, respectively.

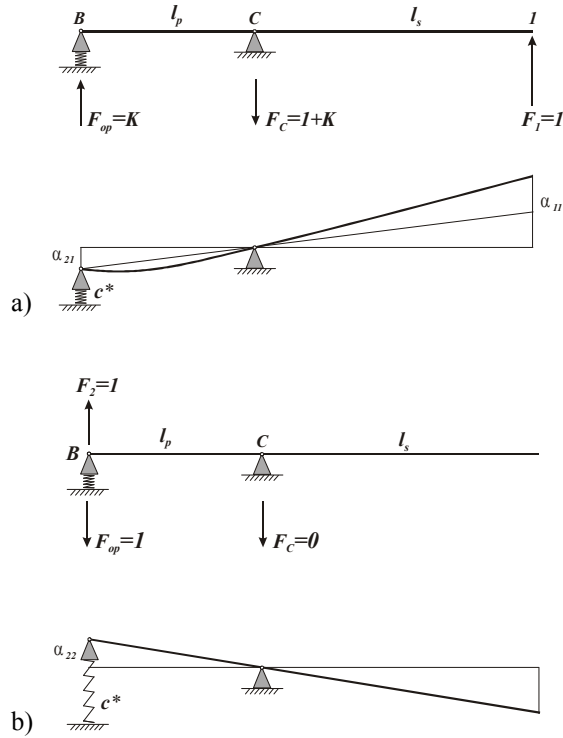


Figure 5. Determination of influential coefficients

According to [4], matrix of influential coefficient is

$$\alpha = \begin{bmatrix} \alpha_{11} & \alpha_{12} \\ \alpha_{21} & \alpha_{22} \end{bmatrix} = \begin{bmatrix} \frac{K^2}{c^*} + \alpha_{11}^* & -\frac{K}{c^*} \\ -\frac{K}{c^*} & \frac{1}{c^*} \end{bmatrix},$$

that is, stiffness matrix of the system

$$C = \alpha^{-1} = \begin{bmatrix} \frac{1}{\alpha_{11}^*} & \frac{K}{\alpha_{11}^*} \\ \frac{K}{\alpha_{11}^*} & \frac{K^2}{\alpha_{11}^*} + c^* \end{bmatrix}.$$

Value α_{11}^* is displacement at outreach end, gained from unit force at outreach end, fig. 6. This value include variability of boom cross-section, presented in [6].

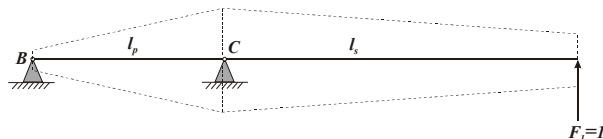
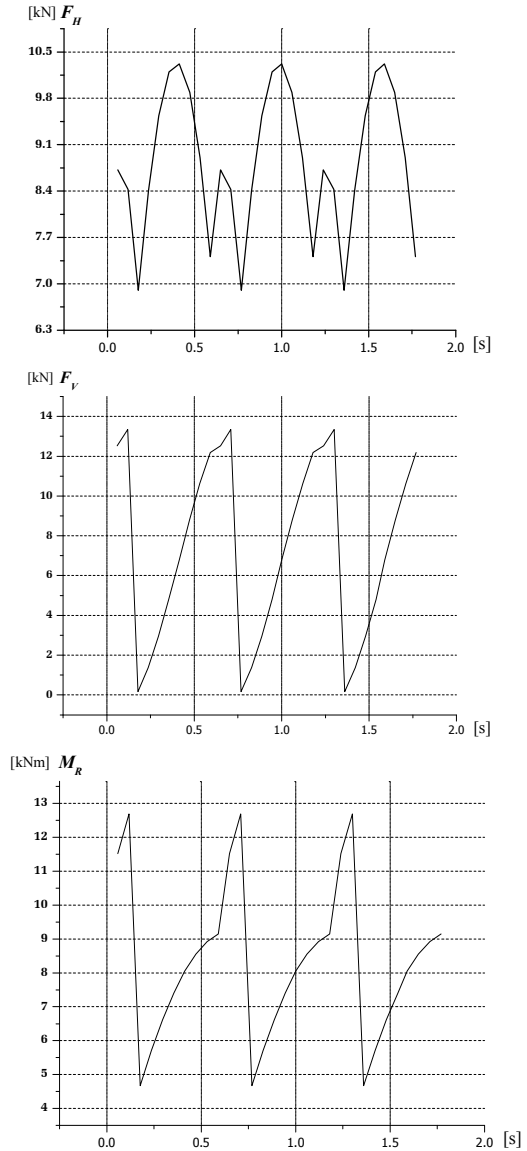


Figure 6. Variability of boom cross-section

3.3 Dynamic loading

Within the coal reclaiming zone, boom is subjected to resistances to coal reclaiming [1]. Dynamic loads acting on boom top are, fig. 3: horizontal force F_H , vertical

force F_V and bending moment M_R . External loads are gained by software [2], and their magnitude charts are presented on following diagrams.



As we can see, they present periodic forcing function and can be described in Fourier series.

Virtual work of forced loading, depending to the boom slope, is given as:

$$\delta A = (-F_H \cos \alpha - F_V \sin \alpha - \frac{M_R}{l_s}) \delta q_1,$$

that is, vector of generalized forces is

$$Q = \begin{bmatrix} -F_H \cos \alpha - F_V \sin \alpha - \frac{M_R}{l_s} \\ 0 \end{bmatrix}$$

Performed harmonic analysis, [4], along with following approximations, give next time functions:

$$F_H(t) = \frac{1}{3} (2F_{H \max} + F_{H \min}) - \frac{4}{\pi^2} (F_{H \max} - F_{H \min}) \cdot \sum_{n=1}^{\infty} \frac{1}{n^2} \cos(n\Omega t)$$

$$F_V(t) = \frac{1}{2} (F_{V \max} + F_{V \min}) - \frac{F_{V \max} - F_{V \min}}{\pi} \cdot \sum_{n=1}^{\infty} \frac{1}{n} \sin(n\Omega t)$$

$$M_R(t) = \frac{1}{2} (M_{R \max} + M_{R \min}) - \frac{M_{R \max} - M_{R \min}}{\pi} \cdot \sum_{n=1}^{\infty} \frac{1}{n} \sin(n\Omega t)$$

4. MATHEMATICAL FORMULATION OF FORCED VIBRATION OF BOOM STRUCTURE

Mathematical model is set through Langranges equations of the second-part that gives differential equation of forced vibration

$$A \cdot \ddot{q} + C \cdot q = Q,$$

After series of well-known transformations in eigenvector analysis, circular frequencies are obtained through next expression

$$\omega_{1,2}^2 = \frac{\left(\frac{m_2 + M}{\alpha_{11}} + m_1 \left(\frac{K^2}{\alpha_{11}^2} + c^* \right) \right) \pm \sqrt{\left(\frac{m_2 + M}{\alpha_{11}} + m_1 \left(\frac{K^2}{\alpha_{11}^2} + c^* \right) \right)^2 - 4 m_1 (m_2 + M) \frac{c^*}{\alpha_{11}}}}{2 m_1 (m_2 + M)}$$

Then, eigenvector coefficients are as follows

$$\eta_{21}^{(i)} = \frac{-\frac{K}{\alpha_{11}^*}}{\frac{K^2}{\alpha_{11}^*} + c^* - (m_1 + M) \omega_{(i)}^2}, \quad i = 1, 2$$

Modal shape matrix is

$$S = \begin{bmatrix} 1 & 1 \\ \eta_{21}^{(1)} & \eta_{21}^{(2)} \end{bmatrix}$$

Concerning the fact that in real cases free vibration are easily damped [5], the emphasis here is on forced vibration which presents final solution of differential equation

$$A \ddot{q} + C q = Q_0 + \sum_i Q_C \cos n \Omega t + \sum_i Q_S \sin n \Omega t$$

$$Q_0 = \begin{Bmatrix} -\cos \alpha \frac{1}{3} (2 F_{Hmx} + F_{Hmn}) - \sin \alpha \frac{1}{2} (F_{Vmx} + F_{Vmn}) - \frac{1}{2 l_s} (M_{Rmx} + M_{Rmn}) \\ 0 \end{Bmatrix} = \begin{Bmatrix} Q_{0,I} \\ 0 \end{Bmatrix}$$

$$Q_C = \begin{Bmatrix} -\cos \alpha \frac{-4}{n^2 \pi^2} (F_{Hmx} - F_{Hmn}) \\ 0 \end{Bmatrix} = \begin{Bmatrix} Q_{C,I}^{(n)} \\ 0 \end{Bmatrix}$$

$$Q_S = \begin{Bmatrix} -\sin \alpha \frac{-1}{n \pi} (F_{Vmx} - F_{Vmn}) - \frac{1}{l_s} \frac{(-1)}{n \pi} (M_{Rmx} - M_{Rmn}) \\ 0 \end{Bmatrix} = \begin{Bmatrix} Q_{S,I}^{(n)} \\ 0 \end{Bmatrix}$$

After series of transformations, finally we get

$$q_0 = \begin{bmatrix} \frac{K^2}{c^*} + \alpha_{11}^* & -\frac{K}{c^*} \\ -\frac{K}{c^*} & \frac{1}{c^*} \end{bmatrix} \begin{Bmatrix} Q_{0,I} \\ 0 \end{Bmatrix}$$

$$q_C^{(n)} = \frac{1}{\Delta_{n\Omega}} \begin{bmatrix} \frac{K^2}{\alpha_{11}^*} + c^* - (m_2 + M)(n\Omega)^2 & -\frac{K}{\alpha_{11}^*} \\ -\frac{K}{\alpha_{11}^*} & \frac{1}{\alpha_{11}^*} - m_1(n\Omega)^2 \end{bmatrix} \begin{Bmatrix} Q_{C,I}^{(n)} \\ 0 \end{Bmatrix}$$

$$q_S^{(n)} = \frac{1}{\Delta_{n\Omega}} \begin{bmatrix} \frac{K^2}{\alpha_{11}^*} + c^* - (m_2 + M)(n\Omega)^2 & -\frac{K}{\alpha_{11}^*} \\ -\frac{K}{\alpha_{11}^*} & \frac{1}{\alpha_{11}^*} - m_1(n\Omega)^2 \end{bmatrix} \begin{Bmatrix} Q_{S,I}^{(n)} \\ 0 \end{Bmatrix}$$

where:

$$\Delta_{n\Omega} = \det[C - A(n\Omega)^2] = \left(\frac{1}{\alpha_{11}^*} - m_1(n\Omega)^2 \right) \left(\frac{K}{\alpha_{11}^*} + c^* - (m_2 + M)(n\Omega)^2 \right) - \left(\frac{K}{\alpha_{11}^*} \right)^2$$

Oscilating motion, in non-resonance case $n\Omega \neq \omega_i$, has following form

$$q_p = q_0 + \sum_1^{\infty} q_C^{(n)} \cos n \Omega t + \sum_1^{\infty} q_S^{(n)} \sin n \Omega t$$

This algorithm presents universal solution of forced vibrations of boom structure.

5. CONCLUSION

In this paper it is set up an original dynamic model of boom structure of brydge-type stacker-reclaimer. Adopted model is of enough mathematical volume for solving the desired problem, because it have two degrees of freedom, i.e. deflection of boom top and counterweight deflection. The stiffnes matrix is determined through influence coefficients, along with deformation superposition. Variability of boom section is included in stiffnes matrix of the whole system. Given solution of differential equations has universal character and can performed of similar structures of material handling machines. First, with certain aproximations, it can be used for dynamic analysis of stationary bucket chain elevators. Also, this concept enables further stress/deformation analysis of reclaiming bucket chain booms at unloading bridges.

REFERENCES

- [1] Bošnjak, S.: Bucket wheel trenchers (in Serbian), Faculty of Mechanical Engineering, Belgrade, 2001.
- [2] Bošnjak, S., Jovković, M., Gašić, V.: PREMO, Software for calculating the external loads caused by coal reclaiming process at bridge-type reclaimers, Faculty of Mechanical Engineering, Belgrade, 2004.
- [3] Dedić, S., Petković, Z., Grujić, B.: Design T-107, Working processes of heavy machinery, Faculty of Mechanical Engineering, Belgrade, 1990.
- [4] Gašić V.: Dynamic behaviour identification of bridge type stacker – reclaimer with bucket chain booms in power plants, M. Sc.Thesis, Faculty of Mechanical Engineering, Belgrade, 2004.
- [5] Radosavljević, Lj.: Theory of vibrations (in Serbian), Faculty of Mechanical Engineering, Belgrade 1981.
- [6] Tuma, J., Munshi, R.: Advanced structural analysis, Schaums outline series, McGraw-Hill, Oklahoma 1971.
- [7] Wöhlbier, R.H.: Stacking, Blending, Reclaiming of Bulk Materials, Trans Tech Publications, First Edition 1977.

This paper is a part of the research project TR 6344 "Research, development and construction of machines for handling and stocking of containers and bulk materials, supported by Serbian Ministry of Science and Environmental Protection.

РЕСУРС ДЕТАЛЕЙ ТРАНСПОРТНЫХ МАШИН – В ЗАВИСИМОСТИ ОТ НАГРУЗОЧНЫХ РЕЖИМОВ

Георги Геннадиев¹

Резюме: В докладе рассматривается зависимость технического ресурса деталей транспортных машин от нагрузочного режима, когда разрушительным процессом является изнашивание. Нагрузочные режимы – переменные: смешанные или раздельные. Доказывается преимущество по ресурсу раздельной нагрузки перед смешанной нагрузкой.

Ключевые слова: надежность, ресурс, изнашивание.

1. НАГРУЗКА И РЕСУРС

Влияние нагрузки на ресурс транспортных машин является объектом исследования автора настоящей работы. Преимущество по ресурсу раздельной нагрузки в сравнении со смешанной нагрузкой доказано – обобщено и представлено в [1]:

- в чисто теоретическом аспекте;
- при помощи аналитически-статистических моделей;
- в связи с обработкой результатов статистических наблюдений;
- путем экспериментов разрушения деталей-образцов в стендовых условиях и др.

Здесь будут представлены результаты сравнительных исследований изнашивания деталей и их ресурсов в условиях смешанных и раздельных переменных нагрузочных режимов.

2. ИЗНАШИВАНИЕ И РЕСУРСЫ

Пусть I – означение наличной толщины рабочего слоя новой детали, т.е. это её *физический ресурс*. Этот слой изнашивается (физический ресурс расходуется) со скоростью i . Тогда *технический ресурс* (далее будем называть только ресурс) T можно выразить:

$$(1) \quad T = \frac{I}{i}.$$

Если известны n различных скоростей изнашивания, то им соответствуют различные ресурсы:

$$(2) \quad T_j = \frac{I}{i_j},$$

где i_j – отдельные скорости изнашивания, а T_j – соответствующие им ресурсы ($j = \overline{1, n}$).

Сейчас соображаем другую возможность, когда в расходовании физического ресурса принимают участие отдельные скорости i_j – каждая с относительным участием $\alpha_j^{\text{физ.}}$; формируется смешанный ресурс $T^{\text{смесь}}$:

$$(3) \quad \sum_{j=1}^n \frac{\alpha_j^{\text{физ.}} I}{i_j} = T^{\text{смесь}} = \frac{I}{i^{\text{смесь}}} \left(\sum_{j=1}^n \alpha_j^{\text{физ.}} = 1 \right),$$

где $i^{\text{смесь}}$ – скорость смешанного изнашивания.

¹ Георги Борисов Геннадиев – доц., д-р, инж., Высшее транспортное училище им. Т. Каблешкова, София, Болгария, e-mail: ggenad@abv.bg

Или из (3) и (2):

$$(4) \quad \sum_{j=1}^n \alpha_j^{\text{физ.}} T_j = T^{\text{смесь}}.$$

С расходом относительной части $\alpha_j^{\text{физ.}}$ физического ресурса I – со скоростью i_j , расходуется относительная часть α_j ресурса $T^{\text{смесь}}$, т.е.:

$$(5) \quad \frac{\alpha_j^{\text{физ.}} I}{i_j} = \alpha_j T^{\text{смесь}};$$

$$(6) \quad \alpha_j^{\text{физ.}} T_j = \alpha_j T^{\text{смесь}} \left(\sum_{j=1}^n \alpha_j = 1 \right).$$

Тогда:

$$(7) \quad \alpha_j = \alpha_j^{\text{физ.}} \frac{T_j}{T^{\text{смесь}}};$$

$$(8) \quad \alpha_j^{\text{физ.}} = \alpha_j \frac{T^{\text{смесь}}}{T_j};$$

$$(9) \quad \sum_{j=1}^n \alpha_j T^{\text{смесь}} = T^{\text{смесь}}$$

(вид, принимаемый выражением (4) в соответствии с (6)).

Таблица 1

		$A_p,$ Nm				
		100	200	300	400	500
$i,$ $\times 10^{-2} \mu m / h$	$i_{\text{гильз цил.}}$	1,436	1,607	1,977	2,590	3,489
	$i_{\text{смесь, гильз цил.}}$	2,239				
	$i_{\text{кор. подш.}}$	2,423	2,996	3,875	5,039	6,474
	$i_{\text{смесь, кор. подш.}}$	4,186				
	$i_{\text{шат. шеек}}$	2,980	3,958	5,461	7,453	9,912
	$i_{\text{смесь, шат. шеек}}$	5,818				
$h,$ $\times 10^{-2} \mu m / h$	$h_{\text{шат. подш.}}$	8,700	9,460	10,901	13,101	16,120
	$h_{\text{смесь, шат. подш.}}$	11,992				

Таблица 2

$\alpha^{\text{физ.}}$	$\alpha^{\text{физ., гильз цил.}}$	0,10	0,15	0,20	0,25	0,30
	$\alpha^{\text{физ., кор. подш.}}$					
	$\alpha^{\text{физ., шат. шеек}}$					
	$\alpha^{\text{физ., шат. подш.}}$					

Таблица 3

α	$\alpha_{\text{гильз цил.}}$	0,1559	0,2090	0,2265	0,2161	0,1925
	$\alpha_{\text{кор. подш.}}$	0,1728	0,2096	0,2160	0,2077	0,1940
	$\alpha_{\text{шат. шеек}}$	0,1925	0,2205	0,2131	0,1952	0,1761
	$\alpha_{\text{шат. подш.}}$	0,1378	0,1901	0,2200	0,2288	0,2232

Таблица 4

Ниже средние скобки обозначают численную стоимость вложенных в них физических ресурсов, выраженных в μm .

		$A_p,$ Nm				
		100	200	300	400	500
Ресурси T, h	$T_{\text{гильз.цил.}},$ $\times [I_{\text{гильз.цил.}}]$	69,638	62,228	50,582	38,610	28,661
	$T_{\text{разд.,гильз.цил. ср.}},$ $\times [I_{\text{гильз.цил.}}]$	49,944				
	$T_{\text{смесь,гильз.цил. ср.}},$ $\times [I_{\text{гильз.цил.}}]$	44,665				
	$T_{\text{кор.подш.}},$ $\times [I_{\text{кор.подш.}}]$	41,271	33,378	25,806	19,845	15,446
	$T_{\text{разд.,кор.подш. ср.}},$ $\times [I_{\text{кор.подш.}}]$	27,149				
	$T_{\text{смесь,кор.подш. ср.}},$ $\times [I_{\text{кор.подш.}}]$	23,890				
	$T_{\text{шат.шеек}},$ $\times [I_{\text{шат.шеек}}]$	33,557	25,265	18,312	13,417	10,089
	$T_{\text{разд.,шат.шеек ср.}},$ $\times [I_{\text{шат.шеек}}]$	20,128				
	$T_{\text{смесь,шат.шеек ср.}},$ $\times [I_{\text{шат.шеек}}]$	17,189				
	$T_{\text{шат.подш.}},$ $\times [H_{\text{шат.подш.}}]$	11,494	10,571	9,173	7,633	6,203
	$T_{\text{разд.,шат.подш. ср.}},$ $\times [H_{\text{шат.подш.}}]$	9,015				
	$T_{\text{смесь,шат.подш. ср.}},$ $\times [H_{\text{шат.подш.}}]$	8,339				

Из левой и правой стороны двойного равенства (3) следует, что:

$$(10) \quad \sum_{j=1}^n \frac{\alpha_j^{\text{физ.}}}{i_j} = \frac{1}{i^{\text{смесь}}} ;$$

$$(11) \quad i^{\text{смесь}} = \frac{1}{\sum_{j=1}^n \frac{\alpha_j^{\text{физ.}}}{i_j}} .$$

Тогда правое равенство в (3) в соответствии с (11) принимает вид:

$$(12) \quad T^{\text{смесь}} = \frac{I}{i^{\text{смесь}}} = I \sum_{u=1}^n \frac{\alpha_u^{\text{физ.}}}{i_u} .$$

Пусть так полученное выражение для $T^{\text{смесь}}$ заместим в (5):

$$(13) \quad \frac{\alpha_j^{\text{физ.}} I}{i_j} = \alpha_j T^{\text{смесь}} = \alpha_j \frac{I}{i^{\text{смесь}}} ,$$

откуда и в соответствии с (11):

$$(14) \quad \alpha_j = \frac{i^{\text{смесь}}}{i_j} \alpha_j^{\text{физ.}} = \frac{\alpha_j^{\text{физ.}}}{i_j \sum_{u=1}^n \frac{\alpha_u^{\text{физ.}}}{i_u}} .$$

Возможно и другое представление ресурса $T^{\text{смесь}}$ [1]:

$$(15) \quad T^{\text{смесь}} = \frac{1}{\sum_{j=1}^n \frac{\alpha_j}{T_j}} .$$

Исходя из организационно-эксплуатационным соображениям, можно рассматривать два средних ремонтов – $T_{\text{ср.}}^{\text{смесь}}$ и $T_{\text{ср.}}^{\text{разд.}}$, если режим нагружения соответственно смешанный и раздельный:

$$(16); (17) \quad T_{\text{ср.}}^{\text{смесь}} \equiv T^{\text{смесь}} ; T_{\text{ср.}}^{\text{разд.}} = \frac{\sum_{j=1}^n T_j}{n} .$$

В данных выше выражениях вместо I и i (без индексов или с индексами) могут стоять соответственно H – изменение рабочего зазора, и h (тоже без индексов или с индексами) – скорость изменения зазора.

3. РЕЗУЛЬТАТЫ

Пользуясь экспериментальными зависимостями скоростей i_j и h_j от амплитуды $A_{p,j}$ переменного нагрузочного режима (когда частота f_p этого режима – неизменная) [2], нами получены результаты, представленные в таблицах, где:

- представлены вычисленные параметры изнашивания и ресурсы деталей *гильз цилиндров*, *коренных подшипников*, *шатунных шеек* и *шатунных подшипников* двигателя КамАЗ-740, для которых использованы соответствующие индексы *гильз.цил.*, *кор.подш.*, *шат.ш.еек* и *шат.подш.*;
- отсутствуют нумерации стоимостей – посредством индекса j , т.е. чередование смешивания нагрузочных режимов не оказывает влияние на средние ресурсы;
- в таблице 2 задано относительное участие отдельных скоростей;
- в таблице 1 показаны скорости;
- в таблице 3 видно относительное участие отдельных ресурсов;
- в таблице 4 можно сравнить вычисленные ресурсы.

4. ВЫВОДЫ

- Получены характерные зависимости между ресурсами и скоростями изнашивания.
- В таблице 4 продемонстрировано преимущество по ресурсу раздельного нагрузочного режима перед смешанным нагрузочного режима.

ЛИТЕРАТУРА

- [1] Геннадиев, Г. Изразходване на ресурса на машините и качество на системите за техническо обслужване и ремонт (теоретичен подход). С., ВЦМКНИ, 2004.
- [2] Денисов, А. С., Басков, В. Н. Особенности изнашивания деталей при переменных режимах работы агрегатов. Санкт-Петербург, *Двигателостроение*, № 4, 2003, с. 46-48.

BEHAVIOR OF OVERHEAD TRAVELING CRANE'S CARRYING STRUCTURE DURING JOINT OPERATION OF HOISTING AND TROLLEY MECHANISMS

Miloradović N.,¹ Slavković R.,² Vujanac R.³

Abstract

The paper presents analysis of the stress state of the overhead traveling crane carrying structure during joint operation of hoisting and trolley mechanisms. The crane carrying capacity is 32 tons. It has two main girders with box shaped profiles. Dynamical model is adopted and dynamical equations of motion are set and solved using Newmark step-by-step method. Modeling of the overhead traveling crane carrying structure is performed using shell finite elements. The results of the analysis are shown as effective stress and deformation fields at main girders.

Keywords: overhead traveling crane, carrying structure, Finite element method

1. INTRODUCTION

Exploitation of the overhead traveling cranes has shown that non-stationary operating regimes induce occurrence of variable loads that act on the carrying structure and mechanisms of the crane. Therefore, it is important to establish, as precisely as possible, stress and deformation state at loaded crane's structure.

2. MATHEMATICAL MODEL

Main girders of the overhead traveling crane are represented by beams with constant cross-sections and articulated supports. Considering the importance of transverse vibration of the overhead traveling crane's carrying structure in vertical plane, eigenfrequencies of the unloaded beam are defined by the expression:

$$\omega_i = i^2 \cdot \pi^2 \sqrt{\frac{E \cdot I}{m \cdot l^3}}, \quad i = 1, 2, \dots$$

Forced vibrations of the beam may be represented by equation:

$$M_i \frac{d^2 q_i}{dt^2} + C_i q_i = 2F \sin \frac{i\pi x}{l} \quad (1)$$

For the i-th vibration mode, we have:

$$M_i = \int_0^l \Phi_i(x) m(x) dx, \quad C_i = M_i \omega_i^2 = \frac{i^4 \pi^4 EI}{l^3},$$

$$q_i = q_i(t), \quad F = F(x, t), \\ \phi_i = \sin \frac{i \cdot \pi \cdot x}{l}, \quad i = 1, 2, \dots$$

It is assumed that transverse beam vibrations may be represented by [1]:

$$f(x, t) = \sum_{i=1}^{\infty} [q_i(t) \Phi_i(x)] \quad (2)$$

3. MODELING OF THE CARRYING STRUCTURE USING THE FINITE ELEMENTS

Geometrical model of the carrying structure of overhead traveling crane is formed using the "FEMAP" software. Corresponding model with no loads and deformations is shown in Figure 1.

The model contains four-node shell elements and has 1934 elements and 1598 nodes. The main girders of the crane with corresponding vertical braces are shown in Figure 2. In order to obtain more realistic stress distribution at support areas, triangular shell elements are used.

The first results of the dynamic analysis are the values of eigenfrequencies of the carrying structure of the overhead traveling crane. The first three vibration modes are shown in Figures 3, 4 and 5.

¹ Nenad Miloradović, M. Sc., assistant, The Faculty of Mechanical Engineering, Kragujevac, e-mail: mnenad@kg.ac.yu

² Radovan Slavković, Ph. D., full professor, The Faculty of Mechanical Engineering, Kragujevac, e-mail: radovan@kg.ac.yu

³ Rodoljub Vujanac, B. Sc., assistant, The Faculty of Mechanical Engineering, Kragujevac, e-mail: vujanac@kg.ac.yu

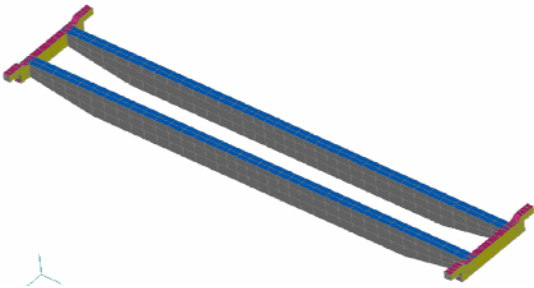


Fig. 1 Geometrical model of the overhead traveling crane

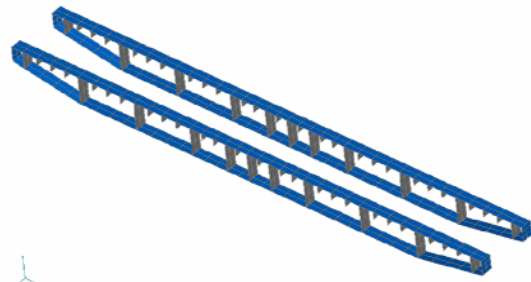
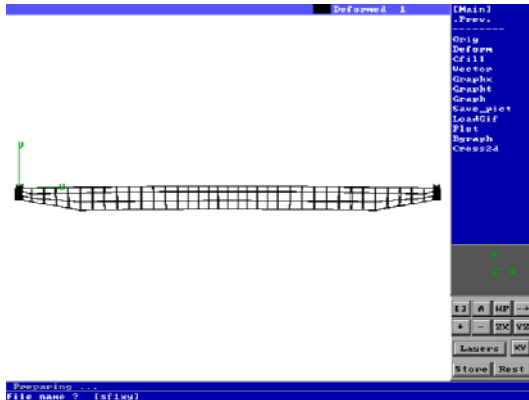
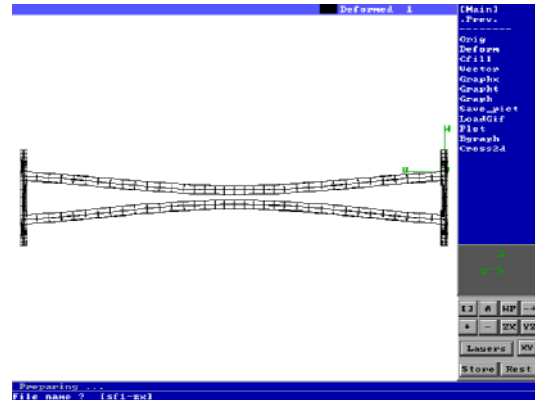


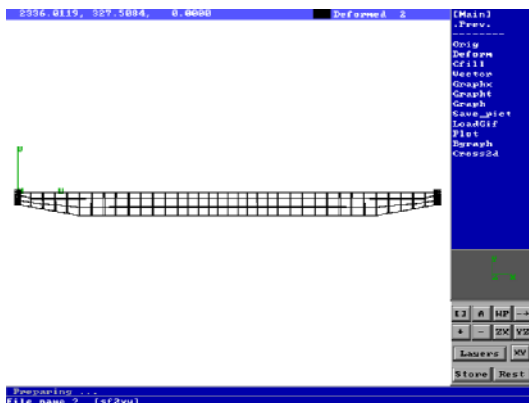
Fig. 2 Main girders of the overhead traveling crane



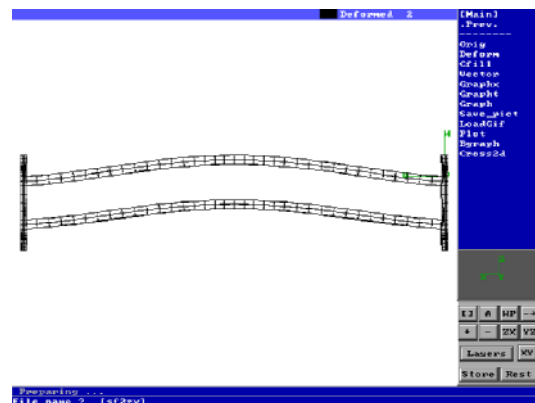
Vertical plane



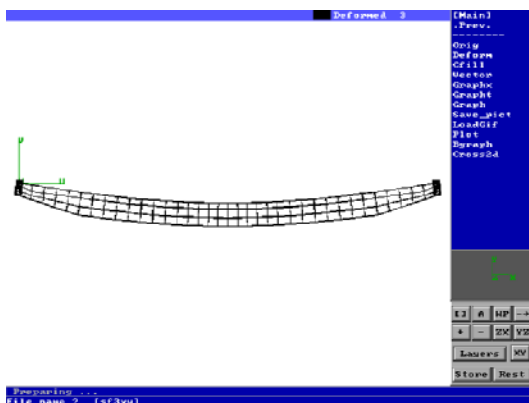
Horizontal plane

Fig. 3 The first vibration mode $\nu_1 = 1.6412$ Hz

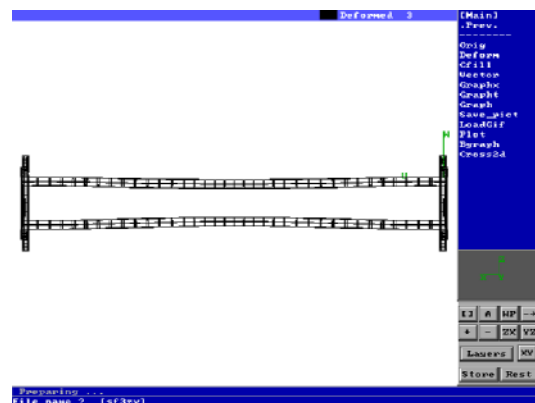
Vertical plane



Horizontal plane

Fig. 4 The second vibration mode $\nu_1 = 1.74459$ Hz

Vertical plane



Horizontal plane

Fig. 5 The third vibration mode $\nu_1 = 2.82646$ Hz

As mentioned before, dynamical loads at cranes appear during non-stationary operating regimes of any mechanism of the crane. According to regulations, the number of simultaneous independent motions of the crane must not exceed two in the case when a man is operating the crane. The larger number of motions is possible to obtain in the case of automated crane operation. The majority of authors consider the problem of dynamical crane loads for each independent motion. A small number of researchers have investigated in detail a problem of joint operation of two crane's mechanisms and possibilities for complete automation of its operation. A case of lifting the load off the ground with joint operation of the trolley mechanism is not considered here, since "the tweaking" of the load off the ground is forbidden.

The essence of the analysis is in the fact that differential equations are formed based on proposed dynamical model. In cases when only hoisting mechanism operates, coordinate x_k has constant value, i.e. the position of the trolley is fixed. During presentation of the results, characteristic positions of the trolley at the carrying structure of the crane will be adopted. If movable load or the following of the trolley's motion along the girders is considered, speed of the trolley is introduced into calculations with the adoption of the expression $x_k = v_k \cdot t$, Figure 6.

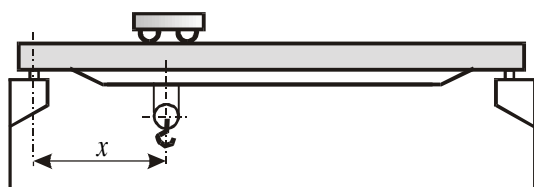


Fig. 6 The position of the trolley

By replacing this expression in the equations of motion, a new system of equations is gained and some of the solutions are presented through the analysis of the results in this paper. Time dependence of the forces that act upon the carrying structure of the crane is obtained as one of the solutions. These time dependences are actuating forces, i.e. they will be used as inputs for the program in the process of numerical analysis using finite elements method.

4. PRESENTATION OF THE RESULTS

Systems of differential equations that describe dynamical behavior of the overhead traveling crane in vertical plane at non-stationary operating regimes are solved using Runge-Kutta numerical method by application of MathLab software. Due to shortage of experimental results, time functions of forces acting upon the carrying structure of the overhead traveling crane are obtained as the results of MathLab simulations. Forces obtained in such a manner are specified at corresponding points of the carrying structure of the model formed using the Finite Element Method (shown in Figure 1). Values of stress and deformation states in all structure elements are obtained using "PAK" software [3]. Fields of displacements and effective stresses are shown at moments when maximal values are obtained for every listed calculation case, Figures 7 and 8. Such values may be compared with allowed stress states at the same elements obtained using JUS standards for cranes.

Actuation forces acting positions, i.e. the number of nodes at which these forces act depending on position of the trolley along the carrying structure, are shown in Figure 9:

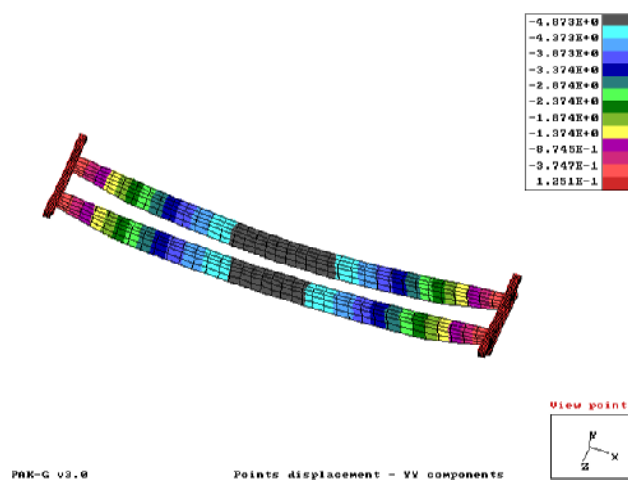


Fig. 7 Displacements in y-direction – deformed model

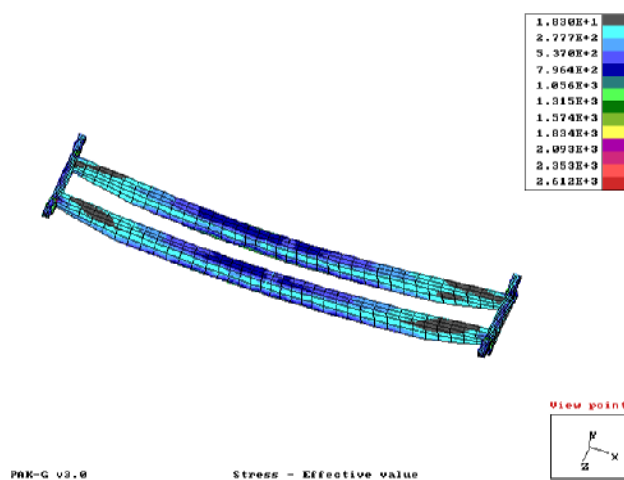


Fig. 8 Effective stress distribution

- a) Trolley position 1 – position of load application
 b) Trolley position 2 – arrows denote forces with which trolley wheel act upon the carrying structure of the crane, numbers beside denote nodes at which mentioned forces act.

- c) Spatial presentation of the carrying structure
- nodes 524 and 530 are at $x=3.647$ m distance from the axis of the crane's left wheel,
 - nodes 791 and 808 are at the middle of the span of the carrying structure.

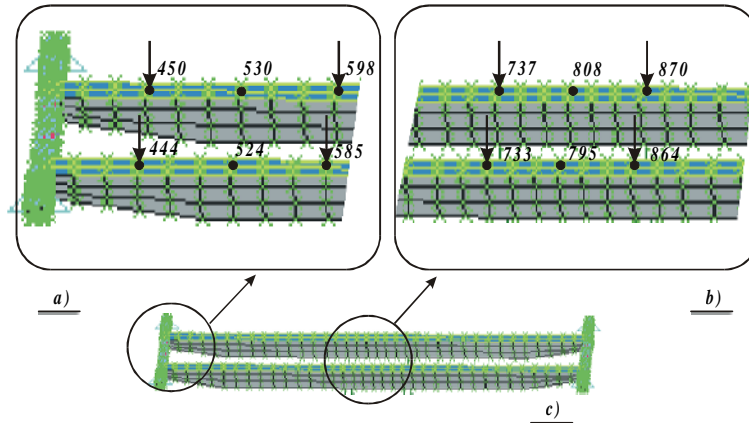


Fig. 9 Loads of the carrying structure of the overhead traveling crane

In order to realistically give the influence of the moving loaded trolley on the carrying structure, vertical force at the trolley's wheel is multiplied at every node by corresponding time function $f(t)$ obtained using "FORTRAN" program. Function $f(t)$ enables that corresponding structure node is loaded depending on instantaneous position of the trolley. For example, if the trolley wheel is positioned immediately above the node, a full scale force is acting on the node, and if movable load is positioned in the area between the nodes, the load is proportionally distributed on nearby nodes. As an illustration, loads at structure nodes in the case of movable unit acting force are presented in Figure 10. Time interval of 18 s denotes time required for the trolley to reach the middle of the span of crane.

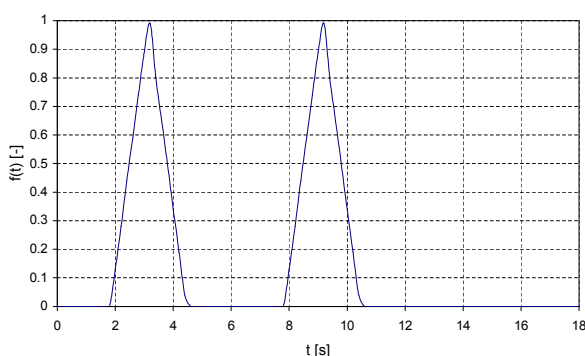


Fig. 10 Distribution function of the movable unit load at the node

5. CONCLUSIONS

Proposed geometrical model of the overhead traveling crane's carrying structure enables the analysis of time variations of various selected quantities (forces, displacements) in the regime of joint operation of the hoisting mechanism and the trolley mechanism of the

crane.

A quick insight on the influence of individual quantities on dynamic behavior of the crane may be obtained with taking into account the variation of the drive force and input parameters, such as stiffness, damping, speed, etc.

With the application of "PAK" ready-to-use modules and some minor model modifications, it might be possible to compare the dynamic behavior of similar crane types.

6. REFERENCES

- [1] Ostric, D.: "Dynamics of overhead traveling cranes", (in Serbian), Faculty of Mechanical Engineering, Belgrade, 1998
- [2] Kojic M., Slavkovic R., Zivkovic M., Grujovic N.: "The Finite Element Method I – Linear Analysis", (in Serbian), Faculty of Mechanical Engineering, Kragujevac, 1998
- [3] Kojic M., Slavkovic R., Zivkovic M., Grujovic N.: "PAK-S Program for FE Structural Analysis", Faculty of Mechanical Engineering, Kragujevac
- [4] Technical documentation of the overhead traveling crane having 32 tons portability, (in Serbian), "Zastava Factory", Kragujevac

ADVANTAGES OF CONTEMPORARY, MODULAR, LIGHTWEIGHT PROFILE BRIDGE CRANE AND MONORAIL SYSTEMS

Brkić A.¹, Petrović Z.², Bugarić U.³

Abstract

This paper presents advantages of modular lightweight crane and monorail solutions. Also it presents Profile Master, user friendly software for preprocessing end-user solutions. With Profile Master monorail systems as well as single girder and double girder systems could be developed.

Keywords: *Modular, lightweight, monorail, double and single girder, bridge crane, solutions, Profile Master*

1. INTRODUCTION

During past decade, there wasn't any relevant investment in industry in Serbia. That was the case in almost all industry branches, but especially in equipment for vertical transportation. As one can see, things are changing and investments in transportation equipment are becoming reality. No one can imagine that final product can be competitive on very rough market as Serbia has become, without efficient transportation systems within workshops. High investments are needed for high quality vertical transportation equipment, but solutions that include modular lightweight crane, or monorail systems are low cost solutions that can fit in almost any warehouse, or workshop. Modular solutions are becoming primary choice when thinking about vertical transportation from 125 – 2000 kg nominal weight.

2. DESCRIPTION

Lightweight profile solutions that are made in SWF Krantechnik facilities, called Profile Master, are used in two ways. First way is monorail hoist that is attached to profile. Trolley is using inside of the profile as railway. That way no dust or metal sawdust can't get inside of the system. No additional lubricating of the wheels is necessary that way. Maximal load of the monorail systems is between 125 and 2000 kg's no matter how many trolleys are running on the same profile. Systems are often used in industrial facilities, for certain technological processes, or as part of maintenance systems in workshops. They are efficient, low costing, and easy to install. On the other hand, if there is need to completely change flow of material within factory or workshop, system can be easily moved to fit current needs. Lightweight modular systems are used in food industry, for production lines in plastic industry, very

often in automotive industry, etc. One of the monorail systems is installed in Peugeot factory in France. Monorail runways can be curved. That way more complex material flow can be accomplished. Standard angles for curved tracks are 10, 15, 30, 45, 60, and 90 degree, with standard radius of 1500 mm. Other radius (e.g. 1000 mm), are available on request.

Advantages of modular lightweight monorail systems are: easy installation, low cost maintenance, system could be installed in almost any condition (attached to roof construction, walls, existing beams, etc.). Main advantage over classic monorail system is that lightweight systems are 30-60% lighter, which means that lightweight system is applicable in situations in which classic monorail systems can't be installed.



Figure 1. Profile Master system in Peugeot factory, France

Second solution is single or double girder bridge cranes. This way whole area of workshop, or warehouse is covered with transportation system. There are some limitations for applying modular lightweight cranes,

¹ Ass. M.Sc.-Ing. Aleksandar Brkić, Faculty of Mech.Engineering, Kraljice Marije 16, 11000 Belgrade, E-mail: abrkić@mas.bg.ac.yu

² Ing. Zoran Petrović, BaTREX, Bulevar Arsenija Čarnojevića 42, 11070 Belgrade, E-mail: zoki99@yubc.net

³ Doc. PhD.-Ing. Uglješa Bugarić, Faculty of Mech.Engineering, Kraljice Marije 16, 11000 Belgrade, ubugaric@mas.bg.ac.yu

concerning length of main girder. Main girder can't be more than six meters long (deflection and torque).

For distances between runways (span) more than six meters, I beam should be used instead of lightweight profile. Double girder bridge cranes are used for spans and loads that are near the limits of lightweight systems (6 meters, 2000 kg's).

Main advantage of lightweight systems is easy installation, and fact that system is adaptable to any type of warehouse or workshop, no matter of it's construction. Suspensions represent maybe most important part of a lightweight systems. Their articulated construction minimizes the horizontal stress transmitted to the building structure. The suspensions are available in different sizes depending on the existing structures and can be connected to any I or H beam, or straight to the ceiling or a wall. Side supports provide a reinforcement against the horizontal stresses and also prevent runaways or monorails from swaying.

2. SOFTWARE FOR PROFILE MASTER (SYSTEM 2000)

Profile Master wouldn't be such easy applicable, and fast installing system without software that helps crane designer to bring optimal solutions in just a second. There are only few input data that are necessary for program to develop optimal transportation system for current project.

When starting System 2000, software for calculating and optimizing lightweight systems, user-friendly window, offers to choose between monorails and cranes.

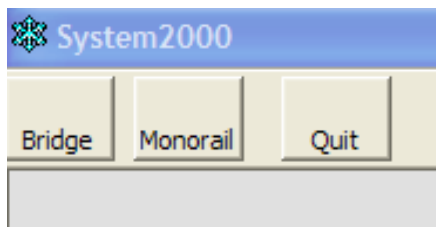


Figure 2. Main window for choosing calculation for Bridge or Monorail system, System 2000, SWF Krantechnik

No matter what has been chosen, input parameters must be defined. When all necessary data entered, System 2000 does basic calculation for type of runaway (UKA20,30 or 40), and the type of main girder (the same profiles), while optimizing solutions.

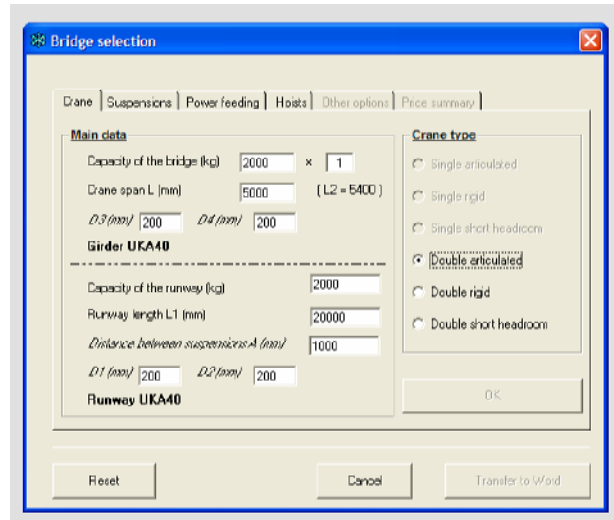


Figure 3. Basic parameters for Bridge crane calculation, System 2000, SWF Krantechnik

In addition to main data, suspension's must be defined. There are 4 main types of suspension's (Short and long ceiling suspensions, short and long articulated suspensions – for walls and ceiling, and special type suspensions for I beams and wood beams and other non-standard solutions).

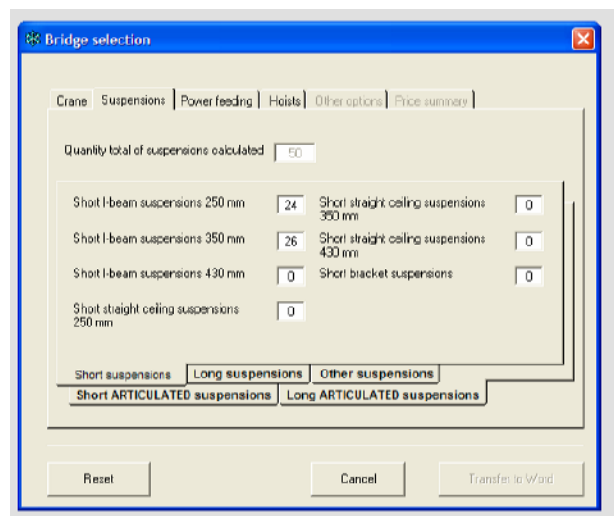


Figure 4. Defining suspensions, System 2000, SWF Krantechnik

With this data runaway is completely defined. Now, crane and trolleys must be chosen. There are many of parameters that should be adjusted. For example, parameters for crane motion (manual, motorized with varying speeds), manual or motorized trolleys, hoisting speed, etc. must be set. One more detail is to choose how crane and hoist should be fed with power.

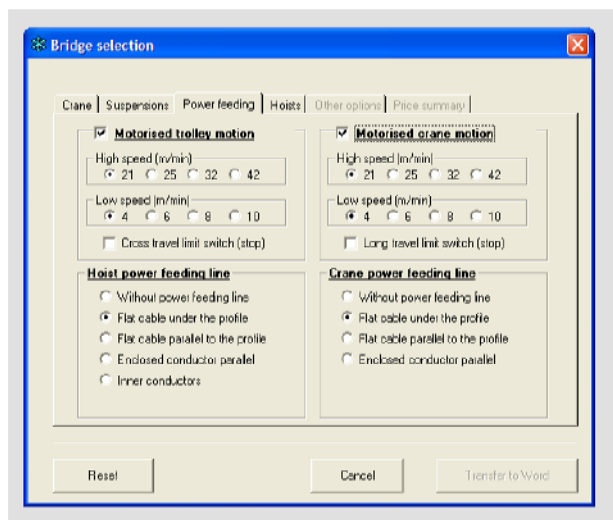


Figure 5. Choosing between various parameters for crane and trolley motion, and power feeding lines, System 2000, SWF Krantechnik

Last data needed for making complete project is defining power supply, and non-standard equipment. There are lot of standard power supplies to choose from, but system could be adjusted to any voltage and/or frequency. Special equipment include thermal overload protector (installed on lifting motor, for protecting it from overheating), time meter (measures operating time, Safe Working Period, etc.), additional main switch with rising cable. Particular advantage of the Profile Master is Radio remote control Radio Master2, that could be installed separately from standard control that comes along with hoist.

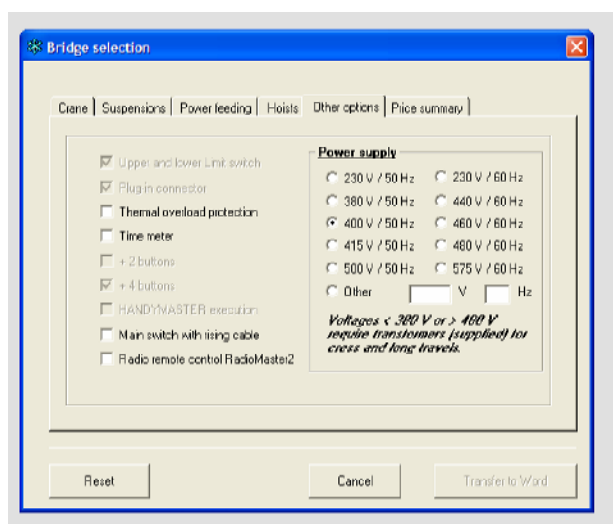


Figure 6. Defining power supply and special equipment, System 2000, SWF Krantechnik

With all data defined optimal solution for current project is calculated. Output of System 2000, is preliminary solution for current project with all necessary technical data.

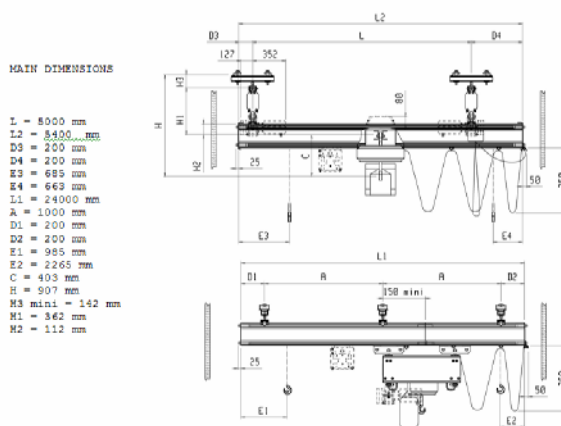


Figure 7. Main technical data as result of calculation, System 2000, SWF Krantechnik

4. CONCLUSION

Flexible and individually adjustable lightweight crane systems are applicable for all types of warehouses, workshops, or any other building. System can be easy installed thanks to system connections (suspensions). With modular system smooth lifting and positioning of loads, can be made with minimum tolerances. Profile Master is suitable for large spans, and also available for various headrooms. Monorails can be design with curves, switch points and turntables. Lightweight systems have prolonged service life combined with low maintenance cost. Main advantage of modular lightweight systems is that they are easy to design with user friendly software solution from SWF Krantechnik, System 2000. That way complete preprocessing project could be finished in very short time, and provide high advantage over competence.

REFERENCES

- [1] SWF Krantechnik.: Technische Daten Profile Master, SWF Krantechnik, 2001.
- [2] Ostrić, D.: Cranes (in Serbian), Faculty of Mechanical Engineering, Belgrade, 1992.
- [3] Petrović, Z.: Design of modular jib cranes with Mechanical Desktop 6.0 - Master thesis, Faculty of Mechanical Engineering, Belgrade, 2003.

ROBUST STABILITY OF NETWORKED CONTROL SYSTEMS BASED ON LYAPUNOV-RAZUMIKHIN THEORY

Vojislav Filipovic

Abstract: A model of the networked control systems (NCS) is considered in the presence of network-induced delay, the data packet dropout in the transmission and unmodeled dynamics. The model is equivalent to a linear system with a bounded time-varying delay. For such system the state feedback controller is proposed. Using Lyapunov-Razumikhin theory stability of system is considered. In the form of theorem the improved delay-dependent stability criteria are formulated.

Key words: Networked control systems, Razumikhin theorem, Stability

1. Introduction

Many modern control systems have some control loops that are closed via a serial communication channel that transmit signals from many sensors and actuators in the system. The examples are well known high-speed LAN such as Ethernet (standard IEEE 802.3) and Token Ring (standard IEEE 802.5)[1]. Networked control systems (NCS) are currently receiving considerable attention in the literature [2]-[4]. The basic problems in NCS are: network induced delay, single-packet or multiple packet transmission of plant inputs and outputs and dropping of network packets [5]. Also, the serial communication channel has many nodes (sensor and actuators) where only one node can report its value at the time so that scheduling of NCS is a very important task [6].

A basic problem in an NCS is the stability of the system. Different approaches exist for such kind of problems. When only messages from a sensor are transmitted through a network the NCS can be approximated by continuous time model, a perturbation method of stability analysis of NCS is considered in [7]. A model based stability of NCS is considered in [8]. Stability problem of NCS, based in hybrid system technique, has been investigated in [5]. Hybrid control systems recently is considered in series of author's papers [9]-[13]. In all of the above works one first designs the controller without taking into account the network and then, in the second step, one determines a design parameter, known as a maximum allowable transfer interval, so that the closed loop remains stable.

The controller design for the NCS, for stochastic control systems, have been proposed in [14] and [15]. The NCS, in the frame of constrained control and estimation, is considered in [16]. Stability and robustness of high-speed networks, using randomized algorithms, is considered in [17]. In [18] the model of the NCSs is provided under consideration of both the network-induced delay and the data packet dropout in the

transmission. The controller design method is based on delay-dependent approach.

Nonlinear NCS have received less attention. Such problems are considered in [19] and [20]. In the reference [20] the result on input-output L_p stability of NCS are presented for a large class of network scheduling protocols. In this paper we will consider the controller design for the NCS in the presence of model uncertainty. The uncertainty is described by affine family of matrices. Also, model includes network-induced delay and data packet dropout in the transmission. As in [18] it is supposed that sensor is clock driven, the controller and actuator are event driven, and the data are transmitted in the form of single packet. In this paper we will improve results from [21].

2. Problem formulation

The continuous system with unmodeled dynamic is given as

$$\dot{x}(t) = A(q)x(t) + Bu(t) \quad (1)$$

$$A(q) = A + \sum_{i=1}^e q_i A_i, \quad q \in Q \quad (2)$$

where $x(t) \in R^n$ and $u(t) \in R^m$ are the state vector and control input respectively. The $A(q)$ is affine family of matrices by which the uncertainty is described. It is supposed that sensor is clock-driven, the controller and actuator are event driven and the data is transmitted as a single packet.

The control input is realised as a zeroth-order hold. That means that the input is piecewise constant function. The system (1), if we take into account network-induced delay and network packet dropout, will take the form [5], [18]

$$\dot{x}(t) = A(q)x(t) + Bu(t), \quad t \in [i_k h + \tau_k, i_{k+1} h + \tau_{k+1}) \quad (3)$$

$$u(t^+) = Kx(t - \tau_k), \quad t \in \{i_k h + \tau_k\}, \quad k = 1, 2, \dots \quad (4)$$

where h is sampling period, $i_k, k = 1, 2, \dots, 3$ are some integers and $\{i_1, i_2, i_3, \dots\} \subset \{0, 1, 2, 3, \dots\}$. The τ_k is the time delay from the sensor to actuator in the control systems. From definition of t in (3) and (4) follows

$$\bigcup_{k=1}^{\infty} [i_k h + \tau_k, i_{k+1} h + \tau_{k+1}) = [t_o, \infty), t_o \geq 0 \quad (5)$$

It is, also, supposed that $u(t_o) = 0$ and that

$$(i_{k+1} - i_k)h + \tau_{k+1} \leq r, \quad \exists r > 0, \quad k = 1, 2, \dots \quad (6)$$

It is not required that $i_{k+1} > i_k$ so that dropout can be described.

From (3) and (6) one can get

$$x(t) = x(t_o - r)e^{A(t-t_o+r)} = \Phi(t), \quad t \in [t - r, t] \quad (7)$$

The $\Phi(t)$ is the initial condition function for the system.

Since

$$x(i_k h) = x[t - (t - i_k h)] \quad (8)$$

$$\tau(t) = t - i_k h, \quad t \in [i_k h + \tau_k, i_{k+1} h + \tau_{k+1}), \quad k = 1, 2, 3, \dots \quad (9)$$

then we have from (3) and (4)

$$\dot{x}(t) = A(q)x(t) + BKx(t - \tau(t)) \quad (10)$$

$$x(t) = \Phi(t), \quad t \in [t_o - r, t_o] \quad (11)$$

The system described by (10) and (11) is the description of NCS and will be topic for analysis in the next subsections.

Remark 1. The form of uncertainty in relation (2) is considered in [23].

3. Delay-dependent stability of the NCS

Less conservative result can be given using information about the time-delay in the system [22] Let us again consider

the system (10) and initial condition (11) where

$$\Phi \in C([- \tau(t), 0], R^n) \quad (12)$$

where $C([a, b], R^n)$ is a set of continuous functions mapping the interval $[a, b]$ to R^n .

Let us observe that for $\forall q \in \mathcal{Q}$

$$\begin{aligned} x(t - \tau(t)) &= x(t) - \int_{\tau(t)}^0 \dot{x}(t + \theta) d\theta = \\ &= x(t) - \int_{-\tau(t)}^0 [A(q)x(t + \theta) + BKx(t + \theta - r(t + \theta))] d\theta \quad (13) \end{aligned}$$

For $t \geq \tau(t)$, system (10) can be rewritten in the next form

$$\dot{x}(t) = (A(q) + BK)x(t) +$$

$$\int_{-\tau(t)}^0 [-BKA(q)x(t + \theta) - (BK)(BK)x(t + \theta - r(t + \theta))] d\theta - \tau(t) \quad (14)$$

with the initial condition

$$x(\theta) = \Psi(\theta), \quad -\tau(t) \leq \theta \leq \tau(t)$$

$$\Psi(\theta) = \Phi(\theta), \quad -\tau(t) \leq \theta \leq 0 \quad (15)$$

$\Psi(\theta)$ is solution of (10)-(11) for $0 < \theta \leq \tau(t)$

System (21) and (22) is the class of system to which is embedded the system (10)-(11) and has the form

$$\dot{x}(t) = \bar{A}(q)x(t) + \int_{-2\tau(t)}^0 A(q, \theta)x(t + r(t, \theta)) d\theta \quad (16)$$

where

$$\bar{A}(q) = A(q) + BK$$

$$A(q, \theta) = -BKA(q), \quad \theta \in [-\tau(t), 0] \quad (17)$$

$$A(q, \theta) = -(BK)^2, \quad \theta \in [-2\tau(t), -\tau(t)]$$

with initial condition

$$x(\theta) = \Psi(\theta), \quad -2\tau(t) \leq \theta \leq 0 \quad (18)$$

The stability of the system (23)-(25), given by transformation of the system (10)-(11), implies the stability of the original systems. For derivation of our results important next theorem.

Theorem 1. (Razumihin, [22]). A time-delay system with maximum time delay τ is asymptotically stable if there exists a bounded quadratic Lyapunov function V such that

$$1^0 \quad V(x(t)) \geq \varepsilon \|x(t)\|^2, \quad \exists \varepsilon > 0$$

$$2^0 \quad \dot{V}(x(t)) \leq -\varepsilon \|x(t)\|^2$$

for

$$V(x(t + \xi)) \leq pV(x(t)), \quad -\tau \leq \xi \leq 0, \quad \exists p > 1 \quad \blacksquare$$

Now we will formulate theorem which guarantees the asymptotic sta

Theorem 2. (Filipovic, [21]). The system described with (23)-(25)

1⁰ time-varying delay is bounded, i.e.

$$0 < \tau(t) \leq \tau_{\max}$$

2⁰ exists a real scalars $\alpha_k, k = 0, 1$ such that

$$\alpha(\theta) = \alpha_0, \quad -\tau(\theta) < \theta \leq 0$$

$$\alpha(\theta) = \alpha_1, \quad -2\tau(t) \leq \theta \leq -\tau(t)$$

3⁰ exists a symmetric matrix P

4⁰ exists a symmetric matrix function $R(\theta)$ such that

$$R(\theta) = R_0, \quad -\tau(\theta) \leq \theta \leq 0$$

$$R(\theta) = R_1, \quad -2\tau(t) \leq \theta \leq -\tau(t)$$

and, also, valid

$$\int_{-2\tau(t)}^0 R(\theta) d\theta = 0$$

$$5^0 \begin{bmatrix} N_k & -P\bar{A}_k(\theta) \\ A_k^T(\theta) & -\alpha(\theta)P \end{bmatrix} < 0$$

for $k=0,1$ and $\forall q \in Q$.

The elements of the matrix are

$$N_0 = \frac{1}{2\tau_{\max}} [P(A(q) + BK) + (A(q) + BK)^T P] + \alpha_0 P + R_0$$

$$N_1 = \frac{1}{2\tau_{\max}} [P(A(q) + BK) + (A(q) + BK)^T P] + \alpha_1 P + R_1$$

$$A_0(\theta) = A(\theta, q) = -BKA(q), \quad -\tau(t) < \theta \leq 0$$

$$A_1(\theta) = A(\theta, q) = -(BK)^2, \quad -2\tau(t) \leq \theta \leq -\tau(t)$$

Then system (23)-(25) and, also, system (10)-(11), is asymptotically stable. ■

Remark 6. Many pessimistic results on the complexity-theoretic barriers for deterministic robustness problem is discovered [23]. One possibility to overcome above problems, is to shift the meaning of the robustness from its usual deterministic sense to a probabilistic one [12].

Remark 7. The local stability and robustness of a discrete-time nonlinear congestion control algorithm in the presence of multiple bottleneck links and non symmetric users, analytic solution is not possible. In that case can be used randomized algorithms [12], [24].

4. The improved delay-dependent stability criteria

For us need result from matrix theory.

Lemma 1 (Schur complement, [23]). The LMI

$$\begin{bmatrix} W_{11}(x) & W_{12}(x) \\ W_{21}(x) & W_{22}(x) \end{bmatrix} > 0$$

$W_{22}(x) = W_{22}^T(x)$, $W_{21}(x) = W_{12}^T(x)$ and $W_{12}(x)$ depend affinely on x . is equivalent to

$$W_{12}(x) > 0, \quad W_{11}(x) - W_{12}(x)W_{22}^{-1}(x)W_{12}^T(x) > 0 \quad \blacksquare$$

Now we will prove next theorem.

Theorem 3. There exists a symmetric matrix R such that for $\forall q \in Q$

$$\begin{bmatrix} N_{0k} + R & -PBKA(q) \\ (-BKA(q))^T P & -\alpha_0 P \end{bmatrix} < 0 \quad (19)$$

$$\begin{bmatrix} N_{1k} - R & -P(BK)^2 \\ -[(BK)^2]^T P & -\alpha_1 P \end{bmatrix} < 0 \quad (20)$$

if and only if

$$\begin{bmatrix} N_{0k} + N_{02} & -PBKA(q) & -P(BK)^2 \\ (-BKA(q))^T P & -\alpha_0 P & 0 \\ -[(BK)^2]^T P & 0 & -\alpha_1 P \end{bmatrix} < 0 \quad (21)$$

$$N_{01} = \frac{1}{2\tau_{\max}} [P(A(q) + BK) + (A(q) + BK)^T P] + \alpha_0 P$$

$$N_{11} = \frac{1}{2\tau_{\max}} [P(A(q) + BK) + (A(q) + BK)^T P] + \alpha_1 P$$

$$R(\theta) = \begin{cases} R & , \quad -\tau(t) < \theta \leq 0 \\ -R & , \quad -2\tau(t) \leq \theta \leq -\tau(t) \end{cases} \quad \blacksquare$$

Proof: Using Lemma 1 we can get from (21)

$$P > 0 \quad (22)$$

$$\Delta = N_{01} + R - \alpha_0 PBK(q)P^{-1}(BKA(q))^T P - \alpha_1 P(BK)^2 P[(BK)^2]^T P < 0 \quad (23)$$

Also, from (19) and (20) we have

$$\Delta_1 = N_{01} + R - \alpha_0 PBK(q)P^{-1}(BKA(q))^T P < 0 \quad (24)$$

$$\Delta_2 = N_{11} - R - \alpha_1 P(BK)^2 P^{-1}[(BK)^2]^T P < 0 \quad (25)$$

We must to show that exists R satisfying (6) and (7) if and only if (5) is satisfying for given P in relation (4). The existence of R for (6) and (7) implies (5) since

$$\Delta = \Delta_1 + \Delta_2 < 0 \quad (26)$$

Also, we have from (8) and (10)

$$\Delta_1 = \Delta - \Delta_2 = \Delta + \varepsilon I < 0 \quad (27)$$

Fallows that (6) and (7) is satisfied. ■

The main result of the paper is formulated in the form of next theorem.

Theorem 4. Let us suppose that exists

1⁰ Symmetric matrix P

2⁰ Scalar α_0 and α_1

3⁰ For $\forall q \in Q$ is

$$\begin{bmatrix} T & -PBKA(q) & -P(BK)^2 \\ (-BKA(q))^T P & -\alpha_0 P & 0 \\ -[(BK)^2]^T P & 0 & -\alpha_1 P \end{bmatrix} < 0$$

where

$$T = \frac{1}{2\tau_{\max}} [P(A(q) + BK) + (A(q) + BK)^T P] + (\alpha_0 + \alpha_1)P$$

Then the system (23)-(25) is asymptotically stable. ■

Proof: Omitted owing the space.

5. Conclusion

In this paper the problem of stability of the networked control systems is considered. The model of the system incorporates network-induced delay and data packet dropout and can be interpreted as a functional differential equation with bounded time-varying delay. Using Lyapunov-Razumikhin theory the stability of system is proved.

6. References

- [1] W. Stallings, *Data and Computer Communications*. New Jersey: Prentice-hall, 2004.
- [2] R.W. Brockett and D. Liberzon, "Quantized stabilization of linear systems", *IEEE Trans. Automat. Control*, vol.45, pp.1279-1289, July 2000.
- [3] N. Eilia and S.K. Mitter, "Stability of linear systems with limited information", *IEEE Trans. Automat. Control*, vol.46, pp. 1348-1400, July 2001.
- [4] S. Tatikonda and S. Mitter, "Control under communication constraints", *IEEE Trans. Automat. Control*, vol.77, pp.1056-1068, September 2004.
- [5] W. Zhang, M.S. Branicky, and S.M. Phillips, "Stability of networked control systems", *IEEE Control Syst. Mag.*, vol.21, pp.84-89, Feb 2001.
- [6] G.C. Walsh and H. Ye, "Scheduling of networked control systems", *IEEE Control Syst. Mag.*, vol.21, pp.57-65, Jan 2001.
- [7] G.C. Walsh, O. Beldiman, and L.G. Bushnell, "Error encoding algorithms for networked control systems", *Automatica*, vol.38, pp. 261-267, 2002.
- [8] L.A. Montestruque and P. Antsaklis, "Stability of model-based networked control systems with time-varying transmission times", *IEEE Trans. Automat. Control*, vol.49, pp. 1562-1572, September 2004.
- [9] V.Z. Filipovic, "Robust hybrid LQ controller", *European Control Conference*, Cambridge, UK, 2003
- [10] V.Z. Filipovic, "Hybrid control of systems with input delay", *16th IFAC World Congress*, Praha, CR, 2005
- [11] V.Z. Filipovic, "Upper bounds of performance guided hybrid controller", *11th IEEE International Conference on Methods and Models in Automation and Robotics*, Miedzydroje, Poland, 2005
- [12] V.Z. Filipovic, "Performance guided hybrid LQ controller for time-delay systems", *15th International Conference on Control Systems and Computer Science*, Bucharest, Romania, 2005
- [13] V.Z. Filipovic, "Robust switching controller in the presence of model uncertainty and saturation", *5th International Conference on System Identification and Control Problems*, Moscow, Russia, 2006
- [14] J. Nilsson, B. Bernhardsson, and B. Wittenmark, "Stochastic analysis and control of real-time systems with random time-delays", *Automatica*, vol.34, pp. 57-64, 1998.
- [15] S.S. Hu and Q.X. Zhu, "Stochastic optimal control and analysis of stability of networked control system with long delays", *Automatica*, vol. 39, pp. 1877-1844, 2003.
- [16] G.C. Goodwin, M.M. Seron and J.A. De Dona, *Constrained Control and Estimation: An Optimization Approach*. Berlin: Springer-Verlag, 2005.
- [17] R. Tempo, G. Calafiore and F. Dabbene. *Randomized Algorithms for Analysis and Control of Uncertain Systems*. Berlin: Springer-Verlag, 2005.
- [18] D. Yue, Q.L. Han, and C. Peng, "State feedback controller design of networked control systems", *IEEE Trans. Circuits and Systems-II*, vol. 51, pp. 640-644, November 2004.
- [19] G.C. Welsh, O. Beldiman, and L.G. Bushnell, "Asymptotic behaviour of nonlinear networked control systems", *IEEE Trans. Automat. Control*, vol.46, pp. 1093-1097, July 2001.
- [20] D. Nešić and A.R. Teel, "Input-output stability properties of networked control systems", *IEEE Trans. Automat. Control*, vol.49, pp. 1650-1667, November 2004.
- [21] V.Z. Filipovic, "Networked control systems with time-varying transmission times and unmodeled dynamics", *11th IEEE International Conference on Methods and Models in Automation and Robotics*, Miedzydroje, Poland, 2005
- [22] B.S. Razumikhin, "On the stability of systems with a delay", *Prikl. Mat. Meh.*, vol.20, pp. 500-512, 1956. (In Russian).
- [23] B.T. Polyak and P.S. Shcherbakov. *Robust Stability and Control*. Moscow: Nauka, 2002. (In Russian)...
- [24] K. Gu, V. Kharitonov, and J. Chen. *Stability of Time-Delay Systems*. Basel: Birkhauser, 2003.
- [25] V.D. Blondel and J.N. Tsitsiklis, "A survey of computational complexity results in systems and control", *Automatica*, vol. 36, pp. 1249-1274, September 2000.
- [26] T. Alpcan, T. Basar, and R. Tempo, "Randomized algorithms for stability and robustness analysis of high speed communication networks", In: *Proceedings IEEE Conference on Control Applications*, pp. 397-403, 2003.

UNIVERSAL EQUATIONS OF UNSTEADY MHD INCOMPRESSIBLE FLOW ON HEATED MOVING PLATE OF FLUID WHICH ELECTRO-CONDUCTIVITY IS FUNCTION OF VELOCITY RATIO

Zoran Boričić, Dragisa Nikodijević, Dragica Milenković and Stamenković Živojin
Faculty of Mechanical Engineering, University of Nis, A.Medvedva 14, 18000 Nis

Abstract

This paper is concerned with the unsteady MHD flow of incompressible and electro-conductive fluid caused by moving of flat plate with variable velocity. The plate is moving in its own plane, and in "undisturbed fluid". Fluid electro-conductivity is function of ratio of longitudinal fluid velocity and plate velocity. The plate temperature is function of longitudinal coordinate and time. External magnetic field is perpendicular to the plate. For solving of described problem in this paper the general similarity method has been used, and universal equations are obtained. Beside these equations the impulse equation of the observed problem has been also developed.

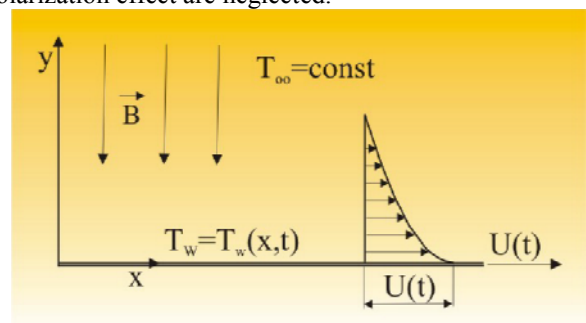
Keywords: magneto hydrodynamics, incompressible, electro-conductive, general similarity method

1. INTRODUCTION

One of the first prospectors who considered natural and forced incompressible viscous fluid flow on the solid plates was Ostrach [1]. Later on Grief with associates [2], Gupta with associates [3] and other scientist are researched fluid flow on inert flat plate. With moving of flat plate or solid surface fluid flow is changing and this flow has been the exploration subject of Sakiadis [4]. In our paper [5] we considered MHD fluid flow caused by constant velocity moving of porous flat plate, and in paper [6] flow caused by variable plate moving. In this paper we will consider unsteady MHD flow of incompressible fluid with variable electro-conductivity caused by moving of flat plate with variable velocity. For contemplation of described problem "universalization" method of laminar boundary layer equations has been used, which is developed by L.G.Loicijanskij [7]. This method has numerous unsuspected benefits in comparison with other approximated methods. By using this method, which is a very important, universal equations of described problem is obtained. Obtained system of universal equations can be once for all numerically integrated by using a computer and during that only snipping of the system has been considered. The results of universal equations integration can be on convenient way saved and then used for general conclusion conveyance about fluid flow and for calculations of particular problems. In this paper we will satisfied with development of fluid flow universal equations of described problem.

2. MATHEMATICAL MODEL

This paper is concerned with the laminar, unsteady flow of viscous, incompressible and electro-conductive fluid caused by variable moving of flat plate along x-axis. The plate is moving in its own plane and in "undisturbed" fluid. Plate velocity is function of time t. Present external magnetic field is perpendicular to the plate and external electric field is neglected. All fluid properties are assumed constant except the fluid electro-conductivity. Plate temperature is function of longitudinal coordinate x and time t. Viscous dissipation, Joule heat, Hole and polarization effect are neglected.



The fluid electro-conductivity can be assumed in the following expression:

$$\sigma = \sigma_0 S\left(\frac{u}{U}\right) \quad (1)$$

where σ_0 -constant fluid electro-conductivity, u -means longitudinal velocity of the fluid, U -means plate moving velocity, $S\left(\frac{u}{U}\right)$ -differential function.

The mathematical model of described problem is expressed by the following equations:

$$\begin{aligned} \frac{\partial u}{\partial t} + u \frac{\partial u}{\partial x} + v \frac{\partial u}{\partial y} &= \frac{\partial U}{\partial t} + \gamma \frac{\partial^2 u}{\partial y^2} + NU \left(S(1) - \frac{u}{U} S\left(\frac{u}{U}\right) \right) \\ \frac{\partial T}{\partial t} + u \frac{\partial T}{\partial x} + v \frac{\partial T}{\partial y} &= \alpha \frac{\partial^2 T}{\partial y^2} \\ \frac{\partial u}{\partial x} + \frac{\partial v}{\partial y} &= 0 \end{aligned} \quad (2)$$

and the boundary and initial conditions:

$$\begin{aligned} u &= U(t), \quad v = 0, \quad T = T_w(x, t) \quad \text{for } y = 0; \\ u &\rightarrow 0, \quad T \rightarrow T_\infty \quad \text{for } y \rightarrow \infty; \\ u &= u_1(x, y), \quad T = T_1(x, y) \quad \text{for } t = t_1; \\ u &= u_0(t, y), \quad T = T_0(t, y) \quad \text{for } x = x_0. \end{aligned} \quad (3)$$

In the equations (2) and the boundary and initial conditions (3) the parameter labelling used is common for the theory of MHD boundary layer: x, y -longitudinal and transversal coordinate respectively; t -time; v -transversal velocity component; γ -coefficient of the kinematics viscosity of fluid, $N = \sigma_0 B^2 / \rho$ where B -magnetic field induction, ρ -density of fluid, α -heat conduction coefficient, T -fluid temperature, T_w -plate temperature; T_∞ -temperature in “undisturbed” fluid; $u_1(x, y)$ and $T_1(x, y)$ - disposition of longitudinal velocity and fluid temperature in time moment $t = t_1$ respectively; $u_0(t, y)$ and $T_0(t, y)$ - disposition of longitudinal velocity and fluid temperature in cross section $x = x_0$.

For further consideration of the described problem for every particular problem i.e. for given values of $S, U, N, T_w, T_\infty, u_1, T_1, u_0, T_0$ the system of equations (2) can be solved with corresponding boundary and initial conditions (3). The results can be used for obtaining of general conclusions about particular fluid flow problem.

3. UNIVERSAL EQUATIONS

In boundary layer theory V.J.Skadov [8], L.G. Loicijanskij [7] and V.N. Saljnikov [9] introduced general similarity method in different forms. With this method with adequate choice of transformations and then similarity parameters universal equations and universal boundary conditions can be obtained. This equations and boundary conditions are independent from particular problems. Because of that very often in literature this method is called “universalization” method.

Considering that general similarity method gives good results not only for simple boundary layer problems also for very complicated [10], [11], [12], in this paper we make attempt to evolve this method in Loicijanskij version [7] on the described problem.

In that sense, following the general similarity method [7], [8], [9], we introduced first flow function $\Psi(x, y, t)$ with relations:

$$\frac{\partial \Psi}{\partial x} = -v, \quad \frac{\partial \Psi}{\partial y} = u, \quad (4)$$

and then new variables in following form:

$$\Phi(x, t, \eta) = \frac{\Psi}{U \delta^{**}}, \quad \eta = \frac{y}{\delta^{**}}, \quad \Theta(x, t, \eta) = \frac{T - T_\infty}{T_w - T_\infty} \quad (5)$$

where δ^{**} - thickness of impulse loss, defined with expression:

$$\delta^{**}(x, t) = \int_0^\infty \frac{u}{U} \left(1 - \frac{u}{U} \right) dy. \quad (6)$$

By using the new variables (5) we transform the system of equations (2) into the equations:

$$\begin{aligned} \frac{\partial^3 \Phi}{\partial \eta^3} + \frac{1}{2} F \Phi \frac{\partial^2 \Phi}{\partial \eta^2} + f_1 \left(1 - \frac{\partial \Phi}{\partial \eta} \right) + \frac{1}{2} \eta p \frac{\partial^2 \Phi}{\partial \eta^2} + \\ + g_{1,0} \left[S(1) - \frac{\partial \Phi}{\partial \eta} S\left(\frac{\partial \Phi}{\partial \eta}\right) \right] &= z \frac{\partial^2 \Phi}{\partial t \partial \eta} + U z X(\eta; x) \\ \frac{1}{Pr} \frac{\partial^2 \Theta}{\partial \eta^2} + \frac{1}{2} F \Phi \frac{\partial \Theta}{\partial \eta} - l_{1,0} \Theta \frac{\partial \Phi}{\partial \eta} - l_{0,1} \Theta + \\ + \frac{1}{2} \eta p \frac{\partial \Theta}{\partial \eta} &= z \frac{\partial \Theta}{\partial t} + U z Y(\eta; x) \end{aligned} \quad (7)$$

where, for the sake of shorter expression, the notations are introduced:

$$\begin{aligned} z &= \frac{\delta^{**2}}{\gamma}, \quad F = U \frac{\partial z}{\partial x}, \quad f_1 = \frac{z}{U} \frac{\partial U}{\partial t}, \\ g_{1,0} &= Nz, \quad Pr = \frac{\gamma}{\alpha} \text{ -Prandtl number,} \\ l_{1,0} &= \frac{Uz}{T_w - T_\infty} \frac{\partial T_w}{\partial x}, \quad l_{0,1} = \frac{z}{T_w - T_\infty} \frac{dT_w}{dt}, \quad p = \frac{\partial z}{\partial t}, \\ X(x_1; x_2) &= \frac{\partial \Phi}{\partial x_1} \frac{\partial^2 \Phi}{\partial \eta \partial x_2} - \frac{\partial \Phi}{\partial x_2} \frac{\partial^2 \Phi}{\partial x_1 \partial \eta}; \\ Y(x_1; x_2) &= \frac{\partial \Phi}{\partial x_1} \frac{\partial \Theta}{\partial x_2} - \frac{\partial \Phi}{\partial x_2} \frac{\partial \Theta}{\partial x_1}. \end{aligned} \quad (8)$$

Corresponding boundary conditions obtained from equations (3) have the following form:

$$\begin{aligned} \Phi &= 0, \quad \frac{\partial \Phi}{\partial \eta} = 1, \quad \Theta = 1 \quad \text{for } \eta = 0; \\ \frac{\partial \Phi}{\partial \eta} &\rightarrow 1, \quad \Theta \rightarrow 0 \quad \text{for } \eta \rightarrow \infty, \\ \frac{\partial \Phi}{\partial \eta} &= \frac{u_1}{U}, \quad \Theta = \frac{T_1 - T_\infty}{T_w - T_\infty} \quad \text{for } t = t_1 \\ \frac{\partial \Phi}{\partial \eta} &= \frac{u_0}{U}, \quad \Theta = \frac{T_0 - T_\infty}{T_w - T_\infty} \quad \text{for } x = x_0. \end{aligned} \quad (9)$$

By further following the “universalization” method we introduced in consideration three sets of parameters:

$$f_k = \frac{1}{U} \frac{d^k U}{dt^k} z^k \quad (k = 1, 2, \dots),$$

$$g_{k,n} = U^{k-1} Z^{k+n} \frac{\partial^{k-1+n} N}{\partial x^{k-1} \partial t^n},$$

$$l_{k,n} = \frac{U^k}{q} \frac{\partial^{k+n} q}{\partial x^k \partial t^n} Z^{k+n},$$

$$(k, n = 0, 1, 2, \dots; k \vee n \neq 0), \quad (10)$$

where $q = T_w - T_\infty$,

$$\text{and constant parameter: } p = \frac{\partial z}{\partial t} = \text{const}, \quad (11)$$

which replace longitudinal coordinate x and time t . By using introduced sets of parameters (10) like new variables we transform equations system (7) unto form:

$$\begin{aligned} \mathfrak{I}_1 + \mathfrak{I}^* &= \sum_{k=1}^{\infty} \left[Q_k X(\eta; f_k) + E_k \frac{\partial^2 \Phi}{\partial \eta \partial f_k} \right] + \\ &+ \sum_{\substack{k,n=0 \\ k \vee n \neq 0}}^{\infty} \left[K_{k,n} X(\eta; g_{k,n}) + M_{k,n} X(\eta; l_{k,n}) \right] \\ &+ \sum_{\substack{k,n=0 \\ k \vee n \neq 0}}^{\infty} \left[L_{k,n} \frac{\partial^2 \Phi}{\partial \eta \partial g_{k,n}} + N_{k,n} \frac{\partial^2 \Phi}{\partial \eta \partial l_{k,n}} \right] \\ \mathfrak{I}_2 &= \sum_{k=1}^{\infty} \left[Q_k Y(\eta; f_k) + E_k \frac{\partial \Theta}{\partial f_k} \right] + \\ &+ \sum_{\substack{k,n=0 \\ k \vee n \neq 0}}^{\infty} \left[K_{k,n} Y(\eta; g_{k,n}) + M_{k,n} Y(\eta; l_{k,n}) \right] \quad (12) \\ &+ \sum_{\substack{k,n=0 \\ k \vee n \neq 0}}^{\infty} \left[L_{k,n} \frac{\partial \Theta}{\partial g_{k,n}} + N_{k,n} \frac{\partial \Theta}{\partial l_{k,n}} \right] \end{aligned}$$

where the following markings have been used for shorter statement: \mathfrak{I}_1 -left side of first equation of system (7) without last addend, \mathfrak{I}^* -last addend on the left side of same equation, \mathfrak{I}_2 - left side of second equation of same system,

$$\begin{aligned} z \frac{\partial f_k}{\partial t} &= f_k (kp - f_1) + f_{k+1} = E_k; \\ Uz \frac{\partial g_{k,n}}{\partial x} &= (k+n) g_{k,n} F + g_{k+1,n} = K_{k,n}, \\ z \frac{\partial g_{k,n}}{\partial t} &= [(k-1)f_1 + (k+n)p] g_{k,n} + g_{k,n+1} = L_{k,n} \\ Uz \frac{\partial l_{k,n}}{\partial x} &= [-l_{1,0} + (k+n)F] l_{k,n} + l_{k+1,n} = M_{k,n} \\ z \frac{\partial l_{k,n}}{\partial t} &= [kf_1 - l_{0,1} + (k+n)p] l_{k,n} + l_{k,n+1} = N_{k,n}. \\ Uz \frac{\partial f_k}{\partial x} &= kF f_k = Q_k; \quad (13) \end{aligned}$$

Boundary conditions which are appropriate to equations (13) have the form:

$$\Phi = 0 \frac{\partial \Phi}{\partial \eta} = 1, \Theta = 1 \text{ for } \eta = 0;$$

$$\begin{aligned} \frac{\partial \Phi}{\partial \eta} &\rightarrow 0, \Theta \rightarrow 0 \text{ for } \eta \rightarrow \infty; \\ \Phi &= \Phi_0, \Theta = \Theta_0 \text{ for } f_k = 0 \text{ (} k = 1, 2, \dots \text{)}, \\ g_{k,n} &= 0, l_{k,n} = 0 \text{ (} k, n = 0, 1, 2, \dots; k \vee n \neq 0 \text{)}, \quad (14) \end{aligned}$$

where Φ_0, Θ_0 are solutions of following system of equations:

$$\begin{aligned} \frac{\partial^3 \Phi}{\partial \eta^3} + \frac{1}{2} F \Phi \frac{\partial^2 \Phi}{\partial \eta^2} &= 0, \\ \frac{1}{Pr} \frac{\partial^2 \Theta}{\partial \eta^2} + \frac{1}{2} F \Phi \frac{\partial \Theta}{\partial \eta} &= 0. \quad (15) \end{aligned}$$

Obtained system of equations (12) is not “universal” because it contain values F, S and Pr . In respect to values S and Pr obtained system can not be universal, but after their imposing, system is universal if value F is function only from introduced sets of parameters. In order to prove that we start from impulse equation of described problem:

$$\frac{\partial}{\partial t} (U \delta^*) + \frac{\partial}{\partial x} (U^2 \delta^{**}) + NU \delta_1 = -\gamma \left(\frac{\partial u}{\partial y} \right)_{\infty}, \quad (16)$$

in which:

$$\delta^* = \int_0^{\infty} \left(1 - \frac{u}{U} \right) dy, \delta_1 = \int_0^{\infty} S(1) - \frac{u}{U} S \left(\frac{u}{U} \right) dy. \quad (17)$$

After introducing new variables (10) in equation (16) obtained equation have the following form:

$$\begin{aligned} F &= -2 \left[\zeta + H \left(f_1 + \frac{1}{2} p \right) + H_1 g_{1,0} - \lambda_{0,0} + \right. \\ &+ \sum_{k=1}^n E_k \frac{\partial H}{\partial f_k} + \sum_{\substack{k,n=0 \\ k \vee n \neq 0}}^{\infty} \left(L_{k,n} \frac{\partial H}{\partial g_{k,n}} + N_{k,n} \frac{\partial H}{\partial l_{k,n}} \right) \left. \right], \quad (18) \end{aligned}$$

where, for the sake of brevity, the notation is introduced:

$$\begin{aligned} \zeta &= \left(\frac{\partial^2 \Phi}{\partial \eta^2} \right)_{\infty}; H = \frac{\delta^*}{\delta^{**}} = \int_0^{\infty} \left(1 - \frac{\partial \Phi}{\partial \eta} \right) d\eta; \\ H_1 &= \frac{\delta_1}{\delta^{**}} = \int_0^{\infty} \left[S(1) - \frac{\partial \Phi}{\partial \eta} S \left(\frac{\partial \Phi}{\partial \eta} \right) \right] d\eta \quad (19) \end{aligned}$$

Values ζ, H and H_1 depend only from parameters (10), if function S is known function, and that mean also for value F which is expressed with equation (18), so the system of equations (12) is universal system of equations of observed problem.

Equations system (12) with boundary conditions (14), for exact value of Pr and function S can be integrated by computer using and during that only “snipping” of equations has been considered. Obtained results can be on convenient way saved and then used for general conclusion conveyance about fluid flow and for calculations of particular problems.

4. APPROXIMATED UNIVERSAL EQUATIONS

Actual solving of equations (12) requires limitation of independent variables number. This leads us to indispensable application of sector method which consists of neglecting of all parameters starting with some index. That brings us to approximated universal equations of described problem. If we retain influence of parameters $f_1; g_{1,0}; l_{1,0}$ and neglect influence of the rest of parameters and their derivatives we obtain the system of universal equations in three-parameter approximation.

$$\begin{aligned}\mathfrak{T}_1 + \mathfrak{T}^* &= Ff_1X(\eta; f_1) + (p - f_1)f_1 \frac{\partial^2 \Phi}{\partial \eta \partial f_1} + \\ &+ g_{1,0}FX(\eta; g_{1,0}) + l_{1,0}(F - l_{1,0})X(\eta; l_{1,0}) + \\ &+ g_{1,0}p \frac{\partial^2 \Phi}{\partial \eta \partial g_{1,0}} + (f_1 + p)l_{1,0} \frac{\partial^2 \Phi}{\partial \eta \partial l_{1,0}} \\ \mathfrak{T}_2 &= Ff_1Y(\eta; f_1) + (p - f_1)f_1 \frac{\partial \Theta}{\partial f_1} + \\ &+ Fg_{1,0}Y(\eta; g_{1,0}) + (F - l_{1,0})l_{1,0}Y(\eta; l_{1,0}) + \\ &+ pg_{1,0} \frac{\partial \Theta}{\partial g_{1,0}} + (p + f_1)l_{1,0} \frac{\partial \Theta}{\partial l_{1,0}}\end{aligned}\quad (20)$$

Corresponding boundary conditions for equations (20) have the following form:

$$\begin{aligned}\frac{\partial \Phi}{\partial \eta} &= 1, \Phi = 0, \Theta = 1 \text{ for } \eta = 0; \\ \frac{\partial \Phi}{\partial \eta} &\rightarrow 0, \Theta \rightarrow 0 \text{ for } \eta \rightarrow \infty; \\ \Phi &= \Phi_0, \Theta = \Theta_0 \text{ for} \\ f_1 &= 0, g_{1,0} = 0, l_{1,0} = 0, p = 0,\end{aligned}\quad (21)$$

where Φ_0, Θ_0 represent solution of system of equations (15).

On the same way we can acquire other approximated equations of described problem.

For some actual changing of fluid electro-conductivity we obtain:

- for $\sigma = 0$ $\mathfrak{T}^* = 0$
- for $\sigma = \sigma_0 = \text{const}$ $\mathfrak{T}^* = g_{1,0} \left(1 - \frac{\partial \Phi}{\partial \eta} \right)$
- for $\sigma = \sigma_0 \left(1 - \frac{u}{U} \right)$ $\mathfrak{T}^* = -g_{1,0} \frac{\partial \Phi}{\partial \eta} \left(1 - \frac{\partial \Phi}{\partial \eta} \right)$

5. CONCLUSION

This paper is concerned with unsteady MHD flow of incompressible fluid caused by moving of flat plate with variable velocity. The flat plate moves in its own plane in and in “undisturbed” fluid. The fluid electro-conductivity is function of velocity ratio.

Present external magnetic field is perpendicular to the plate, and electric field is neglected. Variable plate temperature is function of longitudinal coordinate and time. For consideration of described problem general similarity method is used and universal equations are obtained. Beside the general universal equations in this paper some approximated equations are given and equations for actual alteration of fluid electro-conductivity.

REFERENCES

- [1] Ostrach, S.; (1954), NACA. PN, p-3141.
- [2] Grief, R.; Habib, I.S. and Lin, J.C. (1971): J.Fluid Mech, 46, p-513.
- [3] Gupta, P.S. and Gupta, A.S., (1974), Int. J. Heat mass Transfer 17, p-14-37.
- [4] Sakiadis, B.C., (1961), AICHE 7m, 26, 221, p-467.
- [5] Boričić Z., Nikodijević D., Milenković D., Stamenković Ž., Univerzalne jednačine MHD strujanja nestišljive tečnosti na zagrejanoj poroznoj pokretnoj ploči, Fourth International Conference Heavy Machinery-HM'02 Kraljevo, 27-30 June 2002, HM-02, Proceedings B.9-B.13. Mataruška Banja, 2002.
- [6] Boričić Z., Nikodijević D., Milenković D., Stamenković Ž., Univerzalne jednačine nestacionarnog MHD strujanja nestišljivog fluida na zagrejanoj pokretnoj ploči Zbornik radova, HIPNEF, Vrnjačka Banja, 2002.
- [7] Л.Г.Лойцянский, Универсальные уравнения и параметрические приближения в теории ламинарного пограничного слоя, Академия Наук СССР, Прикладная математика и механика, Том 29, выпуск 1, 1965., 70-87.
- [8] В. Шкадов, Пограничный слой с градиентом давления в потоке сжимаемой жидкости, Изв. АН ССР, ОТН, Механика и машиностроение, No 2, 1963, 28-32.
- [9] V. N. Saljnikov, A Contribution to Universal Solutions of the Boundary Layer Theory, Theoretical and Applied Mechanics 4, 1978., 139 - 163.
- [10] B. Obrović, Equations of ionised gas boundary layer and their parametric solutions, Facta Universitatis, Vol.1, No 5, 1995, pp.619-629
- [11] V. Saljnikov, Z. Boričić, D. Nikodijević, Generalised similarity solutions for 3-D laminar compressible boundary layer flows on swept profiled cylinders, Acta Mechanica, 1994, Suppl.4, 389-399, Springer-Verlag 1994.
- [12] D. Ivanović, On unsteady laminar two-dimensional boundary layer of incompressible flow for airfoils, Proceedings of the Yuctam, B8-B13, Nis, 1995.

CONVENTIONAL AND INTELLIGENT TEMPERATURE CONTROL COMPARISON FOR THE MULTIZONE CRYSTAL GROWTH FURNACE

Vlastimir Nikolić, Žarko Čojbašić and Katarina Aleksić

Abstract

In this paper two PI controller design schemes for the control of crystal growth of semiconductor materials have been presented. In the process of crystal growth different types of time-dependent convections and heater temperature fluctuations cause growth anomalies, resulting in possible appearance of striations, inclusions, and structural defects in the crystal. The constancy of the applied temperature field is therefore an essential parameter to be addressed for the sake of achieving crystals of high purity and homogeneity. In this paper the seven zone crystal growth furnace is considered, actually representing seven-input seven-output multivariable system. The system has firstly been decoupled, then a time domain optimal tuning PI controller for each subsystem has been designed. Based on the relationship with conventional PID controller, fuzzy incremental PI controllers have also been considered. The performance of the proposed controllers has been compared by extensive computer simulations.

Keywords: temperature control, multizone crystal growth furnace, PI controller, fuzzy PI controller

1. INTRODUCTION

In the process of crystal growth of semiconductor materials, different types of time-dependent convections and fluctuations in the heater temperature can cause growth inhomogeneities. As a consequence striations, inclusions, and structural defects in the crystal might appear. The constancy of the applied temperature field is therefore an essential parameter to be addressed for the sake of achieving crystals of high purity and homogeneity.

In order to establish a well-defined and controlled thermal profile in the sample the use of multizone furnaces for materials processing has become very attractive in recent years [1][7]. In these furnaces the temperature of each zone can be adjusted individually by a respective power setting. This paper describes an attempt to apply both controllers to multizone furnace: time-domain optimal PI controllers and incremental fuzzy PI controller.

This paper is organized as follows. The mathematical model of the multi-zone furnace and the identification of model parameters are described in the Section 2. In Section 3 the controller structure which consists of main controller and decoupling controller is given. The optimal PI controller is presented in Section 4. Fuzzy incremental controller design is given Section 5. Simulation results are presented in Section 6. Conclusions are formulated in the last section.

2. SYSTEM MODELLING

The basis of the high-stability temperature control is an accurate mathematical model of the multizone-furnace, which has to take all the thermal couplings between the zones and the environment into account [6]. The structure of the model, which is determined by the physical conditions, turns out to be V-canonical [5], i.e. the state in a zone is determined by the heating power of the zone and all the other zone states (but not their heating power). With the couplings being induced by heat radiation and heat conductance the model results in a nonlinear system of ordinary differential equations (ODEs):

$$\underbrace{C \dot{\theta}_i}_{\text{change of heat content}} = \underbrace{\sum_{\substack{j=1 \\ j \neq i}}^n S_{ij} (\theta_j^4 - \theta_i^4)}_{\text{internal radiation}} + \underbrace{\sum_{\substack{j=1 \\ j \neq i}}^n L_{ij} (\theta_j - \theta_i)}_{\text{internal conductance}} + \underbrace{S_{i,env} (\theta_{env}^4 - \theta_i^4)}_{\text{external radiation}} + \underbrace{L_{i,env} (\theta_{env} - \theta_i)}_{\text{external conductance}} + \underbrace{W_i q_i}_{\text{source}} \quad (1)$$

with θ_i and q_i denoting temperature and electrical power in zone i . The linearization of the system of ODEs in a steady operating point $\theta_{i,0}$, $q_{i,0}$ leads to

$$T_i \dot{v}_i + v_i - \sum_{\substack{j=1 \\ j \neq i}}^n K_i V_{ij} v_j = K_i p_i, \quad (2)$$

where $v_i = \theta_i - \theta_{i,0}$ (in [K]) and $p_i = q_i - q_{i,0}$ denote the deviations from the operating point.

With the structure of the model being determined the model parameters (W_i, C_i, S_{ij}, L_{ij} in the nonlinear and K_i, T_i, V_{ij} in the linear case) have to be identified experimentally. A theoretical derivation could only be achieved by taking all the material and geometrical properties of the furnace into account what seems to be hardly practical.

The identification of the model parameters is based on a fixed sequence of test signals of the electrical power input and the excited temperature response as the output signal. With the temperature response being measured at the sample points kT_a (T_a sampling time, $k=1, \dots, k_{max}$), the output-least-squares parameter identification method can be formulated as the optimization problem:

$$\sum_{k=1}^{k_{max}} \sum_{i=1}^n |v_i(kT_a) - \bar{v}_i^k|^2 \rightarrow \min_x, \text{ for } x_l \leq x \leq x_u. \quad (3)$$

The pattern of test signals of the electrical power has to be chosen carefully for successful identification of the model. Pseudo-random multi-level (PRMS) signals are appropriate for the identification of strongly coupled multivariable systems. A PRMS is sequence of square signals with features resembling to those of white noise. The magnitude of the signals should cover the whole feasible range of the linearized model for sufficient excitation. Primary requirement for a test signal is even excitation within the whole frequency domain and a noise-to-signal ratio as small as possible. Both demands are in cross-purpose because great frequency rates give only small contributions to excitation. To find a compromise, lot of experiments were undertaken. The calculation of the parameters has been done by applying software tools for solving nonlinear least squares problem.

3. DECOUPLING CONTROLLER

A popular approach to dealing with control loop interactions is to design no interacting or decoupling control schemes. Here, the objective is to eliminate completely the effects of loop interactions. This is achieved via the specification of compensations networks known as decouplers, so that the multivariable process can be controlled using independent loop controller.

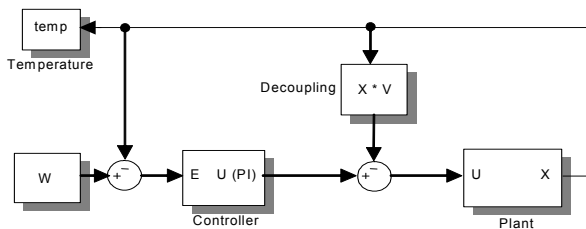


Fig. 1. Block diagram of the closed loop system

Figure 1. gives the block-diagram for the closed loop system. Controller consists of one main (PI) controller for each zone and decoupling controller between zones. The effects of the loop interactions are completely eliminated by decoupling controller. Therefore the system is decomposed into a series of seven independent single-loop sub-systems and the problem of the controller design is reduced to tuning seven independent PI controllers.

4. TIME-DOMAIN OPTIMAL PI CONTROLLER

In the time domain, specifications for a control system design involve certain requirements associated with the time response of the system. The requirements are often expressed in terms of the standard quantities on the rise time, settling time, overshoot, peak time, and steady state error of a step response. In order to have a good closed-loop time response, the following performance function needs to be considered during the design of PI controller:

$$J(K_p, K_I) = \int_0^{\infty} (y_{step}(t) - y_{step}^d(t))^2 dt \quad (4)$$

where $y_{step}^d(t)$ is the desired response and $y_{step}(t)$ the step response of the system with the PI controller. Since it is often not allowed to tray different PI controller parameters on the plant for the sake of safety, $y_{step}(t)$ is replaced by the step response of the model with the PID controller. Thus the optimal PI controller design may be stated as

$$\min_{K_p, K_I} J(K_p, K_I) \quad (5)$$

based on the linearized model of the multizone furnace. The parameters K_p and K_I are optimized using the MATLAB routine "lsqnonlin". This routine actually performs least squares fit on the tracking of the output.

5. INCREMENTAL FUZZY PI CONTROLLER

The classical PI controller in the system is replaced with the incremental Fuzzy PI controller. An incremental controller adds control signal change to the current control signal value [3][4].

$$u_n = u_{n-1} + \Delta u_n \Rightarrow \Delta u_n = K_p(e_n - e_{n-1} + \frac{1}{T_i} e_n T_s). \quad (6)$$

The control signal U_n is the sum of all previous increments,

$$U_n = \sum_i (cu_i \cdot GCU \cdot T_s). \quad (7)$$

The linear approximation to this controller is:

$$\begin{aligned}
U_n &= \sum_{i=1}^n (E_i + CE_i) \cdot GCU \cdot T_s \\
&= GCU \cdot \sum_{i=1}^n \left[GE \cdot e_i + GCE \cdot \frac{e_i - e_{i-1}}{T_s} \right] \cdot T_s \\
&= GCU \cdot \left[GE \cdot \sum_{i=1}^n e_i \cdot T_s + GCE \cdot \sum_{i=1}^n (e_i - e_{i-1}) \right] \\
&= GCE \cdot GCU \left[\frac{GE}{GCE} \sum_{i=1}^n e_i \cdot T_s + e_n \right].
\end{aligned} \quad (8)$$

It is obvious that the gains of the classical PI controller and the normalization gains of fuzzy incremental PI controller are related in the following way:

$$GCE \cdot GCU = K_p, \quad \frac{GE}{GCE} = \frac{1}{T_i}. \quad (9)$$

Notice that the proportional gain depends on GCE and the integral action is determined by the ratio between two inputs gains. The input variables are the deviation from the desired value and its derivative, and the output variable is the increment of the operating value.

The signal flow is as follows: the error signal and the time derivative of the error are first normalized to the range

$[-1 \ 1]$ by multiplying with scaling factors, namely input gains GE and GCE , and are fed into the Fuzzy controller; the output variable ΔU is fed out from the Fuzzy controller and turned back to the non-scaled value Δu by multiplying with the output gain GCU and finally this non-scaled value is integrated to obtain the practical control value which is fed into plant.

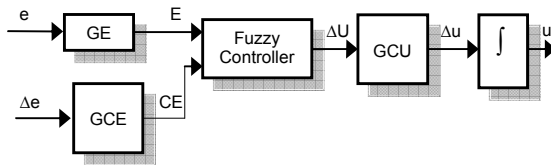


Fig. 2. Fuzzy incremental controller

The Rule Base is given in Table 1. where PB, PM, PS are labels of the fuzzy sets meaning positive big, positive medium and positive small, ZO is zero, NS is negative small, NM negative medium and NB denotes negative big.

		ΔE						
		NS	NM	NS	ZE	PS	PM	PB
E	NB	NB	NB	NM	NM	NM	NS	ZE
	NM	NB	NM	NM	NM	NS	ZE	PM
	NS	NM	NM	NS	NS	ZE	PS	PM
	ZE	NM	NM	NS	ZE	PS	PS	PS
	PS	NS	NS	ZE	PS	PS	PS	PS
	PM	NS	ZE	PS	PM	PM	PM	PB
	PB	ZE	PS	PM	PM	PM	PB	PB

Table 1. The fuzzy rules table

The membership functions of input and output variables are Gaussian functions. Membership functions of the input variables are selected to be of different widths (that is narrowest are ZO fuzzy sets, and the widest are PB and NB fuzzy sets, etc.), as shown in Figure 3. By this fine control has been provided for the small deviations while for the larger deviations the control action is more aggressive.

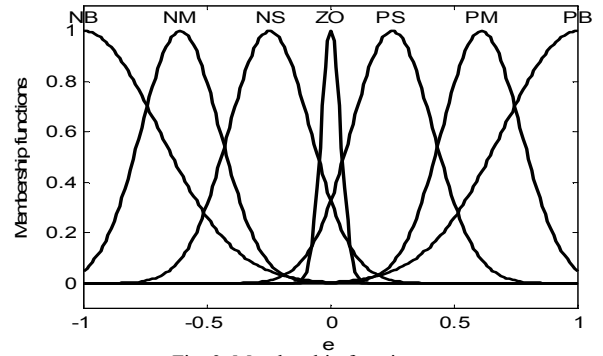


Fig. 3. Membership functions

6. SIMULATION RESULTS

Both proposed control strategies are applied to the considered multizone furnace. Temperature response of optimal PI controller is shown in Figure 4. Since an overshoot in the step response occurs, the modification of the control law has been performed by multiplying the reference signal by the constant parameter b .

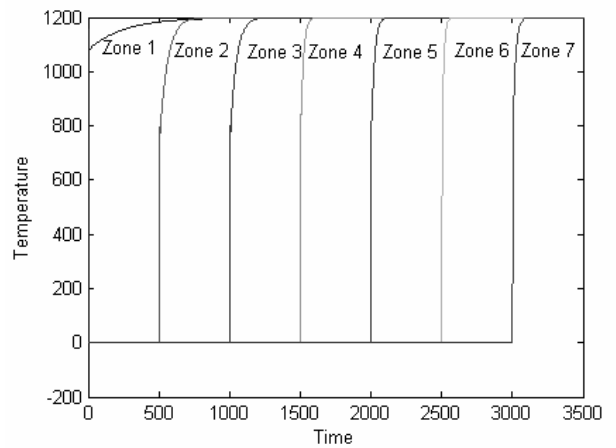


Fig. 4. Temperature response of optimal PI controller

Simulation results obtained by application of the incremental fuzzy PI controller are shown in Figure 5. The two input normalization gains and output denormalization gain were determined based on the previously obtained gains of the conventional PI controller. GE , the input gain with respect to the deviation E , was set equal to $1/(\text{desired value})$, where GCE and GCU are determined from the equations (9). Since the first zone reacts slowly because of the construction of the furnace, the scaling factor GCE was fine tuned to the $GCE/15$ to accelerate the response of the first zone.

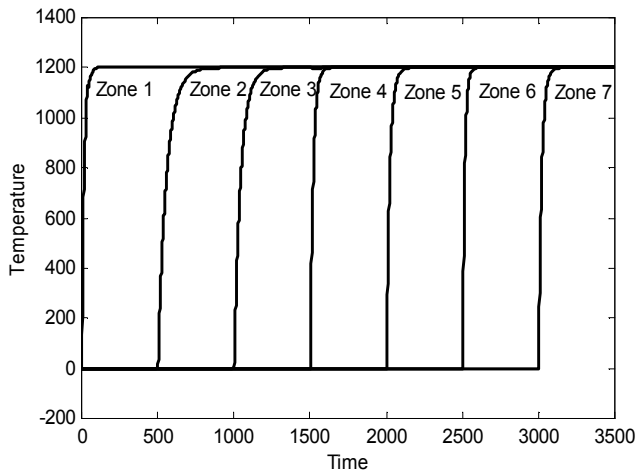


Fig. 5. Temperature step response of the fuzzy incremental PI controller

The simulations presented in Fig. 5. show that the fuzzy incremental PI controller gives the faster response and there was also no need to do the modification of control law (multiplication by b). Although the structure of the fuzzy controller is far more complicated than the one of the classical controller, it has been shown that fuzzy controller design is convenient in this case and that the large number of the adjustable parameters gives a lot of possibilities for tuning and achievement of good control strategy.

7. CONCLUSIONS

In this paper two PI controller design schemes for temperature control of the crystal growth furnace have been considered: time domain optimal PI controller and incremental PI fuzzy controller. The optimal tuning mechanism finds optimal parameters for the PI controller so that the desired system specifications are satisfied. The scaling factors of the fuzzy controller are determined from the gains of the conventional PI controller. The shapes of membership functions were fine tuned to improve steady state error and overall performance.

Simulation results confirm that the fuzzy logic approach is feasible and convenient in this case, and can be an interesting alternative to conventional control despite the fact that model is known and linear. Implemented fuzzy incremental PI controller presented a slightly superior dynamic performance when compared with conventional PI controller, in terms of better response speed and overshoot reduction.

REFERENCES

- [1] C. Batur, W. M. B. Duval and R. J. Bennett, "Control and design of crystal growth furnace", ISA Transactions, vol 38, p.p. 73-85, 1999.
- [2] G.P. Liu, S. Daley "Optimal-tuning PID control for industrial systems", Control Engineering Practice vol 9, p.p. 1185-1194, 2001
- [3] M. Kinouchi, I. Hayashi, N. Iwatsuki, K. Morikawa, J. Shibata, and K. Suzuki, "Application of Fuzzy PI control to improve the positioning accuracy of a rotary-linear motor driven by two-dimensional ultrasonic actuators", Microprocessors and Microsystems, vol 24, p.p. 105-112, 2000.
- [4] W. Li, "Design of Hybrid Fuzzy Logic Proportional Plus Conventional Integral-Derivative Controller", IEEE Transactions of Fuzzy Systems, vol 6, no 4, p.p. 449-464, November 1998
- [5] V. Nikolić, and K. Aleksić, "Identification and control of multizone Furnace", PAMM Bulltens for applied and computational mathematics, p.p.100-106, Hungary, 2003.
- [6] S. Rohani, M. Haeri, and H. C. Wood, "Modeling and control of a continuous crystallization process Part 1. Linear and non-linear modeling", Computers and Chemical Engineering, vol 23, p.p. 263-277, 1999.
- [7] S. Rohani, M. Haeri, H. C. Wood, "Modeling and control of a continuous crystallization process Part 2. Model predictive control", Computers and Chemical Engineering, vol 23, p.p. 279-286, 1999

DYNAMIC PROCESSES OF BRAKING THE VEHICLE WITH THE HYDRAULIC BRAKING SYSTEM

Bogdevicius Marijonas.¹

Abstract

Transport traffic safety depends on many factors; one of them being the efficiency of the vehicle braking. The efficiency of the vehicle depends on the reaction of the driver, the braking system, the quality of tires, the characteristics of the road surface. The quarter of the vehicle with the hydraulic braking system and disc brake with the wheel has been investigated. The dynamic models of the disk brake assembly and the wheel have been constructed. The dynamic models of disk brake evaluate elastic, damping and frictional properties of the pad and the hosting. The dynamic model of the vehicle quarter takes the dynamic properties of the suspension and the tire, the tire-road friction coefficient that depends on the longitudinal tire slip and the linear velocity of the wheel into account. The systems of equation of dynamic models' motions are solved by numerical methods. The dynamic characteristics of the braking system of the automobile are obtained.

Keywords: braking system, suspension, tire, hydraulic system, numerical method

1. INTRODUCTION

The modern automotive braking system has been refined for over 100 years and has become extremely dependable and efficient. The typical disc braking system consists of a disc (rotor), caliper housing, a piston, seal and pads. When braking, the system generates fluid pressure that pushes the piston towards the shoe with lining, forcing the shoe with lining to rub against the disk and generating the braking torque to stop the vehicle.

When studying the dynamics of the vehicle braking process, the impact of the most important parameters of the braking system on the braking process shall be taken into consideration [1,2,3]. The following parameters of the braking system may be considered as the most important: the hydraulic system, brake fuel physical characteristics, caliper housing, elastic and damping characteristics of braking pads, the initial distance and friction coefficient between the pad and the disc, the characteristics of the vehicle suspension, the interaction between the wheel and road surface.

This article deals with the vehicle quarter with the hydraulic braking system, the suspension as well as the dynamic processes of the interaction between the wheel and road surface.

2. THE DYNAMIC MODEL OF THE BRAKING SYSTEM

The dynamic model of the braking system includes the brake rotor, housing, piston, pads, hydraulic cylinder, wheel and part of the suspension (Fig. 1).

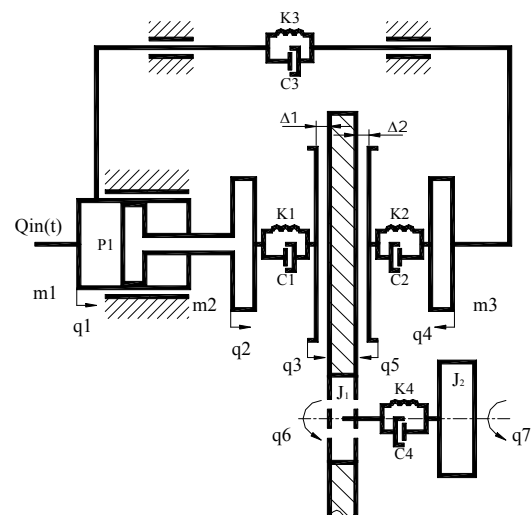


Figure 1 The main scheme of the braking system

¹ Professor habil dr Marijonas Bogdevicius, Vilnius Gediminas Technical University, Department of Transport Technological Equipment, e-mail: marius@ti.vtu.lt

The system of equations of the caliper disk brake may be written as follows:

$$m_1 \ddot{q}_1 = -pS_1 - k_3(q_1 + q_4) - c_3(\dot{q}_1 + \dot{q}_4) - F_{fr12} \text{sign}(\dot{q}_1 - \dot{q}_2) - F_{fr14} \text{sign}(\dot{q}_1 + \dot{q}_4), \quad (1)$$

$$m_2 \ddot{q}_2 = pS_1 - F_{fr12} \text{sign}(\dot{q}_2 - \dot{q}_1) - F_{N1}, \quad (2)$$

$$F_{N1} = \begin{cases} 0, & q_3 \leq \Delta_1 \\ k_1(q_2 - (q_3 - \Delta_1)) + c_1(\dot{q}_2 - \dot{q}_3) & q_3 > \Delta_1 \end{cases}$$

$$m_3 \ddot{q}_4 = -k_3(q_4 + q_1) - c_3(\dot{q}_4 + \dot{q}_1) - F_{N2} - F_{fr14} \text{sign}(\dot{q}_1 + \dot{q}_4), \quad (3)$$

$$F_{N2} = \begin{cases} 0, & q_5 \leq \Delta_2 \\ k_2(q_4 - (q_5 - \Delta_2)) + c_2(\dot{q}_4 - \dot{q}_5) & q_5 > \Delta_2 \end{cases};$$

$$\dot{p} = \frac{K(p)}{V_0 + S(q_2 - q_1)}(Q_{in} - S(\dot{q}_2 - \dot{q}_1));$$

$$J_1 \ddot{q}_6 = -M_b \text{sign}(\dot{q}_6) - k_4(q_6 - q_7) - c_4(\dot{q}_6 - \dot{q}_7); \quad (4)$$

$$M_b = R_a(F_{N1} + F_{N2})f,$$

where m_1 is the mass of a hydraulic cylinder; m_2, m_3 are masses of pads; J_1, J_2 are inertia mass moments of disk and tire; k_1, k_2 and c_1, c_2 are stiffness and damping coefficients of inner pads, respectively; k_3, c_3 are stiffness and damping coefficients of housing; Δ_1, Δ_2 are initial gaps between a pad and a disk; $Q(t)$ is discharge of fluid; F_{fr12} is friction force between a cylinder and a piston; F_{fr14} is friction force between a cylinder and a pad; F_{N1}, F_{N2} are normal forces between pads and the disk; S is a cross-section area of the piston; V_0 is initial volume of the cylinder; M_b is a brake torque; R_a is an average radius; f is friction coefficient between pad and disk; q_1, q_2, \dots, q_7 are generalized coordinates;

The system of equations of the dynamic model of the vehicle quarter is presented. The wheel rotational dynamics is expressed by the following equation:

$$J_2 \ddot{q}_7 = -R_d F_T(\mu) - k_4(q_7 - q_6) - c_4(\dot{q}_7 - \dot{q}_6) \quad (5)$$

where k_4, c_4 are stiffness and damping coefficients of the wheel; R_d is the dynamic radius of the wheel,

$R_d = R_0 + q_9 - z(t)$; R_0 is the initial radius of the wheel; $F_T(\mu)$ is traction/braking force; μ is tire/road friction coefficient.

The vehicle quarter motion in the longitudinal direction on the road plane is described by the following equation, in which the effect of aerodynamic, drag and rolling resistance are estimated:

$$(m_4 + m_5) \ddot{q}_8 = F_T(\mu) - a_1 \dot{q}_8 - a_2 \dot{q}_8^2 \text{sign}(\dot{q}_8) \quad (6)$$

where m_4 is the mass of the wheel; m_5 is mass of vehicle quarter; a_1, a_2 are coefficients of resistance to movement.

The following system of equations of the suspension is given:

$$m_4 \ddot{q}_9 = -k_5(q_9 - z(t)) - c_5(\dot{q}_9 - \dot{z}(t)) - m_4 g - k_6(q_9 - q_{10}) - c_6(\dot{q}_9 - \dot{q}_{10}) - F_{fr5} \text{sign}(\dot{q}_9 - \dot{q}_{10}); \quad (7)$$

$$m_5 \ddot{q}_{10} = -k_6(q_{10} - q_9) - c_6(\dot{q}_{10} - \dot{q}_9) - m_5 g - F_{fr5} \text{sign}(\dot{q}_{10} - \dot{q}_9) \quad (8)$$

where m_5 is the mass of vehicle quarter; $k_5, c_5, k_6, c_6, F_{fr5}$ are stiffness and damping coefficients and friction force of suspension, respectively.

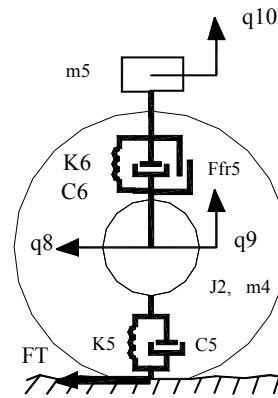


Figure. 2 The calculated circuit of the quarter vehicle

The tire friction force depends on the vertical force, longitudinal tire slip (λ), velocity ($v = \dot{q}_8$) and is equal to the slip angel (α)

$$F_T = F_N \mu(\lambda, v, \alpha),$$

where F_N is a vertical force,

$$F_N = -k_5(q_9 - z(t)) - c_9(\dot{q}_9 - \dot{z}(t)).$$

The friction coefficient between the tire and the road is equal :

$$\begin{aligned} \mu(\lambda, v, \alpha) &= \\ b_0 \exp(b_1 + b_2 \lambda) \lambda^{b_3 + b_4 \lambda} \exp(b_5 v) \exp(b_6 \alpha) & \text{ when } \lambda > 0; \\ \mu(\lambda, v, \alpha) &= \\ -d_0 \exp(d_1 + d_2 |\lambda|) |\lambda|^{d_3 + d_4 |\lambda|} \exp(d_5 v) \exp(d_6 \alpha) & \text{ when } \lambda < 0; \\ \mu(\lambda, v, \alpha) &= 0, \text{ when } \lambda = 0, \end{aligned} \quad (9)$$

where b_i and d_i ($i = 0, 1, \dots, 6$) are known coefficients. Figure 3 shows the function coefficient curve. It is evident that the peak of the friction coefficient varies between 0.10 and 0.20.

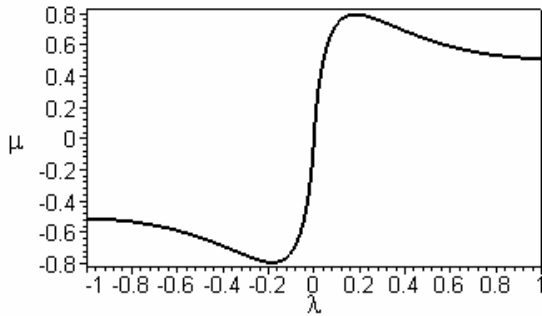


Figure 3. Friction coefficient curve

When studying the dynamics of the vehicle, the intricate interaction between the wheel and the road surface, i.e. the characteristics of the tire to even the initial stochastic road surface is taken into account. The effectiveness of the tire evening characteristics high frequency components (harmonics) of the surface are not taken into consideration. If stochastic road surface characteristics are known, stochastic signals may be generated. Thus the algorithm, which is based on the linear transformation of the sequence of independent numbers $\xi[n]$, is used when the numbers of the sequence distribute according to the normal distribution into sequence $f[n]$ which correlates according to the following law:

$$R_{ff}[n] = M\{f[k]f[k+n]\} = R_{ff}[nz] \quad (10)$$

$n = 0, 1, 2, \dots$

here z is the height of the road surface; t is discretion step.

Then, non-inertial non-linear transformation is used to obtain the required law $f[n]$. To create the most widely spread correlation functions, the effective discrete modelling algorithms are written in the following form:

$$f[n] = \sum_{k=0}^l a_k \xi[n-k] - \sum_{k=1}^m b_k f[n-k]. \quad (11)$$

The stochastic road surface is described by the following correlation function:

$$\begin{aligned} R(\tau) &= \sigma_1^2 \exp(-\alpha_{s1}|\tau|) + \\ &\sigma_2^2 \exp(-\alpha_{s2}|\tau|) \cos(\beta\tau). \end{aligned} \quad (12)$$

The results obtained when modelling the road surface stochastic grading are shown in Figure 4.

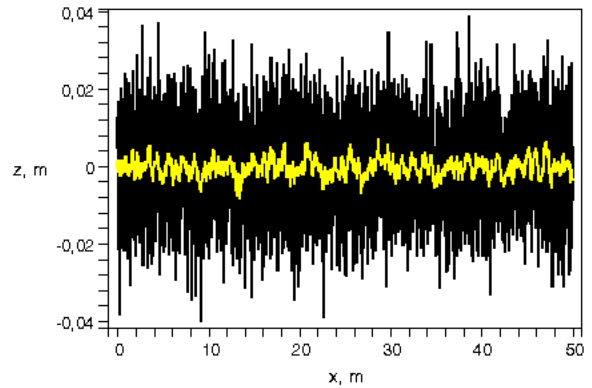


Figure 4. Road surface grading:

$$\begin{aligned} \sigma_1 &= 0.005 \text{ m}; \alpha_{s1} = 20.0 \text{ m}^{-1}; \\ \sigma_2 &= 3.87 \cdot 10^{-3} \text{ m}; \alpha_{s2} = 15.0 \text{ m}^{-1}; \\ \beta &= 60.0 \text{ m}^{-1} \end{aligned}$$

3. RESULTS

The vehicle braking process is studied when the vehicle moves on the asphalt concrete pavement and the initial speed is equal to $\dot{q}_8 = 80 \text{ km/h}$. The vehicle's dynamic model parameters are as follows:

$$\begin{aligned} m_1 &= m_2 = 0.5 \text{ kg}; m_3 = 1.0 \text{ kg}; m_4 = 30.0 \text{ kg}; \\ m_5 &= 250.0 \text{ kg}; \\ J_1 &= 0.30 \text{ kgm}^2; J_2 = 0.350 \text{ kgm}^2; \\ k_1 &= 5.0 \cdot 10^6 \text{ N/m}; k_1 = k_2 = 5.0 \cdot 10^6 \text{ N/m}; \\ k_3 &= 5.0 \cdot 10^8 \text{ N/m}; k_4 = 5.0 \cdot 10^6 \text{ Nm/rad}; \\ k_5 &= 160.0 \cdot 10^3 \text{ N/m}; k_6 = 10^6 \text{ N/m}; \end{aligned}$$

$$c_1 = c_2 = c_3 = 40.0 \text{ Ns/m}; c_4 = 0.50 \text{ Nms/rad};$$

$$c_5 = 2.50 \cdot 10^3 \text{ Ns/m}; c_6 = 10.0 \cdot 10^3 \text{ Ns/m};$$

$$k_5 = 160.0 \cdot 10^3 \text{ N/m}; k_6 = 10^6 \text{ N/m};$$

$$F_{fr5} = 30 \text{ N}; f = 0.45.$$

The dependence of the vehicle braking distance $L(t)$ on time is shown in Figure 5. The dependence of the vehicle braking acceleration on time is shown in Figure 6. The dependence of the wheel angular acceleration on time is shown in Figure 7

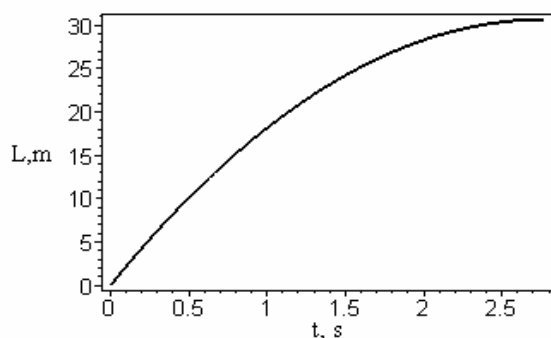


Figure 5. Dependence of braking distance on time

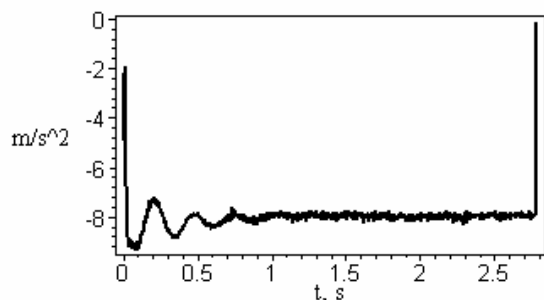


Figure 6. Dependence of braking acceleration on time

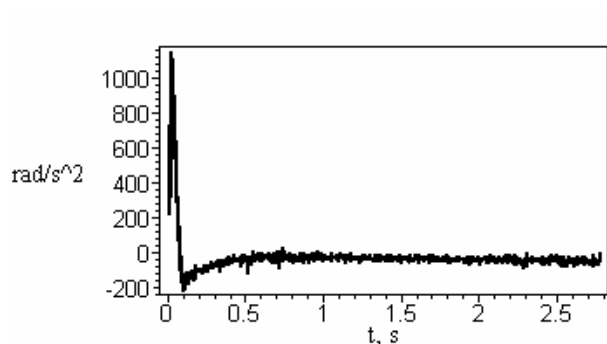


Figure 7. Dependence of wheel angular acceleration on time

4. CONCLUSION

1. The dynamic model of the interaction between the vehicle hydraulic system and the wheel, which takes the main parameters of this system influencing on the dynamics of the vehicle braking process into account, has been constructed.
2. The dynamic characteristics of the braking process were obtained and the impact of the main parameters of the hydraulic braking system on the efficiency of the braking process was estimated through the use of this dynamic model

5. REFERENCES

1. Bogdevicius M., Vladimirov V. Simulation of Automobile Hydraulic Brake System // *Mechanika*, Nr.3 (35). Kaunas: Technologija, 2002, p. 67 – 70.
2. Bogdevicius M., Vladimirov V. Dynamic processes in the hydraulic braking system of transport vehicle // *The Fourth International Conference "Heavy Machinery HM 2002"*, Kraljevo, 28-30 June 2002 : proceedings / Fakultety of Mechanical Engineering Kraljevo, University of Kragujevac. Kraljevo : Riza, 2002. ISBN 86-82631-15-6. p. 37-40.
3. Bogdevicius M., Vladimirov O. Investigation of Dynamic Processes in the Hydraulic Braking System of Transport Vehicle with Anti-lock Brake System. // *Transport and Telecommunication*. Riga, Vol.5, Nr.1, 2004, p. 85-90.
4. Aladjev V., Bogdevicius M. *Maple 6: Solution of the Mathematical, Statistical and Engineering – Physical Problems*. Moscow: Laboratory of Basic Knowledge, 2001, p.864 (in Russian).

A NEW SYSTEM FOR TEXTILE WEB FEEDING AT CALENDERING LINES IN TIREFMAKING INDUSTRY

Ž. Jakovljević, P. B. Petrović¹

Abstract

In this paper a new system for control of textile web feeding into the calendering process is presented. It consists of three stages: textile web centering, web center spreading and web edges spreading. The control of these processes is based on information on cords distribution and orientation obtained from vision sensors. Acquired vision signal processing is based on two-dimensional discrete wavelet transform. Experimental verification of this method has shown satisfactory results when real-world disturbances and real-time applicability are considered.

Key words: Calendering process, web feeding, vision sensor, discrete wavelet transform

1. INTRODUCTION

Passenger vehicle and truck tires are made of steel or textile cord, which is layered by rubber compound.

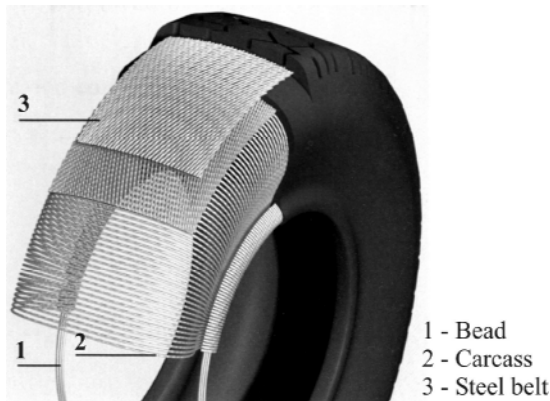


Figure 1. An example of steel cords location in truck's tire

The role of steel or textile cord is to carry the load, while the rubber compound ensures spatial position of fibers and makes the final shape of tire. An example of steel cords arrangement in truck pneumatic is shown in Figure 1. The regularity of cords distribution, their preload and mechanical bonding of textile/steel to the rubber are of the most importance for the quality of final product.

Ruberrized steel/textile cord sheets are produced using calendering technique. A pre-set number of steel cords or textile web is introduced into calender, which usually consists of 4 steel rolls in S configuration revolving in opposite direction. Rubber compound is added to the opening area between the first two rollers and it is pressed into, on the top of and on the bottom of the steel/textile cords. Continuous sheet of thus obtained composite is put trough several more rollers where, using friction and rolling, good penetration and bonding between rubber and cords is ensured.

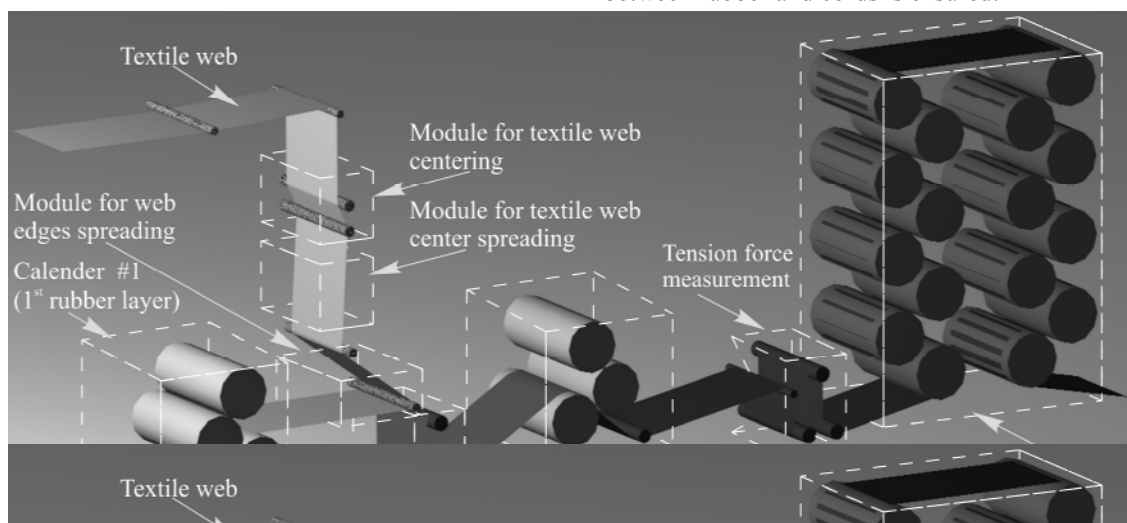


Figure 2. Flowchart of line for textile cord calendering with flowchart of textile web feeding (the line consists of 2 three-roll calenders).

¹ Živana Jakovljević, M.Sc. (ME), Faculty of Mechanical Engineering, 11 000 Belgrade, Kraljice Marije 16, e-mail: zjakovljevic@mas.bg.ac.yu
Professor Dr. Petar B. Petrović, Faculty of Mechanical Engineering, 11 000 Belgrade, Kraljice Marije 16, e-mail: pbpetrovic@mas.bg.ac.yu

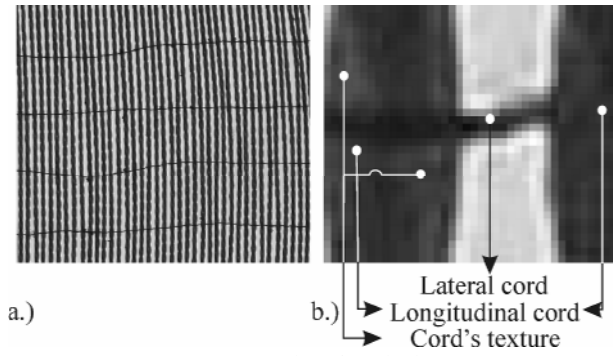


Figure 3. A shot of textile sheet

Flow chart of calendering process is shown in Figure 2, on an example of calendering line LPK-80-1800, produced in Russia, which is based on two 3-roll calenders. When steel cord is calendered, each cord is introduced into calendering process separately. Textile cord, on the other hand, is introduced in the form of textile web (fabric) – longitudinal cords are weaved with lateral. Uniform distribution of textile cords along the whole width of the web (including its edges) is crucial for the quality of final product. A shot of textile sheet is shown in Figure 3.a. It is made of dense longitudinal cords (usually 1000 cords per 1m), weaved with relatively rare lateral cords. Deformability of lateral cords disables maintaining of pre-set geometry of textile webs. Due to unequal web spreading and due to the uneven friction torque along transport rolls, the position of longitudinal cords is lost – they become accumulated or rarefied in some areas (usually at web edges), they become inclined relative to the feeding axis, or even they can get curved shape in extreme cases. For these reasons, some corrective actions using special equipment must be carried out just before rubberizing.

In conventional systems for feeding of textile web into the process, all corrective actions of mechanisms for web centering and spreading, besides contact sensors for web edges detection, are based on a priori given parameters, following general experience rules.

In this paper, an approach to the control of uniformity of cord distribution in textile web is proposed. It is based on real time identification of cord distribution using vision sensors and two-dimensional wavelet transform of acquired signal (image).

2 SYSTEM FOR CONTROL OF TEXTILE WEB FEEDING

A flowchart of proposed system for textile web feeding control is shown in Figure 4.

Acquired vision signal (image) is processed in order to obtain the information on cords distribution and orientation based on which corrective actions using feeding mechanism are carried out.

2.1. Signal processing

Identification of spacing between longitudinal cords and their orientation in respect to the longitudinal axis implies identification of each cord on static scene. This

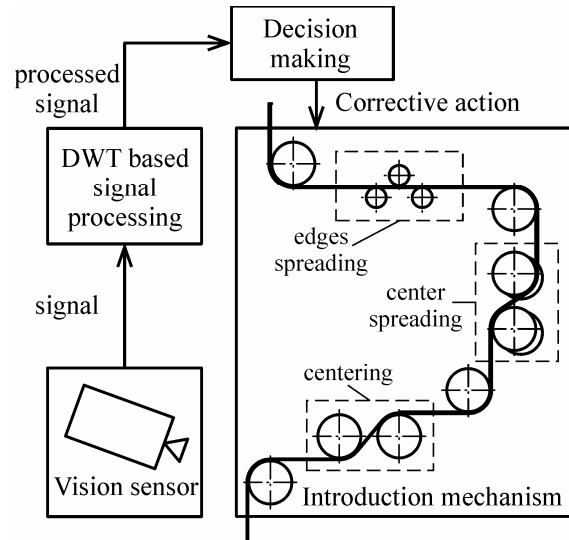


Figure 4. A flowchart of proposed control system

can be done by identification of left or right edge of the cord. Algorithm for identification of vertical edges interlaced with horizontal ones, in the presence of bordering noise on the edges, cord texture, as well as individual fibers stepping out, (Fig. 3.b.) is not straightforward and cannot be based on simple threshold method. Even if all edges were isolated, determining which edge belongs to the longitudinal and which one to the lateral cord (taking gradient method, e.g.) would've been extremely slow from the real time applicability point of view, and especially when the number of cords is considered.

For these reasons algorithm for cord identification is based on two-dimensional discrete wavelet transform (DWT). Using DWT signal is presented as superposition of wavelets, functions, which are obtained by translation and dilatation (in discrete steps) of single function called “mother wavelet” [1, 2, 3]. Mother wavelet and wavelets are non-periodic functions, which can be compactly supported (defined in finite time/space interval) and can be of asymmetric, irregular shapes. Thanks to these properties of wavelets, DWT is especially suitable for detection of stepwise changes in signal (such as edges in image) and their localization in time or space [3,5,6].

Multiresolution analysis (MRA) [2, 3, 4] gives fast algorithms for direct and inverse DWT computation called subband filtering scheme. Its main results can be formulated as follows. If a sequence of resolutions 2^{-j} , $j \in (0, -\infty)$ is taken, then each signal can be represented as the sum of its approximation on resolution $J - Af$ and details $D_j f$, $j \in [1, J]$ taken from it during passing from higher level of approximation (resolution) to the lower one:

$$f = A_J f + \sum_{j=1}^J D_j f = \sum_n a_n^J \phi_{J,n} + \sum_{j=1}^J \sum_n d_n^j \psi_{j,n} \quad (3)$$

where a_n^J are the approximation and d_n^j the detail coefficients, computed by above-mentioned subband filtering scheme, $\{\psi_{j,n}, n \in \mathbb{Z}\}$ are the families of ortho-

normal wavelet bases and $\{\phi_{j,n}, n \in \mathbb{Z}\}$ is the family of corresponding scaling functions orthonormal basis [4].

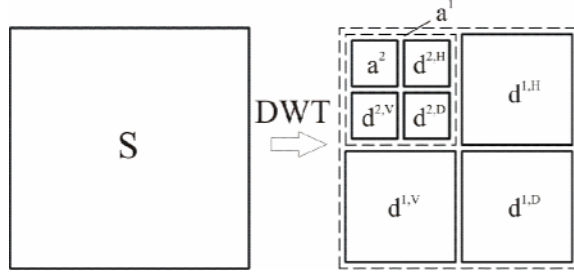


Figure 5. Two-dimensional DWT visualization

If an image is considered as two-dimensional signal (represented by matrix S with dimensions $m \times n$, where m is the number of rows, and n the number of columns), then the edge on image can be considered as an abrupt change in space and it can be localized using two-dimensional DWT. Two-dimensional DWT is also carried out using subband filtering scheme in following two steps:

Step 1: One-dimensional DWT of each row of matrix S

Step 2: One-dimensional DWT of columns computed in step 1.

Two-level DWT of image S can be visualized as shown in Figure 5. Approximation coefficients a^1 and a^2 represent versions of starting image at 2 and 4 times lower resolutions. Detail coefficients $d^{i,H}$, $d^{i,V}$ and $d^{i,D}$ carry information on horizontal, vertical and diagonal edges in image, respectively. These matrices have 2^n (n is the level of transformation) smaller dimensions than original matrix, thus making further analysis faster, which is extremely significant from real-time applicability point of view.

2.2. Identification of distance between cords

As mentioned above, identification of spacing between longitudinal cords and their orientation in respect to the longitudinal axis is based on identification of edge of each cord. In method used here it is done in three main steps [5].

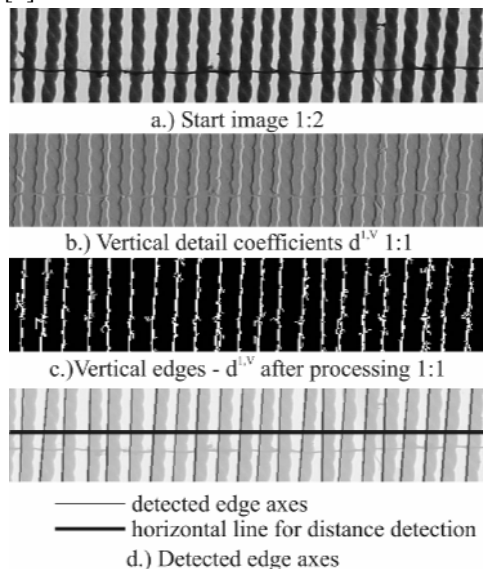


Figure 6. Steps in proposed edges detection method

First, one level DWT of original image (Figure 6.a.) using 'haar' wavelet [1, 2, 5] is carried out in order to obtain vertical detail coefficients (Figure 6.b.). Maximal values of $d^{1,V}$ (the lightest pixels in Figure 6.b.) correspond to the left, and minimal (the darkest pixels in Figure 6.b.) to the right cord edges.

Afterwards, applying threshold method on $d^{1,V}$ and putting thus obtained matrix through some additional processing [5] and low-pass filter will lead to image shown in Figure 6.c., which represents detected left edges of cords.

In third step, centroid and the angle between horizontal line and main axis of ellipse of inertia of each object on scene, that is, of each edge is computed. In this way, position and orientation of each edge on scene is determined.

Based on detected position and orientation of cord edges, their axes are determined (Figure 6.d.). The distance between cords is calculated using the distance between intersections of axis of each edge and horizontal reference line as shown in Figure 6.d. By translation of vision sensor along the web width, several images are obtained. Combining information gained from these images, the profile of longitudinal cord distribution along lateral section of textile web, that is, the profile of cords density is obtained.

2.3. Mechanism for textile web feeding

Sensory information obtained as described above, makes basis for implementation of system for control of textile web feeding into the calendaring process. Corrective actions are carried out using mechanisms dedicated for textile web centering, for textile web center spreading and for textile web edges spreading.

Due to the long infeed paths, textile web is usually inclined in infeed plane. The information on angle of inclination - α (Figure 7.) is obtained from information on cord orientation. Based on this information corrective actions are carried out using mechanism for textile web centering (Figure 7.). Main parts of this mechanism are

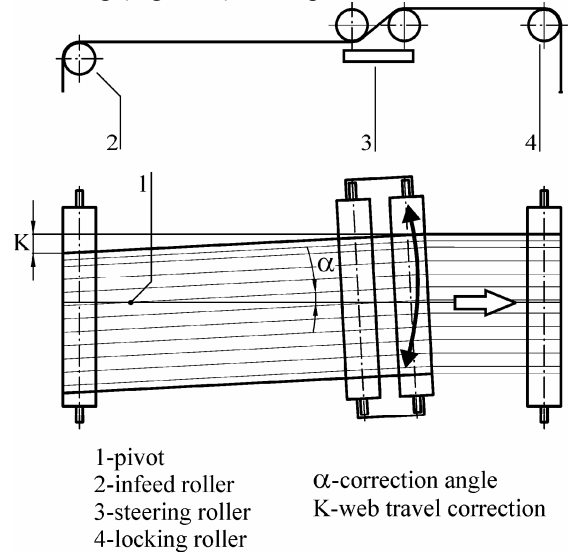


Figure 7. Mechanism for textile web centering

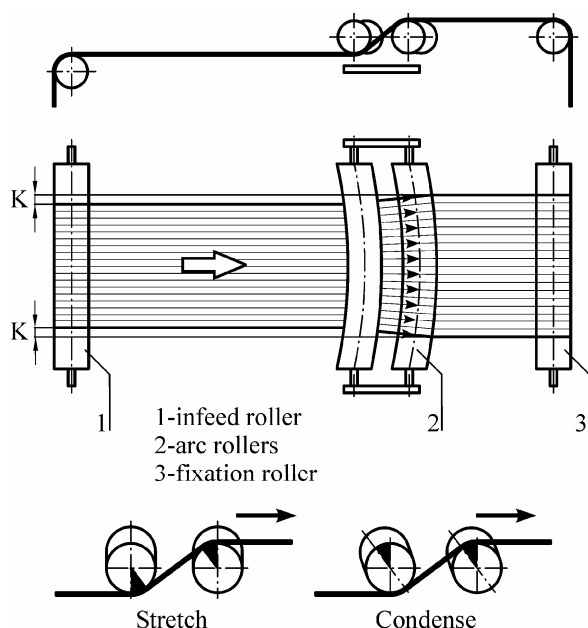


Figure 8. Mechanism for textile web center spreading

guide rollers, which rotate in infeed plane. Depending on the change of angle between guide rollers and infeed direction, the tension distribution along lateral section of web is changed, thus forcing the cords to change their direction. In this way, textile web takes demanded orientation.

Although the web is now well centered, its width and the distribution of cords within it are yet to be corrected. The mechanism for web center spreading (Figure 8.) has, as main elements, two arc (banana) rollers, separated in the center, each of them operating independently. Pivot angle between arc rollers is computed from information on cords distribution. Depending on this angle textile web is either stretched or condensed thus fixing cords distribution.

Since, due to the nature of textile web, the main errors in cord distribution appear at the web edges where the cords are usually extremely condensed, for web edges spreading special mechanism is introduced (Figure 9.). It consists of two independent three-finger rollers, which spread the cords according to its distribution obtained from vision sensor signals. Two of three rollers are fixed and are always in contact with the web, while the third is movable. The width of the web is controlled by changing the bite angle of the movable (middle) roller (β). Spreading is controlled by changing the cant angle α , while the range of influence towards the center of the web can be adjusted by changing the center gap between movable roller and web plane (G).

3. CONCLUSION

This paper gives a new approach to the control of textile web feeding into the calendaring process based on textile web condition monitoring using vision sensor signal. Proposed DWT based method for monitoring of condition of textile web before its entering into the

calendaring process has given good results on considered textile web samples. Two-dimensional DWT

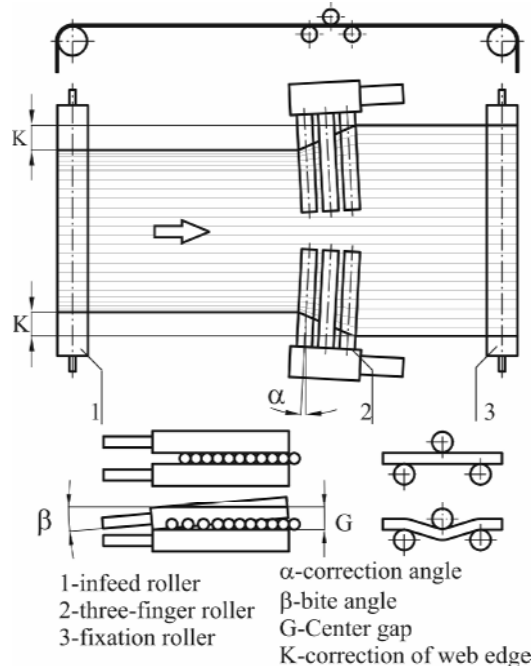


Figure 9. Mechanism for textile web edges spreading

represents efficient means for detection of edges of longitudinal cords in presence of noise, lateral cords, cords texture and other real-world disturbances in image. Besides, it makes good basis for fast real-time computing of longitudinal cords distribution profile and their orientation in infeed plane. This information can be efficiently utilized for corrective actions using various mechanical mechanisms for textile web centering and spreading, as described.

REFERENCES

- [1] Daubechies, I., Ten Lectures on Wavelets, CBMS-NSF regional conference series in applied mathematics, 61, Society for Industrial and Applied Mathematics, Philadelphia, Pennsylvania, 1992.
- [2] Daubechies, I., The Wavelet Transform, Time-Frequency Localization and Signal Analysis, IEEE Transactions on Information Theory, Vol.36, No.5, pp.961-1004, September 1990
- [3] Jakovljević, Ž., Petrović, P., B., Primena vejvlet transformacije u detekciji diskontinuiteta u signalu, 30. JUPITER konferencija, Zbornik radova, pp. 4.17-4.22., Beograd, april 2004.
- [4] Mallat, S., G., A Theory for Multiresolution Signal Decomposition: The Wavelet Representation, IEEE Transaction on Pattern Analysis and Machine Intelligence, Vol II, No. 7, pp. 674-693, July 1989.
- [5] Jakovljević, Ž., Petrović, P., B., Identifikacija profila gustine niti po poprečnom preseku tekstilnog platna primenom senzora veštačkog gledanja i diskretne vejvlet transformacije, 31. JUPITER konferencija, Zbornik radova, pp. 3.50-3.55., Zlatibor, april 2005.
- [6] Walker, J., S., A Primer on Wavelets and their Scientific Applications, ISBN 0-8493-8276-9, Chapman & Hall/CRC, New York, 199

FEEDBACK OVER WIRELESS CHANNEL

Vojislav Filipovic

Abstract. *Motivated by practical problem (control of water distribution system with radio feedback signal) we consider the problem of performing state estimation with intermittent observations. The dynamical systems consist of state equation which is given by a linear stochastic differential equation and noisy measurement occurs at discrete times, in correspondence of the arrivals of Poisson process. In our context measurement noise has non-Gaussian distribution. For such case it is derived approximate non Gaussian filter. From that result we get robust Kalman filter using Huber's min-max methodology. Then is proved that sequence of estimation error covariance matrices is a homogenous Markov process. Finally, the P controller is formulated.*

Key words: *Wireless channel, intermittent observations, filtering, control*

1. INTRODUCTION

The major topic in the field of applied sciences now is convergence of control, communication and computer sciences[1]. In this paper we will consider the connection of control and communication (wireless). In the distributed and networked control systems communication is very important component[2]. In the reference [2] the problem of stabilizing a linear system with unmodeled dynamics, through feedback under constraints on the bit-rate of the feedback loop, is considered. The control network is wire (not wireless).

Consideration of a distributed control system supported by a wireless network is an important task that requires a new design approach to both systems. Control systems and communication networks are designed using different principles. The control theory requires the feedback data to be accurate, timely and lossless. In communication network design the random delay and packet loss are generally accepted. This delay and loss is much more pronounced in wireless networks. The area of wireless communication has very intensive research [3]-[5]. Now is well known that wireless networks have limited spectrum and power, time-varying channel gains and interference. In distributed control systems, from the control perspective, the more the controller knows about the system, the better the control performance is. This can be done by increasing the number of sensors or sending sensors measurement more frequently. But, this increases the communication demand on the network and the network may become congested. This introduces longer delays and more packet losses which degrade the control performance. Because a joint design of the network and controller is necessary [6], [7].

¹In several papers the state estimation in the case of missing observations is considered. The dynamical system where the state equation is given by a linear

stochastic equation and noisy measurement occur at discrete times, in correspondence of the arrivals of Poisson process is presented in [8]. It is proposed Kalman filter-based state estimation algorithm. The sequence of estimation error covariance matrices is not deterministic as for the ordinary Kalman filter, but is a stochastic process itself. In [9] the problem of performing Kalman filtering with intermittent observation is considered. The arrival of the observation is modeled as a random process. It is assumed that observation events have independent Bernoulli probabilities. The observation measurement are either received in full or completely lost. In [10] the partial observation losses are considered. The Kalman filter and its error covariance matrix iteration become stochastic, since they now depend on the random packet arrivals of sensor measurements, which can be lost or delayed when transmitted over communication network. In [11] the moving horizon Monte Carlo state estimation is proposed. Measurements are quantized prior to transmission.

In [12] the power control in wireless networks is considered. Controlling transmitted power in a wireless network is critical for maintaining quality of service, maximizing channel utilization and minimizing near-for effect for suboptimal receivers. Depending on the prevailing channel conditions, it selects appropriate controller and places it in the feedback loop. The algorithm is superior in comparison with well known distributed power control algorithm.

In this paper we will consider packet wireless network [13]. The packet arrivals of the sensor measurement is modeled as a Poisson process. We will consider more difficult problem than in [8]. Namely, it is supposed that measurement noise, in the stochastic model, has non-Gaussian distribution. The resulting filter has a nonlinear transformation of production errors and that transformation depends from non-Gaussian distribution of observations. Non trivial difference in comparison

¹ RCT, PO Box 126, Y15300 Loznica, Yugoslavia Fax:++381 15 874 995, E-mail: vfilip@eunet.yu

with the result in [14] is fact that filter is stochastic process itself. Filter is derived using Bayesian methodology [15]. Further we suppose that a priori is known that probability of observation belongs to the known class of distributions. So is given robust stochastic filter with nontrivial difference in comparison with [16]. The main goal of this investigations is to apply results to problem of water distributions control where the feedback signal is given by radio link.

2. PRACTICAL MOTIVATION FOR PROBLEM

The water distribution problem in town Loznica is very jagged. The pipeline of system has length of 750 km and air distance between outer most points is 30km. Project in [17] defines 50 LAN-s and all LAN-s is connected by radio link with the dispatcher center. The one node in the network is presented on the next figure.

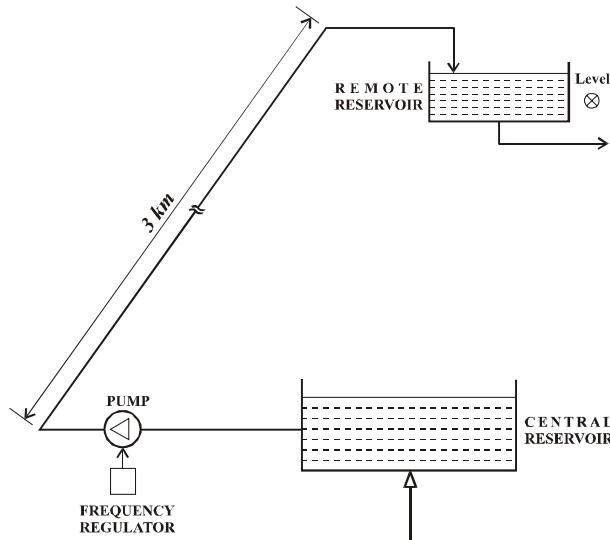


Fig.1. The one node in water distribution system

The purpose of control system is to control of level in the remote reservoir by pump on the position of central reservoir. For that we must use feedback signal (level measurement) from remote reservoir. Distance is about 3 km. To use telephone line is unsuitable in this case and expensive. Our intention is to use feedback signal in the form of radio link. Because we have control system with feedback over wireless channel as is showed in the next figure.

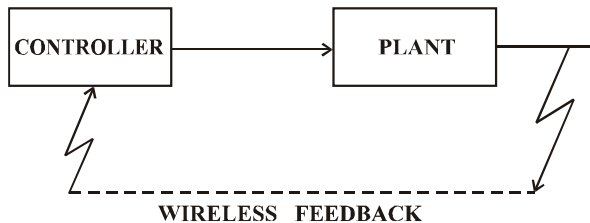


Fig.2. The control loop with wireless feedback

The radio link is a very complex [18]. The main sources of RF interference are: another radio user operating close by on the same frequency of the system, noisy transmitters that emit spurious frequencies outside their allocated bandwidth and intermodulation.

3. FORMAL PROBLEM DESCRIPTION

We will suppose that system under consideration can be described by next stochastic differential equation [19]

$$dx(t) = Fx(t)dt + Gu(t)dt + r(t)dt \quad (1)$$

$$y(t) = Cx(t) + v(t) \quad (2)$$

where $x \in R^n, u \in R^m, y \in R^p$ and $F \in R^{n \times n}, G \in R^{n \times m}$ are known time – invariant real matrices. The stochastic process $r(t)$ is Gaussian with covariance Q , i.e.

$$E\{r(t)r^T(\tau)\} = Q\delta(t - \tau) \quad (3)$$

where $\delta(\cdot)$ is Dirac function. The process $v(t)$ is non-Gaussian.

Let us suppose that packets arrival occur at time instants $\{t_k\}_{k=1}^{\infty}$ which are positively ordered ($t_{k+1} > t_k, \forall k \in N$) and are such that time intervals.

$$T_o = t_1, T_k = t_{k+1} - t_k, k \geq 1 \quad (4)$$

are i.i.d. exponential random variables. The time instants $\{t_k\}_{k=1}^{\infty}$ are the arrivals of Poisson process [20] with the intensity λ . Now system (1) and (2) we can rewrite in the next form

$$\dot{x}(t) = Fx(t) + Gu(t) + r(t) \quad (5)$$

$$y(t_k) = Cx(t_k) + v(t_k) \quad (6)$$

For system (5) and (6) we will find the sampled version whereby sampling period is stochastic.

The discrete –time, stochastic system has a form

$$x(t_{k+1}) = A_k x(t_k) + B_k u(t_k) + w(t_k) \quad (7)$$

where

$$A_k = e^{F(t_{k+1}-t_k)} = e^{FT_k}$$

$$B_k = \int_0^{T_k} e^{F\tau} G d\tau$$

$$w(t_k) = \int_0^{T_k} e^{F\tau} r(t_{k+1} - \tau) d\tau$$

We can see that matrices A_k and B_k are random. Now we will find the mean and covariance matrix of $w(t_k)$. Proofs for all lemmas and theorems will be omitted owing the space.

Lemma 1. For given random time interval T_k

$$E\{w(t_k)|T_k\} = 0 \quad \blacksquare$$

Lemma 2. Let the matrix Q_k is defined as

$$Q_k = E\{w(t_k)w^T(t_k)|T_k\}.$$

$$\dot{Q}(t) = FQ(t) + Q(t)F^T + S$$

where $E\{r(t)r^T(\tau)\} = S\delta(t - \tau)$. \blacksquare

Lemma 3. For $j \neq k$ is

$$E\{w(t_k)w^T(t_j)|T_k, T_j\} = 0. \quad \blacksquare$$

From lemmas follows that $w(t_k)$ conditioned on $\{T_j\}_{j=0}^\infty$ is Gaussian noise, i.e.

$$w(t_k)|T_k \sim N(0, Q_k)$$

4. STATE ESTIMATION ALGORITHM

As a optimal estimator, for system (6) and (7), will used the minimum variance estimator which is given by the conditional expectation.

$$\hat{x}_k = E\{x(t_k) | [y(t_j), T_{j-1}]_{j \leq k}\} \quad (8)$$

We now will formulate the next theorem.

Theorem 1. Asume that

- 1° probability density $p\{x(t_k) | [y(t_j), T_{j-1}]_{j \leq k-1}\}$ is Gaussian with mean \bar{x}_k and covariance matrix M_k
- 2° probability density $p\{y(t_k) | [y(t_j), T_{j-1}]_{j \leq k-1}\}$ exists and twice differentiable
- 3° $E\{w(t_k)w^T(t_k) | T_k\} = Q_k$
- 4° the $w(t_k)$ and $w(t_n)$ are zero mean independent sequences
- 5° the initial state x_0 is independent of the future disturbances $w(t_k)$ and $w(t_n)$
- 6° the observation expectation \hat{x}_k and its conditional covariance

$P_k = E\{(\hat{x}_k - x(t_k))(\hat{x}_k - x(t_k))^T | [y(t_j), T_{j-1}]_{j \leq k}\}$ satisfy

$$\hat{x}_k = \bar{x}_k + M_k C^T G_k(y(t_k)) C M_k$$

$$M_k = A_{k-1} P_{k-1} A_{k-1}^T + Q_{k-1}$$

where $g_k(y(t_k))$ is a column vector with components

$$[g_k(y(t_k))]_i = - \left[\frac{\partial p(y(t_k) | [y(t_j), T_{j-1}]_{j \leq k-1})}{\partial y(t_k)_i} \right] \cdot \left[p(y(t_k) | [y(t_j), T_{j-1}]_{j \leq k-1}) \right]^{-1}$$

and $G_k(y(t_k))$ is a matrix with elements

$$[G_k(y(t_k))]_{ij} = \frac{\partial [g_k(y(t_k))]_i}{\partial y(t_k)_j}. \quad \blacksquare$$

Remark 1: When the noise $v(t_k)$ has Gaussian distribution then this theorem converts to results in [8]. If, additionally, T_k is deterministic from theorem one can get Kalman filter [21].

5. ROBUST STATE ESTIMATION

Let us suppose that \mathbf{T} is class of estimates, \mathbf{F} is a class of distribution and $V(T, F)$ the asymptotic variance of $T \in \mathbf{T}$ when the distribution is $F \in \mathbf{F}$. Consider the game in

which we chose $T \in \mathbf{T}$, nature chooses $F \in \mathbf{F}$ and $V(T, F)$ is the payoff. This game has a saddle point pair (T_o, F_o) if T_o and F_o satisfy

$$\min_{T \in \mathbf{T}} \max_{F \in \mathbf{F}} V(T, F) = V(T_o, F_o) = \max_{F \in \mathbf{F}} \min_{T \in \mathbf{T}} V(T, F) \quad (9)$$

The estimate T_o is min-max, robust estimate. F_o is a least favourable distribution [22]. In this paper we will

consider family \mathbf{F}_ε

$$\mathbf{F}_\varepsilon = \{F | F = (1-\varepsilon)\Phi + \varepsilon H, 0 < \varepsilon < 1, H \text{ symmetric}\} \quad (10)$$

where Φ is normal distribution. For such case the nonlinear transformation of prediction error is next nonlinear function [23], [24].

$$\psi(t) = \begin{cases} t & |t| \leq K \\ K \operatorname{sgn}(t) & |t| > K \end{cases} \quad (10)$$

Now we will formulate, in the form of theorem, the robust filter for our problem.

Theorem 2. Consider the relation (6) to (8). The covariance matrix Q_n is determined by Lemma 1. Let us suppose that next is valid

- 1° distribution F_v of transformed prediction errors $v_n = V_k y_n - V_n C x_n$ satisfies

$$a) f(v_1, \dots, v_b, \dots, v_r) = f(v_1, \dots, -v_b, \dots, v_r) \text{ for each } i=1, 2, \dots, r, \text{ where } f(\cdot) \text{ is the } r\text{-dimensional density associated with } F$$

$$b) \text{ all marginal distributions for } F \text{ are members of } \mathbf{F}_\varepsilon$$

- 2° prior density of x_k be Gaussian with mean and covariance matrix M_k , i.e.

$$x_k \sim N(\bar{x}_k, M_k)$$

Then the robust filter is

$$\hat{x}_k = \bar{x}_k + B_k u_k + M_k C^T V_k \psi(v_k)$$

$$\bar{x}_k = A_k \hat{x}_{k-1}$$

$$v_k = V_k(y_k - C \bar{x}_k)$$

$$M_k = A_{k-1} P_{k-1} A_{k-1}^T + Q_{k-1}$$

and the filter covariance

$$P_k = E\{(\hat{x}_k - x_k)(\hat{x}_k - x_k)^T\} \text{ satisfies}$$

$$P_k = M_k - M_k C^T V_k^T V_k C M_k E_{F_o} \{\psi'(v_k)\}$$

where F_o is least favorable distribution. \blacksquare

Remark 2: When the sampling period T_k is deterministic and F_o is normal distribution, the filter, formulated by Theorem 2, is Kalman filter.

The matrix P_k in the last theorem is random. In classical Kalman filter this matrix is deterministic. Properties of random matrix P_k are described in the next theorem.

Theorem 3. Let us suppose that next is valid

- 1° the random sampling period T_k is i.i.d. random variables

- 2° $r(\cdot)$ is Gaussian noise

3° the random covariance matrix for estimates is

$$P_k = A_{k-1}P_{k-1}A_{k-1}^T - A_{k-1}P_{k-1}A_{k-1}^T C^T V_k^T V_k C A_{k-1}P_{k-1}A_{k-1}^T \cdot E_{F_o} \{ \psi'(\nu_k) \}$$

Process $\{P_k\}_{k=0}^{\infty}$ is homogenous Markov process. ■

The result of this theorem is very important. Such result has interesting consequences in statistical descriptions of relevant quantities of robust estimator.

6. CONTROLLER DESIGN

The feedback law for system with wireless feedback is given by

$$u_k = -K\hat{x}_k \quad (11)$$

The controller (11) is P controller. It means that always present static error. For our problem that is enough. But, not any problems to modify control law (11) in such way that be included I and/or D action.

7. CONCLUSION

In this paper the problem of system control with feedback over wireless channel is considered. The urgent problems which must be resolved are: statistical description of the estimator and lower bound of the sampling rate that makes it possible to keep the estimation error variance below a given threshold. Investigations are in the progress.

8. REFERENCES

- [1] R.M. Murray, *Control in Information Rich World: Report of the Panel of Future Directions in Control, Dynamics and Systems*, SIAM, Philadelphia, 2003
- [2] V.Z. Filipovic, "Communication limited stabilization of Linear Systems in the Presence of Uncertainty", *SAUM Conference, Belgrade, SCG*, pp. ,2004
- [3] S. Haykin and M. Moher, *Modern Wireless Communication*, New Jersey, Prentice-Hall, 2005
- [4] D. Tsf and P. Viswanath, *Fundamentals of Wireless Communication*, Cambridge, Cambridge University Press, 2005
- [5] A. Goldsmith, *Wireless Communications*, Cambridge, Cambridge University Press, 2005
- [6] X. Liu and A.Goldsmith, "Wireless network design for distributed control", *IEEE Conference on Decision and Control*, USA, 2004
- [7] L. Xiao, M.Johansson, H.Hindi, S. Boyd and A. Goldsmith, "Joint optimization of communication rates and linear systems", *IEEE Trans. Automatic Control*, vol. 48, pp. 148-153, 2003
- [8] M. Micheli and M.I. Jordan, "Random sampling of a Continuous time Stochastic Dynamical Systems", *Proc. of 15th International Symposium on the Mathematical theory of Networks and Systems, USA*, pp. 1-15,2002
- [9] B. Snippily, L. Schemata, M. Franceschetti, K.Poola, M. Jordan and S. Sastry, "Kalman filtering with intermittent observations", *IEEE Trans. Automatic Control*, vol49, pp. 1453-1464, 2004
- [10] X. Liu and A. Goldsmith, "Kalman filtering with partial observation losses", *IEEE Trans. Automatic Control*, 2005, Submitted
- [11] G.C. Goodwin, H.Haimovich, D.E. Quevedo and J. Welsh, "A moving horizon approach to networked control system design", *IEEE Trans. Automatic Control*, vol. 49, pp. 1427-1445, 2004
- [12] V. Filipovic, "Hybrid power control in wireless networks", 2005, *To be published*
- [13] W. Stallings, *Wireless Communication and Networks*, New Jersey, Prentice-Hall, 2002
- [14] C.J. Masreliez, "Approximate non-Gaussian filtering with linear state and observation relations", *IEEE Trans. Automatic Control*, vol. 19, pp. 107-110, 1975
- [15] A.P. Sage and J.L. Melsa, *Estimation theory with Application in Communication and Control*, New York, McGraw Hill, 1972
- [16] S.J. Masreliez and R.D. Martin, "Robust bayesian estimation for the linear model and robustifying the Kalman filter", *IEEE Trans. Automatic Control*, vol. 20, pp361-371, 1977
- [17] *Control of Water Distribution Systems*, RPC Soft, Project, 2004
- [18] H. Sizon, *Radio Wave Propagation for Telecommunication Application*, Berlin, Springer-Verlag, 2005
- [19] B. Oksendal, *Stochastic Differential Equations. An Introduction with Applications*, Berlin, Springer-Verlag, 1998
- [20] D.J. Daley and D. Vere-Jones, *An Introduction to the Theory of Point Processes I*, Berlin, Springer-Verlag, 2002
- [21] T. Kailath, A.H. Sayed and B. Hassibi, *Linear Estimation*, New Jersey, Prentice-Hall, 2000
- [22] P. Huber, *Robust Statistic*, New York, Wiley, 2003
- [23] V.Z. Filipovic, "Robust adaptive one-step ahead predictor", *IMA Journal of Mathematical Control and Information*, vol. 18, pp.491-50, 2001
- [24] V.Z. Filipovic, "Stochastic multivariable self-tuning tracker for non-Gaussian Systems", *International Journal of Applied Mathematics and Computer Science*, 2005, Submitted

COMPUTER PROGRAM FOR MATHEMATICAL MODELING AND IDENTIFICATION OF HYDRODINAMIC PROCESSES OF A PISTON RADIAL PUMP¹⁾

Radovan Petrovic, Svetislav Cantrak, Zoran Glavcic²⁾

Abstract

Fundamental basis in developing the piston-radial pumps presents an experimental research and mathematical modeling of non stationary high dynamic hydraulic processes in the pump cylinder, discharge space and intake and discharge pipe line in the function of the action angle of the shaft. Based on the experimental research results and the results of the mathematical modeling, developing and application of the identification method of unknown parameters of a mathematical model, the computer RADIP program has been developed which enables sufficiently exact determination of some parameters of working processes of piston radial pumps.

Key words: piston radial pump, mathematical modeling, hydrodinamic processes, velocity of sound

1. INTRODUCTION

Modern design of a piston radial pump, based on computer aided design (CAD), requires description of the all processes and parameters in the pump. Complexity of hydrodynamic and dynamic processes in a piston-radial pump (pump cylinder, intake and discharge space, discharge valve and pipeline of high pressure) demands very studious physical and mathematical analysis the same processes. Fundamental basis, in order to solve this problem, presents experimental research, based on the ultra-speed measurement system, mathematical modeling of non stationary high dynamic processes and optimization technique.

2. MATHEMATICAL MODEL

For mathematical modeling of hydrodynamic and dynamic processes in a piston-radial pump (pump cylinder, intake and discharge space, discharge valve and a pipeline of high pressure). Fig. 1, the following general suppositions have been adapted [1]:

- a) Changes of the fluid state are pseudo stationary, except in the discharge pipeline;
- b) Kinetic energy of fluid in each control space, except in the discharge pipeline, is neglected.*)
- c) Fluid flow through clearances (crevices between the piston and cylinder, the flow through a split panel and discharge valve) is pseudo stationary;
- d) The processes in the control spaces are isothermic or isentropic.

2.1 MATHEMATICAL MODEL OF A PUMP PROCESS

Mathematical model is given for each element, considering the complexly of some processes and their mutual dependence as well as the need for further mathematical modeling. This makes programming module and their further improvement and monitoring much easier [1].

- mass flow through the opening 1, on the entrance place into the intake space of the pump of fluid, Fig. 1:

$$\frac{dm_1}{dt} = \sigma_1 \mu_1 A_1 \sqrt{2\rho_s |p_u - p_s|},$$

where are: $\sigma_1=1$ for $p_u \geq p_s$, $\sigma_1=-1$ for $p_u < p_s$
 A_1 - geometrical flow section of the intake pipe.

- mass flow of fluid through the split pump organ during filling one of the pump cylinders:

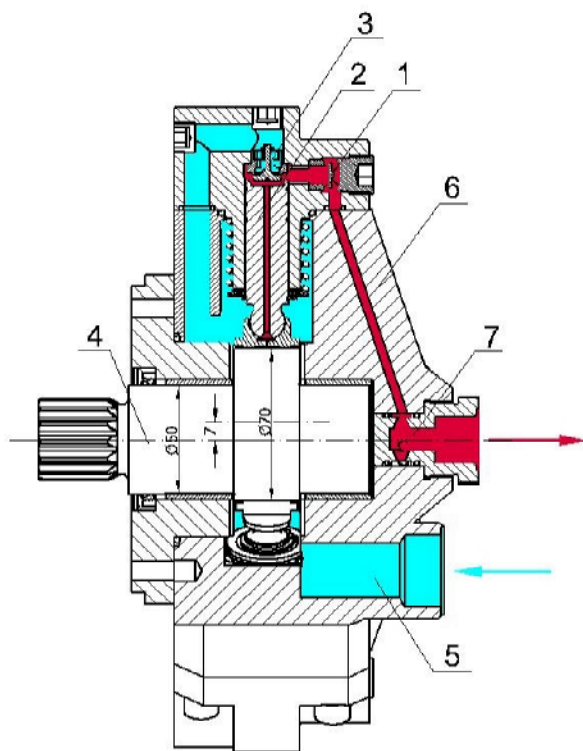
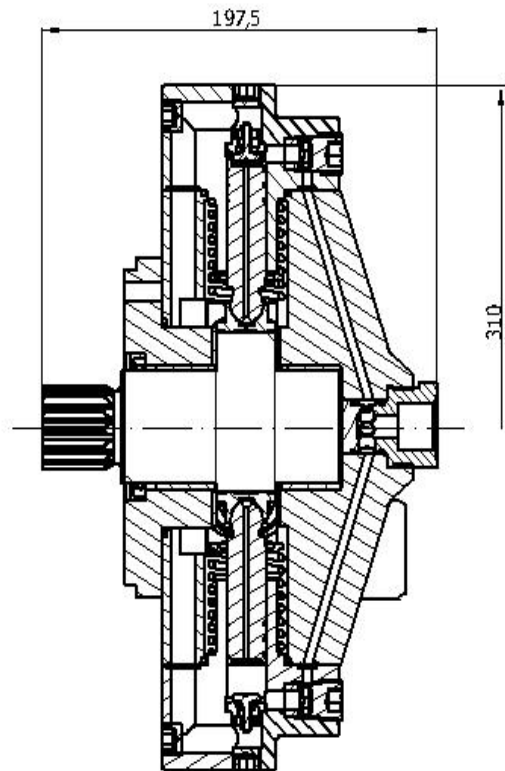
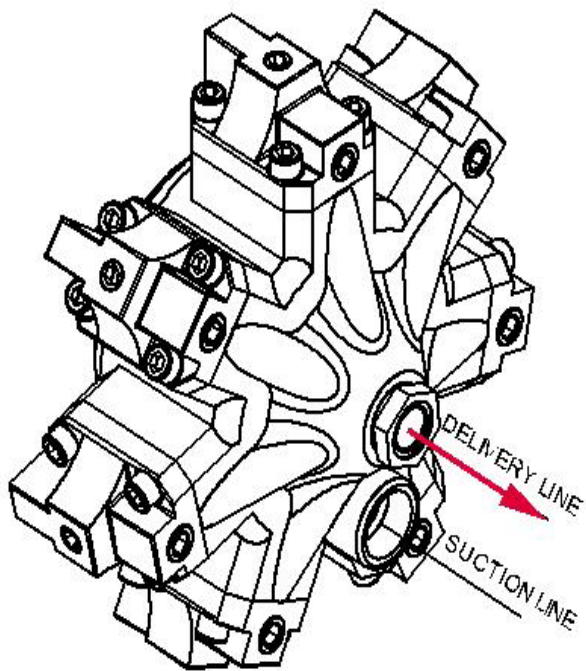
$$\frac{dm_u}{dt} = \sigma_u \mu_u A_u \sqrt{2\rho_s |p_s - p_c|},$$

where are:

$\sigma_u=1$ for $p_s \geq p_c$, $\sigma_u=-1$ for

1) This work is part of the scientific and research project that is co-financed by Ministry of Science and Environmental Protection of the Republic of Serbia for period 2003-2005, evidention number 3.07.0090A

2) Doc. dr Radovan Petrović, grad. mech. engineer, Faculty of Mechanical Engineering Kraljevo, Dositejeva 19, 36000 Kraljevo,
 Prof. dr Svetislav Cantrak grad. mech. engineer, Faculty of Mechanical Engineering Beograd, 27. marta 80, 11000 Beograd,
 Mr Zoran Glavčić, grad. mech. engineer, Faculty of Mechanical Engineering Kraljevo, Dositejeva 19, 36000 Kraljevo,



1. pressure valve
2. piston
3. suction valve
4. the pump shaft
5. intake space of the pump
6. cylinder block
7. discharge space of the pump

- mass balance of the intake space is:

$$\frac{dm_s}{dt} = \frac{dm_1}{dt} - \sum_{j=1}^{z_c} \frac{dm_{u,j}}{dt},$$

where are:

$j=1,2,\dots, z_c$ order number of cylinder,

z_c the numbers of cylinders.

- differential pressure equation in the intake pump space:

$$\frac{dp_s}{d\varphi} = \frac{E}{V_s \rho_s} \left(\frac{dm_1}{d\varphi} - \sum_{j=1}^{z_c} \frac{dm_{u,j}}{d\varphi} \right)$$

- differential pressure equation in the pump cylinder

$$\frac{dp_c}{d\varphi} = \frac{E}{V_c} \left[\frac{A_c v_k}{\omega} + \frac{1}{\rho_c} \left(\frac{dm_u}{d\varphi} - \frac{dm_i}{d\varphi} \right) \right]$$

where are:

$V_c = V_{c\min} + V_{cx}$; $V_{cx} = A_c \cdot x_k$; - immediate volume of the cylinder; the change of the volume of the pump cylinder caused by piston moving:

$$\frac{dV_c}{dt} = -A_c v_k,$$

x_k - immediate displacement of the piston.

- mass balance of the discharge space is:

$$\frac{dm_v}{dt} = \sum_{j=1}^{z_c} \frac{dm_{i,j}}{dt} - \frac{dm_2}{dt},$$

where are:

$j=1,2,\dots, z_c$ order number of cylinder, z_c the numbers of cylinders.

- mass flow streaming out of the discharge space into the discharge pipe is:

$$\frac{dm_2}{dt} = \sigma_2 \mu_2 A_2 \sqrt{2\rho_l |p_v - p_n|},$$

where are:

$\sigma_2=1$ for $p_v \geq p_n$, $\sigma_2 = -1$ for $p_v < p_n$

A_2 - geometrical flow section of the discharge pipe line.

- differential pressure equation in the discharge pump space:

$$\frac{dp_v}{d\varphi} = \frac{E}{V_v \rho_v} \left(\sum_{j=1}^{z_c} \frac{dm_{i,j}}{d\varphi} - \frac{dm_2}{d\varphi} \right)$$

- mass flow through a concentric clearance between

the cylinder and the piston:

$$\frac{dm_z}{dt} = \frac{\pi \cdot D_c \cdot \Delta r^3}{12 \cdot \eta \cdot x_k(\varphi)} \cdot (p_c - p_s) \cdot \rho_c$$

where are:

D_c - diameter of cylinder, Δ - radial clearance between the piston and the cylinder, η - dynamic viscosity, $x_k(\varphi)$ - immediate displacement of the piston, p_c - the pressure in the cylinder, p_s - the pressure in the intake space, ρ_c - the density of the fluid in the cylinder.

2.2 MODELING THE STREAMING IN THE INTAKE AND DISCHARGE PIPE LINE OF THE PUMP

During mathematical modeling of a process in a pump, it is also necessary to include and consider a series of suppositions for a process modeling occurring in the intake and discharge pipe line of the pump.

For the most general model the following suppositions for streaming of the operational fluid in the intake and discharge pipe line are taken and considered:

- The fluid streaming is one-dimensional. The pipes are of a constant cross section. Temperature and streaming fields per cross section of the pipe are homogeneous. Velocity vector laps the direction of the axis of the pipe at any moment and in any section.
- Viscosity friction between some layers of the fluid inside the pipe is neglected. The friction forces appear on the inside walls of the pipe.
- The processes in the pipes are isentropic. The change of entropy caused by friction, heat and mixing of fluid parts are neglected.
- Forces of the field (gravitational, magnetic, etc) are neglected.

In the scope of dynamic of one-dimensional streaming, such streaming are considered as "non stationary streaming in a streaming fiber".

Equation Quantity Of Moving

The equation of continuity of pressed fluid with functions p , w , ρ at the isentropic change of the state:

$$\frac{\partial p}{\partial t} + w \frac{\partial p}{\partial x} + a^2 \rho \frac{\partial w}{\partial x} = 0$$

where are:

p and w – values of density and velocity of fluid per cross section of the pipe,

$a = \sqrt{\left(\frac{\partial p}{\partial \rho} \right)_s}$, the velocity of sound in the fluid,

where are:

$p = p(t, x)$ and $\rho = \rho(t, x)$ functions of time t and coordinate x .

Equation Quantity Of Moving

$$w \frac{\partial \rho}{\partial t} + \rho \frac{\partial w}{\partial t} + w \frac{\partial}{\partial x} (\rho w) + \rho w \frac{\partial w}{\partial x} + \frac{\partial p}{\partial x} = -f_r \rho$$

where is: f_r – friction force per mass unit.

3. STRUCTURE AND ORGANISATION OF THE COMPUTER PROGRAM “RADIP”

Simultaneous integration of the previous non linear differential equations of boundary conditions and partial differential equations of streaming in a discharge pipeline required the application of computer and a corresponding computer program.

The program connecting and solving simultaneously all listed differential equations, the equations of change of characteristic flow sections and changes of physical characteristics of fluid, required a corresponding structure and organization. The program was written in the programming language Digital Visual Fortran 5.0. and realized on the measuring and controlling system ADS 2000 [2]. The principles of structural and modular programming were used. The programming consists of the main program and a module.

The more important programs were written as complete modules mutually connected or with the main program, but they can be used individually as well.

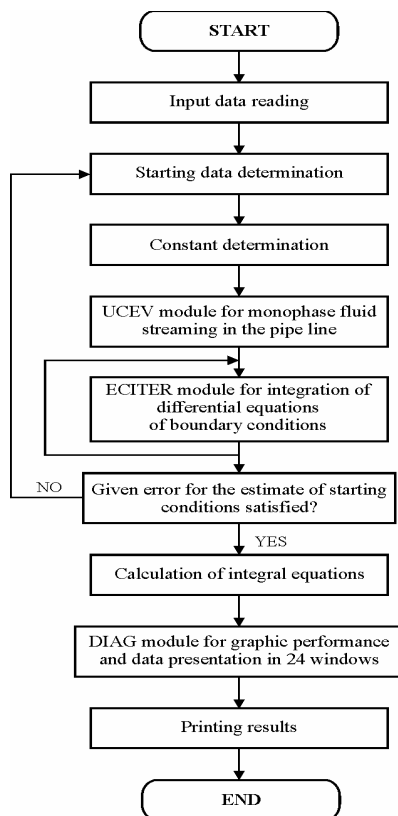


Fig.2: Structure of the main RADIP program for calculation of working parameters of the piston-radial pump

On the basis of the previous equations a program system was developed named RADIP for mathematical modeling of streaming and hydro-dynamic processes for the complete time cycle of a piston-radial pump with combined distribution of working fluid. RADIP program is modular outlined and consists of the main RADIP program and its modules.

Some program modules consisted of one or more programs but perform exactly a fixed number of operations. A simplified scheme of RADIP program can be seen in Fig. 2

4. CONCLUSION

It is not possible to give a precise determination of parameters of hydrodynamic processes of a piston radial pump neither experimentally nor by a mere mathematical modeling only. Sufficiently exact parameters can be obtained by combining the application of measuring the pressure flow in the cylinder, mathematical modeling of a real hydrodynamic process and the method of nonlinear optimisation which enables, at the same time, the determination of systemic measuring errors and unknown parameters.

Further research is possible in the construction of the piston-radial pumps with a bent cylinder block and splitting of working fluid by means of a split panel. Mathematical model would be, in that case, expanded by a dynamic cylinder block and a hydrodynamic processes in clearances between the cylinder block and the split panel.

5. LITERATURE

- [1] PETROVIC R., 1999, "Mathematical modeling and identification of multicylindrical axial piston pump parameters", PhD, Faculty of Mechanical Engineering, Belgrade, 1999. (in Serbian).
- [2] JANKOV R., 1989, "Development of new generation of ultra fast acquisition and control system ADS 2000", "Science and vehicle", Belgrade, (in Serbian).
- [3] NEDIC N., BUCEVAC Z., PRSIC D., 1996, "Experimental analysis and identification of axial piston pump BPV100", International Conference Heavy Machinery HM'96, Kraljevo, 28-30 Jun

MATHEMATICAL MODEL OF THE VANE PUMP WORKING FLUID¹⁾

Radovan Petrovic, Zoran Glavcic, Nebojsa Zdravkovic²⁾

Abstract

Hydrodynamic processes in vane pumps require knowledge of certain characteristics of the working fluid as a homogenous mono-phase medium or homogenous two-phases medium containing gas, depending on applied model. Proper physical characteristics of the working fluid are as follows: coefficient of compressibility, density, coefficient of viscosity, and velocity of sound running in fluid.

Key words: gas, two-phases medium, coefficient of compressibility, density, coefficient of viscosity, velocity of sound

1. INTRODUCTION

Hydrodynamic processes in vane pumps require knowledge of certain characteristics of the working fluid as a homogenous mono-phase medium or homogenous two-phases medium containing gas, depending on applied model.

Proper physical characteristics of the working fluid are as follows: coefficient of compressibility, density, coefficient of viscosity, and velocity of sound running in fluid. Great number of specialists published the results of experimental determination of these values (2, 3, 4) where the results (1) were used.

2. MATHEMATIC MODEL OF THE WORKING FLUID

Approximate formulas obtained based on experimental curves with application of MATLAB and ORIGIN programs were used for practical performance. Function $H(p)$ was determined by numerical integration where Runge-Kuta method in MATLAB program were used.

In this way, obtained were formulas which show following dependence of certain characteristics of working fluid:

- Dependence of sound velocity and pressure:

$$a(p) = \frac{A_0 - A_1}{1 + \left(\frac{p}{A_2}\right)^K} + A_1 \quad (1)$$

- Dependence of sound velocity and $H(p)$ function:

$$a(H) = \frac{A_0 - A_1}{1 + \left(\frac{H}{A_2}\right)^K} + A_1 \quad (2)$$

- Dependence of pressure and $H(p)$ function:

$$p(H) = A_0 + A_1 \cdot H + A_2 \cdot H^2 \quad (3)$$

- Dependence of $H(p)$ function on pressure:

$$H(p) = A_0 + A_1 \cdot p + A_2 \cdot p^2 \quad (4)$$

A_0, A_1, A_2 and K coefficients in (1) – (4) formulas are given in the Tables No. 1 and No. 2, depending on the chosen model (either mono-phase, or two-phase) of the working fluid.

3. CHARACTERISTICS OF MONO-PHASE WORKING FLUID

Characteristics of mono-phase (liquid) working fluid necessary for calculation could be found in the literature (2, 3).

The work (3) gives empiric dependence among modulus of elasticity and pressure in the form:

1) This work is part of the scientific and research project that is co-financed by Ministry of Science and Environmental Protection of the Republic of Serbia for period 2005-2007, evidention number TR 6371A

2) **Doc. dr Radovan Petrović**, grad. mech. engineer, Faculty of Mechanical Engineering Kraljevo, Dositejeva 19, 36000 Kraljevo, petrovic.r@maskv.edu.yu

Mr Zoran Glavčić, grad. mech. engineer, Faculty of Mechanical Engineering Kraljevo, Dositejeva 19, 36000 Kraljevo, glavcic.z@maskv.edu.yu

$$E = E_0 \left(1 - e^{(-0,4-0,02p)} \right) \quad (5)$$

where are:

p - pressure expressed in bars,

$E = 1,4 \cdot 10^9$ - reference modulus of elasticity for the working fluid having P0 density expressed in N/m²

The same literature shows dependence of density in pressure function:

$$\rho = \rho_0 + 0,0575p \quad (6)$$

where are:

p – pressure expressed in bars

$\rho_0 = 858 \text{ kg/m}^3$ – density of working fluid at p=0 bar.

Kinematics viscosity according to (3) expressed in pressure function is:

$$\nu = (36 + 0,0875p) \cdot 10^{-6} \text{ m}^2/\text{s} \quad (7)$$

It is generally known the connection among kinematics viscosity and the density in the form of:

$$\eta = \nu \cdot \rho \quad (8)$$

Speed velocity is expressed with the exponent :

$$a = \sqrt{\frac{E}{\rho}} \quad (9)$$

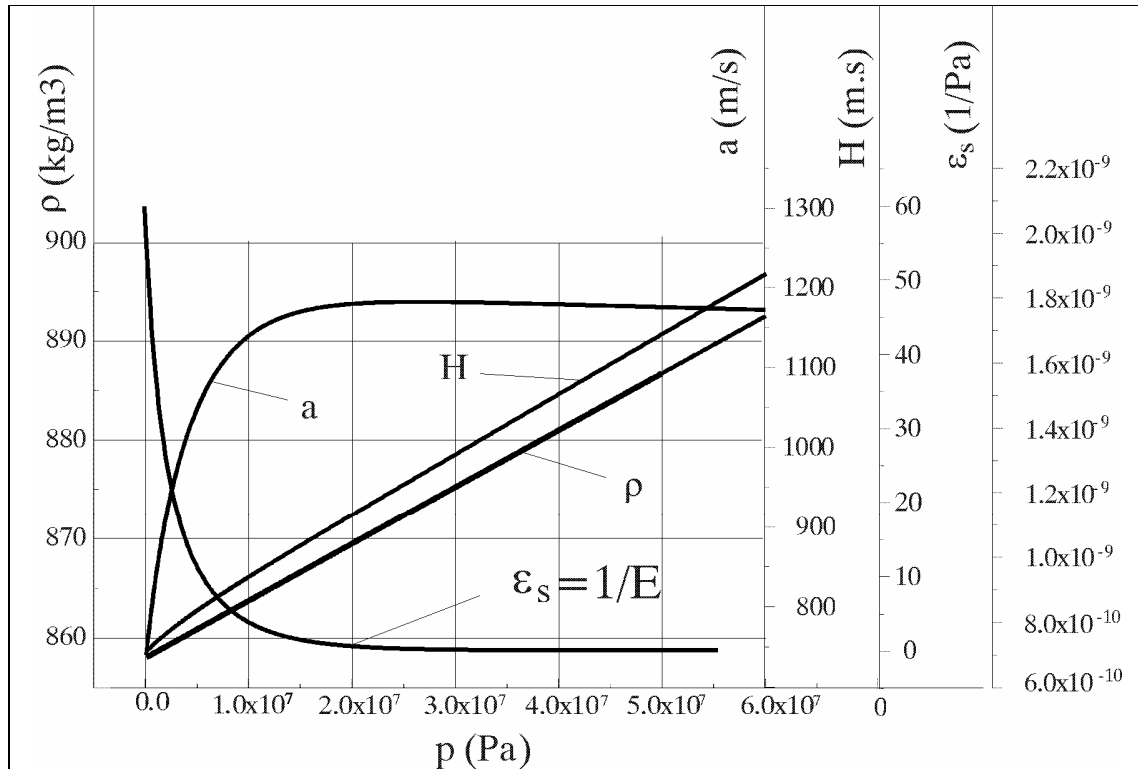


Fig. 1 Characteristics of mono-phase fluid in the pressure function

Table No. 1: Coefficient values A_0 , A_1 , A_2 , and K for mono-phase fluid.

	A_0	A_1	A_2	K
a(p) (m/s)	74	1264	$3,57 \cdot 10^6$	1,95
a(H) (m/s)	748	1264	4,0	2,25
p(H) (N/m ²)	$-1,034434 \cdot 10^6$	$1,0223881 \cdot 10^6$	1199,5611	-
H(p) (m/s)	1,0468142	$9,701916 \cdot 10^{-7}$	$9,0373647 \cdot 10^{-16}$	-

Coefficient values A_0 , A_1 , A_2 , and K in formulas (1) to (4) are given in table No. 1.

4. CHARACTERISTICS OF TWO-PHASE WORKING FLUID

Presence of gas bubbles highly influences sound speed in working speed, and, at the same time, coefficient of compressibility. They are present in the whole high-pressure volume, Therefore, justified is the hypothesis that the working fluid could be observed as a homogenous mixture of gas and liquid phases.

Dependence of modulus of elasticity, pressure and gas content is shown in literature (3) with the following empirical formula:

$$E = \frac{E_0}{1 + \gamma \left[\frac{E_0}{k \cdot p} - 1 \right] \cdot \left[\frac{p_0}{p} \right]^{\frac{1}{k}}} \quad (10)$$

where are:

p – pressure expressed in (N/m² = Pa),

$E_0 = 1,8 \cdot 10^9$ (N/m²) - modulus of elasticity of examined working fluid,

- $k = 1,4$ - for two-atoms gases,

- $p_0 = \text{bar}$ - atmospheric pressure,

- $\gamma = \frac{V_g}{V_g + V_t}$ - volume part of gas phase in two-phase fluid,

fluid,

- V_g - volume of the gas phase,

- V_t - liquid phase volume.

Density of two-phase fluid is determined according to formula (8):

$$\rho = (\rho_0 + 0,0575p) \cdot (1 - \gamma) \quad (11)$$

Figures 2 to 10 show three-dimensions coordinates system of interecine dependence of homogenous two-phase fluid characteristics.

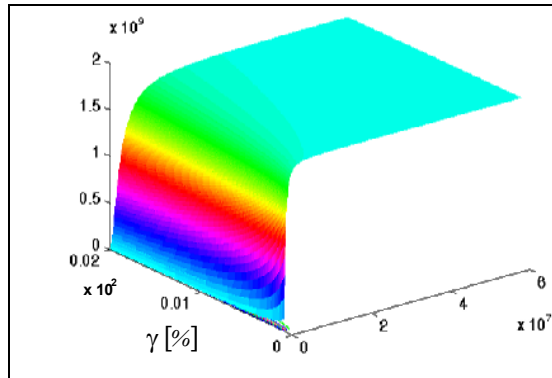


Fig. 2 Modulus of elasticity in dependence of pressure and gas content

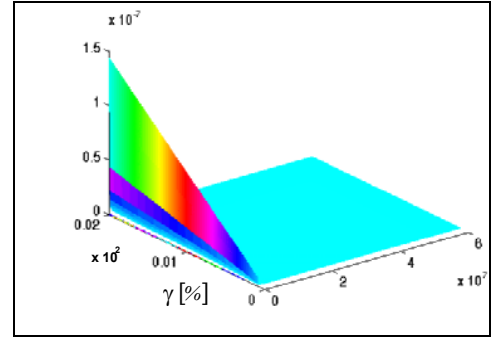


Fig. 3 Coefficient of compressibility in dependence of pressure and gas content

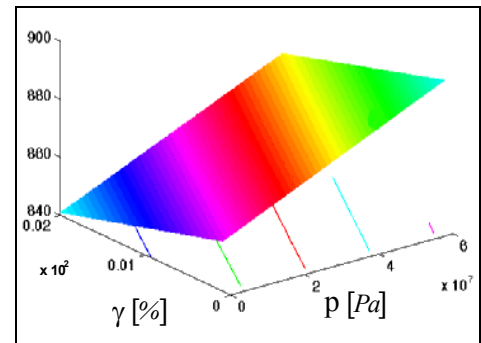


Fig. 4 Fluid density in dependence of pressure and gas content

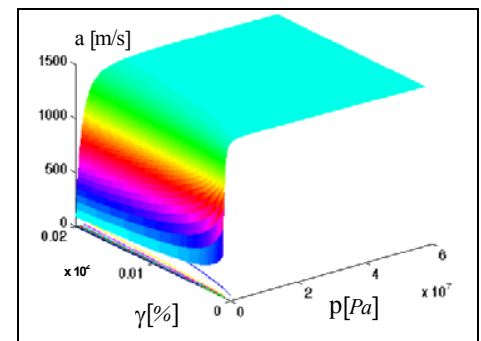


Fig. 5 Sound speed in fluid depending on pressure and gas content

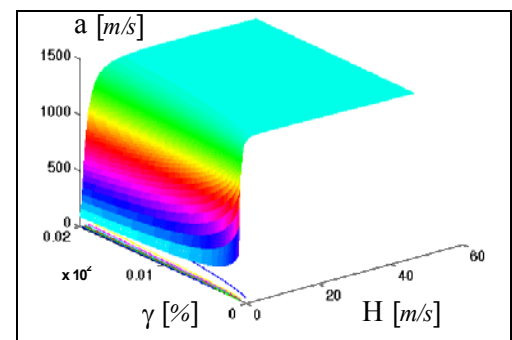


Fig. 6 Sound speed in fluid in dependence of H-function and gas content

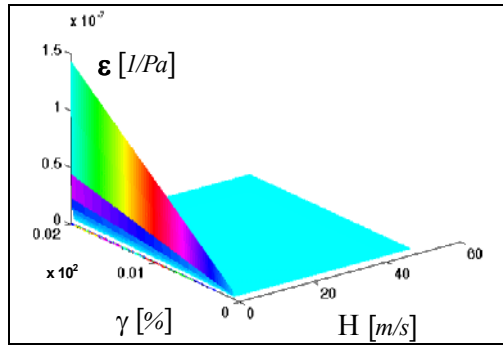


Fig. 7 Coefficient of compressibility in dependence of H-function and gas content

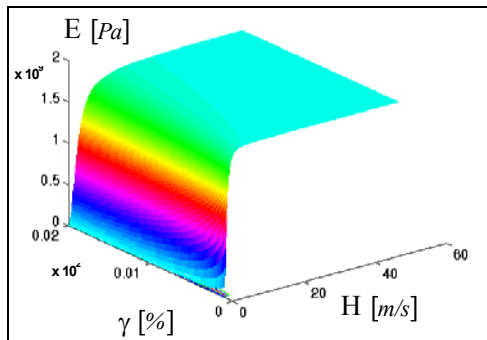


Fig. 8 Modulus of elasticity in dependence of H-function and gas content

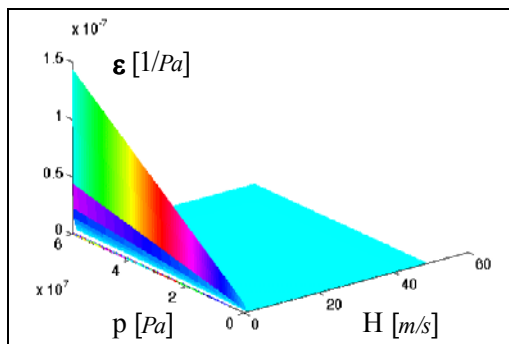


Fig. 9 Dependence of fluid compressibility coefficient on H-function and pressure

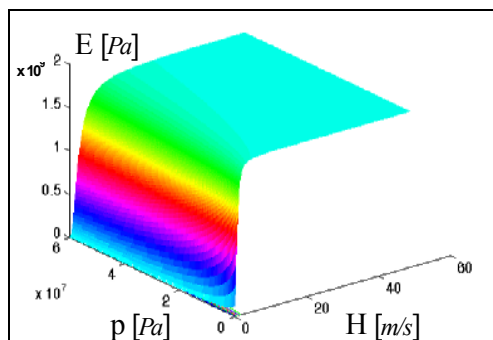


Fig. 10 Dependence of fluid elasticity modulus on H-function and pressure

Characteristics of two-phase fluid in the function of pressure and gas content are given in Fig. 11.

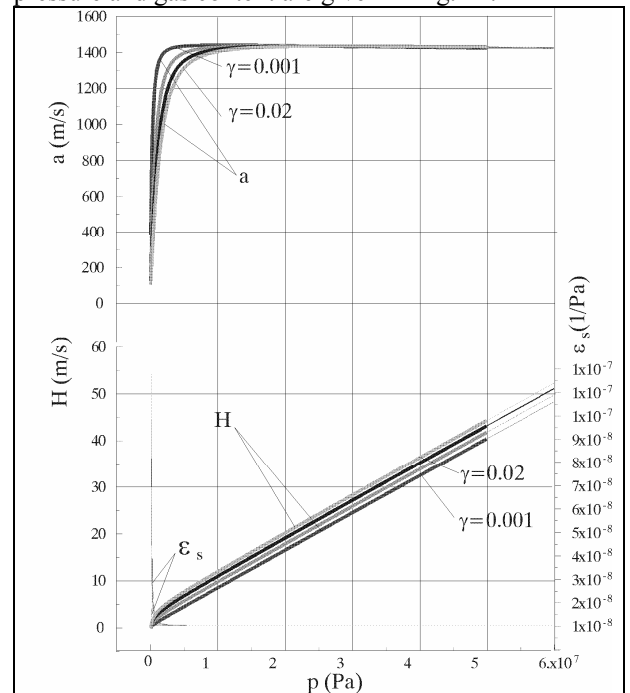


Fig. 11 Characteristics of homogenous two-phase fluid

5. CONCLUSION

For very complexed non-stationary streaming of the working fluid in suction and force pipeline, developed is mathematic model based on one-dimension compressed fluid with friction. Considered was possible content of dissolved gas in the working fluid. Special numerical characteristics method for partial equation and iteration predictor-corrector procedure for limit conditions was used for solving obtained system of non-linear partial differential equations of processes in pipelines together with non-linear ordinary differential equations of changeable structures at limit points (in cylinder, suction, and force area).

6. LITERATURE

- [1] R. Petrovic, "Mathematical Modeling and Identification of High-cylindrical Piston-Axial Pump Parameters", doctor's degree dissertation, Mechanical Faculty in Belgrade, November 1999.
- [2] H. Oswald, "Primarmanahme yur Gerausminderung an verstellbaren Axialkolbenpumpen", O.P. Olhidraulic und Pneumatic, 1978.
- [3] M. Bergemann, "Systematische Untersuchung des Gerausverhaltens von Kolbenpumpen mit ungerader Kolbenanzahl", Verlag Mainz, 1994.
- [4] W. Hoffman, "Dynamisches Verhalten hydraulischer systeme Automatischer Modellaufbau und digitale Simulation", Dissertation TH Aachen 1981.

NUMERICAL AND EXPERIMENTAL DETERMINATION OF VENTURI TUBE FLOWMETER DISCHARGE COEFFICIENT

Zoran Boričić, Dragisa Nikodijević, Dragica Milenković and Stamenković Živojin

Abstract

This paper consider possibility of numerical determination of Venturi meter discharge coefficient (calibration of orifice flow meter). Discharge coefficient for this measuring device is usually determined according to standard JUS L.H2.015, but this standard is valid only for limited area of application (diameters from 50 to 1200mm, Re number grater then 3150 and controlled laboratory conditions with fully developed flow upstream of the Venturi meter). Problem appears when some of this conditions are not satisfied, and specifically when the orifice meter can not be volumetric calibrated.

Modern CFD software's for fluid dynamics problems solving (in this paper Phoenix) enable obtaining of very precise results for velocity and pressure fields in specific flow space. In this paper analysis of different numerical models of turbulent flow was conducted and compatibility of numerically obtained results and experimental results is very satisfied. Discharge coefficient is determined for one type of Venturi flowmeter and results are given in function of Re number.

Keywords: Venturi meter, discharge coefficient, CFD, Phoenix

1. INTRODUCTION

The most commonly used method for metering large fluid flows uses an Venturi meter, which is geometrically simple device. Venturi tube and other differential pressure flowmeters is implemented in accordance with international standard ISO 5167-1 and in our country with JUS L.H2.015 [1]. The discharge coefficients α for orifice meters are normally obtained using empirical equations.

$$\alpha = CE, \quad (1)$$

where C is discharge factor and E inflowing factor of upstream velocity.

These quantities are determined according to the following equations:

$$E = \left(1 - \beta^4\right)^{\frac{1}{2}}, \quad (2)$$

$$\text{where} \quad \beta = \frac{d}{D}, \quad (3)$$

$d(m)$ -diameter of orifice hole and $D(m)$ - pipe diameter.

Re	C
5×10^4	0.970
1×10^5	0.977
2×10^5	0.992
3×10^5	0.998
5×10^5	0.995

Table 1. Discharge factor in function of Re

In table 1 Re is Reynolds which can be determined according to the well known equation: $Re = \frac{uD}{\nu}$, where $u(m/s)$ -fluid velocity and $\nu(m^2/s)$ - kinematic viscosity of fluid.

Equation for flow trough venture tube has the following form:

$$q_v = \frac{\pi}{4} d^2 \sqrt{\frac{2\Delta p}{\rho}} \alpha, \quad (6)$$

where $\Delta p(Pa)$ is orifice pressure drop and $\rho(kg/m^3)$ fluid density.

Previous equations are based on experimental data that are derived under controlled laboratory conditions with fully developed flow upstream of Venturi meter.

Standard JUS L.H2.015 for production and application of Venturi meters is valid only for limited area of application. This standard restricts production and application of Venturi tube with machining convergent part, throat and inlet cylinder according to the following criterions:

- Pipe diameter must be in range from 50 to 250 mm.
- β ratios is defined with following values $0.4 \leq \beta \leq 0.75$.
- Reynolds number is limited between the values: $2 \times 10^5 \leq \beta \leq 1 \times 10^6$
- Flow conditions must be ideal, i.e. flow must be fully developed flow upstream of Venturi meter.

The axisymmetric Venturi tube was investigated in this paper. The pressure drop at the connectors of the Venturi tube has been measured. These measurements were carried out in a 50mm diameter (D) smooth pipe. The Venturi tube consists of a throat with a diameter $d=30\text{mm}$, giving a β ratio of 0.6. The figure 1 shows the geometry and 3D model of Venturi tube.

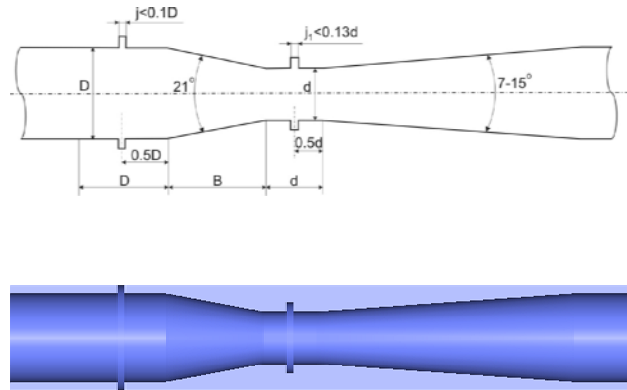


Figure 1. Geometry of orifice plate and 3D model

1.1 Literature review

To help to improve metering technology, computational fluid dynamics (CFD) models have been tested in recent years to study trends and to provide insight into the flow physics [2,3]. The use of such codes by the engineering community has increased dramatically in past few years. In this paper is adopted the general purpose Phoenix 3.6 software.

Information on the predicted flow structure downstream of Venturi tube is scarce in the literature. Cockrell and Markland [4] researched flow in diffusers. In a couple papers, Reader-Harris et al. [5, 6] have studied experimentally the discharge coefficients of Venturi tubes with beta ratios from 0.4 to 0.75 and with standard and non-standard convergent angles. Terkriwal [7] used Fluent to model pressured drop in converging-diverging nozzles. He studied six different nozzles with Reynolds number $Re \approx 6 \times 10^5$ and found good agreement between the calculation using $k-\epsilon$ turbulence model and the measurements, but the pressure drop over the Venturi tube was not reported. Most of the other researchers who have published numerical calculations on this subject have been interested in metering and have focused on the pressure drop over an Venturi tube. Yongtao et al. [8] carried out calibration of D_N 1400mm Venturi tube on large scale water rig. Spencer et al. [9] made intercomparasion on LDA and hot-wire measurement with computation of velocity distribution through a contraction and diffuser. They studied effects of disturbances on Venturi flowmeter performance. many researchers has also used CFD to study differential pressure flowmeters, primarily the discharge coefficient and the wall pressure distribution through the contraction or diffuser. Several authors have used CFD for parametric

studies and many researchers have measured the flow field downstream of an Venturi tube.. Erdal and Andersson [10] used Phoenix to investigate whether is possible to simulate metering stations that include flow conditioners.

2. COMPUTATIONAL CODE

The Phoenix computer code, version 3.6, was used to simulate the flow through the Venturi tube. This software is applicable to steady or unsteady, one-, two- and three-dimensional turbulent or laminar flows using Cartesian, cylindrical-polar or curvilinear coordinates (BFC). In this paper, it has been used to calculate three-dimensional turbulent flow with Cartesian coordinates. Phoenix uses the finite-volume method, in which the original partial differential equations are converted into algebraic finite-volume equations with the aid of discretisation assumptions.

The partial differential equations for all variables are integrated over each control volume to obtain finite-volume equations. Central differencing is employed for the diffusion terms. The convection terms are discretised using HYBRID schemes. The simple algorithm is then used to solve the finite-volume equations. For elliptic calculations, like flow trough the Venturi tube, many sweeps are carried out until the solutions converges. In addition, the pressure equation is solved in a simultaneous whole-filed manner at the end of each sweep.

Appropriate relaxation of the flow variables is necessary in order to obtain convergence. Both internal and linear relaxations are employed. The former is normally applied to velocity variables, whereas the latter is applied to pressure and turbulent kinetic energy and its dissipation rate.

Phoenix was run until the sum of the absolute residual sources over the whole solution domain was less than a half per cent of the reference quantities, based on the total inflow of the variables in question. In addition, checks were made to see that the dependent variables at some selected locations fluctuated less than 0.1% between successive iteration cycles.

2.1 Turbulence models

In this paper standard $k-\epsilon$ model and its modification are used for numerical prediction of flow in Venturi tube. Following models are used for simulations:

- The $k-\epsilon$ model;
- The Chen-Kim modified $k-\epsilon$ turbulence model;
- RNG-derived $k-\epsilon$ turbulence model;
- Two-Layer $k-\epsilon$ turbulence model

The $k-\epsilon$ turbulence model proposed by Harlow and Nakayama in 1968 is by far the most widely-used two-equation eddy-viscosity turbulence model. Phoenix provides the standard high-Reynolds-number form of the $k-\epsilon$ model, as presented by Launder and Spalding [1974].

The model $k-\epsilon$ employs a single time scale (k/ϵ) to characterize the various dynamic processes occurring in

turbulent flows. Accordingly, the source, sink and transport terms contained in the closed set of model equations are held to proceed at rates proportional to ε/k . Turbulence, however, comprises fluctuating motions with a spectrum of time scales, and a single-scale approach is unlikely to be adequate under all circumstances because different turbulence interactions are associated with different parts of the spectrum.

In order to remedy this deficiency in the standard model, Chen and Kim [1987] proposed a modification which improves the dynamic response of the ε equation by introducing an additional time scale (k/P_k), where P_k is the volumetric production rate of k .

Yakhot and Orszag [1986] derived a k - ε model based on Renormalization Group (RNG) methods. In this approach, RNG techniques are used to develop a theory for the large scales in which the effects of the small scales are represented by modified transport coefficients.

For example, a modified eddy viscosity is the parameter appearing in the momentum equations through which the high-wave-number modes (i.e. small scales) affect the retained larger scales.

The low-Re k - ε model has the undesirable feature of requiring very high numerical resolution near the wall because of the steep gradient of the dissipation rate ε , for which an equation is solved. Also, the models have been found to perform rather poorly in adverse-pressure-gradient boundary layers; and the damping functions are not always well-behaved in separated flows.

Hence, in order to save mesh points and improve convergence rates, and also to introduce the fairly well-established length scale (l) distribution very near the wall, one alternative is the use a two-layer k - ε model (Elhadidy [1980] and Rodi [1991]).

The two-layer k - ε model uses the high-Re k - ε model only away from the wall in the fully-turbulent region, and the near-wall viscosity-affected layer is resolved with a one-equation model involving a length-scale prescription.

Phoenics has been equipped with the two-layer model of Rodi [1991] which employs the one-equation model of Norris and Reynolds [1975] in the near-wall region.

The basic equations [11] which describe the k - ε turbulence model beside the time averaged continuity equation and Navier-Stokes equations are:

$$\begin{aligned} (\rho \bar{U}_j k)_{,j} &= \left[\left(\mu + \frac{\mu_t}{\sigma_k} \right) k_{,j} \right]_{,j} + P_k - \rho \frac{k^2}{l} \\ (\rho \bar{U}_j \varepsilon)_{,j} &= \left[\left(\mu + \frac{\mu_t}{\sigma_\varepsilon} \right) \varepsilon_{,j} \right]_{,j} + P_\varepsilon - c_{\varepsilon 2} \rho \frac{\varepsilon^2}{k} \\ P_k &= \mu_t (\bar{U}_{i,j} + \bar{U}_{j,i}) \bar{U}_{i,j}; \\ P_\varepsilon &= c_{\varepsilon 1} (\varepsilon/k) P_k \\ l &= \frac{k^2}{\varepsilon}; \mu_t = \rho c_\mu \frac{k^2}{\varepsilon}. \end{aligned} \quad (7)$$

In the equations (7) the parameter labeling used is common for the theory of turbulent flow modeling: \bar{U}_j - time averaged velocity in x_j direction, k -turbulent kinetic energy, ε -dissipation, μ -dynamic viscosity, μ_t -dynamic turbulent viscosity, $(\cdot)_{,j}$ -derivation with respect to x_j , l -turbulent length scale and five constants: $c_\mu = 0.09, c_{\varepsilon 1} = 1.44, c_{\varepsilon 2} = 1.92, \sigma_k = 1.0, \sigma_\varepsilon = 1.31$.

3. RESULTS

Experimentally obtained results for discharge coefficients and results obtained on the base of empirical equations defined by standard JUS L.H2.015 have very satisfactory agreement for different values of Reynolds number. Higher errors can be perceived for higher values of Reynolds number ($Re > 200000$).

Numerically obtained discharge coefficients for different turbulence models are given on the figure 2 and they are compared with discharge coefficients calculated with empirical equations which are defined with standard for differential pressure flowmeters design.

The best results are obtained with RNG-derived k - ε turbulence model. This model gives same difference in results compared with empirical equations for the Reynolds number in the range $5 \cdot 10^3$ to 10^6 . A numerical simulation in Phoenics was conducted with mesh of 135000 nodes ($150 \times 30 \times 30$) and the difference in results can be assigned to inadequate grid density. Figure 3 presents the results for pressure and velocity obtained with numerical simulations in Phoenics.

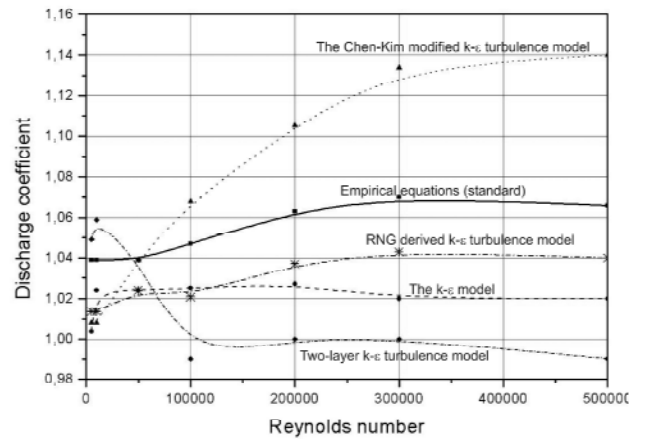


Figure 2. Discharge coefficients obtained by empirical equation and different turbulence models

Simulations with sufficiently fine mesh require considerable computer time and this simulations and simulations of real conditions on metering stations will be subject of future research.

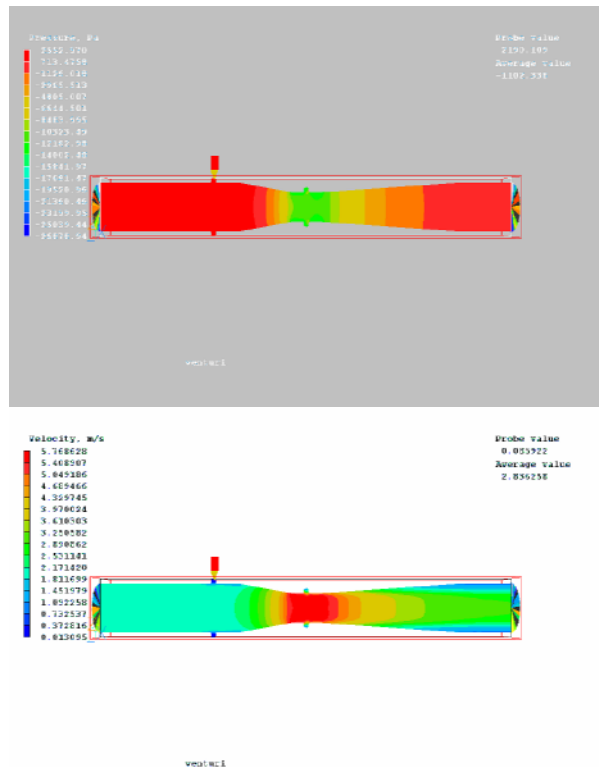


Figure 3 Pressure and velocity distribution in flow domain

4. CONCLUSION

The use of computational fluid dynamics (CFD) tools for modeling and analyzing process systems has increased in recent years. In this paper we attempt to investigate whether is possible to simulate metering stations that include Venturi tube. This study was initiated prior to the start of full pipe simulation to investigate various grid effects, coordinate arrangements, differencing schemes and turbulence models and to compare obtained results with JUS L.H2.015 standard regulation for differential pressure flowmeters production. Obtained results, especially for RNG k-ε model, have very satisfactory agreement between computed and experimental discharge

coefficients for the Reynolds number in the range $5 \cdot 10^3$ to 10^6 . However, more information and validation are required in several areas before the technique can be fully exploited.

REFERENCES

- [1] Standard: Merenje protoka fluida mernim blendama, mlaznicama i venturijevim cevima ugrađenim u cevovode kružnog poprečnog preseka, JUS L.H2.015, 1989.
- [2] Proceedings: Erdal A., Torbergesen, L. E. Rimestad, S. and Krogstad, P. A. Evaluation of a CFD model for simulation of simplified flow conditioners, Fluid Flow Measurement 3rd International Symposium, San Antonio, March 1995.
- [3] Proceedings: Thomassen, D., Langsholt, M. and Sakariassen, R., Flow conditions in a gas metering station, North Sea Flow Measurement Workshop, Oktober 1992.
- [4] Journal: Cockrell D.J., Markland E., A review of incompressible diffuser flow, Aircraft Engineering, pp. 286-292, 1963.
- [5] Proceedings: Reader-Harris M.J., Bruntor W.C., Gibson J.J., Hodges D., Nicholson I.G., Venturi tube discharge coefficients, In Proc. 4th International Symposium on fluid flow measurement, Denver, 1999.
- [6] Journal: Reader-Harris M.J., Bruntor W.C., Gibson J.J., Hodges D., Nicholson I.G., Discharge coefficients of Venturi tubes with standard and non-standard convergent angles, Flow measurement and instrumentation, pp. 135-145, 2001.
- [7] Technical report: Tekriwal P.K., Pressure drop calculation and measurement in converging-diverging nozzles, report number 96CRD157, 18 pages, 1996.
- [8] Journal: Yongtao Han, Shufang Han, Ling-an Xu, The practice on DN 1400mm Venturi tubes, Flow measurement and instrumentation, pp. 11-23, 1998.
- [9] Journal: Spencer E.A., Heitor M.V., Castro I.P., Intercomparasion of measurements and computations of flow through a contraction and a diffuser, Flow measurement and instrumentation, Vol. 6, pp. 3-14, 1995.
- [10] Journal: Erdal, A. and Andersson, H. I., Numerical aspects of flow computation through orifices, Flow Measurement and Instrumentation, Vol. 8, No. 1, pp. 27-37, 1997.
- [11] Report: Lars Davidson, An Introduction of Turbulence Models, Department of Thermo and Fluid Dynamics, Chalmers University of Technology, Goteborg, Sweden, January 2003.

CAUSALITY OF 0-JUNCTIONS IN ENERGY BASED MODELING

D.H. Pršić and N.N. Nedić

Abstract

The paper considers flow activities at determination of computational causality 0-junction bond graph physical system model. At first, it says about responsibility question, then about the algorithm for causality determination. Particularly this work considers the case 0-junction with one input and two output of energetic flow. here are included the flow activities for effort and flow causality of the input bond.

Keywords: bond graph model, 0-junction, causality

1. INTRODUCTION

A model always represents only some a real system abstraction, depending on the intended usage. From control point of view, energetic aspect of system description, based on bond graph method is useful [1-4]. Creation of the simulation model is structured by the few abstraction levels which create hierarchy in the sense that the degree of details increases from physical component level to the mathematical level. At the last step, in order to have quantitative system analyses, it is necessary to define mathematical relations which describes physical mechanisms from previous phase. These relations are denoted as constitutive relations.

In general, the mathematical abstraction process can be divided into two steps [2]:

- Definition of constitutive relations
- Mathematical causalities determination

Should be noticed, that constitutive relations are given in declarative way, not as assign statements. This intensify flexibility and possibility of repeat use of the model. [5, 6]. In the next step, depending of the context model application, we have to definition causality.

2. CAUSALITY

Causality plays an important role in any aspect of model based reasoning about physical system. In prediction or simulation, causality controls the propagation of information. In explanation of behavior it is used to describe the propagation of effects, etc. It has two sides: mathematical and physical. From mathematical point of view it refers order of computations, from physical point of view it refers to an interpretation of this ordering in physical terms.

The main concept of the notion of causality is the concept of computational causality. For example, if we consider the flow through the resistance with turbulent regime which can be described by:

$$Q := k\sqrt{\Delta p} \quad (1)$$

Mathematical abstraction of resistance given in the equation form (1) presents its essence and doesn't depend from application. It only claims that the relation between flow and pressure drop must to be satisfied in any moment. It doesn't say anything about what happens: the flow determines the pressure drop or the pressure drop determines the flow. But, in implementation phase to this relation the computational direction must to be define. Here two cases are possible (Fig.1)

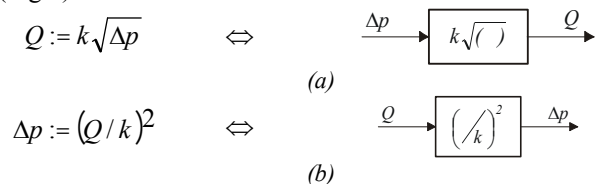


Fig. 1 Two computational directions of turbulent resistance constitutive relation

In order to make explicit computational direction, assignment statement ($:=$) instead equality relation ($=$) is used. In the first case (a) the pressure drop (Δp) is used as input (independent) variable by which output (dependent) variable Q is calculated. In second case (b) we use second form of constitutive relation with the exchanged role of variables Δp and Q .

The question is how for one functional block (FB) to define calculation order? In fact, the first question is who is responsible for calculation direction determination? From previous it can be seen that causality is defined in relation on variables with FB has communication with output world. It is independent from the FB constitutive relation. It means that we can't say nothing about causality of FB but in the context of the output world in which it is. In other words, causality is global system property of all system, but not of the system parts. Therefore the question is how to make the model library because we don't know in advance the

application context. Fortunately, reference approach ontology [2] has more simple communication with outer world via power ports. That means, from outside world there are only two possibilities: effort exogenous and flow endogenous or vice-versa.

3. 0 - JUNCTION

By 0-junction we make conception of the parallel connections of the energetic flows in a system [7-9]. The 0-junction represents a node at which all efforts of the connecting bonds are equal:

$$e_1 = e_2 = \dots = e_n \quad (2)$$

Therefore this connection is called the effort junction. From the structural model view, 0-junction can be consider as presentation of characteristic values of effort variables. For example, in some hydraulic system, all flow connections (disconnections) can be modeled by this mechanism.

Base on power continuity conditions (3)

$$\sum_{i=1}^n e_i f_i = 0 \quad (3)$$

we have that flow variables satisfied condition:

$$f_1 + f_2 + \dots + f_n = 0 \quad (4)$$

i.e. algebraic sum of the flows connecting bonds is zero. The power direction determines the sign of the flows: all inward pointing bonds get a plus and all outward pointing bonds get a minus.

Expressions (3) and (4) presents constitutive relations of 0-junction. In other word, energetic variables from (3) and (4) can be on any way to be joined with the ports in the connection. It means, that space system topology can be straightforward, mathematical described by ports number and connection type. In Fig 2a it is showed the electrical circuit with three parallel connected branches. Throw each of three branches passing one energetic flow which in this case presents one mechanism. In Fig.2b it is showed the bond graph model of 0-junction (not all circuit) of the circuit from Fig. 2a. Power variables for each port are branch current and potential difference, that is, voltage between the connected node. Therefore 0-junction presents point of characteristic potential (node A) in circuit. Figure Fig. 2c shows block diagram expansion of 0-junction.

Base on power continuity defined by relation (3) follows that in each distribution mechanism must to be at list one port through which energy coming and list one port through which energy leaving from the mechanism. In contrast, we will have some energy accumulation what is in contrast with the base mechanism concept.

For case 0-junction with three ports we coming up to two possible forms in function of the third bond direction (Fig.3).

The next step presents the causality determination. From application aspect, in order to determine mathematical

causality, two conditions must be satisfied [2]:

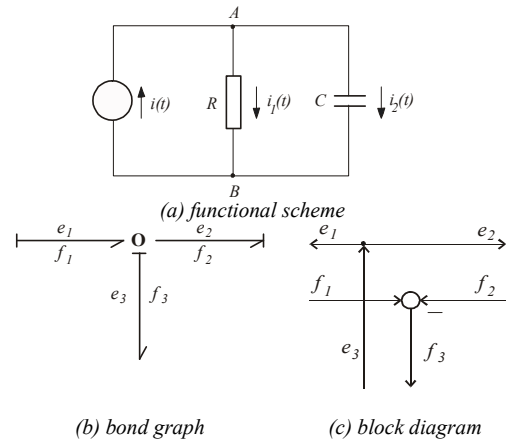


Fig.2 0 - junction with three branches

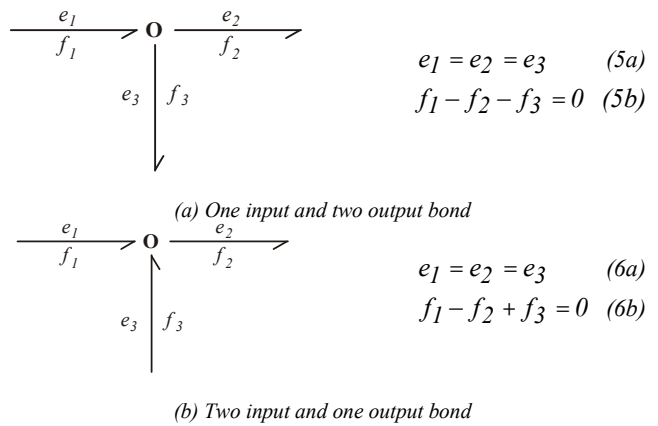


Fig.3 Two forms of 0-junction with one input bond

- Consistency condition: no variable may be the dependent variable of more then one constitutive relation
- Computability condition: for each relation, it should be possible to compute the values of the dependent variables from the values of the independent variables.

The consistency constraints the choice of computational directions in a way such that whenever a direction has been determined for one relation this will propagate and restrict the choice of direction of other relations. The computability condition rule out those directions for which the values of the variables defined as dependent can not be computed from the variables defined as independent.

In system model the distribution mechanism has role of causality propagators and for it is not defined default causality.

With consistency condition generalization on 0-junction we coming up to constraint that only one effort and (n-1) flow variables can be independent. In other words, outer world can only on one port change independent effort, on all rest ports the effort variables are dependent.

At realization there is essential difference between distributor with one and two input ports. In the case with

two input ports, it is necessary to ensure synchronization of input messages, it is not case at the mechanism with one stimulus. Therefore these two cases we consider separately.

4. CAUSALITY 0-JUNCTION WITH ONE INPUT BOND

When at the input port there is e -causality it means that outer call as input parameter forward effort (Fig.4).

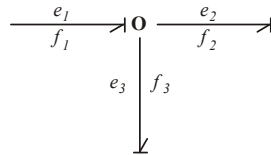
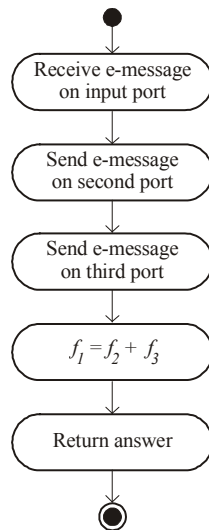


Fig.4 0-junction with e -causality input port

Base on consistency condition causality from input is propagated to two output ports such that causality of mechanism is straightforward determined. In that case flow activities in class for realization of this concept looks like Fig.5.



Sl.5 0-junction with one e -causality input port activity flow diagram

Incoming message from environment initiates activity for handle of that event. Effort variable 0-junction propagate to two output ports request flow variables f_2 and f_3 . After adding their values, mechanism returns answer on outer call function $KRelacija()$. Like this for port 1, activities for rest of two ports looks like with change role of power variables. It is obvious that mechanism is invariant on choice of input port.

Realization of constitutive relation of input port with e -causality is given in Fig.6.

In the case when initiate call forward flow as input variable then on input port we have f -causality (Fig.7). In that case the situation isn't so straightforward as at e -causality, that is, there are more scenarios at exchange energy. However, constraint that exactly one of the rest two ports must to have e -causality is further valid. For example, it doesn't allow that are both ports connected

with integral form I-storage because in that case the effort variable will be undefined. Like, by reason consistency condition it doesn't allow the presence of integral form of C-storage on both ports.

```
public boolean kRelacija(double t, Effort e1, Flow f1){
    //iz spoljnjeg sveta stize e
    tekuceVreme=t;
    e.setVal(e1.getVal());
    portP[1].connectTo.kR.kRelacija(t,e,f);
    f1.setVal(f.getVal());
    portP[2].connectTo.kR.kRelacija(t,e,f);
    f1.setVal(f1.getVal()+f.getVal());
    return true;
};
```

Fig.6 Processing 0-junction input port e -message

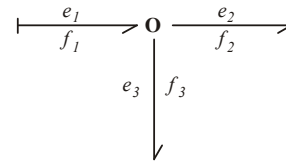


Fig.7 0-junction with f -causality input port

In order to establish which of the causal forms are possible on the output ports 0-junction, with 1 is coded the possibility of some causality on the port, respectively with 0 impossibility. In that case, the combination table of possible causality forms on the output ports of 0-junction, looking from inside of the mechanism, looks as:

Dec.No.	e_2	f_2	e_3	f_3
6	0	1	1	0
7	0	1	1	1
9	1	0	0	1
11	1	0	1	1
13	1	1	0	1
14	1	1	1	0
15	1	1	1	1

Table 1. Combination table of possible causal forms 0-junction output ports

From altogether 16 combinations 7 combinations are possible. The pairs "00" are not allowed, because for each port must to be at least one causal form. Beside, the consistency condition don't allow combinations: 0101 and 1010. The pairs "11" mean that the both causal forms are possible on the port.

Base on combination table, in Fig.8 the causal form of the output ports of 0-junction are graphical presented. If there is not causal stroke on the bond it means that their causality is ambiguously.

From figure can be seen that combinations 6 and 9 are dual forms with exchanged ports role. Like means for combinations 7-13 and 11-14. It means that on output ports of 0-junction with one input bond we can have one of four causal forms:

- both port have determined and different causality (6,9);
- on one port there is f -causality, but on the other

- port both causality forms are possible (7,13);
- on one port there is e -causality, but on the other port both causality forms are possible (11,14);
- on both ports the both forms are possible (15).

Having in mind the previous, from 0-junction point of view, always two actions going on with the same order (Fig.9).

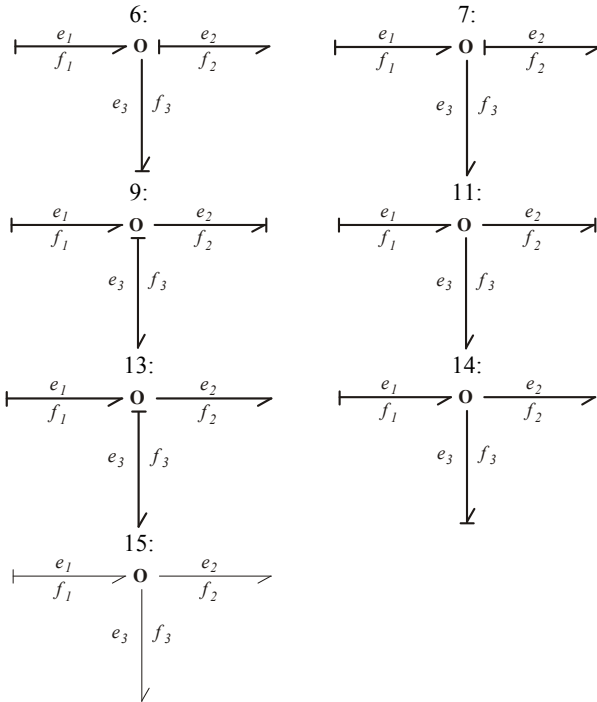


Fig.8 Causal forms 0-junction output ports

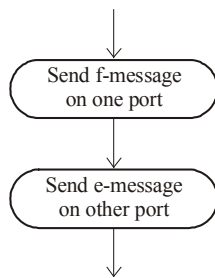


Fig.9 Action sequence 0-junction with one f -causal input port

How is use case initialized by the message which forward flow, the mechanism can ask one or another port with the same or modified e -message. When the first part returns effort variable, then it can ask the second port with e -message. In fact, the order of the actions is the same without of output causality. Only is variable the order of port asking in function of output causality*. For example, if port 2 has f -causality it is port whom the first message will be forward. If port 2 has e -causality then to the third port the first message will be forward.

From the previous it can be concluded that concept

* From Fig.5 it can be seen that at 0-junction with e -input port order of port polling is not defined.

NulaVeza1U by whom 0-junction with one port is abstracted, has one more responsibility to outer world: determination causality, that is port polling order definition. Since there are only two output ports, the order definition means definition of the first port.

Should observe that the new responsibility it is not obliged to particular multiport, but to the model as whole. This coming from that that causality is global model property. It means that distribution mechanism initiate should be the matter of the model constructor (component or system) but not of some multiport constructor.

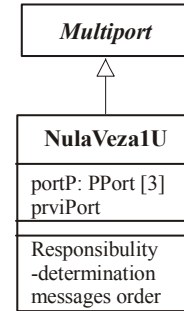


Fig.10 Concept 0-junction with one input port

V. CONCLUSION

Causality is the global model property, not a particular mechanism as a part of a model. Causality determination is in function of modeling aim and concepts introduced on higher level of abstraction. The same concept can have different causality in different context. Therefore, it is necessary that the model has possibility of self tuning depending of particular case. Distribution mechanism demands to consider a few scenarios in communication with environment. In general there are two cases: mechanism with one and more input ports. In case of more inputs must to be ensured input messages synchronization. At mechanism with one input causality determination depends from input bond causality. Since 1-junction presents dual form of 0-junction for causality determination can be used the same algorithms.

REFERENCES

- [1] D. Karnopp, D. Margolis, R. Rosenberg, "System Dynamics", John Wiley, New York, 2000.
- [2] U. Söderman, "Conceptual Modelling of Physical Systems - a frame of reference", Ph.D. Thesis, Univ. of Linköping, Sweden, 1995.
- [3] D. Pršić, N. Nedić, "Structural Modeling of Hydraulic Systems", Electronics, Vol. 7, No. 1, 2003, University of Banja Luka.
- [4] D. Pršić, N. Nedić, "Bond Graph Concepts in Object Oriented Modeling", VIII Triennial International SAUM Conference, Belgrade 2004.
- [5] D. Pršić, N. Nedić, "Object-oriented modeling of Hydraulic Systems", VII International SAUM Conference, V. Banja, 2001.
- [6] D. Pršić, N. Nedić, "Modeling of hydraulic system using object-oriented language Modelica", (On Serbian) Infoteh 2002, Jahorina 2002.
- [7] D. Karnopp, D. Margolis, R. Rosenberg, "System Dynamics", John Wiley, New York, 2000.
- [8] J.F. Broenink, "Introduction to Physical Systems Modelling with Bond Graphs", University of Twente, Netherlands.
- [9] D. Antić, B. Danković, "Modeling and Simulation of Dynamic Systems", (On Serbian) Faculty of Electronics Nis, Nis, 2001.

EXPERIMENTAL ANALYSIS OF FIRE CONTROL SYSTEM

S. Lj. Biočanin, V. D. Veljković

Abstract

Increase in efficiency of air target firings mostly depends on dynamic characteristics of the Fire Control System. Fire Control Systems embody all complexity of concept solutions and advancement in application of the latest technologies, including a series of characteristics, which only refer to them. Analytical descriptive approach of dynamic Fire Control System features is mostly very complex one. Therefore, research work has proved that experimental analysis of dynamic Fire Control System features should be also conducted, besides analytical analysis for the purpose of comparing their results. This paper deals with experimental analysis of the System with hydroelectric servo system as an executive organ. Analysis is supported by created applications of software package for graphic programming Lab view IV.

Keywords: Fire Control System, experimental tests and hydroelectric servo system.

1. INTRODUCTION

The objective of this paper is to take into consideration an experimental method, which will serve for determination of dynamic features of an Anti-tank Fire Control System. Above all, the said method has emerged due to arisen need for testing Fire Control System after completed overhaul operations of an air defense unit. For the purpose of meeting the test requirements, special test, measuring and computer equipment have been defined.

2. TESTING SYSTEM

Test, measuring and computer equipment have been connected per Block Diagram shown in Figure 1. Data acquisition system, Computer System A2, through demodulator and modulator, has been connected to the Gun's Fire Control System via connecting box. Gun's carrying signal has amounted to 6.6 V, 400 Hz. Electric power supply system source can be either Gun's electric generating set or supplied from electric network 3x220V/50 Hz.

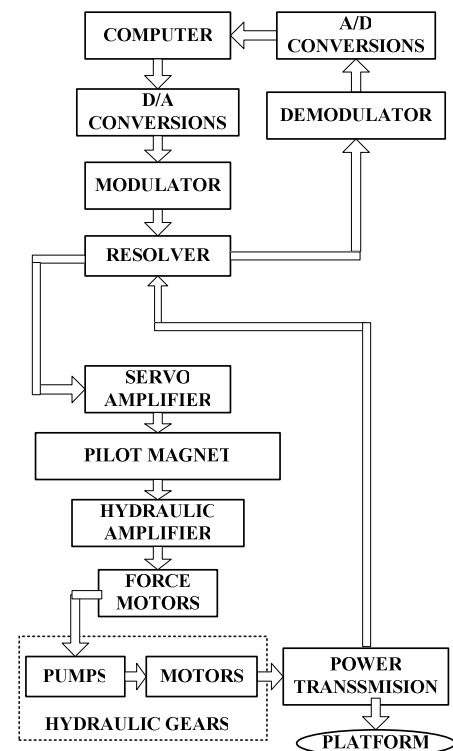


Figure 1 – Block diagram for measuring equipment connection

MEASUREMENT RESULTS

The quoted experimental method can serve for a great number of measurements. Some of these results are provided herein. number of measurements. Some of these results are provided herein. Determining the scope of error signals ε_{sv} and ε_{hv}

Control signals and signals measured as system echo, are voltage signals. Gun's echo is manifested as angle change. It is necessary to establish the relation between voltage and angle, the so called ratio factor. Gun is subjected to step impulse of 10 mrad for the purpose of recoding Gun's echo, namely error signal (error signal should be amplified for 10 times). In the first instance, when error signal is maximal, the voltage value of error signal corresponds to 10 mrad angle. Figure 2 shows the voltage value of error signal and its figure is used for computation of ratio factor.

$$\begin{aligned} 10 \text{ mrad} &= 387\text{mV}/10 \\ 1 \text{ mrad} &= 3,87\text{mV} \\ 1\text{mrad} &\sim 4\text{mV} \end{aligned}$$

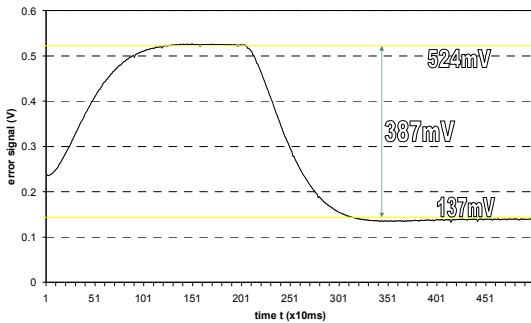


Figure 2 – Determination of ratio factor

Gun's maximum speed per traverse measured in both directions must be minimum 85°/s

The Gun is subjected to 1600 mrad impulse. The Gun cannot achieve this speed, but it will move with its maximum speed. Position of the Gun is recorded (x and y coordinates). These records serve for computation of maximum speed per traverse.

Diagram of changes of x-axis position serves for reading of time needed to the Gun to travel 360 degrees (Figures 3 and 4). X-axis serves to denote the number of measurements. Time between two measurements is 10ms.

$$\begin{aligned} V_{\max} &= 360^{\circ}/(591-198) \times 10\text{ms} = 91,6^{\circ}/\text{s} \\ V_{\max} &= 360^{\circ}/(607-214) \times 10\text{ms} = 91,6^{\circ}/\text{s} \end{aligned}$$

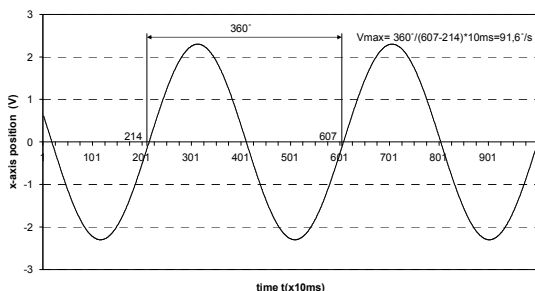


Figure 3 – Determining of maximum speed per traverse in clock direction

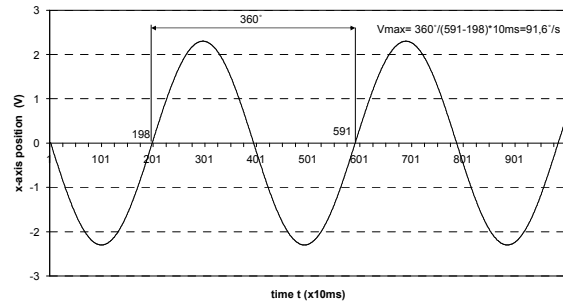


Figure 4 – Determining of Gun's maximum speed per traverse in counter clock direction

Gun's maximum speed per elevation measured during upward and downward movements must be minimum 45°/s

The Gun is subjected to 1100 mrad. The Gun cannot achieve this speed, but it will move with its maximum, possible speed. Position of the Gun is recorded (x, y and z coordinates). Gun's angle is computed as $\arctg z/x$. These diagrams serve for computation of maximum speed per elevation based on tilt (change of angle per time). X-axis serves to denote the number of measurements. Time between two measurements is 10ms (Figures 5 and 6).

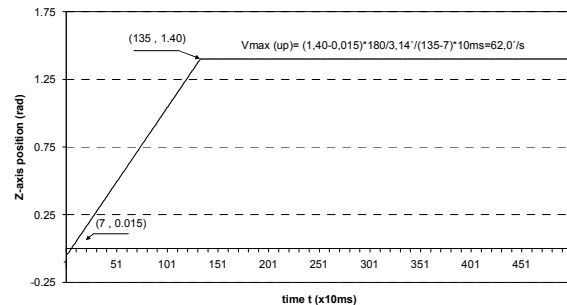


Figure 5 – Determining of Gun's maximum speed per elevation in upward direction

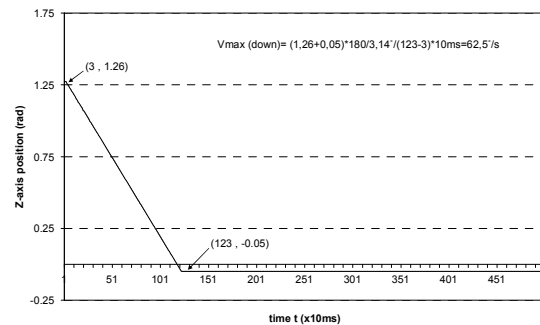


Figure 6 – Determining of Gun's maximum speed per elevation in downward direction

$$V_{\max} (\downarrow) = (1,26+0,05) \times 180/3,14^{\circ}/(123-3) \times 10\text{ms} = 62,5^{\circ}/\text{s}$$

$$V_{\max} (\uparrow) = (1,40-0,015) \times 180/3,14^{\circ}/(135-7) \times 10\text{ms} = 62,0^{\circ}/\text{s}$$

Error signal of traverse during Gun's travel with constant speed ranging from 1-2mrad/s must be less than 0.5mrad, 1mrad (Figure 7)

The Gun is subjected to constant speed of travel and error signal is recorded. The recorded signal is divided with ratio factor in order to obtain the value in mrad. Diagram will serve to us to determine the distance between minimum and maximum value in the zone when travel becomes stable.

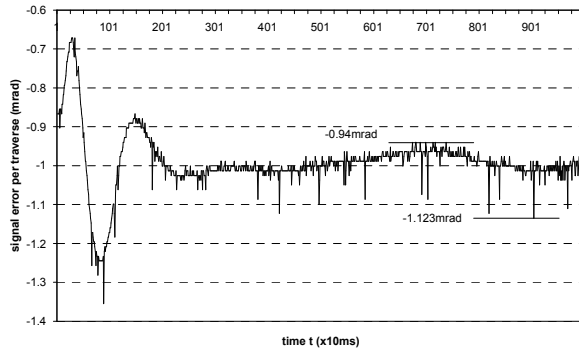


Figure 7 – Determining of signal error per traverse

Error signal of elevation during Gun's travel with constant speed ranging from 1-2mrad/s, must be less than 0.5mrad (Figure 8)

The Gun is subjected to constant speed of travel and error signal is recorded. The recorded signal is divided with ratio factor in order to obtain the value in mrad. Diagram will serve to us to determine the distance between minimum and maximum value in the zone when travel becomes stable.

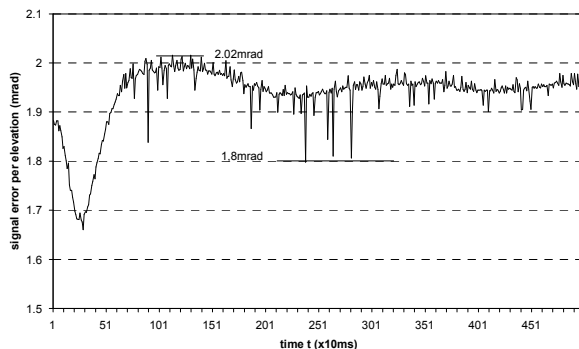


Figure 8 – Determining of signal error per elevation

Error signal of system echo traverse to sinus function of frequency 0.1Hz and amplitude of 15° (261.8mrad) must be less than 5mrad pp (Figure 9)

The Gun is subjected to sinus impulse of the above-mentioned characteristics and error signal is recorded. The recorded signal is divided with ratio factor in order to obtain the value in mrad. Diagram will serve to us to determine the distance between minimum and maximum value.

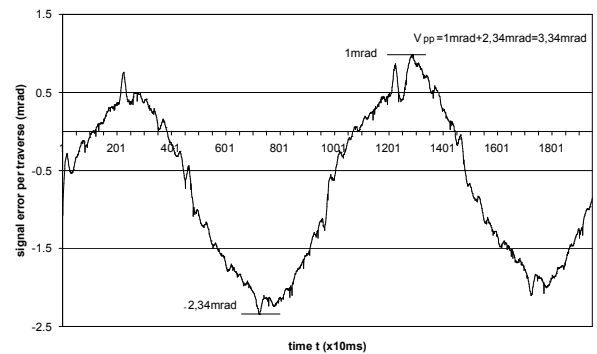


Figure 9 – Error signal of system echo traverse to sinus function

$$V_{pp} = 3.34 \text{ mrad}$$

Error signal of system echo elevation to sinus function of frequency 0.1Hz and amplitude of 15° (261.8mrad) must be less than 5mrad pp (Figure 10)

The Gun is subjected to sinus impulse of the above-mentioned characteristics and error signal is recorded. The recorded signal is divided with ratio factor in order to obtain the value in mrad. Diagram will serve to us to determine the distance between minimum and maximum value.

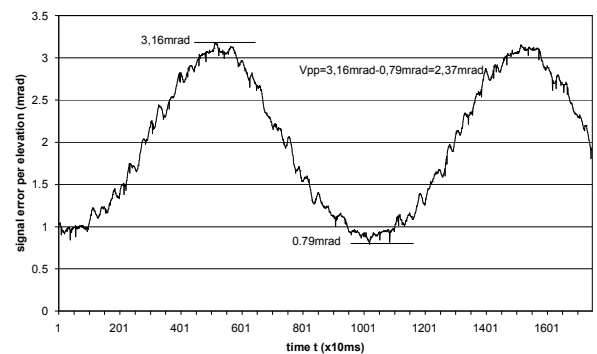


Figure 10 – Error signal of system echo elevation to sinus function

$$V_{pp} = 2.37 \text{ mrad}$$

Dynamic echo of the Gun to step function per traverse must be such that time of recording (defined as the time when impulse is set up to the time when the position error per traverse is beyond 2mrad) is less than:

- 100 mrad 1.0 s
- 200 mrad 1.5 s
- 1000 mrad 3.0 s

The Gun is subjected to step impulse and error signal is recorded. The Figure serves for reading of time during which error signal drops beyond 2 mrad. (Figure 11)

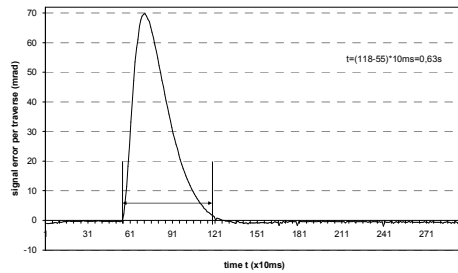


Figure 11 – Dynamic echo of the Gun per traverse to step impulse of 100 mrad

Dynamic echo of the Gun to step function per elevation must be such that time of recording stabilization (defined as the time when impulse is set up to the time when the position error per elevation is beyond 2 mrad) is less than:

- 100 mrad 1.0 s
- 200 mrad 1.5 s
- 1000 mrad 3.0 s

The Gun is subjected to step impulse and error signal is recorded. The Figure serves for reading of time during which error signal drops beyond 2 mrad (Figures 12)

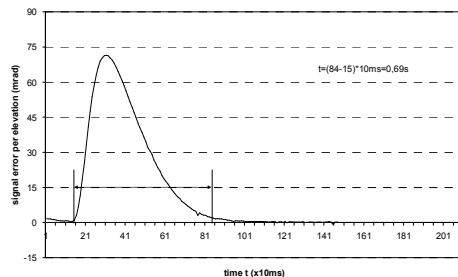


Figure 12 – Dynamic echo of the Gun per elevation to step impulse of 100 mrad

Maximum acceleration of the Gun per traverse should be such that set step impulse of 1600mrad/s should be achieved in 1.0s to 1.65s

The Gun is subjected to travel with its maximum speed in both directions. The signal is recorded from speed lever synchro of hydraulic gears. The signal is recorded from speed lever synchro of hydraulic gears (Fig. 13).

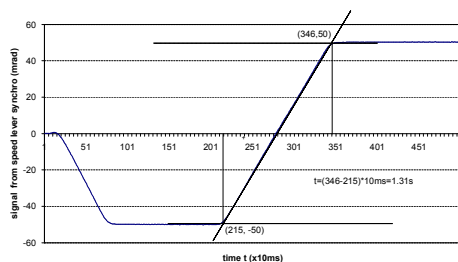


Figure 13 – Maximum acceleration of the Gun per traverse

Maximum acceleration of the Gun per elevation should be such that set step impulse of 1200mrad/s should be achieved in 0.5s to 0.80s

The Gun is subjected to travel with its maximum speed in both directions. The signal is recorded from speed lever synchro of hydraulic gears. The signal is recorded from speed lever synchro of hydraulic gears (Figure 14).

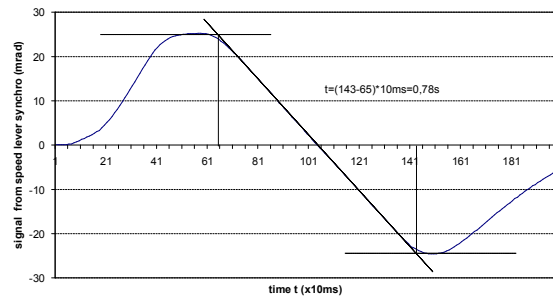


Figure 14 – maximum acceleration of the gun per elevation

4. CONCLUSION

This experimental method, including minor supplements and changes, has been also applied for tests covering several types of Fire Control Systems.

REFERENCES

- [1] Hydro-electric servo system for travel control of platform of air defense unit. Master of Science thesis is in course of elaboration.
- [2] User's Instructions of air defense unit (Volume 1-3)
- [3] Overhaul Manual, (second part)
- [4] User Manual. Lab VIEW, National Instruments (Ivuser.pdf)
- [5] Measurements Manual, Lab VIEW, National Instruments (Ivmeas.pdf)
- [6] User Manual, Master Link Software Libraries (PCI-20369S and PCI-20485S) for DOS, Windows 3.x and Win32 (ED LInk_V3.0.pdf)
- [7] User and Reference Manual, Master Link Software Drivers For National Instruments LabVIEW, Data Acquisition VI Library PCI-20496 (Mlink for LabVIEW.pdf)
- [8] User Manual, ED System Check (ED SYSTEM CHECK_V.2.3.pdf)

SIMULATION MODEL FOR THE ANALYSIS OF BEHAVIOUR OF HYDROSTATIC FORCE TRANSDUCER (HFT)

M. Živković¹⁾, G. Mihajlović¹⁾, D. Golubović²⁾

Abstract

Calculating simulation has become an inevitable method for analysis of work and behaviour of technical systems in all working regimes. It was enabled, in previous years, by very intensive development of computer science and software and by automatic data processing, too (ADP). Thus it is nowadays more and more used in designing as the means of fast prototype making on the basis of models.

Simulation equation for HFT behaviour in MATLAB was according to simulation scheme in SIMULINK. It will be built in mechatronic device of "MEHATRONIK TF 1000/12" calibrator, which is developed in the Faculty of Technical Sciences in Čačak, and it will be used for force detection during program testing and calibration. Analysis of behaviour was done for slope input function, [5,7].

Key words: mathematical model, simulation model, hydrostatic force transducer

1. INTRODUCTION

Mathematical modelling and simulation are certainly the most important assumptions for successful development of science and technique. They enable the analysis and synthesis i.e. the most favourable alternative, confirming the proven, as well as new scientific inventions and relations. The model generally means the physical or abstract creations that in certain circumstances has the characteristics of the problem being researched.

Application of model is not invention of up-to-date science, so the model development can be observed along with development of science and technique. Mathematical models were more applied because of development of computer technologies, which enabled development of simulation methods, too.

Mathematical model is derived analytically using available theoretic knowledge's on observed process of experimentally finding the functional dependence between input and output values. Each study of the given process or technical problem by means of models is called simulation.

Mathematical modelling relies, as mentioned above, on simulation by means of the computers. It enables mathematical modelling to be confirmed as a scientific method. By simulation and automatic data processing (ADP) it is possible, with detailed analysis, to develop analysis with more parameters (without economic consequences).

In the beginning of 19th century physical effects were discovered and by development of measurement instruments the measurement of no electric values was enabled as well as their identification into adequate electric ones. The components that convert no electric

values into electric ones are usually called transducers (Massumformer in German), [8].

In this paper mathematical modelling of hydrostatic force transducer (HFT) was done as well as its simulation by analysis of its behaviour while device for various program stresses was working. The basic reason for its development is a high price of force transducer produced by TIGRP and HBM, [7].

2. MATHEMATICAL MODEL OF HYDRO- STATIC FORCE TRANSDUCER

In the 60es of last century, by invention and development of measuring tape, an important application of electric methods for force measurement began. Beside measuring tapes inductive and magnetic converters are used for force measurement. However, by using well known advantages of hydrostatics mathematical analysis of behaviour and identification of functional HFT parameters started [3,5,7,8].

Depending on the working force at F_R transducer (the force that should be measured) being tensile or compressive, deformations of bolts and fluid will always be at the same direction (figure 1). It means that either simultaneous lengthening of both bolts and fluid is present (when tensile force acts on transducer) or simultaneous shortening of both bolts and fluid (when compressive force acts on transducer). If we assume that the bolts deform as "metal spring" when mentioned forces act on them and that fluid deforms as "liquid spring" then it can be noticed that both bolts and fluid can be treated as a mechanical mass system m and dissipated characteristic k made of two parallel connected springs. Rigidity of all bolts (c_b) and fluid (c_f) according to, [3,6] is:

¹⁾ Mr Milutin Živković, dipl. ing. mašinstva, VTMS – Trstenik, Radoja Krstića 19, e-mail: vtmsts@ptt.yu

¹⁾ Mr Goran Mihajlović, prof., VTMS – Trstenik, Radoja Krstića 19, e-mail: vtmsts@ptt.yu

²⁾ Dr Dragan Golubović, red. prof., Tehnički fakultet – Čačak, Svetog Save 65, e-mail: mehatron@ptt.yu

$$c_z = z \cdot E_z \cdot \frac{A_z}{l_z} \quad (1)$$

$$c_f = E_f \cdot \frac{A_f}{h} = E_f \cdot \frac{(d_k^2 \cdot \pi) / 4}{h} = E_f \cdot \frac{d_k^2 \cdot \pi}{4h} \quad (2)$$

where z - total number of bolts; E_z - elastic modulus of bolt material; E_f - fluid elastic modulus; A_z - sectional area of bolt body; A_f - fluid sectional area contacting the piston whose diameter is d_k ; l_z - bolt length between the piston head and contacting piston plane and cylinder; h - fluid height; F_R - working (external) force registered by transducer.

In private enterprise "AM-Hidraulik" in Trstenik prototype of hydrostatic force transducer (HFT) is developed and it will serve for measurement of tensile forces up to 250kN and compressive forces up to 180kN. Schematic presentation of developed transducer with main parts is shown on fig.1, while the principle of its work and parameters influential on sensitivity and width of measurement range are explained in details in [3,5,7].

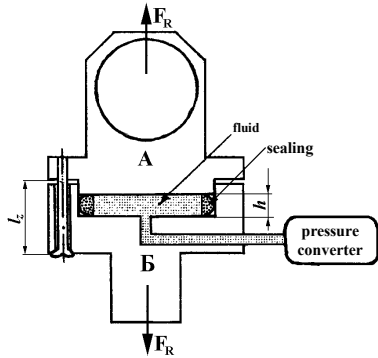
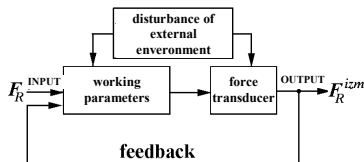


Fig. 1. Schematic presentation of HFT (A-piston, B-cylinder, F_R -working force)

For analysis of the set problem: measurement of external working force by means of hydrostatic transducer the following system: **external environment-transducer-working parameters** must be observed as well as function of each part while this complex measurement chain (fig.2) is working, where [6,7]:

$x(t)$ - input value that is to be measured i.e. external working force at F_R transducer;

$y(t)$ - output value i.e. value of external working force F_R^{izm} at determined working regimes of transducer.



a)

b)

Fig. 2. Structural system scheme: external environment-transducer-working parameters (a) and block system diagram (b)

Mechanical model of system of measures for force measurement by means of hydrostatic transducer is shown in fig. 3.

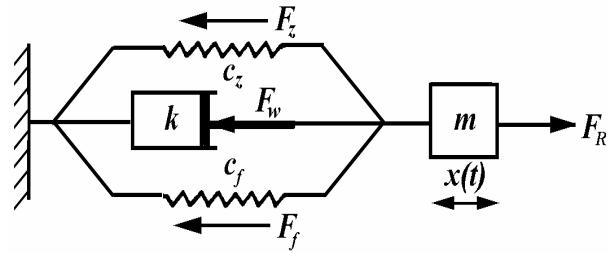


Fig. 3. Mechanical model of system of measures with hydrostatic force transducer

Mechanical model of system of measures shown in fig. 3 can be mathematically expressed by differential equation (3), [4].

$$m \frac{dv}{dt} + k \cdot v + c_z \int_0^t v \cdot dt + F(0) + c_f \int_0^t v \cdot dt + F(0) = F_R \quad (3)$$

Having in mind that for $t=0$ the force in "springs" (in bolts and in fluid) is not zero but tightening force F_p as well as:

$$v = \frac{dy}{dt}, \quad \text{i.e.:} \quad a = \frac{dv}{dt} = \frac{d}{dt} \left(\frac{dy}{dt} \right) = \frac{d^2 y}{dt^2},$$

equation (3) will have the following form:

$$m \frac{d^2 y(t)}{dt^2} + k \cdot \frac{dy(t)}{dt} + c_z \int_0^t \frac{dy(t)}{dt} dt + F_p + c_f \int_0^t \frac{dy(t)}{dt} dt + F_p = x(t) \quad (4.1)$$

$$\frac{d^2 y(t)}{dt^2} + \frac{1}{m} \cdot k \cdot \frac{dy(t)}{dt} + \frac{1}{m} \cdot (c_z + c_f) \cdot y(t) + \frac{2F_p}{m} = \frac{1}{m} \cdot x(t) \quad (4.2)$$

$$\frac{d^2 y(t)}{dt^2} + K_I \cdot k \cdot \frac{dy(t)}{dt} + K_I \cdot c_u \cdot y(t) + 2 \cdot K_I \cdot F_p = K_I \cdot x(t) \quad (4.3)$$

$[c_z + c_f = c_u$ - total rigidity of transducer];

$\left[\frac{1}{m} = K_I$ - inertial constant of system of measures]

(because it has $l/kg = kg^{-1}$ dimension).

Equation (4.3) is differential equation of the second order and it presents **mathematical model of hydrostatic force transducer functioning in course of time**. On that basis examination of dynamic behaviour of the system: external environment-transducer-working parameters can be done.

3. SELECTION OF EXCITATION FUNCTION OF HYDRO-STATIC FORCE TRANSDUCER

As the transducer is meant for registration of forces that in the course of measurement change the most favourable excitation function at the system "input" can be the *slope function* $x(t)$ because its change in the course of time is almost same as the change of measured force intensity. Slope function in linear system theory is defined by integral of unit step function $\sigma(t)$, i.e.:

$$x(t) = \int_0^t \sigma(t) \cdot dt = \int_0^t \delta(t) \cdot dt = t \quad (5.1)$$

$$x(t) = \int_0^t \sigma(t) \cdot dt = \int_0^t 1 \cdot dt = t \quad (5.2)$$

When inclination or pulse function $x(t)$ acts as excitation function then mathematical model of HFT expressed by (4.3) can be presented with fig. 5, 6.

4. SIMULATION ANALYSIS

Simulation can be realized on devices specially made for that purpose or as mentioned above by means of digital computer. Both approaches are important and the adopted methodology must depend on the application area. The analysis of HFT behaviour was done by simulation of equation (4.3) in MATLAB according to simulation scheme (fig. 4) in SIMULINK [1,2].

Estimation of relevant system characteristics is done on the basis of system properties manifested while known excitation function acts, which is shown in fig. 5, 6.

In simulation analysis masses of all movable carrying elements of calibrator are taken into account so $m=1090\text{kg}$ [4].

$$c_z=4,386 \cdot 10^6 \text{ N/mm}; \quad c_f=15,086 \cdot 10^6 \text{ N/mm};$$

$$c_f/c_z=3,44;$$

$$K_I=1/m=9,2 \cdot 10^{-4} \text{ kg}^{-1}$$

$$E_z=2,15 \cdot 10^5 \text{ MPa (steel);}$$

$$E_f=4900 \text{ MPa (glycerine)}$$

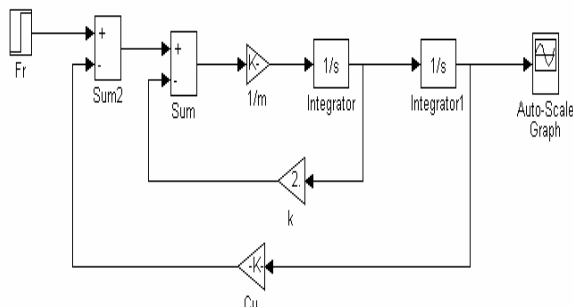


Fig. 4. Simulation scheme in SIMULINK

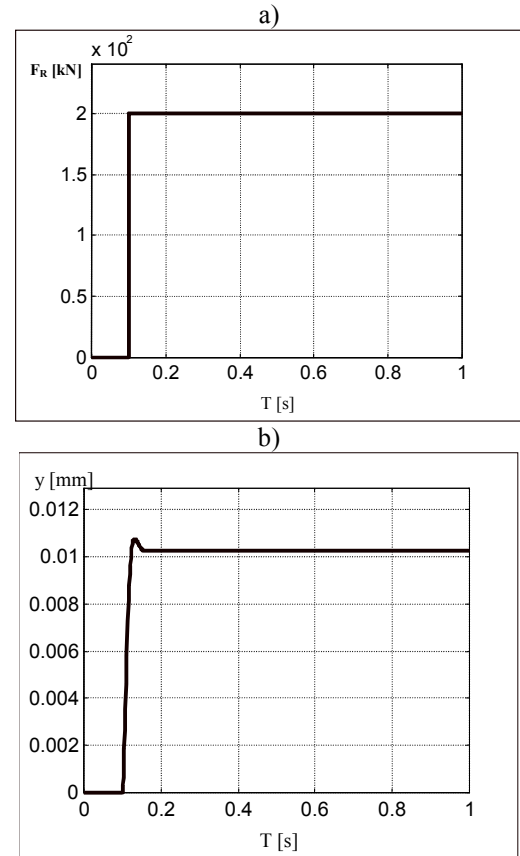


Fig. 5. Time response of system with HFT built in pulse change of external force

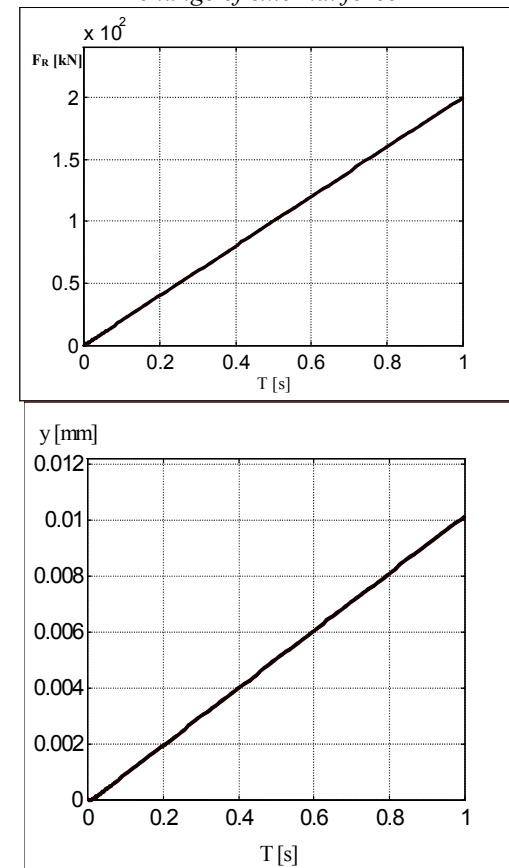
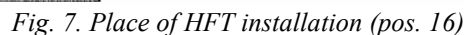


Fig. 6. Time response of system with HFT built in: a) inclination input; b) inclination input response



- Mathematical modelling and computer simulation are used in technique as a kind of help in decision making as well as the basis for calculation and designing.
- Results obtained by coordinate use of experimental techniques and computer simulation often offer the insight that cannot be reached by conventional experiments.
- Simulation can be observed as an experimental process with mathematical model.
- Elastic part of HFT converter expresses external measurement force and equivalent state of deformability through its volume deformation.
- By analysis of transfer system characteristics when inclination input function acts it can be concluded that the mentioned system will satisfy its purpose [6,7].

[1] Antić D., Vidojković B.: Bondsim-simulink biblioteka za modeliranje i simulaciju primenom bond grafova, časopis Tehnika-Elektrotehnika 47 (1998.) 3 (UDC: 681.324/325:519.171.1=891), naučni rad, str. E1÷E6.

- [2] Antić D.: Priručnik za modeliranje i simulaciju dinamičkih sistema, Elektronski fakultet u Nišu, 1999., (str. 315).
- [3] Mihajlović G, **Živković M.**, Golubović: Optimizacija senzitivnih parametara hidrostatičkog davača sile za industrijske aplikacije, NSS – IRMES '04, 16÷17.09.2004., Kragujevac, MF Kragujevac i JUDEKO (str. 105÷110).
- [4] **Živković M.**, Golubović: Sopstvena frekvencija linearnih servomotora, V međunarodno savetovanje o dostignućima elektro i mašinske industrije DEMI 2002., Banja Luka, 25÷26.04.2002.(str. 199÷204).
- [5] **Živković M.**, Mihajlović G, Golubović D: Dinamička analiza merno-kontrolnih sistema sa ugrađenim hidrostatičkim davačem sile, NSS – IRMES '04, 16÷17.09.2004., Kragujevac, MF Kragujevac i JUDEKO (str. 527÷532).
- [6] H. Kazerooni, M. Evans, J. Jones: *Hydrostatic force sensor for robotic applications*, Journal of dynamic systems, measurment and control, pages 115...119, MARCH 1997.
- [7] **Golubović D.**, Živković M: Kidalica - kalibrator MEHATRONIK TF 1000/8 (elaborat dogradnje, Tehnički fakultet Čačak, 2003 (str.35).
- [8] Simić D.: *Osnovi automatskog upravljanja*, Građevinska knjiga, Beograd, 1984.

PRESSURE EQUIPMENTS SAFETY UNITS TESTING ACCORDING TO EUROPEAN DIRECTIVE (PED) 97/23 EC*

N.N.Nedić, D.H.Pršić, L.J.M.Dubonjić

Abstract

This paper presents the problems, development and application of the methods and procedures of safety units testing according to European directive of pressure equipment PED 97/23 EC.

Keywords: European directive, pressure equipment, safety units

I. INTRODUCTION

Free movements of goods in EU countries, without Technical barriers to trade, is based on the acceptance of technical requirements, based on "European Union Council resolution in New approach to technical harmonisation and standardisation"(1985) and "Global approach" for accreditation and certification (1989). After that we have the series standards EN ISO 9000 (quality management) and EN 45000 (accreditation and certification). After that (1993) accreditation, in EU countries, is recommended as a common approach to demonstrate technical competence of notified bodies [1]. Adapting this approach, SRJ declared Law on Standardization (16 May, 1996), vice-law conformity

assessment) [3] and is formed Yugoslav Accreditation Body JUAT (1998). Faculty of Mechanical Engineering Kraljevo- Center for automatic control and fluid technics was among of the first who started to prepare for laboratories accreditation (1999) JUAT declared accreditation of Laboratory for testing on the Faculty of Mechanical Engineering (2001) according to JUS ISO /IEC, Guide 25 and JUS EN 45001.

In mean time, EU Council declared 21 directives. Those have the law capability in EU. Directives of New Approach define the requirements for safety of products and a manufacturer became responsible for the performance of quality assessment of products to EU market.

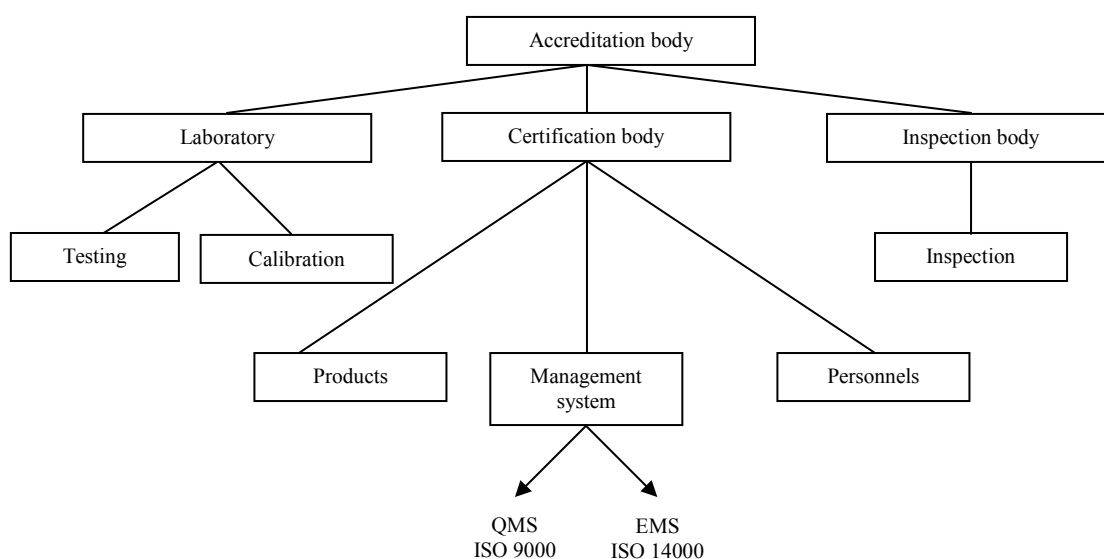


Fig.1. Types of accreditation

The key in obtaining the CE work is implementation of directives based on the New and Global approach through harmonized standards and conformity assessment (testing, inspection, certification and accreditation) [7]. The types of accreditation are given in Fig.1.

The base standards for the accreditation process are (ISO/IEC 17011):

- ISO/IEC/EN 17025 - Testing Laboratories (ISO/IEC Guide 58')
- EN 45004 (ISO/IEC 17020)- Inspection body (Guide 65)
- EN 45011 Certification body for the products (ISO/IEC Guide 65)
- EN 45012 (ISO/IEC 17021) Certification body for QMS (ISO/IEC Guide 62)

Our country, so far, has not accepted New directives in our legislature, but there are "draft laws":

- Law on Technical requirement of products
- Law on Standardization
- Law on Accreditation
- Law on Metrology

and we expect they to be declared soon. However, EU through European agency for Reconstruction (EAR) initiated the project "SCG-Quality" which should contribute to development of the quality infrastructure (standardization, accreditation, metrology, conformity assessment) in order to be our country prepared for CE marking.

One of the New directives is directive 97/23 EC Pressure Equipments.

II. EUROPEAN DIRECTIVE 97/23 EC AND PRESSURE EQUIPMENT SAFETY UNITS

European directive 97/23 ES defines work with pressure equipments where is an internal ganged pressure greater than 0,5 bar as are: vessels, boilers, storage water heaters, industrial valves, refrigerating systems, pipes, regulators etc. [8]. This directive began in November 1999. but all manufacturers and accreditation institutions must were to be adapted until November 2002. Having in mind that this directive covers many industrial branches, as are: oil, gas, water works, chemical industry, heating and refrigerating systems etc it is obvious what is importance of this directive. So far, there are over 120 harmonized standards in relation to pressure equipment. Summary list titles and references in relation to these are given in [9]. If one wants to comply requirements of this directive and harmonized standards it must to pass a number of the steps as are:

- analysis requirements
- project (construction) verification including supply and embed safety components on/or devices in product/machine
- type certification

- production certification (QMS, personnel licenses etc)
- end verification of the safety requirements

These requirements have of different shades and it depends of risk degree, pressure, temperature, fluid etc. Annexes I and II of this directive more close explain technical requirements and modul selection.

In order to ensure the safety of a pressure equipment every pressure device must to have a safety unit (valve) if in that device is possible pressure increasing without some work material incoming (heating or chemical reaction) [10]. Safety valves are define by JUS ISO 4126-1 [11]. Types of the valve according to action are:

- valve with direct action
- valve with command
- valve with extra load
- valve with control

There are many forms and sizes of these valves in regard with particular application. Until today, there are not harmonized standards in relation to safety valves, but in our country there are a few manufacturers ("Prva Iskra"-Barič, "Fabrika vagona"-Kraljevo, "Borac"-Beograd, "Rankomil-armature"-Beograd etc.). Special interest in our country there is for production of electrical storage water heaters. They needs very high quality safety unit.

III. ELECTRICAL STORAGE WATER HEATERS SAFETY UNITS

Electrical storage water heaters safety units in our country, are define by JUS M.C5.750 from 1991, with obliged application from 1992-02-08. With this standard is replaced standard JUS. M.C5.310 from 1967 and JUS M.C5.311 from 1967. The new standard defines in detail the safety unit testing (mechanical, hydraulic, dynamic) and technical requirement for every element. It consists:

- shutoff valve
- one-side valve
- safety valve
- window for one-side valve control

This standard is one of "the most rigorous" standard for safety unit in EU.

Electrical storage water heaters are defined by JUS M. E2.950, JUS M.E.2.951 and JUS E2.952 (1996) and JUS N.M1.100 (1989). The law on Technical requirements of electrical storage water heaters says that the closed electrical storage water heaters must to heave the safety unit for the pressure growth protection in the closed vessel. The safety unit must to be according to JUS M.C5.750. Electrical storage water heaters must to be completed.

In fact, this standard for the safety unit makes more safety electrical storage water heaters and it is on the European way in relation to product safety.

In the our electrical storage water heaters market there are many different safety unit from export and domestic.

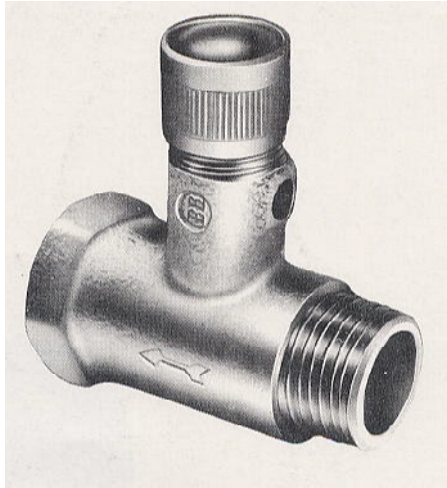


Fig. 2. "Old type" safety valve

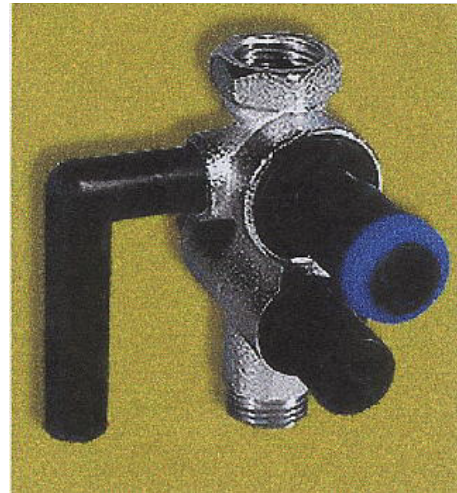


Fig. 3. "New type" safety unit

Typical safety valve in relation to "previous" standard is given in Fig.2 and safety unit in relation with the standard from 1991 is given in Fig. 3.

In the our market there is resistance in application of the new safety unit because it's price is higher.

IV. TESTING LABORATORY

In Faculty of Mechanical Engineering Kraljevo- Center for automatic control and fluid technics, Laboratory for

testing was accredited by JUAT (2001) according to JUS ISO/IEC Guide 25 and JUS EN 45001 for electrical storage water heaters safety unit (JUS M.C5.750 (1991)) and pressure reduction water valve (JUS M.C5.260(1998)) [12]. After that , according to the new accreditation requirements (ISO/IEC/EN 17025), the laboratory was again accredited by Accreditation body of Serbia and Montenegro [13]. Out look view of the Laboratory for testing is given in Fig.4.



Fig. 4. Accredited laboratory for testing

V. CONCLUSIONS

According to European New and Global Approach and the pressure equipment directive (PED 97/23 EC) and our research we can conclude:

- This directive is important for our domestic industry.
- The domestic Quality Infrastructure is "very poor".
- It is necessary urgent to prepared to make "common" notification body for this directive.
- Our domestic industry must to adapt in relation to this directive (CE marking) in production of the some product as are: vessels, safety units, storage water heaters etc.
- Faculty of Mechanical Engineering Kraljevo-Center for automatic control and fluid technics working on complement of the Laboratory for testing of safety units for pressure equipments.

REFERENCES

- [1] P.Popović, LJ.Kovačević, "Accreditation of Conformity Assessment Bodies Basis for Notification Process", Festival kvaliteta 2005, Kragujevac, 19-21 May 2005.
- [2] "Law on Standardization" "Službeni list SRJ", 28 June 1996, No. 30.
- [3] "Procedures for conformity assessment and inspection" "Službeni list SRJ", 7 November 1997, No. 55.
- [4] V.Zeljковиć, M.Đapić, S.Uzunović, G.Đinović, "CE Mark: Verification of the Safety Requirements", Festival kvaliteta 2005, Kragujevac, 19-21 May 2005.
- [5] P.Vasić, T.Janković and Z.Radojević, "Procedure for Attestation of Conformity of Clay Masonry Units According to Relevant Standards", Festival kvaliteta 2005, Kragujevac, 19-21 May 2005.
- [6] K.Kanjevac, J.Milivojević, "Technical Barriers to Trade, Directives New Approach and CE Marking", Festival kvaliteta 2005, Kragujevac, 19-21 May 2005.
- [7] M.Đapić and V.Zeljковиć, "Accreditation Role in the Conformity Assessment Body Notification ", Festival kvaliteta 2005, Kragujevac, 19-21 May 2005.
- [8] Directive 97/23 EC of the European Parliament and of the Council
- [9] Summary list of titles and references to harmonized standards in relation to pressure equipment published in the official Journal of the European Union.
- [10] M.Isailović, M. Bogner, "Technical regulation of pressure equipment" SMEITS 2003. (in Serbian).
- [11] Safety valves, Part 1: General requirements JUS ISO 4126-1,1998, Yugoslav Standard (in Serbian)
- [12] Accreditation Diploma for Laboratory for testing No. 01-03/2001, JUAT, Belgrade, 2001-04-12.
- [13] Accreditation Diploma for Laboratory for testing No. 01-005/1, Accreditation body for Serbia and Montenegro, Belgrade, 29.9.2003.

ДИНАМИЧЕСКИЕ ПРОЦЕССЫ В КОМБИНИРОВАННОМ ПРИВОДЕ МАШИН С СУММИРОВАНИЕМ ПАРАЛЛЕЛЬНЫХ СИЛОВЫХ ПОТОКОВ

В.П. Баранчик, д-р техн. наук, профессор,
В.А. Васильев, инженер

Анализируются колебательные процессы и потери мощности в приводе транспортной машины с суммированием потоков мощности при параллельной работе двигателя внутреннего сгорания и электрического двигателя.

Силовой поток, узловая точка, комплексная амплитуда, комплексная жесткость, упругий и диссипативный моменты, внешняя скоростная характеристика двигателя, передаточные отношения планетарной передачи, тяговая характеристика транспортной машины

Комбинированная энергосиловая установка (КЭСУ) на транспортных машинах (автомобилях, тракторах, самоходных строительных машинах) включает в себя параллельно работающие двигатель внутреннего сгорания (ДВС) и электрический двигатель (ЭД), питаемый от аккумуляторов, которые, в свою очередь, заряжаются от генератора. Генератор приводится от того же ДВС. Основная идея применения КЭСУ заключается в снижении вредных выбросов ДВС за счет использования сравнительно более экологически чистого ЭД. Электродвигатель имеет преимущество в тяговой характеристике при пуске и в начале движения машины. Для повышения КПД целесообразно передавать мощность параллельными потоками от ДВС и от ЭД, при этом потоки мощности суммируются в редукторе и передаются в трансмиссию (Рис.1).

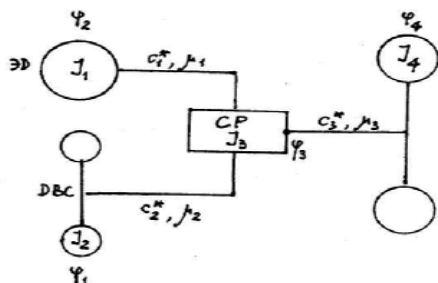


Рис. 1. Схема привода с параллельными потоками мощности

где: $\varphi_1 \varphi_2 \varphi_3 \varphi_4$ - углы поворота масс ЭД, ДВС, ведомого вала СР, ведущего колеса соответственно;

$I_1 I_2 I_3 I_4$ - моменты инерции вращающихся масс ЭД, ДВС, СР (относительно ведомого вала) и поступательно движущейся массы автомобиля (относительно оси ведущего колеса);

$c_1 c_2 c_3$ - коэффициенты упругого сопротивления участков привода;

$\mu_1 \mu_2 \mu_3$ - коэффициенты вязкого сопротивления участков привода;

Суммирующий редуктор (СР) является обобщенной узловой точкой силовых потоков ДВС и ЭД. Частота вращения выходного вала СР одинакова для обоих потоков, а вращающие моменты при данной частоте должны быть постоянны по величине и по знаку. Вращающий момент ДВС при постоянной частоте вращения представляет сумму среднего момента и целого ряда гармонических моментов, поэтому суммирование его с постоянным моментом ЭД неизбежно приведет к возмущению колебаний, динамическим нагрузкам и потерям мощности в трансмиссии. Динамические процессы, происходящие в СР, могут быть исследованы при помощи математических моделей, в основу которых положен метод комплексных амплитуд

[1], позволяющий учесть внутреннее трение в материале при закручивании валов и вязкое трение в передачах, муфтах и в других элементах привода. Считаем, что трение в материале пропорционально деформации и сдвинуто относительно упругого момента на 90 градусов [2]. Конструкционное трение считаем пропорциональным скорости деформации [1].

Независимыми координатами являются углы поворота вращающихся масс. Вращающиеся массы соединены упруго-диссипативными линейными связями. Например, комплексная жесткость 1-ой связи содержит упругую и диссипативную составляющую и равна

$$c_1^* = c_1^*(1 + i\gamma_1), \quad (1)$$

где: c_1 - действительная жесткость связи 1;

γ_1 - коэффициент внутреннего трения в материале связи 1;

i - мнимая единица.

Аналогично выражаются комплексные жесткости остальных связей. Будем считать, что коэффициент внутреннего трения одинаков для всех звеньев, т.е. редуктор изготовлен из однородного материала коэффициентом внутреннего трения γ .

В соответствии с целью исследования рассматриваем колебания масс относительно положения статического равновесия. Причиной колебаний являются гармонические составляющие вращающего момента ДВС. Момент на валу ЭД и момент полезного сопротивления на колесе считаем постоянными.

Для составления дифференциальных уравнений движения используем принцип Даламбера.

Решение отыскивается в виде

$$\varphi = \Phi e^{i\omega t}.$$

Продифференцировав дважды по времени, получим

$$\dot{\varphi} = \Phi i\omega e^{i\omega t}, \quad \ddot{\varphi} = -\Phi\omega^2 e^{i\omega t},$$

где: Φ - комплексная амплитуда,
 $\Phi = U + iV$;

U, V - действительная и мнимая части комплексной амплитуды.

Преобразуем систему уравнений с комплексными коэффициентами в систему уравнений 8-го порядка с действительными коэффициентами относительно U, V .

В матричной форме система уравнений движения может быть записана в виде:

$$\begin{matrix} C - \omega^2 A & -(\omega B + \gamma C) \\ \omega B + \gamma C & C - \omega^2 A \end{matrix} \times \begin{matrix} U \\ V \end{matrix} = \begin{matrix} M \\ 0 \end{matrix}$$

где: A, B, C - матрицы масс, демпфирования и жесткости;

ω - угловая частота гармонической составляющей вращающего момента ДВС;

γ - коэффициент внутреннего трения в материале.

Модуль амплитуды колебаний вычисляется по формуле

$$\Phi = \sqrt{U^2 + V^2},$$

Величины U и V определяются в результате решения системы.

Адекватность математической модели проверена расчетно-экспериментальными методами при проектировании опытных образцов гибридного автомобиля Иж-21261. Математическая модель позволяет исследовать динамические процессы при различных схемах СР. На графиках приведены некоторые результаты расчетов с использованием разработанной математической модели. Расчеты проведены для схемы, в которой ЭД приводился к сцеплению через шестеренчатый редуктор с передаточным отношением $i_g = 1,4$. ДВС непосредственно соединялся со сцеплением ($i_p = 1$).

По найденным значениям Φ могут быть определены амплитудные значения углов закручивания участков, упругих и диссипативных моментов, мощности колебательного процесса, мощности потерь и другие величины, являющиеся функциями независимых координат (углов поворота масс). Например, упругий и диссипативный момент на валу ЭД определяются следующими зависимостями:

$$M_{упр1} = c_1(\Phi_1 - \Phi_3 i_3 i_p)$$

$$M_{сorp2} = \mu\omega(\Phi_1 - \Phi_3 i_3 i_p)$$

Упругие моменты, возникающие при закручивании участков привода, соизмеримы со средним значением момента полезного сопротивления (Рис.2).

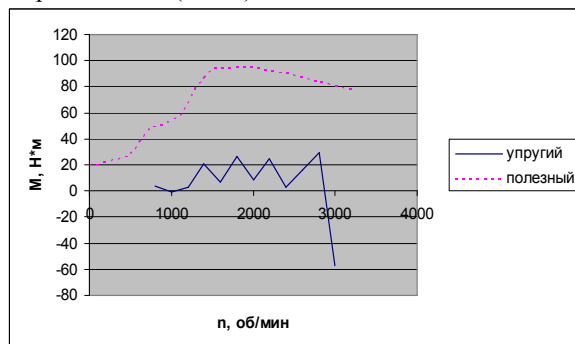


Рис. 2. Упругий момент (сплошная линия) и момент полезного сопротивления (пунктир) на ведомом валу суммирующего редуктора (и вала ДВС)

Для уменьшения динамических нагрузок необходимо уменьшить взаимовлияние силовых потоков ЭД и ДВС. Применение планетарного редуктора, имеющего две степени свободы, позволяет в значительной мере упростить управление ДВС и ЭД.

В рассматриваемом примере передаточное отношение от звена СР, на котором установлен ДВС, до выходного вала СР должно быть не менее $5500 / 4300 = 1,279$.

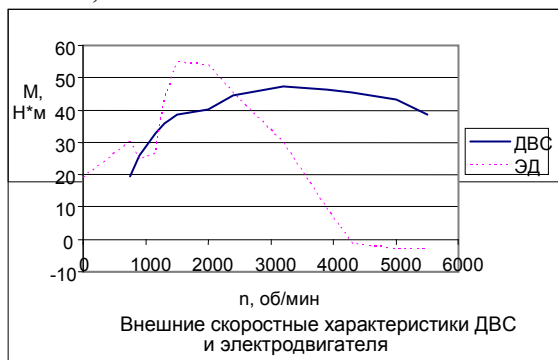


Рис. 5. Внешние скоростные характеристики ДВС и ЭД

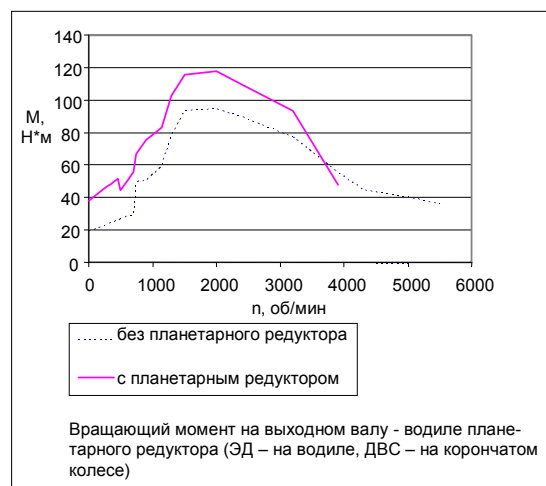


Рис. 6. Тяговая характеристика комбинированного привода

Заключение:

1. Упругие и диссипативные моменты в приводе соизмеримы с моментом полезного сопротивления.
2. Представленная математическая модель позволяет управлять динамическими процессами в приводе.
3. Планетарный редуктор в приводе автомобиля с комбинированной энергетической силовой установкой целесообразно использовать для разделения силовых потоков от ДВС и от электродвигателя, что создает предпосылки для упрощения системы управления двигателями.
4. Электродвигатель целесообразно устанавливать на выходном валу, а ДВС – на том звене планетарной передачи, передаточное отношение к выходному валу которого соответствует отношению максимальных оборотов ДВС и электродвигателя. Максимальные обороты электродвигателя должны отвечать тяговому режиму работы электрической машины.

Литература

1. Вибрации в технике: Справочник в 6-ти томах. Т.1./Под ред. В.В. Болотина -М.: :Машиностроение,1981.
2. Сорокин Е.С. К теории внутреннего трения при колебаниях упругих систем.-М.: Стройиздат, 1960.
3. Баранчик В.П., Васильев В.А. Математическая модель для исследования динамических процессов в приводе машин с параллельными силовыми потоками.- Труды МНТК «Интерстроймех 2005».-Тюмень: ТюмГНГУ, 2005.
4. Баранчик В.П., Васильев В.А. Выбор схемы комбинированной энергосиловой установки машины с планетарным согласующим редуктором.- Труды МНТК «Интерстроймех 2005».-Тюмень: ТюмГНГУ, 2005.

THE ELEMENT-FREE GALERKIN METHOD

Miroslav Zivkovic¹, Milos Kojic², Vlade Vukadinovic³, Ivo Vlastelica⁴

Abstract

In this paper, theoretical backgrounds of the element-free Galerkin method are presented. Since this is a relatively new method, it has not been investigated sufficiently yet. There are several forms of weight functions and a large number of coefficients which are adopted according to experience, whereat the authors give various recommendations for values of those coefficients. In this paper, weight function, which gives the best results in solving strength of displayed 2D problems, was defined, as well as its parameters.

Key words: The element-free Galerkin method, structural analysis, optimization of parameters

1. INTRODUCTION

Development of computers in the last few decades was followed by a very fast development of computer methods and appropriate software. The finite element method (FEM) is the most universal and the best-known among those methods. However, for solving the problems with specific conditions, such as singularities in the case of fracture mechanics, methods which have advantages in comparison to FEM were developed, e.g. the element-free Galerkin method (EFG).

2. MOVING LEAST-SQUARE APPROXIMATION

In EFG method, due to the application of MLS (moving least-square) approximation, the function of moving $u^h(x, y, z) = u^h(\mathbf{x})$ is (Vukadinovic 2005):

$$u^h(\mathbf{x}) = \sum_{j=1}^m p_j(\mathbf{x}) a_j(\mathbf{x}) = \mathbf{p}^T(\mathbf{x}) \mathbf{a}(\mathbf{x}) \quad (2.1)$$

where $p_j(\mathbf{x})$ are basis functions of coordinates of free points, and $a_j(\mathbf{x})$ are coefficients, which are the functions of spatial coordinates \mathbf{x} . In general case, basis functions for two-dimensional problems:

$$\mathbf{p}^T(\mathbf{x}) = [1, x, y] \quad (m=3, \text{ linear}) \quad (2.2)$$

$$\mathbf{p}^T(\mathbf{x}) = [1, x, y, x^2, xy, y^2] \quad (m=6, \text{ square}) \quad (2.3)$$

Coefficients $\mathbf{a}(\mathbf{x})$ in (2.1) for every point \mathbf{x} are obtained by minimization of middling form:

$$J(\mathbf{x}) = \sum_{I=1}^n w_I(\mathbf{x}) [\mathbf{p}^T(\mathbf{x}_I) \mathbf{a}(\mathbf{x}) - \tilde{u}^I]^2 \quad (2.4)$$

and have the value:

$$\mathbf{a}(\mathbf{x}) = \mathbf{A}^{-1}(\mathbf{x}) \mathbf{P}^T \mathbf{W}(\mathbf{x}) \tilde{\mathbf{u}}, \quad (2.5)$$

where: \tilde{u}^I is movement of I -point, $w_I(\mathbf{x})$ weight function of point I , and n is the number of free points which influence the integration point \mathbf{x} (figure 2.1).

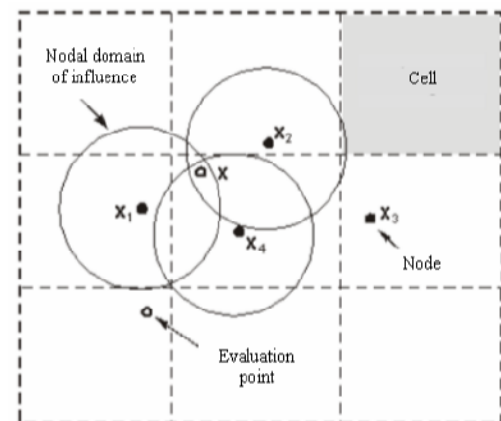


Figure 2.1 Display of free points domain in relation to integration point of cell

3. WEIGHT FUNCTIONS

In EFG method, the weight functions $w_I(\mathbf{x})$ are in general case monotonously falling functions of distance $\|\mathbf{x} - \mathbf{x}_I\|$. These functions influence the functions of movement $u^h(\mathbf{x})$ which is obvious when $\mathbf{a}(\mathbf{x})$ from (2.4) is replaced in (2.1).

The most common forms of weight functions are:

¹ Dr Miroslav Zivkovic, Associate Professor, The Faculty of Mechanical Engineering in Kragujevac, Sestre Janjic 6, 34000 Kragujevac, JMZ@EUNET.YU

² Dr Milos Kojic, Full-time Professor, The Faculty of Mechanical Engineering in Kragujevac, Sestre Janjic 6, 34000 Kragujevac, mkojic@hsph.harvard.edu

³ Vlade Vukadinovic, grad. eng., The Faculty of Mechanical Engineering in Kragujevac, Sestre Janjic 6, 34000 Kragujevac, vukadinac@yahoo.com

⁴ Dr Ivo Vlastelica, Senior Lecturer, Technical College Cacak, 32000 Cacak, ivovl@ptt.yu

(a) polynomial form, Beissel et al. (1996)

$$w_I(d_I) = \begin{cases} 1 - 6\left(\frac{d_I}{d_{\max_I}}\right)^2 + 8\left(\frac{d_I}{d_{\max_I}}\right)^3 - 3\left(\frac{d_I}{d_{\max_I}}\right)^4 & d_I \leq d_{\max_I} \\ 0 & d_I > d_{\max_I} \end{cases} \quad (3.1)$$

(b) exponential form, Belytschko et al. (1993)

$$w_I(d_I) = \begin{cases} \frac{e^{-\left(\frac{d_I}{c}\right)^{2K_I}} - e^{-\left(\frac{d_{\max_I}}{c}\right)^{2K_I}}}{1 - e^{-\left(\frac{d_{\max_I}}{c}\right)^{2K_I}}} & d_I \leq d_{\max_I} \\ 0 & d_I > d_{\max_I} \end{cases} \quad (3.2)$$

where $d_I = \|\mathbf{x} - \mathbf{x}_I\|$ is distance from free point \mathbf{x}_I to interpolation point \mathbf{x} , and d_{\max_I} defines the maximal area of weight function influence for each free point – influence radius.

Coefficient c has been differently defined in literature, so we have the definitions:

-According to Hegen

$$\frac{d_{\max_I}}{c} \geq 4; \quad c \leq \frac{d_{\max_I}}{4} \quad (3.3)$$

-According to Belytschko et al. (1993):

$$c = \alpha c_I \quad (3.4)$$

where $c_I = \max\{\|\mathbf{x}_J - \mathbf{x}_I\|, J = 1, n\}$ represents the maximal distance between I -point and all other free points which act upon the same integration point. Coefficient α is within range $1 \leq \alpha \leq 2$; α about 1 is adopted for singular problems and large gradients, and $\alpha = 2$ for smooth solutions.

-According to Du (1998):

$$c = c_I / k_{ch} \quad (3.5)$$

where c_I is defined in two ways, and consequently, so is the value k_{ch} . According to the first method c_I is defined as maximal distance between I -point and other free points which act upon one integration point.

$$c_I = \max\{\|\mathbf{x}_J - \mathbf{x}_I\|, J = 1, n\} \quad (3.6)$$

In this case, it was recommended that the value k_{ch} is within range 9-12.

According to the second method, c_I is defined as mean distance between I -point and other free points which act upon one integration point.

$$c_I = \frac{1}{n} \sum_{J=1}^n \|\mathbf{x}_J - \mathbf{x}_I\| \quad (3.7)$$

Here, the recommendation is that k_{ch} is selected within range 7-8.

-According to Askes et al. (1998):

$$c = \alpha d_{\max_I} \quad (3.8)$$

whereat it is recommended that $\alpha = 1/3$.

-According to Belytschko et al. (1996)

$$c = \alpha d_{\max_I} \quad (3.9)$$

Here, however, unlike the previous case, the recommendation for the value of α is 0.4.

It can be observed that the last two theories are a special case of Hegen's theory.

All aforementioned theories adopt the coefficient $K_I = 1$.

4. ALGORITHM OF PROBLEM SOLVING

When solving the problem, we begin with balanced equation

$$\mathbf{K} \cdot \mathbf{U} = \mathbf{F} \quad (4.1)$$

where:

$$\mathbf{K} = \int_V \mathbf{B}^T \mathbf{C} \mathbf{B} dV \quad (4.2)$$

and \mathbf{F} is vector of external forces.

Having solved the movement, we determine the strain field by applying the equation

$$\mathbf{e} = \mathbf{B} \mathbf{U} \quad (4.3)$$

and stress in each integration point

$$\boldsymbol{\sigma} = \mathbf{C} \mathbf{e} \quad (4.4)$$

Movement vector is defined in the same way as in finite elements

$$\mathbf{u} = \Phi \mathbf{U} \quad (4.5)$$

Matrix of derivatives of interpolation functions is

$$\mathbf{B} = [\mathbf{B}^1 \quad \dots \quad \mathbf{B}^n] \quad (4.6)$$

where:

$$\mathbf{B}^I = \begin{bmatrix} \Phi_{I,x} & 0 \\ 0 & \Phi_{I,y} \\ \Phi_{I,y} & \Phi_{I,x} \end{bmatrix} \quad (4.7)$$

Interpolation functions $\Phi(\mathbf{x})$ are determined with:

$$\Phi_I(\mathbf{x}) = p_I(\mathbf{x}) A_{ij}^{-1} P_{Ij} w_I \quad (I=1, \dots, n; i,j=1, \dots, m) \quad (4.8)$$

And derivatives of interpolation factors according to Cartesian's coordinates:

$$\frac{\partial \Phi_I(\mathbf{x})}{\partial x_i} = \frac{\partial p_k(\mathbf{x})}{\partial x_i} A_{ij}^{-1}(\mathbf{x}) P_{Ij} w_I(\mathbf{x}) + p_k(\mathbf{x}) \cdot \left[\frac{\partial A_{kj}^{-1}(\mathbf{x})}{\partial x_i} P_{Ij} w_I(\mathbf{x}) + A_{kj}^{-1}(\mathbf{x}) P_{Ij} \frac{\partial w_I(\mathbf{x})}{\partial x_i} \right] \quad (4.9)$$

Matrix \mathbf{A} was defined in the following way:

$$\mathbf{A}(\mathbf{x}) = \mathbf{P}^T \mathbf{W}(\mathbf{x}) \mathbf{P} \quad (4.10)$$

$$\text{where: } w_{IJ} = w_J(\mathbf{x} - \mathbf{x}_J) \delta_{IJ} \quad (4.11)$$

Derivatives from A_{kj}^{-1} are calculated as:

$$\mathbf{A}_{ji}^{-1}(\mathbf{x}) = -\mathbf{A}^{-1}(\mathbf{x}) \mathbf{A}_{ji}(\mathbf{x}) \mathbf{A}^{-1}(\mathbf{x}) \quad (4.12)$$

where derivatives from A_{sk} are calculated according to:

$$\frac{\partial \mathbf{A}}{\partial x_i} = \mathbf{P}^T \frac{\partial \mathbf{W}}{\partial x_i} \mathbf{P} \quad (4.13)$$

The values used in previous expressions were defined as:

$$\mathbf{P} = \begin{bmatrix} p_1^T \\ p_2^T \\ \vdots \\ p_n^T \end{bmatrix} = \begin{bmatrix} 1 & x_1 & y_1 \\ 1 & x_2 & y_2 \\ \vdots & \vdots & \vdots \\ 1 & x_n & y_n \end{bmatrix} \quad (4.14)$$

where n is the number of free points which influence one integration point. w_i represents weight function (3.1) or

(3.2), and $\frac{\partial w_i}{\partial x_i}$ derivatives of weight functions according to Cartesian's coordinates.

- Derivative of polynomial form of weight function:

$$\frac{\partial w_i}{\partial x_i}(d_i) = \frac{12}{d_{\max_i}^2} d_i \left(-1 + 2 \frac{d_i}{d_{\max_i}} - \frac{d_i^2}{d_{\max_i}^2} \right) \frac{\partial d_i}{\partial x_i} \quad (4.15)$$

- Derivative of exponential form of weight function:

$$\frac{\partial w_i}{\partial x_i} = -\frac{2K_i}{c_i^{2K_i}} d_i^{2K_i-1} \frac{e^{-\left(\frac{d_i}{c_i}\right)^{2K_i}}}{D_i} \frac{\partial d_i}{\partial x_i} \quad (4.16)$$

where:

$$D_i = 1 - e^{-\left(\frac{d_{\max_i}}{c_i}\right)^{2K_i}} \quad (4.17)$$

For 2D problems, radius d_i is defined by expression:

$$d_i = \sqrt{(x - x_i)^2 + (y - y_i)^2} \quad (4.18)$$

5. EXAMPLES

5.1 Console bending

Console loaded by force at its loose end is observed. The aspect of console is given in *figure 5.1*.

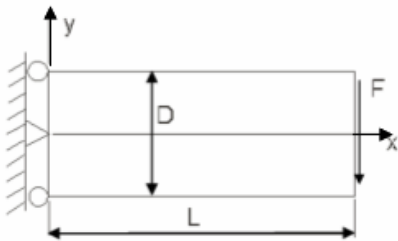


Figure 5.1 Console loaded by force at its loose end

Material and geometrical data are:

$$L = 48 \text{ in}, \quad D = 12 \text{ in}$$

$$E = 3.0 \cdot 10^7 \text{ psi} \quad \nu = 0.3$$

$$F = 1000 \text{ lbf}$$

$$1 \text{ in} = 25.4 \text{ mm}, \quad 1 \text{ lbf} = 4.44822 \text{ N}, \quad 1 \text{ psi} = 6.89476 \cdot 10^3 \text{ Pa}$$

For the analysis of beam bending, GML method was used with various weight functions, i.e. with adopted various coefficients of weight function. Beam was discretized with 231 free points and with 192 cells (2D four-node elements) *figure 5.2*. The number of Gauss' integration points is 6x6.



Figure 5.2 Model of beam discretized by free points and cells

Comparative results for vertical movement u_y are given in **table 5.1**. In addition to the results of numerical calculations, the analytical solution is also given, as well as solution deviation from analytical in percentages, for possible comparison and establishment of accuracy.

For the analysis of movement, linear base and weight functions of exponential and polynomial form are used, whereat for weight functions of exponential form we adopt various values of coefficient α by which we perceive its influence on obtained solutions.

Table 5.1 Comparative results for vertical movement U_y of loose end of beam

	Analytic	Weight function of exponential form			Weight function of polynomial form
		$\alpha = 1/4$	$\alpha = 1/3$	$\alpha = 0.4$	
σ_y [MPa]	3	2.738	2.855	2.964	3.266
(%)	-	91.26	95.17	98.8	108.87

Figure 5.3 shows the solutions which match the analytical solution best (weight function of exponential form and $\alpha = 1/3$).

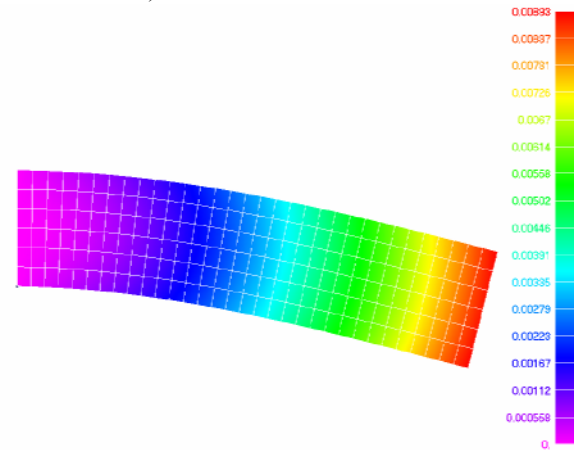


Figure 5.3 Displacement field in strained configuration

5.2 Slab with opening

Slab with opening is tension-loaded in y direction by continual load $\sigma = 1 \text{ psi}$. *Figure 5.4* shows

one quarter of the slab discretized with 156 free points and 132 cells (2D four-node elements). The same figure includes material and geometrical properties, as well as appropriate limitations and loads.

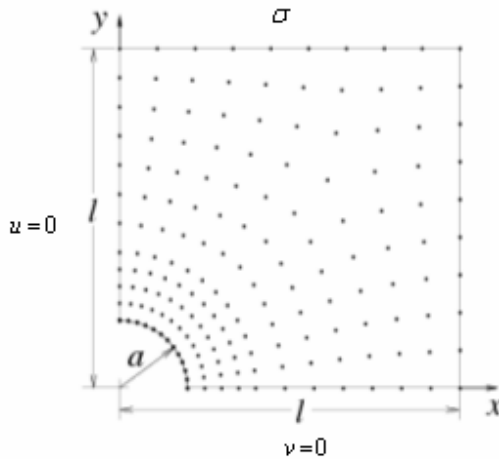


Figure 5.4 Discretized model of one quarter of the slab with opening

$$E = 3.0 \cdot 10^7 \text{ psi}, \quad \nu = 0.3$$

$$a = 1 \text{ in}, \quad l = 5 \text{ in}$$

$$\sigma = 1 \text{ psi}$$

$$1 \text{ in} = 25.4 \text{ mm}, \quad 1 \text{ lbf} = 4.44822 \text{ N}, \quad 1 \text{ psi} = 6.89476 \cdot 10^3 \text{ Pa}$$

For the analysis of the movement, linear base and weight functions of exponential and polynomial form are used, whereat for weight functions of exponential form we adopt various values of coefficient α by which we perceive its influence on obtained solutions.

Table 5.2 Comparative results for stress σ_{yy} on the edge of opening

	Analytic	Weight function of exponential form			Weight function of polynomial form
		$\alpha = 1/4$	$\alpha = 1/3$	$\alpha = 0.4$	
σ_{yy} [MPa]	3	2.738	2.855	2.964	3.266
(%)	-	91.26	95.17	98.8	108.87

Figure 5.5 shows the solutions which match the analytical solution best (weight function of exponential form and $\alpha = 0.4$).

6. CONCLUSION

With the aim of investigating the weight functions and its influence, the programme was written in Fortran and installed in PAK, containing various forms of the same functions. By using the various forms of weight functions, the results were compared and the following conclusion was made: polynomial form of weight function can give satisfactory solutions, but it often doesn't, which makes it unreliable for practical application. Unlike this one, exponential form of weight function gives satisfactory solutions for all three values of coefficients,

whereat the solutions with $\alpha = 1/3$ and $\alpha = 0.4$ are prominent for its accuracy. Whether the solutions will be better with one or the other value of coefficient varies from one example to another, so in practical application both values can be applied, or some values in-between the same ones might be tried, which could be the subject of some further investigations.

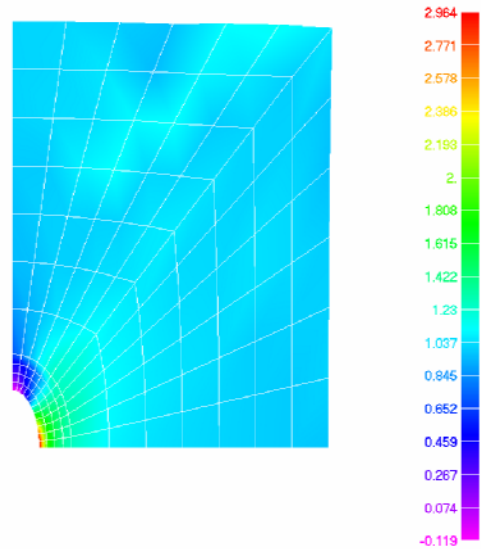


Figure 5.5 Stress field σ_{yy} in strained configuration

7. LITERATURE

- Organ J.D., (1996), Numerical Solutions to Dynamic Fracture Problems Using the Element-Free Galerkin Method, Northwestern university, Evanston, USA, PhD thesis
- Beissel S., Belytschko T., (1996) 'Nodal integration of the element-free Galerkin method', Northwestern university, Evanston, USA
- Belytschko T., Gu L., Lu Y.Y., (1993) 'Fracture and crack growth by element free Galerkin methods', Northwestern university, Evanston, USA
- Du C., (1998) An element-free Galerkin method for simulation of station of stationary two-dimensional shallow water flows in rivers', University of Karlsruhe, Karlsruhe, Germany
- Askes H., de Borst R., Heeres O., (1998) 'Conditions for locking-free elasto-plastic analyses in the Element-Free Galerkin method', Delft University of Technology, Delft, The Netherlands
- Belytschko T., Krongaus Y., Organ D., Fleming M., Krysl P., (1996) 'Meshless methods: An overview and recent developments, Northwestern University, Evanston, USA
- Vukadinovic V., (2004) The Element-Free Galerkin Method, Faculty of Mechanical Engineering in Kragujevac, Final exam

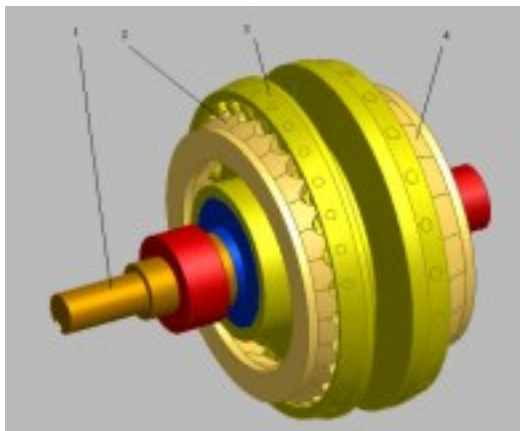
INFLUENCE OF THE GEOMETRICAL PARAMETERS CONCERNING THE DISTRIBUTION OF MESHING FORCES ON HARMONICAL GEARINGS WITH RIGID FRONTAL ELEMENT

Prof. Dr. Adrian BRUJA
Marian DIMA
Catalin FRANCU

Abstract: In this report is presented a study of how geometrical parameters influences the distribution of meshing forces of harmonical gearing with rigid frontal element. Parameters that were studied are: angle between the axes, number of teeth of the wheels, median radius of the wheels (radius of the sphere where takes place the meshing), vertex angle of the satellite's rolls and profile's angular displacement. Values are in numerical and grafical form.

Keywords: Harmonical, Central wheel, Mesh forces

Harmonical gearings with rigid frontal element are used in designing of frontal harmonical transmissions with rigid elements, which can be: gear reducers, differential gears, gearboxes and continuously variable transmissions. In figure 1a is represented a harmonical reductor with double satellite and in figure 1b is represented the kinematic diagram.

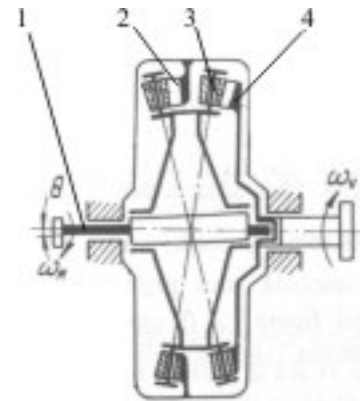


(a)

Satellite toothing is realised in shape of conical rolls disposed regularly on the lateral surface of the rolling cone and which has the cone-points at the intersection of the axes of gear wheels. The fixed central wheel's toothing flank has the mating profile shape of conical rolls. The number of teeth of the satellite is greater by 1 than the central wheel's number of teeth.

Figure 2 presents the harmonic gearing's conjunction with the sphere on which the meshing takes place and points out the central wheel's profile, the satellite's rolls and the line of contact. The line of contact's parametric equation were determined based on fundamental law of meshing:

$$\begin{aligned} z_l &= \frac{-b - \sqrt{b^2 - 4ac}}{2a}; \\ y_l &= \frac{2z_l(n_z x_1 - n_x z_1) + n_x(x_1^2 + y_1^2 + z_1^2 + r^2 - \rho'^2)}{2(n_x y_1 - n_y x_1)}; \\ x_l &= -\frac{n_z z_l + n_y y_l}{n_x}, \quad \varphi_s \in (0, 2\pi), \text{ and } = ct. \end{aligned} \quad (1)$$



(b)

Figure 1 Harmonical reductor with rigid frontal element with double satellite.

1- input shaft, 2- fixed central wheel, 3- double satellite, 4- driven central wheel (fixed with output shaft)

where:

$$\begin{aligned} a &= 4(n_x^2 + n_y^2)(n_z x_1 - n_x z_1)^2 + 4(n_x^2 + n_y^2)(n_x y_1 - n_y x_1)^2 + \\ &8n_y n_z (n_z x_1 - n_x z_1)^2 \\ b &= 4n_x(n_x^2 + n_y^2)(n_z x_1 - n_x z_1)(x_1^2 + y_1^2 + z_1^2 + r^2 - \rho'^2) + \\ &4n_x n_y n_z (n_x y_1 - n_y x_1)(x_1^2 + y_1^2 + z_1^2 + r^2 - \rho'^2) \end{aligned} \quad (2)$$

$c = n_x^2(n_x^2 + n_y^2)(n_z x_1 - n_x z_1)(x_1^2 + y_1^2 + z_1^2 + r^2 - \rho'^2)^2 - 4r^2 n_x^2 (n_x y_1 - n_y x_1)^2$;

where:

x_1, y_1, z_1 represents the coordinates of center of satellite's roll;

n_x, n_y, n_z are the parameters of the common normal \vec{n} of the flanks in the point of contact

r – radius of the sphere on which takes place the meshing
 ρ' – radius of the satellite's roll.

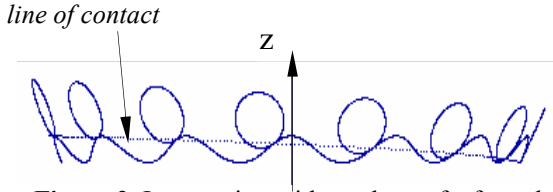


Figure 2 Intersection with a sphere of a frontal harmonical transmission mesh rigid element

As you can see in figure 2 during operation all the teeth are in contact and half of those are transmitting the motion. As of this, the problem of determining the forces that appear in the points of contact of the teeth, on the line of contact, is a redundant problem, and the degree of indeterminacy, is equal with the number of meshing teeth decreased by 1. The problem can be solved taking into account the elastic deformations of the teeth flanks in the points of contact, assuming that these deformations are proportional with the values of those forces. Expression of the force can be determined, for every point of contact, p .

$$F_p = \frac{M_c \cdot (x_l n_{ry} - y_l n_{rx})_p^n}{\sum_{p=1}^m (x_l n_{ry} - y_l n_{rx})_p^{n+1}} \quad (3)$$

where:

M_c transmitted moment of twisting;

x_l, y_l - the coordinates of points of contact (placed on the line of contact);

n_{rx}, n_{ry} - parameters of direction of force in meshing;

$$n = 10/9;$$

m – number of pairs of teeth that are transmitting the motion; numbering of the pairs of teeth starts from the roll that is on the bottom between 2 teeth of central wheel.

Values of the \bar{F}_p forces and their number depend by the values of geometrical and kinematical parameters of the gearing: angle between the axes, number of teeth of the wheels, median radius of the wheels (radius of the sphere where takes place the

meshing), vertex angle of the satellite's rolls and profile's angular displacement (defined as the difference of the half vertex angles of cone's surface on which are disposed satellite's rolls).

For a frontal harmonical reducer, having the following parameters: angle between the axes $\theta = 2.5^\circ$, number of teeth of the central wheel $z_c = 29$, number of rolls of the satellite $z_s = 30$, median radius of meshing sphere $r = 85mm$, vertex angle of the satellite's rolls $\alpha = 2.4^\circ$ and profile's angular displacement $\delta = 2.4^\circ$, Maximum transmitted moment of twisting at the output shaft $M_c = 240Nm$, has been written a computer program that can determine the values of forces in meshing and the modification of the geometrical and kinematical parameters.

For a clear interpretation of the results each of the 5 parameters taken into account was modified.

Next is presented the influence of every parameter.

For the angle between the axes θ , were taken into account: 2° , 2.5° and 3° , results are presented both as a chart and as a table in figure 3. You can observe that the values for the angle θ of 2° and 2.5° are meshing 15 pairs of teeth and for the value of θ of 3° are meshing 13 pairs of teeth. This fact happens because for an angle greater than $\theta = 2.5^\circ$, interference is showing up at the top of the teeth, which decreases the number of pairs of teeth in contact. We can observe that for $\theta = 2.5^\circ$ values of meshing forces are smaller than for $\theta = 2^\circ$.

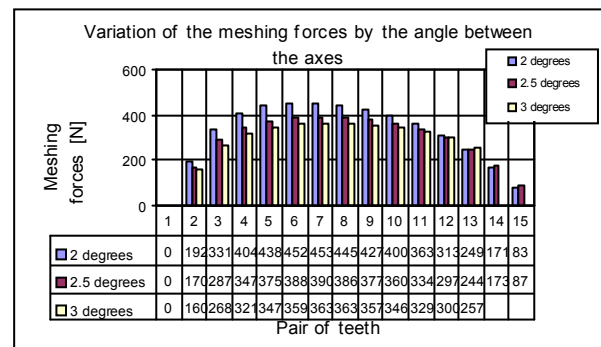


Figure 3

Figure 4 represents distribution of the meshing forces by the number of satellite's rolls. The analysis of figure 4 returns as expected the fact that the meshing forces are decreasing when the number of the teeth is increasing with the restriction that the interference would not show up (32 rolls case)

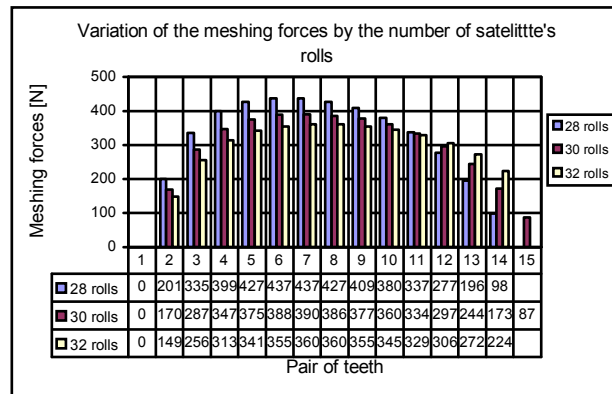


Figure 4

In figure 5, sphere's meshing radius growth indicates a decrease in meshing forces because of the fact that moment arms to the central wheel's axis of

rotation are increasing. We can observe that variation of the force is strictly proportional with the variation of the parameter, for every tooth.

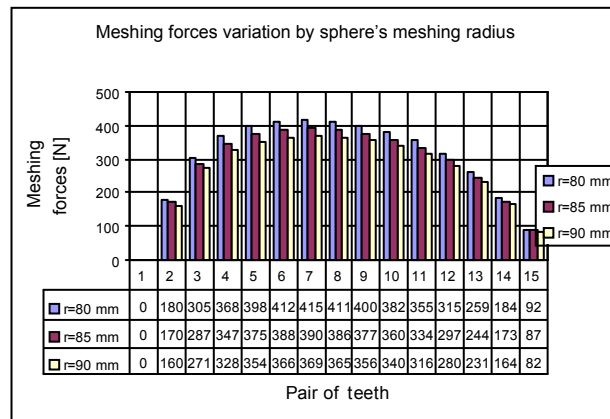


Figure 5

Vertex angle of the satellite's rolls has the greatest influence over the distribution of meshing forces in the frontal harmonical reducer figure 6. Increasing the vertex angle of the satellite's rolls over

$\theta = 2,5^\circ$ makes the interference to show up, and this wears the teeth, and therefore number of pairs of teeth in contact is decreasing.

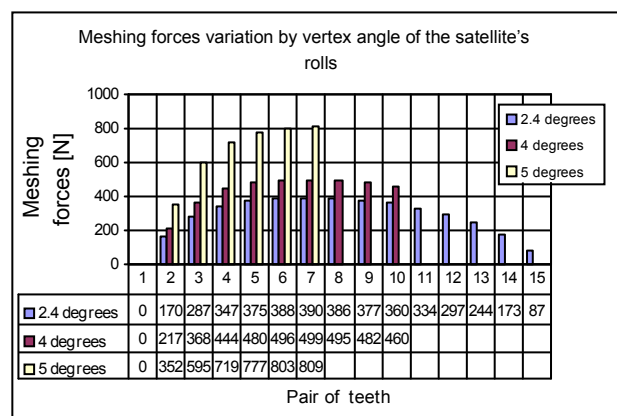


Figure 6

Profile's angular displacement influences the conditions in which meshing takes place and therefore influences the distribution of the meshing forces on every pair of teeth in contact. We can see in figure 7 that a smaller value of angular displacement makes the distribution of the meshing forces more asymmetrical, and a higher value may have negative consequences by decreasing the pairs of teeth in contact.

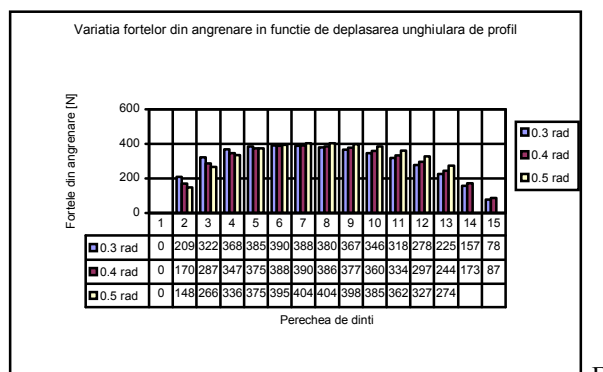


figure 7

By looking the 3...7 figures some conclusions arise:

- For a gearing with a known reduction ratio, we can choose values for geometrical parameters, to distribute the meshing forces over the highest number of pairs of teeth in contact; The maximum number of teeth in contact is half of central wheel's number of teeth.
- Distribution of the meshing forces in points of contact has the shape of a second-degree curve slightly asymmetrical, values being higher when the contact is on the bottom of the tooth, and smaller when the contact is on the top of the tooth.

References

[1]. Bruja Adrian, Dima Marian – La détermination de la ligne d'action pour l'angrenage avec mouvement de précession. Articol, Analele Universității "Dunărea de Jos", Fascicola XIV, pag. 17-20, Galați, 1999, ISSN 1224-5615.

[2]. Bruja Adrian, Dima Marian – L'influence des paramètres de la transmission par mouvement de précession sur le profil des dents de la roue centrale. Articol, Analele Universității "Dunărea de Jos", Fascicola XIV, pag. 17-20, Galați, 1999, ISSN 1224-5615.

[3]. Bruja Adrian, Dima Marian – La cynétostatique de l'engrenage avec mouvement de précession. Articol, Analele Universității "Dunărea de Jos", Fascicola XIV, Galați, 2000, ISSN 1224-5615.

[4]. Bruja Adrian, Dima Marian – La repartition de la charge sur les dents des engrenages et la détermination des forces qui agissent sur les éléments composant de la transmissions harmonique frontale avec élément rigide. Comunicare, XVI International Conference on "MATERIAL FLOW, MACHINES AND DEVICES IN INDUSTRY" University of Belgrade 7-8 dec. 2000, pag 5.57-5.60.

[5] Adrian Bruja, Marian Dima - La détermination des forces qui agissent sur les dents de l'engrenage harmonique avec élément frontal rigide. Articol. Al VIII-lea Simpozion Internațional de Teoria Mașinilor și Mecanismelor IFToMM, SYROM 2001, vol. III, pag. 91-96, ISBN 973-8143-38-1, ISBN 973-8143-27-6, București, 28 aug. - 1 sept 2001

[6] Adrian Bruja, Marian Dima - Ascuțirea dinților și interferența în cazul angrenajului armonic frontal cu element rigid. Articol, Sesiunea de comunicări științifice a Catedrei de Mecanică Tehnică și Mecanisme, SIMEC 2002, 29 martie 2002, ISBN 973-8165-20-2, pag. 23-26.

GEAR HOUSING MODAL BEHAVIOUR AND NOISE EMISSION

Ognjanović M.* and Čirić-Kostić S.**

Noise emission of gear drives is proportional to the value of disturbance power in gear teeth meshes, bearing contacts, etc., as well as to gear housing noise isolation ability and gear housing modal behaviour. A few specific approaches to this analysis are very briefly presented in this paper. Gear vibrations are treated like free restorable vibrations. These vibrations are restored when every tooth entering the mesh and comes into impact at this moment. A detailed experimental analysis and results modelling in this sense are worked out. A gear housing modal analysis by using FEM and modal testing with the aim to define mechanisms of certain modal vibration disturbing are carried out. Effects of gear housing modal behaviour are presented by definition of disturbance energy transmission through gear drive structure and through frequency spectrum range.

Key words: Gear, Vibration, Modal analysis

1. Introduction

Gear vibrations have been studied intensively for many years. They are mainly treated as forced damped vibrations caused by stiffness fluctuation of the gear teeth in mesh. Such an approach gives good results in the sub-critical and resonant mesh frequency range. In the super-critical frequency range, the vibration level slightly increases with the increase of the gear speed of rotation. Modern gear calculations [5] include these effects obtained by the experimental approach. A model which supports the measurement results in all three frequency ranges, sub-critical, resonant and

supercritical, is presented by [8]. The starting point of this paper is the assumption that the gear vibrations are free damped and the excitation is repeated by teeth impact at entering of each tooth into meshing (Fig.1). The process of teeth meshing is presented as a singular process and the gear vibration is presented as restorable free vibrations. The latest gear dynamic research in the calculation of models of forced gear vibration includes effects of bearings [7], effects of sliding friction and non-linearities [4], and gives more precise calculation models in the range of sub-critical and critical teeth mesh-frequency range.

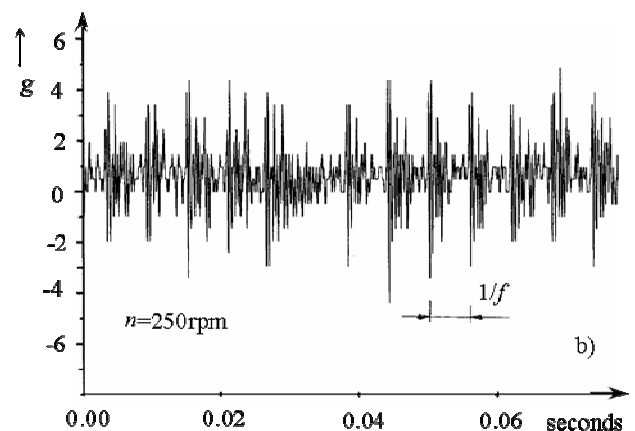
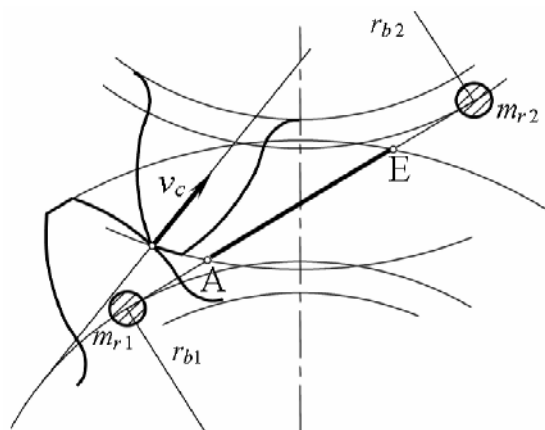


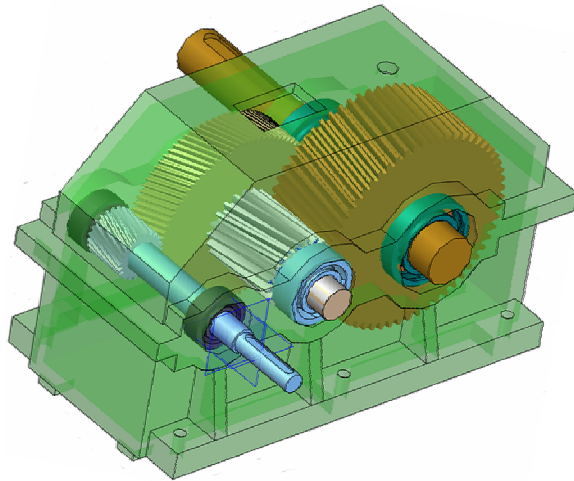
Figure 1: Restorable free vibration excited by gear teeth impact

* Prof. dr Milosav Ognjanovic, Faculty of Mechanical Engineering, University of Belgrade, ognjen@Eunet.yu mognjanovic@mas.bg.ac.yu

** MSc Snežana Čirić-Kostić, Faculty of Mechanical Engineering Kraljevo, University of Kragujevac, cirickostic.s@maskv.edu.yu

The disturbance energy caused by teeth impacts and by fluctuation of teeth deformations is the potential energy which is transmitted by elastic waves through the gear transmission structure. A part of this energy gets into gear drive surroundings in the form of acoustic wave energy. These waves are emitted by the gear housing walls. The acoustic emission caused by the gear drives is especially presented in articles [1] and [2]. The role of gear housing modal behaviour is extremely important. The modal analysis by using FEM method is presented in article [6]. The results shown give some of the necessary explanations which are presented in the following part of this chapter. Additional spreading of those results is worked out by using the experimental research presented in this paper.

Figure 2a presents the chosen example of the gear drive system (reducer) [6]. The massive housing is made of cast iron and designed with thick walls and ribs. By using FEM method, 88 modal shapes and natural frequencies in the frequency range to 3000 Hz are obtained. Further analysis is directed to mechanisms of certain modal shapes and natural frequency excitation.



Elastic deformation of the chosen modal shapes is simulated and analysed. Waves of elastic deformation spreading in the elastic structure of the gear housing are the main objective. Nodal areas of elastic deformations and standing waves (Fig. 2b) can be created by the disturbance energy carried into the elastic structure by disturbances in teeth meshes. The analysis includes the place and direction of the deformation which excites a certain modal shape, then excitation frequencies which can excite a certain modal shape, and the effect of internal damping in the housing walls. Complex distribution of elastic deformation and transfer of disturbance energy from one frequency to another make the modal exciting mechanism very difficult to understand. Besides this, internal damping of material has considerably different effects for different modal shapes. By direct integration, by using FEM method and disturbance by pulls force, it is not possible to disturb many of natural frequencies and modal shapes. In the continuation, with the support of modal testing, a modal excitation mechanism will be completed. Disturbance energy transmission through the elastic structure and the frequency spectrum will be analysed.

b)

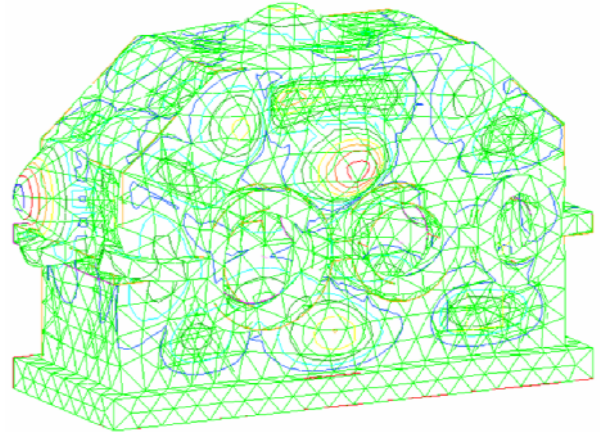


Figure 2: Restorable free vibration of the gear housing walls

1. Disturbance energy transmission in the machine system structure

The disturbance energy absorbed by gear teeth meshing is proportional to the teeth deformation amplitude x_{a0} and the teeth in mesh stiffness c_γ , i.e. $E_p = c_\gamma x_{a0}^2 / 2$. With the increase of the speed of rotation n , the teeth mesh frequency $f = nz/60$ increases together with the disturbance power in the gearbox $W_d = \sum_{i=1}^k E_{pi} f_i$,

where z corresponds to the gear teeth number, and k is the number of teeth meshes in the gearbox. If the gearbox sound power W_s is obtained by measurement, the disturbance power losses can be

determined in the form of the transmissibility factor $\zeta_T = W_s / W_d$. This ratio is, by the rule, very small. Many effects help to reduce the sound power [2], but the housing walls have a predominant role. The total sound power is $W_s = W_{s1} + W_{s2} + W_{s3}$. One part of the sound energy (W_{s1}) represents a part of the inside sound energy which comes through the walls. This energy transmission is realized by elastic waves through the wall thickness. The sound reduction is proportional to the sound frequency and the wall thickness. Another part of sound radiation, in the form of elastic waves, is transmitted from the gear contacts with the surfaces of the housing

walls end emitted into the surroundings (W_{s2}). The first two parts of the sound power create forced waves in the elastic structure of the walls which radiate sound into the surroundings. The third part of the sound power is a result of natural free vibrations, i.e. elastic waves of the housing walls (W_{s3}) (Fig.2b). By using the measured modal damping (Fig.3), the modal kinetic energy can be calculated by means of FEM method. In this case, the total kinetic energy is equal to the sum of the kinetic energy E_{kj} of all modal shapes for a certain disturbance. If this disturbance is caused by gear meshing, the power of modal vibration is

$$W_n = \sum_{j=1}^q W_{nj} = \sum_{j=1}^q E_{kj} f_{nj},$$

where q – the number of modal shapes and f_{nj} – the natural frequency. It is possible to divide the total power transmission factor into two parts:

$$\zeta_T = \frac{W_s}{W_d} = \frac{W_s}{W_d} \frac{W_v}{W_v} = \frac{W_v}{W_d} \frac{W_s}{W_v} = \zeta_{T1} \zeta_{T2}$$

where W_v is the total wall vibration power. The first

part of the transmission factor is proportional to the vibration power ratio $\zeta_{T1} = W_v/W_d$, and the second one ζ_{T2} is proportional to the sound radiation in comparison with the wall vibration. The transmission factor ζ_{T2} is smaller if the material density ρ_2 of the surroundings is smaller in comparison with the wall density. Housing walls are made of cast iron or from steel with high level of density ρ_1 and with high elastic wave speed c_{w1} . Acoustic space are presented with much more less density ρ_2 and wave speed c_{w2} for the air. The simplified formula of the power transmission from walls in surroundings (Fig. 3b) are

$$\zeta_{T2} = \frac{W_s}{W_v} = \frac{1}{1 + \frac{1}{4} \left(\frac{\rho_2 c_{w2}}{\rho_1 c_{w1}} + \frac{\rho_1 c_{w1}}{\rho_2 c_{w2}} \right)^2}$$

Using this formula and values of density and wave speed for the steel and for the air, obtains ratio between sound power and wall vibration power $\zeta_{T2} = 4 \cdot 10^{-10}$. This means that extremely small part of vibration energy transmits into sound energy i.e. sound power.

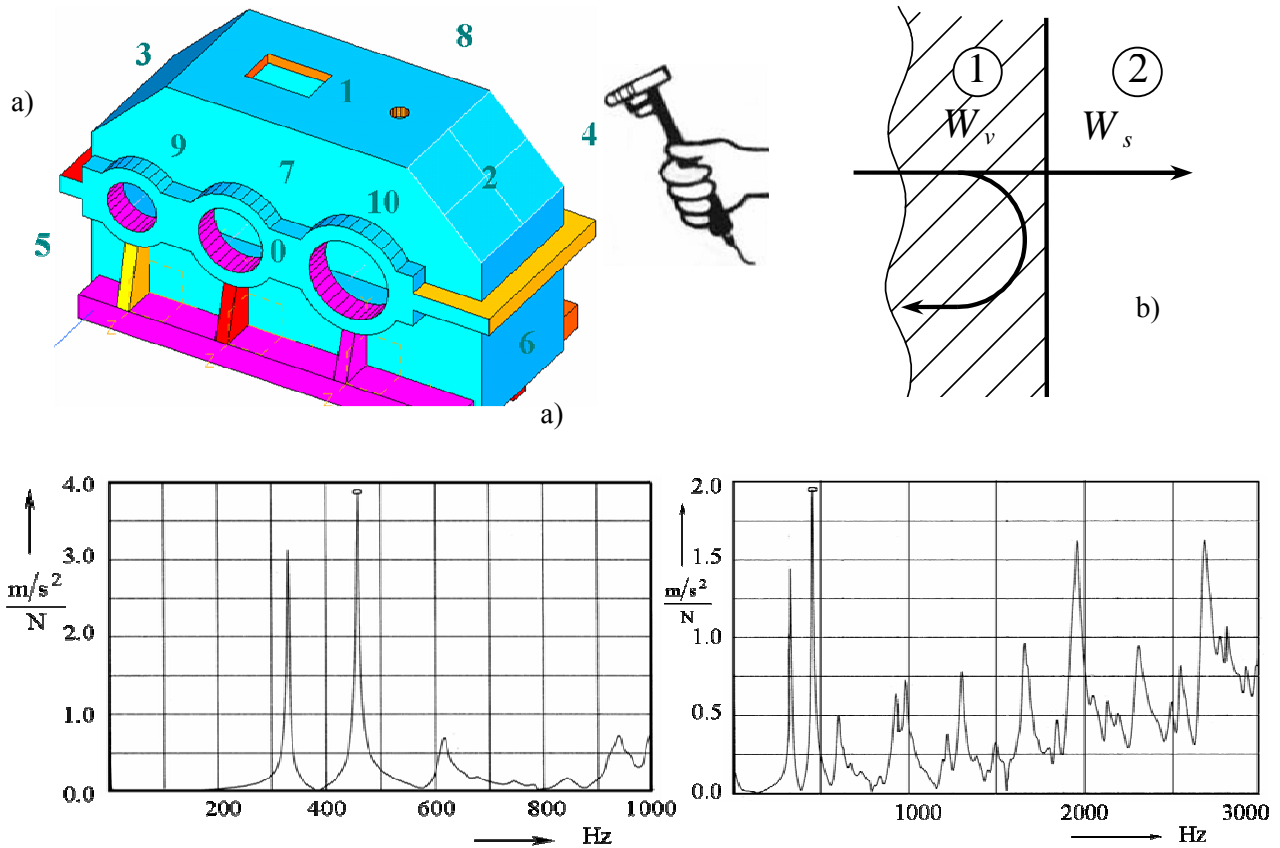


Figure 3. a) Modal testing of the gear housing and b) noise emission

3. Disturbance energy transmission in the frequency spectrum

Disturbance energy in the elastic structure of a gear drive, in the form of disturbance power W_d , is carried in the teeth gear meshing with the mesh frequency f . If this frequency is equal to some of the natural frequencies f_{nj} , the whole disturbance energy is spent to disturb that natural frequency. The result of this disturbance is the vibration power W_v , equal to the vibration power of this natural frequency W_{nj} . If there is no equality between the disturbance frequency f and any of the natural frequencies f_{nj} , the disturbance energy is spent to disturb a number of natural frequencies. If some of the natural frequencies are close to the frequency of disturbance repetition f , the disturbance effect is stronger for this frequency. In case of a great difference between the mesh frequency f and the naturals, the disturbance energy dissipates to natural vibrations in a very complex way which is very difficult to define.

In modal behaviour of mechanical structures exists one great problem more. The modal frequencies disturbs in the random way. Every modal impact (Fig.3a) disturbing some natural frequencies or response for some of them are different. Presented modal testing shows very interesting results in this view. By modal analysis using FEM method 88 modal frequencies in the range 0-3000 Hz is obtained. This is just possibilities, and by testing it is possible to obtain about 20 of them. Possibilities of modal excitation is presented in [6]. With modal testing repetition it is very difficult to obtain the same natural frequencies. Existing displacement of natural frequencies of a few Hz in the frequency spectrum. The next what it is possible to notice that some of frequencies disappear and some new arise. Some of response values fluctuates too. Response diagrams in Figure 3a is obtained for the same disturbance conditions. The first presents frequency range to 1kHz and second one to 3kHz. Response frequencies not exactly the same and response values for some frequencies not the same too. Response for the first two frequencies is about the two times is different.

Randomness in modal disturbance, randomness in modal response and randomness in disturbance energy transmission to the number of natural frequencies creates housing walls vibration random. This is stationary random vibration. Modal parameters (frequencies, responses and modal damping) are random values. For numerical calculation of the natural vibration or noise emission it is necessary to identify statistical parameters of modal parameters fluctuation.

4. Conclusions

Noise emission of gear drives is proportional to the disturbance power W_d generation, the housing noise isolation ability and especially to the housing modal behaviour. This behaviour defines a number of natural frequencies and possibilities to attenuate natural frequencies. The housing effect at the noise emission is defined by the disturbance energy transmissibility which consists of two parts: the disturbance energy transmission to housing walls vibrations and the transmission of vibration energy to sound energy. An additional analysis includes dissipation of disturbance energy to the housing walls natural vibration.

Disturbance process are random and parameters of natural vibrations are random too. Transmission process from disturbance in the gear meshes to the surrounding (the noise emission) is defined by transmission parameters.

5. References

- [1] Sabot J.: Integrated vibroacoustic approach to compute and reduce gear transmissions noise, - Proceeding of the International conference on Power transmission, Paris 1999, p.p. 2039-2050.
- [2] Ognjanovic M.: Propagation of disturbance energy and noise emission by gear transmission structures, - Proceedings of the International conference of Power transmission, Paris 1999, pp 1895-1908.
- [3] Huang K.J., Liu T.S.: Dynamic analysis of a spur gear by the dynamic stiffness method, - Journal of Sound and Vibration (2000) 234(2), 311-329.
- [4] Vaishya M., Singh R.: Sliding friction-induced non-linearity and parametric effects in gear dynamics, Journal of Sound and Vibration 248(4) (2001), pp 671-694.
- [5] Höhn B.R.: Modern gear calculation, - Proceeding of the International conference on gears, VDI-Brioche NR.1665, Munich 2002. Vol.1, pp. 23-43.
- [6] Ćirić-Kostić, S., Ognjanović, M.: Nature and mechanism of modal displacement excitation in gear housing walls, - Proceedings of the International conference "Power Transmissions '03", Varna-Bulgaria, 2003, pp 77-81.
- [7] Verdmar L., Andersson A.: A method to determine dynamic loads on spur gear teeth and on bearings, - Journal of Sound and Vibrat. 267 (2003) 1065-1084.
- [8] Agemi F., Ognjanovic M. : Gear Vibration in Supercritical Mesh-Frequency Range, - Journal FME-Transactions, Vol.32, No.2, (2004) pp 87-94.
- [9] G. Pavic, The role of damping on energy and power in vibrating systems, *Journal of Sound and Vibration* 281 (2005) 45-71.

OPTIMUM DESIGN OF MULTISPEED GEARBOXES AND MODELING OF TRANSMISSION COMPONENTS

Prof. dr Božidar Rosić, dr Aleksandar Marinkovic, mr Aleksandar Venc

Abstract: By applying the optimum design in the field of gear transmission design it is possible to define the optimal relations between the parameters of the complete gear transmission, and of each transmission stage separately. This paper presents a one criterion procedure for gear transmission optimization and multicriterion optimization procedure for each transmission stage. Second part of the paper is focused on modeling of cylindrical gears that are common used machine elements and main parts of gear transmissions. These models are made using part and assembly design module in CATIA V5R11 software. On the end of paper some applications of models in finite elements analysis and optimization are also described

Keywords: optimum design, multistage gearbox, computer added design, gears modeling, CATIA

1. Introduction

Concept from optimization and decision theory can play an important role in all stages the design process. The optimizing design theory applying and methodology will be illustrated on a multispeed gearbox example. Gearboxes present a very important group of machine members, which are utilized in a great number of engineering fields and which must satisfy very rigorous technical requirements regarding reliability, efficiency, precise manufacturing of gears, bearing, etc. In addition, the latest achievements in the fields of technology and testing of the preciseness of manufacturing gears, bearings, etc., have been applied to the manufacturing process.

The development of the computer technology, together with the corresponding computer programs (AutoCAD, Solid Works, CATIA, etc.), have very quickly found their place in the development of the expert system for gearbox design at a high technical level. Thus, it can freely be said nowadays that the gearbox design is no longer a "routine job", which in most cases based upon the designer's experience and knowledge.

This paper demonstrates the application of a nonlinear multicriteria optimization method, with the purpose to build such a powerful method as a module into the gearbox design expert system. The introduction of some criteria considering the desirable performances, combined with high quality gearbox component modeling represents a significant step towards the reality of a gear train model.

2. Gearbox decomposition

Gearboxes represent complex mechanical systems that can be decomposed into the corresponding number of gears with corresponding interaction. This means that the procedure for multistage gearbox

optimization can also be carried out through the corresponding number of stages. During the first optimization stage, characterized by comparatively small number variables, the distribution of transmission ratio per gearbox stages is defined from the conditions of the minimal volume of the gear sets. During the second stage, the multicriteria optimization problem is solved by introducing a greater number of criteria which represent the essential gearbox performances. Thereby, it is necessary to satisfy the restrictions from the following aspects: load distribution, stresses, kinematics and correct conjugate gear action.

The target function for multistage gearbox representing the volume of the gear sets can be written in the form the following relation [1]:

$$f(x) = 0.25\pi d_1^3 j_I ((1+u_I^2) + j_{II} d_3^2 / d_1^2 j_I (1+u_{II}^2) + \dots) \quad (1)$$

where:

u_I, u_{II} – the transmission ration for particular transmission stages of multistage gearbox;

d_1, d_3 – diameters of kinematics circles of the driver gears;

$j = b/d_1$ – ratio of width of the gear and diameter of the driver gear kinematics circle.

For the target function stated, it is also necessary to define the functional restrictions from the standpoint of the surface strength for the first stage of gearing, which can be written in the following form:

$$g'(x) = Z \cdot \frac{2 \cdot K \cdot T_1}{d_1^3} \cdot \frac{u_I + 1}{u_I} \leq \frac{[s_H]_I}{S_H} \quad (2)$$

and, from the standpoint of the volume strength:

$$g''(x) = K \cdot Y \cdot \frac{2 \cdot T_1}{\varphi_1 \cdot d_1^2 \cdot m_I} \leq \frac{[\sigma_F]_I}{S_F} \quad (3)$$

In the exactly analogous way, the functional restrictions from the standpoint of the surface and volume strength for other transmission stages of gearboxes are determined.

Commencing from the technical requirement concerning the transmission ratio of a gearbox, it is also necessary to determine the functional restriction in the form of the equation [2]:

$$h_I(x) = u - u_I \cdot u_{II} \cdot \dots \cdot u_N = 0 \quad (4)$$

Basing upon the determined target function and the restrictions, it can be noticed that this problem belongs to the field of nonlinear optimization with the restrictions in the form of inequalities. For the solution of this problem, the computer program SUMT, based on the mixed penalty functions, has been applied. Fig. 1 shows a graphic representation of the results of the computer program SUMT. Basing upon the section of the corresponding functions, the domains of the optimum transmission ratios for the multistage gearboxes are defined in the following way:

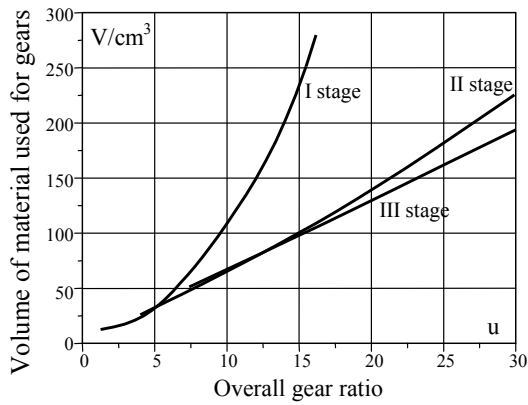


Figure.1: The relation between the volume of gear train and overall gear ratio.

To complete this analysis of decomposed gearbox, here are added a pair of restrictions in the form of inequalities, based on stress restrictions [3]:

- tooth gear stress for I stage gear

$$g_3(\bar{x}) = \sigma_{F1} = K \cdot Y \frac{2 \cdot T_1}{\varphi_I \cdot d_1^2 \cdot m_I} \leq \frac{[\sigma_F]_I}{S_F} \quad (5)$$

- tooth-root gear stress for II stage gear

$$g_4(\bar{x}) = \sigma_{F3} = K \cdot Y \frac{2 \cdot T_1 \cdot u_I}{\varphi_{II} \cdot d_3^2 \cdot m_{II}} \leq \frac{[\sigma_F]_{II}}{S_F} \quad (6)$$

Based on gear stress relations the value of gear module is determined:

- for contact stress

$$m \geq \left(\frac{2 \cdot K \cdot T_1 \cdot (u_I + 1) \cdot Z^2 \cdot S_H^2}{\varphi_I \cdot [\sigma_H]_I^2 \cdot u_I \cdot z_1^3} \right)^{\frac{1}{3}} \quad (7)$$

- for tooth-root stress

$$m \geq \left(\frac{2 \cdot K \cdot T_1 \cdot Y \cdot S_F}{\varphi_I \cdot z_1^2 \cdot [\sigma_F]_I} \right)^{\frac{1}{3}} \quad (8)$$

Fig. 2 shows graphical interpretation of relations (7) and (8) in function of tooth number Z_1 . Upper of two lines on the Fig. 2 presents values of gear module determined on contact stress and lower one for values determined on tooth-root stress. The lines and admissible space on Fig. 2. indicate that contact stress relation for gear module (7) is prior and is to be used for gear dimensions dermination.

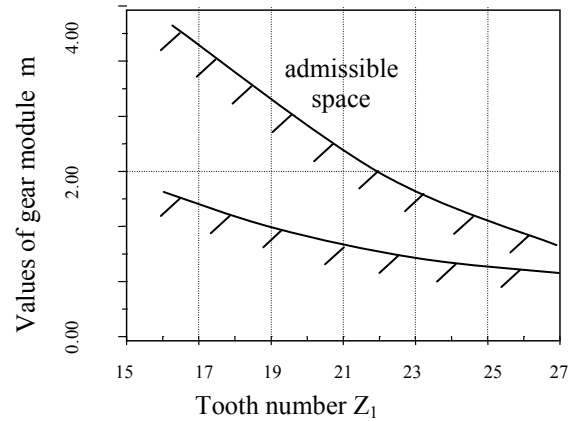


Figure. 2: Diagram of module values up to tooth number

3. Gears modeling

Gears are very important machine elements today and they are common used in different kinds of gearboxes and transmissions. Especially cylindrical gears are most applicable because of their very high efficiency and not complicated production. Modeling of cylindrical gears is very important process in machine design, as for making real model of gearbox, such for gear and transmission structure analysis and optimization. Last years this process can be done very fast and qualitative using new software tools such as **CATIA**. This software is very complex, but some main modules like **Part design** and **Assembly design** are in use for cylindrical gear modeling. The main problem in any gears modeling is to define a real gear tooth and after that to import it into gear body making. Cylindrical gears modeling consists of several phases, depends from gear body and kind of its production:

- The first phase of gear modeling is definition and making real involute gear teeth profile.
- The second phase, in case of cutting or pressed gear body, is to use Part design CATIA module to make gear body.
- The third phase, only in case of welding way made gear body, is to use Assembly design module to connect all its parts.

All this phases consists of several operations and it will be described separately in followed chapters.

Every chapter gives principal facts of general modeling, some special operations with advantages of using CATIA software in gears modeling and examples of different cylindrical gears that are modeled.

In analysis of internal and external gear profiles there are four different lines in one pitch, which defines complete profile of gear. So there are the involute profile arc, profile foot circle arc, addendum circle arc and trochoid arc as a connection [4]. In analytic-kinematics way for profile definition is to define a lot of restrictions and constrains for setting parameter equations each of this profile arcs and angles. After some matrix transformations matrix parameter equation for contact line of engaged gear tooth profiles can be determined. Based on this analytic-kinematics model computer program is developed to define points of gear profiles [5].

Gears modelling is very useful and important, as to make real gear transmission simulation, so for lot of other analysis. Different software tools are in use today for machine design and machine elements modelling, as ACAD, Mechanical Desktop, Pro Engineer and last years Solid Works, CATIA etc. But it can be seen that gear modelling (especially internal gears) with real profiles is more complicated compared with modelling of all other machine elements. Here will be presented the possibilities of cylindrical gears modelling using CATIA V5R11 software. Depends of production way and form of gear body it is possible to use **Part design** module or **Assembly design** module of CATIA software.

For designing simplest cylindrical gear (flat) first step is to define correct sketch, where involute profile tooth coordinates (from first phase) should be imported. After that designer can apply Sketch based features (Create pad), to get cuted gear model as is shown at Fig. 3.

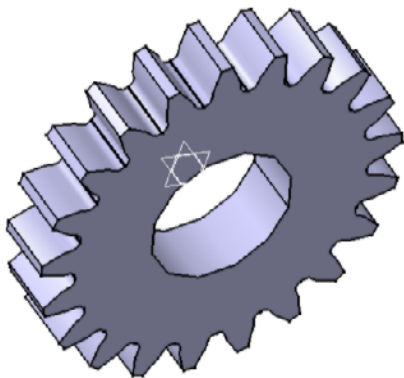


Figure 3: Simplest model of cylindrical gear

One step forward is designing a press made gear body, that could be modeled by rotating sketch made figure, or like simulation of production process. On Fig. 4 it is given a gear model made also by using sketch and few Sketch-Based, Dress-Up and Transformation Features. Presented gears are common in use and they have an external involute profile. But in some cases, like planetary gear train designing [6], it is necessary to make a model of internal profiled gear. For this purpose designer has to calculate a new table with involute profile coordinates, by using external gear as a tool for making internal profile.

After that properly sketch and other features as for other cylindrical gears modelling has to be used.

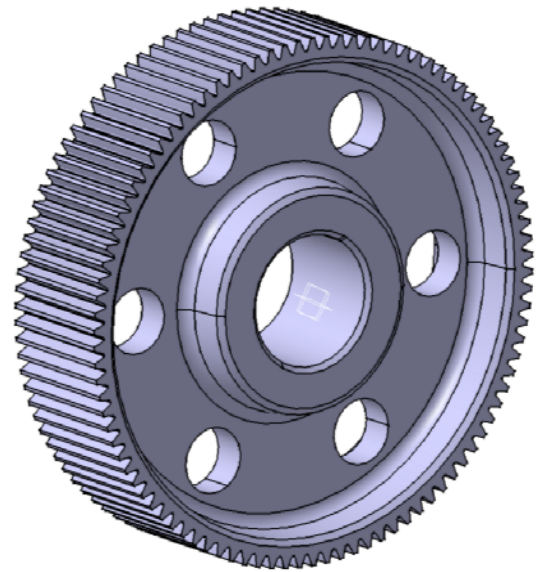


Figure 4: Press made model of cylindrical gear

Assembly design is another module in CATIA which is in use in aim to complete all parts and standard elements that are already modelled in Part or Shape design modules. Besides that it is possible to insert new bodies in existing assembly and also to do Boolean Operations between bodies if it is necessary. These Boolean operations between bodies are Assemble Bodies, Intersect Bodies, Add Bodies, Remove Bodies, Trim Bodies, Remove Lumps, etc.

The best sample of using Assembly design is cylindrical gear made by welding number of separated elements [7]. It means that this type of gear consists of many elements that are modelled in Part design. The main part is outer plate with involute profiles that are welded with central cylinder with two circle plates and six stiffeners at both sides (Fig. 5).

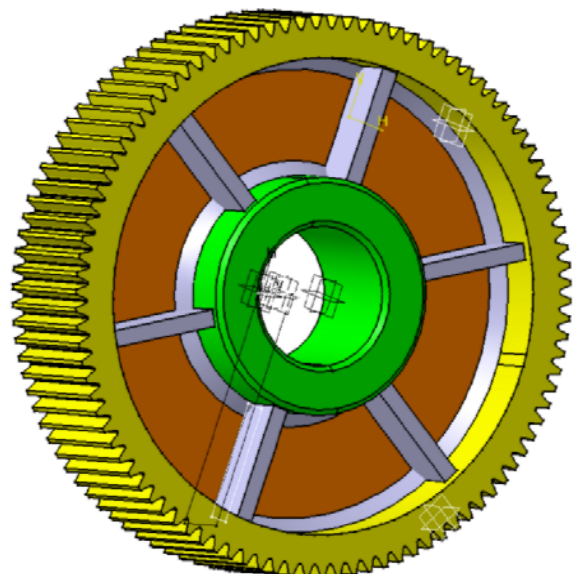


Figure 5: Cylindrical gear made by welding

A gear modeling is very significant because of many applications that could be done:

- After completing assembly it is possible to do kinematics simulations, using another CATIA module DMU.
- Internal and external gears models can be used for solving a lot of problems in mechanical engineering, such as **structural analysis**, contact pressure between corresponding gears and also thermal and many other analyses [8]. A typical example for this could be following structural analysis made using finite element method, where Fig. 6 shows gear model made of 77633 tetrahedrons which makes 18965 nodes.

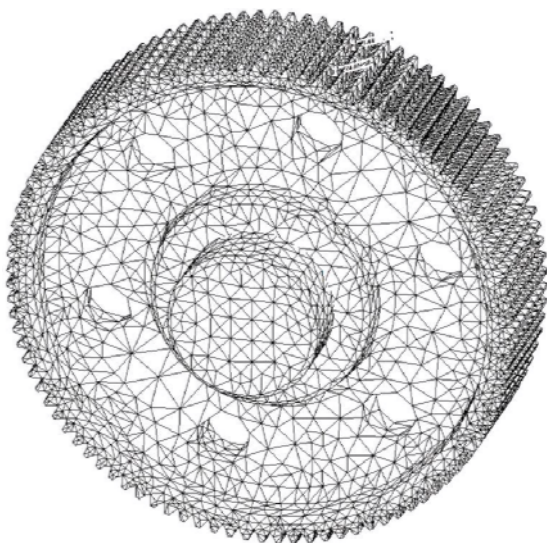


Figure 7: Gear model in form of finite element net

Stress values (Fig. 7) represent critical constructive points where gear is high loaded which could be also very useful in design and optimization process and procedure.

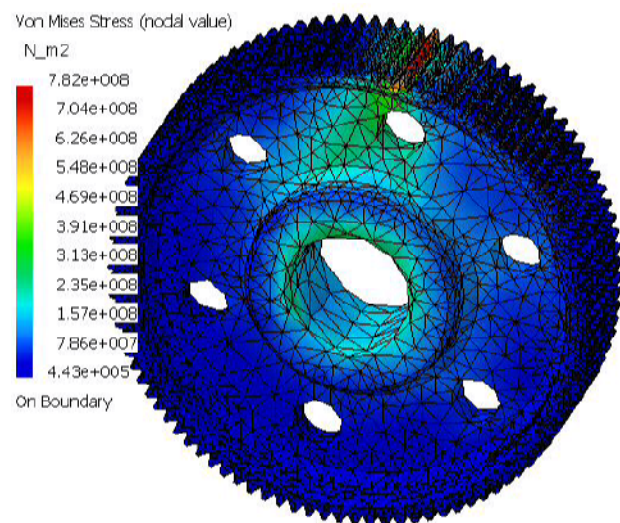


Figure 7: Stress values of loaded gear model calculated in structural analysis

4. Conclusion

The paper represents a brief illustration of a wider study undertaken with the aim of building the powerful multicriteria optimization methods into the expert system for gearbox design. It points out the necessity of decomposition multistage gearboxes as complex mechanical systems. In the way, the gearboxes optimization procedure is also carried out through the corresponding number of stages. In this first optimization stage, the domains of the practical application of gearboxes are defined, whereas, during the second stage, the multicriteria optimization problem is solved.

To resume the point of this modeling part of paper, here could be said that it presents only a brief of cylindrical gears modeling possibilities in CATIA software. Besides presentation of modeling in Part and Assembly design modules, at the end of this paper it is to add that CATIA is powerful and today may be the completest design software in engineering with wide range of applications.

References

- [1] Rosić B., 1993.: *Parameter Investigation and Optimization of Planetary Gear Train Transmission*, Ph.D Thesis, Mechanical Engineering Faculty, University of Belgrade
- [2] Arora J.S., 1989.: *Introduction to optimum design*, McGraw-Hill Book Company, New York
- [3] Rosić B., Marinković A.: *Planetary gear transmission as a tribosystem: Efficiency calculation and simulation*, ÖTG Jahres Symposium, Wien, November 2003.
- [4] Colbourne, J. R., 1987: *The geometry of Involute gears*, Springer-Verlag, New York
- [5] Rosić B., Rinkovec B., Marinković A., Pavlović N.: *The analytical-kinematics method for definition of internal cylindric gears*, Yugoslav Conference "IRMES 2002", Faculty of Mechanical Engineering Srpsko Sarajevo, Jahorina – BIH, September 2002, Proceedings, pp. 625-630.
- [6] Rosić B.: *Planetary gear trains*, Monography, Faculty of Mechanical Engineering, University of Belgrade, edited in year 2003.
- [7] Rosić B., Marinković A., Vencl A., 2004.: *Cylindrical Gears modeling using CATIA software*, 4th International Conference "RADMI 04", Zlatibor, Serbia and Montenegro, August-September 2004., Proceedings on CD, pp. 73-77.
- [8] Rosić B., Marinković A., Vencl A., 2004.: *Modeling and Structural Optimization of Cylindrical Gears construction profiles*, Yugoslav Conference "IRMES 04", Faculty of Mechanical Engineering Kragujevac, Kragujevac, September 2004, Proceedings, pp. 173-178.

ANALYSIS OF THE INDUCED STRESS AND STRAIN OF TEETH FLANKS OF FRONTAL HARMONIC GEARINGS WITH RIGID ELEMENT

Prof. Dr. Adrian BRUJA
Marian DIMA
Catalin FRANCU

Abstract: This paper presents the way of determining of induced stress and strain (deformations) of toothings of frontal harmonic gearings with rigid element. Chosen analysis methods are analytical and FEA. Studied Wheel is the fixed central wheel of a frontal harmonical reducer with double satellite. Induced stress and strain of this wheel were also studied experimentally.

Keywords: Stress, Strain,

1. Introduction

Frontal harmonical transmissions with rigid elements have bevel planetary gearing that have the shape of conical rolls, (1), figure 1, and central wheel's external toothings mating profile (2), with the satellite's rolls motion on the sphere.

While working, the main loads to which are subjected central wheel's teeth, is stress contact.

The induced stress and strain of the studied gearing was analysed by three ways: analytical – using equations in elastic theory, Finite Element Analysis method and experimental method – in figure 2 is presents where was placed the bonded strain gauge.

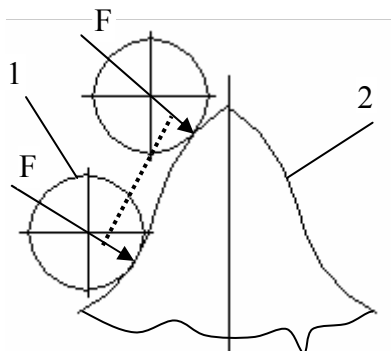


Fig. 1

2. Analytical analysis of induced stress and strain

2.1. Stress and strain on contact surface

Analysis of the stress starts with choosing a reference system oriented with the x axis through the length of contact surface, on its middle line, y axis is perpendicular on the middle line contained in the plane of surface contact and the z axis is perpendicular on the contact surface plane and directed to the inside of the equivalent cylinder of the cone. Because of the fact

that the length of cylinders in contact, are supposed to be infinite, then the origin of the coordinates can be any point on the middle line of the contact surface. In other words, the induced stress of the bodies in case of linear contact doesn't depend of the x coordinate.



Figure 2

For steel bodies ($\mu_1 = \mu_2 = 0,3$) we can evaluate:

a) half-width of the contact surface

$$b = 1,522 \sqrt{\frac{q}{E} \cdot \frac{R_2 R_1}{R_2 + R_1}}, \quad (1)$$

b) maximum contact pressure

$$p_0 = 0,4180 \sqrt{qE \cdot \frac{R_2 + R_1}{R_2 R_1}}, \quad (2)$$

c) proximity of the bodies

$$\delta = 0,579 \frac{q}{E} \left(\ln \frac{4R_1 R_2}{b^2} + 0,814 \right). \quad (3)$$

where:

q – compression load on length unit;

E - length strain magnitude;

R_1, R_2 - radius of curvature.

2.2. Stress within the bodies in contact

The induced stress of any point inside a body

is:

$$\begin{aligned}\sigma_x &= -p_0 \cdot 2\mu \frac{z}{b} \left[\sqrt{\frac{b^2 + \lambda}{\lambda}} - 1 \right] \\ \sigma_y &= -p_0 \frac{z}{b} \left[\sqrt{\frac{b^2 + \lambda}{\lambda}} \left(2 - \frac{b^2 z^2}{\lambda^2 + b^2 z^2} \right) - 2 \right] \\ \sigma_z &= -p_0 \frac{b z^3}{\lambda^2 + b^2 z^2} \sqrt{\frac{b^2 + \lambda}{\lambda}} \\ \tau_{yz} &= \tau_{zy} = -p_0 \frac{b y z^2}{\lambda^2 + b^2 z^2} \sqrt{\frac{\lambda}{b^2 + \lambda}} \\ \tau_{xy} &= \tau_{yx} = 0 \quad \tau_{zx} = \tau_{xz} = 0.\end{aligned}\quad (4)$$

Parameter λ (eq. 4) is the highest root of the following equation (5) :

$$\frac{y^2}{b^2 + \lambda^2} + \frac{z^2}{\lambda} = 1. \quad (5)$$

Using the equations (1)..(5) were evaluated induced stress and strain, where was placed the bonded strain gauge on the central wheel, for different positions of the force throughout the length of the profile's tooth starting from the bottom of the tooth. Results are shown in table 1. Measurement units for induced stress are [N/mm²], values for strain are multiplied by 10⁻⁶ for linear deformations and multiplied by 10⁻⁵ for angle of shearing deformations.

3. Analysis by FEA

3.1 Creation of 3D model of central wheel

To create the 3D model of the central wheel we've started from parametrical equations of the central wheel's profile evaluated in grid coordinates [1]. Using Turbo Pascal programming language we've calculated the coordinates of the points from the central wheel's profile. The obtained results were written in a data file as real-valued number list.

The profile of the central wheel was sketched in MDT6 using an AutoLISP subroutine that reads the data file. AutoLISP subroutine follows:

```
(defun tprofil29 ()
  (setq fis (open "c:\supr29.dat" "r"))
  (command "spline")
  (setq i 1)
  (while (< i 361)
    (setq lin (read-line fis))
    (setq x (atof (substr lin 1 10)))
    (setq y (atof (substr lin 11 10)))
    (setq z (atof (substr lin 21 10)))
  )
  (command (list x y z))
  (setq i (1+ i))
)
```

Table1

Force pos	F[N]	R[mm]	σ_u	σ_v	σ_w	τ_{uv}	τ_{vw}	τ_{wu}	ϵ_u	ϵ_v	ϵ_w	γ_{uv}	γ_{vw}	γ_{wu}
1	157.4 2	8.12 (-)	- 0.393	- 1.824	- 1.824	0	- 1.824	0	3.339	- 5.517	- 5.517	0	- 2.258	0
2	265.2 5	11.02 (-)	- 0.516	- 3.259	- 3.259	0	- 3.259	0	6.853	- 10.12	- 10.12	0	- 4.034	0
3	319.1 9	13.98 (-)	- 0.535	- 3.811	- 3.811	0	- 3.811	0	8.341	- 11.94	- 11.94	0	- 4.718	0
4	344.6 6	17.70 (-)	0.517	3.887	3.887	0	3.887	0	- 8.644	12.22	12.22	0	4.812	0
5	355.6 1	26.25 (-)	0.488	3.839	3.839	0	3.839	0	- 8.643	12.1	12.1	0	4.752	0
6	358.0 7	27.00 (+)	0.456	3.379	3.379	0	3.379	0	- 7.483	10.61	10.61	0	4.184	0
7	354.3 6	15.20 (+)	0.424	2.948	2.948	0	2.948	0	- 6.402	9.219	9.219	0	3.649	0
8	344.9 8	13.70 (+)	0.393	2.896	2.896	0	2.896	0	- 6.401	9.09	9.09	0	3.585	0
9	329.2 5	1.70 (+)	0.361	2.031	2.031	0	2.031	0	- 4.084	6.254	6.254	0	2.515	0

Wheel's geometry was defined using 3D modelling commands in MDT6.

3.2 Model pre-processing

The model of the wheel defined previously was loaded with meshing forces, forces that were calculated using equations presented in [1]. This forces are distributed on the line of elastic contact between the flanks of meshing teeth. It was also considered that the wheel is fixed on a circular surface. Results are presented in figure 3.

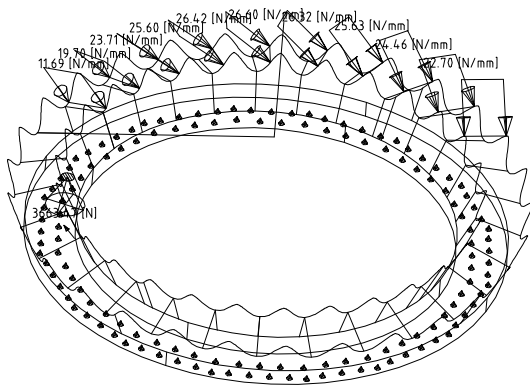


Figure 3

Central wheel's model was digitised using tetrahedron elements. The obtained digitisation is presented in figure 4.

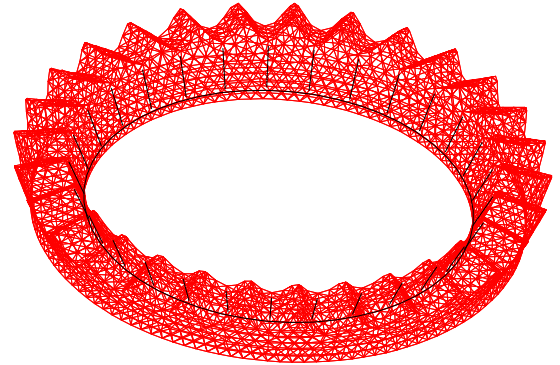


Figure 4

3.3 Model post-processing

After processing results in figure 5 are presented displacements, and in figure 6 the induced stress (Von Mises), figure 6; both presented in colour codes.

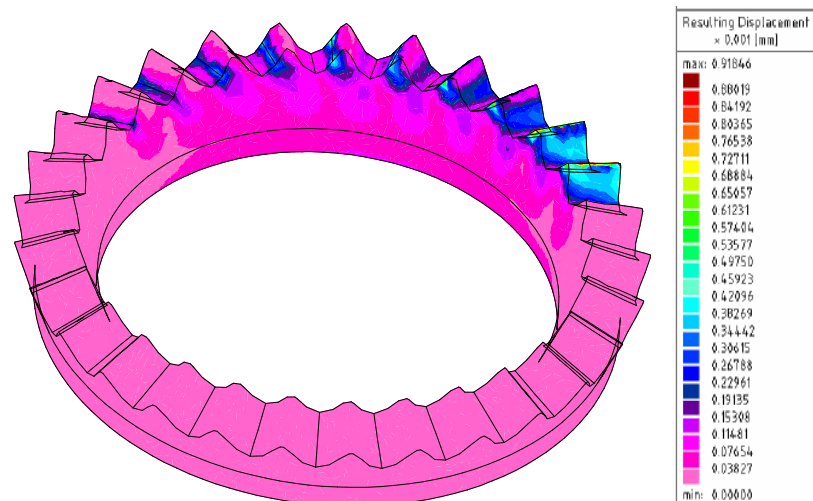


Figure 5

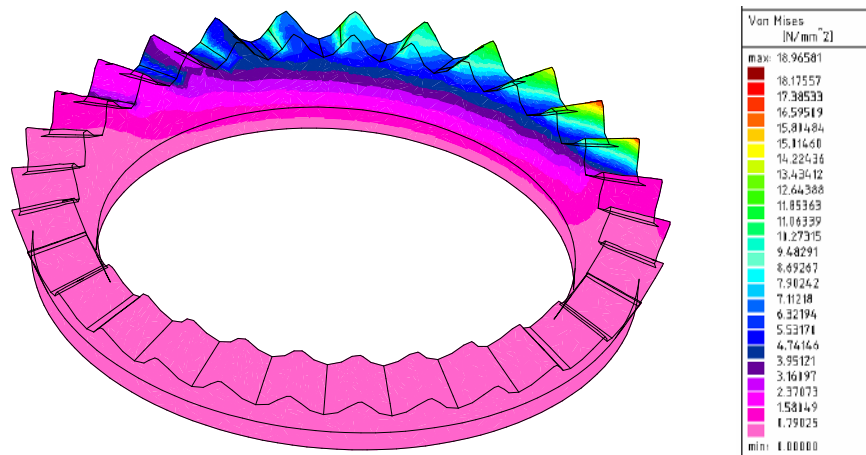


Figure 6

Maximum obtained numerical values are: 19 N/mm² for equivalent stress and 1 μm linear displacement. These values are close to the ones obtained experimentally and aren't dangerous to the central wheel's teeth.

References

- [1] Bruja Adrian, Dima Marian – La détermination de la ligne d'action pour l'engrenage avec mouvement de précession. Articol, Analele Universității "Dunărea de Jos", Fascicola XIV, pag. 17-20, Galați, 1999, ISSN 1224-5615.
- [2] Bruja Adrian, Dima Marian – L'influence des paramètres de la transmission par mouvement de précession sur le profil des dents de la roue centrale. Articol, Analele Universității "Dunărea de Jos", Fascicola XIV, pag. 17-20, Galați, 1999, ISSN 1224-5615.
- [3] Marian Dima, Adrian Bruja - Studiul stărilor de tensiuni și deformații prin metoda elementului finit la roțile dințate ale angrenajului armonic frontal cu elemente rigide Articol, Sesiunea de comunicări științifice a Catedrei de Mecanică Tehnică și Mecanisme, SIMEC 2004, 26 martie 2004, ISBN 973-8165-92-X, pag. 82-85.

CRITICAL TRANSVERSE PRESSURE OF A COMPOSITE PLATE WITH MID-LAYER MADE OF LONGITUDINAL STRIPS

Dr Milorad Milovančević⁽¹⁾, Dr Milan Dedić⁽²⁾

Summary

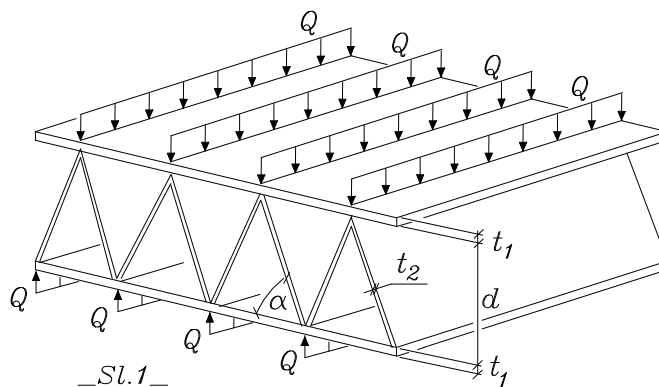
This paper analyzes the calculation of critical value of transverse pressure applied to a composite plate. The plate is made of two outer layers of thin plates and a mid-layer made of longitudinal strips connected in triangles. The analysis may be applied to both isotropic or orthotropic material, and different layers can have different mechanical properties. The loss of stability considered is caused by local buckling of the longitudinal strips in their cross-section plane. The calculation of the critical buckling load is done analytically. Deformations are in elastic domain. The loss of stability is studied for the cases with free and restricted deformations of the outer layers.

Key words: *Buckling of plates, Composite plates, Cellular plates*

1. Introduction

Let us consider composite three layered plate of the type shown in Fig.1. The mid-layer is made of longitudinal strips connected in triangles. This type of plates may have significant strength to weight ratio, particularly good bending stiffness in longitudinal direction. An interest for this type of plates has been increasing recent decades with need for ever lighter structural elements. However, calculation of their capacity to carry

with open cross-section, and in $/4/$ in case of close-walled element. Referring to the structure in Fig.1, we shall assume in this paper that: a) thicknesses of all elements are small compared to d , so that deformations are linear elastic, b) outer plates have the same thickness t_1 and all mid-layer strips thickness t_2 b) all joints are rigid, c) geometric quantities and load are constant throughout the plate d) all triangles formed by strips are alike, and one deformation pattern in the course of



transverse compressive load must take into account the possibility of failure due to local buckling.

Buckling and bending of plates has been discussed in a vast number of references. We shall mention here only $/1/$, $/2/$ in which buckling of plates and bars and its interaction with other resisting structural elements is described. This aspect of structural behavior was analyzed in $/3/$ in case of thin-walled structural element

buckling extends through all the cross-section plane. Furthermore, we shall assume that material is isotropic, although the analysis that follows may easily be extended to orthotropic material with one principal material axis in longitudinal direction.

Under these assumptions we may take that all elements in buckled state undergo cylindrical bending in cross-section plane (front plane, Fig.1), and that we can

⁽¹⁾ Milorad Milovančević, Associated Professor, Faculty of Mechanical Engineering, University of Belgrade, Serbia and Montenegro, E-mail: mmilovancevic@mas.bg.ac.yu

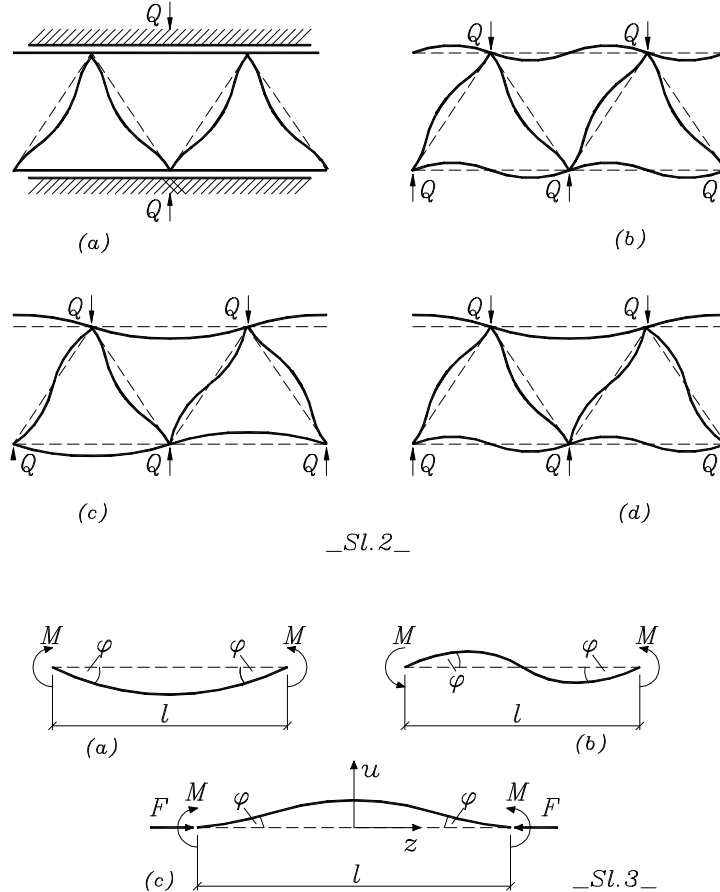
⁽²⁾ Milan Dedić, Associated Professor, Faculty of Mechanical Engineering in Kraljevo, University of Kragujevac, Serbia and Montenegro, E-mail: dedic.m@maskv.edu.yu

take for the plate bending stiffness per unit length $D = Et_i^3/12(1-\nu_i^2)$, Ref./1/, where t_i denotes thickness and ν_i Poisson's ratio of i -th element. If compressed transversely by rigid bodies, Fig.2a, outer plates will be prevented to bend, and strips will buckle cylindrically as rods clamped on both ends, at the maximum value of buckling force. More interesting cases are those when load inducing elements, not shown in Fig.1 and 2, do not

It has been shown in paper /3/ that end slopes and moments of a cylindrically bent plate in symmetric and antisymmetric mode, Fig.3a,b are related respectively:

$$\varphi = \frac{Ml}{2D} \quad \varphi = \frac{Ml}{6D} \quad (1), (2)$$

Cylindrical buckling of a strip compressed by force F (per unit length of loaded edge) implies that normal



—Sl. 2—

—Sl. 3—

prevent bending of outer plates, allowing strips to buckle at significantly lower values of load force Q , Fig.2b,c,d. These cases occur when Q is uniform along joint lines as in Fig.1. As always when multiple buckling modes are possible, all modes must be analyzed in order to find the one with the lowest value of critical force.

2. The first mode of buckling

Let us first consider mode in Fig.2b. Several adjacent strips of in-layer and outer plates are shown apart in Fig.4. Observing only moments and rotations in the central joint we may say that strips (2) and (3) buckle elastically resisted by strips (1) and (4). It is important to notice that elastic lines of all the strips are symmetrical, and we assume that this deformation pattern repeats in all triangles to the left and right.

displacement is function only of coordinate z in cross-section plane, i.e. $u = u(z)$. Consequently, buckling equation in that particular case can be obtained from the general (two-dimensional) equation by dropping the members with derivatives of u in direction of axis normal to the cross-section plane. That way we come to:

$$u(z)^{IV} + k^2 u(z)'' = 0, \quad \text{with } k^2 = F/D \quad (3)$$

It's general solution has the form:

$$u(z) = C_1 \cos kz + C_2 \sin kz + C_3 z + C_4 \quad (4)$$

Boundary conditions $u(-l/2) = 0$, $u(+l/2) = 0$, and $M(-l/2) = M(+l/2)$ eliminate three unknown integral constants, and we come to:

$$u(z) = [\cos kz - \cos kl/2] C_1 \quad (5)$$

So, the moment and slope at the left end, $z = -l/2$, are:

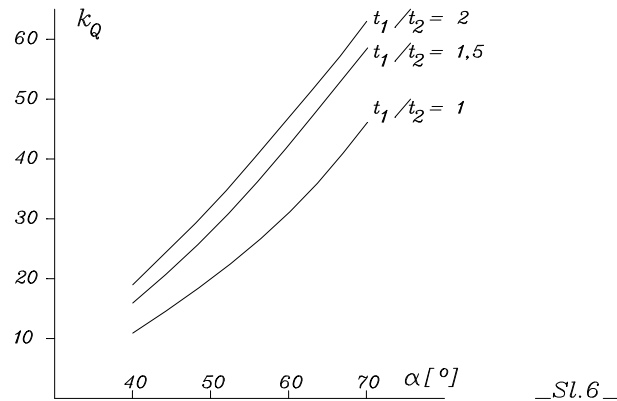
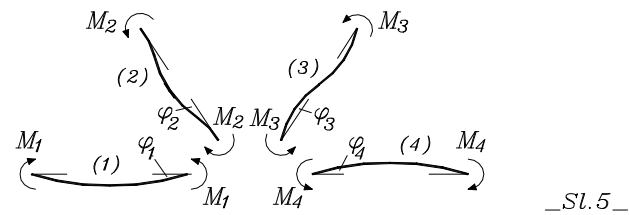
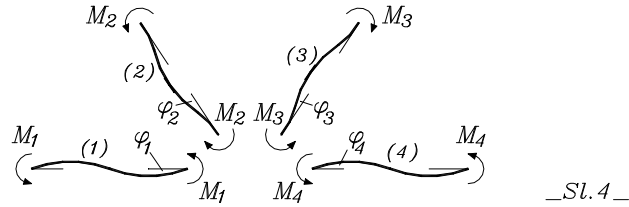
$$M = -Du''(z) = -D k^2 \cos \frac{kl}{2} C_1 \quad (6)$$

$$\varphi = u'(z) = k \sin \frac{kl}{2} C_1 \quad (7)$$

With the above relations let us now observe the joint in

$$\frac{6D_1}{l_1} \varphi_1 - \left[-k_2^2 D_2 \cos \frac{k_2 l_2}{2} \right] C_1 = 0 \quad (11)$$

Relations (10) and (11) make system of two homogeneous equations in two unknowns φ_1 and C_1 . It can have *nontrivial* solution only if its determinant Δ equals



which strips (1) to (4) meet, Fig.4. They are drawn in deformed state, and separately to indicate end moments and angles. Regular pattern of deformation, spreading all along the cross-section to the left and right in Fig.5, implies: $M_3 = M_2$, $M_4 = M_1$ as well as $\varphi_3 = \varphi_2$, $\varphi_4 = \varphi_1$, so that compatibility and equilibrium conditions will read:

$$\varphi_1 = \varphi_2 \quad (8)$$

$$M_1 - M_2 = 0 \quad (9)$$

Changing M_1 from (1) and φ_2 and M_2 from (6) and (7) into (8) and (9) we obtain:

$$\varphi_1 - \left[k_2 \sin \frac{k_2 l_2}{2} \right] C_1 = 0 \quad (10)$$

zero:

$$\Delta = \begin{vmatrix} 1 & -k_2 \sin \frac{k_2 l_2}{2} \\ \frac{6D_1}{l_1} & -k_2^2 D_2 \cos \frac{k_2 l_2}{2} \end{vmatrix} = 0 \quad (12)$$

After some calculations that can be put in the form:

$$\Delta = (k_2 l_2) \cos \frac{k_2 l_2}{2} + 6 \frac{l_2}{l_1} \frac{D_1}{D_2} \sin \frac{k_2 l_2}{2} = 0 \quad (13)$$

We see that Δ is an equation in k_2 as the only unknown. Its smallest positive non-zero solution k_2 gives, via (3), the critical force at which strip (2) buckles: $F_{cr2} = k_2^2 D_2$. Finally, from force equilibrium condition of vertical forces in joint $\sum Y_i = 0$ we have the load force:

$$Q_{cr} = \frac{F_{cr2}}{2 \sin \alpha} \quad (14)$$

and the problem is solved. Additionally, one must always check if these results lay within the elastic domain of deformations. Numerical results for non-dimensional load:

$$k_Q = \frac{Q_{cr}}{2 (k_2 l_2)^2 \sin^3 \alpha (B_2 / d^2)} \quad (15)$$

versus angle α and $t_1 / t_2 = 1, 1.5$ and 2 , which corresponds to $D_1 / D_2 = 1, 3.38$ and 8 respectively, and for $E_1 = E_2$, are given in Fig.6. More detailed insight indicates that for $t_1 / t_2 \geq 2$, F_{cr2} is close to the value of the strip clamped on both ends!

3. The second and third mode

The mode in Fig.2.c, shown with strips apart in Fig.5, occurs when strip (2) buckles elastically resisted by strip (1) in symmetric bending, Fig.3a., and strip (3) in anti-symmetric bending, Fig.3b. Assuming that $M_4 = M_1$ and $\varphi_4 = \varphi_1$ (due to repeating pattern of deformation along the whole cross-section) compatibility and equilibrium conditions would read:

$$\varphi_1 = \varphi_2 \quad (16)$$

$$\varphi_1 = \varphi_3 \quad (17)$$

$$2M_1 - M_2 + M_3 = 0 \quad (18)$$

Using relations (1), (2), (6) and (7), and repeating the same procedure as above, we come to the system of three homogeneous equations in three unknowns φ_1 and C_1 and φ_3 . Numerical calculations show that this case give five to seven percent higher F_{cr2} than previous case for $t_1 / t_2 = 1$, and approximately equal values for t_1 / t_2 tending to 2.

Finally we can analyze the mode in Fig.2d. To shorten the argument we shall say here only that all the

strips undergo unsymmetrical buckling or bending. Compatibility and equilibrium conditions must be written for three joints. There will be seven conditions with seven unknown deformation. Again we get critical force higher than in the first mode.

4. Conclusion

Numerical results indicate that the first mode of freely deformed structure gives the lowest values of critical load for outer plates and inner strips of approximately equal sizes. One explanation can be found by comparing the ratio of number of the resisting strips N_r to the number of buckled strips N_b . Observing Fig.2b,c,d we find out that for the cases one to three ratios N_r / N_b are respectively 1/1, 3/1 and 3/1. Thus, the first case is obviously the least stiffened, and it therefore gives the lowest buckling force. The fact that for $t_1 / t_2 \geq 2$ inner strips tend to buckle as being clamped on both ends, at the highest value of F_{cr2} , indicates to optimum thickness ratio t_1 / t_2 for this type of structure.

5. References

1. Timoshenko S., Woinowski-Krieger S., "Theory of Plates and Shells", McGraw-Hill Book Company Inc., 1959.
2. Brush D. O., Almroth B. O., "Buckling of Bars, Plates, and Shells", McGraw-Hill Book Company Inc., 1975.
3. Dedic M., "The Optimum Shape of Open Thin-Walled Beam in Local Buckling due to Compression", Proceedings of Third International Conference Heavy Machinery – HM '99, Kraljevo, 1999.
4. Dedic M., Ruzic D., "Buckling of Closed Thin-Walled Beam with Curved Side Plates Subjected to Bending", Proceedings of Fourth International Conference Heavy Machinery – HM '02, Kraljevo, 2002.

THE ANALYSIS OF DESIGNING COLUMNS CENTRICALLY LOADED BY AXIAL COMPRESSIVE LOAD

Ruzica R. Nikolic¹, Jelena M. Veljkovic²

Abstract: In this paper is analyzed design of columns centrically loaded by axial compressive load, by using the ω -procedure and by using the standard procedure JUS U.E7.081. This analysis will be presented on an example of a column with the complex cross-section. By comparison between the calculated normal stresses and allowable stress for both procedures, it can be seen that the stresses calculated using the standard procedure are significantly smaller than stresses calculated using the theoretical procedure. This shows that the standard procedure is much more on the safety side.

1. INTRODUCTION

Load-carrying capacity of axially loaded columns, with single-part cross-section, by using the standard procedure JUS U. E7. 081/198, is written as:

$$\sigma_N = \frac{N}{A} \leq \sigma_{i,dop} = \chi \sigma_{dop}, \quad (1)$$

where is: N - calculated normal force for appropriated case of loading, A - the cross-sectional area, σ_N - calculated normal stress, $\sigma_{i,dop}$ - allowable buckling stress, σ_{dop} - allowable normal stress, χ - dimensionless slenderness ratio which depends on relative slenderness $\bar{\lambda}$, shape of cross-section and degree of equivalent geometric imperfections.

Dependence of the column's cross section and degree of equivalent geometric imperfections are expressed by column belonging to one of the buckling curves, A_0 , A , B , C or D , [5].

Relative slenderness ratio $\bar{\lambda}$ is the relation between the effective slenderness ratio λ and slenderness ratio at yield strength, λ_v :

$$\bar{\lambda} = \frac{\lambda}{\lambda_v} \quad (2)$$

Effective slenderness ratio is a quotient of the effective length of the column, ℓ_{ki} and competent radius of gyration i :

$$\lambda = \frac{\ell_{ki}}{i}. \quad (3)$$

Load-carrying capacity of axially loaded columns, by using the ω -procedure, is written as:

$$\sigma_{\omega} = \frac{N}{A} \omega \leq \sigma_{dop} \quad (4)$$

where coefficient ω depends on effective slenderness ratio, λ .

¹ Prof. Dr. Ruzica R. Nikolic, Faculty of Mechanical Engineering, University of Kragujevac, Sestre Janjic 6, YU34000 Kragujevac, Serbia and Montenegro

tel. ++381-34-335-990, fax. ++381-34-333-1992, E-mail: inikoli@ptt.yu

² Dr. Ing. Jelena M. Veljkovic, Research Associate, "ZASTAVA Machines" Factory, Trg Topolivca 4, YU34000 Kragujevac, Serbia and Montenegro

tel. ++381-34-334-613, fax. ++381-34-333-627, E-mail: vkatarina@ptt.yu

2. THE DESIGN OF COLUMNS CENTRICALLY LOADED BY COMPRESSIVE LOAD

The cross section of the multi-part columns is characterized by the material and non-material (free) axes. The former crosses all the individual parts of the cross section, while the latter does not necessarily pass through all the parts of cross section. The lace sheets and truss bars are positioned perpendicular to the free axis.

The individual element axis is the axis that corresponds to the minimum gyration ratio. The carrying capacity control of centrically compressed columns, of the constant, multi-part cross-section, enhances the control of buckling carrying capacity both around the material and non-material axes.

The problem of design centrically loaded column by compressive load will be illustrated on an example of a column with cross-section shown in Figure 1. The column height is $h=7$ m, and axial compressive force is $F=840$ kN. The material is Č 0361.

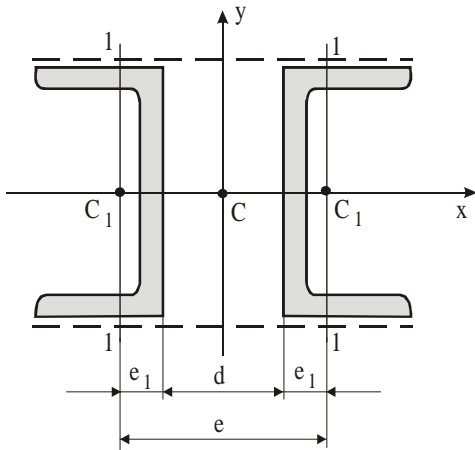


Figure 1. Cross-section of a column

In the first place, dimensions necessary to carry actual load, will be determined using the ω - procedure.

Firstly, is selected U24, with the following data (Figure 1):

$$I_{x_1} = 3600 \text{ cm}^4, \quad I_{y_1} = 248 \text{ cm}^4, \quad A_1 = 42.3 \text{ cm}^2, \\ e_1 = 2.23 \text{ cm}, \quad i_{y_1} = i_1 = 2.42 \text{ cm}, \quad i_{x_1} = 9.22 \text{ cm}$$

For 2U24 column cross-section is:

$$I_x = 2 \cdot I_{x_1} = 2 \cdot 3600 = 7200 \text{ cm}^4$$

$$i_x = \sqrt{\frac{I_x}{A}} = \sqrt{\frac{2 \cdot I_{x_1}}{2 \cdot A_1}} = \sqrt{\frac{I_{x_1}}{A_1}} = i_{x_1} = 9.22 \text{ cm}$$

$$\lambda_x = \frac{h}{i_x} = \frac{700}{9.22} = 75.92 \Rightarrow$$

$$\lambda_x = 76 \xrightarrow{\text{Table}} \omega_x = 1.46$$

$$\sigma_{\omega_x} = \frac{F}{2 \cdot A_1} \cdot \omega_x = \frac{840}{2 \cdot 42.3} \cdot 1.46 =$$

$$= 14.5 \frac{\text{kN}}{\text{cm}^2} = 145 \text{ MPa}$$

$$\sigma_{\omega_x} = 145 \text{ MPa} < \sigma_{dop} = 160 \text{ MPa}.$$

The 2U24 cross-section is well selected in view of buckling stability around the x-x axis. It is necessary to check validity of criterion of stability around the y-y axis. Lattice e , namely, d is unknown, and will be determined under condition that the material is utilized by buckling around that axis up to $\sigma_{dop}=160$ Mpa, [2].

$$\sigma_{\omega_y} = \frac{F}{A} \cdot \omega_{y_i} = \sigma_{dop}$$

$$\omega_{y_i} = \frac{2 \cdot A_1 \cdot \sigma_{dop}}{F} = \frac{2 \cdot 42.3 \cdot 16}{840} = 1.61 \rightarrow \lambda_{y_i} = 85, \\ \text{ (Table [5])}.$$

$$\lambda_1 = \frac{c}{i_1} = \frac{100}{2.42} = 41.32 \approx 41 \quad \text{ - (distance}$$

between two lacing bars is $c=100$ cm).

$$\lambda_{y_i} = \sqrt{\lambda_{y_1}^2 + \lambda_1^2} \Rightarrow$$

$$\lambda_{y_1} = \sqrt{\lambda_{y_i}^2 - \lambda_1^2} = \sqrt{85^2 - 41^2} = 74.4$$

$$\lambda_{y_1} = \frac{\ell_{ky}}{i_{y_1}} = \frac{h}{i_{y_1}}$$

$$i_{y_1} = \frac{h}{\lambda_{y_1}} = \frac{700}{74.4} = 9.41 \text{ cm}$$

$$I_{y_1} = i_{y_1}^2 \cdot A = 9.41^2 \cdot 2 \cdot 42.3 = 7490 \text{ cm}^4$$

$$I_y = 2 \cdot \left(I_{y_1} + x_{C_1}^2 \cdot A_1 \right) = 2 \cdot \left(I_{y_1} + \frac{e^2}{4} \cdot A_1 \right)$$

$$I_y = 2 \cdot I_{y_1} + \frac{e^2}{2} \cdot A_1 \Rightarrow$$

$$e^2 \cdot \frac{A_1}{2} = I_y - 2 \cdot I_{y_1} \Rightarrow$$

$$e = \sqrt{\frac{2 \cdot (I_y - 2 \cdot I_{y_1})}{A_1}}$$

$$e = \sqrt{\frac{2 \cdot (7490 - 2 \cdot 248)}{42.3}} = 18.2 \text{ cm}$$

for

$$e = 18.2 \Rightarrow d = e - 2 \cdot e_1 = , \\ = 18.2 - 2 \cdot 2.23 = 13.74 \text{ cm}$$

thus the value of $d=16$ cm is adopted.

For $d = 16 \text{ cm} \Rightarrow$

$$e = d + 2 \cdot e_1 = 16 + 2 \cdot 2.23 = 20.46 \text{ cm}$$

$$I_y = 2 \cdot \left(248 + \frac{20.46^2}{4} \cdot 42.3 \right) = 9340 \text{ cm}^4$$

$$i_y = \sqrt{\frac{I_y}{A}} = \sqrt{\frac{9340}{2 \cdot 42.3}} = 10.5 \text{ cm}$$

$$\lambda_y = \frac{h}{i_y} = \frac{700}{10.5} = 67$$

Control of buckling stability around the y-y axis:

$$\lambda_{y_i} = \sqrt{\lambda_y^2 + \lambda_1^2} = \sqrt{67^2 + 41^2} = 79$$

$$\lambda_{y_i} = 79 \rightarrow \omega_{y_i} = 1.51, \text{ (Table, [5])}.$$

$$\sigma_{\omega_y} = \frac{F}{A} \cdot \omega_{y_i} = \frac{840}{2 \cdot 42.3} \cdot 1.51 = 15.0 \frac{\text{kN}}{\text{cm}^2} = 150 \text{ MPa}$$

$\sigma_{\omega_y} = 150 \text{ MPa} < \sigma_{dop} = 160 \text{ MPa}$, thus the stability checks.

Control of the distance between two lacing bars:

$$\lambda_1 = \frac{c}{i_1} \leq 50 \cdot \left(4 - 3 \cdot \frac{\sigma_{\omega}}{\sigma_{dop}} \right) = \\ = 50 \cdot \left(4 - 3 \cdot \frac{150}{160} \right) = 59 \\ \lambda_1 = 41 < 59.$$

The cross-section 2U24 is selected with lattice $d=16$ cm.

Design of centrically loaded column, by using the standard procedure JUS U. E7. 081, will be shown in further analysis.

The proof of load-carrying capacity around the material axis (JUS U. E7. 081), is as follows:

$$\lambda_{i,x} = \frac{\ell_{i,x}}{i_x} = \frac{700}{9.22} = 75.92$$

$$\bar{\lambda}_x = \frac{\lambda_{i,x}}{\lambda_v} = \frac{75.92}{92.9} = 0.82 \rightarrow \chi = 0.65, \quad (\text{Curve "C", [5]}).$$

Allowable buckling stress is:

$$\sigma_{i,dop} = \chi \cdot \sigma_{dop} = 0.65 \cdot 160 = 104 \text{ MPa}$$

Calculated normal stress is:

$$\sigma_N = \frac{N}{A} = \frac{840}{84.6} = 99.3 \text{ MPa} < \sigma_{i,dop} = 104 \text{ MPa}$$

thus it is less than the allowable stress.

The proof of the load-carrying capacity around nonmaterial axis, as follows:

$$\lambda_y = \frac{\ell_{i,y}}{i_y} = \frac{700}{10.5} = 67$$

$$\lambda_{y_i} = \sqrt{\lambda_y^2 + \frac{m}{2} \lambda_1^2} = \sqrt{67^2 + \frac{2}{2} \cdot 41^2} = 78.55$$

$m=2$ - number of single elements in complex cross-section

$$\lambda_1 = \frac{c}{i_1} = \frac{100}{2.42} = 41.32 \approx 41$$

$$\bar{\lambda}_{y_i} = \frac{\lambda_{y_i}}{\lambda_v} = \frac{78.55}{92.9} = 0.85 \rightarrow \chi = 0.63,$$

(Curve "C", [5]).

Allowable buckling stress is:

$$\sigma_{i,dop} = \chi \cdot \sigma_{dop} = 0.63 \cdot 160 = 100.8 \text{ MPa},$$

while the calculated normal stress is:

$$\sigma_N = \frac{N}{A} = \frac{840}{84.6} = 99.3 \text{ MPa} <$$

$$< \sigma_{i,dop} = 100.8 \text{ MPa}$$

3. CONCLUSION

By comparing the calculated normal stress to the allowable stress according to the ω - procedure and the standard procedure, it can be seen that the stresses obtained by using the standard procedure are significantly smaller than stresses obtained by using the theoretical procedure. This shows that the standard procedure is much more on the safety side. The reason for this difference in stresses' values (up to 40 %) is that the calculation by the ω - procedure is done under an assumption that the material is utilized by buckling up to allowable stress, while calculation done by the standard procedure does not consider the aforementioned assumption.

4. REFERENCES

- [1] Milosavljevic M., M. Radojkovic, B. Kuzmanovic, Fundamentals of Steel Constructions, Gradjevinska knjiga, Belgrade, 1986.
- [2] Nikolic R., V. Marjanovic, Metal Constructions - Handbook, Faculty of Mechanical Engineering, Kragujevac, 1998.
- [3] **Group of standards JUS M.B1.**, JUS standards for construction elements, materials allowable stresses, ..., National institution for standardization, Belgrade.
- [4] Ostric D., Metal constructions, Faculty of mechanical engineering, Belgrade, 1988.
- [5] Petkovic Z., D. Ostric, Metal Constructions in Engineering Mechanics 1, Institute of Mechanization, Faculty of Mechanical Engineering, Belgrade, 1996.

AN ANALYSIS OF LOCAL STABILITY OF COMPOSITE PLATE WITH STRIPPED MID-LAYER

Dr Milan Dedic ⁽¹⁾

Summary

In this paper an analysis of local stability of a composite plate in longitudinal compression is presented. The plate is made of two outer layers and a mid-layer of strips linked in triangular pattern. The load acts in the direction of strips. Material is isotropic or orthotropic, and different layers of the plate can have different mechanical properties. Buckling is in linear elastic domain of deformations. The calculation of the critical buckling force is analytical. The case of destabilizing due to buckling of outer layers and due to buckling of strips are considered.

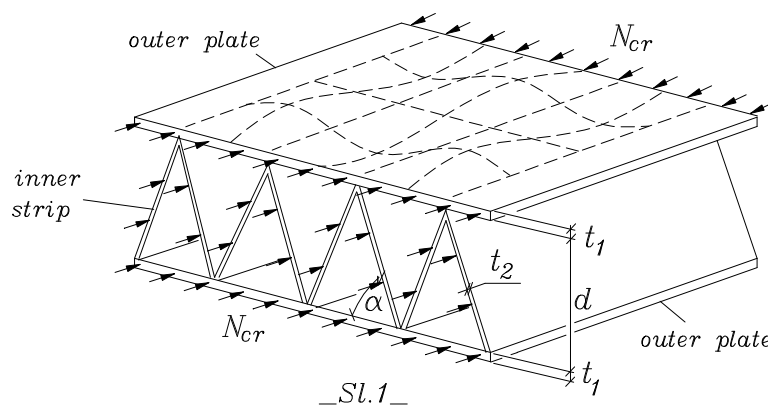
Key words: Buckling of plates, Composite plates, Cellular plates

1. Introduction

Composite plates with cellular inner layer, as the one in Fig.1 with inner strips connected in triangles, may have good global longitudinal buckling strength to weight ratio. However, if parts of the plate are very thin, i.e. dimensions t_1 and t_2 are small compared to apparent thickness d , local buckling, indicated by dashed lines on the figure may occur. This paper presents a calculation of the critical longitudinal compressive stress σ_{cr} in local buckling of this type of plates comprising both buckling in outer plates and inner strips.

whole is symmetric to its mid surface both geometrically and materially – although outer plates and strips may have different material properties. Thus, flexural rigidity of i -th part may be written: $D_i = E_i h_i^3/12(1-\nu_i^2)$. Compressive stress is assumed to be uniformly distributed over loaded edges, and acting along longitudinal axis of strips. Outer plates are free to deform in direction normal to their surface.

Different buckling modes give different values of critical stress. For example, mode (a) in Fig.2 can occur only if rigidity D_1 of outer parts is much greater then D_2 of strips. Conversely, if $D_2 \gg D_1$, mod (b) will occur.



2. Definition of the plate structure and load

In the following analysis we assume that: all the parts are straight and flat in unloaded state and without any irregularity, strips are rigidly connected to outer plates. Outer plates have the same thickness t_1 and all the strips have the same thickness t_2 . So, plate as a

In reality, if rigidities are of the same order- which is most likely, all the parts will undergo some kind of deformation, and modes (c) and (d) should be considered. Of course, calculation procedure for a given example should be performed for all possible modes until the one with the smallest critical stress is found! In this paper mod (c) will be analyzed in two variants.

⁽¹⁾ Milan Dedić, Associated Professor, Faculty of Mechanical Engineering in Kraljevo, University of Kragujevac, Serbia and Montenegro, E-mail: dedic.m@maskv.edu.yu

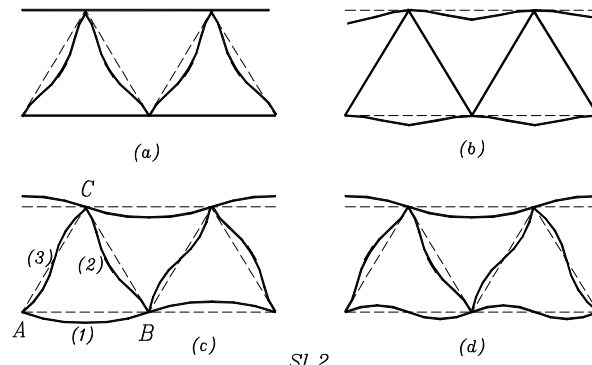
3. Buckling mod (c)

Let us observe a triangle ABC , Fig.2, consisting of part (1) of the outer plate, and parts (2) and (3) of adjacent strips. Let all parts undergo deformation, so that parts (1) and (2) have *symmetric* deformation and part (3) *antisymmetric* deformation. Let us further assume that part (1) buckles, Fig.3a, being elastically restricted by parts (2), Fig.3b, and part (3), Fig.3c. We shall suppose that all parts behave like thin plates in domain of elastic deformations. Accordingly to /1/ and /2/ for buckling of part (1), and to /3/ for bending of parts (2) and (3), deformations will be governed by equations:

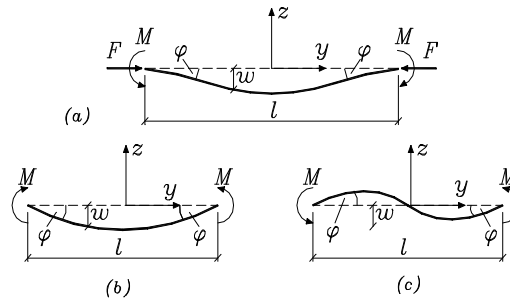
$$w_I'''' + 2w_I'' w_{I'xy} + w_I'' w_{I'yyy} = -\frac{N_{crI}}{D_I} w_I'' \quad (1)$$

$$w_i'''' + 2w_i'' w_{i'xy} + w_i'' w_{i'yyy} = 0 \quad i = 2, 3 \quad (2),(3)$$

where x, y denote axes in longitudinal and transverse



—Sl.2—



—Sl.3—

direction, w_i denotes displacement normal to the outer plate or inner strip surface, (see Fig.3.a), prime denotes differentiation with respect to variables following it, and N_{crI} critical buckling force per unit length of the loaded edge of first part (a strip of outer plate between two adjacent joints). Equations for $i = 2, 3$ are obtained putting for the transverse load $p = p(x, z) = 0$. Solution of this type of problem was discussed in /4/ and /5/. We take solution to the above equations in the general form:

$$w_i(x, y) = C_i \sin \frac{m\pi x}{a} f_i(y) \quad (4)$$

where m and a are number of sinusoidal halfwaves of the buckled surface and length of composite plate in longitudinal direction. After putting $\lambda = m\pi/a$ solution routines lead to:

$$f_1 = C_{11} \operatorname{ch} \alpha_1 y + C_{12} \operatorname{sh} \alpha_1 y + C_{13} \cos \beta_1 y + C_{14} \sin \beta_1 y \quad (5)_1$$

$$\alpha_1 = \sqrt{+\lambda^2 + \lambda \sqrt{N_{crI}/D_I}} \quad (5)_2$$

$$\beta_1 = \sqrt{-\lambda^2 + \lambda \sqrt{N_{crI}/D_I}} \quad (5)_3$$

$$f_2 = C_{21} \operatorname{ch} \alpha_2 y + C_{22} \operatorname{sh} \alpha_2 y + C_{23} y \operatorname{ch} \alpha_2 y + C_{24} y \operatorname{sh} \alpha_2 y \quad \alpha_2 = \lambda \quad (6)$$

$$f_3 = C_{31} \operatorname{ch} \alpha_3 y + C_{32} \operatorname{sh} \alpha_3 y + C_{33} y \operatorname{ch} \alpha_3 y + C_{34} y \operatorname{sh} \alpha_3 y \quad \alpha_3 = \lambda \quad (7)$$

Constants C_{ij} are determined from boundary conditions.

For all parts w_i equals null along longitudinal edges, i.e. for $y = \pm b_i/2$, where b_i denotes width of i -th part. That gives six equations:

$$f_i\left(+\frac{b_i}{2}\right) = 0 \quad f_i\left(-\frac{b_i}{2}\right) = 0 \quad i = 1, 2, 3 \quad (8)$$

Three more equations are obtained from the conditions of symmetric deformation of parts (1) and (2), and antisymmetric deformation of part (3) expressed in terms of edge rotations $\varphi_i = w_{i,y}$:

$$\varphi_i\left(-\frac{b_i}{2}\right) = -\varphi_i\left(+\frac{b_i}{2}\right) \quad i = 1, 2 \quad (9), (10)$$

$$\varphi_3\left(-\frac{b_3}{2}\right) = \varphi_3\left(+\frac{b_3}{2}\right) \quad (11)$$

The previous nine equations lead to the following three expressions for buckled plate (1) and bent plates (2) and (3) with only one integral constant remained in each one:

$$f_1(y) = \left[-\frac{\cos B_1}{ch A_1} ch \alpha_1 y + \cos \beta_1 y \right] C_{13} \quad (12)$$

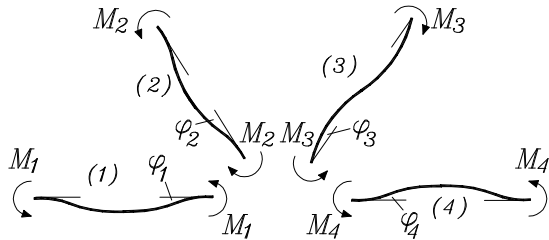
$$A_1 = \alpha_1 b_1 / 2 \quad B_1 = \beta_1 b_1 / 2$$

$$f_2(y) = \left[ch \alpha_2 y - \frac{2}{b_2} \frac{ch A_2}{sh A_2} y sh \alpha_2 y \right] C_{21} \quad (13)$$

$$A_2 = \alpha_2 b_2 / 2$$

$$f_3(y) = \left[sh \alpha_3 y - \frac{2}{b_3} \frac{sh A_3}{ch A_3} y ch \alpha_3 y \right] C_{32} \quad (14)$$

$$A_3 = \alpha_3 b_3 / 2$$



—Sl. 4—

Observing Fig. 4 with parts meeting in joint B shown apart, we see that deformations in that joint must satisfy the following two compatibility conditions in terms of edge rotations and one in terms of edge moments:

$$\varphi_{1B} = \varphi_{2B} \quad (15)$$

$$\varphi_{1B} = \varphi_{3B} \quad (16)$$

$$2M_{1B} - M_{2B} - M_{3B} = 0 \quad (17)$$

provided that joint B is acted to by end moments M_{1B} of two adjacent horizontal parts. Regarding (12) to (14) rotations in the above equations can be expressed as:

$$\varphi_{1B} = w_{1'y} \Big|_{y=b_1/2} = \sin \frac{m\pi x}{a} f_1'{}_B C_{13} \quad (18)$$

$$\varphi_{2B} = w_{2'y} \Big|_{y=-b_2/2} = \sin \frac{m\pi x}{a} f_2'{}_B C_{21} \quad (19)$$

$$\varphi_{3B} = w_{3'y} \Big|_{y=-b_3/2} = \sin \frac{m\pi x}{a} f_3'{}_B C_{32} \quad (20)$$

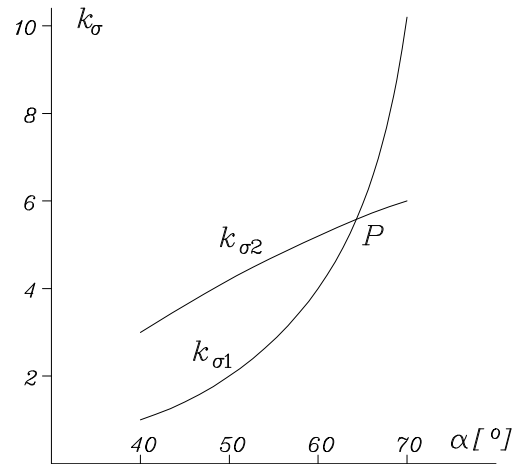
where quantities $f_i'{}_B$ denote derivatives of functions f_i in (12) to (14) calculated in B. Similarly edge moments can be expressed as:

$$M_{1B} = -D_1 w_{1''yy} \Big|_{y=b_1/2} = -D_1 \sin \frac{m\pi x}{a} f_1''{}_B C_{13} \quad (21)$$

$$M_{2B} = -D_2 w_{2''yy} \Big|_{y=-b_2/2} = -D_2 \sin \frac{m\pi x}{a} f_2''{}_B C_{21} \quad (22)$$

$$M_{3B} = -D_3 w_{3''yy} \Big|_{y=-b_3/2} = -D_3 \sin \frac{m\pi x}{a} f_3''{}_B C_{32} \quad (23)$$

where $f_i''{}_B$ denote second derivatives of functions f_i in B. Changing expressions (18) to (23) in relations (15) to (17), after canceling term containing sine function, we



—Sl. 5—

come to system of three homogeneous equations in the unknowns C_{13} , C_{21} and C_{32} :

$$f_1'{}_B C_{13} - f_2'{}_B C_{21} = 0 \quad (24)$$

$$f_1'{}_B C_{13} - f_3'{}_B C_{32} = 0 \quad (25)$$

$$2D_1 f_1''{}_B C_{13} - D_2 f_2''{}_B C_{21} - D_3 f_3''{}_B C_{32} = 0 \quad (26)$$

The nontrivial solution of that system can exist only if the determinant of the system equals zero:

$$\Delta = \begin{vmatrix} f_1'{}_B & -f_2'{}_B & 0 \\ f_1'{}_B & 0 & -f_3'{}_B \\ 2D_1 f_1''{}_B & -D_2 f_2''{}_B & -D_3 f_3''{}_B \end{vmatrix} = 0 \quad (27)$$

Regarding that N_{cr1} enters (27) through α_l and β_l , see (5)₂ and (5)₃, and through A_l and B_l , see (12), it is obvious that (27) is an equation in N_{cr1} as the only unknown. The smallest (positive) value of N_{cr1} obtained from it, is the critical buckling force. In theory, however, rather than N_{cr1} a nondimensional buckling force k_l is calculated:

$$k_l = \frac{N_{cr1}}{(\pi^2 D_l / b_l^2)} \quad (28)$$

so that the critical stress can be written:

$$\sigma_{cr} = \frac{N_{cr1}}{t_1} = k_l \frac{\pi^2 D_l}{t_1 b_l^2} = k_{\sigma 1} \frac{\pi^2 E_1}{12(1-\nu_1^2)} \quad (29)$$

where $k_{\sigma 1}$ is new nondimensional factor that reads:

$$k_{\sigma 1} = k_l \frac{t_1^2}{b_l^2} = k_l \frac{t_1^2}{d^2} 4tg^2 \alpha \quad (30)$$

Numerical results for $k_{\sigma 1}$ versus angle α are plotted in Fig.5 for $t_1/d = t_2/d = 0,01$ and $E_1 = E_2$.

Previous text explains how we proceed when part (1) buckles elastically restricted by parts (2) and (3). In the same manner we could calculate the critical stress assuming that part (2) buckle elastically restricted by (1) and (3) to see which mode yields lower value of critical stress for given structural parameters. Proceeding as described above, instead of (29) and (30), we would have:

$$\sigma_{cr} = \frac{N_{cr2}}{t_2} = k_2 \frac{\pi^2 D_2}{t_2 b_2^2} = k_{\sigma 2} \frac{\pi^2 E_2}{12(1-\nu_2^2)} \quad (31)$$

with:

$$k_{\sigma 2} = k_2 \frac{t_2^2}{b_2^2} = k_2 \frac{t_2^2}{d^2} \sin^2 \alpha \quad (32)$$

Corresponding curve is also plotted in Fig.5 for the same geometric parameters as $k_{\sigma 1}$.

Finally, as a third possibility we could make attempt with part (3) buckling and parts (1) and (2) resisting it.

However, regarding that buckling of part (3) in anti-symmetric mode will always result in critical stress of

several times higher value than part (2) buckling in symmetric mode, we can simply drop that possibility out, and restrict our attention to the previous two modes.

4. Conclusion

Results in Fig.5 show variation of nondimensional critical stress $k_{\sigma 1}$ and $k_{\sigma 2}$ with angle of mid-layer strips α , see Fig.1. Curve $k_{\sigma 1}(\alpha)$ raises progressively with α because width of part (1) decreases, and it becomes more stiffened (relative thickness t_1/b_1 increases also). Till the intersection point P at angle of $\alpha \approx 63^\circ$, as one may expect, $k_{\sigma 1}(\alpha)$ is less than $k_{\sigma 2}(\alpha)$, and the composite plate will loose stability due to buckling of part (1). For $\alpha > 63^\circ$ $k_{\sigma 2}(\alpha)$ becomes less than $k_{\sigma 1}(\alpha)$, and part (2) will buckle first. So for $\alpha < 63^\circ$ we should take $\sigma_{cr} = \sigma_{cr1}$, and for $\alpha > 63^\circ$ we should take $\sigma_{cr} = \sigma_{cr2}$.

For different geometric (t_i/d) and material parameters (E_i, ν_i) curves of nondimensional stress will be slightly different, and point P will shift to the left or to the right. Again, critical stress obtained this way must be checked if it falls within elastic buckling domain.

4. References

1. Timoshenko S., "Theory of Elastic Stability", McGraw-Hill Book Company Inc., 1936.
2. Brush D. O., Almroth B. O., "Buckling of Bars, Plates, and Shells", McGraw-Hill Book Company Inc., 1975.
3. Timoshenko S., Woinowski-Krieger S., "Theory of Plates and Shells", McGraw-Hill Book Company Inc., 1959.
4. Dedic M. "The Optimum Shape of Open Thin-Walled Beam in Local Buckling due to Compression", Proceedings of Third International Conference Heavy Machinery – HM '99, Kraljevo, 1999.
5. Dedic M., Ruzic D., "Buckling of Closed Thin-Walled Beam with Curved Side Plates Subjected to Bending", Proceedings of Fourth International Conference Heavy Machinery – HM '02, Kraljevo, 2002.

APPLICATION OF DYNAMICS OF RIGID BODIES TO MECHANISMS WITH CLOSED CHAIN FORMS

Svetislav Radovic⁽¹⁾

SUMMARY: This paper considers the problem of forming equations of differential constraints of systems of rigid bodies connected in such a way that they form a closed kinematic chain (mechanism). The method orientated to the application of computer is presented. By a suitable approach to the problem –cutting the chain in a joint 0 the closed chain is considered as open one. Introducing and keeping overplus generalized coordinates on the point where the chain is cut, we obtain such a form of motion, form a complete system. Thus, we obtain a closed system of equations for determination of all generalized coordinates, i.e. both independent and overplus. The exposed method is suitable for forming equations of differential constraints and robot systems of closed kinematic chain form.

Keywords: closed kinematic chain, excess, coordinates.

1. INTRODUCTION

Studying of motion of a system of rigid bodies connected in such a way that they form a closed kinematic chain is the most complex problem in the theory of mechanisms and machines. This complexity is reflected in the fact that closing of chains imposes additional constraints on generalized coordinates and velocities whose forming represents a necessary condition for forming of equations of motion of such systems. Different the system with kinematic chain form 2, 3, 9 etc. Are found in the literature but the constraints are always supposed to be known in advance and independent. Meanwhile, in the application of those methods to real technical objects (mechanisms, robots, etc.) , insurmountable difficulties are some – times encountered while forming the equations of

such system constraints which are the result of kinematic chain closing. Difficulties most frequently among the equations of constraints formed in that way, which means that there are dependent generalized coordinates and velocities as well, and it is difficult, sometimes even impossible, to recognize dependent coordinates and velocities in the set of all generalized coordinates and velocities and separate them from independent ones. It is especially difficult by a computer because the computer cannot “recognize” dependent generalized parameters.

This paper presents a method for forming of equations of such system constraints in their differential form without elimination of dependent ones. Such approach to the problem enables forming of equations of motion in the known form 7 – as equations in excess coordinates. This results in a closed system of equations for determination of all generalized coordinates and velocities, which

⁽¹⁾ **Svetislav Radovic**, Associated Professor, Faculty of Mechanical Engineering in Kraljevo, University of Kragujevac, Dositejeva 19, 36000 Kraljevo, Serbia and Montenegro, e-mail radovic.s@maskv.edu.yu

represents an algorithm suitable for computer application because it is not necessary to “recognize” and eliminate dependent generalized coordinates and velocities.

2.EQUATIONS OF CONSTRAINTS IN EXCESS COORDINATES

Let us consider a system of rigid bodies connected in such a way that they form the closed kinematic chain shown in Fig.1.

Let us introduce the following system of denotations:

q_a^α ($\alpha = 1, \dots, s_a \leq 6, a = 1, \dots, N$) - relative coordinates,
 $0, 1, \dots, a, \dots, i, \dots, N-1, N$ - denotations for bodies,

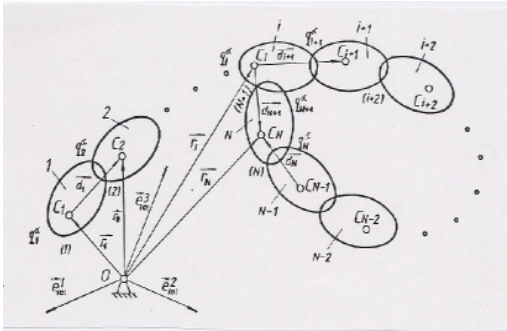


Fig.1.

(1), ..., (a), ..., (i), ..., (N-1), (N), (N+1) - denotations for joints,

$C_0, C_1, \dots, C_a, \dots, C_N$ - centres of body masses,

$\vec{p}_{a,a}, \dots, \vec{p}_{e,e}, \dots, \vec{p}_{N,N}$ - vectors of positions of

centres of body masses in relation to inertial basis.

The system consists of N rigid bodies connected by joints in such a way that the body with the denotation N is connected with the body with denotation i by means of the joint with the denotation $(N+1)$, where N is always $> i$. For the variables of the state, let us choose relative coordinates between two adjacent bodies, i.e. q_a^α , as well

as the corresponding velocities \dot{q}_a^α ($\alpha = 1, 2, \dots, s_a \leq 6, a = 0, 1, \dots, N$), where s_a represents the number of degrees of freedom in the joint with the denotation (a) . The excess joint $(N+1)$ in relation to the corresponding open kinematic chain is formed by closing the kinematic chain.

Closing of the chain, i.e. forming of the joint $(N+1)$ imposes the constraints to the state variables so that there are dependent ones among them. If we want to write the equations of motion with the minimum number of state variables, it is necessary to elimination of dependent generalized coordinates is difficult and the overcoming of that problem is approached in different ways.

This paper will present an idea for overcoming the problem of elimination of dependent generalized coordinates-the equations of motion will be formed without their elimination. Dependent values of the state will be called excess, and the rest of them will be called independent. The equations of motion will be formed not with total member of them whose number is equal to the number of values of the described system state.

For the purpose of realization of the exposed idea, we shall consider the open chain – instead of the closed kinematic chain – requiring it to be dynamical – cutting the closed chain in a joint, for example $(N+1)$, and the by forming the constraints in their differential form which describe the condition for chain closing. The equations of motion are written in excess coordinates and joined by the equations of constraints, of all coordinates.

In a general case, closing of the kinematic chain imposes six constraints to the system.

- there constraints which express the condition that the difference between the absolute angle velocities of the body with the denotation N and the body with denotation I is equal to the relative angle velocity between those two bodies.
- Three constraints which express the condition that the difference between the absolute velocities of the centers of masses of the body with the denotation N and the body with the denotation I is equal to the relative velocity between those two bodies.

The conditions a) and b) may be formulated in another way.

If $\dot{\varphi}$ denotes the relative angle velocity in the joint with the denotation (a) , then the constraints of the form a) can be expressed as

$$\vec{\omega}_{r,i+1} + \vec{\omega}_{r,i+2} + \dots + \vec{\omega}_{r,N} + \vec{\omega}_{r,N+1} = 0. \quad (1)$$

If \vec{d} denotes the vectors between the centres of mass of two adjacent bodies (see Figure 1.), then the conditions b) can be expressed as

$$\vec{d}_{N+1} = \vec{d}_{i+1} + \vec{d}_{i+2} + \dots + \vec{d}_N. \quad (2)$$

Projecting the expressions (1) and (2) to the system of base vectors, we obtain six scalar equations which represent six constraints of the forms a) and b). Those constraints are not always independent – there may also be dependent ones among them. How many dependent ones and how many independent ones there are among the previously stated constraints depends on how many degrees of freedom of motion are allowed by the joint with the denotation $(N+1)$, because

$$s+r=6, \quad (3)$$

where: s – number of degrees of freedom in the joint $(N+1)$, r – number of independent constraints.

For the purpose of considering the closed kinematic chain as open, it is necessary to express the vector of the position on the centre of mass of the body N as the function of all generalized coordinates. Firstly, we shall divide all generalized coordinates q_a^α ($\alpha = 1, 2, \dots, s_a \leq 6, a = 0, 1, \dots, N$) into two groups:

1) Independent generalized coordinates

$$q_a^\alpha \quad (\alpha = 1, 2, \dots, s_a \leq 6, a = 0, 1, \dots, N)$$

2) excess generalized coordinates

where n – total number of generalized coordinates, including the joint $(N+1)$.

The vector of the position of the body N in relation to the inertial basis can be written in the form

$$\vec{r}_N(q_1^\alpha, \dots, q_N^\alpha, q_{N+1}^\alpha) = \frac{1}{2} [\vec{r}_N(q_1^\alpha, \dots, q_N^\alpha) + \vec{r}_N(q_1^\alpha, \dots, q_{N+1}^\alpha)] \quad (4)$$

where (see Fig.1.).

$$\vec{r}_N(q_1^\alpha, \dots, q_N^\alpha) = \vec{r}_0 + \vec{d}_1 + \dots + \vec{d}_N$$

$$\vec{r}_N(q_1^\alpha, \dots, q_{N+1}^\alpha) = \vec{r}_0 + \vec{d}_1 + \dots + \vec{d}_i + \vec{d}_{N+1}$$

Taking into consideration that

$$\vec{r}_N = \vec{r}_i + \vec{d}_{N+1} \quad (5)$$

the expression (4) obtains the form

$$\vec{r}_N(q_1^\alpha, \dots, q_N^\alpha, q_{N+1}^\alpha) = \frac{1}{2} [\vec{r}_N(q_1^\alpha, \dots, q_N^\alpha) + \vec{r}_i(q_1^\alpha, \dots, q_i^\alpha) + \vec{d}_{N+1}(q_1^\alpha, \dots, q_{N+1}^\alpha)] \quad (6)$$

3.KINETIC ENERGY OF A SYSTEM IN EXCESS COORDINATES

Let us now consider forming of the expression for kinetic energy of a system which is also written in the function of all generalized coordinates. Kinetic energy of a system of rigid bodies with m degrees of freedom of motion is

$$T = T(q, \dot{q}), \quad (q = q^1, \dots, q^m, \dot{q} = \dot{q}^1, \dots, \dot{q}^m) \quad (7)$$

Let us note the function of the form

$$T' = T'(q, \dot{q}, q', \dot{q}'),$$

$$(q' = q^{m+1}, \dots, q^{m+l=n}, \dot{q}' = \dot{q}^{m+1}, \dots, \dot{q}^{m+l=n}) \quad (8)$$

Let us assume that there is a system of finite constraints of the form

$$F_\nu(q, q') = 0, \quad (\nu = m+1, \dots, m+l=n) \quad (9)$$

Let us assume that the system (9) is solvable in relation to q , i.e.

$$q^\nu = f^\nu(q^\alpha),$$

$$(\alpha = 1, \dots, m, \nu = m+1, \dots, m+l=n). \quad (10)$$

Differentiation of the expression (10) results in

$$\dot{q}^\nu = b_\alpha^\nu(q, q') \dot{q}^\alpha \quad (11)$$

where

$$b_\alpha^\nu = \frac{\partial f^\nu}{\partial q^\alpha}, \quad (\alpha = 1, \dots, m, \nu = m+1, \dots, m+l=n).$$

It is known from analytic mechanics that since

$$T'[q, \dot{q}, q'(q), \dot{q}'(q, \dot{q})] = T(q, \dot{q}), \quad (12)$$

the system of differential equations of the form

$$\frac{d}{dt} \frac{\partial T}{\partial \dot{q}^\alpha} - \frac{\partial T}{\partial q^\alpha} = Q_\alpha, \quad (\alpha = 1, \dots, m) \quad (13)$$

is equivalent to the system

$$\frac{d}{dt} \frac{\partial T}{\partial \dot{q}^\alpha} - \frac{\partial T}{\partial q^\alpha} - Q_\alpha + b_\nu^\alpha \left(\frac{d}{dt} \frac{\partial T}{\partial \dot{q}^\nu} - \frac{\partial T}{\partial q^\nu} - Q_\nu \right) = 0,$$

$$\dot{q}^\nu = b_\alpha^\nu \dot{q}^\alpha, \quad (\alpha = 1, \dots, m, \nu = m+1, \dots, m+l=n). \quad (14)$$

$$F_\nu(q^\alpha, q^\nu) = 0$$

The previous statement directly follows from the known statements exposed in many textbooks on analytic mechanics 4, 5. The proof is in the elimination of q and \dot{q} from the system (14) by (10) and (11), which results in the system (13).

Using these known facts, we shall write the expression for kinetic energy of the considered system in the form

$$T' = T_1 + T_2 + \dots + T_i + \dots + T_{N-1} + \frac{1}{2}(T_N + T'_N) \quad (15)$$

where

$$T_N = T_N(q_1^\alpha, \dots, q_N^\alpha, \dot{q}_1^\alpha, \dots, \dot{q}_N^\alpha)$$

$$T'_N = T'_N(q_1^\alpha, \dots, q_i^\alpha, q_{N+1}^\alpha, \dot{q}_1^\alpha, \dots, \dot{q}_i^\alpha, \dot{q}_{N+1}^\alpha),$$

and where

$$T'[q^\alpha, \dot{q}^\alpha, q^\nu = f^\nu(q^\alpha), \dot{q}^\nu = b_\nu^\alpha(q^\alpha, q^\nu) \dot{q}^\alpha] = T \quad (16)$$

It means that the conditions (12) are satisfied, and the equations of motion can be written in the form (14).

4. EXAMPLE

For the robot system with two closed kinematic chains, shown in Fig.2, form the equations of constraints in their differential form

In this case:

- number of bodies _____ 7,
- number of joints _____ 9,
- 9 relative coordinates, where q is the angle between the body 0 and the body 1, q is the angle between the body 0 and the body 2, etc. (see Fig.2.), q is angle between the body 6 and the body 7.

The conditions of chain closeness are

$$\vec{\rho}_1 + \vec{\rho}_4 + \vec{\rho}_6 + \vec{\rho}_7' + \vec{\rho}_2 + \vec{O_0O_1} = 0 \quad (a)$$

$$\vec{\rho}_3 + \vec{\rho}_5 + \vec{\rho}_7'' + \vec{\rho}_2 + \vec{O_0O_3} = 0$$

Differentiation of expression (a) in relation to time results in

$$\vec{\omega}_{10} \times \vec{\rho}_1 + \vec{\omega}_{40} \times \vec{\rho}_4 + \vec{\omega}_{60} \times \vec{\rho}_6 + \vec{\omega}_{70} \times \vec{\rho}_7' + \vec{\omega}_{20} \times \vec{\rho}_2 = 0 \quad (b)$$

$$\vec{\omega}_{30} \times \vec{\rho}_3 + \vec{\omega}_{50} \times \vec{\rho}_5 + \vec{\omega}_{70} \times \vec{\rho}_7'' + \vec{\omega}_{20} \times \vec{\rho}_2 = 0$$

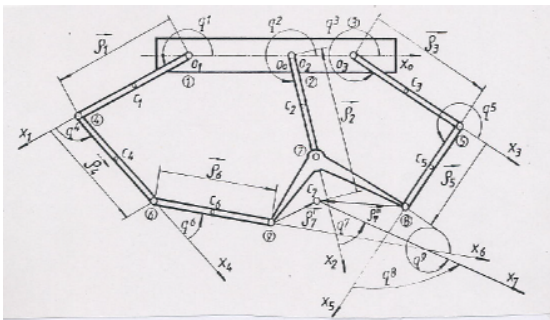


Fig.2.

Since,

$$\vec{\omega}_{10} \times \vec{\rho}_1 = \dot{q}^1 (\vec{k} \times \vec{\rho}_1)$$

$$\vec{\omega}_{40} \times \vec{\rho}_4 = (\dot{q}^1 + \dot{q}^4) (\vec{k} \times \vec{\rho}_4)$$

$$\dots \dots \dots \vec{\omega}_{20} \times \vec{\rho}_2 = (\dot{q}^1 + \dot{q}^4 + \dot{q}^6 + \dot{q}^7 + \dot{q}^2) (\vec{k} \times \vec{\rho}_2)$$

the expression (b) obtains the form

$$\dot{q}^1 (\vec{k} \times \vec{\rho}_1) + \dots + (\dot{q}^3 + \dot{q}^5 + \dot{q}^7 + \dot{q}^2) (\vec{k} \times \vec{\rho}_2) = 0. \quad (c)$$

The conditions on angle velocities are

$$\vec{\omega}_{r,1} + \vec{\omega}_{r,4} + \vec{\omega}_{r,6} + \vec{\omega}_{r,7} + \vec{\omega}_{r,2} = 0,$$

$$\vec{\omega}_{r,3} + \vec{\omega}_{r,5} + \vec{\omega}_{r,7} + \vec{\omega}_{r,2} = 0, \quad (d)$$

that is

$$\dot{q}^1 \vec{k} + \dot{q}^4 \vec{k} + \dot{q}^6 \vec{k} + \dot{q}^7 \vec{k} - \dot{q}^2 \vec{k} = 0 \quad (e)$$

$$\dot{q}^3 \vec{k} + \dot{q}^5 \vec{k} + \dot{q}^7 \vec{k} - \dot{q}^2 \vec{k} = 0$$

or finally

$$\dot{q}^1 + \dot{q}^4 + \dot{q}^6 + \dot{q}^7 - \dot{q}^2 = 0, \quad (f)$$

$$\dot{q}^3 + \dot{q}^5 + \dot{q}^7 - \dot{q}^2 = 0$$

The equations (f) give constraints on generalized velocities.

REFERENCES

1. **Veskovik M., Radovic S.**, Contribution of Dynamics of Systems of Rigid Bodies, Proceedings of XIX Yugoslav Congress on Theoretical and Applied Mechanics, Ohrid 1990.
2. **Vitenburg I.**, Dinamika sistem tverdih tel, Mir, Moskva, 1980.
3. **Lilov L.**, Struktura, kinematika i dinamika sistem tverdih tel, Uspehi mehaniki, Moskva, 1983.
4. **Radovic S.**, Contribution to Dynamic Analysis of Motion of Technical Systems with Nonholonomic Constraints, Doctor 's Dissertation, The Faculty of Mechanical Engineering Belgrade, 1991.
5. **Radovic S.**, Equations of Differential Constraints of Mechanisms which are the results of closing of Kinematic, Proceedings of IV Congress SAUM, Kragujevac, 1992.
6. **Covic V.**, On First Integrals of Differential Equations of Motion of Nonholonomic Systems, XIV Yugoslav Congress on Rational and Applied Mechanics, Portoroz, 1978.
7. **Covic V., Rusov S.**, On a Mechanical Model of Industrial Robots as the Simplest System of Rigid Bodies, International seminar and symposium "Automation and robot", Belgrade, 1987.

USING QUALITY METHODOLOGIES FOR INNOVATIVE DESIGN

Cristiano Fragassa, Leonardo Frizziero, Martin Villanueva¹

Introduction. This work is a sample of designing a simple object, just like a coffee machine, using innovative methodologies as Quality Function Deployment, Value Analysis and Design for Assembly. These are three methods which serve to improve quality during the process of design; they are part of the famous designing technique which is named Concurrent Engineering. The first one, Quality Function Deployment, is the structuralization of all the information which come along with each design project; the second one, Value Analysis, is about the evaluation of all the costs that our project implicates; the last one, Design for Assembly, is a methodology oriented to direct the design process towards the exemplification of all the components' shapes: in this way, we can obtain a product easy to be assembled. In the next paragraph, we analyze more deeply the features of the over shown methodologies.

Key Words: Design, coffee machine, QFD, VA, Design for Assembly, CAD, Rendering.

Three methodologies: QFD, VA and DfA

QFD) Quality Function Deployment (QFD) is the structuralization of the information flow which comes along with each design project. QFD is a system for translating customer requirements into appropriate companies' requirements at every stage, from research through production design and development, to manufacture, distribution, installation, sales and services. It was developed to bring this personal interface to modern manufacturing and business processes. In modern industrial society, where the growing distance between producers and users is a gap to reduce, QFD links the needs of the customer (and user) with design, development, engineering, manufacturing, and service functions. It helps designers seeking out both spoken and unspoken needs, translating these into actions and designs, and focusing various business functions toward achieving this common goal. QFD empowers companies to exceed normal expectations and provide a level of unanticipated excitement that generates value.

QFD is:

1. Understanding the requirements of the customers;
2. Improving quality systems thinking + psychology + knowledge/epistemology;
3. Maximizing positive quality that adds value;
4. Realizing comprehensive quality system for customers' satisfaction;
5. Creating strategy to stay ahead of the competitive game.

This method starts with the *explanation of the task* which is formed by the following important steps:

- 1) Analysis of the marketing environment;
- 2) Analysis of the competitors products;
- 3) The six questions to characterize the products;
- 4) The evaluation and comparative matrixes.

Then we arrive at the definition of the technical requirements, which will be adopted to design our product.

The explanation of the task is one of the most important aspects of QFD. The problem must be completely defined as clear as possible so that the corrections in it will be afterwards limited. The analysis of the environment and the six questions are part of the explanation of the task. In fact "planning activity is not only a scientific-technique, but also a humanistic one. Planning of design is the synthesis between two cultures: the technical one and the humanistic one".

- 1) *Analysis of the environment:* it is important to understand which is the area of our product and what kind of characteristics it has to own.
- 2) *Analysis of the competitors products:* it is important also to understand how the competitors were able to design a similar object; we can improve their lacks.

¹ D.I.E.M. – Department of Mechanical Engineering – University of Bologna Viale del Risorgimento, 2
leonardo.frizziero@mail.ing.unibo.it

3) *Six questions*: The *six questions* serve to immediately characterize those characteristics that the object to design must necessarily possess. They are:

- 1) **Who**: Who uses our product?
- 2) **What**: What is the use of the product?
- 3) **Where**: Where is it used?
- 4) **When**: When is it used?
- 5) **Why**: Why is it used?
- 6) **How**: How is it used?

4) *The evaluation matrixes*: in order to estimate the relative importance of the requirements defined before, the *interrelation matrix* is used. The interrelation matrix is an instrument which evaluates the relationships of dependency (*first kind of employing*) and/or of relative importance (*second kind of employing*) among various requirements or concepts; the instrument is also used to define the priorities and to establish the optimal sequences of actions.

In the first employment, the variables on the columns must be considered as the causes and the same ones, on the rows, as the effects. The dependence between the requirements can be weak, medium or strong: it can be amountable, for example, with the following conventional values: 1, 3, 9.

Instead, in the second employment, the matrix is used to give an evaluation of relative importance to the “independent” variables. For the relative importance analysis, the following conventional votes are used:

- 1** if the row element has the same importance of the column one;
- 0** if the row element is most important than the column one;
- 2** if the column element is most important than the row one.

All the votes can be obtained by market analysis upon a large sample of people.

Using this instrument, the highest values of the sums per rows indicate which is the most important variable among the “independent” ones (i.e. those which have more influence on the others).

Finally, after explanation of the task, we can start with the conceptual design at first, and then with the constructive one. In our sample, we will realize conceptual design through the What/How Matrix and the constructive design through the Morphological Matrix and the CAD drawings (after that, we will make also some rendering pictures).

VA) The Analysis of the Value is the most effective instrument for the management of the Value. Value

(Index of Value) V is the ratio between the minimal estimated price W that we are disposed to pay in order to obtain the function in examination, in a determined place and in determined circumstances, and the total production cost C (cost).

In synthesis the Analysis of the Value is an operating methodological instrument for obtaining Quality (excellence) through placing maximum attention on the functions and the relationships of indices of value (V, W and C).

Moreover, by VA we can analyze all the cost voices: we can know all the percentage of each one of them, being able to reduce the highest one through technical interventions.

DfA) During the design process, it is very important not to forget the assembly simplicity. This methodology is known as “design for assembly” and, together with value analysis, it is the most important technique for reaching a great result for industrializing a product. Every component must be designed to be easily assembled with the others.

The example of a coffee machine design

1) Analysis of the environment: In our analysis we noticed five mode to prepare coffee, which are the following ones:



1. MOKA MODE



2. NAPLES MODE



3. TURKISH MODE



4. FILTER MODE



5. “ESPRESSO” MODE

We chose to design an “Espresso” machine because it can be a product which brings together both aesthetical and mechanical features. So, it is the best one where we can operate a design project, among the others over.

2) *Analysis of the competitors products*: through this analysis, we can observe how the competitors were able to design a similar object and what is present on the market today; we can improve the lacks of these products, making something new not existing yet.



Spiral boiler



Self grinding



A Richard Sapper design with self grinding mechanism



Sophisticated materials and design

3) *Six questions*: now we can apply these *six questions* to the case of the coffee machine; then we will answer the questions and we will be able to find out the requirements wanted:

- 1) **Who**: Who uses the coffee machine?
- 2) **What**: What is the use of the product?
- 3) **Where**: Where is it used?
- 4) **When**: When is it used?
- 5) **Why**: Why is it used?
- 6) **How**: How is it used?

The answers below were given by a selected group of people:

1. Who uses the coffee machine? *Families*, which are composed by different people, with different attitudes: we need a *very simple, ergonomic* and *economical* machine.

2. What is the function of the coffee machine? It has to make a good coffee: *good functionality*.

3. Where is it used? Usually *in a kitchen*, which is a wet and warm environment: *dampness and heat resistant, solid*.

4. When is it used and how many times? It is used *3/4 times a day* for *8/9 years*: *resistant, solid, easy to clean, echo-compatible*.

5. Why is it used? It is used for drinking the coffee, which is a relaxing moment: *good-looking*.

6. How is it used? It is used for making espresso coffee: *high speed*.

From these answers we can obtain the most important characteristics which the coffee machine has to own:

1. Solidity

2. Functionality

3. Simplicity

4. Maintenance

5. Dampness and Heat Resistance

6. Handiness

7. Design

8. Ergonomics

9. Velocity

10. Stability

11. Economy

12. Echo-compatibility.

4) *The evaluation matrixes*: below we can read the *interrelation matrixes*, used in both kinds of employment for the coffee machine case.

The 1st use												
1. Solidity	1	2	3	4	5	6	7	8	9	10	11	12
2. Functionality	2	1	3	4	5	6	7	8	9	10	11	12
3. Simplicity	3	3	1	2	4	5	6	7	8	9	10	11
4. Maintenance	4	4	2	1	3	5	6	7	8	9	10	11
5. Dampness and Heat Resistance	5	5	4	3	1	2	6	7	8	9	10	11
6. Handiness	6	6	5	6	6	5	1	2	3	4	5	6
7. Design	7	7	7	7	7	7	2	1	2	3	4	5
8. Ergonomics	8	8	8	8	8	8	3	2	1	2	3	4
9. Velocity	9	9	9	9	9	9	4	3	2	1	2	3
10. Stability	10	10	10	10	10	10	5	4	3	2	1	2
11. Economy	11	11	11	11	11	11	6	5	4	3	2	1
12. Echo-compatibility	12	12	12	12	12	12	7	6	5	4	3	2

Resistance and Economy are the most dependent

Handiness and Ergonomics are the most independent and influential

The 2nd use												
1. Solidity	1	2	3	4	5	6	7	8	9	10	11	12
2. Functionality	2	1	3	4	5	6	7	8	9	10	11	12
3. Simplicity	3	3	1	2	4	5	6	7	8	9	10	11
4. Maintenance	4	4	2	1	3	5	6	7	8	9	10	11
5. Dampness and Heat Resistance	5	5	4	3	1	2	6	7	8	9	10	11
6. Handiness	6	6	5	6	6	5	1	2	3	4	5	6
7. Design	7	7	7	7	7	7	2	1	2	3	4	5
8. Ergonomics	8	8	8	8	8	8	3	2	1	2	3	4
9. Velocity	9	9	9	9	9	9	4	3	2	1	2	3
10. Stability	10	10	10	10	10	10	5	4	3	2	1	2
11. Economy	11	11	11	11	11	11	6	5	4	3	2	1
12. Echo-compatibility	12	12	12	12	12	12	7	6	5	4	3	2

This matrix shows that the most relative important requirements are: *Functionality* and *Resistance* again

By the evaluation matrixes, we can affirm that the main properties of our coffee machine must be: easy to handle, functional, resistant and good-looking.

Then we have the Relationships Matrix (What/How Matrix): this matrix, named also *What/How Matrix*, links the technical solutions to the requirements obtained from the preceding analysis. It explains HOW realizing WHAT we want to design!

Matrice di relazione COSA/COME												
1. Solidità	1	2	3	4	5	6	7	8	9	10	11	12
2. Funzionalità	2	1	3	4	5	6	7	8	9	10	11	12
3. Semplicità	3	3	1	2	4	5	6	7	8	9	10	11
4. Manutenzione	4	4	2	1	3	5	6	7	8	9	10	11
5. Resistenza al calore e all'umidità	5	5	4	3	1	2	6	7	8	9	10	11
6. Maneggevolezza	6	6	5	6	6	5	1	2	3	4	5	6
7. Design	7	7	7	7	7	7	2	1	2	3	4	5
8. Ergonomia	8	8	8	8	8	8	3	2	1	2	3	4
9. Velocità	9	9	9	9	9	9	4	3	2	1	2	3
10. Stabilità	10	10	10	10	10	10	5	4	3	2	1	2
11. Economicità	11	11	11	11	11	11	6	5	4	3	2	1
12. Compatibilità ambientale	12	12	12	12	12	12	7	6	5	4	3	2

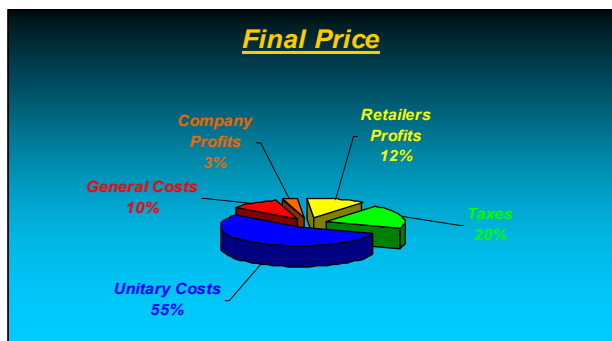
The last matrix used is the morphological one: it indicates all the technical requirements evaluated to design the machine and the path chosen, which corresponds to the final project.

Morphological Matrix			
Funzioni	Soluzioni		
	S1	S2	S3
1. Piastra scaldavivande	Acciaio	Alluminio	Lega metallica
2. Vasoio portafiltro	Plastica termoresistente	Alluminio	Lega metallica
3. Sistema produzione caffè	Per grandi quantità (a espulsione)	Per quantità ridotte (a boiler)	
4. Sistema produzione vapore	Pressione H2O calda		
5. Illuminazione sistemi lead	Lampadine	Illuminazione diffusa	
6. Comandi	Automatici	Semiautomatici	Manuali
7. Manico con aggancio	A pressione manuale	Viti	Bottoni
8. Contenitore acqua	Piccolo	Medio	Grande
9. Vaschetta residui caffè	Apribile	Semiapribile	Chiusa

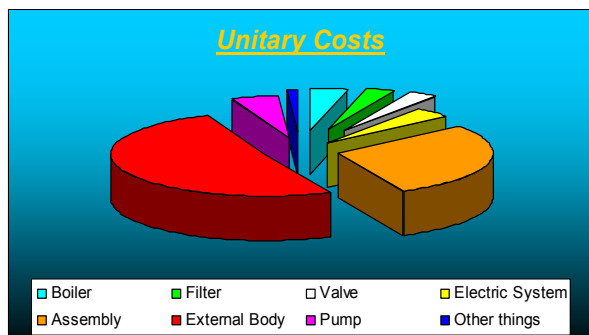
Industrialization of the product: Value Analysis and “design for assembly”

How can we apply this methodology to our coffee machine? We must begin from the Value Analysis of our product; then we can optimize the process, basing upon the results obtained.

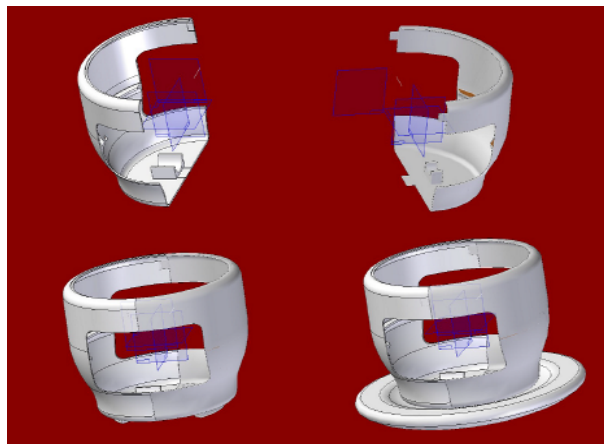
Value Analysis of the coffee machine: the final price of our coffee machine can be evaluated as we can see in the picture below. In the following picture there is the subdivision of all the costs forming final price:



In the next picture, instead, we have the subdivision of the unitary costs, which are the greatest ones:



“Design for Assembly”: for executing DfA in our coffee machine, we decided to realize an external body made only by two shells: the assembly of these two components is permitted by a forced connection; there are three plugs on the first one and three cavities on the other one. The assembly finishes with the connection of the plate, on the basis of the two shells connected. We can see it in the following pictures:

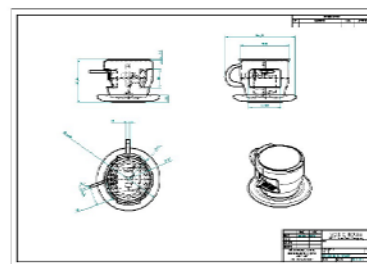


The Final Pictures

Through CAD applications (Solid Edge), we are able to define both 2D drawings and 3D pictures. This is an

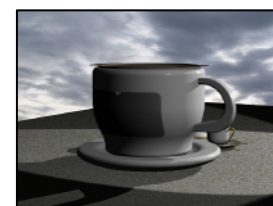
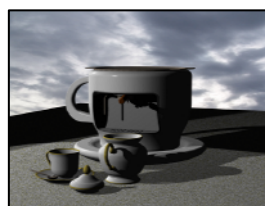
important point of the design process: in fact for the first time we can visualize our object as we imagined before and we can define the constructive design.

2D Drawings and 3D Pictures



Rendering Pictures

Rendering is the last phase of the project: it concerns the insertion of the new virtual object into a real environment, with real lights and shadows and real materials. In the following pictures, we can observe the rendering of our coffee machine.



Conclusions

This work is a sample of designing a simple object, using innovative methodologies as QFD, VA and DfA, which serve to improve quality during the process of design; they are part of the famous designing technique named Concurrent Engineering. QFD orders all the information which come along with each design project; VA evaluates all the costs that our project implicates; finally, DfA directs the design process towards the exemplification of all the components' shapes: in this way, we can obtain a product easy to be assembled.

Essential bibliography

[1] Alessandro Freddi, “Imparare a progettare”, Pitagora Editrice, Bologna 2005. [2] Bruno Munari, “Da cosa nasce cosa”, Editore Laterza, Bari 2002. [3] Bruno Munari, Design e comunicazione visiva. Economica Laterza. [4] Paolo Tedeschi. Disegno industriale. Edizioni Calderini Bologna. [5] Paola Biondi. Il Design in Italia dell'arredamento domestico. Giuliana Graminia. Umberto Allemandi & C. [6] Atlante del design italiano. Grassi, Pansera. Gruppo editoriale Fabbri

THE MODEL FOR GENERATING THE STRUCTURE OF THE NEURO – FAZI INFERENCE SYSTEM

M.Sc. Boban Andjelković, Ph. D. Vlastimir Đokić, Ph. D. Dragan Milčić¹

Resume: Mechanical elements design process has some critical variables, like coefficient of friction. This variable accuracy determines minimal working force for many mechanical connections based on friction. This coefficient is the function of many arguments. There are many theory for calculation for this coefficient. In this paper the two phases model of generating the neuro – fuzzy inference system is suggested: the prediction phase and the phase of application the knowledge gathered in this way in the proceedings of the adjustement of neuro – fuzzy systems.

Keywords: neural network, fuzzy logic, mechanical design, data structure recognition¹⁾

INTRODUCTION

Fuzzy inference systems and neural networks are an new aspect of reality comprehension and relations between phenomenons.

Fuzzy systems are working with rules in the parallel level. Complete rules base set includes all combinations of fuzzy inputs values. The size of the rule base increases exponentially with the number of fuzzy sistem inputs. The complete rule base of the Mamdani or the Takagi - Sugeno fuzzy inference system with n inputs and m linguistics values would be m^n rules. The big number rules calculations, including calculations in fuzzyfication phase and defuzzyfication phase, makes real working time of this composed system significantly long and unacceptable.

Compared to fuzzy inference systems, neural network provides hight level of accuracy [2]. But in spite of all already mentioned, some significant shortages were noticed:

- The small number of experimental data doesn't provide the set of informations for complete neural network education, good enough. The result of this fact indicates that there is a set of input data for which the neural network is not able enough to compute, even approximately, acceptable output results.
- The great complexity of received neural network doesn't provide interpretability of received results. In the other way, it is not

possible to create new scientific facts or conclusions, based on the neural networks structure and its function only.

THE NEW MODEL

These conclusions indicate that some of algorithms, already existed, could be used as knowlegde creation algoritms based on already existed experimental data and that final fuzzy inference system generation could be done based on the collected knowlegde and other hybrid neural – fuzzy and fuzzy – neural models. In this way, the newly created konwlegde, received in the first phase, could be, in the mostly effective way, build in the new fuzzy system. In the same time, a unwanted influence of experimental data set, with small number of elements, would be avoided.

The new estimation model structure (fig. 1):

The Prediction Phase

- Creating the set of experimental data for the phase of the konwlegde creation
- Collecting and the systematization the present knowlegde in the algorithm form.
- Algorithm for the knowlegde generation with the lot of technics application:
 - The technique of the reduction the number of input variables

¹ M. Sc. Boban Andjelković, Mechanical faculty, Niš, bandjel@mail.ru
Ph. D. Vlastimir Đokić, Mechanical faculty, Niš, dzul@mail.ru
Ph. D. Dragan Milčić, Mechanical faculty, Niš, dmilcic@ptt.yu

- The technique of the deduction the number of inference rules
- The technique of the fuzzy set reduction, based on their similarities.
- The phase of the induced knowledge synthesis and the synthesis of adaptable neural – fuzzy systems in the course of the new neural – fuzzy inference system development.

The Final Phase

- Creating a set of the final neural – fuzzy system education data
- The final neural – fuzzy system synthesis
- The neural – fuzzy optimisation based on new knowledges (transformational techniques)

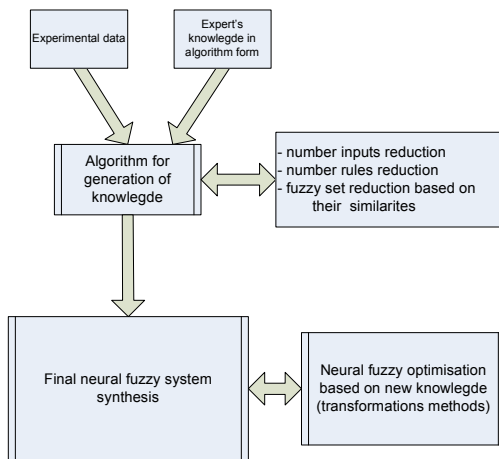


fig. 1 New model estimation structure

If rules, based on empirical facts or knowledge, are defined as a part of the initial fuzzy logical systems, this system could be used for education. This is also usable in the cases when we are not sure of the rule correctness.

CLASSICAL ALGORITHM FOR THE FRICTION COEFFICIENT ESTIMATION

The model for the neural – fuzzy system, we described here, is tested on the problem of the ordering the variable coefficient of press fits.

Theoretical searchings of the friction coefficient are based on experimental data. It is possible to separate three groups of influential factors:

- The roughness of surfaces of contact
- The surfaces of contact hardness. This factor hasn't an homogeneous influence on the friction coefficient value.
- The surfaces of cleanliness.

During the process of impressing a hard element in a soft one, deformations of a hard element are less than

deformations of a soft. According to this, characteristics of the element whose surface shows a higher level of hardness, are decisive for this estimate. The one of algorithms for the estimation of the friction coefficient value [1] we can show at the fig. 2.

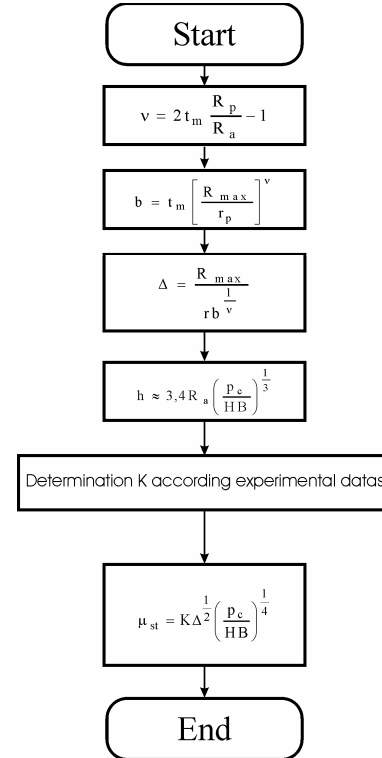


fig. 2 The classical algorithm for the friction coefficient estimation

THE APPLICATION AND RESULTS

The new model for the estimation was applied on the set of experimental data, received by examination of press fits on the occasion of separating the cartridge case from the shaft. Friction coefficient was measured indirectly by measuring the maximal force on the occasion of the fit disassembling process. Since the surface of contact value is known as well as the value of the surface pressure, the value of the friction coefficient is calculated according to:

$$\mu = \frac{F}{p \pi d l} \quad (1)$$

The application of the expert's knowledge and already existed algorithm models (fig. 2) leads to the basic fuzzy inference model creating with 18 rules.

By the reduction of input variables (aggregation methods), the number of the fuzzy sets, based on the similarity and different methods of the rule number reduction, the initial fuzzy system is simplified in the system of four rules only. The fuzzy surface we received is showed at the fig. 3 [4].

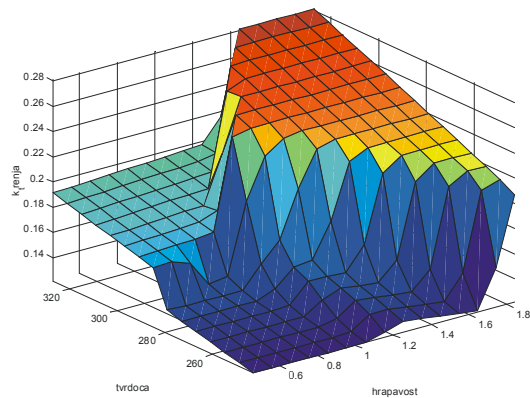


fig. 3 The FIS surface of the system with two input data, one output variable and with four rules

According to the analyze of this FIS surface it is possible to make a conclusion as follows:

- The sudden rise of the friction coefficient value, existence in the narrow zone of the roughness change and the material surfaces hardness, is the result of the small number of data set which were used in the FIS surface creating. This rise makes the surface received unreliable for a practical use.
- The connection between the friction coefficient value, at the one side, and the contact fits roughness and the surface's hardness, at the other, is noticeable. This connection is possible to show in the following way:

With the rise of the effective roughness value and the surface's hardness, the value of the friction coefficient rises too

The existence of such relation makes it possible to direct correctly the course of the other experimental data set processing, in the *final phase*.

In order to achieve better characteristics the initial neural fuzzy system has some weight factors. Two group of factors are included:

- the level of the fuzzy rules education and
- the level of the articles function education

These factors have the role of weight factors and make it possible different influences of particular fuzzy rule in the final fuzzy conclusion.

After the neural fuzzy system education, the final fuzzy inference system showed on the fig. 4 and fig. 5, was received. This system consists of 9 rules i.

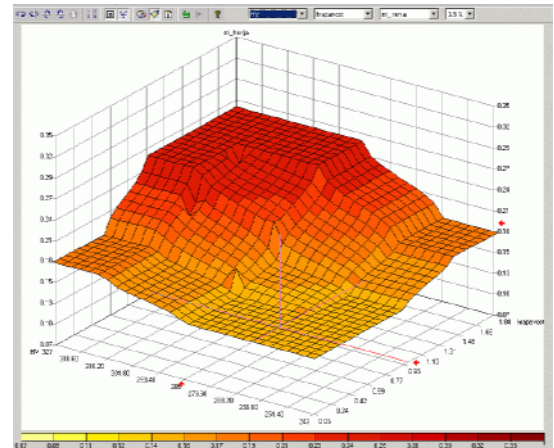


fig. 4 The final fuzzy surface

#	IF	THEN
1	hrapavost [1.00] tvrdoca [1.00]	k_tg [1.00]
2	hrapavost [1.00] tvrdoca [1.00]	k_tg [1.00]
3	hrapavost [1.00] tvrdoca [1.00]	k_tg [1.00]
4	hrapavost [1.00] tvrdoca [1.00]	k_tg [1.00]
5	hrapavost [1.00] tvrdoca [1.00]	k_tg [1.00]
6	hrapavost [1.00] tvrdoca [1.00]	k_tg [1.00]
7	hrapavost [1.00] tvrdoca [1.00]	k_tg [1.00]
8	hrapavost [1.00] tvrdoca [1.00]	k_tg [1.00]
9	hrapavost [1.00] tvrdoca [1.00]	k_tg [1.00]

fig. 5 Fuzzy rules of the final inference system

The final searching form was carried out in the form of the computer program (fig. 6) able enough to determine of friction coefficient value, for assigned input roughness values and for surface's hardness of both elements in press fit.

During program developing, the full attention was payed about modulated structure (fig. 7) in the way to accomplish the fuzzy inference system as an independent unit, who permits a dynamic calls trough the appropriate function library.

The modulated organisation enables the independence of the program code from the code who performs fuzzy calculations. It is possible, in this way, to change the whole program in a easy way by changing only one segment intended for fuzzy calculations.



fig. 6 Accomplished program based on the carried out researchings

THE CONCLUSION

Results received by using a limited experimental data set with small number of datas, are very optimistic. Applied data set enables creating an scientific relation, in the *predictional phase*, who applies successfully in all following phases and who enables the development of the neural fuzzy inference system. On the other hand, it

wouldn't possible to reach usable neural fuzzy system by usual proceedings of experimental data analyze.

LITERATURA

- [1] D. Stamenković: **Press fits capacity researching as a tribo - system in the scope of railroad vehicles driving system**, Niš, 1999
- [2] Ilić, V.: **The neural nets education for cyrillic letters recognizing**, master of science thesis, Tehnički Fakultet "Mihajlo Pupin", Zrenjanin, 1999
- [3] Miltenović V., Milčić D.: **Aplication artifical intelligence for the gear power transmitters design**. The Third International Conference "HEAVY MACHINERY 'HM 99", Proceedings, Kraljevo, 28 – 30 October 1999, s. 7.15 – 7.20.
- [4] Olaf Wolkenhauer: **Fuzzy Toolbox for use with Matlab / Simulink**, 1996
- [5] Claudio Moraga: **Neuro – Fuzzy Modeling between minimum and maximum**, Computational Intelligence – Theory and Applications, February 27, 2001, Niš, pp. 21 – 2

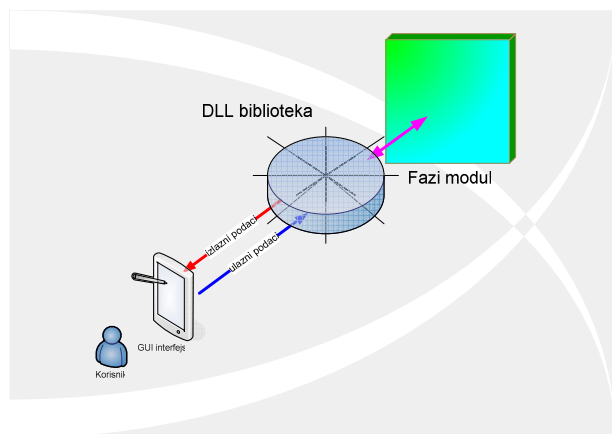


fig. 7 The structure of the program for the fuzzy estimation of the friction coefficient value

NONLINEAR CONTACT ANALYSIS OF THE HEAVY STRUCTURE SUPPORT

Jovanović M., Milić P., Mijajlović D.

The paper deals with contact problem in huge rolling supports, used in industry and buildings. One of the main questions is the choice of the analysis type for the carrying elements check. In this paper nonlinear contact static analysis was applied. Nonlinear analysis better define the stress distribution in the structure, because it uses variable boundary conditions, friction, sliding and the rigidity of bodies in contact. The results are given graphically and numerically. The finite element mesh, the model properties and composite stresses in contact zones are shown. The objective evaluation of these analyses gave the support behavior in practice.

Key words: Contact analysis, FEM, heavy support

1. INTRODUCTION

The structural analysis of the biggest rolling supports is an exclusive category with the demand of highest engineering reliability. Therefore numerical solutions using Finite Element Method were calculated. The technical solution for the given support [5] was used for the analysis, formed of two flat plates with the rolling body in between. The plates and the rolling body are massive constructive elements of alloy steel, fig. 1. How much engineering solutions of the model can differ is the most important question. This question can be directly answered if number of contact analyses is done. Real industrial tasks overreach the complexity of *Hertz's* model because of the bending as an additive influence. Furthermore, plastic deformation can appear in the construction, which inducts sliding of the contact surfaces. The solution of one real task and the solution model are shown in the following text.

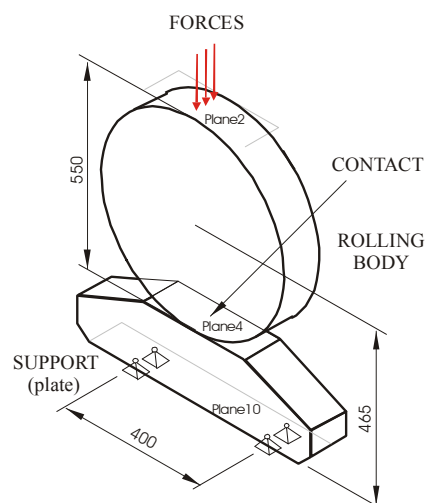


Figure 1. The analysed rolling support geometry

2. NONLINEAR CONTACT ANALYSIS

The basic reason for nonlinearity of contact task is caused by the boundary conditions change during the contact force initiation (growth). The modern contact tasks analysis is realized using **method of direct constraints**. It is realized using contact pairs [4, 5]. The contact pairs in the cylinder and surface contact are **contact surfaces**. Hereby the **target** and **contact** surfaces are defined. The method follows the kinematics of the contact surface, resulting in boundary conditions defining in the moment of contact, along with the further movement restriction. In the touching nodes contact forces F_i are applied. This method determines: the collective of finite elements where the bodies are in contact, the collectives of nodes that potentially can get in touch and the edges that potentially get in touch.

The given discrete 3D mesh passes through these contact boundary surfaces. The nodes in the contact area are the contact analysis carriers. To this nodes the spherical (pinball) tolerant potential contact areas are assigned, fig 2.

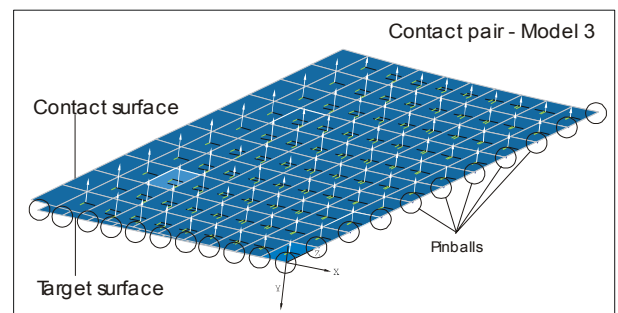


Figure 2. Contact model "surface-to-surface"

When the node of other contact surface enters tolerant area, the mechanical conditions of the contact are placed.

The way of pressure realization, the movement direction, possible sliding, and the target surface nodes rigidity is defined.

This is realized using *Gaussian* method. It identifies the Gaussian points that are in contact, which ones are out of contact, and which ones are near contact. This way the non-linear analysis boundary conditions were defined, which do not depend on the initial assumptions about the contact pair rigidity. The real contact points' rigidity is determined in details in every analysis step. This way the assumptions about the model rigidity are eliminated and the real contact points' rigidity is used. The solution is obtained using *Full Newton-Raphson method*. The *Penalty method* can also be used.

The second reason of model nonlinearity is induced by the plastic material deformations caused by the possible excess of nominal stresses allowed. It can happen at constructions in civil engineering which duration period is 50 to 100 years. Supporting structures are exposed to unpredicted-incidental events.

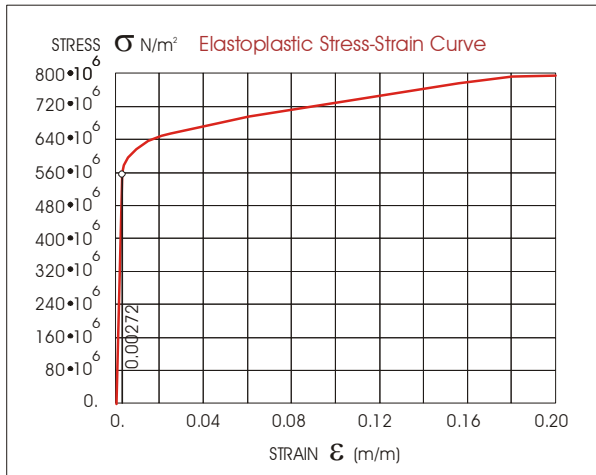


Figure 3. Curve of elasto-plastic stress-strain material (Chrome-nickel steel)

According to *Prandtl-Reuss* elasto-plastic problem generalization, the plastic deformations are proportional to the stress deviator [2]. Appropriate to this model, the total stress state was determined according to the equivalent increment of plastic deformation and equivalent stress. The equivalent stress in plastic area σ_e corresponds to the normal component stresses $\sigma_x, \sigma_y, \sigma_z$ and tangent stresses $\tau_{xy}, \tau_{yz}, \tau_{xz}$, and also is proportional to the octaedic shear stress $\tau_{okt}^{(1)}$, as shown in relation (1):

$$\sigma_e = \frac{1}{\sqrt{2}} \cdot \left[(\sigma_x - \sigma_y)^2 + (\sigma_y - \sigma_z)^2 + (\sigma_z - \sigma_x)^2 + 6 \cdot \tau_{xy}^2 + 6 \cdot \tau_{yz}^2 + 6 \cdot \tau_{xz}^2 \right]^{0.5} = \frac{3}{\sqrt{2}} \cdot \tau_{okt} \quad (1)$$

¹ Octaedic shear stress is dependant on plasticity

The task was solved using full incremental *Newton-Raphson* method. The displacements until reaching the contact are large. The procedure is based on iterative solutions of the equation:

$$[K_{n,i}^T] \cdot \{\Delta u_i\} = \{F_n^a\} - \{F_{n,i}^{nr}\} \quad (2)$$

In the equation (2) $[K_{n,i}^T]$ is the Tangent rigidity matrix for the step n in the iteration i in *Newton-Raphson* method. $\{F_n^a\}$ is overall (absolute) force vector in the step n , while $\{F_{n,i}^{nr}\}$ is force vector for the step n in the iteration i . $\{\Delta u_i\}$ is the vector of the searched solutions for node displacements of the discrete system. *Newton-Raphson* large displacements method (*The large strain analysis*) is always recommended when as the consequence of the contact bodies results in their shape change or change of the contact surfaces orientations.

The iterative process convergence is achieved when residuum is less then the tolerance for the given value. Default tolerance value is 0.001. The convergence was checked using L2 norm (Euclid norm), which is formed as a square root of the sum of unbalanced forces, squares R_i , in all degrees of freedom given in the equation.

$$L_{2\text{norm}} = \|\{R\}\|_2 = \left(\sum R_i^2 \right)^{0.5} \quad (3)$$

The ANSYS software uses contact *Augmented Lagrange algorithm*. The concept of Gauss allows modeling of different mechanical models contact situations. These are the situations of penetration, the preceding penetration, possibility/impossibility of separation, large/small contact deformations. In the tetrahedral or wedge elements application, the contact surfaces are triangles and they do not have to obtain the full topological contact up to the element edges. As a result, the nonsymmetry of the finite elements engaged appears in the contact pair. This possibility is given by the analysis algorithm, which improves the numerical stability. Also, in this kind of analysis the initial closing can be given – the dimension of the contact applied. This eliminates the situation, that the Gaussian points do not identify the whole contact area, or that they pass one through another without cutting in the two neighboring iterations.

The tribological phenomena of inner friction are implemented in the the contact task using exponential function (4), [4]:

$$\mu = \mu_d \cdot \left[1 + (k-1)^{-d \cdot v} \right] \quad (4)$$

In the equation (4), μ is the theoretical friction coefficient, μ_d is the dynamic friction coefficient, k is

the static and dynamic friction quotient, d is decay coefficient (sec/m), v is the slip rate ($\mu=0.2$).

The given task of the MODEL-3 has 10150 3D solid basic elements, 100 contact elements **TARGE 170** and 100 contact elements **CONTA 174**. Taking into account the model symmetry, the problem was described with 12155 nodes and 34425 degrees of freedom. Figs. 4 and 5 illustrate details of the non-linear contact analysis results for the whole MODEL-3 (shown on fig.1). The analysis comprises the both contact bodies.

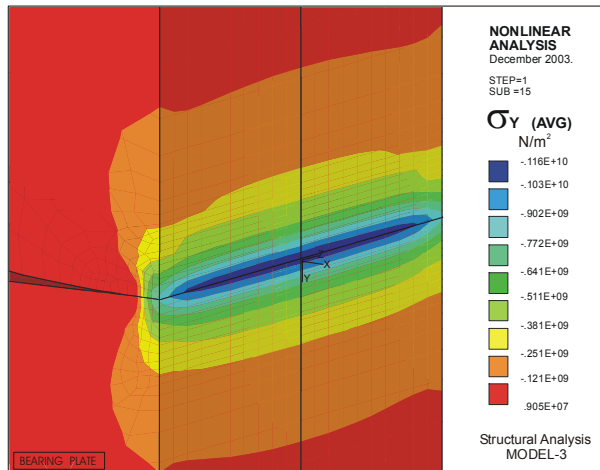


Figure 4. The contact zone detail - normal component stresses σ_Y (MODEL-3)

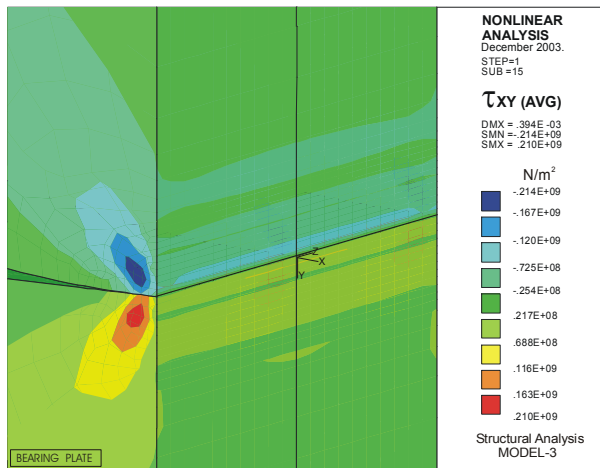


Figure 5. The contact zone detail - tangent component stresses τ_{XY} (MODEL-3)

Fig. 4 shows the area of the maximal normal component stresses, which amounts $1160 \cdot 10^6$ N/m². Fig. 5 shows the area of the maximal tangent component stresses for the both elements in connection.

This way the complexity of the contact geometry mechanism was improved. The friction characterized with the "steel-to-steel" model was involved, as used in friction joints. The use of the real material characteristics gives the realistic picture of stresses

(fig. 5Error! Reference source not found.), based on numerically determined deformations. It primarily refers to the situation of elasto-plastic deformations state, which is identified in this analysis and experimentally found damages on the real object, [6].

3. THE RESULTS OF ANALYSIS

The calculated results for the stresses and deformations give the basis for the contact pair accuracy evaluation. Deformations are non-adequate evaluation criterion, because the reliance conditions for the models used differ significantly. Therefore the equivalent stresses calculated according to the theory of the biggest deformation work used for shape deformation (*Hencky-Hubert-Mises*, better known as *Von Mises*) are the basic criterion for the engineering model validity evaluation. Principal stresses σ_1 , σ_2 , σ_3 are calculated based on component stresses σ_x , σ_y , σ_z , τ_{xy} , τ_{yz} , τ_{xz} and maximal tangent τ_{MAX} . The following table T1 gives the overview of the analysis.

Fig. 6 shows the equivalent stresses for the MODEL-3.

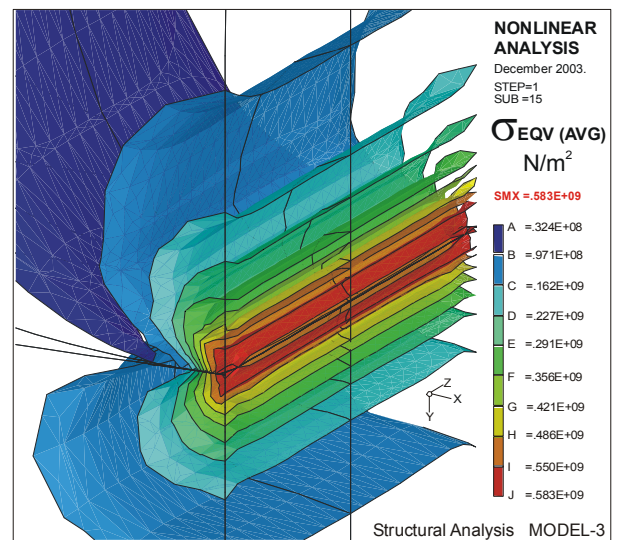


Figure 6. The equivalent stresses in non-linear analysis (MODEL-3)

Table T1

Model for analysis	MODEL-3
Number of elements (3D)	10150
Number of gap/contact elements (1D)	200
Number of nodes	12155
Degrees of freedom (DOF)	34425
Max. Equivalent stress in contact area	563340000 (N/m ²)
Max. Tangential stress in contact area	210000000 (N/m ²)
Deformation Δy	0.000394 (m)

The calculated equivalent stresses in non-linear analyses MODEL-3 are $563.000 \cdot 10^6 \text{ N/m}^2$ and they are caused by different contact rigidity. The calculated contact stresses aren't only the consequence of the contact pressure, but also the plate bending. In the analysis MODEL-3 the friction stresses of lower order showed up, fig. 8. The equivalent plasticity stresses (in the contact zone) of MODEL-3 are given on fig. 7.

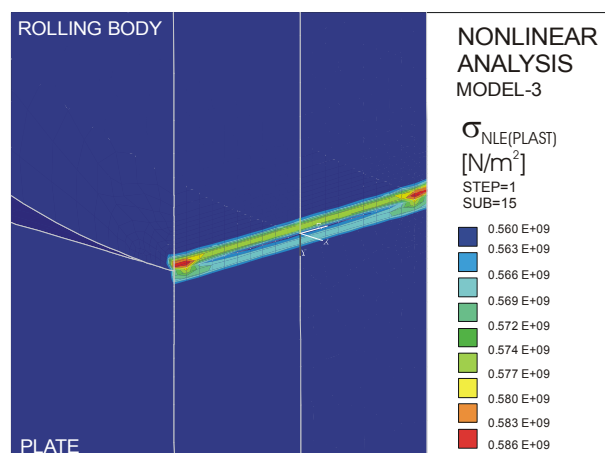


Figure 7. The equivalent plastic stresses in (MODEL-3) (in the contact zone)

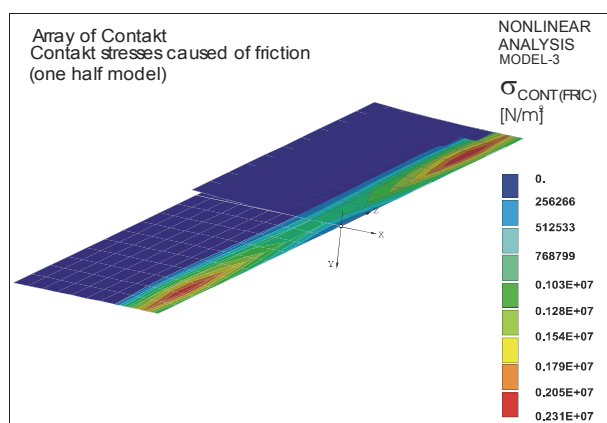


Figure 8. Contact friction stresses in MODEL-3 (the contact zone)

4. CONCLUSION

The whole analysis is the example of complex responsible structure treatment. The contact zone is the place of the highest stress in the support plate. The stresses of this analysis gave, represent the spatial state

of stresses which comprises the plate deflection influence (as global deformation) and contact pressure (as local deformation). The classical *Hertz* theory and the existing regulations for constructions offer safety coefficients and allowed stresses for the tensile, bending, shear, contact pressure cases, but not for combination of influences of bending and surface pressure for the spatial state of stresses.

The obtained maximal stress $\sigma_{\text{VON MISES}} = 595295008 \text{ N/m}^2$ in the previously performed linear contact analysis is larger than contact stress in the non-linear analyses [6] as the consequence of plastic material deformation. The appearance of large stresses points out to the existence of plastic yield stresses and the risk which brings along the linear analysis. The compound stress is, on the other hand, much larger then the bending stresses, calculated using the classical bending theory procedure ($\sigma_s = 125 \cdot 10^6 \text{ N/m}^2$). The combination of contact influence and bending of the plate for now can only be viewed through equivalent stress. The comprehension for the shearing and normal stresses influence and the plastic states elimination is the necessary category for definition of the contact element construction. This can be efficiently realized using the contact analyses group for the known geometry whose maximal structural action is searched for.

REFERENCES

- [1] Timoshenko S., STRENGTH OF MATERIALS, Part II, Princeton, New Jersey, 1956.
- [2] Kojić M.: APPLIED THEORY PLASTICITY, University of Kragujevac, 1979.
- [3] Jovanović M., Vacev T., Jovanović M.: Stress-Strain Sliding-Plate support Analysis of the middle head, Naval shiping port the Power-station "ĐERDAP-1" Kladovo, Report, MININSTITUT, MIN Holding Co., Niš, 1998.
- [4] ANSYS - Release 7.0, Theory Reference, Nonlinear Structural Analysis, 2000.
- [5] MSC/NASTRAN for Windows V 4.0, Theory Reference, FEMAP, 1998.
- [6] Jovanović M., Milić P., Mijajlović D.: THE APPROXIMATE CONTACT MODELS OF THE ROLLING SUPPORTS, Facta Universitates – Mechanical Engineering Series, vol. 2, University of Niš, 2004.

CALCULATION OF DOUBLE PARABOLOID SPRINGS

Nikola Janković¹

Abstract

In this paper, calculation of double paraboloid springs are presented. Springs are very important element, because large movement in elastic joint, accumulation of energy and depreciation of shock are enabled. In any examples in practise, it is very useful to appliance springs with nonlinear characteristic.

In this paper, special care is based on calculation of flexion, calculation of forces, calculation of stress and geometry calculation of double paraboloid spring. All results with corresponding tables and figures are presented.

Key words: spring, nonlinear characteristic, flexion, stress, spring geometry, Arhimed's spiral, hiperboloid

1.0 INTRODUCTION

Double paraboloid springs are wire with very little value of diameter and very large value of length, which is wind like shape of Arhimed's spiral. At this type of springs, large value of deformation are enabled.

Double paraboloid springs have shape of parabola which make nonlinear characteristic with large value of loads. Diameter of coil is less by degrees from middle of spring to spring seat. Coil with bigger diameter have bigger deformation from coil with less diameter. When the load increase deformation increase linearly by the moment when the coils with the biggest diameter start to seat on surface of contact. This coils don't participate in deformation of spring, number of active coils is less and rigidity is progressive increase. In diagram of spring characteristic have two different part. The first part of curve is linear by the moment when one coil start seat on another coil, and the second part of curve have progressive increase.

There are two type of coil snug. The first type is that coils seat on another coils, and the second type is that coils enter in another coils. In the second type, spring have shape of Arhimed's spiral. In this case there are less number of active coils z_a and less value of diameter D_v , and it makes to progressive increase of springs rigidity.

In the example which is presented in this paper, spring are made by steel wire with diameter $d = 5,6$ mm,

free length of spring $L_0 = 200$ mm, number of active coils $z_a = 6$, diameters of spring $D_m = 35$ mm, $D_v = 86,6$ mm and $\alpha = 30 \div 26^\circ$.

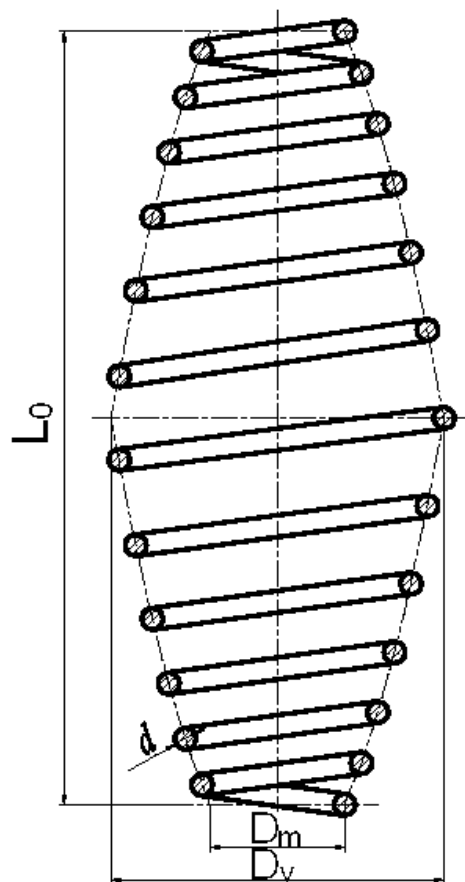


Figure 1. Design of double paraboloid spring

¹ Nikola Janković, dipl. maš. ing., Mašinski fakultet u Kragujevcu, Sestre Janjić 6, 34000 Kragujevac

2.0 CALCULATION OF FLEXION AND FORCES IN SPRING

Requirement: $D_v - D_m = 51,6$ mm

$$d \cdot z_a = 33,6 \text{ mm}$$

$51,6 > 33,6 \Rightarrow$ Type R of double paraboloid spring is used.

Geometry rate of arithmetic means:

$$q = \frac{D_m}{D_v} = 0,4042$$

Flexion of spring on the end of lineary part:

$$f_2 = \frac{(1 + q^2) \cdot L_0}{2} = 116,3343 \text{ mm}$$

Force of spring on the end of linear part:

$$F_2 = \frac{G \cdot d^4 \cdot L_0}{4 \cdot z_a \cdot D_v^2 \cdot (D_m + D_v)} = 745,8983 \text{ N}$$

where:

$G = 83000$ N/mm² – modules of elasticity in shear.

Rigidity of spring in linear range:

$$c_2 = \frac{F_2}{f_2} = 6,4117 \text{ N/mm}$$

Force in spring with maximal flexion:

$$F_B < \frac{F_2}{q^2} = 4566,4562 \text{ N} \Rightarrow F_B \approx 4,57 \text{ kN}$$

Forces and flexions at progressive part of characteristic:

$$f_n = \frac{L_0}{2 \cdot (1 - q^2)} \cdot \left(2 - \frac{F_2}{F_n} - \frac{F_n}{F_2} \cdot q^4 \right)$$

Table 1. Value of flexion and forces in spring

α [°]	f_n [mm]	F [N]	F_n [N]
30	116,3343	745,898	745,898
29	121,4843	778,918	780,494
28	126,4843	810,977	817,403
27	131,3143	841,945	856,658
26	135,9943	871,952	898,618

where:

f - flexion of spring

F - theoretic force in spring ($F = f \cdot c$)

F_n - really force in spring

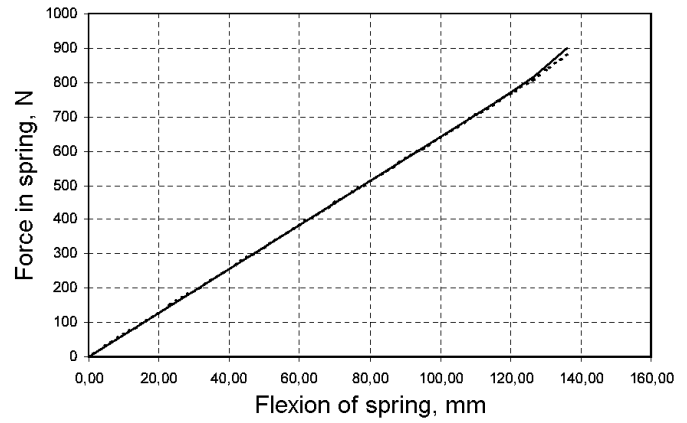


Figure 2. Characteristic of spring

In diagram with characteristic of spring, with broken line is shown characteristic of ideally, and with solid line is shown characteristic of really spring.

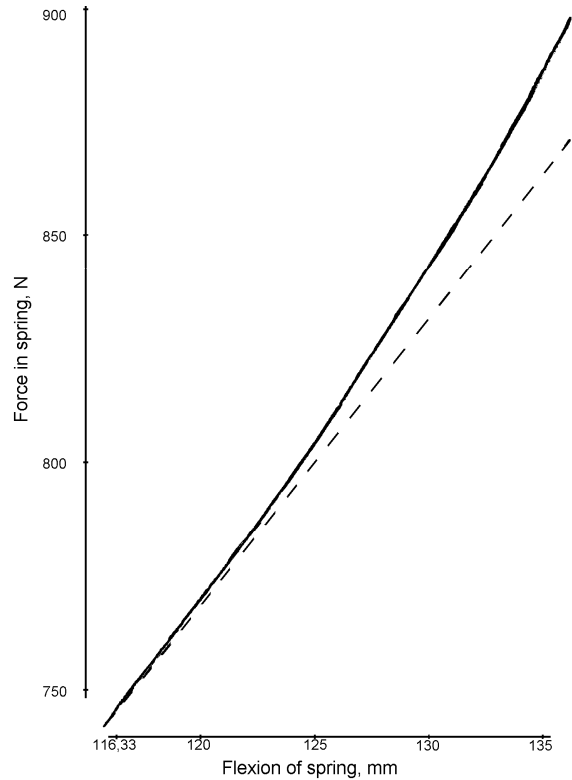


Figure 3. Progressive part of characteristic

3.0 CALCULATION OF STRESS IN SPRING

Double paraboloid spring have unequal value of stress. Stress is comparatively with diameter of coil and with rate of diameters $K=D/d$. Coil with the biggest diameter have the biggest value of stress, too. If diameter D is less then coefficient k will increase so this observation must not be true. Comparison between value of stress at the end of spring and in the middle part of spring is necessary.

The biggest value of theoretic force in spring:

$$F = 871,952 \text{ N}$$

Arithmetic mean of diameter:

$$D_{sr} = \frac{D_m + D_v}{2} = 60,8 \text{ mm}$$

Maximal torsional stress:

$$\tau_{idop} = 0,56 \cdot \sigma_M = 884,8 \text{ N/mm}^2$$

where $\sigma_M = 1580 \text{ N/mm}^2$ - minimal value of tensile strength of wire

Coefficient k:

$$k = \frac{4 \cdot K - 1}{4 \cdot K - 4} + \frac{0,615}{K} = 0,133$$

$$\text{where } K = \frac{D_{sr}}{d} = 10,8571$$

Ideally torsional stress:

$$\tau_i = \frac{8 \cdot D_{sr} \cdot F}{\pi \cdot d^3} = 768,727 \text{ N/mm}^2$$

Requirement $\tau_i < \tau_{idop}$

$768,727 < 884,8 \Rightarrow$ Requirement is complete.

Maximal torsional stress:

$$\tau_{max} = k \cdot \tau_i = 870,968 \text{ N/mm}^2$$

4.0 GEOMETRY CALCULATION

Selection of dimension of double paraboloid spring is based on necessary condition of work, necessary rigidity and necessary safe in work.

In this part, equation of Arhimed's spiral and equation of paraboloid are defined, and Arhimed's spiral and paraboloid are constructed.

4.1 Equation of Arhimed's spiral

$$D_{mi} = D_m + \frac{D_v - D_m}{2 \cdot \pi \cdot z_a} \cdot \varphi$$

$$R_{mi} = R_m + \frac{R_v - R_m}{2 \cdot \pi \cdot z_a} \cdot \varphi$$

where: R_{mi} - radial of arhimed's spiral

φ - angle

Table 2. Value of radius of Arhimed's spiral

φ	R_{mi}
0	17,50
$\pi / 4$	18,04
$\pi / 2$	18,57
$3\pi / 4$	19,11
π	19,65
$5\pi / 4$	20,19
$3\pi / 2$	20,72
$7\pi / 4$	21,26
2π	21,80

For drawing Arhimed's spiral nine points are defined, with jumping change angle of Arhimed's spiral with value of $\pi / 4$.

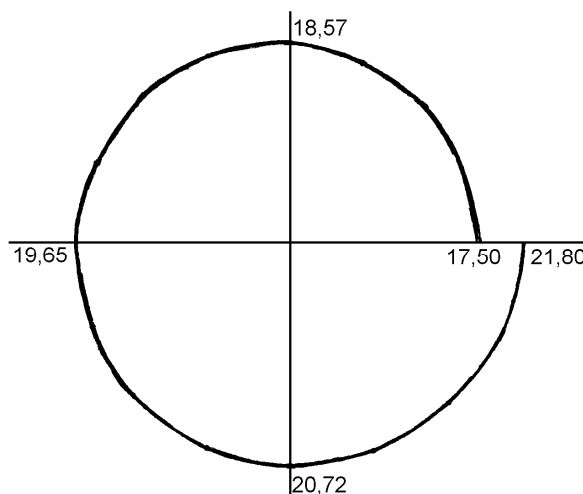


Figure 4. Arhimed's spiral

4.2 Equation of paraboloid

$$L_{y1} = \frac{L_0 \cdot D_m^2}{2 \cdot (D_v^2 - D_m^2)} = 19,5233 \text{ mm}$$

$$a = \sqrt{\frac{D_m^2}{4 \cdot L_{y1}}} = 3,9606$$

$$L_{yli} = \frac{D_{mi}^2}{4 \cdot a^2}$$

where: L_{yli} - height of paraboloid which depend from radius of paraboloid

Table 3. Value of height paraboloid

D_{mi} [mm]	L_{yli} [mm]
35	19,52
40	25,50
45	32,27
50	39,84
55	48,21
60	57,37
65	67,33
70	78,09
75	89,65
80	102,00
85	115,15
86,6	119,52

For drawing paraboloid twelve points are defined, with jumping change diameter of Arhimed's spiral with value of 5 mm.

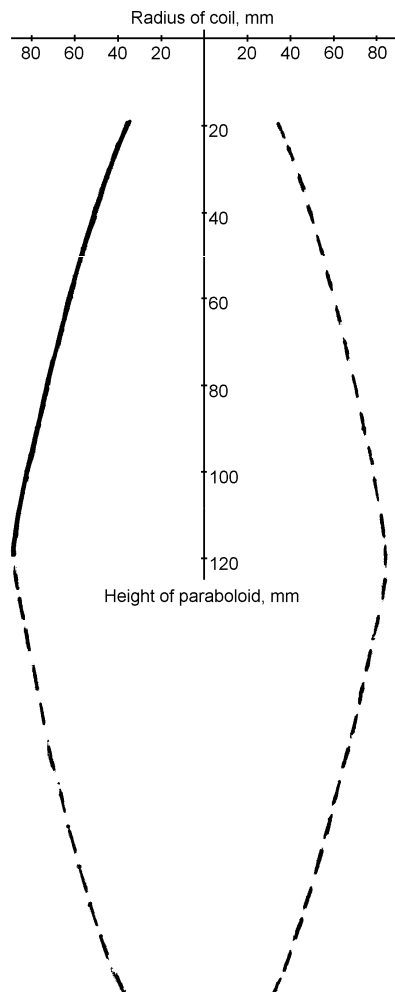


Figure 5. Shape of paraboloid

5.0 CONCLUSION

Double paraboloid spring have very specific shape, which made it possible for large deformation. This type of spring may have very small height at the moment when all active coils are blocked.

It is very useful to apply double paraboloid springs in case when it is necessary progressive increase of rigidity during work. Figure 2 shown characteristic of double paraboloid spring. The first part of this characteristic is linear curve. If the value of loads increase, then this characteristic will be progressive.

Coils with bigger diameter are much easy deformed from coils with less diameter. When load increase, than deformation linearly increase, while coils with the biggest diameter start to seat on surface of contact. This coils are blocked, than number of active coils are less and rigidity of spring progressive increase, which means that this characteristic become nonlinear

The biggest value of stress is placed on coil with the biggest diameter. Depending from value of coefficient k , maximal value of stress may be placed on some other coil.

LITERATURE

- [1] Janković N., Primena novih oblika zavojnih opruga sa nelinearnom karakteristikom na vozila, Diplomski rad, Kragujevac, 2002.
- [2] Ognjanović M., V. Miltenović, Mašinski elementi I – Mašinski spojevi, Mašinski fakultet Beograd – Niš, 1996.
- [3] Decker K. H., Elementi strojeva, Tehnička knjiga, Zagreb, 1987.

DYNAMIC ANALYSIS OF MULTIPLY GEAR

Ana Pavlović,
Prof. dr Vera Nikolić-Stanojević, Dipl. Eng.
Mr. Dejan Dimitrijević

1. Abstract

New technology and development of new software have been enabled a big step in research of mechanical systems and their components. Porous of this paper is to show us dynamical analysis of multiply gear. Dynamical forces have much more affect than static on efficient work of a system and therefore, this paper is dedicated to that analysis. The exploitation show that the level of noise and vibration also depend on this kind of load. The efficiency and precision of one mechanical part depends on well checked dynamic analysis. For this analysis have been used various software for modeling (Autodesk-Mechanical Desktop, Autodesk Inventor Professional 9) and construction analysis (COSMOS/M, ANSYS).

2.1. Basic equations for dynamic analysis

Important time dependence in dynamic analysis is movement of observed part according to variable load. Dynamical forces also called *motivation forces* because the responses of system affected with, are very complicated.

The mathematical expressions shown bellow have more importance for this analysis. The basic equation is **equation of moving** from where we can get movement in time:

Starting from Hamilton's

$$\int_{t_1}^{t_2} \delta(E_k - \Pi) dt + \int_{t_1}^{t_2} \delta W dt = 0 \quad (1)$$

And D'Alamber's principle

$$F_{st} + F_{in} = 0 \quad (2)$$

E_k —all kinetic energy

Π -- All potential energy of internal and external forces

W —doing of unconservation forces

$L = E_k - \Pi + W$ -----functional of Lagrange

Hamilton's principle shown that real movement is those for witch LaGrange's function has a static value:

$$\delta \Pi = 0 \quad (3)$$

$$E_k = E_k(q_i, \dot{q}_i) \quad \Pi = \Pi(q_i) \quad \delta W = Q_i \delta q_i \quad (4)$$

For $\delta q_i(t_1) = \delta q_i(t_2) = 0$ from this we have:

Equation of Lagrange of second rang

$$\frac{d}{dt} \left(\frac{\partial E_k}{\partial \dot{q}_i} \right) - \frac{\partial E_k}{\partial q_i} + \frac{\partial \Pi}{\partial q_i} = 0 \quad (5)$$

Generic coordinates have been used in dynamic analysis because it's easy to determinate position of system in any moment of time.

For system without suppression we have **equation in matrix shape**:

$$[m] \ddot{q} + [k] q = \{Q\} \quad (6)$$

$[m]$ - Mass matrix

$[k]$ - Rigidity matrix

$\{Q\}$ - Vector of generated forces

The only forces that affect on all masses of system are those which set-up under influence of inner forces.

According that equation (6) becomes:

$$[m] \ddot{q} + [k] q = 0 \quad (7)$$

This equation represents **differential equation of proper oscillation**. According to D'Alamber's principle, inner forces are in balance with inertial forces, so we have:

$$-[m] \ddot{q} = [k] q \quad (8)$$

The free frequency of the system and their main shapes has been gotten from **equation of frequency**:

1) Student of 5th year on Faculty of Mechanical Engineering in Kragujevac,
University of Kragujevac Bunjevačka 2, 34000 Kragujevac, Serbia and Montenegro, (miakg@eunet.yu)
2) Faculty of Mechanical Engineering in Kragujevac, Sestre Janić 6,
34000 Kragujevac, Serbia and Montenegro

QUALITATIVE PARAMETRES OF THE REGENERATION OF THE DAMAGED GEARS OF THE FIRST GEAR AND REVERSE IN GEAR BOX OF THE HEAVY LOAD TRUCKS

Dr Svetislav Lj. Markovic, Dr Danica Josifovic, Dr Slobodan Tanasijevic, M.Sc. Snezana Ciric-Kostic*

Abstract: In this paper are given some fundamental considerations about gears regeneration, and the general technological procedure of damaged gears regeneration is explained. The hard facing of damaged gears' teeth is usually done by the MMA welding procedure. Regenerated gears are then relaxed, mechanically machined, and by thermal treatment teeth working surfaces hardness is brought to values that are prescribed by technical documentation. Besides that, in the paper are presented results of testing the cylindrical involute spur gears, and the survey is given of the regenerated gears quality parameters. It was show that, gears that had different types of damages, can, by application of hard facing be reliably and economically efficiently regenerated.

Key words: Gear teeth hard facing, gear regeneration, economic efficiency.

1. INTRODUCTION

Irregularities that occur on gears during exploitation can be divided into: damages of the gear hub (wear of holes, wedge grooves or grooved holes, cracks, etc.), of the gear body (cracks at spokes, radial and axial eccentricity), and of the gear teeth. Gear damages can be divided into three groups: wear, plastic deformation and teeth fracture. The large number of types of wear was identified, but the predominant influence on loss of the working capabilities of gears has the destructive pitting. Plastically deformed teeth worsen the conjugate action and contribute to appearance of internal damages. The teeth fracture can be complete or partial fracture of one tooth or several teeth. Fracture of the whole tooth causes immediate withdrawal of a gear from exploitation and by that also of a transmitter to which it belongs. The working ability of gears frequently determines the working life of the belonging machine system. Today

exists the whole series of methods for more or less successful regeneration of damaged teeth. Most frequently applied are the following:

- hard facing of grooves,
- inserts of additional bushes,
- welding of cracks,
- placing of inserts and additions of different shapes and with several ways of fastening,
- placing of the new toothed rim,
- hard facing,
- hard facing with a template
- additional – repair correction of teeth,
- thermit pouring,
- pressing – extrusion.

* Dr Svetislav Lj. Markovic, Professor, Higher Technical School, Svetog Save 65, YU-32000 Cacak, Serbia and Montenegro, e-mail: svetom@ptt.yu.
Dr Danica Josifovic, Professor, Faculty of Mechanical Engineering, University of Kragujevac, Sestre Janjic 6, YU-34000 Kragujevac, Serbia and Montenegro.
Dr Slobodan Tanasijevic, Professor, Faculty of Mechanical Engineering, University of Kragujevac, Sestre Janjic 6, YU-34000 Kragujevac, Serbia and Montenegro.
M.Sc. Snezana Ciric-Kostic, asistent, Faculty of Mechanical Engineering Kraljevo, University of Kragujevac, YU-36000 Kraljevo, Serbia and Montenegro, e-mail: cirickostic.s@maskv.edu.yu.

2. TECHNOLOGICAL PROCEDURE OF TEETH REGENERATION

Teeth regeneration includes damages detection, causes of their appearance and their character, application of the most rational and most reliable method of regeneration and method of teeth working surfaces hardening. Most of gears that are withdrawn from exploitation can be successfully and reliably regenerated.

As regeneration of the damaged teeth is assumed the exact sequence of technological operations, whose objective is renewal of the lost working characteristics. Regeneration must provide for the nominal sizes and required quality of surface machining, regular geometric shapes, required kinematics and dynamic characteristics and preservation (or even improvement) of basic mechanical characteristics of the regenerated gear material.

Technological process of gear regeneration consists of the following operations:

- cleaning, washing and degreasing of gears,
- identification of type, size, character and position of damages (defects detection),
- classification of gears according to comparison of results defects detection and requirements from technical documentation to: proper gears, gears predicted for regeneration and gears predicted for discard (waste),
- choice of optimal regeneration method,
- design of regeneration technological procedure,
- preparation for regeneration,
- realization of the prescribed regeneration procedure,
- machining of the regenerated surfaces,
- realization of the procedure for hardening of the damaged gear parts and other functional surfaces,
- final machining – grinding,
- final control and testing of the regenerated gear.

3. REGENERATION OF THE GEAR TEETH BY HARD FACING

The most modern way of damaged gear teeth regeneration is hard facing. Regeneration of dimensions of the steel gear worn teeth is done by hard facing. Hard facing can be done as arc welding, manual or semiautomatic, gas welding, or oxyacetylene. Arc hard facing is done with usual common welding electrodes or with special electrodes for hard facing with thick shield. Surface aimed for hard facing is previously prepared by cleaning with a steel brush until the metal shine is obtained. Preparation of teeth for hard facing, besides removing grease, oxides and anti-corrosive coatings, also includes removal of cracks and damaged parts of teeth, as well as potential sources of stress concentrations – sharp edges. In this phase is also removed the hardened (cemented) layer from the teeth

working surfaces. These preparation operations are done mechanically, usually by grinding.

Arc welding hard facing is done at current intensity of 150 to 250 A, in a single layer, whose thickness, after mechanical machining must be at least 1,5 mm. In the hard faced layer it is necessary to leave a small addition for cleaning and machining of the hard-faced tooth. The tooth shape is controlled by a template. When small module teeth are hard faced (to $5 \div 6$ mm), the whole gear is constantly heated with hot water, to avoid deformation due to thermal effects.

To avoid eccentricity of the gear, hard facing of teeth is not performed consecutively, one tooth after the other, but every 5 to 10 teeth. In order to avoid eccentricity (warping), the gear is submerged into water in such a way that only the place that is hard-faced remains not molten. It is covered by the asbestos tape with a cut slot for hard facing. Besides that, it is also possible to preheat the gear up to $200 \div 300^\circ\text{C}$. Preheating is done in order to decrease hardenability of the parent metal and hard faced layer, to decrease stresses due to hard facing and deformation of both teeth and gears, to prevent appearance of gas bubbles and cracks in the hard faced layer and heat affected zone, as well as to increase the ability of bonding the parent metal and the hard faced layer.

Basic requirements in performing the hard facing procedure are that the heat is brought as uniformly as possible (in order to avoid local thermal stresses), and that the hard facing is done from the parts of larger width toward the thinner ones. Teeth of greater length are hard faced in the direction from the imagined symmetry axis towards the ends, and from the tooth dedendum towards the addendum. The hard facing direction must be perpendicular to the slip direction in order to increase the hard-faced layer wear resistance.

After hard facing the gear is tempered to remove stresses caused by hard facing, provided that the teeth working surfaces high hardness is not required. Then the mechanical machining and thermal treatment are performed. In some cases, when the high accuracy is not required, manual machining of teeth is also possible, by file or manual electrical grinders.

For gears with small module ($m < 5$ mm), hard facing of individual teeth is substituted by hard facing of the teeth rim, that is done over the whole perimeter. Then the teeth are cut in.

In regeneration of high module gears is desirable to hard face teeth with help of a template, made of copper or brass (Figure 1). The template with the regenerated tooth constitutes a closed volume which is filled with the molten metal. To maintain the hollow between teeth the template must have support on the neighboring tooth.

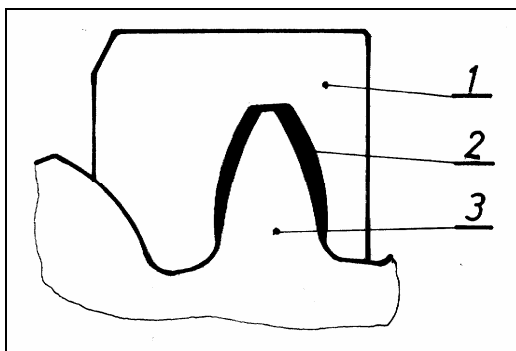


Figure 1. Scheme of gear teeth hard facing with use of a template: 1 – template, 2 – hard faced layer, 3 – regenerated gear

If the gear was previously thermally treated (quenched), it is necessary to also quench the new teeth. They are heated by the gas burner up to $750\div 820^{\circ}\text{C}$. The neighboring teeth must be covered by the protective grease. After heating, teeth are cooled quickly with water and then cleaned by abrasive grinding wheel.

Gears, that are regenerated by hard facing are then tempered, mechanically machined and thermally treated, so the working surfaces hardness is brought to prescribed values given in drawings or technical recommendations. Hardness, on the average, must be HRC 30÷45, for gears made of constructive carbon steels (C0545, C0645), and for gears made of alloyed steels HRC 45÷65. Regenerated gears, that are subjected to one sense load, should be, if it is constructively possible, mounted into mechanisms rotated for 180° . In that way it would be achieved that the regenerated surfaces become idle, and teeth surfaces with unchanged structure would become the working ones.

4. REGENERATED GEARS QUALITY PARAMETERS

Quality parameters characteristics were determine on samples of the regenerated spur gears: gears of the first gear and reverse in the gear box of the heavy load trucks were rejected from exploitation due to inadmissible wear and pitting of the teeth working surfaces,

Arc welding (AW) hard facing was chosen as the optimum and most reliable method for their regeneration. In regeneration of all samples the protection of neighboring surfaces was strictly kept in mind, as well as preparation of samples for hard facing, and the schedule of teeth for hard facing, so the cemented layer would not be reheated, and other damages would not be induced by thermal influences of hard facing.

Mentioned samples were regenerated by the following procedures gears exposed to wear and pitting were regenerated by AW hard facing of the teeth flanks in two ways:

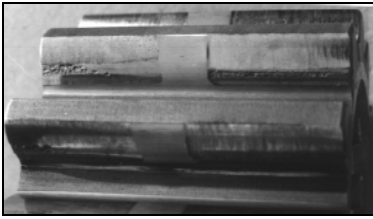
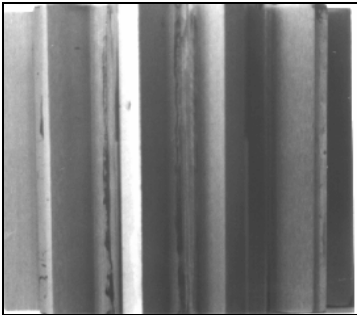
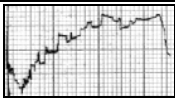
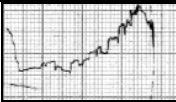
- I. By the Castolin 2 electrode
- II. Tooth addendum and dedendum were hard faced with the Castolin 680S electrode, and the surface

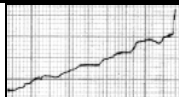
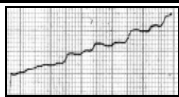
between them with the Castolin 2 electrode, what produces higher resistance of tooth to bending.

The regeneration procedures are almost identical and they consist of: degreasing, determination of the technical state (damage detection), grinding for removing the damaged cemented layer, hard facing, and lock-smith works – bringing of teeth to the approximate shape by manual electric grinder and final grinding of teeth – peripheral, frontal and side surfaces.

The appearance, basic geometric and kinematic characteristics, and results obtained by control and testing of regenerated gears are presented in Table 1. It is obvious that the tested quality parameters are within the prescribed limits.

Table 1. Quality parameters of regenerated teeth

N ^o	Controlled and tested parameters	Required/obtained values on characteristic samples	
		I method	II method
1.	Appearance of gear rejected from exploitation		
2.	Material	C5421	
3.	Basic geometric parameters	$m = 9, \quad z = 12,$ $\alpha_0 = 20^{\circ}, \quad x_m = +2,7 \text{ mm},$	
4.	Damage detection report	Teeth wear and teeth working surfaces pitting around and below the pitch circle	
5.	Appearance of the regenerated gear		
6.	Voids and cracks (Ferro-flux)	None	None
7.	Addendum circle d_k	$d_k = 127,8_{-0,5} \text{ mm}$ $d_k = 127,4 \text{ mm}$	$d_k = 127,8_{-0,5} \text{ mm}$ $d_k = 127,5 \text{ mm}$
8.	Measure across tooth W	$W_2 = 43,2132_{-0,088}^{+0,088}$ $W_2 = 42,92 \text{ mm}$	$W_2 = 43,2132_{-0,088}^{+0,088}$ $W_2 = 42,92 \text{ mm}$
9.	Tooth profile tolerance T_{ev}	 $T_{ev} = 18 \mu\text{m}$ $T_{ev} = 16 \mu\text{m}$	 $T_{ev} = 18 \mu\text{m}$ $T_{ev} = 15 \mu\text{m}$

10.	Tooth flank line tolerance T_{β}	 $T_{\beta}=18 \mu\text{m}$ $T_{\beta}=13 \mu\text{m}$	 $T_{\beta}=18 \mu\text{m}$ $T_{\beta}=14 \mu\text{m}$
11.	Teeth radial eccentricity T_r	$T_r=78 \mu\text{m}$ $T_r=20 \mu\text{m}$	$T_r=78 \mu\text{m}$ $T_r=18 \mu\text{m}$
12.	Regenerated surfaces machining quality	N7 $R_a=1,60 \mu\text{m} - \text{N7}$	N7 $R_a=1,60 \mu\text{m} - \text{N7}$
13.	Surface hardness	HRC \geq 56 HRC=55,9	HRC \geq 56 HRC=56,2

In order to prove economic effectiveness of the regeneration procedure, in Table 2 is given comparison of the regeneration prices and of the newly made gears. Savings is calculated according to expression:

$$U = \frac{C_{ni} - C_r}{C_{ni}} 100 (\%)$$

where: C_{ni} (DEM) – is the price of the newly produced gear,

C_r (DEM) – is the price of regeneration.

Table 2. Indicators of economic efficiency of gears regeneration

Indicator	Method I	Method II
Regeneration time	19,2 NH (192 DM)	20,0 NH (200 DM)
Material needed for regeneration	Castolin 2, ϕ 3,2 mm, 300 gr (70 DM)	Castolin 2, ϕ 3,2 mm, 180 gr, Castolin 680S, ϕ 3,2 mm, 120 gr (70 DM)
Total price of regeneration	262 DM	270 DM
The new production procedure	Turning operations, milling operations, planing operations, thermal treatment and grinding	
Time of new production	43,5 NH (435 DM)	
Material needed for new production	C5421, ϕ 130x110 mm, 12 kg (35 DM)	
Total price of new production	470 DM	
Savings	44,3 %	42,6 %

5. CONCLUSION

Regeneration of damaged gears is necessary in many cases, like: impossibility of purchasing the new product (spare part), nonexistence of technical documentation, impossibility of purchasing the adequate material for manufacturing, complexity of technological procedure for manufacturing the new gear, etc.

Geometric characteristics, prescribed tolerances and deviations, required mechanical characteristics, as well as the surfaces machining quality of the regenerated gears completely comply with prescribed and standardized values of the newly produced gears. Regeneration is more economically efficient with respect to the new production for about 50 %, for the given examples of spur evolvent gears, of pretty simple construction. If the gears are larger and of more complex shape, savings with regeneration compared to new production are even greater.

Regeneration should not be performed in cases where economic indicators do not recommend it, than for very complex shapes that are not suitable for any of the known regeneration procedures, and when the damage degree of the gear is so high that it is more optimal to make a new gear.

6. REFERENCES

- [1] Markovic S., Josifovic D.: *Savings in Material and Machining costs of the Work Tooth Gears by the Regeneration Method*, Tribologie in Industry, vol. 4, 1995, p. 120-126.
- [2] Markovic S., Josifovic D.: *Regeneration of Gears*, Monograph, Yugoslav Society for Tribology, Kragujevac, 1998, 145 p.
- [3] Josifovic D., Markovic S.: *Hard facing damaged teeth - the optimal method for gear regeneration*, 5. International Conference on Advanced Mechanical Engineering & Technology "AMTECH '99", Proceedings, Vol. II, Plovdiv, Bulgaria, 23-25. June 1999, p. 474-479.
- [4] Josifovic D., Markovic S., Ciric-Kostic S., Ciric R.: *Technical and economic justification of offacing of regeneration of damaged gear teeth*, The third international congress – Mechanical engineering technologies MT'01, Sofia-Bulgaria, 24-26. 06. 2001, p. C-III-58.

PRESENT STATE OF RAILWAY VEHICLES CENTER KRALJEVO

Ranko Rakanović¹

Abstract

This review paper presents current state of Railway Vehicles Center of Faculty of Mechanical Engineering Kraljevo and Wagon Factory Kraljevo. It presents organization, resources and status changes, current project and plans for further development of Railway Vehicles Center.

Key words: Wagon testing, static and dynamic behavior of wagons

INTRODUCTION

Railway Vehicles Center is joint laboratory of Faculty of Mechanical Engineering and Wagon Factory from Kraljevo. It consists of personnel involved in work of Department for Railway Vehicles at Faculty of Mechanical Engineering and Test Center of Wagon factory, but temporarily includes personnel from other departments of Faculty.

Department for Railway Vehicles of Faculty of Mechanical Engineering is concerned with education of department's students in area of design, calculation and investigation of freight wagons. Besides, the department is also concerned with research work in respective area.

Test Center of Wagon Factory is concerned with investigation of wagons and heavy machinery

structures manufactured at Wagon Factory and other manufacturers. Its work also concerns with research and development of measurement methods needed for the investigation.

The history of joint work began in late 1960s and during this period the organization had been changed, but permanent activity resulted in more than 150 research and investigation projects and development of original measurement methods and equipment.

The work and capabilities has been previously presented to the public at the Conference [1], and therefore in this paper the recent development will be presented, with only general overview of key points previously described.

RESOURCES

¹ Dr Ranko Rakanović, Full Prof, Faculty of Mechanical Engineering Kraljevo, Dositejeva 19, 36000 Kraljevo, Serbia and Montenegro, rakanovic.r@maskv.edu.yu

The basis of the work of the Railway Vehicle Center is in its human and material resources.

One of the most important concepts applied in the work of the Center is that human resources are key component of work: stuff has to be carefully selected, permanently trained and always kept in work process. Unfortunately, during 1990's, economic crisis and international isolation critically reduced market demands and endangered the second and third request of human resources management concept of the Center. Current stuff of the Center consists of:

- 3 doctors of technical sciences
- 4 engineers
- 2 technicians

It is of vital importance that even five members of the staff were students of Department for Railway Vehicles at Faculty of Mechanical Engineering at Kraljevo, which demonstrates live connection between studies and practice.

Material resources of the Center consist of laboratory, wagon laboratory and test and measurement equipment.

Laboratory is located at Test center of the Wagon factory. It has room and equipment necessary for testing and calibration of measurement equipment. Although it has some capabilities for manufacturing of sensors, the capabilities of other branches of Wagon Factory Kraljevo and other manufacturers are usually used for such purposes. Besides, the Center also uses facility for experimental investigation of fatigue of mechanical structures at "Prva petoletka" factory in Trstenik near Kraljevo.

Wagon laboratory is placed within modified passenger wagon of Li type, designed for speeds up to 120 km/h. It is capable of carrying all equipment needed for running wagon tests.

Test and measurement equipment consists of test stands, sensors and data acquisition systems.

The Center has the following test stands:

- Test stand for investigation of static behavior of wagons;
- Test stand for investigation of torque rigidity of wagons;
- Test stand for investigation of impact behavior of wagons;
- Test stand for investigation of static behavior of bogies.

In course of the investigations, the Center applies both commercial sensors and sensors developed of its own design. Commercial sensors that are applied are strain gauges, displacement and acceleration sensors, mainly products of German manufacturer HBM.

Recently, the Center provided commercial system PIKO 20V, manufactured by "MZT Hepos" manufacturer from Skopje, Macedonia. PIKO 20V is portable system designed for investigation of brake systems during test rides. It enables measurement of pneumatic system pressures, braking forces, brake temperatures, speed of the wagon, and braking path length of wagon. The important feature of the system is that it has wireless transmission of the signal from the sensors mounted at investigated wagon to the main unit, which of considerable importance in running wagon tests when main unit is located within wagon laboratory. The system has nine input channels that enable measurement with

- 5 pressure sensors with measurement range 0-10 bar
- 2 braking force sensors with measurement range 0-50 kN
- 1 sensor for measurement of normal component of force acting on brake disc with measurement range 0-50 kN
- 1 sensor for measurement of tangent component of force acting on brake disc with measurement range 0-10 kN
- 1 sensor for measurement of speed with measurement range 0-250 km/h

Besides, the system is accompanied with software that enables fully automated testing of brake process according UIC regulations.

On the other side, sensors specific for wagon testing are the designed by Center itself:

- Dynamometers for measurement of static brake forces;
- Dynamometers for measurement of static vertical loads of wheels during torque rigidity tests;
- Dynamometers for measurement of buffer forces during impact of wagons;
- Dynamometers for measurement of lateral forces H during running tests.

Recently, the Center also developed sensor for measurement of the path length of the wagon. It is based on application of proximity sensor that detects changes of the wagon position with error less than quarter of wagon wheel turn length. Used with wagon laboratory, it means determination of path length with error less than 0,75 m. The sensor is used for determination of instant speed and position of the wagon during test rides.

The Center has wide range of data acquisition equipment capable of acquiring signals of various natures and range. During the long period, the Center is provided with several generations of measurement equipment, each capable of acquiring

data according UIC regulations. The old generation, aimed for analog signal processing included:

- HBM KWS analog amplifiers
- HP analog filters
- HP signal analyzers
- Honeywell magnetic tape recorder

The new generation of data acquisition equipment is based on digital signal processing equipment, and it consists of:

- HBM UPM 100 data acquisition system for static signals acquisition and processing;
- HBM MGC Plus data acquisition system for dynamic signals acquisition and processing;

Up to now, the Center used only new generation of equipment that enabled static behavior investigation with simultaneous measurement of up to 100 signal channels and dynamic measurements of up to 16 signal channels (10 channels for sensors based on strain gauges and 6 channels for sensors based on inductive principles).

Recently, the Center developed new measurement equipment concept that enables simultaneous application of both old and new generation of equipment. The main idea is to insert digitalization element in measurement chain of old generation measurement equipment. By application of 16-channel A/D converter, measurement signals provided from HBM KWS analog amplifiers are digitalized and stored at computer memory. Being that one channel is used for synchronization purposes, applied concept added 15 digital channels to present data acquisition scheme.

As an example, Fig. 1 presents current scheme for running behavior investigations. In the scheme, magnetic tape recorder system is used for filtering purposes, being that UIC regulations request analog filtering of signals.

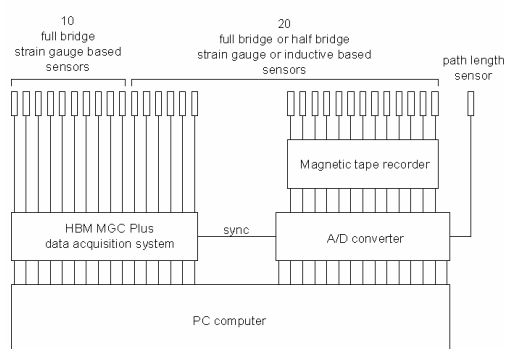


Fig. 1.

As it is shown, the system is extended so as to provide capabilities for simultaneous measurement of up to thirty mechanical quantities and measurement of path length.

METHODS

Railway Vehicles Center develops methodologies for both calculation and investigation of railway wagons.

Calculation methods include:

- Calculations of vehicle gauge
- Calculations of wagon structure rigidity
- Calculations of wagon structure fatigue
- Static and dynamic calculations of wagon structure

All calculations may be performed by both classical means and application of finite elements methods.

The main area of work of the Center is development and application of methods for investigation of freight wagons according UIC recommendations and regulations. The center developed the following wagon testing methodologies:

- Investigations of static properties of wagon
- Torque rigidity investigations
- Static brake testing
- Running tests of brake system
- Impact test of wagons
- Running behavior test
- Estimation of fatigue of mechanical components and systems

Recently, the Center has obtained the permanent Technical Certificate of the Community of Yugoslav Railways, which acknowledges the Center as leading institution in Serbia in area of wagon testing and investigation methodologies research, development and application.

PROJECTS

The Center currently works on two projects, one national, and the other international.

National project "Improvements of suspension systems of coal transport Fbd and car transport Ddam freight wagons is financed by Serbian Ministry of Science and Environment Protection. It employs experiences gained through previous projects and investigations in order to find solutions for suspension system problems occurring at both heavy and light transport freight wagons.

International project "Establishment of Regional Railway Transport Research and Education Center" is performed in cooperation with Bulgarian University of Transport "Todor Kableshkov" from Sofia and is aimed to establishment of joined institution that will coordinate research and development efforts of railway transport researchers of all Balkan countries. The project is financed by

European Commission as part of FP6 "Integration of European Research Area" project.

PLANS

The future development plans include development of all aspects presented here.

Organizational changes that both Serbian Ministry of Science and Technology and Ministry of Higher Education are making should lead to establishment of the Center as independent legal subject within Faculty; so far, all legal regulations are not defined, and such organization changes will wait until legal circumstances are defined.

The most important improvement considering resources of the center is provision and preparation of new wagon laboratory; it is expected that passenger wagon capable of running with speeds up to 160 km/h will be available during next year.

In the area of design and calculations the Center is researching and developing methodology of modular design of wagons.

The most important methodology that is researched in area of measurement is development of methodology of direct measurement of lateral and vertical forces in rail-wheel contact.

The Center is currently in process of preparation for verification by international railway organization (TÜV). It will enable re-establishment of international co-operation which was interrupted during international isolation of Serbia. The Center for Railway Vehicles expects that the co-operation will include common education of students, research and development activities and common projects with international education and research institutions.

LITERATURE

[1] R. Rakanović, Proceedings of XIII Scientific Conference «Transport 2003», p.139, Sofia (2003)

A MODEL FOR DYNAMICS OF WAGON-TRACK SYSTEMS

Dobrinka Borisova Atmadzhova¹

This paper presents a three-dimensional wagon-track system dynamics (WTSD) model developed from first principles for understanding the vertical and the lateral responses of various components of the wagon and track system. The model consists of a full wagon with 37 degrees of freedom (DOF), a four-layer track with discretely supported rails and a wheel-rail interface representing Kalker's creep and Hertzian contact parameters. The model has been validated using two sets of field data: one dealing with vertical impact due to the flat wheel and the other dealing with lateral hunting.

Keywords: wagon, track, wheel-rail irregularities, Kalker's creep, hunting, lateral impact, vertical impact

1 INTRODUCTION

There are several commercial computer simulation packages available for the analysis of wagon dynamics (e.g. VAMPIRE, ADAMS/RAIL, MEDYNA and UMLAB). These packages are capable of handling very detailed three-dimensional models of wagons to evaluate their vertical and lateral dynamics including hunting, curving and derailment potential. However, these packages consider the track either as rigid or as a uniform elastic foundation.

Track dynamics is generally investigated using two dimensional models [1-18]. These models provide only the vertical impact force at the wheel-rail interface, the rail seat, the sleepers, the ballast and the sub grade. The two-dimensional models have other inherent limitations in that they only examine the effect of defects in the wheel and/or the rail symmetric to the track centre-line. Such models can predict neither the dynamic responses due to lateral uneven loading nor the lateral hunting of wagon body or bogies.

The three-dimensional wagon models, the other hand, consider the track as rigid or elastic with a uniform track modulus.

2 THREE-DIMENSIONAL SYSTEM MODEL

The three-dimensional WTSD model includes three subsystems: the wagon subsystem, the track subsystem and the wheel-rail interface subsystem. Detailed formulation of the basic governing equations is similar to a simplified two-dimensional version of this model that has recently been published [16].

2.1 Wagon subsystem

Wagon subsystems include one wagon car body containing two bolsters and two bogies. Each bogie consists of two secondary suspension elements, two side frames, four primary suspension elements and two wheelsets, as shown in Fig. 1a and b. The wagon car body rests on the secondary suspension elements through the bolsters. The side frame is an intermediate structure that

provides seating for the secondary suspension element and connects to the wheelsets through the primary suspension elements and wheel bearing.

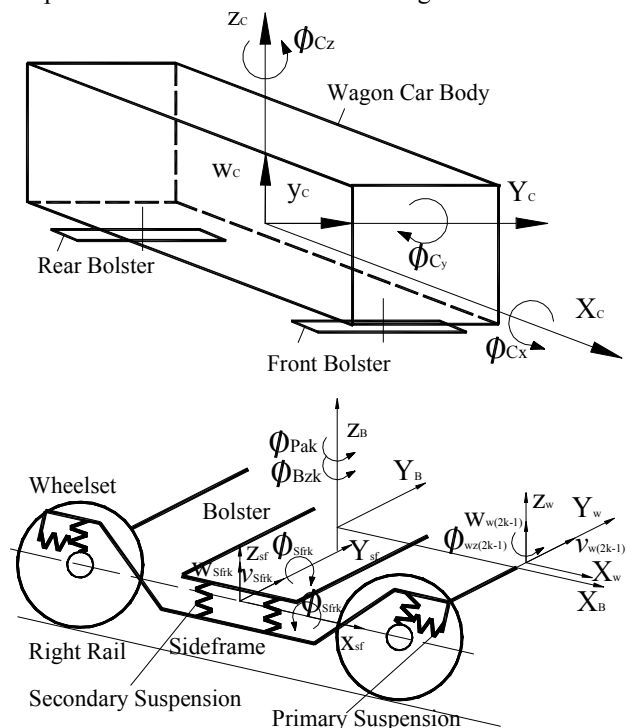


Fig. 1 Schematic diagram of the wagon subsystem: wagon car body and bogie

(u , v and w - linear displacements and ϕ_x , ϕ_y , and ϕ_z are the rotations about the X, Y and Z axes respectively, and ϕ_{Pa} is the parallelogram motion of the bogie frame about the vertical (Z) axis.)

The primary suspension is also represented by linear spring and damper elements which provide longitudinal, lateral and vertical viscoelasticity. The secondary suspension is represented by linear spring and damper elements which provide lateral and vertical

¹ Dobrinka Borisova Atmadzhova, Ph. D. VTU "T. Kableshev", www.vtu.bg, Department of Transport Equipment, Sofia, 158 Geo Milev, Bulgaria, atmadzhova@abv.bg

viscoelasticity. All the other components of the wagon are considered as rigid bodies with masses and mass inertia moments along the three Cartesian coordinate directions. Owing to the special connection between the wagon car body and the bogie frames (bolster and two side frames), the bogie frame exhibits relative rotation against the wagon car body, known as parallelogram rotation or lozenging of the bogie frame. Therefore, there are two rotations of the bogie frame about the vertical axis considered in the modelling: yaw rotation and parallelogram rotation or lozenging. The total degrees of freedom (DOF) required describing the lateral and the vertical displacements and rotations of the full wagon. As shown, 37 DOF are required to define the wagon dynamics fully.

The equations of dynamic equilibrium can be written using the multi-body mechanics method as shown below:

$$\mathbf{M}_W \cdot \ddot{\mathbf{d}}_W + \mathbf{C}_W \cdot \dot{\mathbf{d}}_W + \mathbf{K}_W \cdot \mathbf{d}_W = \mathbf{F}_{WT} \quad (1)$$

where \mathbf{M}_W , \mathbf{C}_W and \mathbf{K}_W are the mass, damping and stiffness matrices of the wagon subsystem (these matrices are 37×37 or 15×15 for bogies with or without primary suspension respectively), \mathbf{d}_W is the displacement vector of the wagon subsystem and \mathbf{F}_{WT} is the interface force vector between the wagon and the track subsystems consisting of the wheel-rail normal contact forces, tangent creep forces and creep moments about the normal direction in the wheel-rail contact plane.

2.2 Track subsystem

The track subsystem model containing four layers is based on the discretely supported distributed parameter approach [3-5]. The track subsystem comprises two rails, n_s sleepers (n_s is the number of sleepers considered), $4 \times n_s$ fastener and pad assemblies, $2 \times n_s$ ballast blocks, $2 \times n_s$ sub ballast blocks and sub grade.

The lateral and the vertical bending and shear deformations of the rail beam are described using Timoshenko beam theory [20] extended by considering the torque of the rail beam. Thus, five DOF at any point along the longitudinal neutral axis of the rail beam, namely lateral and vertical displacements and rotations about the lateral (Y) and vertical (Z) axes and torsional rotation about the longitudinal (X) axis, are used in the formulation of the rail beam. For simplicity, the dynamic equilibrium equations of the rail beam have been expanded using Fourier series in the longitudinal (X) direction by assigning an equal number of terms (nm , also known as the number of modes of the rail beam) for both the linear displacements and the angular rotations.

The sleepers are considered as deformable short beams resting on an elastic foundation [21] and represented by their mass and viscoelastic properties at the rail seat location and represented by three DOF per sleeper, namely the lateral and vertical displacements and the rotation about the longitudinal (X) direction. The ballast and the sub ballast layers are represented by their mass and viscoelastic properties with only one vertical displacement DOF per block. The properties of the ballast and sub ballast have been determined from a pyramidal model that is widely reported in the literature [8, 10, 16].

The ballast and the sub ballast layers are connected in the vertical and the horizontal (both longitudinal and lateral) directions to depict continuity of these layers as shown in Figs 2a and b. The upgrade (formation) is represented by its viscoelastic properties without mass. The equations of dynamic equilibrium of the sleepers, the ballast, the sub ballast and the sub grade are assembled using multi-body mechanics methods. The governing equations of dynamic equilibrium for the track (rail and all other track components) are expressed in the following matrix form:

$$\mathbf{M}_T \cdot \ddot{\mathbf{d}}_T + \mathbf{C}_T \cdot \dot{\mathbf{d}}_T + \mathbf{K}_T \cdot \mathbf{d}_T = \mathbf{F}^*_{WT} \quad (2)$$

in which \mathbf{M}_T , \mathbf{C}_T and \mathbf{K}_T are the mass, damping and stiffness matrices of the track subsystem. The vector \mathbf{d}_T contains the displacement of the track subsystem which includes the modal and physical displacements, and \mathbf{F}^*_{WT} is the combined interface force vector between the wagon and the track subsystems.

Selection of n_s and nm depends on the required length of travel of the wagon to be simulated. For a travelling distance of 40 sleeper spacings it was found that at least a track length of 120 sleeper spacings should be considered for the results not to be affected by the boundary conditions of the rail beams and the initial conditions used in the dynamic simulation. Therefore, n_s was chosen as 120.

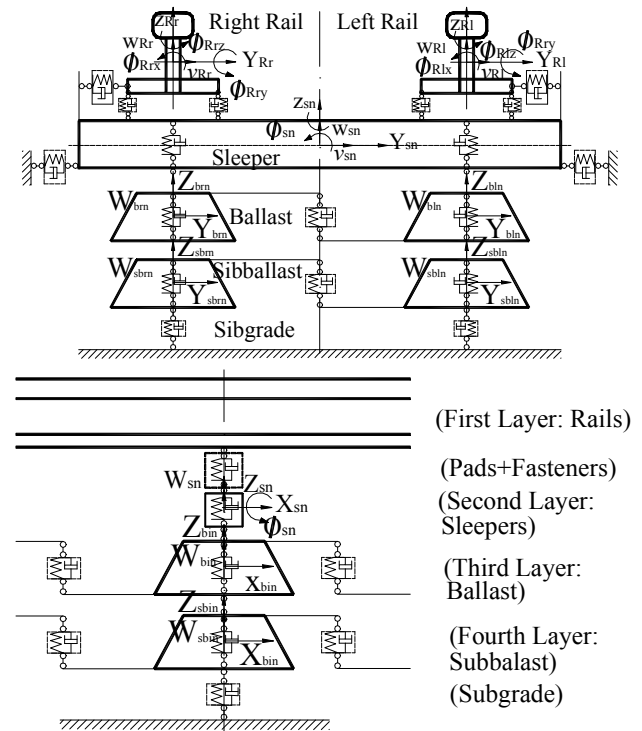


Fig. 2 Schematic diagram of the track subsystem: cross-section and longitudinal section

2.3 Wheel-rail interface subsystem

Generally, wheelsets with shaped wheels UIC. A gap exists between the flanges of the wheelset and the gauge faces of the railhead, which allows lateral shift of the wheelset during longitudinal rolling without flange contact. The longitudinal motion of the wheelsets filled to a wagon through the suspensions does not exhibit pure rolling owing to the effect of creep forces tangential to the

wheel-rail contact plane. The wheelsets in a wagon are also allowed to move laterally (hunting) and to rotate about the vertical axis (yaw) on the rails owing to lateral disturbance from their dynamic equilibrium position.

Under rolling contact, the wheel and the rail produce contact forces in the normal direction on the wheel-rail contact plane. The creep forces are generated in the longitudinal and the lateral directions tangential to the contacting plane, and a creep moment about the normal direction. The method for determining stiffness coefficient of the Hertzian contact spring elements was adopted from reference [6].

The creep forces and the creep moments are determined using Kalker's linear creep theory. The creep forces and moments are usually calculated without due consideration to the velocities of the rail [22], in other words, considering the track as rigid. However, in the three-dimensional WTSD model the velocities of the rail in the lateral and spin directions are included in these calculations of creepages. Expressions for modified longitudinal, lateral and spin creepages at the wheel-rail contact plane are as follows:

$$\begin{aligned}\xi_{ix} &= \frac{1}{V} \cdot \left[V \cdot \left(1 - \frac{r_i}{r_0} \right) \mp y_{wi} \cdot \dot{\phi}_{wz} \right] \\ \xi_{iy} &= \frac{1}{V} \cdot \left[(v_w + r_i \cdot \dot{\phi}_{wz} - V \cdot \dot{\phi}_{wz}) - (v_{Ri} - z_{Ri} \cdot \dot{\phi}_{Rix}) \right] \\ \xi_{isp} &= \frac{1}{V} \cdot \left[\dot{\phi}_{wz} \mp \frac{\delta_i \cdot V}{r_0} - \dot{\phi}_{Rix} \right] \quad (3)\end{aligned}$$

in which V is the wagon speed, subscript i is either l for the left or r for the right wheel, r_i and y_{wi} are the wheel radius and the lateral coordinate of the wheelset at the centroid of the contact patch respectively, r_0 is the wheel nominal radius, z_{Ri} is the vertical coordinate of the rail at the centroid of the contact patch, δ_i is the wheel-rail contact angle at the centroid of the contact patch and the symbol $-/+$ is negative when $i = l$ and positive when $i = r$. As Kalker's linear theory best defines the creep forces only when the creepages are very small, Johnson-Vermeulen's approach presented in reference [22] is used to modify the creep forces further.

2.4 Solution technique

The equations of dynamic equilibrium for the wagon and track subsystem provided in equations (1) and (2) respectively are solved in the time domain.

3 VALIDATION OF THE THREE-DIMENSIONAL WTSD MODEL

The three-dimensional WTSD model has been validated by comparing the filed data published in the literature with the results of the simulation. Two examples were selected for the validation. The first example provides validation of the vertical dynamic responses and impact

due to a flat wheel contacting a defect-free rail [12], and the second example describes the lateral dynamic response due to wagon hunting instability [19].

Example 1: flat wheel [12]

Fermer and Nielsen [12] reported data from their field testing carried out on the Swedish railway network. The experiments were carried out with wheelflats on an instrumented wheelset, on which wheelflats were artificially ground with an initial length of 40mm and a depth of 0.35mm. Such length is the condemning limit for flat wheels in the Swedish Railways. The main objective of the experiments was to examine the influence of the wagon speed, the axle load and the rail pad stiffness on the dynamic response of the wagon and the track.

The dynamic response of the whole wagon-track system was simulated with the wagon travelling at a constant speed of 70km/h. The two wheels of the leading wheelset on the front bogie were assumed to contain flats (40mm long, 0.35mm deep) laterally symmetric to the mass centre of the wheelset.

The dynamic impact force was output at the wheel-rail contact patch for the full period of the simulation.

The measured and simulated contact forces are plotted in Fig. 3, showing that the magnitude and frequency of the simulated and measured impact forces are in reasonable agreement with each other. The impact forces (simulated and measured) are about 50 per cent greater than that of the static wheel load. In the no peak region there is a difference between the measured and the simulated frequencies of the dynamic contact forces. The frequency of the vibration that follows the impact corresponds to the natural frequency of the coupled wagon and rail track system.

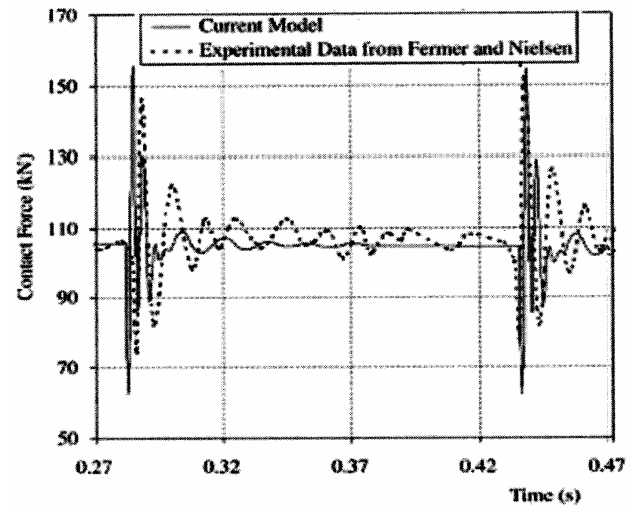


Fig. 3 Comparison of the contact force measured by Fermer and Nielsen [12] and predicted by the current model

In addition to the contact force, the dynamic response of the track components was also monitored at a reference section, mid-way between the full travel distances. Figure 6 shows the impact force factor (ratio of the dynamic wheel load to the static wheel load) between the railhead and wheel, the pad and sleeper, the sleeper and ballast and

the ballast and sub ballast at the reference section. The impact force factor at the first peak between the railhead and the wheel flat is approximately 1.50, which corresponds to the magnitude of the impact force time series shown in Fig. 3.

The vertical impact magnitude drops rapidly from the contact point on the railhead to the pad, as observed in Figs 3 and 4 (approximately, the force factor drops from 1.50 to 0.75).

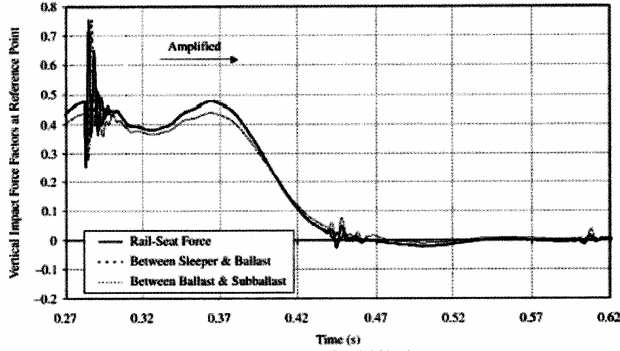


Fig. 4 Force factors for the track components at the reference section predicted by the three-dimensional WTSD model

Example 2: wagon hunting [19]

This example deals with the field observation of empty wagons with two three-piece bogies [19] (without primary suspension) that displayed a hunting response at an operating speed of 75.4 km/h.

By applying the modified Newmark- β method to the 11 DOF model, the time histories of the lateral displacements of the wagon body and two bogies were determined. An initial condition of 0.2mm lateral displacement as disturbance to the leading wheelset of the front bogie was applied for this purpose. Several simulations were carried out at operating speeds in the range 70-85km/h.

The lateral accelerations of the wagon body and two bogies at operating speeds of 75, 79 and 85km/h are shown in Figs 5a to c respectively. From these figures it can be seen that, when the wagon speed is 75 km/h, the wagon system regains lateral dynamic stability in spite of the initial lateral disturbance. At 79 km/h, sustained lateral instability (hunting) occurs, and at 85 km/h, hunting increases with time. It is therefore concluded that the onset of hunting speed determined by the simplified wagon-rigid track model is 79 km/h.

4 EFFECT OF TRACK MODELLING ON WAGON HUNTING

Example 2 was used to demonstrate the effect of detailed track modelling on the simulation of wagon hunting. A three-dimensional WTSD model was used in which the wagon subsystem was described with 15 DOF and the track was modelled as a three-layer subsystem in which the ballast and the subballast were lumped as a single ballast layer. From these figures it can be seen that when wagon speed is 70 km/h, the wagon system regains lateral dynamic stability in spite of the initial lateral disturbance.

This simplification was necessitated as the ballast and sub ballast layers were provided with only vertical DOF (Fig. 2).

For the calculations using the three-dimensional WTSD model, an initial condition of 0.2mm lateral displacement as disturbance of the leading wheel in the front bogie was used.

Several simulations were carried out at operating speeds in the range 70-80 km/h. The lateral accelerations of the wagon body and two bogies at operating speeds of 70, 74 and 78km/h are shown in Figs 6a to c respectively.

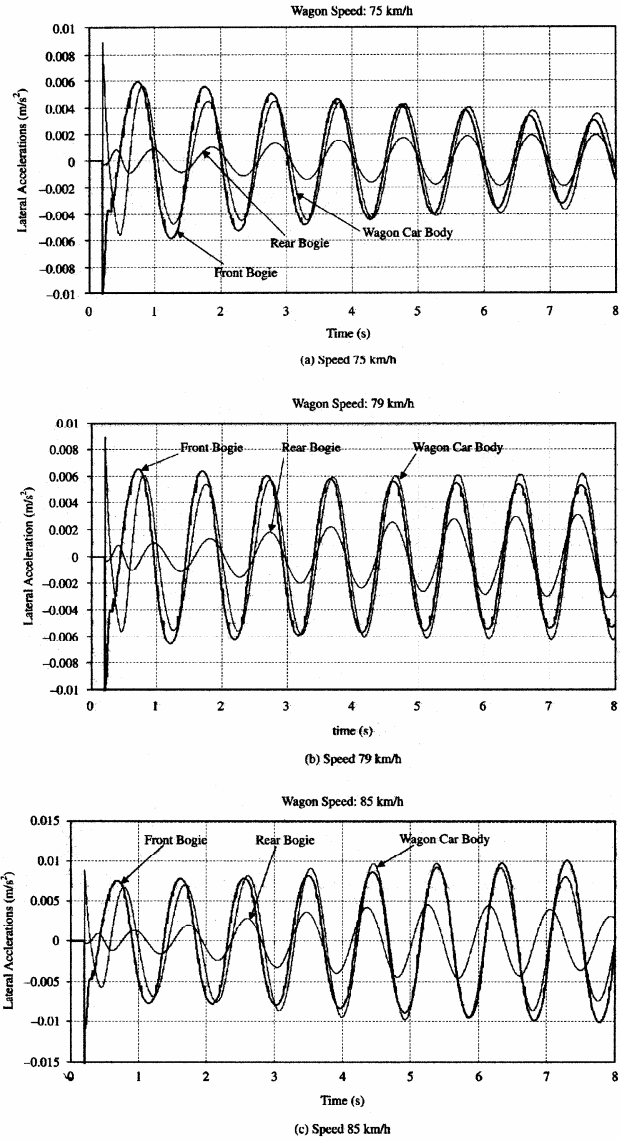


Fig. 5 Predicted time histories of lateral accelerations subballast layer were calculated as follows:

At 74 km/h, sustained lateral instability (hunting) occurs, and at 85km/h, hunting increases with time. It is therefore concluded that the onset of hunting speed determined by the 15 DOF wagon-three-layer track model is 74 km/h, which is close to the operating speed of 75.5 km/h [19]. From Fig. 6b the frequency at hunting was calculated as 1.08 Hz, which compares reasonably well with the reported hunting frequency from field measurement of 1 Hz [19].

5 THE LATERAL IMPACT

It is well known that severe wagon hunting leads to lateral impact of the wheel flange on the gauge face of the railhead and potential wagon derailment. For this purpose, simulation was carried out with the wagon running at 95 km/h (much higher than the critical speed of 74 km/h) (Fig. 7). The wagon body and bogies hunt at the same frequency without any phase shift. The magnitude of the lateral displacement of the wagon car body is much greater than that of the bogies allowing for roll rotation.

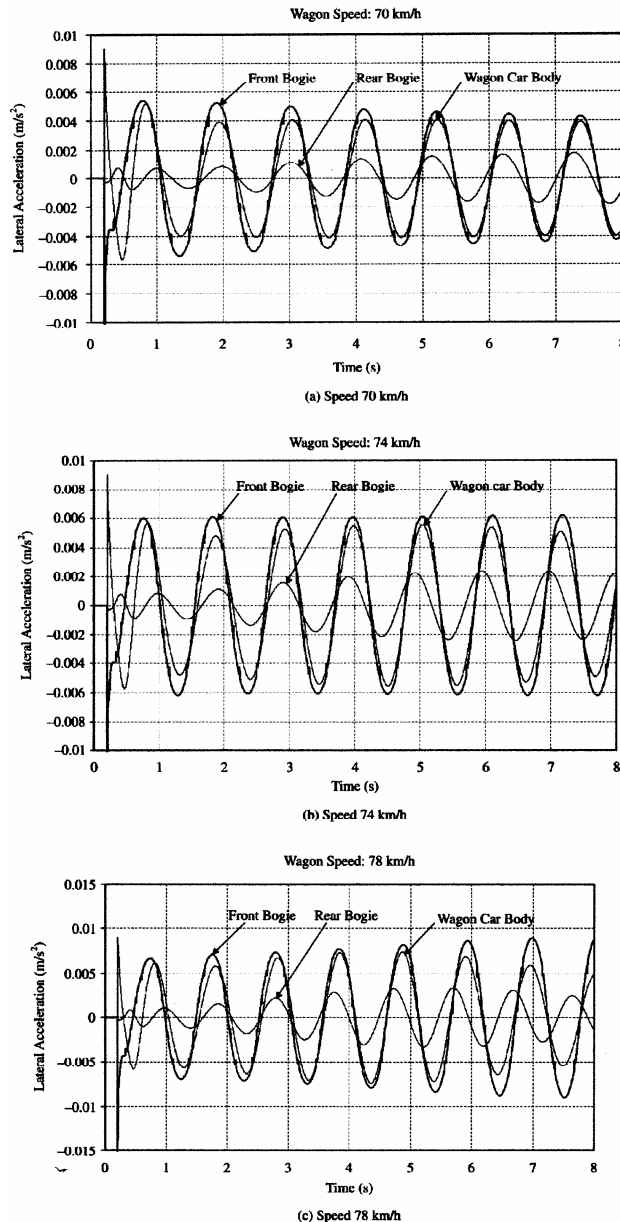


Fig. 6 Time histories of lateral accelerations predicted by the three-dimensional WTSD model

As there existed a maximum clear gap of 6.8 mm between the wheel flange and the gauge face of the railhead, lateral movement less than the clear gap did not introduce lateral impact. The first lateral impact occurred around 8.7 s after the commencement of the wagon travel, and the left rail received the first impact from the leading wheelset of the front bogie. The second impact occurred at the right rail with a much higher magnitude, approximately 65 per cent

of the static vertical load. The impact occurred on the leading wheel of the front bogie. The trailing wheel of the front bogie also impacted the rail at a much smaller magnitude. The magnitude of the maximum lateral impact predicted was approximately 74 per cent of the vertical static wheel load, and the frequency was approximately 1 Hz.

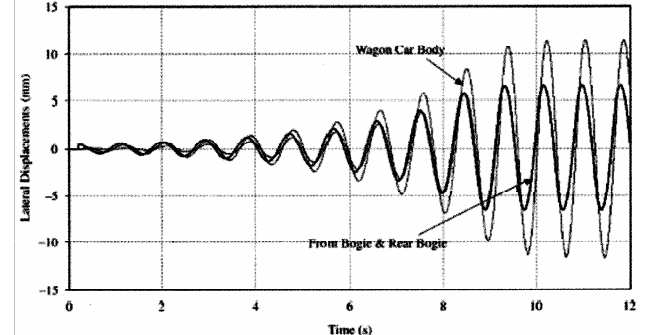


Fig. 7 Time histories during flange contact at a speed of 95 km/h

6 CONCLUSIONS

The model consists of a full wagon defined by 37 degrees of freedom (DOF), a four-layer track with discretely supported rails and a wheel-rail interface representing Kalker's creep and Hertzian contact parameters.

The model has been validated using two sets of field data: one dealing with vertical impact due to a flat wheel and the other dealing with lateral hunting of the wagon body and bogies.

This model can be used to determine both the lateral and the vertical dynamics of the wagon and track system components. This model could deal with discontinuities at the wheel-rail interface that may be either symmetric or unsymmetrical to the track geometry. Uneven loading could also be considered. The model has the potential to predict tangent track derailment due to wheel flange climb on the railhead.

REFERENCES

- 1 Jenkins, H. H., Stephenson, J. E., Clayton, G. A., Morland, G. W. and Lyon, D. The effect of track and vehicle parameters on wheel/rail vertical dynamic forces. *Railway Engng J.*, 1974, **3**(1), 2-16.
- 2 Sato, Y. High frequency track vibration and characteristics of various tracks. *Permanent Way*, 1977, 1-8.
- 3 Newton, S. G. and Clark, R. A. An investigation into the dynamic effects on the track of wheelflats on railway wagon. *J. Mech. Engng Sci.*, 1979, **21**(4), 287-297.
- 4 Clark, R. A., Dean, P. A., Elkins, J. A. and Newton S. G. An investigation into the dynamic effects of railway vehicles running on corrugated rails. *J. Mech. Engng Sci.*, 1982, **24**(2), 65-76.
- 5 Cai, A. and Raymond, G. P. Modelling the dynamic response of railway track to wheel/rail impact loading. *Struct. Engng and Mechanics*, 1994, **2**(1), 95-112.
- 6 Dong, R. G., Sankar, S. and Dukkupati, R. V. A finite element model of railway track and its application to the wheelflat problem. *Proc. Instn Mech. Engrs, Part F: J. Rail and Rapid Transit*, 1994, **208**(F1), 61-72.

- 7 Dahlberg, T.** Vertical dynamic train/track interaction verifying a theoretical model by full-scale experiments. *Veh. Syst. Dynamics Suppl.*, 1995, **24**, 45-57.
- 8 Ahlbeck, D. R., Meacham, H. C. and Prause, R. H.** The development of analytical models for railroad track dynamics. In Proceedings of Symposium on *Railroad Track Mechanics*, 1975, pp. 239-263 (Pergamon Press, Oxford).
- 9 Cai, A. and Raymond, G. P.** Theoretical model for dynamic wheel/rail and track interaction. In Proceedings of International Wheelset Congress, Sydney, Australia, 1992, pp. 127-131.
- 10 Zhai, W. and Sun, X.** A detailed model for investigating interaction between railway vehicle and track. In Proceedings of 13th IAVSD Symposium, 1993, pp. 603-614.
- 11 Ripke, B. and Knothe, K.** Simulation of high frequency wagon-track interactions. *Veh. Syst. Dynamics Suppl.*, 1995, **24**, 72-85.
- 12 Fermer, M. and Nielsen, J. C. O.** Vertical interaction between train and track with soft and stiff railpads-full-scale experiments and theory. *Proc. Instn Mech. Engrs, Part F: J. Rail and Rapid Transit*, 1995, **209**(F1), 39-47.
- 13 Zhai, W.** Locomotive-and-track system coupling dynamics and its application to the study of locomotive performance (in Chinese). *J. China Railway Sci.*, 1996, **17**(2), 58-73.
- 14 Igeland, A.** Railhead corrugation growth explained by dynamic interaction between track and bogie wheelsets. *Proc. Instn Mech. Engrs, Part F: J. Rail and Rapid Transit*, 1996, **210**(F1), 11-19.
- 15 Ishida, M., Uchida, M. and Ono, S.** Prediction of the growth of track irregularity using a track dynamic model. In Proceedings of 7th International Heavy Haul Conference, Brisbane, Australia, 2001, pp. 541-549.
- 16 Sun, Y. Q. and Dhanasekar, M.** A dynamic model for the vertical interaction of the rail track and wagon system. *Int. J. Solids Structs*, 2002, **39**, 1337-1359.
- 17 Jaschinski, A. and Duffek, W.** Evaluation of bogie models with respect to dynamic curving performance of rail vehicles. In Proceedings of 8th IAVSD Symposium, 1983, pp. 266-279.
- 18 Sauvage, G. and Pascal, J. P.** Solution of multiple wheel and rail contact dynamic problem. *Veh. Syst. Dynamics*, 1990, **19**, 257-272.
- 19 McClanachan, M. J.** Investigation of extreme wagon dynamics in Central Queensland coal trains. Master thesis, Central Queensland University, Australia, 1999.
- 20 Dym, C. L.** *Solid Mechanics: A Variational Approach*, 1973 (McGraw-Hill, New York).
- 21 Profillidis, V. A.** *Railway Engineering*, 2000 (University Press, Cambridge).
- 22 Garg, V. K. and Dukkipati, R. V.** *Dynamics of Railway Vehicle Systems*, 1984 (Academic Press, Canada).

THE DETERMINING OF THE PERMITTED VELOCITY OF RAILWAY VEHICLES OVER SWITCHES

Marko Djukić¹
Srdjan Rusov²

Summary – This paper shows the method for determining the permitted velocity of railway vehicles over switches. It shows the complexity of problem and the analysis of parameters that influence the value of permitted velocity over switches. On the basis of analyzed parameters and according to appropriate criterion the value of permitted velocity is estimated as well as the analysis of safety and side vehicle stability during the entry into curve.

Key words – switch, curve, velocity, blow, railway vehicle

1. INTRODUCTION

To permit the switch from one track to another, it is necessary to make the connection between them through appropriate equipment. This equipment differentiates on the basis of whether the moving of vehicle stops during the switching from one track to another, or not.

Turntables and carriers represent the equipment where the switching from one track to another is done by stopping the moving. This equipment has a moving construction where the part of track is and which length is enough for placing some vehicles. By rectilinear or rotational moving of mobile construction and depending on the carriers or turntables, the switching from one track to another is done.

Switches represent the equipment that connects tracks and enables the switching from one track to another without stopping the moving. Using them the most complete track connection is done, because the carrying of complete sets of trains is enabled.

Switch construction causes the reducing of railway vehicle velocity during the turning.

This work shows the method for determining and evaluation of permitted railway vehicle velocity over switches as well as the analysis of side stability when train comes to a switch.

Because of the complexity of the problem, the subject of discussion will only be the single switches, i.e. the switches where only one track is separated from the original track into turning. These switches are the most simple of all switches and that is why they are only used for the mutual track connection.

2. THE CHARACTERISTICS OF SINGLE SWITCHES

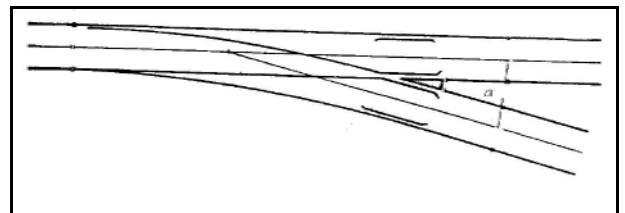
Using the switch one track is separated from another at a certain angle. If that angle is bigger, the switch is shorter and the radius of the curve is smaller.

In Public firm “RAILWAY OF SERBIA” the following parameters are accepted:

- turning angle of 7° and curve radius of 180 m;
- turning angle of 6° and curve radius of 200 m;
- turning angle of 6° and curve radius of 300 m.

It is necessary to mention that on the railways of this firm there are also the non-standard types of switches that were installed during the II World War. Today they can be seen only on some secondary lines, industrial and work tracks. They are known for their bigger turning angle and smaller curve radius.

On main lines, because of reaching the higher velocity into turning, the turntables with smaller turning angle and bigger curve radius are used.



Pic. 1. Single switch

The curve of diverted track ends at a distance of 1 to 3 m in front of the switch common crossing, in order to get the quieter driving over the common crossing that is right. In this case the common crossing angle is equal to switch angle. The track in turning curve has no superelevation but both rails are on the same height. In that way the turntable construction is simplified, but during the driving into curve the velocity must be lowered.

Because of the velocity increasing during driving into curve the switches with outside rail superelevation in the curve are also controlled. With this switches the diverted track curve goes through the switch common crossing, has a bigger radius and the turning angle is smaller so they are longer than the usual switches.

¹ Marko Djukić grad. eng., RAILWAYS OF SERBIA, NEMANJINA 6, 11000 Belgrade, markorail@yahoo.co.uk

² PhD Srdjan Rusov, FACULTY OF TRAFFIC ENGINEERING, VOJVODE STEPE 305, 11000 Belgrade, s.rusov@sf.bg.ac.yu

3. THE CRITERIA FOR DETERMINING THE PERMITTED VELOCITY OVER SWITCHES

The constructive characteristics of switches (curve radius from 180 to 300 m, non-existence of transitional curves and superelevations of outside rail in the curve) cause the necessity for lowering the train vehicle velocity during driving into turning.

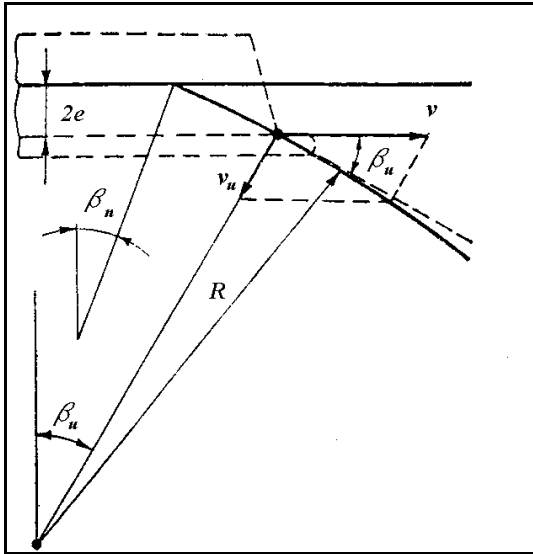
The permitted railway vehicle velocity over switches is calculated on the basis of:

1. permitted blow force of railway vehicle wheel flange against the switch tongue;
2. permitted non-canceled side acceleration that occurs during the vehicle turning through the curve;
3. velocity of non-canceled side acceleration change-side twitches during the vehicle moving through the curve.

The blow force of railway vehicle wheel flange against the switch tongue is proportional to kinetic energy of $0,5mv^2$ where m is the vehicle mass. The blow velocity of wheel flange against the switch tongue is:

$$v_u = v \sin \beta_u [m/s], \quad (1)$$

where β_u is the blow angle (pic. 2).



Pic. 2. Wheel position of railway vehicle during the running into switch tongue

The size of blow angle depends on the curve radius R and angle β_n between main rail and the beginning of switch tongue, with distance of $2e$ between the contact point of wheel flange with switch tongue and main rail and can be obtained from:

$$\beta_u = \sqrt{\sin^2 \beta_n + \frac{4e}{R}}. \quad (2)$$

The blow force of wheel flange against the rail is proportional to size:

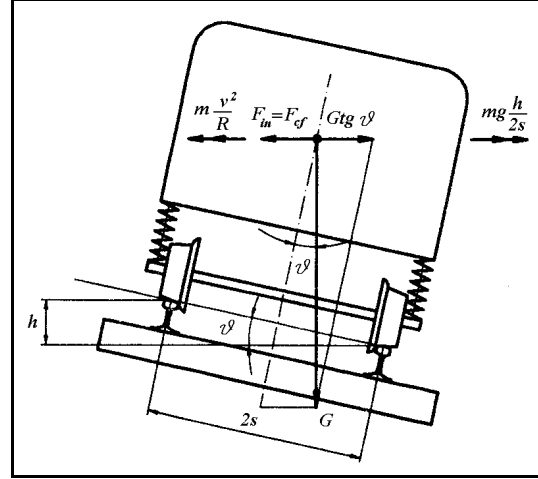
$$\omega = v^2 \sin^2 \beta_u \approx v^2 \beta_u^2, \quad (3)$$

where $\sin \beta_u \approx \beta_u$.

The researches have shown that size ω moves from $0,045$ to $0,061 \text{ m}^2/\text{s}^2$, so the velocity can be found from:

$$v = 3,6 \sqrt{\frac{0,045 \div 0,061}{\sin^2 \beta_n + \frac{4e}{R}}} [km/h]. \quad (4)$$

If $\beta_n = 30' \div 40'$ and $2e = 40 \div 50 \text{ mm}$ the moving velocity over switches goes from 35 km/h (for $R = 180 \text{ m}$) to 50 km/h (for $R = 300 \text{ m}$).



Pic. 3. Position of railway vehicle in transversal surface during moving through curve

Because of the influence of inertial (side) centrifugal forces that occur during the moving of vehicle through the curve the superelevation of outside rail is done in order to reach the balance of these forces (pic. 3.). The non-canceled side acceleration that occurs is obtained from:

$$a_{np} = \frac{v^2}{R} - \frac{h}{2s} g [m/s^2], \quad (5)$$

where h is the superelevation size of outside rail and, $2s$ the distance between the surfaces of wheel rolling. The first article in expression is the acceleration that comes from the centrifugal force - F_{cf} (proportional to square velocity and opposite proportional to curve radius) and the second the acute angle acceleration projection of earth's gravitation. The intensity of permitted non-canceled acceleration goes from $0,65$ to $0,85 \text{ m/s}^2$. Because of the non-canceled side acceleration the balance of inertial centrifugal forces take on the side forces in the zone of wheel-rail contact.

The ideal superelevation h is got for the value of non-canceled side acceleration $a_{np} = 0$ and it is only for one velocity so it can be used with railways with uniform traffic. In general sense where trains operate in different velocities, the superelevation of outside rail in curve is never done to compensate the maximal inertial force that appears with trains with the highest velocity, but it is constructed according to some lower velocity. In that way the excessive inner rail wearing out is stopped that could be caused by the superelevation exceeding for slower trains. According to railway regulations the size of maximal superelevations can not exceed the value of 150 mm.

From (5) we get the highest velocity:

$$v_{gr} = 3,6\sqrt{R(a_n + \frac{h}{2s}g)}[km/h]. \quad (6)$$

Since the switch curves without superelevation are the most frequent, i.e. $h=0$, for non-canceled side acceleration normal value of $0,65 \text{ m/s}^2$, the highest vehicle velocity is got, during driving into curve:

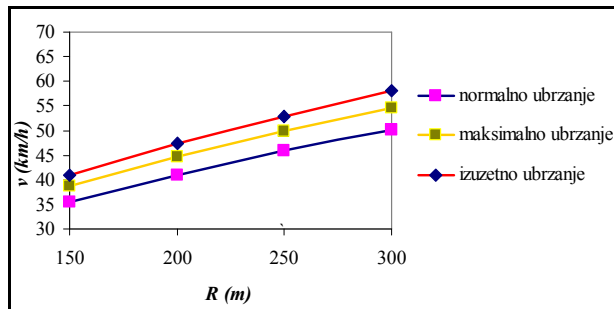
$$v \approx 2,90\sqrt{R}[km/h]. \quad (7)$$

If for the calculation the maximal value of non-canceled side acceleration for velocity over switches is used - $0,75 \text{ m/s}^2$, or exceptional - $0,85 \text{ m/s}^2$ we get:

$$v \approx 3,12\sqrt{R}[km/h], \text{ for maximal value } a_{np} \text{ and}$$

$$v \approx 3,32\sqrt{R}[km/h], \text{ for exceptional value } a_{np},$$

which is shown on pic. 4.



Pic. 4. Permitted velocity over switches depending on curve radius according to criterion of non-canceled side acceleration

For normal non-canceled side acceleration value the velocity of railway vehicles over switches and depending on curve radius, goes from 35 to 50 km/h.

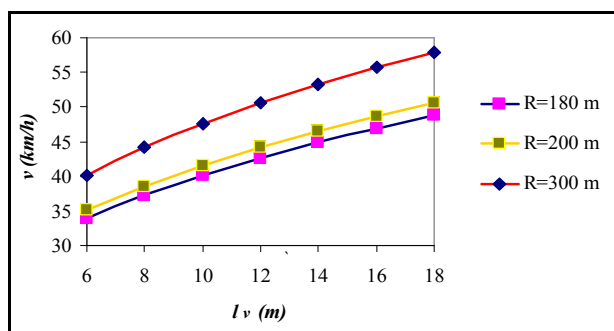
The increase velocity of non-canceled side acceleration value during the entering of vehicle into curve - side switch should go from permitted value of $0,6$ to $0,8 \text{ m/s}^3$. We get the side switch on the basis of:

$$\Psi = \frac{v^3}{Rl_v}[m/s^3], \quad (8)$$

where l_v is distance between railway vehicle body supports. It follows that:

$$v = 3,6\sqrt[3]{\Psi R l_v} \approx 3,25\sqrt{R l_v}[km/h]. \quad (9)$$

The value of train vehicle permitted velocity over switches depending on distance between railway vehicle body supports and according to the criterion of permitted side switch is shown on pic. 5.



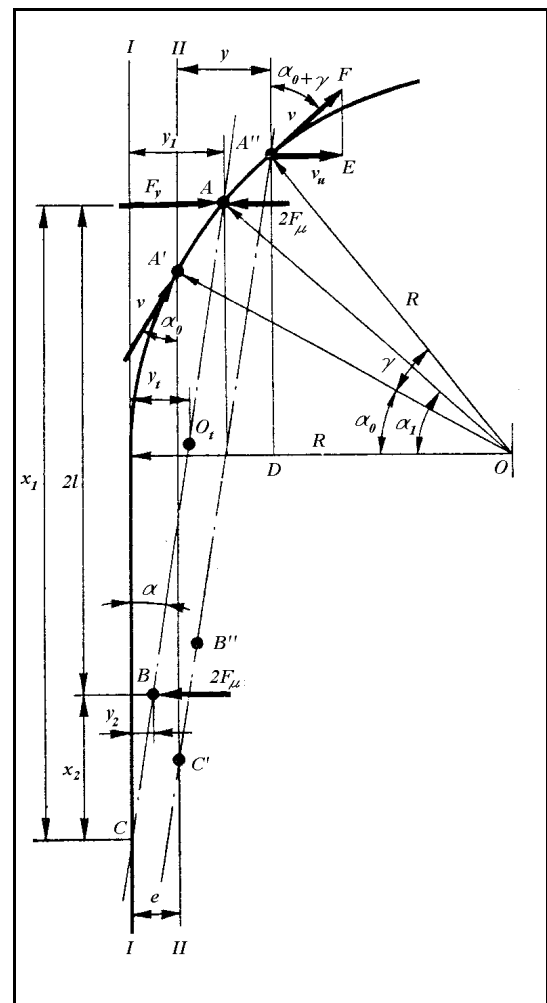
Pic. 5. Dependence of permitted velocity over switches from distance between railway vehicle body supports

according to permitted side switch criterion

4. VEHICLE SAFETY AND SIDE STABILITY

The entering of vehicle into curve without transition curve is followed by horizontal railway vehicle wheel flange blow against the rail head and in that way the sharp turning of vehicle in longitudinal surface. With the analysis of vehicle stability and safety against the derailment of a train it is necessary to take into consideration the forces of mutual effect that occur in that case where the side reactions F_y are primary, because they keep the vehicle on a track.

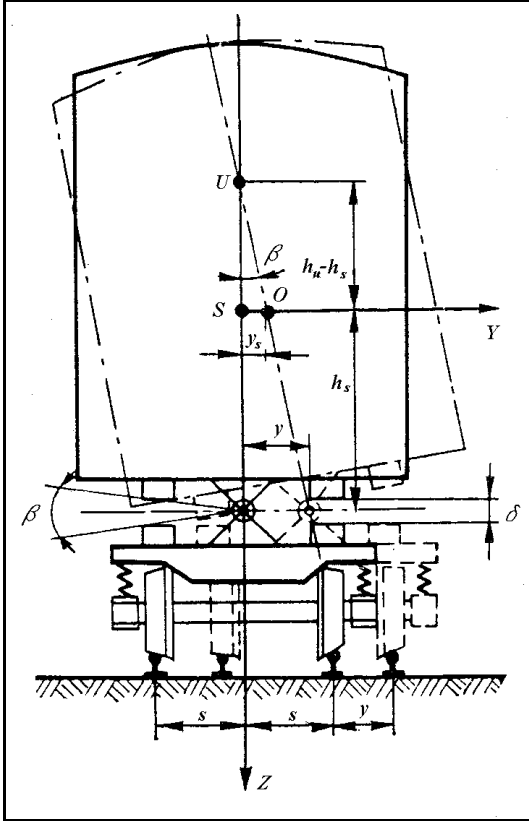
With the train meeting a curve, the front bogie gets the centrifugal acceleration v^2/R . Under the effect of inertial force and horizontal reactions in the zone of wheel-rail contact it comes to the rejection of front bogie for value y_1 , i. e. turning for angle value α_1 . There is also the turning and sliding of back bogie B, where the vehicle body turns for angle α in longitudinal surface (pic. 6.).



Pic. 6. Moving of vehicle axes in longitudinal surface with wheel flange meeting a curve

In transversal surface because of rejecting and turning of the front bogie A comes to the bending of

body for angle β (pic. 7.).



Pic. 7. Body turning in vertical transversal surface with immediate rejection of bogies

Ignoring the deformities of suspension elements the total side force of mutual action of front wheel-running bogie and outside rail – F_y , can be found from Dalmber's balance conditions:

$$\begin{aligned} \sum Y = 0 &\Rightarrow F_y + F_{y1} + F_{y2} + F_{ys} - 4F_\mu = 0, \\ \sum M_c = 0 &\Rightarrow F_y x_1 + F_{y1} x_1 + F_{y2} x_2 + F_{ys}(x_1 - l) + \\ &+ M_{iz} - 2F_\mu(x_1 + x_2) = 0, \\ \sum M_{ox} = 0 &\Rightarrow F_{ys} h_s - M_{ix} = 0, \end{aligned} \quad (10)$$

where:

F_{y1} , F_{y2} , F_{ys} are the side forces of first and second bogies (mass $m_{1t}=m_{2t}=m_t$), i.e. the vehicle body (mass m_s), where:

$$F_{y1} = -m_t \ddot{y}_1, F_{y2} = -m_t \ddot{y}_2, F_{ys} = -m_s \ddot{y}_s; \quad (11)$$

M_{iz} , M_{ix} – moments of body inertial forces according to axes O_z and O_x , where:

$$M_{iz} = -m_s r_z^2 \ddot{\alpha}, M_{ix} = -m_s r_x^2 \ddot{\beta}; \quad (12)$$

r_x , r_z – radius of body inertial mass according to axes O_x and O_z ;

F_μ – friction force of sliding for one pair of wheels;

x_1 , x_2 – distance of bogies from immediate centre of rotation across the longitudinal vehicle axis;

h_s – height of vehicle body centre.

Analyzing the turning of vehicle body in longitudinal and transversal surface we get the following dependences:

$$\begin{aligned} y_1 &= \alpha x_1, y_2 = \alpha x_2, y_s = y_t - \beta h_s; \\ y_t &= \frac{1}{2}(y_1 + y_2), \end{aligned} \quad (13)$$

where y_1 , y_2 , y_t , y_s – transversal moving of supports of front and back bogie, center O_t between them and vehicle body centre S.

From (10), (11) i (12) get:

$$F_y = F_{cf} \frac{(x_1 - l)[(r_x^2 + h_s^2)(m_s + 2m_t) - h_s^2 m_s]}{m_s x_1 (r_x^2 + h_s^2)} + 4F_\mu \quad (14),$$

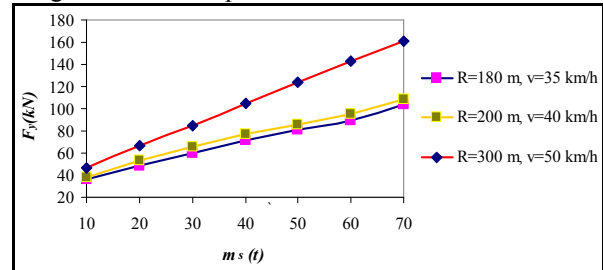
and

$$x_1 = \frac{F_{cf}[(r_x^2 + h_s^2)(l^2(m_s + 4m_t) + r_z^2 m_s) - h_s^2 m_s l^2]}{l[(r_x^2 + h_s^2)(F_{cf}(m_s + 2m_t) + 4F_\mu m_s) - h_s^2 m_s F_{cf}]}. \quad (15)$$

where:

$$F_{cf} = m_s \ddot{y}_1 = m_s \frac{v^2}{R}, 4F_\mu = \mu(m_s + 2m_t)g. \quad (16)$$

For vehicle whose parameters are $2l=8,5$ m, $h_s=1,3$ m, $m_t=4,8$ t, $I_x=1 \cdot 10^5$ kgm², $I_z=1 \cdot 10^6$ kgm², $\mu=0,2$ the dependence of total side force from vehicle body gross weight is shown on pic. 8.



Pic. 8 Dependence of total side force from vehicle body gross weight

Because of the more detailed analysis of safety and side vehicle stability while entering into curve the forces of suspension elements deformation can also be taken into consideration.

5. CONCLUSION

The determining of the permitted velocity of railway vehicles over switches is a very complex problem which is the result of number of different railway vehicle types on one hand, i.e. different track parameters on the other.

This work shows the methodology for determining the permitted railway vehicle velocity over switches where the special attention is dedicated to the analysis of safety and side vehicle stability. The analysis of parameters is done and their dynamic-exploitation factor dependence is shown.

LITERATURE

- [1] Milošević B.: "POSTROJENJA ZA VEZU KOLOSEKA", Faculty of Traffic Engineering, Belgrade (1977.);
- [2] Rusov L.: „MEHANIKA III DINAMIKA“, Naučna knjiga, Belgrade (1994.);
- [3] Rusov S.: „DINAMIKA VOZOVA“, textbook working material;
- [4] Torlaković-Tomičić M., Ranković S.: „GORNJI STROJ ŽELEZNICA“, Belgrade University (1996.);
- [5] Vershinskij S. V., Danilov V. N., Chelnokov I. I.: „DINAMIKA VAGONA“, Transport, Moscow (1978.).

FUNDAMENTAL PROBLEMS IN THE MODELLING OF WAGONS' DYNAMICS

Nebojša Ivković¹⁾, Zoran Marinković²⁾

Abstract: *The aim of the investigation of wagons oscillation is the explanation of the physical nature of oscillations and the consequences they cause, the establishment of the allowed level of occurrence, their dynamic actions, and the development of recommendations for selection of constructive parameters of wagons, which will provide their high dynamic qualities in exploitation. In this paper, the classical modelling methods and modern software package, which enable the analysis of real construction of wagons, are used. The results of such an analysis can give estimation about the quality of wagons even in the phase of projection.*

Key words: modelling, wagons, dynamics, oscillations

1. INTRODUCTION

The safety of movement and the yield of a wagon work depend on its construction and the quality of tracks. In the phase of wagons projecting, it is possible to assess their quality in such a way that wagons together with the railroad tracks are presented as one discrete mechanical system [1]. In real conditions, tracks with curves and wheels have rough spots on the surfaces. Therefore, different oscillations emerge on mobile parts of the wagons, and among them dynamic forces of mutual action. Reduction of these forces can be achieved by better construction of tracks and parts of the wagon, and by their good technical maintenance during exploitation.

The fundamental task of the study of dynamic processes in the system *wagon-track* is the determination of the optimal parameters of that system (geometry, mass, movement, stiffness, etc.), which enable minimal values of oscillations and dynamic forces in the constructions of the wagons parts and tracks. Prior to that, the following should be considered: (i) the solution of problems by study of oscillation processes of wagon and its constituent parts, (ii) the establishment of the criterion for estimation of riding stability, (iii) determination of stability against derail, turn-over and thrust in the train's composition, (iv) analysis of the ability of wagon's movement in the curves and vibrations of its elements, taking into account mutual influences.

2. Dynamic characteristics of tracks

Tracks as part of the mechanical system *wagon-track* can be represented by characteristics that are divided into two groups: characteristics determined by the track's reaction to the dynamic action of the wheel, and characteristics defined by lagging deformations, which emerge from the action of mobile elements. Due to the action of the wagon's wheels, the elasticity forces, inertia forces, and friction forces emerge on the upper structure of the track.

The elasticity consists of dynamic reactions of the track. In the majority of cases, for approximate calculation, it is assumed that the settling of the track is directly proportional to the dynamic pressure of the wheel. The friction forces, which depend on the construction of the track, are based on complex laws. Approximately, they can be classified in two parts: forces of dry friction, proportional to the quantity of the track's settling, and forces of viscous friction, proportional to the rate of change of the track's settling. The inertial forces appear in the upper structure of the tracks during movement through the impact of wheels and tracks on the connection points. Therefore, during the interaction between the wheel and the track, the inertial force on the track at the connection point varies.

The reaction of the track to the dynamic action of the wheel depends to a significant degree on the composition of the upper structure of the track. During its movement on the tracks, under the action of the wheels, there is a continuous gathering of remnant deformations, with the accumulation quantity being different in different points of the railway's tracks. Due to rough spots, the wheels are gradually driven from the equilibrium state, and in that way oscillations appear during the motion. Thus, the roughness of the tracks, which emerges due to the unequal hardness in the upper structure of the track, leads to the accumulation of lagging deformations in the tracks, and this is one of the main causes for the wagon's oscillations.

3. Dynamic characteristics of wagons

A wagon can be represented as a system consisting of a certain number of physical bodies and connections between them. In such systems, bodies have certain motions in different directions. In parallel with the direction of the wagon's motion, the movement of its trunk and bogie due to oscillations should be taken into account. Figure 1 shows a wagon and Cartesian coordinate system, which is used for obtaining the equations of motion for trunk and bogie of the wagon.

Coordinates x , y , z represent linear, while θ , φ , and ψ are angular coordinates. Indexes in the notations mark

¹⁾ Nebojša Ivković, dipl. maš.ing., B. Krsmanovića 18/45 18000 Niš, nzivkovic@ptt.yu

²⁾ prof. dr. Zoran Marinković, Mašinski fakultet Niš, A. Medveda 14 18000 Niš, zoranm@masfak.ni.ac.yu

part of the system they refer to (s – trunk, op – bogie), and standard notations are used (c and β) for the marking of hardness and damping. The distance between central bolts (l) is equal to the sum of distances between the mean vertical transversal axis of the wagon and each central bolt itself ($l = l_1 + l_2$). The transversal distance between suspended sets in the same plane is noted by b , and the distance between axis in the bogie and the bolt is noted by l_{op} .



Figure 1 System of coordinate axes of a wagon

Rigid bodies are characterized by mass, by coordinates of the inertia centre or centre of gravity, by axial and centrifugal inertia momentums (I_{x_0} , I_{y_0} , I_{z_0} , I_{xy_0} , I_{yz_0} and I_{xz_0}). Peaceful motion of the wagon on the real rough tracks is provided by the system of suspended hanging, which comprises the elastic elements and the oscillations dumper.

Certain movements are limited or largely excluded due to the motion of constructive connections between certain parts of the wagon. The connections by springs and other similar mechanisms transfer the force of mutual action between separated masses by jamming their relative movements, but without changing thereby the degree of the movement's freedom. The degree of freedom for all systems is equal to the sum of the degrees of freedom for motion of separated constituent elements.

During motion, own and forced oscillations emerge in the wagon. The first ones appear in the system that is driven out of the equilibrium state for any reason (due to instantaneous transition from the state of rest). Such oscillations are gradually stopped. The latter ones emerge and are continuously supported by action of any source of induction during any considered moment of time.

As a consequence of oscillation processes and other types of non-uniform motion of inertial masses at wagons movements, the dynamic forces appear. The values of oscillation's frequency and its form in the first place determine dynamic features of the wagons: size, peaceful operation, stability and movement, and also the magnitude of forces defining the hardness of the wagon's elements and railway tracks.

For the investigation of the wagons' oscillations, the theoretical and experimental methods have been used. The theoretical ones set the general laws between oscillations and load, which emerge in the system *wagon-track*, by taking into account constructive parameters and conditions of motion, while the experimental ones determine the concrete meaning of these parameters, set the laws by processing results, and establish the methods of calculation.

Theoretical methods are based on the theory and the equations of analytical mechanics. They usually simplify a given complex system of *wagon-track*, where ideal calculation schemes are obtained through the adaptation of

basic dynamic properties of the system. In further considering the parameters and characteristics of the system elements, differential equations of motion are set, equal in number with the degrees of freedom that the system exhibits. In the given example, the d'Alembert method is used, which helps us obtain equations of the dynamic equilibrium of the system by reference to mass inertia forces.

For the chosen calculation scheme and the given coordinates system according to this method, it is recommended setting the differential equations of motion in conjunction with geometrical, physical, and statistical rules. For that, the following is necessary:

- To determine the geometrical ratio of the coordinates of concentrated masses;
- To establishment of the reaction of connection and action on the observed body of the system; inertia forces and momentums due to deformations, increasing coordinates, their speeds and accelerations;
- To replacement of the physical model by a scheme of forces, in which the rejected connections are replaced by reactions, and the inertia forces and momentums of inertia forces are added to the mass center; the system of equations of static equilibrium should be written by adding factors of inertia forces to act as in actual case.

The number of differential equations is equal to the number of degrees of freedom for the movement of the observed system. So, which reduces the study of dynamic processes of the system to putting together and analyzing differential equations that process is described.

The calculation scheme *wagon-track*, after simplification, presents a big number of degrees of freedom for movement, whose elastic connections are often non-linear. Integration of such a complex system is possible only using a computer. Therefore these studies help towards the simplification of schemes with smaller number of degrees of freedom.

4. Model of the system wagon-track

Figure 2 shows the equivalent model of a four-axial wagon with stiff trunk and part of the upper structure of the track. With this type of model, which deals with a mass supported by the elastic base, different oscillations can generally occur.

During the motion of such a system, if there is roughness on the tracks, several types of forced oscillations will appear interacting with each other. The own oscillations with certain frequencies and periods are obtained by driving the system out of the state of rest using impulses of any kind. In such a case, the movements in all possible parts of suspended, tracks and base of the tracks are obtained.

When the wagon is observed as a constituent part of the train, the occurrence of side oscillations should also be taken into account.

In the example, the observed wagon is moving on the tracks with vertical roughness η , which is equal for both wheels ($\eta_1 = \eta'_1$; $\eta_2 = \eta'_2$ itd.).

Using the d'Alembert method, according to Fig. 2, the following relations can be written:

- Movement in the direction y and z in suspended complete sets:

$$\xi_I = z_s - l_1 \varphi_s + b_1 \theta_s - z_{opl}; \gamma_I = y_s - h \theta_s + l_1 \psi_s - y_{opl};$$

$$\begin{aligned}\xi_{II} &= z_s + l_2 \varphi_s + b_1 \theta_s - z_{op2}; \gamma_{II} = y_s - h \theta_s - l_2 \psi_s - y_{op2}; \\ \xi_I' &= z_s - l_1 \varphi_s - b_1 \theta_s - z_{op1}; \gamma_I' = y_s - h \theta_s + l_1 \psi_s - y_{op1};\end{aligned}$$

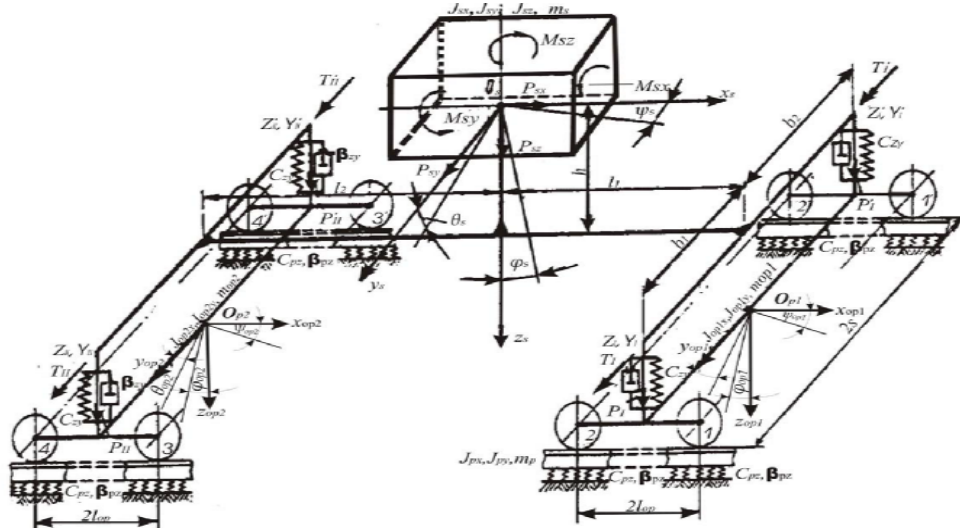


Figure 2 The equivalent model of four-axial wagon

- Movement in direction of y and z for elastic base of the road:

$$\begin{aligned}\xi_{p1} &= \xi_{p1} = z_{op1} - l_{op1} \varphi_{op1} - \eta_1; \xi_{p3} = \xi_{p3} = z_{op2} - l_{op2} \varphi_{op2} - \eta_3; \\ \xi_{p2} &= \xi_{p2} = z_{op2} - l_{op2} \varphi_{op2} - \eta_2; \xi_{p4} = \xi_{p4} = z_{op2} - l_{op2} \varphi_{op2} - \eta_4;\end{aligned}$$

Forces which act on elements of the system:

- Force of reaction of connections in suspended sets:

$$\begin{aligned}P_I &= -c_z \xi_I - \beta_z \dot{\xi}_I; T_I = -c_y \gamma_I - \beta_y \dot{\gamma}_I; \\ P_{II} &= -c_z \xi_{II} - \beta_z \dot{\xi}_{II}; T_{II} = -c_y \gamma_{II} - \beta_y \dot{\gamma}_{II}; \\ P_I' &= -c_z \xi_I' - \beta_z \dot{\xi}_I'; T_I' = -c_y \gamma_I' - \beta_y \dot{\gamma}_I'; \\ P_{II}' &= -c_z \xi_{II}' - \beta_z \dot{\xi}_{II}'; T_{II}' = -c_y \gamma_{II}' - \beta_y \dot{\gamma}_{II}';\end{aligned}$$

- Force in the base of the road:

$$\begin{aligned}P_{p1} &= P_{p1} = -c_{pz} \xi_{p1} - \beta_{pz} \dot{\xi}_{p1}; P_{p3} = P_{p3} = -c_{pz} \xi_{p3} - \beta_{pz} \dot{\xi}_{p3}; \\ P_{p2} &= P_{p2} = -c_{pz} \xi_{p2} - \beta_{pz} \dot{\xi}_{p2}; P_{p4} = P_{p4} = -c_{pz} \xi_{p4} - \beta_{pz} \dot{\xi}_{p4};\end{aligned}$$

- Force and momentums of inertia which act on trunk:

$$\begin{aligned}P_{sy} &= -m_s \ddot{y}_s; P_{sz} = -m_s \ddot{z}_s; \\ M_{sx} &= -I_{sx} \ddot{\theta}_s; M_{sy} = -I_{sy} \ddot{\varphi}_s; M_{sz} = -I_{sz} \ddot{\psi}_s;\end{aligned}$$

- On bogie:

$$\begin{aligned}P_{op1z} &= -m_{op1} \ddot{z}_{op1}; P_{op2z} = -m_{op1} \ddot{z}_{op1}; \\ M_{op1y} &= -I_{op1y} \ddot{\varphi}_{op1}; M_{op2y} = -I_{op2y} \ddot{\varphi}_{op2};\end{aligned}$$

The equation of motion:

- For trunk:

$$\begin{aligned}\Sigma Y &= 0; P_{sy} + T_I + T_I' + T_{II} + T_{II}'; \\ \Sigma Z &= 0; P_{sz} + P_I + P_{II} + P_I' + P_{II}'; \\ \Sigma M_x &= 0; M_{sx} + (P_I + P_{II})b_1 + (P_I' + P_{II}')b_1 - (T_I + T_{II} + T_I' + T_{II}')h = 0; \\ \Sigma M_y &= 0; M_{sy} + (P_I + P_{II})l_1 + (P_I' + P_{II}')l_2 = 0; \\ \Sigma M_y &= 0; M_{sy} + (P_I + P_{II})l_1 + (P_I' + P_{II}')l_2 = 0; \\ \Sigma M_z &= 0; M_{sz} + (T_I + T_I')l_1 + (T_{II} + T_{II}')l_2 = 0;\end{aligned}$$

- For first bogie:

$$\begin{aligned}\Sigma Z &= 0; P_{op1z} + P_{p1} + P_{p1}' + P_{p2} + P_{p2}' - P_I - P_I' = 0; \\ \Sigma M_y &= 0; M_{op1y} - (P_{p1} + P_{p1}' + P_{p2} + P_{p2}')l_{op} = 0;\end{aligned}$$

- For second bogie:

$$\begin{aligned}\Sigma Z &= 0; P_{op2z} + P_{p3} + P_{p3}' + P_{p4} + P_{p4}' - P_{II} - P_{II}' = 0; \\ \Sigma M_y &= 0; M_{op2y} - (P_{p3} + P_{p3}' + P_{p4} + P_{p4}')l_{op} = 0;\end{aligned}$$

By replacing the values of forces and momentums in the equations of equilibrium, the system of differential equations of the wagon is obtained:

$$\begin{aligned}a_{11}\ddot{z}_s + b_{11}\dot{z}_s + c_{11}z_s + b_{12}\dot{\varphi}_s + c_{12}\varphi_s + b_{13}\dot{\theta}_s + c_{13}\theta_s + \\ b_{14}\dot{z}_{op1} + c_{14}z_{op1} + b_{15}\dot{z}_{op2} + c_{15}z_{op2} &= 0; \\ a_{21}\ddot{y}_s + b_{21}\dot{y}_s + c_{21}y_s + b_{22}\dot{\theta}_s + c_{22}\theta_s + b_{23}\dot{\varphi}_s + c_{23}\varphi_s &= 0; \\ a_{31}\ddot{\theta}_s + b_{31}\dot{\theta}_s + c_{31}\theta_s + b_{32}\dot{\varphi}_s + c_{32}\varphi_s + b_{33}\dot{y}_s + c_{33}y_s + \\ b_{34}\dot{z}_s + c_{34}z_s + b_{35}\dot{\varphi}_s + c_{35}\varphi_s + b_{36}\dot{z}_{op1} + c_{37}z_{op1} + \\ c_{37}z_{op2} &= 0; \\ a_{41}\ddot{\varphi}_s + b_{41}\dot{\varphi}_s + c_{41}\varphi_s + b_{42}\dot{z}_s + c_{42}z_s + b_{43}\dot{\theta}_s + c_{43}\theta_s + \\ b_{44}\dot{z}_{op1} + c_{44}z_{op1} + b_{45}\dot{z}_{op2} + c_{45}z_{op2} &= 0; \\ a_{51}\ddot{\psi}_s + b_{51}\dot{\psi}_s + c_{51}\psi_s + b_{52}\dot{y}_s + c_{42}y_s + b_{53}\dot{\theta}_s + c_{53}\theta_s &= 0; \\ a_{61}\ddot{z}_{op1} + b_{61}\dot{z}_{op1} + c_{61}z_{op1} + b_{62}\dot{y}_s + c_{62}y_s + b_{63}\dot{\theta}_s + \\ c_{63}\theta_s + b_{64}\dot{\varphi}_s + c_{64}\varphi_s &= b_{65}(\dot{\eta}_1 + \dot{\eta}_2) + c_{65}(\eta_1 + \eta_2); \\ a_{71}\ddot{\varphi}_{op1} + b_{71}\dot{\varphi}_{op1} + c_{71}\varphi_{op1} &= b_{72}(\dot{\eta}_2 - \dot{\eta}_1) + c_{72}(\eta_2 - \eta_1); \\ a_{81}\ddot{z}_{op2} + b_{81}\dot{z}_{op2} + c_{81}z_{op2} + b_{82}\dot{z}_s + c_{82}z_s + b_{83}\dot{\theta}_s + c_{83}\theta_s + \\ b_{84}\dot{\varphi}_s + c_{84}\varphi_s &= b_{85}(\dot{\eta}_3 + \dot{\eta}_4) + c_{85}(\eta_3 + \eta_4); \\ a_{91}\ddot{\varphi}_{op2} + b_{91}\dot{\varphi}_{op2} + c_{91}\varphi_{op2} &= b_{82}(\dot{\eta}_4 - \dot{\eta}_3) + c_{72}(\eta_4 - \eta_3); \\ a_{11} &= a_{21} = m_s; a_{31} = I_{sx}; a_{41} = I_{sz}; a_{51} = I_{kz}; a_{61} = m_{op1}; \\ a_{71} &= I_{op1y}; a_{81} = m_{op2}; a_{91} = I_{op2y}; b_{11} = 4\beta_z; b_{12} = -2\beta_z(l_1 - l_2); \\ b_{13} &= -2\beta_z(b_2 - b_1); b_{14} = b_{15} = -2\beta_z; b_{21} = 4\beta_y; b_{22} = -4\beta_y h; \\ b_{23} &= 2\beta_y(l_1 - l_2); b_{31} = 2[\beta_z(b_1^2 + b_2^2) + 2\beta_y h^2]; b_{32} = \beta_z(b_1 - b_2) + \\ (l_2 - l_1); b_{33} &= -4\beta_y h; b_{34} = 2\beta_y(b_1 - b_2); b_{35} = -2\beta_y h(l_1 - l_2); \\ b_{36} &= b_{37} = \beta_z(b_2 - b_1); b_{41} = 2\beta_z(l_1^2 + l_2^2); b_{42} = -2\beta_z(l_2 - l_1); \\ b_{43} &= -\beta_z(l_1 - l_2)(b_1 - b_2); b_{44} = -2\beta_z l_1; b_{45} = -2\beta_z l_2;\end{aligned}$$

$$\begin{aligned} b_{51} &= 2\beta_y(l_1^2 + l_2^2); b_{52} = 2\beta_z(l_1 - l_2); b_{53} = 2\beta_y(l_1 - l_2)l; \\ b_{61} &= 2(2\beta_{pz} + \beta_z); b_{62} = -2\beta_z; b_{43} = -\beta_z(b_1 - b_2); b_{64} = 2\beta_z l_1; \\ b_{65} &= 2\beta_{pz}; b_{71} = \beta_{pz}(2l)^2; b_{72} = 2l\beta_{pz}; b_{81} = 2(2\beta_{pz} + \beta_z); \\ b_{82} &= -\beta_z; b_{83} = -\beta_z(b_1 - b_2); b_{84} = -2\beta_z l_1; b_{85} = 2\beta_{pz}; b_{91} = \beta_{pz}(2l)^2; \\ b_{92} &= 2\beta_{op} l_T; [1]. \end{aligned}$$

The values of coefficients C_{ij} can be obtained from expression for b_{ij} by replacing their values c by values β with corresponding numerical indices.

Solving such systems is quite cumbersome and practically can be achieved only by computers, but even in that case, the analysis of obtained results (for mutual influences of oscillations with different frequencies and phases) is difficult. In particular it is difficult to decode notes of results for solutions of equations, in parts where the roughness of the track (η) was introduced, and which is nearer to real value having many types of harmonics of different wave lengths and amplitudes.

For a more thorough study of obtained oscillations for complex systems, some simplifications are introduced. Very often due to the symmetry of construction and the distribution of load, we can start from the assumption that $l_1=l_2=l$, $b_1=b_2=b$, and so making the coefficients $b_{12}, b_{13}, c_{12}, c_{13}, b_{23}, c_{23}, b_{32}, c_{32}, b_{34}, c_{34}, b_{35}, c_{35}, b_{36}, c_{36}, b_{37}, c_{37}, b_{42}, c_{42}, b_{52}, c_{52}, b_{53}, c_{53}, c_{63}, b_{63}, c_{83}, b_{83}$ to be equal to 0. Then, the system is divided into several simpler groups, which have the form:

$$\begin{aligned} a_{11}\ddot{z}_s + b_{11}\dot{z}_s + c_{11}z_s + b_{14}\dot{z}_{op1} + c_{14}z_{op1} + b_{15}\dot{z}_{op2} + c_{15}z_{op2} &= 0; \\ a_{41}\ddot{\phi}_s + b_{41}\dot{\phi}_s + c_{41}\phi_s + b_{44}\dot{z}_{op1} + c_{44}z_{op1} + b_{45}\dot{z}_{op2} + c_{45}z_{op2} &= 0; \\ a_{61}\ddot{z}_{op1} + b_{61}\dot{z}_{op1} + c_{61}z_{op1} + b_{62}\dot{z}_s + c_{62}z_s + b_{64}\dot{\phi}_s + & \\ c_{64}\phi_s = b_{65}(\dot{\eta}_1 + \dot{\eta}_2) + c_{65}(\eta_1 + \eta_2); & \\ a_{81}\ddot{z}_{op2} + b_{81}\dot{z}_{op2} + c_{81}z_{op2} + b_{82}\dot{z}_s + c_{82}z_s + b_{84}\dot{\phi}_s + & \\ c_{84}\phi_s = b_{85}(\dot{\eta}_3 + \dot{\eta}_4) + c_{85}(\eta_3 + \eta_4); & \\ a_{21}\ddot{y}_s + b_{21}\dot{y}_s + c_{21}y_s + b_{22}\dot{\theta}_s + c_{22}\theta_s &= 0; \\ a_{31}\ddot{\theta}_s + b_{31}\dot{\theta}_s + c_{31}\theta_s + b_{33}\dot{y}_s + c_{33}y_s &= 0; \\ a_{51}\ddot{\psi}_s + b_{51}\dot{\psi}_s + c_{51}\psi_s &= 0; \\ a_{71}\ddot{\phi}_{op1} + b_{71}\dot{\phi}_{op1} + c_{71}\phi_{op1} = b_{72}(\dot{\eta}_2 - \dot{\eta}_1) + c_{72}(\eta_2 - \eta_1); & \\ a_{91}\ddot{\phi}_{op2} + b_{91}\dot{\phi}_{op2} + c_{91}\phi_{op2} = b_{82}(\dot{\eta}_4 - \dot{\eta}_3) + c_{72}(\eta_4 - \eta_3); & \end{aligned}$$

The first group of equations describes vertical movement of trunk and bogie in side vertical plane of symmetry. The mentioned oscillations consist of vertical symmetrical and non-symmetrical oscillations, which can be noted in the following way:

$$z_{op} = (z_{op1} + z_{op2})/2; \phi_{op} = (z_{op1} - z_{op2})/2l.$$

By equating these expressions, the movements of bogies in horizontal direction are obtained:

$$z_{op1} = z_{op} + l\phi_{op}; z_{op2} = z_{op} - l\phi_{op}.$$

By replacing the expressions for z_{op1} and z_{op2} in the system of first four equations new system of differential equations is obtained:

$$\begin{aligned} m_s \ddot{z}_s + 4\beta_z \dot{z}_s + 4c_z z_s - 4\beta_y z_{op} - 4c_z z_{op} &= 0; \\ 2m_{op} \ddot{z}_{op} + 4(\beta_z + 2\beta_{pz}) \dot{z}_{op} + 4(c_z + 2c_{pz}) z_{op} - 4\beta_z \dot{z}_s - & \\ 4c_z z_s = 8\beta_{pz} \dot{\eta}_c + 8c_{pz} \eta_c; & \\ I_{sy} \ddot{\phi}_s + 4\beta_z l^2 \dot{\phi}_s + 4c_z l^2 \phi_s - 4\beta_z l \dot{z}_{op} - 4c_z l z_{op} &= 0; \\ 2m_{op} l^2 \ddot{\phi}_{op} + 4l^2 (\beta_z + 2\beta_{pz}) \dot{\phi}_{op} + 4l^2 (c_z + 2c_{pz}) \phi_{op} + & \\ 4\beta_z l^2 \dot{\phi}_s + 4c_z l^2 \phi_s = 8\beta_{pz} l^2 \dot{\phi}_{pc} + 8c_{pz} l^2 \phi_{pc}; & \end{aligned}$$

where: $2m_{op}$ – is the mass of two bogies, η_c – mean vertical movement of railroad pair of wagons due to roughness of the road, ϕ_{pc} – angle of slope of the trunk induced by roughness of the road.

From the aforementioned it follows that first two differential equations of the system describe symmetric oscillations of trunk with bogie. Furthermore it will be considered case of symmetric oscillations for certain type of freight wagon on shorter distance, where the influence of the dumper is neglected ($\beta_z = \beta_{pz} = 0$).

Then, the corresponding differential equations are:

$$\ddot{z}_s + v_1^2 z_s - v_1^2 z_{op} = 0 \text{ and } \ddot{z}_{op} + v_2^2 z_{op} - v_3^2 z_s = u \eta_c,$$

where: $v_1^2 = 4c_z / m_s$; $v_2^2 = 2(c_z + 2c_{pz}) / m_{op}$;

$$v_3^2 = 2c_z / m_s; u = 4c_{pz} / m_{op}.$$

If the symmetric oscillations are singled out from the general process for which the system of differential equations is written, preliminary presented complex calculation scheme of wagon can be replaced by simpler scheme (Fig. 3a), which provides, without a significant error, an insight into wagons oscillations. At times the solving of such systems posed the problem. By applying modern software packages this kind of problems are solved easily and quickly. An example of such solution in graphical way is given in Fig. 3b, where the movements of trunk and bogie for defined time are shown [2].

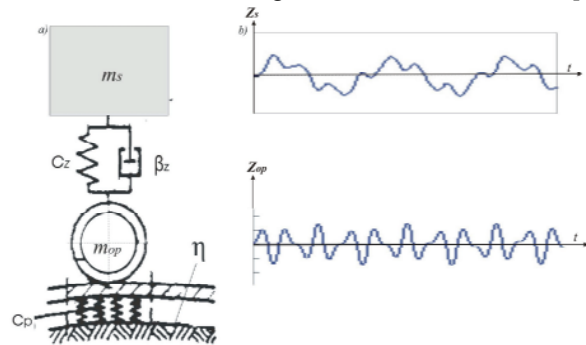


Figure 3 Scheme for calculation of wagons oscillations (a) and graph of oscillations of wagon's trunk and bogie (b).

5. Conclusion

The aim of the type of modelling, simulations and analysis presented in this paper is the possibility of better understanding of wagons performance in exploitation. Nowadays modern software packages can solve complex wagon's dynamic models, which would be difficult to resolve using classical analytical methods. Therefore this technology is a way towards better and cheaper products, which characteristics are analyzed in the phase of projecting wagons without high expenses for test investigations, and when the changes are still possible [3].

Literatura:

- [1] Veršinskij S. V: *Dinamika vagona*, Moskva, Transport, 1978.
- [2] Ivković Nebojša: *Dinamika teretnih vagona*, seminarski rad, Mašinski fakultet Niš, 2005.
- [3] Čalasan Latinka: *Matlab i dodatni moduli*, Mikroknjiga, Beograd, 1996.

ВЛИЯНИЕ ПАРАМЕТРОВ ТРАССЫ ПРИ ПРОЕКТИРОВАНИИ ЖЕЛЕЗНОДОРОЖНОГО ПУТИ

Майя Г. Иванова

Аннотация:

В докладе рассмотрено влияние параметров трассы при проектировании железнодорожного пути. Как основным показателем принят средневзвешенный наклон местности.

Ключевые слова: Трасса, железны дороги, влияние параметров

Существующие у нас железнодорожные пути имеют невысокие технические параметры. Железнодорожный путь Видин – София, принятый в качестве характерного примера, не делает исключение. Маленькие радиусы кривых и большие продольные наклоны определяют маленькую скорость и продолжительное время пути. Вопросы, связанные с проектированием и строительством этого железнодорожного пути, должны решиться до эксплуатационного пуска Дунав мост-2, чтобы не уменьшить значение его построения.

Некоторые основные показатели, которые имеют влияние на технико-экономическое сравнение проектных вариантов:

- фактическая длина железнодорожного пути;
- коэффициент развития ;
- длина прямых участков;
- длина кривых участков;
- число и длина сооружений;
- объем земляных работ;
- время пути.

Именно эти показатели определяют качество каждого проектного варианта.

Так как выбор параметров железной дороги зависит как от проектной скорости, так и от характера местности, поэтому основным показателем принят средневзвешенный наклон местности. Для определения его стоимости использованы данные участков местности соответствующего продольного профиля. Средневзвешенный наклон местности влияет

существенно на технические показатели проектных вариантов.

Общая длина рассмотренных проектных вариантов (489,98 км), их число, как и исключительно разнообразный характер местности, дают основание сделать сравнительно достоверные обобщения некоторой зависимости между различными параметрами трассы.

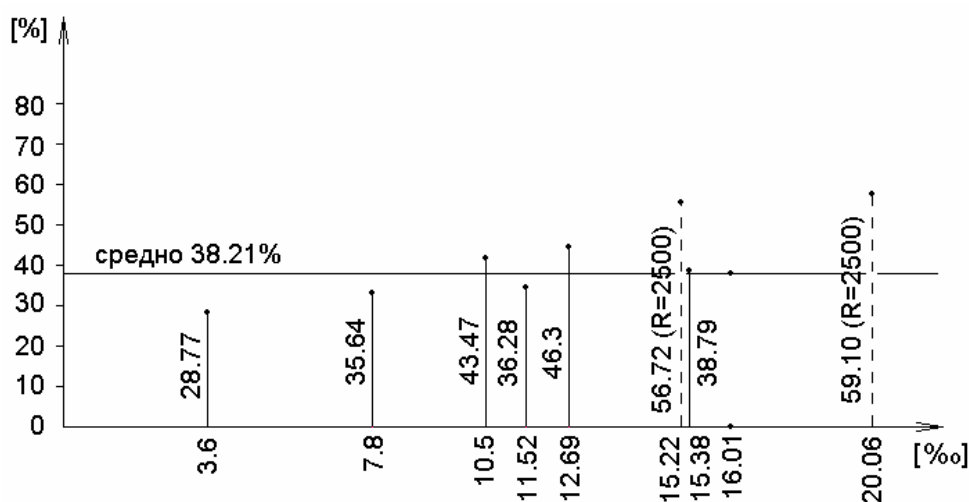
1. ДЛИНА КРИВЫХ УЧАСТКОВ В [%] ОТ ОБЩЕЙ ДЛИННЫ ЖЕЛЕЗНОЙ ДОРОГИ

Этот показатель очень важен при определении качества очередного проектного варианта, так как наличие большего числа кривых ухудшают условия движения (наличие центробежных сил, дополнительного сопротивления), а также увеличивают эксплуатационные расходы.

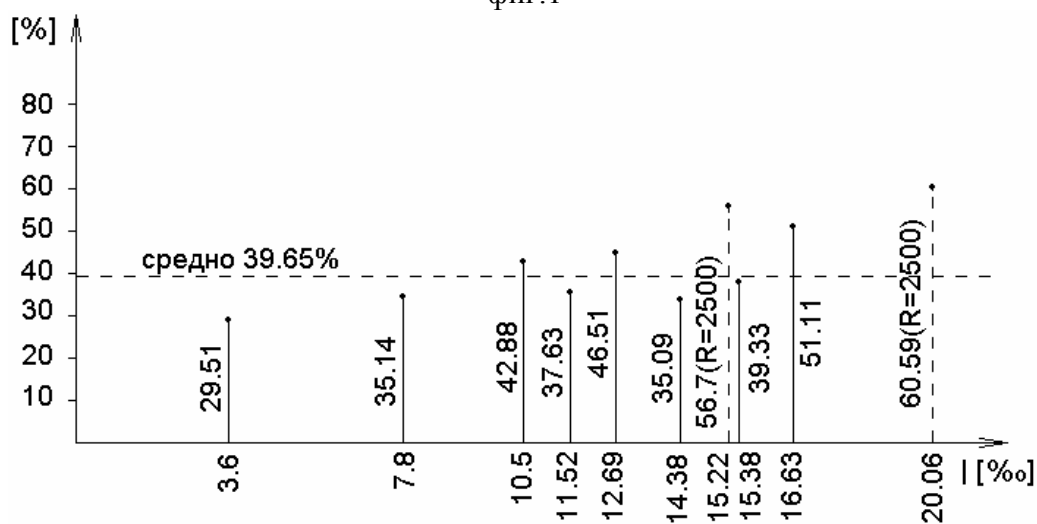
При сравнении рассмотренных вариантов по этому показателю установлено, что величина главного наклона оказывает влияние на соотношение между элементами железной дороги в кривом и прямом участках.

При $I = 15$ длина кривых участков в [%] от общей длинны железной дороги при $R = 1500$ m в среднем 38,21%(фиг.1). При этом же радиусе и $I = 20$ этот процент 39,65%(фиг.2).

Этот же показатель в обоих вариантах с $R = 800$ m и $I = 25$ в среднем 37,37%, т.е. он не отличается существенно от вариантов с $R = 1500$ m



фиг.1



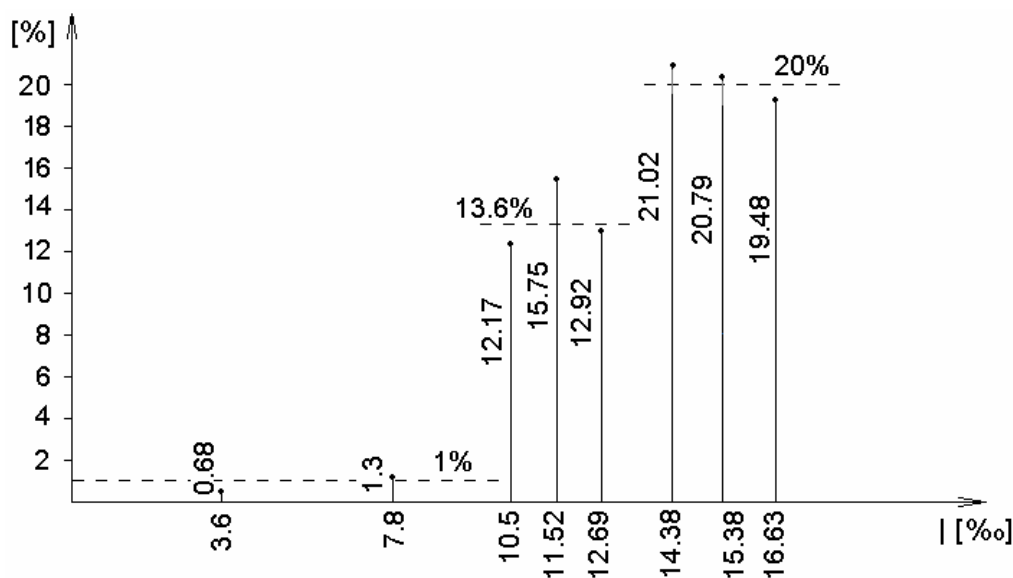
фиг.2

Впечатляет, что процент кривых участков нарастает существенно при увеличении $R = 2500 \text{ m}$, а при продольных наклонах $I = 15$ и $I = 20$, он существенно не различается. Средняя стоимость этого показателя для четырех вариантов с $R = 2500 \text{ m}$ равна 58,28%.

Можно сделать заключение, что при проектировании железнодорожного пути для скорости 200 km/h ($R = 2500 \text{ m}$), процент кривых участков нарастает приблизительно на 20%, сравнивая с процентом для скорости 160 km/h ($R = 1500 \text{ m}$). Уменьшение радиуса меньше, чем 1500 m (респективно скорости), а также и увеличения максимального продольного наклона не приводит к существенному изменению этого показателя.

2. ДЛИННА СООРУЖЕНИЙ В [%] ОТ ОБЩЕЙ ДЛИННЫ ЖЛЕЗНОЙ ДОРОГИ

Стоимости этих показателей не влияют существенно от минимального радиуса и максимального продольного наклона. Самым осезательным влиянием является естественный наклон местности (фиг. 1). Впечатляет резкое изменение (со скоком) средних стоимостей при увеличении естественного наклона.



фиг.3

На фиг. 3 видно, что при естественном наклоне до 10, процент сооружений около 1%. При наклоне местности от 10 до 14, этот процент порядка 13,6%. При естественном наклоне больше, чем 14, длина сооружений занимает около 20% общей длины железной дороги.

Если допустить, что при естественном наклоне местности, большем, чем 10 и длиной сооружений в [%] от общей длины железной дороги существует функциональная зависимость, то она бы могла установиться методом наименьших квадратов. Аппроксимация будет следующего вида:

$$(1) y = 6,5 \cdot 2^{0,1x}$$

Средняя квадратическая ошибка равна:

$$(2) m = \pm \sqrt{\frac{[(y_1 - f(x_i))^2]}{n}} = 2,13\%$$

Относительная ошибка: 12,5 [%].

Аналогичным образом можно найти зависимость длины сооружений в [%] от общей длины железной дороги при $R = 1500 \text{ mm}$ и $I = 15$ (фиг.2). Функция имеет вид:

$$(3) y = 4,6 \cdot 2^{0,14x}$$

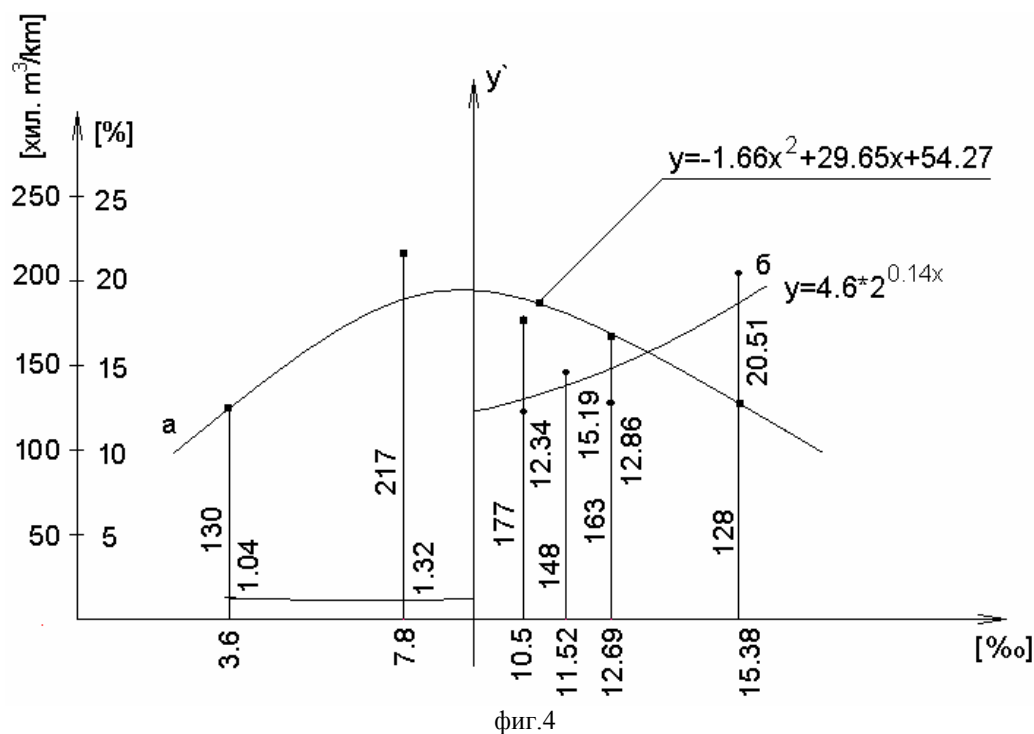
Средняя квадратическая ошибка равна:

$$(4) m = \sqrt{\frac{[(y_1 - f(x_i))^2]}{n}} = 1,56\%$$

Относительная ошибка: 9,9 [%].

3. ВЛИЯНИЕ ПАРАМЕТРОВ ТРАССЫ НА ОБЪЕМ ЗЕМЛЯНЫХ РАБОТ

Объем землянных работ, вместе с сооружениями, определяется для необходимых инвестиций при построении железнодорожного пути. Их величина отнесенная к километру железной дороги, проявляет существенное влияние от естественного наклона местности, а также от числа сооружений. Она нарастает при увеличении естественного наклона и уменьшается при увеличении длины сооружений. Стоимость естественного наклона местности порядка 10 является критической точкой. Землянные работы на километр железной дороги начинают уменьшаться параллельно резкому росту процента сооружений (фиг.4.)



По методу наименьших квадратов можно найти и функциональную зависимость между естественным наклоном местности (x) и объемом землянных работ на километр железной дороги (y). Функция имеет вид:

$$(5) y = -1,66x^2 + 29,65x + 54,27$$

Средняя квадратическая ошибка равна:

$$(6) m = \sqrt{\frac{\sum (y_i - f(x_i))^2}{n}} = 18,43 \text{ км}^3 / \text{км}$$

Относительная ошибка составляет порядком 11,5%.

Так как объем землянных работ зависит от выбора вида и длины сооружений, его стоимость может быть только относительным критерием для качества данного проектного варианта.

Обобщающим критерием в этом отношении возможно иметь ввиду так названные «привиденные» землянные работы на километр железной дороги. Приведенные землянные работы получаются, если допустить, что нет сооружений, а существуют только выемки и насыпи.

От этого исследования можно сделать вывод, что при выборе параметров трассы нужно подходить внимательно, а также иметь ввиду естественный наклон местности. Во всяком случае вариантные решения максимальной скорости 200 км/ч с $R = 2500 \text{ м}$ не нужно пренебрегать даже при трудных условиях местности, используя крутые продольные наклоны. Это особенно важно для железнодорожного пути, который является частью международного коридора.

СОВРЕМЕННЫЕ ГЕОДЕЗИЧЕСКИЕ ТЕХНОЛОГИИ ДЛЯ ОПРЕДЕЛЕНИЯ ГЕОМЕТРИИ ЖЕЛЕЗНОЙ ДОРОГИ

Румен Иванов *, Валентин Николов *, Коста Костов *

Резюме: Существующие технологии контроля геометрии плана железных дорог основаны на измерении стрел изгиба. Точность определения радиуса по этому методу не может быть выше, чем ± 1 м и, кроме этого с нарастанием радиуса кривой нарастает и его средняя квадратная ошибка. Применение GPS или тотальной станции позволяет избавиться от описанного недостатка. Среднеквадратическая ошибка определения координат этой технологии не выходит за пределы 5-10 мм, что удовлетворяет требованиям геометрии железных дорог.

Ключевые слова: геометрия железных дорог, железные дороги, GPS, тотальная станция

1. КОНТРОЛЬ С ПОМОЩЬЮ СТРЕЛ ПРОГИБОВ

Оценка геометрии железной дороги с помощью стрел прогибов базируется на зависимости между радиусом кривой (R) и измеренной стрелой прогиба [3].

$$(1) \quad R = \frac{a^2}{2f},$$

где используются следующие обозначения:

a – половина длины хорды

f – стоимость измерения стрелы прогиба

Точность определения радиуса по этому методу не может быть выше, чем ± 1 м и, кроме этого, с нарастанием радиуса кривой нарастает и его средняя квадратная ошибка m_R . Этим методом не могут быть удовлетворены современные требования контроля геометрии плана железных дорог, как оценка геометрии железной дороги высокоскоростных линий, быстрый доступ к результатам измерения, небольшие габариты, малые затраты времени для оценки параметров пути, возможность проверки на достоверность получаемых результатов, высокая точность измеренных данных и др.[5]. Эти потребности удовлетворяются современными геодезическими технологиями и, точнее, использованием GPS и тотальных станций.

2. GPS

NAVSTAR GPS это спутниковая навигационная система, находящаяся под командованием Министерства обороны и Министерства транспорта США. GPS обеспечивает высокоточную информацию для определения местоположения, позволяя потребителям системы определить свои пространственные трехмерные декартовы координаты, скорость и время 24 часа в сутки,

независимо от метеорологических условий. Система состоит из космической части, наземной контрольной части и приемника.

Измерения с GPS могут быть классифицированы как статические или кинематические, в зависимости от того, проводятся измерения с неподвижного места или во время движения. Для определения геометрии железной дороги обыкновенно проводятся кинематические измерения в реальном времени (RTK). Аппаратура измерения, кроме GPS, включает в себя и компьютер для регистрации и обработки данных и имеет вид, показанный на фиг.1 [4].

Отклонения между проектным и измеренным положением железной дороги позволяет сделать оценку качества геометрии пути[1].

Планируемая модернизация GPS и развитие европейской системы Galileo увеличит доступность сигналов для пользователей спутниковых навигационных систем и позволит еще более широкому использованию этой технологии для оценки геометрии железной дороги.



Фиг. 1

3. ТОТАЛЬНЫЕ СТАНЦИИ

Новые модели тотальных станций позволяют геодезистам совершать эффективные и высокоточные измерения. Эта генерация новых инструментов с меньшими размерами более современна и уменьшает время измерений. Они в корне изменили работу геодезистов, и тотальные станции заменили в большой степени оптические инструменты. Тотальные станции позволяют получить высокую точность измерений в зонах, в которых GPS не может быть использован. Таким образом, они идеально дополняют GPS технологию, и эта взаимная заменяемость позволяет широко использовать в практике различные комбинации измерения с GPS и тотальной станцией. Аппаратура измерения, кроме отражателя, включает в себя и компьютер для регистрации и обработки данных и имеет вид, показанный на фиг.2 [7].

Во многих измерительных системах имеется и экстензометр для определения междурельсия и наклонотометр для определения поперечного наклона (высотная разница) [6].



Фиг. 2

4. СОЗДАНИЕ ОПОРНОЙ ГЕОДЕЗИЧЕСКОЙ ОСНОВЫ ЖЕЛЕЗНОЙ ДОРОГИ

Реконструкция железных дорог немыслимо без создания близкой около них геодезической сети. Построение геодезической сети можно проводить только с помощью GPS, или только с тотальной станцией. Если построим геодезическую сеть только с помощью GPS технологии, время измерений будет неприемлемо долгим. Цена определения положения одной точки с GPS высока, из-за чего могут дополнительно подорожать проекты. Строя

геодезическую сеть только с тотальной станцией, автоматически увеличиваем число точек, а значит и число измерений. Оптимальным принят вариант построения включенной полигонометрической сети (включенного полигона), на котором крайние и начальные точки измерены с помощью GPS, а для определения координат промежуточных точек проводятся измерения с тотальной станцией [2]. С рабочей основы, созданной таким образом, проводятся съемки и контроль геометрии плана железных дорог.

Литература

1. Але Ф., С. Бет, "Анализ качества железной дороги чрез динамический контроль с помощью GPS" (на болгарском языке), Железнодорожный транспорт, бр. 7/8, 36-39с., 2001 г.
2. Иванов Р., Р. Вилков, "Комбинирование измерений с GPS и тотальной станцией для целей геодезического обеспечения железной дороги", (на болгарском языке), XIV Научная конференция с международным участием "Транспорт 2004", ВТУ "Т. Каблешков", 11-12 ноября 2004, София
3. Костадинов, С., "Численные методы в транспортном строительстве", (на болгарском языке), София, 3-229с., 2004г.
4. Glaus, R., G. PEELS, U. Müller, A. Geiger "Precise Rail Track Surveying", GPS World, 12-18pp., 2004
5. Joch M., D. Jussel, D. Maitz, "Автономные системы оценки параметров пути", (в переводе) Железные дороги мира, N12, 2004
6. Kuhlmann H., "Alignment of rails on slab track with robotic tacheometers", The 3rd International Symposium on Mobile Mapping Technology, Kairo, 1-11pp, 2001.
7. Peels G., S. Dale, "A 'Simple' Approach for Track Renewals and Maintenance from a Surveying Point of View", terra international surveys Ltd, 1-2pp, 2004

¹ Румен Ангелов Иванов, гл.ас.д-р инж., ВТУ "Т. Каблешков", адрес: 1574 София, ул. "Гео Милев" 158, rang75@hotmail.com

¹ Валентин Александров Николов, доц.д-р инж., ВТУ "Т. Каблешков", адрес: 1574 София, ул. "Гео Милев" 158, vaa@vtu.bg

¹ Коста Петров Костов, ст.ас. инж., ВТУ "Т. Каблешков", адрес: 1574 София, ул. "Гео Милев" 158, kkostov@vtu.bg

CHARACTERISTICS OF DANGEROUS GOODS – THE SOURCE OF CONSTRUCTIVE REQUESTS IN PRODUCTION OF RAILWAYS

Professor Dragutin Jovanovic¹, Dr. Sc., colonel of the Serbia and Montenegro Army

ABSTRACT: *Transporting dangerous goods carry out a variety of possible hazards and danger for the environment. Quite a number of these is being transporting by railway. In order to make their transportation safer and secure, a variety of measures is been taken. The character of dangerous goods and the way they behave during the transportation present the source of constructive requests in production of railway vehicles. Only well constructed railway vehicles whose specific constructive characteristics are able to meet physical and chemical character of dangerous goods may contribute to safe and secure transportation.*

KEY WORDS: *railway, transportation, dangerous goods, railway coaches*

1. INTRODUCTION

Development of science, techniques and contemporary technology produces, at the same time, more and more dangerous goods nowadays. The nature of cargo that is being transporting affects the environment in some way. Transporting of dangerous goods, considering their characteristics, implies series of possible hazards for the environment as well as for those who directly participate in process of transporting. Ten percent of total amount of dangerous goods make those goods that are being transporting by railway. There is a need to protect from every possible danger. The matter of protection from action of dangerous goods implies three main groups of activities:

- studying the characteristics of dangerous goods in order to stop their damaging influence,
- defining the precautionary measures for eliminating the possibility of arising an accident as well as for diminution of possible consequences and
- taking all necessary measures for safe transportation.

Safe transportation of dangerous goods by railway vehicles with specific technical characteristics, specially considering physical and chemical ones.

2. CHARACTERISTICS OF DANGEROUS GOODS TRANSPORTATION – THE SOURCE OF CONSTRUCTIVE REQUESTS

Dangerous goods are regarded as all those goods which owing to their specific characteristics may, due to inexpert and irresponsible handling or any other accident during the production, transporting and

storage, invite danger and initiate damaging consequences for health and lives of people.

We use term such as “dangerous goods” considering the position they take during their transporting as packed in special packages or some mean of communication. Regarding United Nations references considering transportation of dangerous goods by different types of transportation means, there are several criteria that define possible damaging influence of dangerous goods.

Term “dangerous goods” includes the substance itself with all its physical and chemical characteristics defined with help of mentioned criteria.

In Europe, of total amount of goods that are being transporting, cargo that is considered as dangerous takes 18 %.

In order to regard possible danger while working with dangerous goods in much more details, it is necessary to analyze its physical and chemical characteristics.

In fact, to classify dangerous goods it is necessary to pay attention to its physical condition, viscosity, density, tension of vapour, boiling temperature, melting temperature, incendiary temperature, self-incendiary temperature, explosive admixture limits, reactivity in proportion to other substances, etc.

In process of reproduction, dangerous goods exist in several places: in production, reload and transfer, transportation, storage and consumption.

In each mentioned phase there are some specifications considering exposing living and as well as unliving matters to dangerous goods activity. Considering that, all safety measures should be taken to prevent that.

In processes of reload, transport and storage the level of possible danger is higher then in processes of production and consumption. During reloading, transporting and storage hazard of side effects of dangerous goods for people and the environment is highly emphasized.

¹ Professor Dragutin Jovanovic, Dr. Sc., Education Department of Ministry of Defence, 38 Nežnanog Junaka Street, 11000 Belgrade

The consequences may be the result of an accident during the transportation and may spread around through the atmosphere and leave bad influence in running water and other environmental elements, including places on bigger distances in proportion to place of their arising. Because of the very big importance of transportation of dangerous goods, international regulations considering some types of transportation are developed. They served as basis on which the national regulations have been built.

According to international regulations, in our country Dangerous goods transportation statute has been pronounced (Official gazette SFRJ, No 27/90). Legally valid regulation in our country besides includes:

- ***Dangerous goods road and railway transportation regulation*** (Official gazette, No 53/02).

Transfer of dangerous goods in international railway transportation regularizes Book of regulations concerning international railway transportation of dangerous goods.

In order to define precautionary measures considering protection from side effects of dangerous goods, it is necessary to determine, at the very beginning, intensity and type of danger may happen during the transportation. Starting point would be physical and chemical characteristics of dangerous goods and their appearance as well as technology of transportation process. All safety measures should be taken in order to:

- prevent possible accident while handling with dangerous goods or
- diminution of consequences of side effect of possible accident.

Last couple of years in European Union it was proposed a motion for several projects concerning research of the way transportation and communication system in general affect the environment.

Safe transfer of freight and passengers is defined by national and international standards.

International and European standardization covering the area of transportation means, observed from ecologically aspect, present the most valuable factors of international standards and regulations.

Technical committees of International organization for standardization (ISO/TC) study problems of transportation means. Standardization for railway vehicles is been developed within International railway union (UIC). Other standards concerning railway propose ISO and IEC technical committee as it is shown below, figure 1.

Federal institute for standardization and Yugoslav association of railways (ZJŽ) in 1991 entered into contract of compilation of new Yugoslav standards, based on UIC proclamations, which belong to competence of Yugoslav association of railways as branch standards (JŽS), and general standards, as noise and vibration of railway vehicles – based on ISO are remained as Yugoslav standards (JUS).

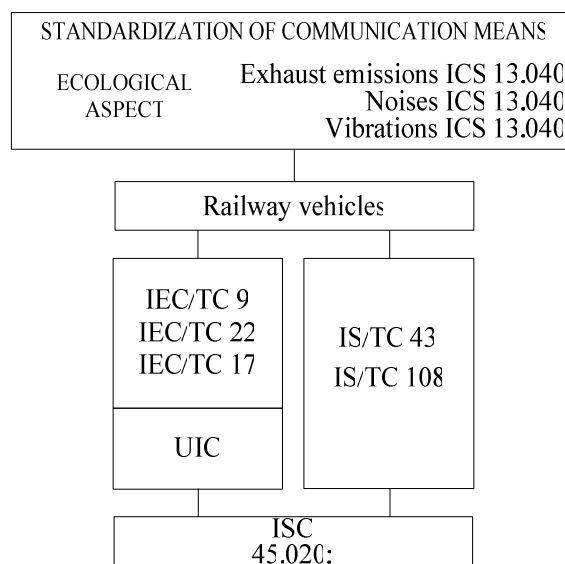


Figure 1. Presentation of technical committees and international organizations which propose standards and technical regulations concerning railway vehicles

3. CONSTRUCTIVE DEMANDS

By cisterns, as specific sort of vessels, liquid, gas, powdery and granular dangerous goods are being transferring. Cisterns consist of one or several vessels with equipment and the carriage. Besides, they possess their own equipment – device for rolling, suspension, traction and bumper device, breaks, loading device, discharging device, ventilation, safeguarding, heating device and device for cavity, external or internal elements for stiffness, fixing and protecting the vessel, some measurement instruments, etc.

Pressure appearing in the vessel depends on level of danger of substance what means that particular attention has to be paid to thickness of the vessel. At the moment of loading or discharging the vessel concerning some types of dangerous goods there may appear specific pressure.

Considering different kinds of dangerous goods, cisterns are made of materials which must be breaking resistant and resistant to tension corrosion in defined temperature regime.

When vessel is welded, it must be paid attention to make joints in accordance with technical rules for complete safety guarantee.

Considering the fact that some of dangerous goods in touch with wall of cistern react dangerously producing dangerous goods or obvious weak material, the best possible material for cistern and adequate internal protection coating. Protection coating must be made in the way by which blocking irrespective of possible deformations during the transfer. When transporting some sorts of dangerous goods, it is possible progressive decreasing of wall thickness, what must be considered when defining the wall thickness, and it have to emphasize for specific value.

Minimal all thickness of cylindrical part of the vessel must fit to the smallest thickness that issues from formula (1)

$$\frac{P_a \times D}{2 \times \sigma \times \lambda} \text{ mm} \quad \frac{P_{bar} \times D}{20 \times \sigma \times \lambda} \text{ mm}$$

where are:

- P_a , calculating pressure (MPa),
- P_{bar} , calculating pressure (bar),
- D , internal gauge of the vessel (mm),
- λ , coefficient of quality of welded joint,
- σ , allowed tension.

Serving devices and equipment of the vessel, or the vessel as the whole, must be made that way which is going to secure transfer without loosing the content of dangerous goods. Besides, railway coaches – cisterns, must, except tension in normal working regime, secure resistance to other possible tensions.

Equipment of cisterns must secure total safety as well as the vessel itself. In other words, it must secure:

- impermeability in normal working conditions as well as in condition of overturning the coaches,
- regular appointing the cap,
- securing from uncovering the cap and system for loading and discharging,
- adequate gap for cleaning the cistern.

Depending on type of dangerous goods, the cistern must be appropriate protected.

Choice of material for making the vessel – cistern and their thickness, depends on extreme temperature during the transport or their loading and discharging.

Except constructive demands to be mentioned, railway coaches – cisterns must satisfy also other numerous special conditions. For example, compact gases transformed in liquid or gases dissolved under the pressure, inflammable liquid substances, inflammable steadily substances, organic peroxides, toxically substances, radioactive substances and corrosion substances.

4. CONCLUSION

Communication system considerably imperils the environment, causing some ecological consequences – air pollution, noise and vibrations, possessing arable areas and disturbing natural ambience.

Transportation of dangerous goods, more and more present nowadays, carry series of hazards for the environment that must be stopped. The most efficient protection would be undertaking all adequate precautionary measures.

By railway is transported enormous quantity of different kinds of dangerous goods. By railway coaches – cisterns

are mostly liquid, gas, granulated and powdery dangerous substances.

A number of different measures are taking for decreasing side effects, considering numerous researches in Europe and worldwide and standards adjusted with international ones.

Railway coaches – cisterns, considering as vessels for transportation with its own equipment, besides general constructive demands, must possess a number of constructive characteristics restricted by specific physical and chemical characteristics of dangerous goods.

REFERENCES

1. *Правилник о међународном и унутрашњем железничком превозу опасних ствари (RID)*, Завод за НИП делатност ЈЖ, Београд, 2003.
2. ISO 14001:1996, *Environmental management systems* – Specification with guidance for use, 1996.
3. ISO 14004:1996, *Environmental management systems* – General guideline on principles, systems and supporting techniques, 1996.
4. ЈОВАНОВИЋ, Д., *Мogućност унапређења квалитета железничке транспортне услуге*, 6. међународна конференција "УПРАВЉАЊЕ КВАЛИТЕТОМ И ПОУЗДАНОШЋУ DQM – 2003", Београд, 2003.
5. ЈОВАНОВИЋ, Д. *Управљање квалитетом услуге у железничком саобраћају и транспорту*, XI НАУЧНОСТРУЧНА КОНФЕРЕНЦИЈА ЖЕЛКОН – 04, Ниш, 2004.
6. ЈОВАНОВИЋ, Д., *Мogućност унапређења квалитета превоза опасних материја железницом*, 7. међународна конференција "УПРАВЉАЊЕ КВАЛИТЕТОМ И ПОУЗДАНОШЋУ DQM – 2004", Београд, 2004.

STATIC AND DYNAMIC THERMAL ENGINEERING TESTS OF RAILWAY VEHICLES

Vladimir Aleksandrov*

ABSTRACT: This paper presents program, methodology and capacities for static and dynamic tests of heating, ventilating and air-conditioning systems in railway vehicles after completion of their prototypes and prior to being put into operation.

KEY WORDS: railway, railway vehicles, heating, ventilating and air-conditioning systems in railway vehicles

1. INTRODUCTION

Competing with other transport modes (air and road traffic), railway generally may fight in four ways: increasing speed, providing adequate comfort to passengers, improving safety and security and forming competitive prices.

From the aspect of comfort improving, railway traffic has an advantage over the air traffic and particularly road traffic.

Comfort may be mainly improved with installation of air-conditioning system in railway vehicles, especially in passenger coaches.

General requirements for construction of heating, ventilating and air-conditioning units are mainly defined in UIC leaflet No. 553. The questions still open are: accommodation of equipment, temperature control system, air distribution and circulation system. Their technical designs result from different requirements and specific features of coach design.

Most common heating system, i.e. air-conditioning system in the coach today is a system with air as a heat carrier. According to UIC regulations, all modern, new coaches equipped with heating, ventilating and air-conditioning units shall be tested to prove functioning and effectiveness of each unit separately as well as thermal engineering test of entire coach shall be made before putting into operation, particularly coaches in international trains. Further on paper deals with the testing methodology, capacities and, in more detail, with testing program (1).

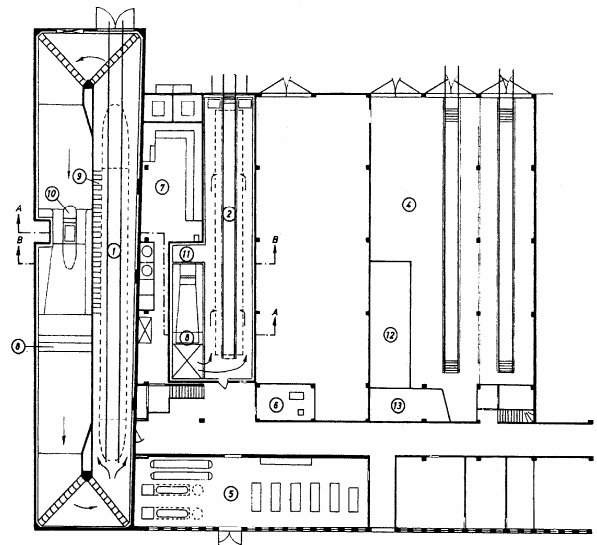
2. METHODOLOGY AND CAPACITIES FOR THERMAL ENGINEERING TESTS OF COACHES

Testing methodology, including type and scope of tests, is defined by provisions specified in UIC leaflet No. 553 (6).

The following issues will be tested in detail: air flow

(external, circulating, entry, exit and condenser cooling air), air velocity (at air inlets, i.e. air outlets, in air ducts and within compartments), pressure (drop) difference (between external air and air in the coach, at different air treatment points, such as: fan, heat exchanger, evaporator, filter, intake grille, etc. as well as in air ducts) (3).

Thermal engineering tests shall be made in special climatic chambers equipped with special equipment and



of railway vehicles in wien-Arsenal, Austria

1. Chamber for dynamic tests, 2. Chamber for static tests, 3. Room for measurements, 4. Hall for preparation of vehicles, 5. Hall with cooling machinery, 6. Hall with heating machinery, 7. Power supply room, 8. Air treatment (drying, cooling, moistening), 9. Solar heaters, 10. Ventilation of chamber for dynamic tests, 11. Ventilation of chamber for static tests, 12. Workshop, 13. Store room for material and equipment measuring instruments. In fact, such climatic chambers are very expensive and complex structures, therefore

* Vladimir Aleksandrov, B. Sc. Mech. Eng. 40a, Prote Mateje street, 11000 Belgrade, Serbia & Montenegro

only few railway administrations possess them and other, mainly neighboring railway administrations use those climatic chambers to test their railway vehicles. One of such plant of special interest for Railways of Serbia is the Center for thermal engineering tests of railway vehicles in Vienna (Wien-Arsenal), Austria, which has been in operation since 1961. It is universal plant that serves for testing of passenger coaches, freight wagons and traction vehicles. In past four decades thousands of railway vehicles passed through testing chambers in this Center (5).

According to articles published in the International Railway Gazette (January 2003), new Center for thermal engineering tests of railway vehicles was commissioned in Floridadorf (also Austria), where characteristics of some new railway vehicles are also tested (e.g. double deck wagons) with simulation of any climatic condition (rain, snow, sun or wind) (4).

Layout of "old" Center in Wien-Arsenal, including typical cross-sections, is shown in the Figure 1.

The station basically consists of: chamber for static tests (Figure 2), chamber for dynamic tests (Figure 3) and test bench for testing of solar radiation effects on coaches (Figure 4).

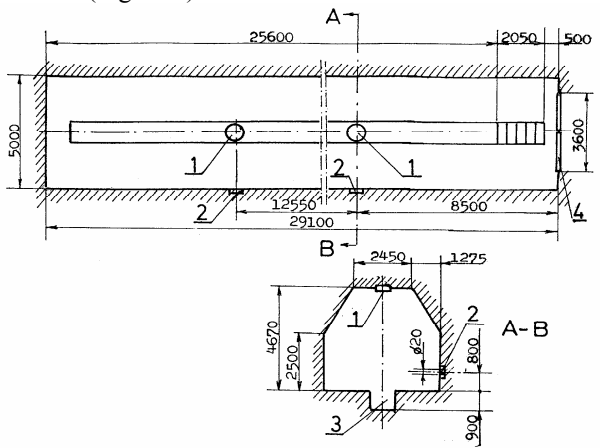


Figure 2: Chamber for static tests of air-conditioning units in railway vehicles

1. Air outlet on ceiling, 2. Air outlet on side wall,
3. Duct in floor, 4. Entry door

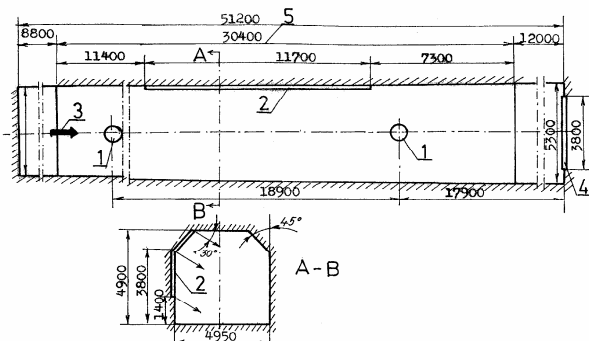


Figure 3: Chamber for dynamic tests of air-conditioning units in railway vehicles

1. Fans on ceiling, 2. Solar heaters, 3. Air inlet, 4. Entry door,
5. Measuring section

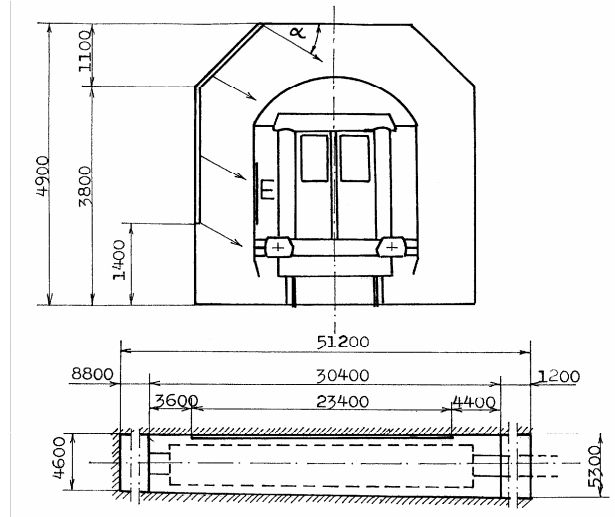


Figure 4: Test bench for testing of solar radiation effects on passenger coaches

3. PROGRAM FOR STATIC AND DYNAMIC THERMAL ENGINEERING TESTS OF COACHES

Program for thermal engineering tests of railway vehicles can be best comprehended through one real diagram of value changes as a function of time in the course of one vehicle test.

Figure 5 shows diagrams of complete programs for static (SVK) and dynamic (FVK) tests of air-conditioning system in one passenger coach according to ORE (ERRI) recommendations. Diagrams actually indicate that temperature changes (θ_i) depend on external temperature (θ_a) and coach running speed (V).

Diagram of static tests is in the upper part of the figure, and diagram of dynamic tests is in the bottom part of the figure. Third diagram (at the very bottom of the figure) indicates change of coach running speed (in fact, air velocity in the chamber for dynamic tests) in km/h as a function of time, expressed in days. Solid line in diagrams indicates change of external temperature and broken line indicates change of internal temperature in coach during the testing. Legend below the figure explains meaning of thermal engineering terms and indicated terms, i.e. magnitudes (numbers in circles) to be tested. Order of tests is the following:

- 1) Test of heating system control (by setting maximum, average and minimum temperature values on the temperature setting unit).
- 2) Preheating test (heating of coach in operation).
- 3) Heat transfer test (at different speeds).
- 4) Critical temperature test (temperature at which installed power may maintain internal temperature $\theta_i = +20^\circ\text{C}$).
- 5) Test of cooling system control.
- 6) Precooling test (coach cooling before operation).
- 7) Test of maximum cooling power.
- 8) Test of comfort.
- 9) Test of needed energy (for heating and cooling).

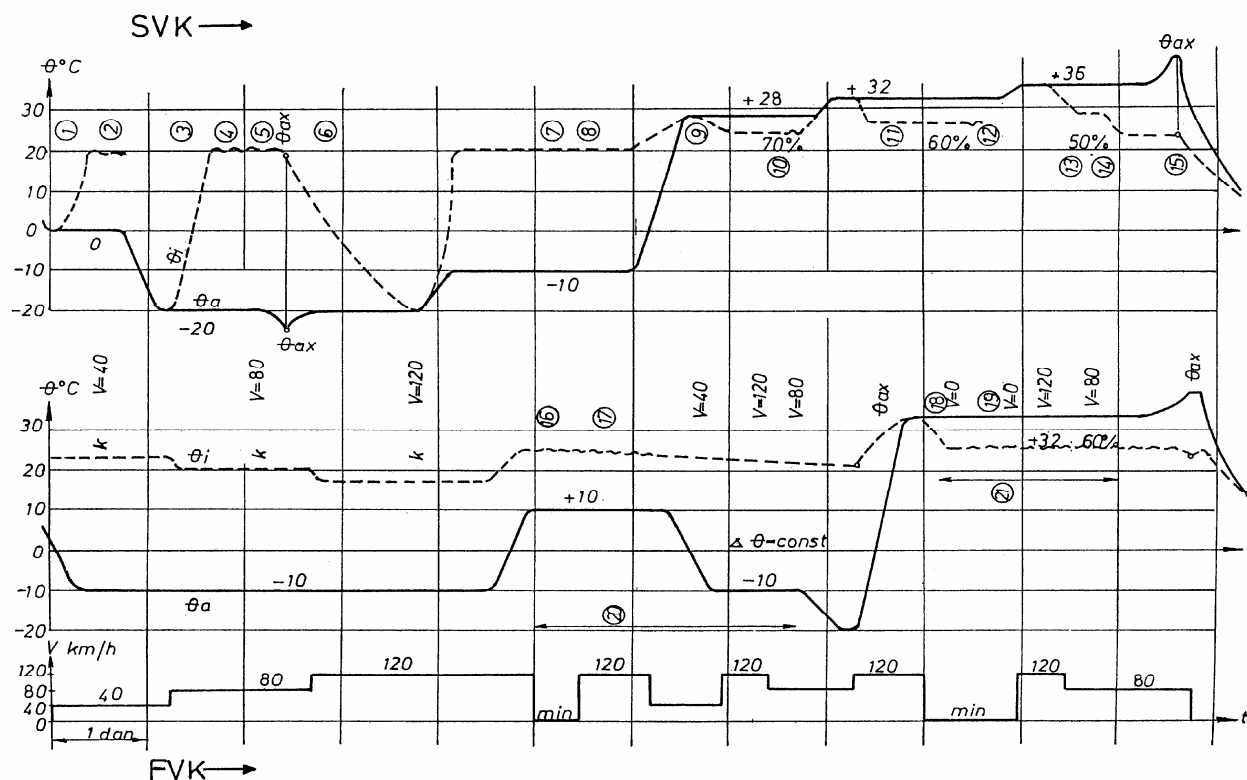


Figure 5: "Standard testing program" for heating and cooling of passenger coaches according to ORE (ERRI)

SVK - static tests, FVK - dynamic tests, θ - temperature in °C, θ_i - mean air temperature in a coach, θ_a - air temperature in the testing chamber, ϕ - relative air humidity in %, t - time in days, v - vehicle speed (velocity of air in chamber) in km/h, k - heat transfer coefficient

- | | |
|------------------------------|---|
| 1 Heating | 12 Control |
| 2 Control | 13 Cooling |
| 3 Comfort | 14 Control |
| 4 Cooling of coach and water | 15 Top temperature limit |
| 5 k-value | 16 With manned compartments |
| 6 Cooling | 17 With manned compartments and solar radiation |
| 7 k-value | 18 With manned compartments |
| 8 Control | 19 With manned compartments and solar radiation |
| 9 Cooling | 20 Testing of heating control |
| 10 Control | 21 Testing of cooling control |
| 11 Cooling | |

- 10) Tests at variable external temperature (switching from cooling operation to heating operation and vice versa).
- 11) Test of wind effects (at simulated vehicle speed).
- 12) Test of solar radiation effects.
- 13) Other tests (protection against freezing).

4. PROCEDURES, INSTRUMENTS AND POINTS OF MEASUREMENTS FOR THERMAL ENGINEERING TESTS

- 1) Measurement of air temperature (with tolerance $\pm 0.5^\circ\text{C}$). To determine air temperature, points of measurement shall be established in passenger compartments and auxiliary rooms at different height above floor level (see Figures 6 and 7)
- 2) Measurement of temperature in different compartment areas.
- 3) Measurement of relative air humidity (minimum at two points, at height of 1.1 m above floor level and at the middle of the coach).
- 4) Measurement of air velocity. Measurement shall be made in two compartments (usually in compartments 3 and 7), i.e. in two corresponding rows of seats in open saloon coach, at passenger head level (1.1 m) and at passenger knees level (0.6 m).
- 5) Measurement of air flow.
- 6) Measurement of noise. Noise shall be measured at height of 1.1 m above floor level - in compartment coaches noise shall be measured at coach ends and in the middle and in open saloon coaches in the middle of the coach.
- 7) Measurement of solar radiation. Solar radiation shall completely comply with UIC leaflet No. 553, Attachment 6.
- 8) Measurement of unit power (constantly, by means of recorder).

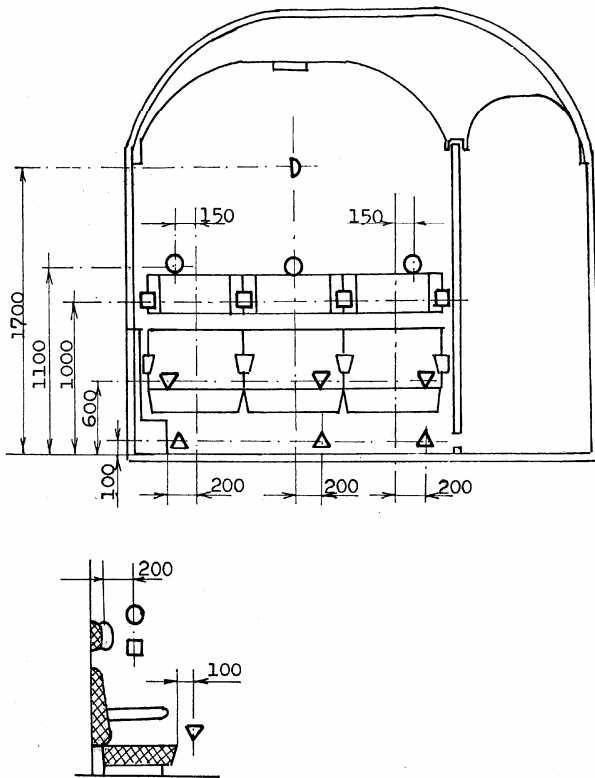


Figure 6: Arrangement of points of measurement for determination of ambient air velocity and temperature in compartment coach

5. CONCLUSION

Considering severe competition between railway traffic and air and road traffic, particularly from the aspect of passenger comfort, air-conditioning of the area where people will spend their travelling time is very important. All modern, new passenger coaches shall not be designed without efficient air-conditioning system, especially in international traffic (2). Before putting those coaches in operation, however, they shall pass rigorous

thermal engineering tests of functioning, which could only be made in specialized centres such as Center in Wien-Arsenal.

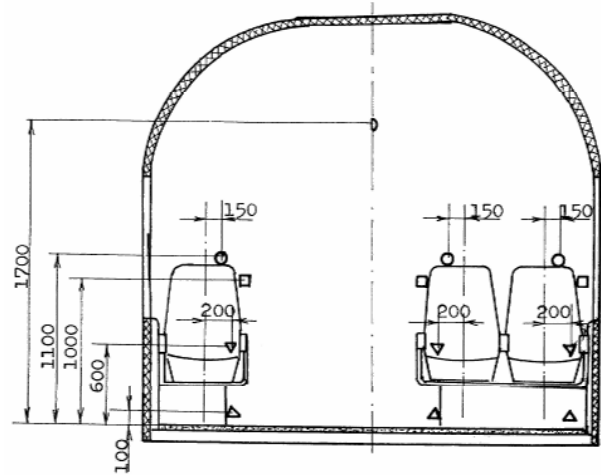


Figure 7: Arrangement of points of measurement for determination of ambient air velocity and temperature in open saloon coach with three-seat rows

BIBLIOGRAPHY

1. Aleksandrov V., Železnička vučena vozila, (Hauled railway vehicles), "Želznid", Belgrade, 2000
2. Aleksandrov, V., Optimizacija sistema za klimatizaciju putničkih kola (Optimization of air-conditioning system for passenger coaches), "Železnice" (Railways journal), 8/1995
3. Aleksandrov, V., Grejanje, provetranje i klimatizacija putničkih kola (Heating, ventilating and air-conditioning of passenger coaches) (monograph pending publication), Belgrade, 2005
4. International Railway Gazette, 1/2003
5. Schausberger, H. Wärme-und Kältetechnische Versuche an Reisezugwagen in der Fahrzeugversuchsanlage Wien-Arsenal, "Kältetechnik und Klimatisierung", 4/1968
6. UIC 553

ИЗМЕРЕНИЕ И ОЦЕНКА ВИБРАЦИЙ В КАБИНЕ ЛОКОМОТИВОВ И МОТОРВАГОННЫХ ПОЕЗДОВ

Иван Миленов, Георги Павлов¹

Резюме: Для получения возможно более полной информации о рабочей среде (кабинах управления тяговым подвижным составом) было проведено ряд измерений некоторых основных параметров - температуры и относительной влажности воздуха, концентрации углеводородов и двуокиси серы, запылённости воздуха, шума в кабине, вибраций пола кабины, вибраций сидений локомотивных машинистов и помощников машинистов, вибраций поездного крана машиниста, вибраций контроллера управления, электромагнитных полей в кабине и в машинном отделении частотой 50 Hz, электрического поля, создаваемого радиостанциями и др.

В данной работе на базе собранного статистического материала представлены некоторые из основных результатов этого исследования в области вибраций, сделаны выводы и предложения.

Ключевые слова: вибрации, виброскорости, метрология, безопасность, рабочая среда, условия труда.

Вибрации бывают общими и локальными. Общими являются те, которые оказывают воздействие на всё тело и воспринимаются нижними конечностями во время работы на вибрирующих поверхностях или передаются сиденьями кресел или стульев. Локальными являются вибрации, воздействие которых воспринимается значительно меньшей частью тела, чаще всего верхними конечностями.

Оказывая воздействие на весь организм, общие вибрации могут вызвать общую вибрационную болезнь. Заболевание характеризуется поражениями периферийной нервной системы и кровеносных сосудов нижних конечностей и изменениями в центральной нервной системе. Обнаруживается пониженная чувствительность нижних конечностей, пониженная температура кожи и атонично-спастические явления в кровеносных сосудах. Наблюдаются общая повышенная утомляемость, головная боль, головокружение и характерные проявления заболеваний вестибулярного аппарата - приступы головокружения в сочетании с упорной головной болью, развивающиеся на фоне астенических и невротических реакций. Возможны поражения среднего уха.

Общая вибрационная болезнь затрагивает, в основном, рабочих предприятий по производству

виброэлементов, рабочих транспорта и др., работающих в местах, где общие вибрации являются неотъемлемой частью технологии и выполняемой трудовой деятельности.

Воздействие локальных вибраций на человеческий организм вызывает локальную вибрационную болезнь. Она - часто встречаемое профессиональное вибрационное заболевание. Самые опасные частоты, причиняющие его, находятся в диапазоне 50 - 250 Hz. Характерными для этого заболевания являются субъективные симптомы: диффузные боли в затронутых конечностях, которые имеют неопределённый характер. Они не могут быть точно локализованы и приводят к очень тяжёлым субъективным ощущениям, наличию парестезий и др. Болезненные приступы в затронутых конечностях возникают обычно в состоянии покоя, очень часто ночью. Наличие влажности и холод провоцируют и усиливают приступы и усугубляют их протекание. Объективно устанавливаются ангиоспазм (сжатие кровеносных сосудов) в затронутых конечностях, изменения в секреторике (повышенное выделение пота) и чувствительности, трофические дегенеративные изменения в затронутой области и др. Сжатие кровеносных сосудов в начальной фазе заболевания определяет внешний вид затронутой руки

¹ Иван Костадинов Миленов – доц., д-р, инж., Высшее транспортное училище им. Т. Каблешкова, София, Болгария, e-mail: milenov55@abv.bg

Георги Митков Павлов – гл. ас., д-р, инж., Высшее транспортное училище им. Т. Каблешкова, София, Болгария, e-mail: g_pavlov61@abv.bg

и объясняет название, под которым описано это заболевание в прошлом – белые пальцы, мёртвые пальцы и др. Появляются: остеопороз верхних конечностей, резорбция суставных хрящей с сужением суставных зазоров, изменения в структуре костей, кисты, остеоартроз и др.

Вибрации исследованы путём измерения вертикальных и горизонтальных виброскоростей согласно требованиям болгарского государственного стандарта (БДС) 1931-79, 16013-84, 12.1.012-80.

Виброскорости измерялись при движении поездных локомотивов и электрического моторвагонного поезда со скоростью 60 - 100 km/h. Маневровые тепловозы двигались со скоростью 20 - 25 km/h, узкоколейные локомотивы - со скоростью 30 km/h. Маневровый электровоз обслуживал поезд со скоростью 40 - 60 km/h.

Проведено измерение виброскоростей пола кабин и сидений машиниста и его помощника. На тепловозах измерялись вибрации без движения локомотива.

Вертикальные, горизонтальные поперечные и горизонтальные продольные виброскорости пола поездных электровозов показаны на фиг. 1 по октавным лентам частот. Допустимые значения для нулевой степени элементов условий труда, которые различны для вертикальных и горизонтальных виброскоростей при разных частотах, также показаны на графике. В целях облегчения сопоставления виброскорости даны в процентах по отношению к норме на фиг. 2. Самыми высокими являются виброскорости при частоте 2 Hz. Вертикальные - $3,72 \text{ m/s} \cdot 10^{-2}$, горизонтальные поперечные - $2,13 \text{ m/s} \cdot 10^{-2}$, горизонтальные продольные - $0,70 \text{ m/s} \cdot 10^{-2}$. По отношению к норме самыми высокими являются вертикальные виброскорости при частоте 8 Hz - 63%, горизонтальные поперечные вибрации достигают 60% (2Hz), самыми низкими являются горизонтальные продольные вибрации - 20% (2 Hz) от предельно допустимой нормы (ПДН). При повышении частоты виброскорости уменьшаются.

Вертикальные и горизонтальные виброскорости пола тепловозов серии 06, 07, 55 показаны на фиг. 3, 4. Эти серии локомотивов находят самое широкое применение на болгарских железных дорогах. Вертикальные и горизонтальные виброскорости меньше нормы для нулевой степени элементов условий труда. Вертикальные виброскорости достигают $6,36 \text{ m/s} \cdot 10^{-2}$ и 90% от нормы (06 серия, 2 Hz), а горизонтальные - $1,23 \text{ m/s} \cdot 10^{-2}$ и 38% от нормы (серия 06, 4 Hz). Самыми высокими являются вертикальные и горизонтальные виброскорости на локомотивах серии 06. Виброскорости на локомотивах серии 07 и 55 серии близки по величине, но нужно отметить, что измерения проводились при различных скоростях.

Виброскорости сидений кресел и стульев машинистов находятся также ниже нормы и также вертикальные больше горизонтальных (фиг. 5, 6). Наибольшими являются виброскорости частотой 2 Hz. Вертикальные виброскорости достигают 67% от ПДН, а горизонтальные - 81% от ПДН.

О динамических качествах стульев персонала локомотива можно судить, если сравнить их виброскорости с виброскоростями пола. Вертикальные виброскорости сидений стульев на локомотивах 44 серии ниже виброскоростей пола на $0,15 - 0,32 \text{ m/s} \cdot 10^{-2}$. В процентах разница при частотах 2 Hz и 4 Hz составляет около 10%, а при частотах 16 Hz достигает 51%. Почти в тех же процентных границах разница при локомотивах серии 07, но виброскорости сидений выше, чем виброскорости пола (за исключением при частоте 16 Hz). Горизонтальные виброскорости сидений при локомотивах обеих серий выше, чем виброскорости пола при частотах 2 Hz и 4 Hz. Разница в пределах 19% - 66%. Следовательно, в большинстве случаев виброскорости сидений выше, чем виброскорости пола. При других сериях тягового подвижного состава ситуация почти такая же. Нет существенной разницы между вибрациями сидений локомотивных машинистов и помощников машинистов.

Локомотивы, находящиеся в эксплуатации на болгарских железных дорогах, имеют неавтоматическое косвенное управление. Для регулирования тяговой и тормозной сил, что производится почти непрерывно, руки машиниста находятся на руле или на секторе контроллера управления и рукоятке крана машиниста поездного пневматического тормоза (реже на рукоятке крана локомотивного тормоза прямого действия).

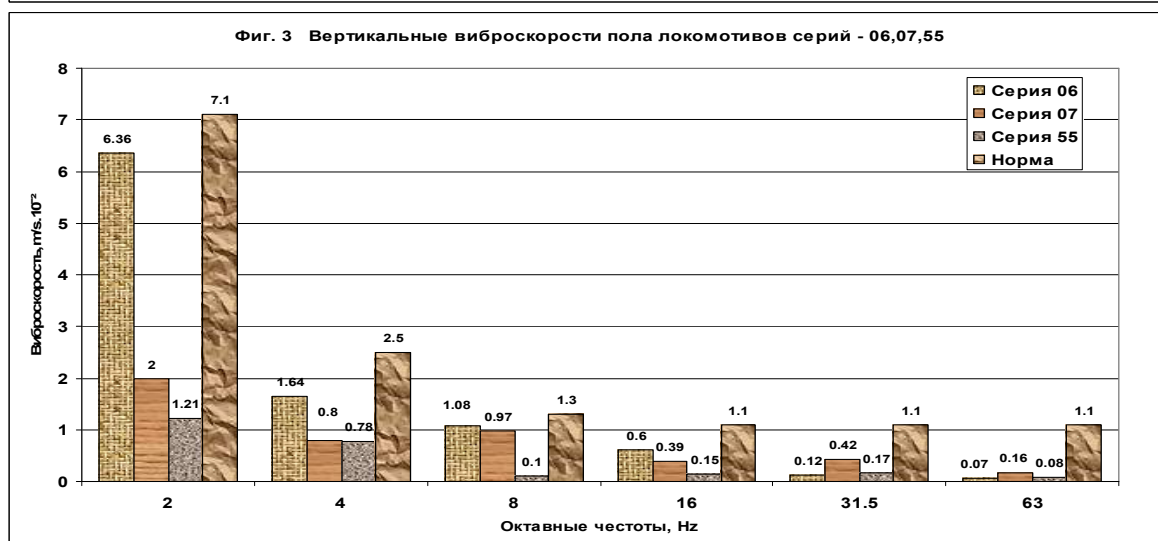
Самыми высокими являются виброскорости при локомотивах серии 07. Они достигают $1,92 \text{ m/s} \cdot 10^{-2}$ (8Hz) и 80% от нормы (16Hz). Горизонтальные виброскорости значительно ниже.

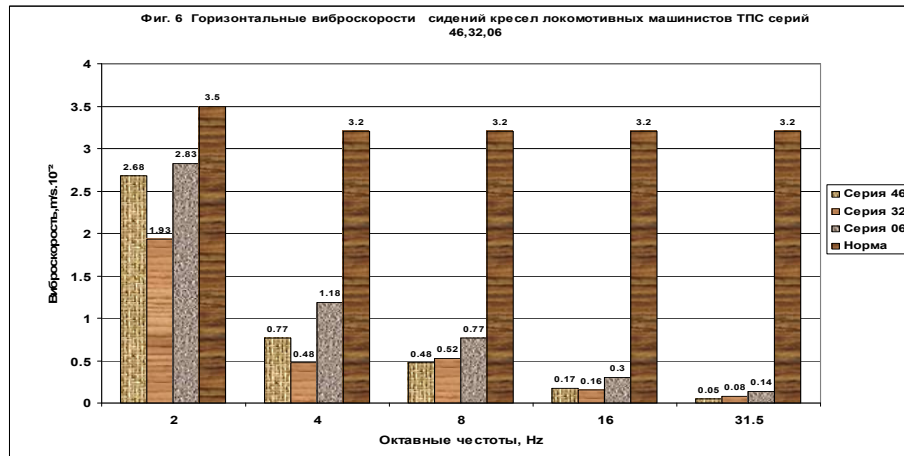
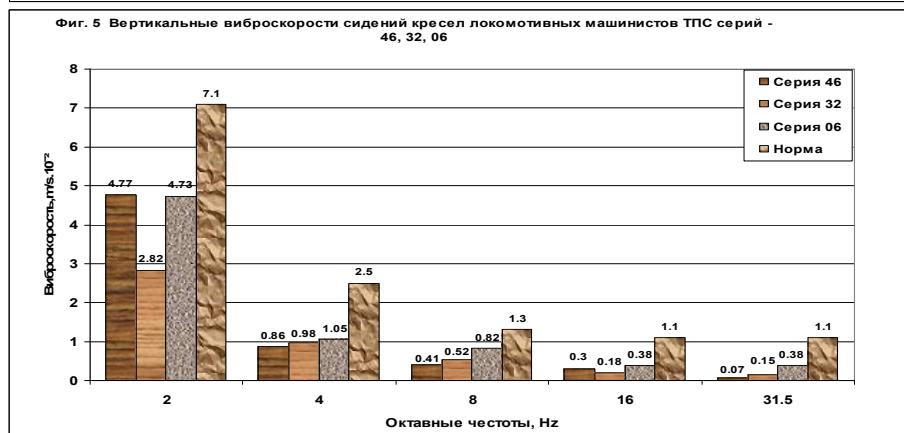
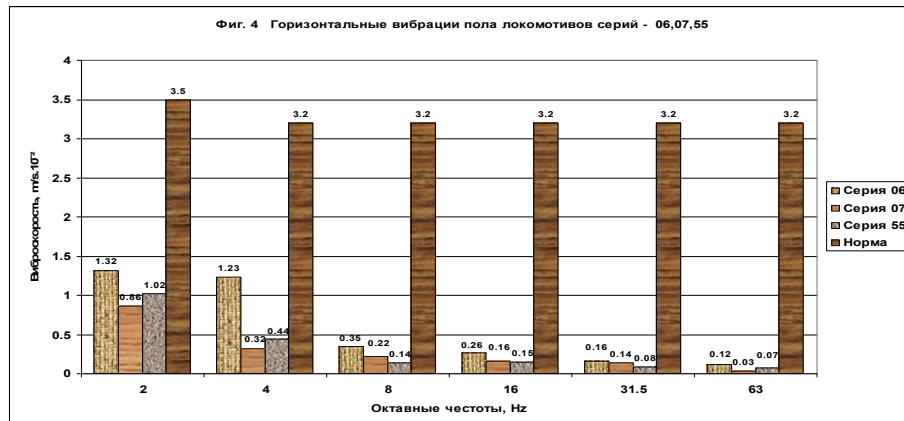
Виброскорости контроллеров ЭПС ниже. Вертикальные виброскорости достигают $0,56 \text{ m/s}$ (серия 44, 8Hz) и 33% от нормы (серия 44, 16Hz). Разницы в виброскоростях отдельных единиц ТПС не превышают 23% от нормы.

Виброскорости крана машиниста ниже виброскоростей контроллеров. То же самое относится и к крану машиниста прямого действия.

Виброскорости вибраций превышают 50% от ПДН, но не превышают норму. Измерены вертикальные виброскорости пола до 90% от ПДН и контроллера управления до 82% от ПДН.

При движении нет существенной разницы в виброскоростях тепловозов и электровозов. На электровозах серии 46.100 измерены вертикальные виброскорости пола $5,85 \text{ m/s} \cdot 10^{-2}$ (82% от ПДН) при частоте 2 Hz. При работающем двигателе без





движения тепловоза самая высокая виброскорость - 15% от ПДН (16 Hz).

Для уменьшения воздействия вибраций необходимо поставить новые кресла для локомотивных бригад.

Необходимо, чтобы кресла отвечали эргономическим требованиям и имели нужные динамические качества. Кресла нужно предвидеть и для помощников машинистов. Не требуется производить замену кресел машинистов локомотивов серии 46.200.

ЛИТЕРАТУРА

- [1] Пантев П. и колл. Исследование влияния рабочей среды и условий труда локомотивных бригад на безопасность движения поездов и принятие практических мер для уменьшения риска. (на болгарском языке). Договор № 04/26.02. 2002г.
- [2] БДС 12.01.069-83 Охрана труда. Вибрации. Измерения на рабочих местах операторов транспортных единиц.

ИЗМЕРЕНИЕ И ОЦЕНКА УРОВНЯ ШУМА В КАБИНАХ ЛОКОМОТИВОВ И МОТОРВАГОННЫХ ПОЕЗДОВ

Георги Павлов, Иван Миленов¹

Резюме: Известно, что шум оказывает неблагоприятное влияние на организм человека. Повышенные значения шумовых воздействий могут привести к поражениям во всех органах и системах организма в целом. В этом аспекте исследование воздействия шума на машинистов и помощников машинистов особенно важно с учётом специфических условий их работы.

В работе представлены некоторые основные результаты, полученные в результате полного исследования параметров рабочей среды и влияния шума на машинистов.

Ключевые слова: шум, метрология, безопасность, рабочая среда, условия труда.

Шум оказывает неблагоприятное влияние на весь организм, что позволяет обособить в качестве профессионального заболевания шумовую болезнь. Начальные её симптомы: повышенная утомляемость, выраженная раздражительность, головная боль, пониженное желание работать и низкая трудоспособность, невозможность сосредоточиться и др. Можно отметить также и ряд объективных изменений, затрагивающих, прежде всего, центральную нервную систему: изменения в условно-рефлекторной деятельности, понижение трудоспособности нервных клеток, нарушение уравновешенности и подвижности основных нервных процессов возбуждения и торможения. Наблюдаются функциональные изменения вегетативной нервной системы - изменения в ритме сердечной деятельности и просвете кровеносных сосудов, нарушения секреторной функции желудка, изменения в зрительном и вестибулярном аппаратах, в железах внутренней секреции и др. Все перечисленные изменения приводят к ослаблению внимания и

невозможности сконцентрироваться, к замедлению психических реакций, к уменьшению тонуса мышц, к расстройству сна и бессоннице, к неприятным ощущениям и боли в области сердца, к потере аппетита и к возникновению функциональных нервных расстройств.

С общим воздействием шума на организм человека связывается ряд заболеваний, которые всё чаще встречаются среди рабочих шумовых производств: заболевания сердечно-сосудистой системы, желудочно-кишечные заболевания (в т.ч. язвенная болезнь); неврозы и психоневрозы и др.

Из сказанного видно, что шум при посредстве центральной нервной системы оказывает неблагоприятное воздействие почти на все органы и системы организма в целом.

Шум оказывает специфическое воздействие на слуховой анализатор, которое выражается в наступлении профессиональной тугоухости. Это

¹ Георги Митков Павлов – гл. ас., д-р, инж., Высшее транспортное училище им. Т. Каблешкова, София, Болгария, e-mail: g_pavlov61@abv.bg

Иван Костадинов Миленов – доц., д-р, инж., Высшее транспортное училище им. Т. Каблешкова, София, Болгария, e-mail: milenov55@abv.bg

заболевание проходит через несколько стадий. На протяжении начальной стадии (адаптация анализатора) слух восстанавливается после прекращения слухового раздражения (после отдыха между сменами). На второй стадии (утомление слухового анализатора) слуховая чувствительность восстанавливается медленно или частично. На третьей стадии (профессиональная тугоухость) изменения в слухе необратимы. Последняя стадия болезни развивается медленно и постепенно и обычно наступает в результате трудовой деятельности в шумовой среде на протяжении 5-10 лет. Начальная профессиональная тугоухость, в отличие от возрастной, характеризуется ухудшением слуха для звуков частотой 4000 – 6000 Hz, что объективно устанавливается путём аудиометрии.

Внезапный сильный шум может вызвать также тяжёлую слуховую травму, при которой может лопнуть барабанная перепонка уха, или могут получиться другие поражения слуха, которые, всё же, редко встречаются в производственных условиях.

Профессиональная глухота наступает вследствие работы в шумовой среде на протяжении многих лет, для наступления общих неблагоприятных изменений в организме достаточно всего несколько месяцев. Шум снижает физическую работоспособность примерно на 30%, а умственную - примерно на 60%.

Измерение, вычисление и нормирование шума проводилось согласно болгарскому государственному стандарту (БДС) 15204-80, 12264-83, 14478-82, 16798-88.

На фиг. 1 показана диаграмма самых высоких средних значений уровня шума в кабинах тягового подвижного состава различных серий (ТПС) при закрытых окнах. Ввиду подобия конструкции локомотивов 42 и 43 серий, локомотивов 44 и 45 серий и моторвагонных поездов 32 и 33 серий результаты их исследований объединены. На фиг 2 самые высокие средние значения уровня шума показаны по рабочим местам. Используются следующие обозначения: ПЭ - для поездных электровозов; ЭМП - для моторвагонных поездов; МЭ - для маневровых электровозов; ПТ - для поездных тепловозов; МТ - для маневровых тепловозов; УТ - для узкоколейных тепловозов. Предельно допустимая норма - 78 dB(A).

Уровень шума в кабинах *электрического подвижного состава* (ЭПС) измерялся в скоростном диапазоне 40 km/h - 100 km/h. Эксплуатационные условия не позволили провести измерения при более высоких скоростях. На маневровом локомотиве 61 серии проводились исследования в поездном режиме при движении со скоростью 60 km/h. Средние значения уровня шума на всех локомотивах при скорости 60 km/h находятся в узких границах 72 - 76 dB(A). При более высоких скоростях уровень шума

повышается. Выше всего он на локомотивах серий 42, 43 - 80,5 dB. Для работающих на локомотивах различных серий машинистов применяется весовой коэффициент. С учётом этого уровень шума для персонала поездных электровозов (ПЭ) составляет 78,5 dB, а для персонала электрических моторвагонных поездов (ЭМП) - 79,3 dB. Оба значения превышают ПДН - 78 dB. Эти значения получены при скоростях 90 km/h для локомотивов "Шкода", 100 km/h - для локомотивов серии 46 и 80 km/h для моторвагонных поездов. При движении с максимальной скоростью на каждом ЭПС уровень шума будет выше. Единственно на маневровых электровозах не следует ожидать превышения ПДН.

При открытых окнах кабины уровень шума повышается на 1-2 dB.

Уровень шума на тепловозах измерялся при скоростях движения от 0 до 90 km/h. При работе двигателя без движения на маневровых локомотивах 55 серии уровень шума достигает 80 dB. Измерения на маневровых локомотивах проводились при скорости 20 km/h, а на поездных локомотивах - при скоростях 60 - 90 km/h. Самые высокие средние значения уровня шума находятся в пределах 80 - 87dB. Они выше среднего уровня и значений, измеренных на электрических поездных локомотивах.

Измерения на узкоколейных локомотивах проводились при уклонах, превышающих 5‰, при кривых с радиусом ниже 1000 m и при рельсах массой меньше 48 kg/m, что является одной из причин, обусловивших более высокие значения уровня шума.

При открытии окон уровень шума повышается на 2 - 6 dB.

При нормировании шума в прошлом исходили из требования не допустить поражений слуха рабочих. Сейчас нормы шума стремятся обеспечить защиту слуха, свободный речевой контакт между рабочими во время производственной деятельности, незначительные физиологические отклонения в организме и относительно хорошее самочувствие.

На тепловозах всех серий самые высокие значения уровня шума в кабинах превышают средний уровень, который составляет 78 dB. На рабочих местах машинистов и помощников машинистов поездных и маневровых тепловозов уровень шума достигает 82 dB (фиг.2). При открытых окнах уровень повышается на 1 - 2 dB. Шум на узкоколейных тепловозах выше.

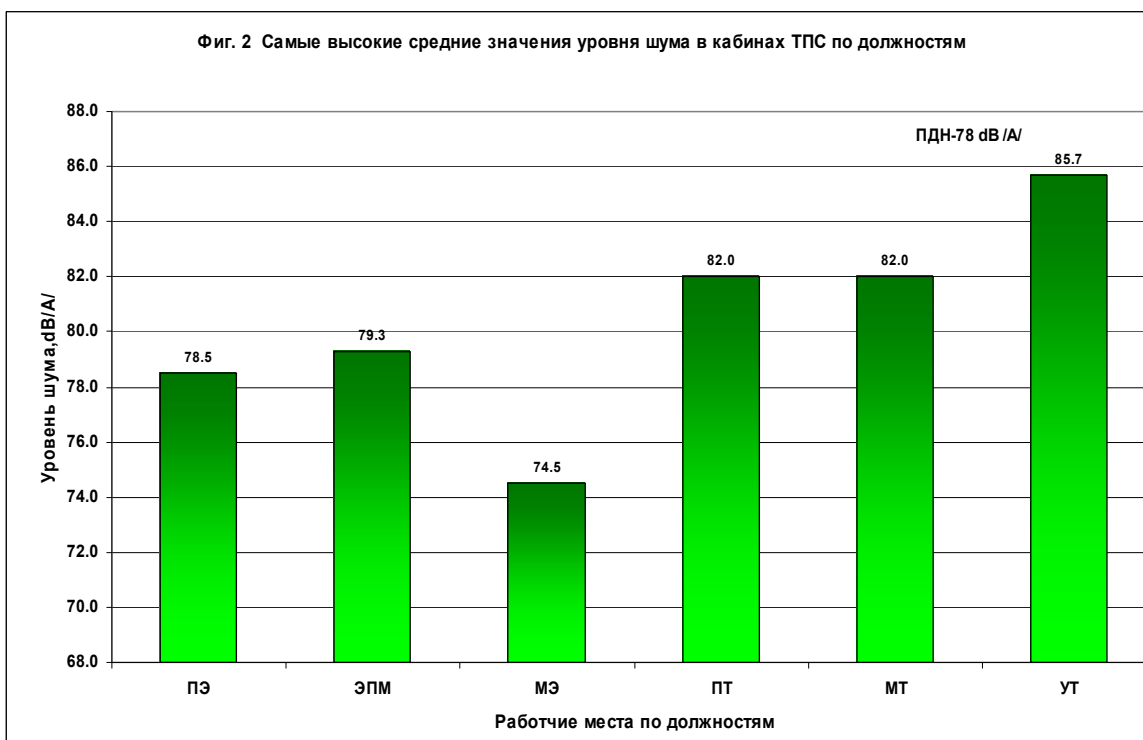
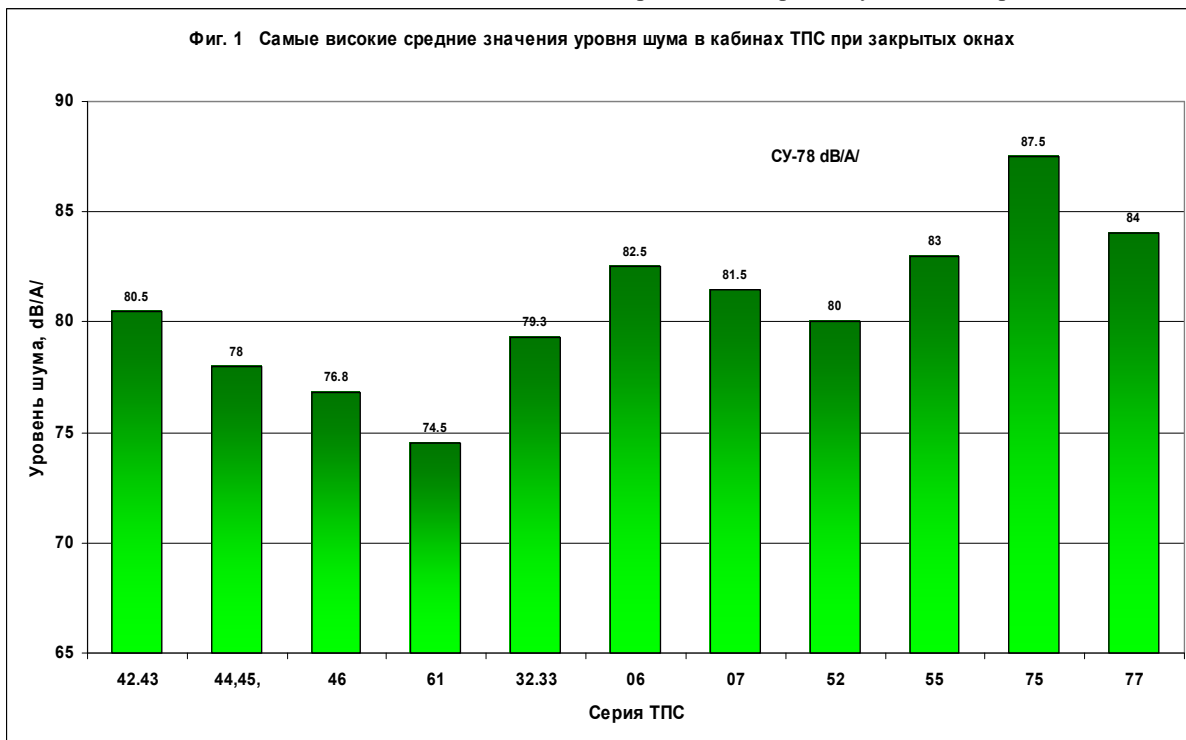
При ЭПС самыми бесшумными являются локомотивы серии 61, но уровень шума - 96% от среднего уровня. Уровень шума при локомотивах серий 44, 45, 46 находится в пределах среднего уровня, но при локомотивах серий 42, 43 и ЭМП серий 32, 33 превышает его. Так как доля локомотивов серии 46 в общем числе локомотивов относительно невелика, средний уровень шума на рабочих местах машинистов

поездных электровозов немного превышает средний уровень.

Для уменьшения воздействия шума необходимо принять следующие меры.

1. Восстановить и улучшить антишумовую изоляцию кабин.

Шум в кабинах, особенно на тепловозах, превышает предельно допустимую норму. Путём материалов проблему можно решить. Особое



внимание нужно уделить стенам между машинными отделениями и кабинами и уплотнениям на дверях в машинные отделения.

1. На тепловозах к личным предохранительным средствам включить антифоны для работы в машинных отделениях.

Необходимо разъяснить эффект от их применения.

ЛИТЕРАТУРА

[1] **Пантев П. и колл.** Исследование влияния рабочей среды и условий труда локомотивных бригад на безопасность движения поездов и принятие практических мер для уменьшения риска. (на болгарском языке). Договор № 04/26.02.2002г.

THE EXPERIENCE OF SERBIA AND THE ESTABLISHMENT OF STATE OWNERSHIP IN THE BULGARIAN RAILWAYS

Anna Dzhaleva-Chonkova¹

The paper presents how the Bulgarian politicians used the experience of Serbia in railway development to avoid the risks of assigning the operation to a foreign private company. It is underlined that the relations between the both countries in the field of railways were marked with high professionalism and considering the mutual interests for further modernization and national prosperity.

Keywords: railway building and operation, Serbia, Bulgaria, state ownership.

1 INTRODUCTION

The railway development on the Balkans began within the boundaries of the Ottoman Empire in the second half of the 19th century. Although the infrastructure plans were considered a substantial part the reforms carried out by the government in Istanbul, they were predominated by the economic and strategic interests of the Great Powers in the region. Being interested in finishing the transcontinental railway line leading westward from Belovo to Vienna, by the Berlin Treaty they assigned that task as a common obligation of four countries: the Ottoman Empire, Austro-Hungary, Serbia and Bulgaria. In 1883 the 3-year long and difficult negotiations of the four countries resulted in signing an agreement known as “*Convention a Quatre*”. It determined the route of the line but did not fix the way of building the sections on the territory of each country. That was an opportunity for Bulgaria to refuse the concession with Baron Hirsch, who was made to declare his resignation. Thus the insistence of the Bulgarian representatives managed to impose the will of the people in the country who knew that the foreign private companies would not perform in favour of national interests. They had witnessed how the companies of Brothers Barclays and Baron Hirsch were building and operating the railways on the purpose of their own profits, neglecting the quality of service, regulations and even the technological requirements.

2 THE DISADVANTAGES OF PRIVATE RAILWAY OPERATION

After the approval of the Convention the Bulgarian Parliament had to promote its implementation by passing the Act of Building the Tsaribrod (now the town of Dimitrovgrad in Serbia)-Vakarel Railway Line. Prior to it, at the end of 1884 the government of the Liberal Party decided that it was necessary to present the draft of a general railway law called *Act of Rail Roads in the*

Principality of Bulgaria. It aimed at establishing the basic principles in the railway development in the country and became one of the most disputable parliamentary acts in the newest Bulgaria history. The debates continued three sessions but eventually the governmental majority achieved its adoption on 31 January 1885.

The attacks of the opposition were directed mainly against the exclusive right of the state to build and operate railroads. The Liberal party lead by Petko Karavelov was accused of presenting a premature law, which the country did not need at that moment. The opposition MPs expressed their distrust in the government's ability to manage such a complex enterprise pointing out that the lack of qualified personnel would result in claims for low quality of transport services. The speakers grounded their statements with negative examples taken from the practice of the railway operation in Serbia. However, the opponents from the Liberal Party objected the opposition statements reminding that they had not taken into account the real situation existing in the neighboring country. It were not the Serbs working as railway officials who had to be blamed for the bad organization of transport services but the management of the foreign company, which operated on the Serbian State Railways. It was also noted that this model was not a free choice of the Parliament (Scupshtina) but had been imposed to it by the Great Powers due to the poor economic condition of the Serbian Kingdom.

Taking up the railway construction a few years later, the Bulgarian politicians had the chance to take warning by the Serbian experience in that field. It showed clearly the risks of assigning the task of railway building and operation to private foreign companies. The contract signed with the so-called General Union from Paris in 1881 brought Serbia nearly to a financial collapse when in 1882 the company unexpectedly went bankrupt. Fortunately, the crisis was escaped by the meddling of France and Austro-Hungary, which helped with the establishment of a new company, Contoir National

¹ Anna Dzhaleva-Chonkova, Ph.D., Senior Lecturer, Department of Humanities, Higher School of Transport, www.vtu.bg, Sofia, 158 Geo Milev, Bulgaria, adzaleva@abv.bg

d'Escompte in order to continued the construction of the line until its opening in September 1884. Yet the operation of the line was assigned to another foreign company, the French Company of Construction and Operation of the Serbian State Railways.

The disadvantages of its management, pointed out as early as during the discussion in the Bulgarian Parliament on the draft Railway Act of 1885, were realized much later by the Serbian government. The operator often violated the economic and railway regulations, hid revenues, did not pay for the transport services on its own purpose as provided in the contract signed. The problems in the relations between the state and the company accumulated with the time and resulted in the idea of changing the situation. On the occasion of studying the reasons for the accident at the station of Grejac, the Minister of Construction proposed to the Serbian government to take up the operation of railway lines by itself. The Decree of the Council of Ministers was signed the same day but announced to the company on the following day, on 21 May 1889. However, Serbia had to pay back for the right of operating its own railways and getting the possibility to use them for the interests of the country. This act confirmed that the policy of the Bulgarian state towards the railway development was the most appropriate for the time being. Moreover, it was in harmony with the European tendency of consolidating the private railway lines into united national systems capable of performing the important task both in economy and as a main strategic means in possible future wars.

3 STATE RAILWAY STRUCTURES AND RELATIONS

The fact that most of the MPs in the Bulgarian Parliament used the Serbian experience to ground their position towards the type of property in railways indicated their thorough knowledge in the railway development in Serbia. That was not amazing because both countries had to meet the requirements of the "*Convention a Quatre*" for connecting their railways thus enabling the traffic along the so-called Orient-Express route. To complete that task, Bulgaria and Serbia signed another document, the Convention of Connecting the Serbian and Bulgarian Railways between Pirot and Tsaribrod that obliged the BDZ authorities to harmonize the internal rules of operation with those existing in Serbia. Considering the above mentioned, it could be supposed that the Bulgarian politicians followed the Serbian example also with creating the governmental structures for coordinating and managing the activities in that field. Analogues to Serbia, the railway department in Bulgaria had existed within the Ministry of Finance before being attached to the Ministry of Public Buildings, Roads and Communications, which was established in 1995. However, it should be said that at first the railway authorities differed in their functions. Unlike the

department with the Serbian Ministry of Construction, which did not deal with operation, the Bulgarian State Railways (BDZ) administration was also the only operator, which soon became one of the three main state-owned enterprises in the country.

Despite the differences existing until 1889, when the operation of the Serbian State Railways was transferred to one of a governmental type, the railway authorities in Bulgaria and Serbia established highly professional relations based on consensus with making decisions and collaboration. Besides the Orient Express and the two conventional trains, they decided to use also mixed trains (local traffic) in order to avoid reloading at the border station by attaching the goods wagons to the post trains of the other country. However, the most impressive fact was the agreement of the two governments to apply a simpler way of trans-border regulation, using one station, Tsaribrod, for changing the trains and customs control. This organization was remarkable not only because of the period it was implemented, only a few years after the war in 1885. It seems even more impressive, if compared with the trans-border conditions on the Mitrovitsa – Vrnja line, where at the border with the Ottoman Empire there were two separate stations (Ristovats and Zibevche), which, by the way, was a widely spread practice all over the Europe. This tradition has been restored recently as a sign of the increasing mutual trust and the improvement of relations between the two neighboring countries.

In conclusion it should be underlined that both Serbia and Bulgaria accepted, although at a different time, the most appropriate type of railway management at the end of 19th century: the state-owned enterprise dealing not only with the infrastructure building and maintenance but also with the railway operation. Another common feature of the state policy in that transport section was that the governments in the both countries, despite of being different in their ideology and international orientation, have always developed the railways as a priority condition for the modernization and future prosperity and for the integration to Europe and the world civilization.

REFERENCES

- [1] Central State Historical Archive of Bulgaria, fund 157.
- [2] Govedarovic, N. & Z. Bundalo, 120 years of the Railway in Nis, Nis, 2004 (in Serbian).
- [3] Dzhaleva-Chonkova, A. & co-authors. History of the Railways in Bulgaria, S., 1997 (in Bulgarian).
- [4] History of Railways. Serbia, Voivodina, Montenegro, Kosovo, Belgrade, 1980 (in Serbian).
- [5] Radev, S. The Founders of Modern Bulgaria, Volume 1, Sofia, 1990 (in Bulgarian).
- [6] Railway Collection, 1896-1900 (in Bulgarian).
- [7] Railway Transport in Bulgaria 1866-1983, S., 1987 (in Bulgarian).
- [8] Stenographic Diaries of the 4th National Assembly, Sofia, 1884-1985 (in Bulgarian).

HARMONIZATION OF THE BULGARIAN TELECOMMUNICATION AND SAFETY SYSTEMS ALONG THE EUROPEAN TRANSPORT CORRIDORS

Margarita Georgieva¹, Ivan Nenov²

The Bulgarian railway network is a part of European corridors of the trans-European railway network and on that reason the projects on railway traffic control system have to meet high operational target parameters and the European requirements of train traffic safety, power efficiency and environmental protection with the railway line operation. The projects must comply with the recommendation for staged implementation of the European ERMTS/ETCS system for control of the automation and traffic processes in the railways. Having in view of actual condition of the railway infrastructure to Bulgaria, managerial system of the motion train and relationship, which are operating, may be offered effective technical and economic decision.

The paper also presents an engineering and expert assessment of the existing safety and telecommunication devices and systems and is proposed effective technical and economic solution.

Keywords: ETCS, ERTMS, traffic safety, telecommunication system, GSM-R, railway transport.

1. INTRODUCTION

There taking into account that the main of corridors of the Trans - European railway network (TEN) pass along the Bulgarian railway network, the automatic control system projects has to meet high operational target parameters and the European requirements of train traffic safety, power efficiency and environmental protection with the railway line operation. Besides that, the project must to comply with the recommendation for staged implementation of the European ERTMS/ETCS system for control of the automation and traffic processes in the railways. The main feature of this system is that it gives the possibility of optimum compatibility between the railway administrations and the railway traffic control systems, so the system is implemented in the most economical and effective way. For that purpose, a multi-functional onboard system on the locomotives has been developed. It can read the information from the track systems and can regulate the train speed according to the safety criteria automatically or semi-automatically, with the participation of the engine driver, i.e. it can provide faultless and regular transport process. Four algorithms (levels) of implementation have been developed which will enable the particular railway administrations to choose the most effective way of implementing the ETCS system and thus to carry out boundary-less train traffic. For that reason, the purpose of this paper is to consider the actual situation in the national railway infrastructure,

i.e. what systems of train traffic control are in operation, what their technical condition is and the possibilities that they be used in the near future. That has imposed the necessity to make an engineering and expert assessment of the existing safety and telecommunication devices and systems and to propose effective technical and economic solution.

The pre-examinations on the state of the safety and telecommunication devices and systems in railway infrastructure have shown that the main technical equipment is of conventional type: station interlocking, relay semi-automated interlocking between stations, automated cross-level devices and train-dispatcher radio connection. There is a modern complex automatic train traffic control system only in the section from Sofia to Plovdiv. An automatic locomotive signaling of point type is under implementation in Plovdiv – Stara Zagora – Bourgas section. This signaling is in compliance with the ETCS, level 1. The existing telecommunication network of the railway transport has been built using analog devices on the base of decade-step switching with a small amount of telematic information of a low reliability. The existing infrastructure is used for technological information with high reliability as the local transmitting tracts for delivery of this information to the center of processing have been built on its basis by a number of devices and software. At the same time there are a

¹ Margarita Georgieva, M.Sc.Senior Lecturer, T. Kableshkov Higher School of Transport, www.vtu.bg, Department of Telecommunication and safety systems, Sofia, 158 Geo Milev , Bulgaria, mgeorgieva@vtu.bg ; margarita_georgieva@abv.bg

² Assoc. prof. Ivan Nenov Ph.D. T. Kableshkov Higher School of Transport, www.vtu.bg, Department of Telecommunication and safety systems, Sofia, 158 Geo Milev , Bulgaria, ivan_nenov33@vtu.bg

number of local computer networks of information processing that exist on a local level.

The existing safety systems of automatic train traffic control systems and the corporate telecommunication network have limited possibilities of development and do not meet the modern European standards.

The modernization and development of transport safety devices without changing the approach and principles of building such systems and telecommunication networks is not reasonable.

2 GENERAL STRUCTURE OF THE SIGNALING AND SAFETY SYSTEMS FOR THE BULGARIAN RAILWAY NETWORK

It is proposed to build a complex system of control automation of train traffic for the maximum speed 160-200 km/h, which will be implemented by stages in separate railway sections according to the Strategy of Transport Development in Bulgaria until 2015.

The system is intended for the actual accomplishment of transportation with the restrictions imposed for strict implementation of the traffic schedule, guaranteed term of goods delivery, providing safety of transportation, comfort of traveling, taking into account the requirements of the market economy and the influence of external disturbance factors.

Due to the territorial de-concentration of the objects under management, control and information and their relative independence, it is necessary that the system has a network structure consisting of three information control centers. They have to be built on a hierarchical principle on two levels: first, for direct control of objects, remote control of a group of objects and second, for generating and optimizing the traffic schedule and coordinating the control on the whole railway network as shown in Fig. 1.

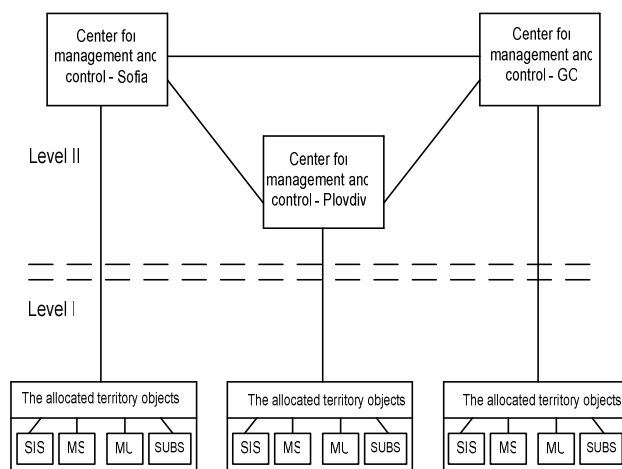


Fig. 1 Structure scheme

On the first level: local systems of local control of objects such as stationary objects (stations, cross-levels); movable units (trains, single locomotives); monitoring stations, ticket offices, offices for freight transportation services, etc.

On the second level: microprocessor radio block centers for management and control of the allocated territory objects by optimizing the traffic schedules along the whole railway network and for providing the traffic safety of the movable transport units.

On the base of the short analysis of the actual state of the national train traffic safety devices and systems and considering that the world has entered in the age of global information society and new achievements in the field of telecommunications and safety equipment, it is necessary to update the concept of processes automation in the railway transport. At that the following facts have to be taken into account:

- principally new equipment and technologies such as ATM, ISDN, GSM, CTC/IR have appeared and are under implementation in the field of telecommunications and computer science;
- the new global information society Internet;
- implementation of mobile telecommunications in the safety systems (GSM-R);
- satellite global positioning system (GPS);
- changes in the part of hardware and software - the equipment is being standardized and the software applications provide the individual specificity of a particular system;
- the area where the fail-safe methods and equipment are applied has been getting narrower at the expense of applying standard equipment and solutions suitable for applying in all fields.

From all of the above it is seen that some prerequisites for a radical change in the principles and technical means used to structure the modern train-control safety systems have been established. By now, the safety systems have been divided into two groups: at stations and between stations, which have definite differences connected with their functional peculiarities and the location of applying to. Now, these differences lose the specific character. For instance, the auto block system is with a centralized location of the equipment; interlocking systems are built up according to the topology of the station (number of the stations) with a distributed location of direct control devices both at the station and between the stations; the safety equipment at big station can control the cites even in sections and dispatching regions.

The appearance of GSM-R, which transmits both voice information and reliable commands of control to fixed sites and trains, creates train-control, dynamic safety traffic intervals without using linking (copper cable) lines but wireless (mobile radio) connectivity.

With the conventional and microprocessors systems, fiber-optic communications have been used more and more widely as well. They use a level of direct control of fixed sites and a level of dispatching control.

The accession of Bulgaria into the European Union imposes the necessity to consider the requirements of compatibility when building the national train-control systems onto the railway transportation technological processes while providing traffic safety in order to avoid problems with train traffic at cross-border train stations. To solve these problems, the EU has already proposed a unified system of railway transport management (ERTMS) with main subsystems – a system of train traffic control (ETCS), GSM-R railway radio system and a system of transport process management ETML. Eurobalise transponders are used to determine the train location /Level 2/. GPS is provided, as an option, which is the main way to determine the location of the trains. There are three levels – Level 1 and 2 are fixed block, while Level 3 is a moving block solution.

These new realities have pre-ordained the use of such an information-and-control system for the railway transport and improvement of the rail transport safety in Bulgaria which is based on the European standards. It is considered expedient to build the system on the base of three basic centers (Sofia, Plovdiv, Gorna Oriahovitsa-GO), between which there is a modern company network to transmit information, including reliable information about the control of the train traffic and other processes. The basic sites, which contain the system of control and safety, can be defined in the following way in [1].

It is recommended to begin with the implementation of ETCS, level 2 that requires minimum costs. Besides that ETCS, level 2 is compatible with ETCS, level 3 and it is easy to drop linear systems and to pass to using GPS. At that it is possible to implement microprocessor interlocking with distributed location of the mechanisms for direct control on sites at stations.

2.1 The results expected are as follows:

- for conditions will be created to integrate the Bulgarian railways into the united railway network of Europe;
- new jobs for workers and specialists will be opened both office and field operation of this system;
- the traffic safety will be considerably improved and optimal schedule of train traffic will be developed;
- the outer devices mounted on the track will be reduced and that will stop vandalism in the railways;
- conditions will be created for certain companies to specialize in and to receive offers to produce devices and systems that will contribute to the economic recovery;
- the passenger comfort and mobility will be improved and conditions will be created to use the housing stock in small villages and towns.

3.CONSTRUCTION OF PRIVATE TELECOMMUNICATION COMPLEX MOBILE RADIO NETWORKS

It is necessary to build a multi-purpose telecommunication network on the principle of using a basic transmitting backbone network intended to transmit voice and highly reliable telematic information with

controlled priority delivery delays and possibilities to introduce wideband, mobile or IP capabilities.

The mobile telecommunications has always played an important part in the railways, that is why various radio systems has been implemented for the different technological processes in the railway transport in the different countries. All these networks operate independently from one another, as most of them have been built according to different technologies and in different railway networks in the range of 450 MHz (UIC75-3) for Europe.

The UIC began standardization at the beginning of 1990s and the EIRENE project developed a catalog of requirements, which are used as a base to specify recommendations now (MORANE project). The functional set includes the functions of GSM-Phase 2+ and additional functions specific or the railways as functionally addressed by subscribers, e.g. trains. The new system has to meet all the requirements with speeds of up to 500 km/h. The European Commission of Frequency Distribution CEPT has separated a frequency band of about 900 MHz with 19 channels for the railways, by which it is achieved:

- interaction on a united telecommunication platform;
- developing a universal radio communication system;
- reducing the costs with using and maintenance while increasing functional possibilities;
- wide application of widely-spread standards;
- reducing the costs by using mass products in the network.

4. TECHNICAL AND TECHNOLOGICAL REQUIREMENTS

The network GSM-R is an official railway system, which provides directly the railway traffic control and safety using different processes, materials and staff with transmitting high-responsible information.

The systems have to provide the achievement of the specific technological activity and the train traffic schedule with high reliability and safety, including under degraded conditions, informing passengers, serving passengers and customers with providing the time of delivery and goods in preserved quality.

The systems have to result in reducing the initial capital expense and future operational costs. The algorithm of operation is determined for all operational activities according to the schedule of the connection of routes, signal indices, switches and the conditions of all objects under control. The schedule will be approved by the National Railway Infrastructure Company.

All systems of tele-control and management of the sites have to be compliance with the requirements provided for the speeds up to 200 km/h and for the functionality and safety according to the EU standards. They have to meet the requirements for safe operation, reliability and adaptability, keeping people healthy and the environment clean. The systems have to meet the requirement for complete operational compatibility of the traffic of all

train types for internal and international communications set in the corresponding directives. The equipment has to possess certificates proving its abilities to be used and to meet the requirement of operational compatibility in the EU countries.

The devices and equipment are to use standard computers. Telecommunications have to be with a standard protocol.

The software is to be compatible with the hardware on different platforms.

The equipment should give a possibility for expansion.

The direct control of point machines, lamps of traffic lights and the railroad sections are to be accomplished by fail-safe controllers, without using relays (with a minimal use of relays) as intermediate elements.

The controllers have to be used for the same purpose at least in one EU country. The protocol of communication between the controllers and devices, which control them, has to be of industrial standard.

During the process of operation, it should have a possibility to deliver spare controlling capacity. The controllers have to be compatible with the other equipment on the level of the communication protocol. The level of compatibility should be pointed out. The system has to meet the standard of safety operation SIL 4.

The external devices of the safety and telecommunication equipment have to be resistant against the vandalism and to have remotely transmitted indication for non-regulated access.

The devices of the external equipment should be provided to operate in the temperature range of from -40 to +80 °C. The life of the system has to be kept for minimum 20 years.

The traffic lights have to give indices in compliance with the speed signaling in BDZ. With the need of track circuits, unlimited track circuits with electrically insulating axle counters have to be used. They can be provided also to control the occupancy of the station tracks and of the tracks between the stations without passing signals.

The man-machine interface should be in Bulgarian in addition to English.

There must be offered a system for the maintenance staff for announcing failures.

The software applied gives a possibility for maintenance and configuration changes. There should be a possibility to add or drop objects. The change with future railway line doubling has to be regulated.

The system has to allow interconnection with other systems on the purpose of providing safety.

The electric supply is to be of UPS type, basically from the catenary's supply and from the AC in reserve, with a possibility to guarantee the operation of the backed-up devices only from batteries for up to 4 hours. The batteries have to be guaranteed for life of at least 15 years. The systems have to be built on the basis of modern components with minimal power consumption, which is to be demonstrated (proven).

The system of train traffic management and control between two stations and at stations has to meet the requirements of ERTMS/ETCS, i.e. Level 2 – a radio based system without signals. It has to allow future capacity expansion and the transition to level 3. The possibilities of expansion and the transition to a higher level should be pointed out as well as the means of changing the traffic capacity of the railway sections. It should be also provided to perform shunting activity with shunting signals by lamps of incandescent wires or by another economical light source.

The track devices for determining the train locations in the sections between the stations have to be compatible with the ones in operation in the railway infrastructure in the Sofia – Plovdiv – Bourgas sections and to meet the European standards of the ERTMS/ETCS system.

The equipment of the working places has to meet the contemporary requirements of ergonomics.

The supervisory signaling (CTC) has a common hardware with the system of train control and the power system of the section. The server has to be mirrored; the work stations have to be identical. It will be necessary to write a complete report about the events, to separate an independent working position for the maintenance staff. The information should be projected on a screen; the number of projectors should be provided with a spare.

The system has to allow using the information available about the train traffic and cargoes from the information system/systems of the carriers to serve passengers and customers.

The necessary heating and air condition systems should be provided as well.

5. CONCLUSIONS

The system of train traffic management and control examined in the paper as a possible solution for the Bulgarian railways meets the standards of ERTMS/ETCS. Its implementation is of vital importance to Bulgaria because of the requirements for the country in connection to its EU accession. The operation of such a system will result in increasing the train traffic safety and improving the railway service as well as in widening the range of transport services and easier information access for people and forwarding companies.

REFERENCES

- 1 ERTMS /ETCS project “EIRENE – MORANE”, 2000-2003.
- 2 Ron Kermisch and Paul Smith, Bain&Company, Making good on telecom convergence. Financial Times, 1/21/2005.
- 3 E. Pencheva, Vavedenie v modernite telekomunikacionni mrezi, Novi Znania, Sofia, 2002 (in Bulgarian).
- 4 Y. Tobita, I. Shimada, K. Ishii, K. Oguma, “New Signaling Systems Featuring Latest Control” Hitachi Review Vol. 53 (2004), No 1, p. 40 [1]

DYNAMICS OF TANK VEHICLES WITH LIQUID CARGO

Rajko Radonjić¹

ABSTRACT. In this paper a method to study interaction of system tank vehicle – liquid cargo is presented. In a general formed simulation model can be included different vehicle parameters, driving state with constant or varying speed, on the straightline or curved road, by vehicle starting and braking. Also, can be considered different tank vehicle configuration with liquid cargo, fuel tanks, fire trucks, containers with liquid foods etc. As example, for a fire truck structure, an appropriate model and parameters are adopted and relevant simulation results are given.

KEY WORDS: vehicle, tank, liquid cargo, interaction, simulation.

1. INTRODUCTION

Different vehicle combination carrying liquid cargo can appear in road traffic. Their handling characteristics may be deteriorated due to the motion of liquid in tank excited from driver's steering, braking, accelerating action in interaction with road geometry, driving on irregularity road surface and from aerodynamical effects, wind forces and moments.

The vehicle excitation will cause liquid free oscillations and/or force full oscillations that influence on the total level of the vehicle oscillations, loads of driver, vehicle and tank components, the lateral and longitudinal stability, in general, on the safety and integrity of total vehicle. Road accidents involving such vehicles lead the most to human injuries, damaging the environment, economic losses.

According to mentioned problems, during development of tank vehicle using efficient methods could provide valuable tools to optimize their dynamic behaviour. The appropriate modeling of vehicle as rigid body structure is based on the multibody system approach. But modeling of rigid body structure with internal sloshing liquids and partially filled tank made very complex problems, requires new approach and simulation methods.

Different approach can find in review of papers from this research field. Multiple linear mass-spring-damper system as equivalent of sloshing liquids is used in paper [1]. A nonlinear pendulum model for the lateral dynamics of liquid load is presented in [2]. A model of fluid components based on Navier-Stokes equations is coupled to a mechanical tank truck system in [3]. The problems of sloshing liquids and vehicle body structure interaction and their solution by combination of computer programme from field fluid dynamics and vehicle dynamics are considered in paper [4].

In present study the attention is concentrated upon relationship between the liquid cargo motion in a tank and vehicle dynamics, therefore, upon their interaction. Investigation are realised by means of simulation models presented in next part of paper, with emphasis possibilities and appropriateness of modern simulation technique to solution these always actual problems.

¹ Prof dr Rajko Radonjić, Faculty of Mechanical Engineering, Kragujevac, Sestre Janjić 6, 34000 Kragujevac, e-mail: rradonjic@kg.ac.yu

2. SIMULATION MODEL

A vehicle - tank system simulation model is shown in Fig .1 . A rigid rectangular tank is mounted on the base a two - axle heavy motor vehicle , with denoted geometric parameters of length , a , height , h , liquid height , h_l and location of liquid center gravity , T_1 . The loaded vehicle center gravity denoted with , T .

The simulation model in Fig. 1 , possessed five degrees of freedom : vertical displacement of unsuspended mass , z_1 , z_2 , respectively , vertical displacement , z , and angular displacement , α , of suspended mass , so called , heave and pitch and displacement of liquid cargo

free surface α_1 , so called , sloshing . Modeling of liquid displacement , in this paper , has been created on the base analogy between liquid mobility and pendulum movement . By modeling is presumed that vehicle operate on the road with different geometry , stationary and non - stationary driving condition , during braking or accelerating , at constant or varying acceleration . For all that , the depth of liquid can vary considerable . The knoweldge of the magnitude of the liquid's natural frequencies is need for creating analogous mechanical models .

In former paper [5] , the natural frequencies of incompressible liquid are obtained from solution of the Laplace equation for rigid boundary conditions and the kinematic condition at the free liquid surface . For a rectangular tank of length , a , width , b and liquid height , h , natural circular frequencies are :

$$\omega_{mn}^2 = gk \left[\sqrt{x} \tanh(h_l k \sqrt{x}) \right] \quad (1)$$

where $k = \pi / ab$, $x = m^2 b^2 + n^2 a^2$, $m, n = 0, 1, 2, \dots$

In the case of an excitation of tank only one direction, will be form only the odd natural frequencies, in longitudinal direction as, $\omega_{2m-10}^2 = gk_1 \tanh(h_l k_1)$, with $k_1 = \pi(2m-1)/a$, and vertical direction as , $\omega_{02n-1}^2 = gk_2 \tanh(h_l k_2)$, with $k_2 = \pi(2n-1)/b$. On the base this relationship an algorithm to determination relevant parameters and creating analogous mechanical model of liquid displacement is formed. Fig. 2, shown graphic relation between natural frequencies of liquid cargo in a partially

filled horizontal rectangular tank, geometrical tank parameters and number of modes, m . As may be seen , natural frequencies increase with the increase height / length ratio , h/a , and increase the mode number , m . Fundamental natural frequency , at mode $m = 1$, increases slower in larger domain of height / length ratio in distinction from heigher order frequencies , $m = 2, 3, \dots$ with rapid increasing in narrow band of h/a . In the case of constant tank length, a , relationship between natural frequencies and liquid height are presented in Fig. 3. The curve shape in this figure follow the curve flows from Fig. 2, sensitivite at low and practical unsensitive at heigher liquid depth.

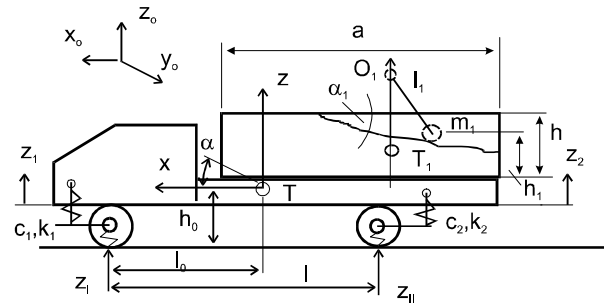


Fig. 1. Vehicle – tank – liquid, simulation model.

Natural frequencies are now basic hydrodynamic parameters to determination equivalent pendulum parameters . According to earlier knoweldge , theoretically , infinite number liquid oscillating modes are possible in a rectangular tank . By means of mentioned determined natural mode frequencies in tank longitudinal direction , equation (1) and results from Fig . 2 , can be calculated the basic liquid model parameters, as equivalent pendulum lenth, corresponding pendulum mass, as part of liquid mass moving relative to tank and part of liquid mass, fixed to tank and vehicle.

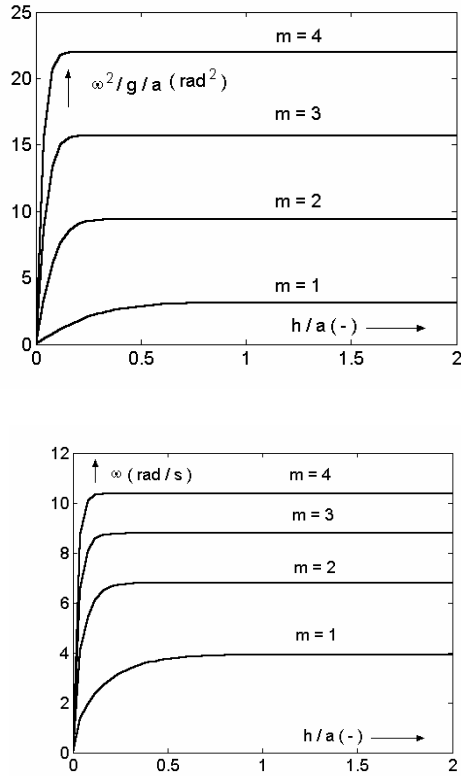


Fig. 2 Relative natural frequencies of liquid cargo in rectangular tank.

Fig.3. Natural frequencies of liquid cargo in rectangular tank.

According to tank vehicle model in Fig. 1 and results in Fig. 2, a simulation model is derived using Lagrange's equations. For a vehicle modified variant with solidified tyre, system differential equations are presented in a condensed implicit form:

$$\begin{aligned}
 E_1 [a_1 \dots a_8, z, \dot{z}, \ddot{z}, \alpha, \dot{\alpha}, \ddot{\alpha}, \alpha_l, \ddot{\alpha}_l] &= F_1 \\
 E_2 [b_1 \dots b_{13}, z, \dot{z}, \ddot{z}, \alpha, \dot{\alpha}, \ddot{\alpha}, \alpha_l, \ddot{\alpha}_l, \ddot{x}] &= F_2 + \\
 + F_3 \ddot{x} \\
 E_3 [c_1 \dots c_9, \ddot{z}, \alpha, \dot{\alpha}, \ddot{\alpha}, \alpha_l, \ddot{\alpha}_l, \ddot{x}] &= 0
 \end{aligned}
 \quad (2)$$

where z, α, α_l in Fig. 1, introduced symbols; F_1, F_2, F_3 , from road to vehicle excitation forces; \ddot{x} – longitudinal vehicle acceleration; a_i, b_i, c_i – coefficients, as interaction of system parameters.

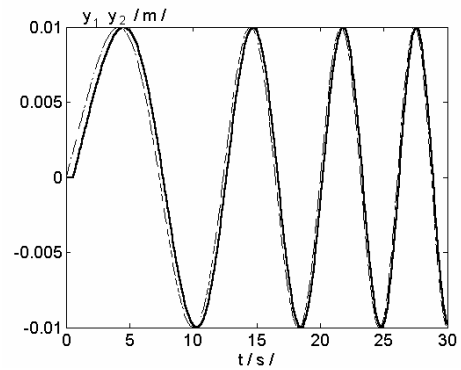
Equations (2) are nonlinear and coupled. The nonlinearities, caused by model structure and eccentricity disposition of the vehicle mass, occur in displacement, velocity and acceleration even in the case of linear characteristics suspended elements.

System equations (2) can not be solved in an analytical closed form. The solution is realised numerically using simulation procedure according to model structure with input variables, the excitation time functions of road irregularity, initial vehicle velocity and longitudinal acceleration.

Model structure and parameters were adopted for a fire truck as example, with basic values: mass of the unloaded truck, 4580 kg; mass of the loaded truck, 8200 kg; truck wheel base, 3 m; tank dimension, length / breadth / height, 2 m / 1.5 m / 1.2 m; liquid in the tank is water. Relationship between excitation forces of vehicle front and rear axle was simulated in this paper, by means of variable transport delay, as shown in Fig. 3.

Fig.4. Time signals of vehicle front and rear axle excitation with variable transport delay.

The plot in Fig. 4 corresponds to the shape of a chirp signal, appropriate to simulation, because of a larger band of



spectral density than proper sinusoidal signal.

Simulation results are given in Fig. 4 and 5.a, b.

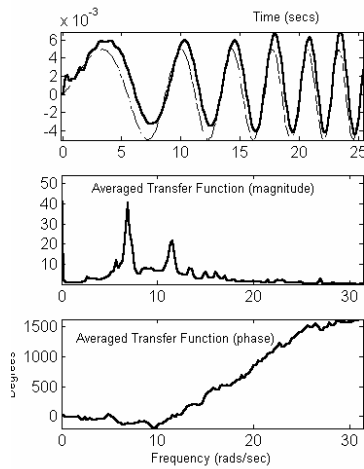
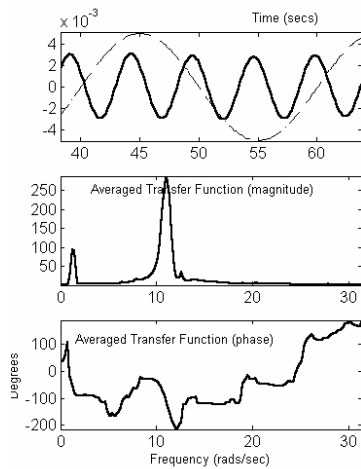
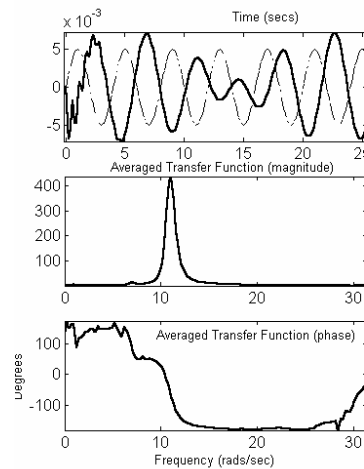


Fig. 5. Relationship between excitation of front axle and vertical displacement of the vehicle centre gravity.



a)

Fig. 6. Relationship between excitation of front axle and displacement of liquid cargo free surface by vehicle initial speed: a) 1m/s, b) 5m/s.



b)

3. CONCLUSION

Investigation of tank vehicle – liquid cargo interaction is a complex research task. Advanced simulation methods can be efficient tools in this research field.

REFERENCES

- [1] Slibar A., Troger H.: Das stationare Fahrverhalten eines Tank-Sattelaufliiegerzuges, *IUTAM Symposium*, Amsterdam, 1976.
- [2] Ranganathan r et al .: Steady turning stability of partially filled tank vehicles with arbitrary tank geometry. *ASME J. Dynam. Systems* 111, 1989.
- [3] Ortiz L et al .: Flexible multibody system interaction. *Internat. J. Numer. Meth. Engrg.* 41, 1998.
- [4] Rauh J., Rill G .: Simulation von Tankfahrzeugen, *VDI Berichte* Nr. 1007, VDI – Verlag, 1992.
- [5] Abramson N .: The dynamic behaviour of liquids in moving containers. *NASA SP-106*, 1966.
- [6] Radonjić R .: Stability of system : tractor – tank semitrailer. *Tractors and power machines*, N 4 / 2002, Novi Sad.

DYNAMICS OF BRAKED VEHICLE ON REAL SURFACE

Lalovic R Ljubica, Lalovic M Dragomir, Knezevic-Miljanovic Julka¹

Abstract

This paper presents effects of front and rear suspension designs as from the aspect of elastic suspension and damping as the way of directing the front and rear wheel to stability of braked vehicle together with effects of uneven road. The general model has been done and applied to two vehicles having the same front suspension concept and different rear suspension concept (one cross and another one longitudinal system) and their effects to braked vehicle stability have been monitored. .

An effective analyze is made where various dynamics forces can be seen on two vehicle axles and with the same slowing down and same uneven roads.

Key words: Dynamics of the vehicle, breaking, uneven road

1. INTRODUCTION

In dynamics of motor vehicles it is usual that dominant vehicle motions are mutual separated and that the straight motion of a vehicle with certain problems are observed.

In practice motions of vehicles caused by various causes of coupling, therefore making of complex models are done.

In this paper the coupling is considered between the vertical motion being caused by uneven roads and the vertical motion caused by the vehicle braking.

In the paper the following designations are used:

$x[m]$ - vehicle longitudinal coordinate
 $y[m]$ - vehicle cross coordinate
 $z[m]$ - vehicle vertical coordinate
 $\theta [rad]$ -rotation angle of vehicle center around cross axle
 $a[m]$ - distance of vehicle center from front axle
 $b[m]$ - distance of vehicle center from rear axle
 $h[m]$ - height of vehicle center
 $g[m/s^2]$ - gravitation acceleration
 $z_1[m]$ displacement of abut mass on front axle
 $z_2[m]$ - displacement of abut mass on rear axle
 $z_{1p}[m]$ - displacement of front wheel center
 $z_{2p}[m]$ -displacement of rear wheel center
 $z_{01}[m]$ -uneven road in point of contact of front wheel and road

$z_{02}[m]$ - uneven road in point of contact of rear wheel and road

$m[kg]$ - vehicle abut mass
 $m_1[kg]$ - abut mass on front axle
 $m_2[kg]$ - abut mass on rear axle
 $m_{1p}[kg]$ - non abut mass on front axle
 $m_{2p}[kg]$ - non abut mass on rear axle
 $I_y[kgm^2]$ - inertia moment for center y-line
 $K_1[Ns/m]$ -characteristics of front suspension damping
 $K_2[Ns/m]$ -characteristics of rear suspension damping
 $C_1[N/m]$ -characteristics of front suspension rigidity
 $C_2[N/m]$ -characteristics of rear suspension rigidity
 $C_{1p}[N/m]$ - characteristics of front wheel rigidity
 $C_{2p}[N/m]$ -characteristics of rear wheel rigidity
 $F_x[N]$ -total longitudinal force
 $F_{x1}[N]$ - brake force on front wheels
 $F_{x2}[N]$ - brake force on rear wheels
 $F_z[N]$ - total vertical force
 $F_{z1}[N]$ - vertical force on front axle
 $F_{z2}[N]$ - vertical force on rear axle
 $\left. \frac{\partial x}{\partial z} \right|_1$ [-]-derivative of front suspension, gradient of change of longitudinal displacement related to vertical one

¹ M.Sc. Lalovic R Ljubica, Faculty of Mechanical Engineering – Kraljevo, e-mail: lalovic.lj@maskv.edu.yu
M.Sc. Lalovic M Dragomir, Zastava-R @ D car institute, e-mail: lale@ia.kg.ac.yu
Prof. Dr Knezevic-Miljanovic Julka, Mathematics faculty-Belgrade, e-mail: knezevic@matf.bg.ac.yu

$\left. \frac{\partial x}{\partial z} \right|_2$ [-]-derivative of rear suspension, gradient of change of longitudinal displacement related to vertical one
 ϕ [-]- coefficient of vehicle longitudinal adherence

Vehicle braking by ideal curve of vehicle braking – figure 1.

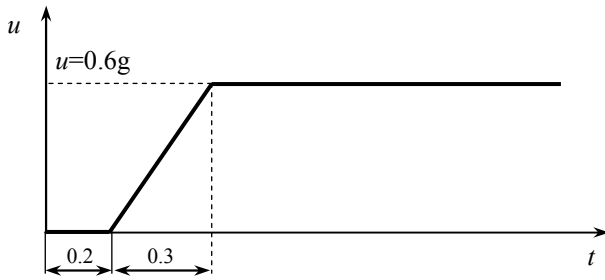


Figure 1 Diagram of vehicle slowing down

Brake force can be described by the equation

$$F_x = \begin{cases} F_x = 0 & 0 \leq t \leq 0.2s \\ F_x = \frac{0.6gm}{0.3}(t-0.3) & 0.2 \leq t \leq 0.5s \\ F_x = 0.6gm & t > 0.5s. \end{cases}$$

Uneven road in contact points of front and rear wheel is described by random function (RND) of amplitude 10mm:

$$z_{01} = 0.01(RND - 0.5)$$

$$z_{02} = 0.01(RND - 0.5)$$

2. DYNAMICS MODEL OF BRAKED VEHICLE

For analyze of braked vehicle stability the braked vehicle model was observed as presented on figure 2 where it is seen that effect of rigidity of front and rear wheel and uneven road are monitored.

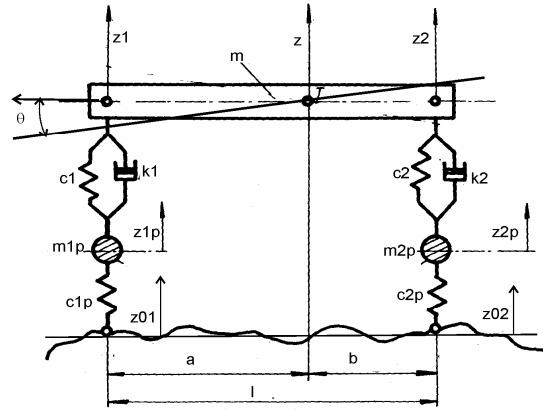


Figure 2 Scheme of oscillating model of braked vehicle

Appropriate system of differential equations are as follows:

$$\begin{aligned} m\ddot{x} &= F_x \\ m\ddot{z} + k_1(\dot{z}_1 - \dot{z}_{1p}) + c_1(z_1 - z_{1p}) + k_2(\dot{z}_2 - \dot{z}_{2p}) + c_2(z_2 - z_{2p}) &= F_z \\ I_y\ddot{\theta} + a[k_1(\dot{z}_1 - \dot{z}_{1p}) + c_1(z_1 - z_{1p})] - b[k_2(\dot{z}_2 - \dot{z}_{2p}) + c_2(z_2 - z_{2p})] &= F_\theta \\ m_{1p}\ddot{z}_{1p} - k_1(\dot{z}_1 - \dot{z}_{1p}) - c_1(z_1 - z_{1p}) + c_{1p}(z_{1p} - z_{01}) &= 0 \\ m_{2p}\ddot{z}_{2p} - k_2(\dot{z}_2 - \dot{z}_{2p}) - c_2(z_2 - z_{2p}) + c_{2p}(z_{2p} - z_{02}) &= 0 \end{aligned} \quad (1)$$

Since

$$\begin{aligned} z_1 &= z - a\theta & \dot{z}_1 &= \dot{z} - a\dot{\theta} \\ z_2 &= z + b\theta & \dot{z}_2 &= \dot{z} + b\dot{\theta} \end{aligned}$$

The system (1) has the following form:

$$\begin{aligned} m\ddot{x} &= F_x \\ m\ddot{z} + (k_1 + k_2)\dot{z} + (-k_1a + k_2b)\dot{\theta} - k_1z_{1p} - k_2z_{2p} + (c_1 + c_2)z + (-c_1a + c_2b) - c_{1p}z_{1p} - c_{2p}z_{2p} &= F_z \\ I_y\ddot{\theta} + (ak_1 - bk_2)\dot{z} + (-a^2k_1 - b^2k_2)\dot{\theta} - ak_1z_{1p} + bk_2z_{2p} + (ac_1 - bc_2)z + (-a^2c_1 - b^2c_2)\theta - ac_1z_{1p} + bc_2z_{2p} &= F_\theta \\ m_{1p}\ddot{z}_{1p} - k_1\dot{z} + k_1a\dot{\theta} + k_1z_{1p} - c_1z + c_1a\theta + (c_1 + c_{1p})z_{1p} &= c_{1p}z_{01} \\ m_{2p}\ddot{z}_{2p} - k_2\dot{z} - k_2b\dot{\theta} + k_2z_{2p} - c_2z - c_2b\theta + (c_2 + c_{2p})z_{2p} &= c_{2p}z_{02} \end{aligned} \quad (2)$$

In matrix form it is as follows:

$$\begin{bmatrix} m & 0 & 0 & 0 & 0 \\ 0 & m & 0 & 0 & 0 \\ 0 & 0 & I_y & 0 & 0 \\ 0 & 0 & 0 & m_{1p} & 0 \\ 0 & 0 & 0 & 0 & m_{2p} \end{bmatrix} \begin{bmatrix} \ddot{x} \\ \ddot{z} \\ \ddot{\theta} \\ \ddot{z}_{1p} \\ \ddot{z}_{2p} \end{bmatrix} + \begin{bmatrix} 0 & 0 & 0 & 0 & 0 \\ 0 & k_1 + k_2 & -k_1a + k_2b & -k_1 & -k_2 \\ 0 & a k_1 - b k_2 & -a^2 k_1 - b^2 k_2 & -a k_1 & b k_2 \\ 0 & -k_1 & a k_1 & k_1 & 0 \\ 0 & -k_2 & -b k_2 & 0 & k_2 \end{bmatrix} \begin{bmatrix} \dot{x} \\ \dot{z} \\ \dot{\theta} \\ \dot{z}_{1p} \\ \dot{z}_{2p} \end{bmatrix} + \begin{bmatrix} 0 & 0 & 0 & 0 & 0 \\ 0 & c_1 + c_2 & -c_1a + c_2b & -c_1 & -c_2 \\ 0 & a c_1 - b c_2 & -a^2 c_1 - b^2 c_2 & -a c_1 & b c_2 \\ 0 & -c_1 & a c_1 & c_1 + c_{1p} & 0 \\ 0 & -c_2 & -b c_2 & 0 & c_2 + c_{2p} \end{bmatrix} \begin{bmatrix} x \\ z \\ \theta \\ z_{1p} \\ z_{2p} \end{bmatrix} = \begin{bmatrix} F_x \\ F_z \\ F_\theta \\ c_{1p}z_{01} \\ c_{2p}z_{02} \end{bmatrix} \quad (3)$$

where:

$$\begin{bmatrix} F_x \\ F_z \\ F_\theta \\ F_{1p} \\ F_{2p} \end{bmatrix} = \begin{bmatrix} F_x \\ F_{x1} \frac{\partial x}{\partial z} \left| 1 + F_{x2} \frac{\partial x}{\partial z} \right| 2 \\ -aF_{x1} \frac{\partial x}{\partial z} \left| 1 + bF_{x2} \frac{\partial x}{\partial z} \right| 2 + (F_{x1} + F_{x2})h \\ c_{1p}z_{01} \\ c_{2p}z_{02} \end{bmatrix} \quad (4)$$

3. CALCULATION RESULTS

The following vehicles were considered:

- 1) S (vehicle with cross front and cross rear driven wheel)
- 2) F (vehicle with cross and longitudinal rear driven wheel)

Solving the above system of equations for the vehicle F and the vehicle S the following results are reached.

For the vehicle S:

$$\frac{\partial x}{\partial z} \Big|_1 = 0 \quad \frac{\partial x}{\partial z} \Big|_2 = 0$$

For the vehicle F:

$$\frac{\partial x}{\partial z} \Big|_1 = 0 \quad \frac{\partial x}{\partial z} \Big|_2 = -0.3$$

The diagram review of uneven road on front and rear wheel is shown on the figures 3 and 4.

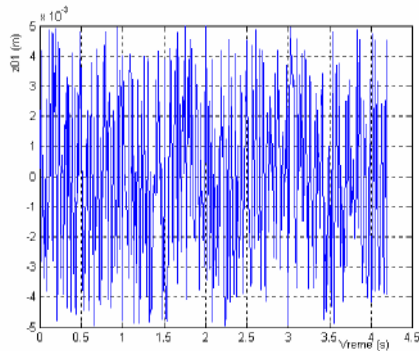


Figure 3 Function of uneven road in the point of contacts of front wheel and the ground

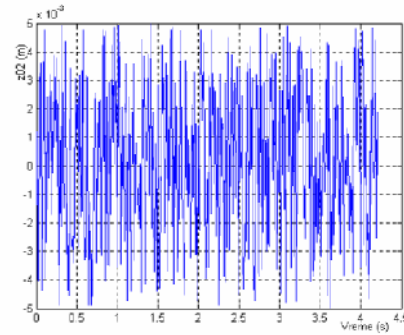


Figure 4 Function of uneven road in the points of contacts of rear wheel and the ground

3.1. Calculation results for the vehicle F

The calculation results for the vehicle F are diagram shown on figures from 5 to 8

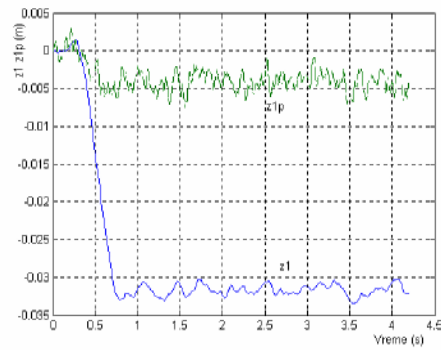


Figure 5 Displacement of abut mass and front wheel center of the vehicle F

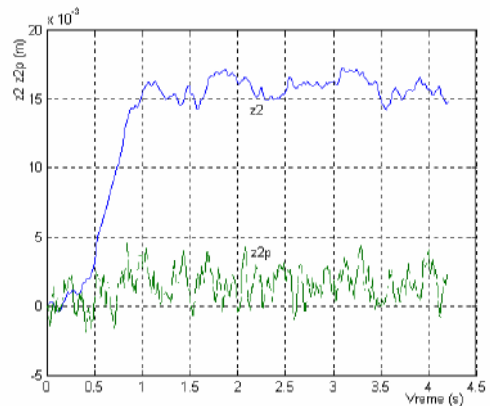


Figure 6 Displacement of abut mass and rear wheel center of the vehicle F

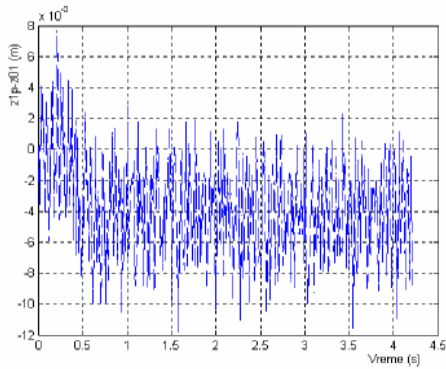


Figure 7 Difference of displacement of wheel center and uneven road on front axle of the vehicle F

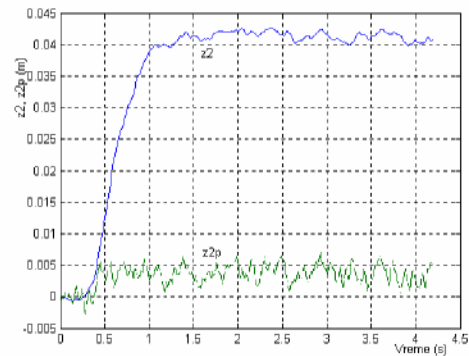


Figure 10 Displacement of abut mass and rear wheel center of the vehicle S

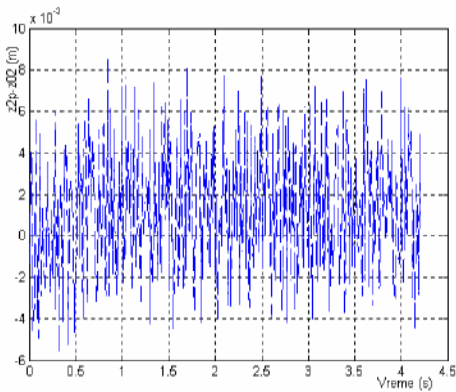


Figure 8 Difference of displacement of wheel center and uneven road on rear axle of the vehicle F

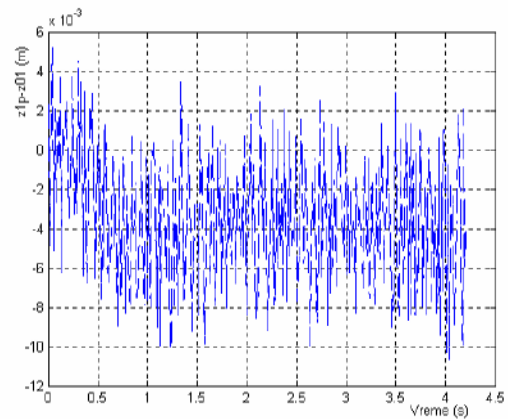


Figure 11 Difference of displacement of wheel center and uneven road on front axle of the vehicle S

3.2. Calculation results for the vehicle S

The calculation results for the vehicle S are diagram shown on figures from 9 to 12

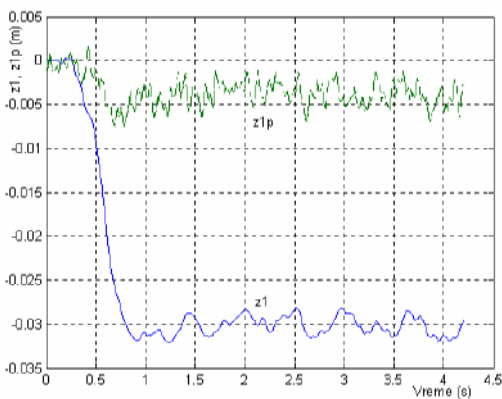


Figure 9 Displacement of abut mass and front wheel center of the vehicle S

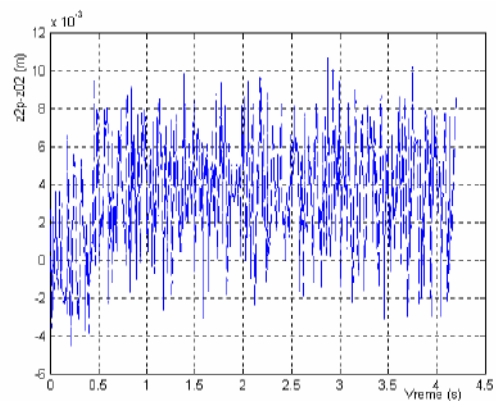


Figure 12 Difference of displacement of wheel center and uneven road on rear axle of the vehicle S

Functions of uneven road in the points of contacts of front and rear wheels and the ground (z_{01} and z_{02}) are given by random functions (RND) being shown on figures 3 and 4 .

Parallel review of displacement of the front wheel center and abut mass on front axle and the rear wheel center and abut mass on rear axle for the vehicles F and S are shown on the figures 5, 6, 9 and 10.

The difference of displacement of front wheel center and uneven road and the rear wheel center and uneven road for the vehicles F and S are shown on figures 7, 8, 11 and 12.

4. EFFECTIVE ANALYZE OF CALCULATED RESULTS

Since the time curve of displacement is in the discrete form the effective value is therefore calculated by the following relation

$$z_{eff} = \sqrt{\frac{1}{N} \sum_{i=1}^N z_i^2(t)} \quad (5)$$

Where: N-number of samples (number of points of signal discretion)

$z_i(t)$ -value of i sample (of i discrete value)

Let's define the effective value of the difference of displacement on front wheel

$$(z_{1p} - z_{01})_{eff} = \sqrt{\frac{1}{N} \sum_{i=1}^N (z_{1pi} - z_{01i})^2} \quad (6)$$

and the effective value of displacement on rear wheel

$$(z_{2p} - z_{02})_{eff} = \sqrt{\frac{1}{N} \sum_{i=1}^N (z_{2pi} - z_{02i})^2} \quad (7)$$

From diagrams on figures 7, 8, 11 and 12 we calculate effective values of displacements in time domain. The reached results are as follows:

For the vehicle F: $(z_{1p} - z_{01})_{eff} = 3.85$ mm

$(z_{2p} - z_{02})_{eff} = 1.76$ mm i

For the vehicle S: $(z_{1p} - z_{01})_{eff} = 3.72$ mm

$(z_{2p} - z_{02})_{eff} = 4.05$ mm

Based on calculated values it is seen the approximate equality of effective values on the front wheel and the difference of effective values on the rear wheel.

Since in both cases the pneumatic is the same (the same rigidity $c_{2p} = 170 \text{ N/mm}$), thus higher effective value of displacement on the vehicle S gives higher dynamics forces.

For example on the rear wheel of the vehicle S

$$F_{d2} = c_{2p} (z_{2p} - z_{02}) = 170 * 4.05 = 688.5 \text{ N} .$$

This force balances the rear axle and considerably reduces stability of the braked vehicle.

On the vehicle F the relevant displacement is $(z_{2p} - z_{02})_{eff} = 1.76$ mm, therefore the dynamics force is lower:

$$F_{d2} = c_{2p} (z_{2p} - z_{02}) = 170 * 1.76 = 299.2 \text{ N} .$$

Therefore the vehicle F is considerably more stable at braking.

5. CONCLUSION

A thorough theoretical approach that takes into consideration the relevant values of the braked vehicles gives as a result the effects of concept of front and rear suspension on longitudinal vehicle stability.

Besides the effects of elastic and damping elements it is also worked out the effect of the driven front and rear wheel on displacement of front and rear axle and abut mass of the vehicle in the whole.

This analyze is done with the effects of uneven road that exists in reality in order to follow jointly any effects of the suspension system concept and uneven roads on longitudinal stability of a vehicle.

The calculations are done for the vehicles F and S from where it can be seen the differences in displacement of rear axle with relation to the car body due to various driven wheels.

The dynamics analyze is presented in the points of contacts of the ground and the wheels pointing out on the differences in dynamics reactions on rear axle of the vehicles F and S.

6. LITERATURE

- [1] Janković D., Todorović J.: Theory of motor vehicle motion, Faculty of Mechanical engineering, Belgrade, 1983.
- [2] Jančićjević N., Janković D., Todorović J.: Design of motor vehicles , Faculty of Mechanical engineering, Belgrade, 1991.
- [3] Matschinsky W.: Die Radführungen der Strassenfahrzeuge, Verlag TUV Rheinland, 1987.
- [4] Ellis J.R.: Vehicle dynamics, Business Books, 1969.

- [5] Burckhardt M.: Fahrwerktechnik: Bremsdynamik und Pkw-Bremsanlagen, Vogel Verlage, Wurzburg, 1991.
- [6] Simić D.: Dynamics of motor vehicles, Science book, Belgrade 1988.
- [7] Radonjić R.: Analyze of mutual effects on braking and suspension systems, MVM 2000, YU-00028, Kragujevac, 2000.
- [8] Rusov L.: Dynamics model and stability of vehicle motion, Collection of papers, Conference on dynamics of objects and stability of their motion, Vrnjačka banja, 9-11 March 1978.

OPTIMIZATION OF VEHICLE SHOCK ABSORBER

Rajko Radonjić

ABSTRACT. In this paper a simulation model to investigation of motor vehicle vibrational processes and comparative analysis of various suspension systems is developed. The potential properties of vehicle passive suspension systems with linear damping and by random excitation from road roughness is studied. By means of inverse equations and with respect to requirements of ride comfort and road holding an optimum form of damper characteristic is derived. The results show that modified damper with nonlinear, unsymmetrical damping provides better isolation from vibration.

KEY WORDS: vehicle, shock absorber, vibration, simulation.

1. INTRODUCTION

A purpose of the suspension system for motor vehicles is to provide better performance: ride comfort, safety, road holding, noise comfort etc. [1], [2]. With modern fixed parameters passive suspension systems it need accomplish the compromise effectively between these conflicting requirements. The limitations of passive suspensions are concerned to, fixed properties, conventional components for energy storage and energy dissipation and dependence damping force only from relative displacement and corresponding velocity. Analysis of the passive suspension limitations and possibilities their improving by means of modified elasto-damping devices is presented in next chapters.

2. LIMITATIONS OF PASSIVE SUSPENSIONS

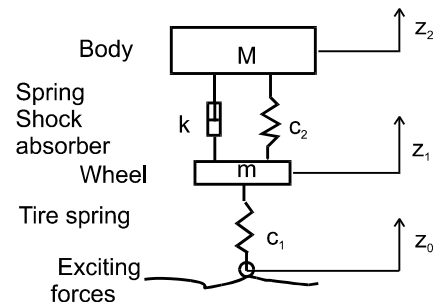
To studies of vehicle vibration has been used so-called the partial vehicle model reduced to one wheel, illustrated in Fig. 1. Wheel and body are connected by means of a conventional spring and a shock absorber. The force which works between the two masses only depends on their relative displacement towards each other and their relative speed. The equations of motion can be written in following form:

$$M \ddot{z}_2 + c_2(z_2 - \dot{z}_1) + k(z_2 - z_1) = 0 \quad (1)$$

$$m \ddot{z}_1 - c_2(z_2 - \dot{z}_1) - k(z_2 - z_1) + c_1(z_1 - \dot{z}_0) = 0 \quad (2)$$

Random exciting forces from road roughness was simulated with a filtered white noise source whose power spectral density curve when plotted on logarithmic coordinates may be approximated by a straight line with the exponential equation:

Fig. 1. A partial vehicle model



$$S(\Omega) = S(\Omega_0) \Omega^{-W} \quad (3)$$

where are: $S(\Omega_0)$, Ω_0 , W – parameters of road roughness, Ω – distance frequency argument. For a vehicle travelling with velocity V it may be shown that the spectral density of corresponding time signal is given by:

$$S(\Omega)V = S(\Omega) \quad (4)$$

¹ Prof. dr Rajko Radonjić, Faculty of Mechanical Engineering, Kragujevac, Sestre Janjić 6, 34000 Kragujevac, e-mail: rradonjic@kg.ac.yu

The limitations of passive suspensions are analysed on the basis of simulation results for partial vehicle model (1), (2) with linear damping. A simulation computer program has been made by SIMULINK interactive circuit in MATLAB environment. By means given random exciting signal and registered output signals the components of transfer function, gain and phase are identified.

3. RESULTS

In figures from 2 to 5, the identification results of vehicle transfer function in respect to the road displacement, with parameters, $S(\Omega_0) = 6.28 \cdot 10^6$, $W = 2$, are presented, as following: body acceleration, suspension working space, shock absorber force and tyre load.

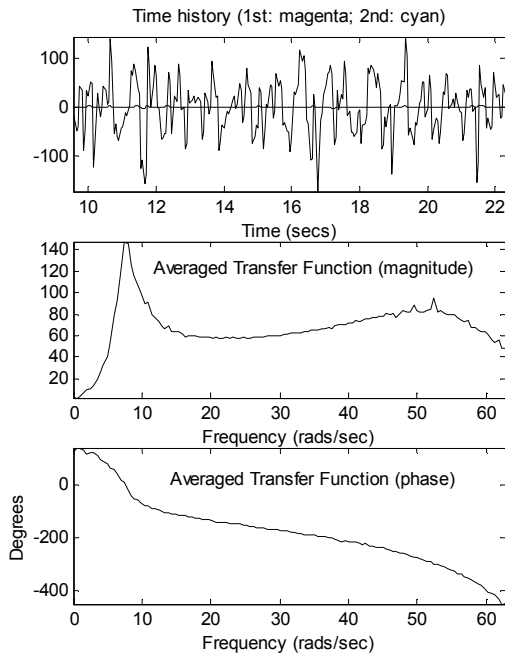


Fig. 2 . Transfer function of body acceleration to road displacement .

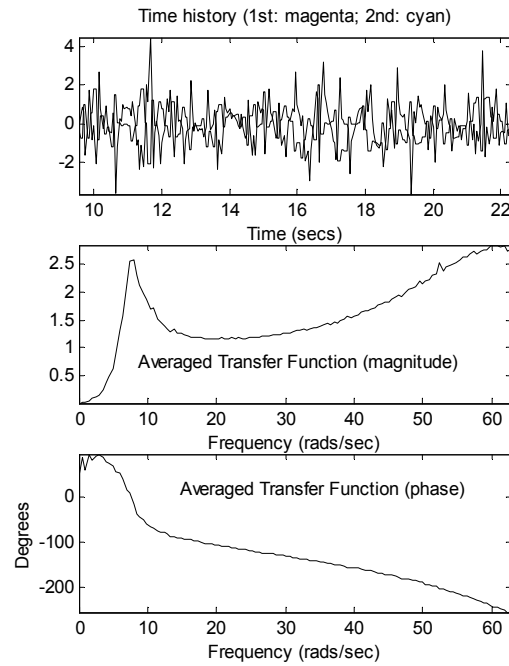


Fig. 3 . Transfer function of suspension working space to road displacement.

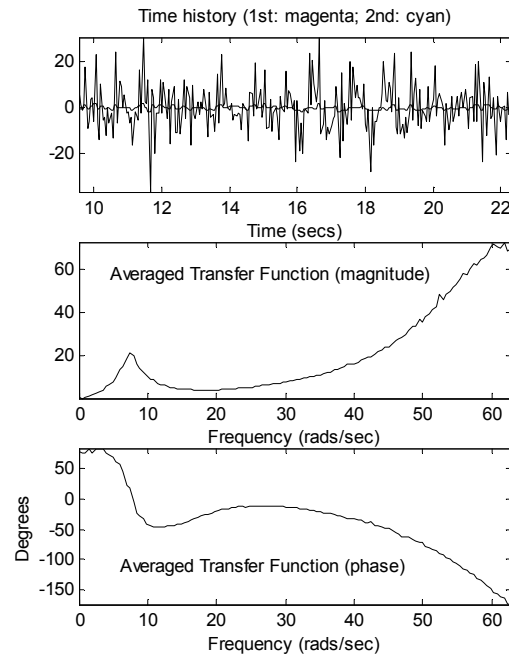


Fig. 4 . Transfer function of shock absorber force to road displacement.

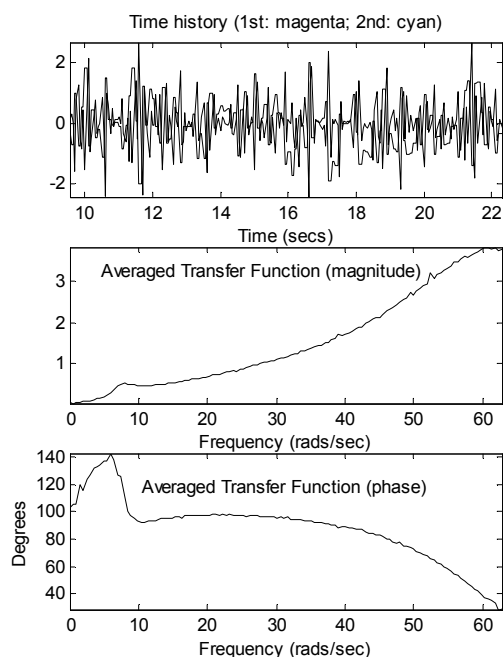


Fig. 5. Transfer function of tyre load to road displacement.

The performance parameters representing comfort, suspension working space and tyre load fluctuations are calculated by means the input spectral density and relevant frequency response function in the frequencies range from 0.25 to 15 Hz. From these relations it can be concluded that: 1/ the main levels of body acceleration, as measure vehicle comfort, are concerned in region of body resonance where is the spring the main force transmitter, 2/ the extreme values of body relative displacement, as measure of used workspace also occurs at body resonance, 3/ the main shock absorber force and tyre load force fluctuation occur at higher frequencies.

To full assessment of the vehicle performance it need in above consideration the phase angle include. In the case of variables, presented in Fig. 2, 3, 4, except by very low frequencies, output variables follow the input variable with time lag. On other hand, variable in Fig. 5 has phase lead.

From above analysis follow conclusion, that it would be advantageous to incorporate the shock absorber with greater damping at low frequencies. In this sense, a proposed procedure to selection the optimum form of shock absorber characteristics with respect to vehicle comfort is presented further. Inverse equations algorithm was used, with input variables, road roughness displacement, weighted body acceleration, and output variables, displacement of unsprung mass, shock absorber force. As result of inverse model

simulation were obtained the shape of an averaging damping characteristics presented in Fig. 6, unsymmetrical, nonlinear, with optimum ratio of damping rates on the rebound and bump strokes.

The derived shock absorber characteristic, in accordance to Fig. 6, has particularly in near the origin a steep slope. The obtained curve can be approximated by a polynomial form of relative velocity power, rational order from eight to ten. The curve fitting model in form of the 8.th order polinom is given below:

$$F = -1.5e+004 * w^8 - 1e+003 * w^7 + 1.5e+004 * w^6 + 1.4e+003 * w^5 - 5e+003 * w^4 - 7e+002 * w^3 + 7e+002 * w^2 + 2.6e+002 * w - 0.93 \quad (5)$$

where is: F – damping force, w – relative velocity
The curve fitting with linear model is appropriate basis to comparative analysis:

$$F = 1.6e+002 * w + 25 \quad (6)$$

The dynamical form of shock absorber damping characteristic is presented in Fig. 7, and correspondig simulation results in Fig. 8, 9, 10, 11.

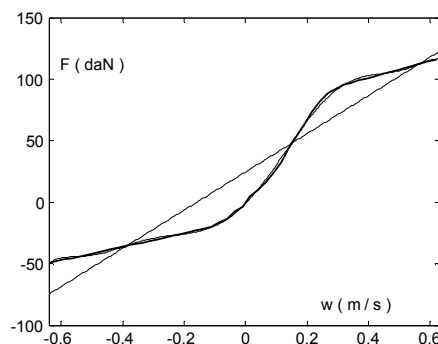


Fig. 6. Damping characteristics of shock absorber derived from inverse vehicle dynamical model.

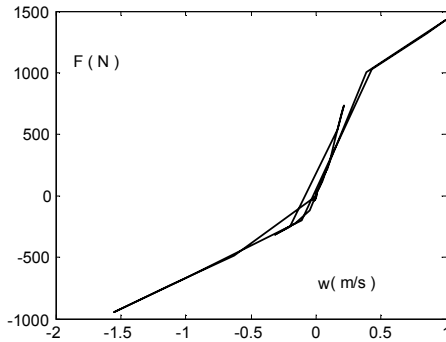


Fig. 7 . Dynamical characteristic of shock absorber derived from inverse vehicle model .

Hysteresis loop of ratio force / velocity, in Fig . 7 is formed by steep exciting from road , height 3 cm .

The curves in Fig . 8 and 9 , shown vertical displacement of spring mass , vehicle body , for linear and nonlinear shock absorber characteristics , respectively . Corresponding curves of vertical acceleration are presented in Fig . 10 and 11 .

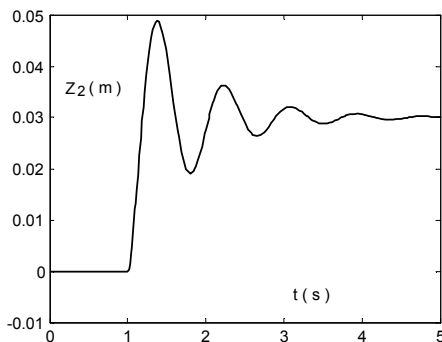


Fig 8 . Displacement of vehicle body - linear damping.

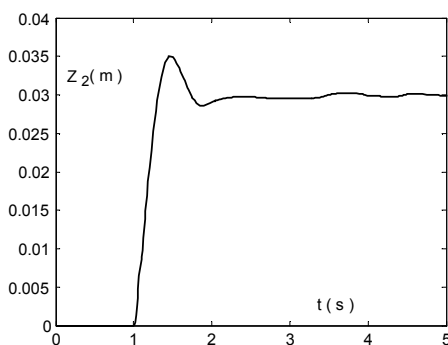


Fig .9 Displacement of vehicle body - nonlinear damping.

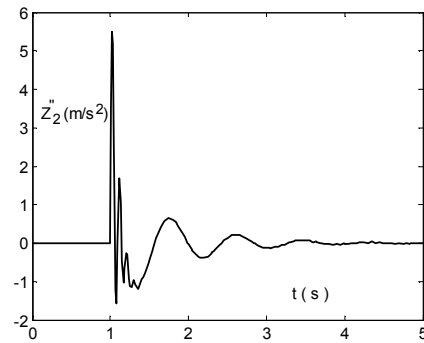


Fig 10. Vehicle body acceleration - linear damping .

The value of standard deviation of vehicle body acceleration is for linear damping 0.7819 m/s^2 , for nonlinear damping 0.6139 m/s^2 .

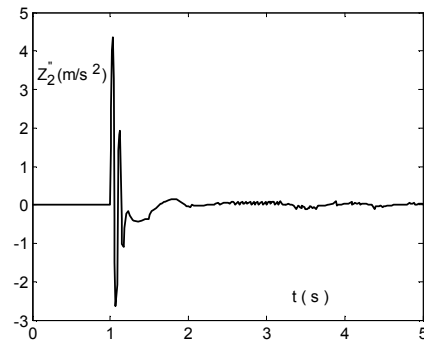


Fig. 11 . Vehicle body acceleration - nonlinear damping .

4. CONCLUSIONS

Simulation procedure with inverse vehicle dynamical model may be used to selection corresponding shock absorber damping characteristics with respect to vehicle comfort , road holding and other conflicting requirements .

REFERENCES

- [1] Thompson A. G., Pearce C. E.: An optimal suspension for an automobil on a random road, *SAE paper 790478*.
- [2] D. Karnopp , “ Active damping in road vehicle suspension system “ , *Vehicle System Dynamics* 12 1993 .

TO DO UP AND GAIN

Dr Tomislav Simović¹

Resume:

The objective of this paper is to point out the possibility of making use of old cars for the production of necessary types by employing limited means and a little more good will to tidy up the environment and employ the car production industry.

The key words are car, secondary raw materials, production, ecology....

1. INTRODUCTION

In the circumstances of a very low economic activity and evident poverty of population it is worth while to stop for a moment and look how far we can go this way, how to discontinue the negative trends and move forward. Our new state is in want, among other things, of natural raw materials, especially iron ore. It means that there is deficiency of home produced materials for the production in heavy and all other machine-building industries. This definitely is to be attributed to the objective circumstances, while to subjective factors our thriftless attitude toward secondary raw materials, i.e. scrap iron is to be attributed.

However, the rich world does not act in this way. Quite the contrary, the world insists on the maximum utilization of recycled materials for, among others, the following reasons:

- preservation of natural resources,
- energy saving,
- environment protection,
- reduction of expenses,
- relief of landfills, etc.

If it is a known fact that the price of steel and iron making from secondary raw materials is by 20 to 30 % lower, then it is not surprising that a country such as Germany makes 44 % of its steel from secondary raw materials. This means that iron scrap is a very much in demand in foreign markets and that it is possible to export all the available quantities – of course, in the absence of the idea to use it somehow on the “home ground”.

The experience the author has acquired in the fields of car-building, energy production and consumption and environment protection entitles him to point out once again before the public the unemployed potentials that offer the opportunity to “kill several birds with one

stone”. The question at issue is a project that should come out as a part of a campaign that is to cover all the possible “nationwide actions for the modernization of the entire economic environment”. Such a project connects directly the needs of our railway transport for freight cars and the opportunity to satisfy such needs using the cars that have been lying idle on our rails for several years.

According to the acquired information, the structure of the 16.000 available freight cars is the following:

- | | |
|------------------|---------|
| - container cars | > 6.000 |
| - open cars | > 7.000 |
| - platform cars | > 900 |
| - special cars | > 1.000 |

Life expectancy for freight cars is 20 years and out of the above indicated number, as much as 52 % is older than that. Approximately 16 % of freight cars in use are older than 30 years. For all these reasons, the railway company ZTP “Beograd” does not use more than 6.000 of freight cars.

Serbia has substantial producing capacities that used to manufacture and export large quantities of cars. Just to remind of some of the freight car manufacturers:

- Car Factory Kraljevo,
- MIN, Nis,
- GOSA, S. Palanka,
- Bratstvo, Subotica,
- ZELVOZ, Smederevo.

The mentioned factories with about 3.000 employees and a capacity to produce between 1.000 and 2.500 cars a year are excessive capacities for our railway transport system. The quantity of cars manufactured in the course of the last ten years has been insignificant, which means that the said factories have been idling all this time being in a position that has only been worsening.

¹ Dr Tomislav Simović, General Manager of MONTINVEST a.d. Belgrade, e-mail: tomislav@montinvest.co.yu

The lack of financial resources and extensive economic difficulties during the former period prevented our railway transport system to satisfy its constant need for 2.000 new and appropriate freight cars.

Taking into consideration the structural discord (excess in number and shortage in function of the available cars), capacities of our car-building industry and needs of our railway transport system, this paper insists upon the realization of a project under the name – OLD FOR NEW. The idea of the proposed project proceeds from the opportunity to assemble one new (needed) car out of several old (unnecessary) without any importation (or very little) whatsoever.

2. PRESENT SITUATION

It has already been said that ZTP “Beograd” possesses 16.000 freight cars approximately, of which 6.000 is unusable. If, for instance, average car weight is 20 tons and its average length 20 m, than we have 120 km of rails (6.000 x 20 m) “seized” by 120.000 tons (6.000 x 20 tons) of scrap iron which our steel works, as a rule, import. Long trains of these cars represent a big disgrace. As already has been said, ZTP “Beograd” is in a continuous need for at least 2.000 freight cars of adequate types, all they together weighting 40.000 tons (2.000 x 20 t) approximately.

3. OBJECTIVE OF THE PROJECT

The objective of the proposed project is:

- securing of the required number of specific types of freight cars,
- employment of our car-building industry and recovery of the employees “manufacturing training”, collecting of scrap iron,
- environment improvement.

4. IMPORTANCE OF THE PROJECT

The importance of the proposed project is manifest through the following:

- increase of number of usable cars,
- employment of our car-building industry in the course of a longer period,
- reduction of iron scrap import,
- freeing of our “seized” rails,
- economic, sociological, ecological, aesthetic effects, etc.

In addition to the rail transport, this project would engage the enterprises such as are:

- car-building industry,
- steel works,
- foundries,
- forge shop,
- paint manufacturers.

5. PROJECT REALIZATION METHOD

In order to successfully accomplish this project, the following needs to be done:

- create a team of experts in different disciplines to manage this project,
- ZTP “Beograd” is to make a list of unnecessary cars (by their type and number) in its possession,
- ZTP “Beograd” is to make a list of necessary cars (by their type and number),
- based on the above data, our freight car manufacturers are to prepare detailed designs for all the needed cars (for the majority of them such designs have already been drawn up),
- commercial banks are to assess the projects and provide minimum financial means, etc.

From the technical point of view, it is practicable to use a large number of members, elements and parts of the existing cars for the incorporation in new cars to be built and to hand over the excessive material to steel works as iron scrap for reprocessing.

A part of the so-called financial construction is based upon the assumption that about 2.000 cars is to be assembled, and for this is needed 40.000 tons of material approximately. It means that out of the 6.000 of the existing cars, 80.000 tons of material will remain and it should be used as iron scrap, which itself is the material in short supply in our country. This, plus little additional means should be used as salaries for the workers engaged in the production of said cars.

6. INSTEAD OF CONCLUSION

In this paper has been in a very simple way explained the idea of production of necessary freight cars with simultaneous removal of those unnecessary from the rails and employment of the free capacities of our car building industry.

The principal places for the realization of this serious yet inexpensive project are ZTP “Beograd” (they will free themselves from waste material, clean rails, get necessary cars), US STEEL SERBIA (they will get the necessary iron scrap and prove the message that they help Serbia), our car building industry (they will employ workers, solve social problems and get back to life), banks (they, finally, will invest in production), citizens (they will have better environment).... The Government, especially its Ministry for Capital Investments, is to inspire all the mentioned subjects.

QUASI-CALIBRATED BRIDGE MEASUREMENT ERRORS

Zlatan Šoškić¹

Abstract

The paper presents estimation of measurement errors made in course of measuring strain and stress by application of modification of standard Wheatstone bridge methodology that is used in Railway Vehicles Center of Faculty of Mechanical Engineering at Kraljevo and Wagon Factory Kraljevo. It is shown that strain measurement error is to be expressed through constant absolute error for small strains and constant relative error for large strains, and those errors together with limiting value separating small and high strains are calculated.

Keywords: Stress measurement, calibration.

1. INTRODUCTION

Strain measurements are standard part of each mechanical engineering measurement methodology and therefore they are well-studied and analyzed in literature [1,2]. Nevertheless, there are numerous modifications of standard methodologies used in practice, and each of them requires its analysis in order to estimate measurement errors, its advantages and drawbacks.

This paper presents methodology applied in Railway Vehicles Center of Faculty of Mechanical Engineering at Kraljevo and Wagon Factory Kraljevo, based on strain gauge methodology and calibration of part of measurement chain by application of high-precision resistor. This method eliminates several electrical sources of measurement errors (error due to finite input impedance of voltage measurement equipment and error due to supply leads), reduces other electrical sources of error (strain gauge non-linearity, errors caused by signal filtering and amplification) and leaves only errors arising due to variations in manufacturing process.

2. MEASUREMENT ERRORS IN STANDARD "QUARTER BRIDGE" METHODOLOGY

Standard strain gauges methodology comprises application of resistors arranged to form Wheatstone bridge. The bridge has power supply (excitation voltage, denoted by V) in one diagonal of the bridge, and output voltage (signal voltage, denoted by v) is measured in the opposite diagonal of the bridge. When the resistors' resistances R_a , R_b , R_c and R_d satisfy condition

$R_a R_c = R_b R_d$ (referred to as *bridge balance equation*), the output voltage v equals zero. If one resistor (for example R_a) is strain gauge sealed to object which strain is to be measured, then its resistance is changed due to deformation of the gauge according to the following equation:

$$\frac{R^*}{R} = k\varepsilon \quad (1)$$

where R^* represents change of the strain gauge resistance R due to the stress ε , and k is strain gauge factor.

There are essentially two ways for measurement of R^* :

- bridge balancing, comprising change of R_b or R_d so as to satisfy bridge balance equation; this is highly-precise method suitable for some laboratory measurements but completely inadequate for high-speed measurements, and
- bridge output voltage measurement, based on the fact that output voltage of the bridge is:

$$v = V \frac{R_a R_c - R_b R_d}{(R_a + R_c)(R_b + R_d)} \quad (2)$$

The standard "quarter bridge" technique consists in application of strain gauges as bridge resistors of the bridge, where one of them (called "*active*" gauge) is sealed to object which strain is to be measured and the others (called "*blind*" gauges) are sealed to the piece of the same material as investigated object and exposed to the same temperature. The aim of such arrangement is to cancel out the effect of temperature on measurement

¹ Zlatan Šoškić, docent, Faculty of Mechanical Engineering Kraljevo, Dositejeva 19, 36000 Kraljevo, Serbia and Montenegro, soskic.z@maskv.edu.yu

object strain, being that temperature causes the same changes to each of R_a , R_b , R_c and R_d . For the case of "quarter bridge" arrangement, equation (2) is approximately reduced to:

$$v \approx \frac{V R^*}{4 R} = \frac{k \varepsilon}{4} V \propto \varepsilon. \quad (3)$$

The obtained linear dependence and temperature independence of equation (3) are the basis for the wide practical application of the strain gauges as strain transducers. Let's now review the errors that are included in application of the equation (3).

2.1. Electrical sources of error

Electrical sources of error are caused by approximations taken into account while calculating output voltage.

2.1.1. Bridge non-linearity

As it has been previously mentioned, equation (3), that is widely used in practice, is merely linearized approximation of equation (2) for the case when Wheatstone bridge is made from strain gauges. The complete expression can be rewritten to have the form:

$$v = \frac{V R^*}{4 R} \frac{1}{\left(1 + \frac{R^*}{2R}\right)} = \frac{V R^*}{4 R} \cdot f_{NL} \quad (4)$$

leading to conclusion that relative error due to bridge non-linearity of expression (3) can be estimated to be:

$$\delta_{NL} \approx \frac{R^*}{2R} = \frac{k \varepsilon}{2}. \quad (5)$$

It is important to notice that non-linearity error depends on measured strain.

2.1.2. Lead supply resistance

The derivation of equation (2) assumes that voltage supply lines have zero resistance, or at least, resistance that could be neglected in comparison to bridge resistance. However, it is often case in practice that voltage supply lines are very long (tens of meters), causing voltage supply lines to have resistances of the order of magnitude of ohm. Being that strain gauge resistance have order of magnitude of hundred ohms, lead supply resistance influence should be calculated in such cases.

Inclusion of non-zero supply resistance (R_{LS}) shows [1] that output voltage for non-zero lead supply resistance (v_{LS}) can be expressed as:

$$v_{LS} = \frac{V R^*}{4 R} \frac{1}{\left(1 + \frac{2R_{LS}}{R}\right)} = \frac{V R^*}{4 R} \cdot f_{LS} \quad (6)$$

leading to conclusion that relative error of expression (3) due to non-zero supply resistance can be estimated to be:

$$\delta_{LS} \approx \frac{2R_{LS}}{R}. \quad (7)$$

2.1.3. Input impedance of voltage measuring device

Besides to neglecting the lead supply voltage, derivation of equation (2) also neglects the influence of input impedance of device that is to measure bridge output voltage. If R_{VM} is input impedance of measurement instrument bridge, output voltage that accounts for finite

impedance of voltage measurement instrument (v_{VM}) can be calculated to be:

$$v_{VM} = \frac{V R^*}{4 R} \frac{1}{\left(1 + \frac{R}{R_{VM}}\right)} = \frac{V R^*}{4 R} \cdot f_{VM} \quad (8)$$

whereas relative error of expression (3) due to finite impedance of can be estimated to be:

$$\delta_{VM} \approx \frac{R}{R_{VM}}. \quad (9)$$

2.1.4. Bridge asymmetry

The expression (3) is also derived under the assumption that unstressed strain gauges have the same resistances R . Due to various reasons in manufacturing process, strain gauge resistances are varying within limits of couple of percents. Therefore, output voltage of bridge is not equal to zero even when active strain gauge is not submitted to strain (bridge offset), and output voltage can be expressed as

$$v_{out} = v + v_0 \quad (10)$$

where v_0 can be estimated from equation (2) to be:

$$v_0 = \frac{\Delta R}{R} V. \quad (11)$$

2.1.5. Electrical induction

The most important sources of electrical induction are long supply and signal cables. However, by taking precautions measures using cables with grounded shield, electrical induction is eliminated as problem.

2.1.6. Voltage supply instability

As it may be seen from equations (2) and (4), output signal is proportional to voltage supply, and therefore all changes of voltage supply are reflected to measured signal, which can produce large errors. Several techniques are applied in order to prevent such errors, one of which will be described in text that follows.

2.2. Mounting sources of error

Mounting sources of error are caused by the fact that gauge stress is slightly different than stress that is being intended to be measured for reasons of creep, moisture effects, poor electrical insulation and misalignment.

2.2.1. Removable sources of mounting errors

Moisture and poor electrical insulation problems may be removed by careful mounting, and creep is easily detected by measurement of bridge offset. Strain gauge that exhibits creep should be replaced.

2.2.2. Misalignment

Effect of misalignment in "quarter bridge" configuration can be estimated on basis of formula

$$\varepsilon_\alpha = \varepsilon_x \cos^2 \alpha + \varepsilon_y \sin^2 \alpha + \beta_{xy} \sin \alpha \cos \alpha \quad (12)$$

where ε_α is the strain at some point along direction making angle α to arbitrary x axes, ε_x and ε_y are strains along directions x and y at the same point, and β_{xy} is shear stress at the point. If strain is caused by single stress, strain gauge should be placed in the direction of the stress. Due to misalignment, the strain gauge is put under the small angle α relative to direction of the stress. Therefore, the actual strain to which strain gauge is submitted is

$$\varepsilon^* = \varepsilon \left[1 - (1 + \mu)\alpha^2 \right] \quad (13)$$

instead of ε , therefore causing relative strain measurement error

$$\delta\varepsilon = (1 + \mu)\alpha^2. \quad (14)$$

3. STRAIN MEASUREMENT CHAIN

Railway Vehicles Center of Faculty of Mechanical Engineering uses data acquisition systems HBM UPM 100 for static strain measurements and HBM MGCPlus for dynamic stress measurements as signal voltage measuring devices. Both system consists of sequence of analog filter, amplifier and analog-to-digital converter that process measured signal and compare it to supply voltage. Instead of displaying measured signal voltage, those data acquisition systems have signal voltage-to-voltage supply ratio

$$y = v / V \quad (15)$$

(measured in mV/V) as output quantity. In this manner, voltage supply instability is removed as an electrical source of error.

Output quantity y of such measurement chain can be expressed in the following form:

$$y = f_{NL}(\varepsilon) f_{LS} f_{VM} f_F(\omega) f_A(\varepsilon) f_{AD} \cdot \frac{k}{4} \varepsilon^* + y_0 \quad (16)$$

where y_0 stands for offset of output quantity due to bridge offset voltage (that is not influenced by other error causes), f_F , f_A and f_{AD} stand for reduced transfer functions of filter, amplifier and digital-to-analog converter, and ω for signal frequency. It should be noted that amplifier introduces non-linearity error and filter introduces frequency dependence in measurement chain. Both acquisition systems display results in digital form and offer possibility of on-line linear scaling of result so that it can be transformed to the form

$$Y = y - y_0 = F(\varepsilon, \omega) \frac{k}{4} \cdot \varepsilon^* \quad (17)$$

before it is displayed or stored into computer's memory.

4. QUASI-CALIBRATION METHOD

Calibration methods are widely used in measurement practice, and they are particularly simple in case when transducer signal is proportional to measured quantity. The general calibration method consists in application of known input to measurement chain while simultaneously measuring output quantity. From the other side, when measuring stress, in majority of cases it is not possible to apply known stress to strain gauge transducer in order to determine output signal.

Nevertheless, there is still possibility to calibrate the part of the strain measurement chain by simulation of change of the gauge resistance; in that case, it is possible to calibrate all parts of measurement chain except strain gauge itself.

The easiest way to do this is to connect resistor of known resistance R_{cal} parallel to active strain gauge; therefore, resistance between strain gauge ends will be reduced for amount

$$R_{cal}^* = \frac{R^2}{R + R_{cal}} \Rightarrow \left(\frac{R_{cal}^*}{R} \right) = \frac{R}{R + R_{cal}}. \quad (18)$$

Now, rewriting equation (16) in the form

$$y = F(\varepsilon, \omega) \cdot \frac{k}{4} \varepsilon + Y_0 = F(\varepsilon, \omega) \cdot \frac{R^*}{R} + y_0 \quad (19)$$

it is possible by two measurements of output quantity y (one with calibration resistor attached, the other without calibration resistor) to determine factor F and constant y_0 to be:

$$y_0 = y(0) \quad F_{cal} = \frac{y_{cal} - y_0}{\left(\frac{R_{cal}^*}{R} \right)} = \frac{Y_{cal}}{\left(\frac{R_{cal}^*}{R} \right)}. \quad (20)$$

It is important to notice that F_{cal} is constant and hence not equal to $F(\varepsilon, \omega)$ being that

$$\frac{F_{cal}}{F(\varepsilon, \omega)} = \frac{f_{NL_{cal}}}{f_{NL}(\varepsilon)} \cdot \frac{f_{A_{cal}}}{f_A(\varepsilon)} \cdot \frac{f_{F_{cal}}}{f_F(\omega)}. \quad (21)$$

Still, adopting F_{cal} instead of $F(\varepsilon, \omega)$, errors due to lead supply resistance and input impedance of voltage measurement instrumentation are completely removed. Hence, quasi-calibration method enables us to calculate measured stress according to:

$$\varepsilon^* = \frac{4}{k} \frac{(R_{cal}^* / R)}{Y_{cal}} Y \quad (22)$$

where Y is instrument reading for measured signal voltage.

5. QUASI-CALIBRATION METHOD MEASUREMENT ERRORS CALCULATION

As usual, measurement errors are classified into systematic and random errors.

5.1 Systematic errors

Quasi-calibration method does not influence to mounting sources of error. Therefore, systematic error of quasi-calibration method may be expressed as

$$\delta\varepsilon_{sys} = \delta\varepsilon_{mis} + \delta\varepsilon_{NL} + \delta\varepsilon_a + \delta\varepsilon_f. \quad (23)$$

where $\delta\varepsilon_{mis}$ is given by equation (14), $\delta\varepsilon_{NL}$ is given by equation (5), while amplifier non-linearity error $\delta\varepsilon_a$ and filtering error $\delta\varepsilon_f$ are given by manufacturer's declaration. Bridge non-linearity can also be expressed in terms of measured voltage as

$$\delta_{NL} = \frac{k\varepsilon}{2} = 2(y - y_0). \quad (24)$$

5.2. Random measurement errors

For the sake of random error calculation, the previous expression for measured strain should be written in the form

$$\varepsilon^* = \frac{4}{k} \frac{R}{(y_{cal} - y_0)(R + R_{cal})} (y - y_0) \quad (25)$$

because these are quantities which measurement errors are known.

Manufacturing errors of strain and calibration resistor can be calculated on basis of manufacturer's declarations where relative errors δk , δR and δR_{cal} are indicated.

Voltage measurement errors are expressed in terms of instrument class of accuracy that determines absolute measurement error as function of measurement range used so that

$$\Delta y = c \cdot y_{\max} . \quad (26)$$

In most cases, $\Delta y \approx y_{\min}$, where y_{\min} is minimal voltage measurable in some measurement range. Relative measurement error δy , as it is always the case with measurement of electrical quantities, depends on measured quantity.

Summing all previously mentioned errors, strain measurement error can be expressed as

$$\delta \varepsilon_{\text{rnd}} = \delta k + \delta R + \delta R_{\text{cal}} + \frac{y_{\min}}{y_{\text{cal}} - y_0} + \frac{y_{\min}}{y - y_0} . \quad (27)$$

5.3 Total measurement error

Total measurement error can be estimated by summing systematic and random measurement errors. Calculated measurement error can be separated into two parts, one of them independent of measured strain and the other that varies depending on measured strain:

$$\delta \varepsilon = \delta \varepsilon_C + \frac{y_{\min}}{y - y_0} + 2(y - y_0) , \quad (28)$$

where constant part is

$$\delta \varepsilon_C = \delta \varepsilon_{\text{mis}} + \delta \varepsilon_a + \delta \varepsilon_f + \delta k + \delta R + \delta R_{\text{cal}} + \frac{y_{\min}}{y_{\text{cal}} - y_0} . \quad (29)$$

Absolute measurement error can then be calculated as:

$$\Delta \varepsilon = \frac{4 \cdot y_{\min}}{k} + \varepsilon \cdot \delta \varepsilon_C + \frac{k \varepsilon^2}{2} . \quad (30)$$

5.4. Error expression analysis

Measurement error presented by equations (28) and (30) has three different ranges separated by two limit

$$\varepsilon_1 = \frac{4 \cdot y_{\min}}{k \delta \varepsilon_C} \text{ and } \varepsilon_2 = \frac{2 \delta \varepsilon_C}{k} . \quad (31)$$

- 1) for strains considerably smaller than ε_1 absolute error is constant;
- 2) for strains considerably larger than ε_2 , but less than ε_1 , relative measurement error is constant;
- 3) for stresses considerably higher than ε_2 non-linearity error should dominate.

Being that $\delta \varepsilon_C$ is generally of the order of magnitude of a percent, non-linearity should be taken into account only when semiconductor strain gauges (having k of the order of magnitude of 100) are used.

Therefore, in vast majority of cases, only constant absolute error and constant relative error ranges are of interest.

6. WAGON SPRING STRESS MEASUREMENTS

As an example, here will be presented results from measurements of wagon spring stresses.

The measurements were performed using strain gauges HBM 10/120 LY11 with resistance $R = (120 \pm 0,35\%) \Omega$ and gauge factor $k = 2,04 \pm 1\%$, and HBM MGCPlus acquisition system with ML30 plug-in module consisting of amplifier with declared non-linearity 0,02%, filter and 16-bit digital to analog converter. Amplifier was set to measuring range from 0,01 mV/V to 3,06 mV/V. Butterworth filter with cut-off frequency

40 Hz was applied that has -1 dB attenuation at frequency 37.5 Hz and overshooting 7%.

While sealing strain gauges, it is estimated that misalignment can be estimated to be less than 0,5 mm from intended orientation, which based on strain gauge length of 18 mm leads to estimation of misalignment angle of 0,03 rad. After connecting the bridge, bridge offset of 2,14 mV/V was measured.

Two resistors were used for calibration purposes, with resistances $(59,88 \pm 0,02\%) \text{ k}\Omega$ and $(29,88 \pm 0,02\%) \text{ k}\Omega$. While connecting them to active strain gauge, signals of 2,65 mV/V and 3,17 mV/V were measured.

Measured voltages varied in amplitude range up to 1 mV/V and frequency range up to 20 Hz.

From the presented data, it can be calculated the following: $\delta \varepsilon_{\text{mis}} \leq 0,2\%$, $\delta \varepsilon_a \leq 0,02\%$, $\delta \varepsilon_f \leq 0,03\%$, $\delta k \leq 1\%$, $\delta R \leq 0,35\%$, $\delta R_{\text{cal}} \leq 0,02\%$, $y_{\min}/(y_{\text{cal}} - y_0) \leq 2\%$ for $R_{\text{cal}} = 59,88 \text{ k}\Omega$ and $y_{\min}/(y_{\text{cal}} - y_0) \leq 1\%$ for $R_{\text{cal}} = 29,88 \text{ k}\Omega$ leading to conclusion that $\delta \varepsilon_C \leq 3\%$ for 59,88 k Ω calibration resistance and 2% for 29,88 k Ω calibration resistance. The results suggests that resistor with smaller resistance is more appropriate be used for of calibration in presented example. In this case, calculations lead to result that limiting stress values are $\varepsilon_1 = 980 \mu\text{m/m}$ and $\varepsilon_2 \approx 20000 \mu\text{m/m}$.

Roughly, absolute measurement error in this example can be considered to be constant and equal to 20 $\mu\text{m/m}$ for strains less than 1000 $\mu\text{m/m}$, and for stresses larger than 1000 $\mu\text{m/m}$, relative error is constant and amounts 2%.

7. CONCLUSION

Summarizing previous analysis, it can be concluded that strain measurements using strain gauges cause both systematic and random errors which are of manufacturing and electrical origins. Because of this fact, strain measurement errors has two different natures that cause that absolute measurement error is constant for small strains and proportional to strain for large strains.

Therefore, strain measurement errors should be expressed by specifying absolute error for small strains and relative error for large strains together with limiting value separating small from large strains.

It can be also concluded that key factor for improving measurements of small strains is improvement of voltage measurement equipment, while measurements of large strains can be improved by application of low-tolerance strain gauges.

ACKNOWLEDGEMENT

The paper presents results which are derivative of investigations on project "Improvements of railway vehicles suspension systems" supported by Ministry of Science and Environment Protection of Republic of Serbia.

LITERATURE

- [1] J. Vaughan, "Strain measurements", Brüel and Kjær, 1975.
- [2] E. Doebelin, "Measurement Systems", McGraw-Hill, 1990.

PROBLEMS AT EXPLOATATION OF DDAM AND FBD WAGONS, AND SUGGESTIONS FOR THEIR RESOLUTIONS¹

Dragan Petrović², Ranko Rakanović, Zlatan Šoškić, Nebojša Bogojević

Abstract

In course of exploitation of freight wagons of railways in the last years, a large number of breaks of suspension system elements have been noticed. This feature is especially reported at four-axled wagon for coal-transport (sign Fbd) and three-axled wagon for transport of cars (sign Ddam). Frequent breaks of suspension system elements decreases efficiency of transport and in some cases causes derailment of wagons and leads to large economic losses.

In this paper, the causes of breakage of suspension at both of wagons have been analyzed, but also the possibilities how to resolve those problems, apropos how to reduce them on the lowest.

Key words: suspension system, experimental analysis, wagons

1. INTRODUCTION

For coal-transport in TE "Nikola Tesla" in Obrenovac, the four-axled wagon (that consists of twin two-axled wagon) is used (type Fbd. Fig. 1.).



Fig. 1.

Wagon for coal-transport with the sign "Fbd" is specialized for the technology of loading and unloading in environment (coalpit-thermoelectric plant). Because of those reasons, the resolution of constructions with specifications in the body, supporting framework and

mechanism for unloading had been resulted. In the floor of wagon, the door with hydropneumatic propulsion is embed. This mechanism provides automatical unloading and closedown after that.

Because of those features and constructions of suspension that is based on laminated spring, declined from standard construction. Remission of the spring length, in regard of standard resolution, has caused stress amplification. Additionally, the operation's loads are more frequent, in compare of exploitation in the Serbian Railway.

Lacks in named system can be noticed at breaking of suspension member and appearance of fracture at supporting framework. The frequent breakages of the main laminated spring minced efficiency of regular coal-transport. The thermoelectric plant "Nikola Tesla" in Obrenovac, has reported an average breakage of suspension of 2,8 at one Fbd wagon yearly (In exploitation are about 400 wagons).

The other problem belongs on car-wagon. For reclamation safety of transport, the existent open wagon (Laaekks) in covered three-axled wagon (Ddam wagon) had been reconstructed (Fig 2.).

Reconstruction consists of adding funicular railing and also the roof on the existent wagon. Moreover, existent

¹ This paper was based on the project "Improvement of suspension systems of freight wagons" N° 006313 financed by the Ministry of Science and Environment Protection

² Dr Dragan Petrović, Docent, Faculty of mechanical engineering Kraljevo, e-mail: petrovic.d@maskv.edu.yu
Dr Ranko Rakanović, Full Prof, Faculty of mechanical engineering Kraljevo, e-mail: rakanovic.r@maskv.edu.yu
Dr Zlatan Šoškić, Docent, Faculty of mechanical engineering Kraljevo, e-mail: soskic.z@maskv.edu.yu
Nebojša Bogojević, Assistant, Faculty of mechanical engineering Kraljevo, e-mail: bogojevic.n@maskv.edu.yu

springs have been reconstructed, but their high has been reduced for 25mm. Because of appearance of breakages, according the fatigue, the main laminas of all springs have been exchanged by news. Owing to reclamation of more efficiency loading and unloading, the reconstruction of floor on the over platform, and also under platform, have been made.

It's very important to mention that the specification of Ddam wagon exerts in elastically connection of the two rigid bodies, above spring of the second wheelset in a middle of car.

Just like in the first case, here, in exploitation, the appearance of spring breakage was noticed. It is noticed primarily on the second axle.



Fig. 2.

2. ANALYSIS OF CAUSES AT BREAKAGES OF SPRINGS

Having released the Fbd wagon from traffic, but also by studying the causes, the following references have been noticed (Tab 1).

Tab. 1.

Breakages	Numbers of appearances	%
Springs	400	67,3
Shackles	125	21,4
Suspension bracket	35	5,9
Locating pin	30	5,4
Σ	590	100

Tab. 2.

Axle	Numbers of appearances
I	148
II	144
III	142
VI	160

The most frequent breakage is related with breakage of the main spring laminas (Fig. 3). In ~70% of cases, laminas being broken in the middle wich is closer to spring buckle, but in ~30% cases the appearance can be noticed on the other half of the spring.

Observed rep axels (Tab. 2), we can conclude that the breakages of elements of the spring of Fbd wagons are equable per axled.



Fig. 3.

Upon primary analyses, large researching of the quality of railway tracks, operation loads, statically and dynamically features of springs and quality of embedded springs had been done. The final results of those researching can be found in literature [2, 3], and here are the conclusions:

- On the railway track, the actable parts in horizontal and vertical course have been observed. The mentioned can qualify the appearance of impact load.
- Unequally load assignment on the wheel had been registered, and that appearance has influence on statically and dynamically strength, but also on the age duration of suspension elements.
- Researching on the fatigue of spring from different producers (Fig. 4.) has shown that the springs haven't had regular durability...
- Based on practiced researching, we do not conclude that, instead of over remarks, nor isn't even quality of spring production safe.

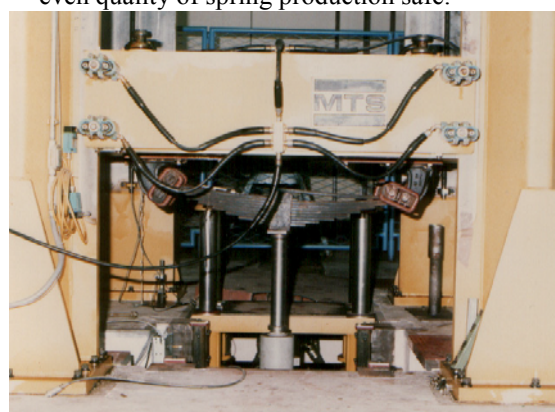


Fig. 4.

Considering wagon exploitation for car-transport (Ddam), community of Serbian railway has registered popping of average one spring per wagon yearly. Nevertheless, average defeasance of wagons from traffic because of exchange of suspension, lasts one month. In a aim to minify breakage of suspension elements, the weight of loaded cars had been relived from 200 kN to

180kN. Meanwhile, nor even that has caused reduction of spring breakages, so it was decided that all Ddam wagons(about 100) canceled from traffic, but also that all necessary researching be accomplished in the aim of rejection named lacks.

Mechanical Faculty of Kraljevo has made researching of load assignment per wheel and axle and researching of torsion stiffness. Based on results that have been given in Tab. 3. , we notice that the torsion stiffness is major than usual. Based on analysis of torsion stiffness of Ddam (tab.3) wagon, we concluded that in ultra causes, the slip of other (middle) wheelset can also be noticed.

Tab. 3.

	C_{tA} [kN/‰]		
	I axle	II axle	III axle
Limit	3,87	2,17	3,87
Experiment	2,43	3,50	2,34

Moreover, worth of stress amplitude and displacement proceeds allowable worth. On diagram that shows amplitude changes of spring stress (Fig. 5), we can notice the frequent appearance of stiff impact of spring buckle at motion limiter (straight places on piques). This appearance can cause the remission of durable dynamical spring strength that is the remission of duration age of spring.

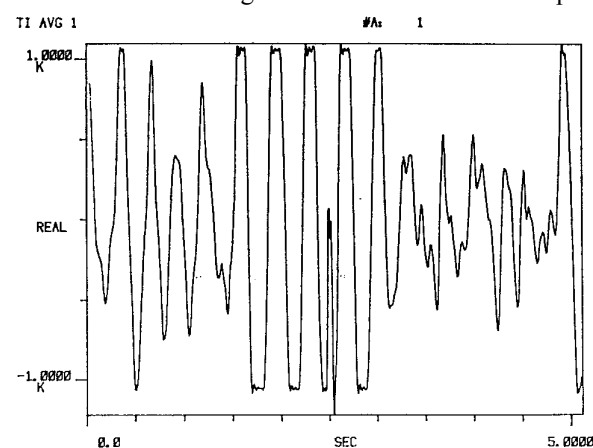


Fig. 5.

3. NATIONAL SOLUTIONS FOR REMISSION OF SPRING BREAKAGES

3.1 Wagon for transport coal Fbd

For resolution the problem of frequent spring breakages, the main base was experimental and service identification of all the parameters that affect on spring fatigue. The named effects, above all expanded loads and stresses, but also unsafe quality of spring products, are the main reasons of appearance of breakages.

Based on attained experimental and service information, the suspension reclamations are projected, with the main aim –to disburden the spring.

A lot of ideas for remission of spring breakages of wagons have been deemed. About Fbd wagons, one of the solutions is incorporation of parabolic springs, but in two variant:

- Gap between spring ear is 1100 mm and
- Gap between spring ears 1200 mm.

The first variant is built in Fbd wagon, but because of reduced gap and bad production in our fabrics, the named variant didn't provide expected results. The second variant in exploitation has shown excellent results, that is, in perennial usage, there were no suspension breakages of wagons. Anyway, this variant dictate important investments in reconstruction of the under wagon platform, but also investments in reconstruction of completely suspension, which is economically impracticable.

Having respected adequate perseverance in existent spring, the resolution with Ferro-rubber elastic element has been projected (Fig. 6).

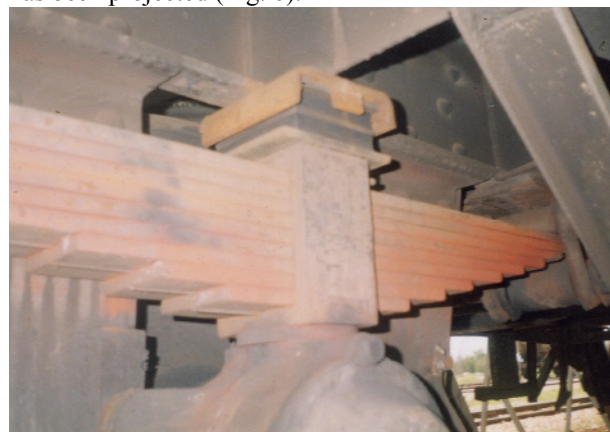


Fig. 6.

Instead of existent metal limiter the elastic element would be laid. This element should have features of stiffness and rigidity, because it has to accept a part of load and disburden present spring. Additionally, dimension of elastic elements have to be projected on that way, that in case of empty wagon, elastic element doesn't touch spring buckle by it's under reef. The elastic element is used only in case when the wagon is laden. Exceptions are springs, whose spring arrow loses projected high, owing to fatigue, that is owing to long exploitation and irregular repair. In that case (and also when the wagon is empty), the elastic element and spring buckle rub each other. That kind of wagon should disable from usage in traffic, but also make spring repair. Projected resolution of Fbd wagon's suspension request the production of probationary samples of elastic elements and accompaniment of presence in exploitation conditions.

Alongside with process of elastic element for spring protection from overload, researching of main spring laminate is observed by welding. As it was mentioned, frequent breakages of the main spring's laminate, their price, and complicated supply, mince efficiency of regular coal transport. All this can qualify research of repair possibilities of springs by welding of main

spring laminate and comparative researching of welded and unwelded springs in laboratory or in exploitation conditions.

Comparative research has been made on: anwelding spring, welded spring which is repaired in fabric "Zelvoz" and on welded spring which is repaired in "Gibnjara" Kraljevo. Program of researching was based on rule UIC, and comprises following activities: researching of geometric accurate, identification of static stiffness, researching for rating of durability (dynamical researching on fatigue) and analyses of results.

Dynamical researching have been made with amplitude ± 15 mm and frequency of 2 Hz. Based on made researching, we can conclude that spring breakage hasn't been emanated in a place of welded splice, that is in a sector of caloric influence (Fig. 7). Expected spring durability of Fbd wagon on fatigue in laboratory researching hasn't been attained, because of unsafe quality embedded material. Unsafe quality of material had been affirmed in earlier researching. It is caused by presence of chemical filths in material



Fig. 7.

3.1 Wagon for car transport DDam

At wagons for DDam-car transport, the way for elastic elements incorporation in suspension hasn't been found. It is because of spring's high arrow remission. Anyway, suspension of DDam wagons gives possibility of exchange of existent springs with parabolic springs. Static feature of parabolic spring can be noticed on Fig.8.

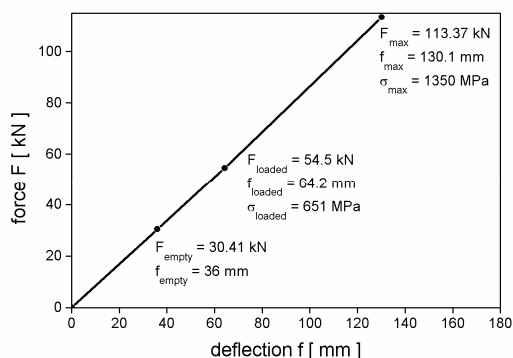


Fig. 8.

The feature of spring has been chosen on that way, to submit all loads that wagon for car-transport has in exploitation. Moreover, those springs have better feature of stiffness, and that feature can influence on more favorable quality and safety of wagon's move.

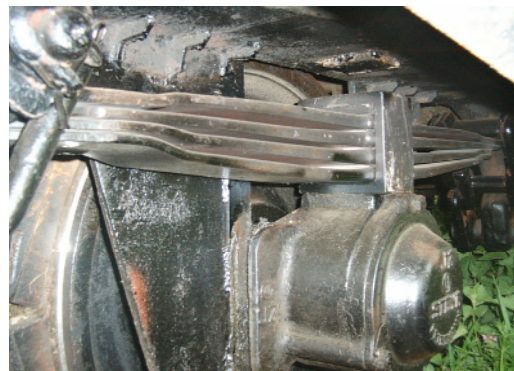


Fig. 9.

4. CONCLUSION

From previously, we conclude:

- Made abstract-experimental research of wagons for coal-transport, with and without projected reclamations, are valuable base for following comparative research in exploitation environment.
- Methodology of welding doesn't have influence on exploitation spring ability, so in Fbd wagons, which transport coal, repatriated springs, which main laminate welded reliance on regular technology, can be embedded.
- Parabolic springs, built in wagon for DDam car-transport, have static feature that can accept exploitation loads. In that case torsional stiffness of wagons is better than preliminary solution.

5. LITERATURE

- [1] Elaborat 4/95, Ispitivanje uvojne krutosti, mirnoce hoda, stabilnosti kretanja i dinamicke cvrstoce elemenata sistema ogibljenja DDam vagona, Masinski fakultet Kraljevo 1995. god.
- [2] Elaborat 67/83, Identifikacija uzroka lomova glavnih listova gibnjeva na Fbd vagonu, Fabrika vagona Kraljevo, Opitni centar 1983.
- [3] Elaborat 1/93 Komparativno ispitivanje zavarenih i nezavarenih gibnjeva, Masinski fakultet Kraljevo 1993.

TORQUE RIGIDITY FOR TRIPL-AXEL WAGONS¹

Nebojša Bogojević², Zlatan Šoškić, Dragan Petrović, Ranko Rakanović

Abstract

Concept for examinations of torque rigidity based on ERRI and UIC regulations applied on triple-axel wagons is described in this paper. Analysis of parameters that has influence on torque rigidity is done and it is given proposition for calculation of torque rigidity for triple-axel wagons. This methodology results are compared with experimental results of DDam wagon examination.

Key words: Torque rigidity, derailment safety, wagons

INTRODUCTION

Torque rigidity test is part of investigations of derailment safety on new or reconstructed wagons. Testing methodology is prescribed by UIC and ERRI regulations [1].

The methodology comprises two kinds of tests:

- Static tests
- Pushing through S-shaped curves

Regulations requests that at least one kind of tests should be applied to wagon for issuing or extension of approval.

Statically tests of torque rigidity consist of experimental determination of torque rigidity C_{tA} of wagon, that is to be compared to its limiting value C_{tA}^{lim} , which in turn are calculated according ERRI recommendations in dependence on geometric characteristics of vehicle and wheel loads.

Wagon derailment at crossing over the distortion of the track (Fig.1) depends from simultaneous appearance of guiding horizontal force and reduction of vertical load on guiding wheel.

In rail/wheel system basic parameters that have influence on wagon derailment are:

- curves
- distortion of the track,
- declination.

On wagon derailment safety at crossing over the distortion of the track main influences are:

- guiding force,
- deviation of wheel load specified for vehicle,
- Variations of wheel load because of distortion of the track and cant track.

Statically method of torque rigidity is established on crossing of wagon over the distortion of the track.

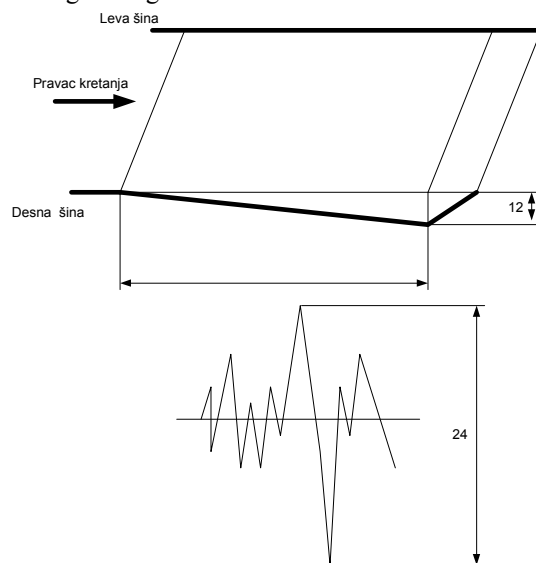


Fig 1. Distortion of the track

¹ This paper was based on the project "Improvement of suspension systems of freight wagons" N°006313 financed by the Ministry of Science and Environment Protection

² Nebojša Bogojević, Assistant, Faculty of mechanical engineering Kraljevo ,e-mail: bogojevic.n@maskv.edu.yu
Dr Zlatan Šoškić, Docent, Faculty of mechanical engineering Kraljevo ,e-mail: soskic.z@maskv.edu.yu
Dr Dragan Petrović, Docent, Faculty of mechanical engineering Kraljevo ,e-mail: petrovic.d@maskv.edu.yu
Dr Ranko Rakanović, Full Prof, Faculty of mechanical engineering Kraljevo ,e-mail: rakanovic.r@maskv.edu.yu

THEORETICAL BASICS

Relation of guiding horizontal force Y with vertical force Q on guiding wheel $\left(\frac{Y}{Q}\right)$ represent basic criteria for estimation of possibility wagon derailment. Wagon derailment safety is provided if limited value is not exceeded:

$$\lim\left(\frac{Y}{Q}\right) < 1,2 \quad (1)$$

Based on major number of standard constructions railway vehicles examinations, a two-axel and bogie vehicle, methodology of wagon derailment is developed.

Railway Vehicle Center on Faculty of mechanical engineering at Kraljevo has been met the problem of examination three-axle Ddam wagon for transportation of automobiles.

DDam is three-axle, two-part, double-deck wagon for transport of automobiles. Its dead weight is 27 t, with carrying capacity of 20 t, designed for speeds up to 120 km/h in S and SS regime.

Model of Ddam wagon is presented on Fig. 2, 3 and 4. Units of wagon are linked between by joint connection which enables rotation over longitudinal body axes within angle of 2° , (Fig. 2) and free rotation over its transversal (Fig. 3) and vertical (Fig. 4) axes.

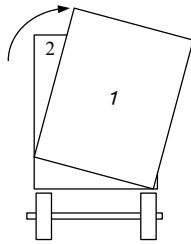


Fig. 2

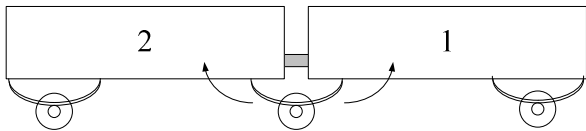


Fig. 3

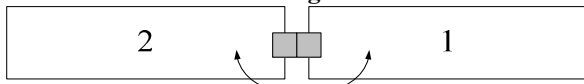


Fig. 4

Characteristic of Ddam wagon is that two units of wagon are connected with laminated spring (Fig. 4).

Basic ERRI recommendations for calculating torque rigidity of wagon are given for two-axel and bogie wagons.

Starting point in development of method for calculation of safety for triple-axle wagons should be torque rigidity for two-axle wagons. If we starting calculation with supposition that torque rigidity depends from variation of wheel load and cantdeficiency which causes that variation then we can write:

$$C_{tA} = \frac{\Delta Q}{g^*} \quad (2)$$

In calculation of wagon torque rigidity it's necessary to identify independent parts of wagon with approximately linear characteristic of rigidity and their influence on wagon torque rigidity. If there is more than one part of wagon which have approximately linear characteristic of rigidity then wagon torque rigidity can be calculated from:

$$\frac{1}{C_e} = \sum_{i=1}^n \frac{1}{C_i} \quad (3)$$

Considering that for different type of wagons there are different constructive solutions (different width of wagons, different distance between springs in suspension system, different wheel-based) to be compared, torque rigidity are wheel-based reduced.

Torque rigidity of two-axle wagon can be estimated:

$$\frac{1}{C_{tA}} = 10^3 \frac{(2b_A^2)}{C_i^*} + \frac{10^3}{2a^*} \frac{b_A^2}{b_z^2} \left(\sum_{i=1}^n \frac{1}{C_{z11}^+} \right) \quad (4)$$

If we analyze equation (4) we can come to conclusion that two-axle wagons have two entireties with approximately linear characteristic of torque rigidity:

1. Torque rigidity of body C_t ,
2. Rigidity of springs in suspension system C_z .

Body rigidity influence on whole torque rigidity of

wagon is taken into consideration as $10^3 \frac{(2b_A^2)}{C_i^*}$, while

influence of springs in suspension system is $\frac{10^3}{2a^*} \frac{b_A^2}{b_z^2} \left(\sum_{i=1}^n \frac{1}{C_{z11}^+} \right)$.

Based on analysis of construction and equation for torque rigidity of two-axle wagons we are trying to estimate torque rigidity of wagon for transport automobiles Ddam.

Body torque rigidity influence of one unit can be expressed as:

$$10^3 \frac{(2b_A^2)}{C_i^*} \quad (5)$$

Spring influence on torque rigidity is double. In one way spring on middle axle have separately influence on every unit of the wagon, and on the other way, because of joint connection, they are connecting influence. Influence of spring on torque rigidity of one unit wagon is:

$$\frac{10^3}{2a^*} \frac{b_A^2}{b_z^2} \left(\frac{2}{C_{z11}^+} + \frac{4}{C_{z22}^+} \right) \quad (6)$$

Where C_{z11} is spring rigidity on first axle, and C_{z22} is spring rigidity on first axle wagon.

When there is direct spring connection between two units of wagon then influence of elastic suspension on wagon torque rigidity we can express as:

$$\frac{10^3}{2a^*} \frac{b_A^2}{b_z^2} \left(\frac{2}{C_{z11}^+} \right) \quad (7)$$

Now wagon torque rigidity for triple-axel wagon we can express as:

$$\frac{1}{C_{tA}} = 10^3 \frac{(2b_A^2)}{C_{r1}^*} + \frac{10^3 b_A^2}{2a^* b_z^2} \left(\frac{2}{C_{z11}} + \frac{4}{C_{z22}} \right) + \frac{10^3 b_A^2}{2a^* b_z^2} \left(\frac{2}{C_{z22}} \right) + 10^3 \frac{(2b_A^2)}{C_{r2}^*} + \frac{10^3 b_A^2}{2a^* b_z^2} \left(\frac{2}{C_{z33}} + \frac{4}{C_{z22}} \right) \quad (8)$$

EXPERIMENT

For examination of DDam wagon, based on ERRI regulations, it is used methodology described in papers [1].

Based the examination of DDam wagon was performed a test of rising one wheel of wagon on the first axel while the variations of vertical loads on others wheels have been measured. Spring in suspension system has not been blocked during the examination. Wagon was raised on horizontal plane. One wheel on the wagon was raised and took down for appropriate limited derailment value.

During the measurement process is registries the raising height of guiding wheel and load variations of wheels on remaining axels. Acquired results are presented on the Fig 5 and 6.

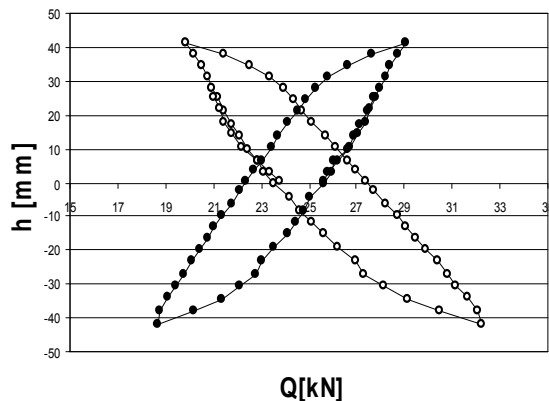


Fig. 5

-Wheel load on second axel while first axel is littered is present on Fig. 5.

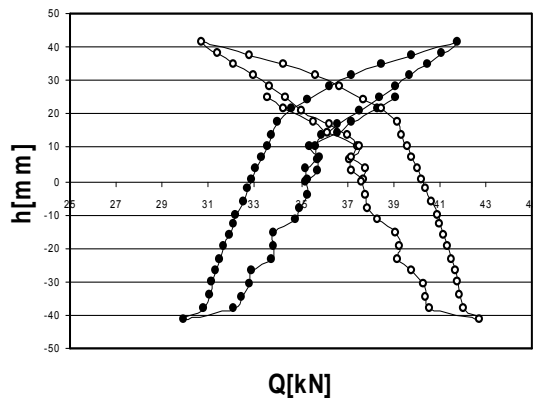


Fig. 6.

-Wheel load on third axel while first axel is littered is present on Fig. 6.

The lifting step adopted was 3 mm. Load forces were measured by dynamometers manufactured at Railway Vehicles Center, with measurement error $\Delta Q = 0,5$ kN, and vertical displacement was measured by inductive displacement transducer Hottinger with measurement error $\Delta h = 0,5$ mm.

ANALISYS

An ERRI recommendation for determination of torque rigidity of wagon is that horizontal forces produced from centrifugal acceleration and body center of gravity position are neglected. Variations of vertical load for guiding wheel, in this experiment are appropriate with buckling which is caused by dropping level of rails or cant deficiency. Since in this experiment work of spring is not blocked therefore diagrams 5 and 6 describes wagon torque rigidity.

From fig 5 we can see that diagram of torque rigidity for the first part of wagon is very similar torque rigidity for two-axel wagons. On the fig 6 diagram of torque rigidity has different form because whole torque rigidity now contains two-pieces of spring between two part of wagons.

Wagon torque rigidity can be determined from equation (2) while limit buckling of wagon and wheel based is calculated from:

$$g^* = \frac{15}{2a^*} + 2 \quad \left[\frac{\circ}{\circ\circ} \right] \quad (9)$$

If we determinate variation of guiding wheel value (ΔQ) from fig 6, for limit buckling g^* we can get wagon torque rigidity calculated towards the equation (2):

$$C_{tA} = \frac{\Delta Q}{g^*} = \frac{4.1}{3.76} = 1.091 \left[\frac{kN}{\frac{\circ}{\circ\circ}} \right] \quad (10)$$

Determination of torque rigidity (equation 8) demands previously determination of torque rigidity for bady of wagon in accordance with ERRI recomandations, based on the methodology that have been described in paper [6] end elaborats 4 and 6. From equation (8) we can get estimated value of wagon torque rigidity:

$$C_{tA} = 0,906 \left[\frac{kN}{\frac{\circ}{\circ\circ}} \right] \quad (11)$$

Experimentl results are different from estimated results for the value 10%.

By the examination methodology described in paper [1] triple-axel Ddam wagon has be examined as two two-axel wagons. Examination results of torque rigidity received from this methodology are shonw in this table:

Axle	C_{tA} [kN/‰]	C_{tA}^{lim} [kN/‰]
Front	2,1	3,8
Middle	1,8	2,2
Rear	2,0	3,8

Torque rigidity of Ddam wagon is determined with equation (8) is $C_{ta} = 1,1 [\text{kN}/\text{‰}]$, while torque rigidity of Ddam wagon acquired as two-axel wagon is $C_{ta} = 1,8 [\text{kN}/\text{‰}]$.

This way of torque rigidity calculation is intensifying the criteria of derailment safety for triple-axel wagons.

CONCLUSION

An ERRI and UIC regulation does not include calculation of torque rigidity for triple-axel wagons.

Calculation of torque rigidity for triple-axel wagons is shown in this paper, while acquired results are based on examination of one type of wagons. To accomplish the aim for receiving better results it is necessary to perform researches for similar types of wagons.

We can come to conclusion that in case of triple-axel wagons it is necessary to develop methodology for determination of torque rigidity. This method of calculation is suggested for triple-axel wagon for transport of automobiles Ddam that was subject of examination. There is a joint connection between two units. It is necessary to expand this examination on other types of triple-axel wagon with joint connections, compare acquired results and eventually try to obtain methodologies for determination torque rigidity for that type of wagons.

LITERATURE

[1] ERRI B12 / DT 135, "Allgemein verwendbare Berechnungsmethoden für die Entwicklung neuer Güterwagenbauarten oder neuer Güterwagenderhgestelle" European Rail Research Institute, Utrecht, 1995.

[2] ORE B 55, "Moyens propres á assurer la circulation normale sur des voies présentant des gauches", ORE de UIC, Utrecht, 1983.

[3] Ахмаджова Д. "Метод за определяне критерия на безопасност срещу дерайлиране при квазистатични условия" VIII НТК на ВВТУ "Т. Каблешков", София, 1995.

[4] R. Rakanović, A. Babić, D. Petrović i dr. Elaborat br. 4/95, "Ispitivanje uvojne krutosti, mirnoce hoda, stabilnosti kretanja i dinamicke cvrstoce elementa sistema ogibljenja Ddam kola", Mašinski Fakultet Kraljevo, Kraljevo, 1995.

[5] R. Rakanović, Z. Šoškić, D. Petrović, N. Bogojević i dr. Elaborat br. 11/5, "Ispitivanje rekonstruisanih/modernizovanih troosovinskih dvospratnih dvočlankastih kola za prevoz putničkih automobila tipa Ddam", Mašinski Fakultet Kraljevo, Kraljevo, 1995.

[6] Nebojša Bogojević, Zlatan Šoškić, Dragan Petrović, Ranko Rakanović "AN EXTENSION TO TORQUE RIGIDITY TEST METHODOLOGY" Proceedings of XIV International Conference "Transport 2004", Sofia 11-12.11.04

TECHNICAL AND ECONOMIC EFFECTS OF ELASTIC ELEMENT BUILT IN SUSPENSION SYSTEMS OF FREIGHT WAGONS¹

R.Rakanović², D.Petrović³, M.Pavličić⁴

Abstract

This paper presents the most important technical and economic effects of innovations on suspension systems of freight wagons. In exploitation of three and four axle freight wagons there is a breakage of suspension system elements especially at the wagons for automobile and coal transportation. This paper gives a technical solution which decreases the possibility of spring breakage at wagons and also removes stagnation in their exploitation, increases safety and transportation speed. There are important economic effects in exploitation and maintenance as well. By theoretic and experimental analysis and economic estimation of the technical solution it can be undoubtedly concluded that innovation at suspension systems of freight wagons is not only financially profitable but necessary as well so that lost permission for this kind of transport vehicles/units could be regained for international traffic.

Key words: suspension systems, exploitation, innovative solution, technical effects, economic effects.

1. INTRODUCTION

A significant attention has always been given to exploitation of traffic units, especially to railway transport vehicles. The attention was undoubtedly caused by exploitation safety and by its financial effects in product and service price on the other hand. In free goods, monetary and traffic communications there is a need for innovative [1] and technical solutions in exploitation of present traffic vehicles. By those solutions our economy would have certain chances for faster joining the European integration, and also for avoiding certain dangers of stagnation in the quality system and standard application which are the pride of European market and prerequisite for equal treatment of our economy system.

One of those innovative solutions is the subject of this paper analysis.

2. SETTING THE PROBLEM AND DEFINING THE TECHNICAL SOLUTION

Research subject of this project is evidention of serious problems in exploitation of freight three axle wagons for

automobile transportation (Ddam wagons) and four axle wagons for coal transportation (Fbd wagons). Both wagons in exploitation have serious problems when passing over skew track and during movement of wagons equipped with automatic clutch on which longitudinal pressure forces act. These two problems cause breaking of suspension system elements, disengagement of wagons so that springs should be replaced (or repaired) and significant economic danger during the repair.

The project has imposed the need for analysis of present solutions for suspension systems of wagons for automobile and coal transportation. The innovative solution had to be efficient, cheap and fast. It could have been defined in making more elastic relation between the springs and metal spring stop. Fig. 1 shows the technical solution that removes metal spring stop (whose height on Fbd wagon is 40mm), and distance between spring buckle and side wagon carrier is increased and its value now is 110m.:

¹ This paper was based on the project "Improvement of suspension systems of freight wagons" N° 006313 financed by the Ministry of Science and Environment Protection

² Dr Ranko Rakanović, full-time professor at the Faculty of Mechanical Engineering in Kraljevo

³ Dr Dragan Petrović, assistant professor at the Faculty of Mechanical Engineering in Kraljevo

⁴ Dr Milorad Pavličić, associate professor at the Faculty of Mechanical Engineering in Kraljevo

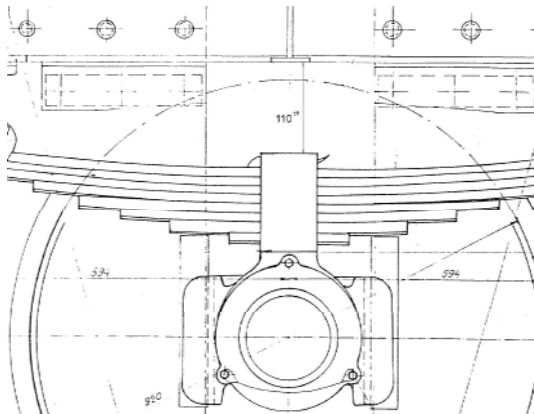


Fig. 1: Designed distance between spring buckle and side carrier (when metal stop is removed)

The stated technical modification in present suspension system enabled the "space" suitable for setting appropriate elastic element so there would be less problems in wagon exploitation while some of the mentioned problems would be totally escaped. The innovative improvement of suspension system is the elastic element made of metal and rubber which takes over part of wagon load and its cargo. Designed height of elastic rubber element is 77mm and height of elastic element holder is 8mm. Maximum clearance between elastic element and holder should be up to 4mm. Regarding appropriate tolerances designed suspension solution allows space between spring buckle and low edge of elastic element to be:

$$a_{\min} = 110 - 5 - (85 + 4) = 16$$

$$a_{\max} = 110 + 5 - (85 + 0) = 30$$

The solution is shown in fig.2:

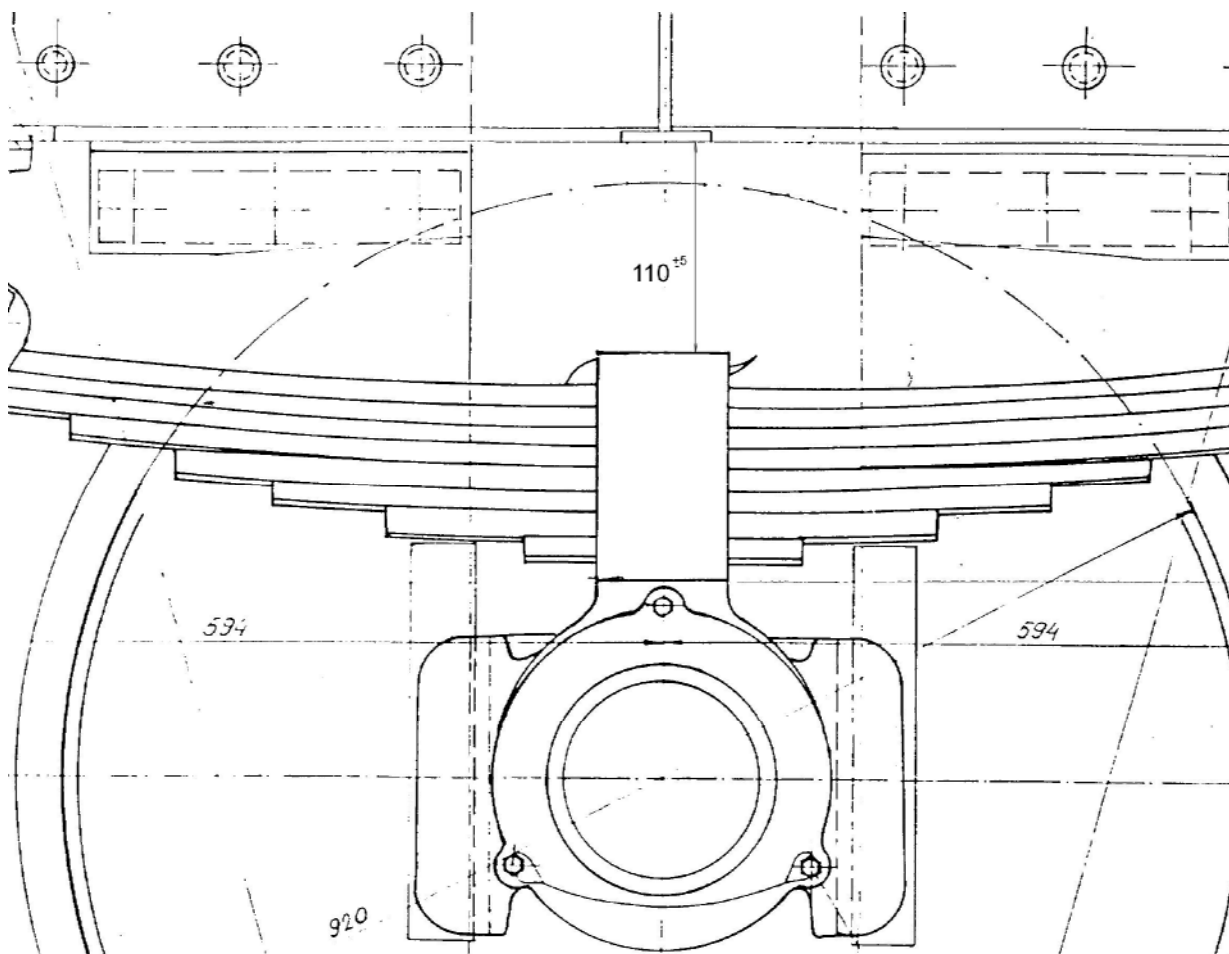


Fig.2 Geometric measures of suspension with elastic element built in

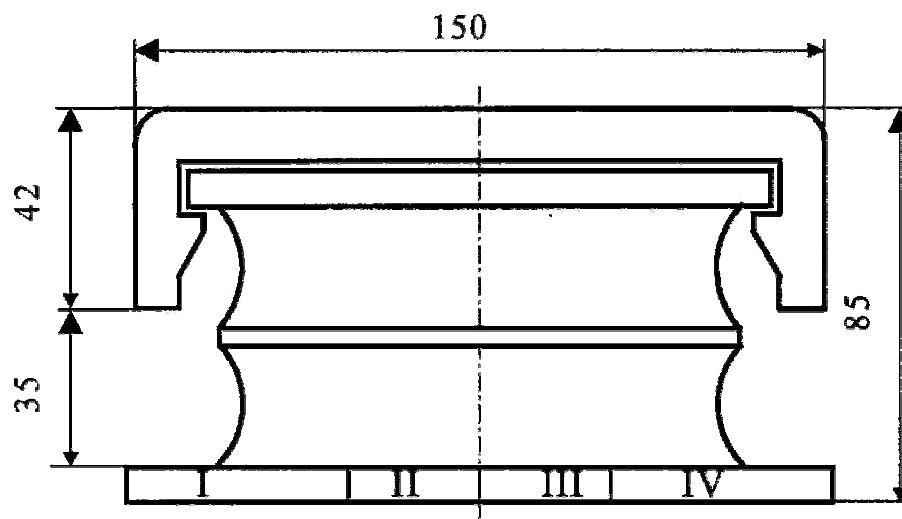


Fig. 3 Elastic element

The stated technical solution has its own technical, protective and economic effects in wagon exploitation.

In case of empty wagon this technical solution makes elastic element not touch spring buckle with its low edge. That makes the technical solution valid and final in normal exploitation conditions.

Technical protection measures of this innovation relate to the cases of wagon exploitation. For example, in case of spring arrow losing designed height, by fatigue, then it is possible for minimum distance between spring and low edge of elastic element to be less than $a_{\min}=16\text{mm}$ for 6-8mm. It is a sign for spring to be replaced.

In case of spring buckle touching low edge of elastic element and wagon being empty, the spring has lost arrow height (i.e. suspension power of spring is pretty decreased) or there are serious skews in construction of wagon sub-frame. In the latter case there can be significant increase of element load and torsional rigidity of wagon can be brought into danger. In this case spring also should be replaced (or repaired, or welded since there are acknowledged technical solutions by which spring vitality is recovered) and distance between spring buckle and low edge of elastic element should be inspected. If mentioned measurements as a result have already defined values there is no need for other technical improvements.

However, if after mentioned intervention elastic element still touches spring buckle that is a reliable sign that wagon is toationally braided and that its geometry must be brought to designed level. In a word, if elastic element of empty wagon touches spring buckle that wagon should be kept out of the traffic and technical overhaul should be carried out.

3. SOME ECONOMIC EFFECTS OF INTRODUCING GIVEN TECHNICAL SOLUTION

The aim of designed solution is decreasing is to keep the freight wagons from element breakage of suspension systems, to decrease the number of element breakages and especially to eliminate the possibility of wagon derailment. A wider technical and social importance of this innovation is to enable wide application in repair of present freight wagons which would significantly increase the regularity of their application as well as their duration and exploitation.

Economic effects of introducing this technical solution are numerous, too.

The mentioned innovation as an investment project needs economic efficiency. Designed solution, according to preliminary estimate, needs an investment of 100.000 euros. Building of elastic element in suspension systems, on average, costs 50 euros per suspension system, or 206.000 euros for all wagons in exploitation. Assembly and installation are relatively simple and fast. Thus, spring breakage and stagnation in wagon exploitation on the whole are eliminated.

For example, on the basis of exact data in exploitation of Fbd wagon for coach transportation, used by steam power station "Nikola Tesla" in Obrenovac, there are, on average 2,83 spring breakages per wagon in a year, and in exploitation of three axle Ddam wagons, used by Serbian and Montenegrin Railways, there is, on average, 1 spring breakage per wagon. In the former case, at 440 four axle wagons (eight suspension systems per wagon), there are 1.250 spring breakages a year, in the latter case at 100 wagons there are 100 spring breakages. Market

price of spring replacement is on the average 500 euros and for the mentioned consumers total cost is cca 675.000 euros.

Direct effects of stagnation are also important. For 100 wagons of Serbian and Montenegrin Railways that are removed from traffic for a month (because of the problems in suspension system) an average lost profit per wagon is 5.000 euros in a year, that is 500.000 euros totally.

In principle, if every investment decision can be observed from strategic and operative point of view the estimation point of this investment version [2] in relation to introducing new suspension system also gives important economic effects. Naimely, suspension system replacement at present freight wagons would be 1.000 euros per wagon, that is 4.1 million euros totally. Taking the price of suspension system replacement and project price into consideration the investment would be repaid in 6 years for Fbd wagons, that is in a year and a half for Ddam wagons, if transportation capacities are fully engaged.

The stated technical solution relates to installation of present elastic element in wagon suspension system. However, at present wagons with already broken springs there could be significant savings. Replacement of broken springs is the simplest but also the most expensive solution. The price of main spring leaf is 18.000 dinars per spring. However, if in stead of spring replacement technology of broken spring repair is improved by introducing welding technology of main spring leaf, than economic savings of this model are also big. Expected price of welding of main spring leaf would be cca 6.000 dinars which is less in relation to replacement which is 12.000 dinars per spring.

Mentioned economic indicators of introducing new technical solutions into improvement of suspension system elements offer direct effects and savings in

exploitation and application which is cca 1 million euros.

4. CONCLUSION

This paper gives the improvement of technical solution of suspension system at special freight wagons for coal transportation in steam power stations. Building of elastic elements in all wagons is expected and their behaviour would be analized in exploitation conditions. On the basis of technical and economic analysis realized in this paper huge savings should be expected in exploitation and maintenance conditions. Along with some modifications this solution can be applied at other freight wagons as well.

5. REFERENCES

- [1] Dr Milorad Pavličić, Preduzetništvo i poslovna politika u malim i srednjim preduzećima, ICIM, Kruševac 2001. god., str. 186.
- [2] Dr Milorad Pavličić, Ekonomika preduzeća-elementi teorije mikroekonomije, ICIM +, Kruševac, 2004. god., str. 65.
- [3] Elaborat 67/83, Identifikacija uzroka lomova glavnih listova gibnjeva na Fbd vagonu, Fabrika vagona Kraljevo, Opitni centar 1983.